ISSN 0021-9673

VOL. 467 NO. 1 APRIL 21, 1989

NAL OF HROMATOGRAPHY

NATIONAL JOURNAL ON CHROMATOGRAPHY, ELECTROPHORESIS AND RELATED METHODS

ELSEVIER

JOURNAL OF CHROMATOGRAPHY

Scope. The *Journal of Chromatography* publishes papers on all aspects of chromatography, electrophoresis and related methods. Contributions consist mainly of research papers dealing with chromatographic theory, instrumental development and their applications. The section *Biomedical Applications*, which is under separate editorship, deals with the following aspects: developments in and applications of chromatographic and electrophoretic techniques related to clinical diagnosis or alterations during medical treatment; screening and profiling of body fluids or tissues with special reference to metabolic disorders; results from basic medical research with direct consequences in clinical practice; drug level monitoring and pharmacokinetic studies; clinical toxicology; analytical studies in occupational medicine.

Submission of Papers. Papers in English, French and German may be submitted, in three copies. Manuscripts should be submitted to: The Editor of *Journal of Chromatography*, P.O. Box 681, 1000 AR Amsterdam, The Netherlands, or to: The Editor of *Journal of Chromatography, Biomedical Applications*, P.O. Box 681, 1000 AR Amsterdam, The Netherlands. Review articles are invited or proposed by letter to the Editors. An outline of the proposed review should first be forwarded to the Editors for preliminary discussion prior to preparation. Submission of an article is understood to imply that the article is original and unpublished and is not being considered for publication elsewhere. For copyright regulations, see below.

Subscription Orders. Subscription orders should be sent to: Elsevier Science Publishers B.V., P.O. Box 211, 1000 AE Amsterdam, The Netherlands, Tel. 5803 911, Telex 18582 ESPA NL. The *Journal of Chromatography* and the *Biomedical Applications* section can be subscribed to separately.

Publication. The *Journal of Chromatography* (incl. *Biomedical Applications*) has 37 volumes in 1989. The subscription prices for 1989 are:

J. Chromatogr. + *Biomed. Appl.* (Vols. 461–497):
Dfl. 6475.00 plus Dfl. 999.00 (p.p.h.) (total *ca.* US$ 3737.00)

J. Chromatogr. only (Vols. 461–486):
Dfl. 5200.00 plus Dfl. 702.00 (p.p.h.) (total *ca.* US$ 2951.00)

Biomed. Appl. only (Vols. 487–497):
Dfl. 2200.00 plus Dfl. 297.00 (p.p.h.) (total *ca.* US$ 1248.50).

Our p.p.h. (postage, package and handling) charge includes surface delivery of all issues, except to subscribers in Argentina, Australia, Brasil, Canada, China, Hong Kong, India, Israel, Malaysia, Mexico, New Zealand, Pakistan, Singapore, South Africa, South Korea, Taiwan, Thailand and the U.S.A. who receive all issues by air delivery (S.A.L. — Surface Air Lifted) at no extra cost. For Japan, air delivery requires 50% additional charge; for all other countries airmail and S.A.L. charges are available upon request. Back volumes of the *Journal of Chromatography* (Vols. 1–460)are available at Dfl. 195.00 (plus postage). Claims for missing issues will be honoured, free of charge, within three months after publication of the issue. Customers in the U.S.A. and Canada wishing information on this and other Elsevier journals, please contact Journal Information Center, Elsevier Science Publishing Co. Inc., 655 Avenue of the Americas, New York, NY 10010. Tel. (212) 633-3750.

Abstracts/Contents Lists published in Analytical Abstracts, ASCA, Biochemical Abstracts, Biological Abstracts, Chemical Abstracts, Chemical Titles, Chromatography Abstracts, Current Contents/Physical, Chemical & Earth Sciences, Current Contents/Life Sciences, Deep-Sea Research/Part B: Oceanographic Literature Review, Excerpta Medica, Index Medicus, Mass Spectrometry Bulletin, PASCAL-CNRS, Referativnyi Zhurnal and Science Citation Index.

See inside back cover for Publication Schedule, Information for Authors and information on Advertisements.

0021-9673/89/$03.50

Printed in The Netherlands

CONTENTS

(Abstracts/Contents Lists published in Analytical Abstracts, ASCA, Biochemical Abstracts, Biological Abstracts, Chemical Abstracts, Chemical Titles, Chromatography Abstracts, Current Contents/Physical, Chemical & Earth Sciences, Current Contents/Life Sciences, Deep-Sea Research/Part B: Oceanographic Literature Review, Excerpta Medica, Index Medicus, Mass Spectrometry Bulletin, PASCAL-CNRS, Referativnyi Zhurnal and Science Citation Index)

(Continued overleaf)

In articles with more than one author, the name of the author to whom correspondence should be addressed is indicated in the article heading by a 6-pointed asterisk (*)

JOURNAL OF CHROMATOGRAPHY

VOL. 467 (1989)

JOURNAL *of* CHROMATOGRAPHY

INTERNATIONAL JOURNAL ON CHROMATOGRAPHY,
ELECTROPHORESIS AND RELATED METHODS

ELSEVIER
AMSTERDAM — OXFORD — NEW YORK — TOKYO

J. Chromatogr., Vol. 467 (1989)

0021-9673/89/$03.50

Printed in The Netherlands

Journal of Chromatography, 467 (1989) 1–14
Elsevier Science Publishers B.V., Amsterdam — Printed in The Netherlands

CHROM. 21 231

GRADIENT FLOW PROGRAMMING: A COUPLING OF GRADIENT ELUTION AND FLOW PROGRAMMING

VIESTURS LESINS[a] and ELI RUCKENSTEIN*
Department of Chemical Engineering, State University of New York at Buffalo, Buffalo, NY 14260 (U.S.A.)
(First received August 30th, 1988; revised manuscript received December 21st, 1988)

SUMMARY

The coupling of flow programming and gradient elution is proposed as an integrated approach to the general elution problem. A model is developed to describe the process in which the flow-rate and mobile phase composition change with time. Experimental results with two model proteins compare favorably with theoretical calculations. A parametric study, experimental and numerical, illustrates the effect of various characteristic parameters. Since initial flow-rates are low, improved front-end resolution can be expected due to an increase in column efficiency. Since the mobile phase composition also changes with time, a wide range of elution strengths can also be applied to the column. This allows for the elution of species which initially are strongly retained.

INTRODUCTION

Even with the judicious selection of operating conditions, the separation of multicomponent mixtures by liquid chromatography (LC) under normal elution is often beset with problems. In many cases, the difficulty is due to the large differences in the relative migration rates of the individual components resulting in what is referred to as the general elution problem. Current methods of attacking the general elution problem include[1–4]: (i) solvent programming; (ii) flow programming; (iii) temperature programming; and (iv) coupled-column operation. In each of these techniques conditions are varied during the separation such that the retention of later eluting bands is reduced as a function of time after sample injection, so that the resolution and widths of early- and late-eluting bands are made more similar.

Few examples have been reported of the combination of two or more of the above individual procedures into a single technique. The purpose of this paper is to explore the feasibility of gradient flow programming (GFP). In this technique gradient elution is coupled with flow programming to yield a new attack on the general elution problem. A mathematical model is developed to describe the procedure. In addition,

[a] Present address: Occidental Chemical Corporation, Development Center, Buffalo Avenue and 53rd St., Niagara Falls, NY 14303, U.S.A.

0021-9673/89/$03.50

a parametric study, both numerical as well as experimental, with two model proteins illustrates the effects of various parameters. Although the present application is restricted to ion-exchange chromatography, GFP can also be applied to other methods.

THEORY

Before considering GFP, it is useful to briefly review its pure constituents, namely, gradient elution and flow programming. For more comprehensive accounts, the interested reader is referred elsewhere[2–4].

Gradient elution is performed by varying the composition of the mobile phase with time so as to provide a continual increase in the solvent strength of the mobile phase entering the column. Thus the initial bands from a normal elution procedure have their migration rates decreased and are separated under more optimal conditions. In addition, since solvent strength increases with time, the final bands from a normal elution procedure have their relative migration rates increased to values near the optimum range. In this manner, all bands migrate through the column with near optimum capacity factor values of about 2–5.

Flow programming is a technique where the flow-rate increases as a function of time. A significant increase in front-end resolution (*i.e.*, the earlier eluting species) from flow programming can be achieved relative to normal elution, due to an increase in column efficiency (*i.e.*, plate number). Although column efficiency is reduced for later eluting components, resolution of these bands is often not a problem.

Although solvent programming is probably the best single method in dealing with the general elution problem, it too can suffer from poor front-end resolution. For example, it may not be possible to obtain mobile-phase conditions so as to significantly increase the retention of early-eluting components. This situation could arise with water as the initial solvent in reversed-phase chromatography or with a plain buffered solution (*i.e.*, no additional electrolyte) in ion-exchange chromatography. In these cases, a decrease in the elution strength of the initial solvent is not possible. In addition, changing to another LC method may not always be practical or feasible for the separation at hand. Thus, to improve resolution of these early eluting species, the column plate number must be increased. In other situations, where the capacity factors between the first and last eluting species differ significantly, front-end resolution may once again suffer if the gradient is too steep. In this case, a compromise must be made between analysis time and resolution. Thus, the coupling of gradient elution with flow programming can be useful in many situations. To understand how this occurs, consider the well-known equation for resolution, R_s, under normal elution conditions[2]:

$$R_s = \underbrace{\frac{1}{4}\left(\sqrt{N_2}\right)}_{\text{I}}\underbrace{\left(\frac{\alpha - 1}{\alpha}\right)}_{\text{II}}\underbrace{\left(\frac{k'_2}{1 + k'_2}\right)}_{\text{III}} \tag{1}$$

where the separation factor $\alpha = k'_2/k'_1$, the capacity factor $k' = (V_R - V_m)/V_m$, subscripts 1 and 2 refer to components 1 and 2, N is the plate number, V_R is the retention volume of the species, and V_m is the void volume.

The three factors (I, II, III) of eqn. 1 describe the contribution of three different effects to resolution which are essentially independent[2]. Consequently, to control resolution, the three factors of eqn. 1 can be adjusted more or less separately. Separation efficiency as measured by N (factor I) is varied by changing column length L or solvent velocity. Column efficiency is increased by increasing column length or by decreasing the flow-rate of the mobile phase, which is the characteristic operating feature of flow programming. The column capacity (factor III) as measured by k' is varied by changing solvent strength, which is the characteristic operating feature of gradient elution. Thus by combining flow programming with gradient elution, one has complete control of the factors involved in resolution as compared to the partial control offered by flow programming (term I) or gradient elution (term III) used alone, on a given column (term II). Hence improved separations can be expected.

In many cases, mobile phase programming is selected through trial and error. However, it would be advantageous to determine elution programming conditions for a given separation *a priori* from a limited knowledge of the properties of the chromatographic system and the components to be separated. Consequently, it is necessary to understand the influence of mobile phase programming on important retention characteristics such as retention volume, bandwidths, and the resolution of sample compounds. This paper quantitatively considers the dependence of the retention volume on various characteristic operating parameters involved in GFP and compares them to experimental results. The effects of operating conditions on bandwidths and resolution are illustrated experimentally and discussed qualitatively.

A schematic illustration of a GFP apparatus is illustrated in Fig. 1. Pump A delivers a chromatographically weak solvent at a constant flow-rate. Pump B delivers a strong solvent, at a flow-rate which increases with time. These solvents are mixed and sent to the column where separation occurs. Retention in ion-exchange chromatography with GFP will now be described. However, GFP has general applicability to any LC technique in which gradients in solvent strength are employed.

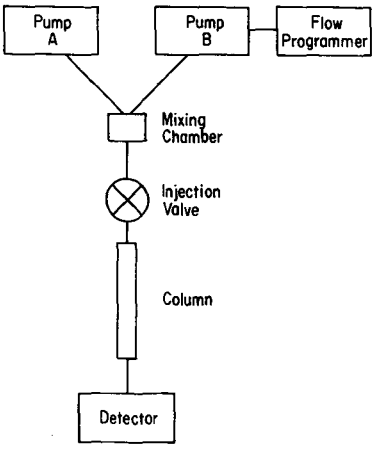

Fig. 1. A schematic illustration of a possible GFP system. In this particular situation, pump A delivers solvent at a constant flow-rate. The flow-rate of the solvent with high elution power increases with time and is delivered by pump B. These solvents are mixed and sent to the column.

MATHEMATICAL MODEL

Volumetric flow-rate

In GFP, the flow-rate and composition are both functions of time. In the present treatment, two solvent-delivery systems are employed to deliver solvent to the column. The flow-rate F_A of the weak solvent is taken as constant:

$$F_A = a = \text{constant} \tag{2}$$

The flow-rate F_B of the strong solvent is assumed to increase linearly with time. In the present situation, we assume that the flow-rate is initially zero and increases linearly with time as

$$F_B = bt \qquad t < t_G \tag{3a}$$

$$F_B = bt_G \qquad t \geqslant t_G \tag{3b}$$

where b is a constant, t is time and t_G is the total gradient time (b could also be a function of time). Also note that b and t_G may be limited by the maximum allowable column pressure. The significance of b and t_G will be discussed later. However, as with gradient elution, times greater than t_G are not advantageous since elution then essentially becomes isocratic in nature. The total flow-rate F to the column is simply

$$F = F_A + F_B = a + bt \qquad t < t_G \tag{4a}$$

$$F = a + bt_G \qquad t \geqslant t_G \tag{4b}$$

Gradient composition

As a specific example, consider ion-exchange chromatography. Let the salt concentrations originating from pumps A and B be denoted by x_A and x_B, respectively. The mobile phase concentration x at the column inlet is therefore given by

$$x = \frac{F_A x_A + F_B x_B}{F_A + F_B} \tag{5}$$

or, by substituting eqns. 2–4 into eqn. 5:

$$x = \frac{ax_A + bx_B t}{a + bt} \qquad t < t_G \tag{6a}$$

$$x_G = \frac{ax_A + bx_B t_G}{a + bt_G} \qquad t \geqslant t_G \tag{6b}$$

Isocratic retention model

Protein retention in ion-exchange chromatography can be represented by an equation of the form[5,6]

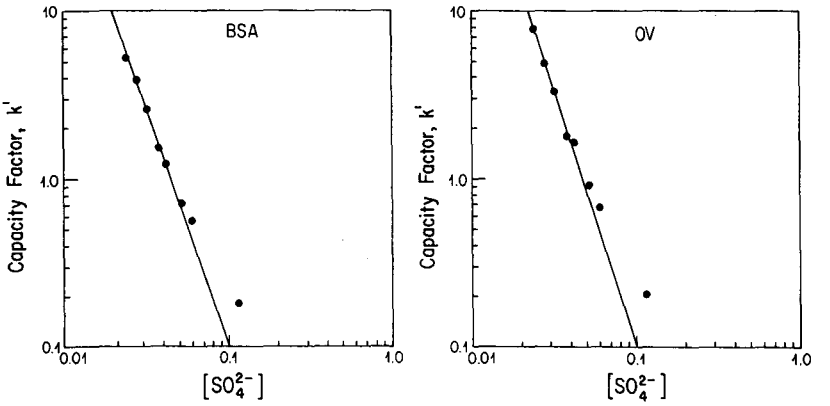

Fig. 2. Isocratic retention data plotted for BSA and OV according to eqn. 7. Isocratic retention parameters derived from linear regression of the data are given in Table I.

$$k' = Kx^m \tag{7}$$

where x is the salt concentration of the mobile phase, K is the equilibrium distribution constant for the ion-exchange process and m is the effective number of charges on the protein which interact with the adsorbent. The parameters m and K are evaluated from the slope and intercept of a plot of log k' *versus* log x, determined under isocratic conditions. The relationship of the capacity factor to the concentration of the displacing ion for bovine serum albumin (BSA) and ovalbumin (OV) is illustrated in Fig. 2.

Linear regression parameters characterizing the isocratic retention parameters of OV and BSA are summarized in Table I. These isocratic retention parameters are necessary for predicting elution in GFP.

Relation of isocratic retention to GFP conditions

The fundamental relationship for gradient elution is given by[3,4]:

$$\int_0^{V_g} \frac{dV}{V_a} = 1 \tag{8}$$

TABLE I

LINEAR REGRESSION PARAMETERS CHARACTERIZING THE ISOCRATIC RETENTION OF BSA AND OV

The error estimates represent the 90% confidence interval.

Protein	*m*	*log K*	*Correlation coefficient*
Bovine serum albumin	-2.83 ± 0.17	-3.83 ± 0.26	0.997
Ovalbumin	-3.04 ± 0.21	-4.02 ± 0.26	0.996

where V is defined by eqn. 10, V_g is the corrected retention volume ($V_g = V_R - V_m$) of the band at elution at its peak maximum, and V_m is the column void volume. The instantaneous value of the corrected retention volume at any given time is represented by V_a, which can be written as

$$V_a = V_m k_a \tag{9}$$

where k_a is the instantaneous value of k' for the band.

Substitution of eqns. 5 and 9 into eqn. 8 with

$$dV = F dt = (a + bt) dt \tag{10}$$

allows eqn. 8 to be rewritten as

$$\int_0^{t_g} \frac{(a + bt)^{m+1}}{(ax_A + bx_B t)^m} dt = KV_m \tag{11}$$

where the time t_g corresponds to the corrected retention volume V_g. At this point it is desirable to define the following dimensionless groups:

$$\tau = \frac{at}{V_m} \tag{12}$$

$$\theta = \frac{x_B}{x_A} \tag{13}$$

$$\kappa = \frac{bV_m}{a^2} \tag{14}$$

Note that τ is the dimensionless time (which compares the time with the void volume residence time at the initial flow-rate), while κ compares the flow-rate of the strong solvent (at a time equal to the residence time of the weak solvent) with the flow-rate of the weak solvent.

Introducing of eqns. 12–14 into eqn. 11 yields

$$\int_0^{\tau_g} \frac{(1 + \kappa\tau)^{m+1}}{(1 + \theta\kappa\tau)^m} d\tau = Kx_A^m \tag{15}$$

where τ_g is the dimensionless retention time corresponding to t_g. Note that the right-hand side of eqn. 15 is simply the capacity factor which would occur with mobile phase A, in other words, the initial capacity factor. To study the effects of θ and κ, which are the fundamental parameters of GFP, a parametric study of these variables was undertaken both numerically as well as experimentally.

MATERIALS AND METHODS

The essential features of the experimental apparatus are shown in Fig. 1. Two Waters Assoc. (Milford, MA, U.S.A.) Model 6000A solvent delivery systems were employed. Pump B was interfaced with a Waters Assoc. Model 660 solvent programmer. A Rheodyne (Cotati, CA, U.S.A.) Model 7125 injection valve with a 20-μl injection loop was employed to load protein onto a Rainin Instruments (Woburn, MA, U.S.A.) Hydropore 300A AX anion-exchange column (25 cm $\times$ 4.6 mm I.D.). Detection was at 280 nm with a Waters Assoc. Model 440 absorbance detector.

Proteins were purchased from Sigma (St. Louis, MO, U.S.A.) and were used without further purification. Other reagents were analytical-reagent grade or of comparable quality. Mobile phases were daily prepared freshly using freshly distilled water from an all-glass still and were passed through a 0.45-μm filter. Eluents were prepared by titrating a 0.0025 *M* sulfuric acid solution with any additional electrolyte required (ammonium sulfate) with imidazole to pH = 7.00 $\pm$ 0.02. Initial and final flow-rates were determined by collecting the column effluent in a buret and timed with a stopwatch. It was assumed that the flow-rate of pump B increased linearly with time. The gradient time, t_G, was monitored with a stopwatch.

RESULTS AND DISCUSSION

The effect of solvent strength ratio θ

Before examining experimental and theoretical results illustrating the effect of θ, it is worthwhile examining the significance of θ and its relation to the separation process. As given by eqn. 13, θ is simply the ratio of salt concentrations in the solvent B reservoir and the solvent A reservoir; thus, θ is a measure of the increase in solvent strength that can be expected. However, in contrast to most gradient elution procedures which vary linearly from pure A to pure B, this situation does not occur in GFP. As shown by eqn. 6, the composition function can be rewritten in terms of the dimensionless variables as

$$x = x_A \frac{1 + \theta\kappa\tau}{1 + \kappa\tau} \qquad \tau < \tau_G \tag{16}$$

Thus, the final composition depends upon the initial concentration x_A, θ, κ, and τ_G (*i.e.*, the dimensionless time corresponding to t_G) and is not x_B as is the general case for most gradient elution procedures.

Although the only absolute requirement on the nature of solvents A and B is that B be chromatographically stronger than A (and that the two be miscible), several other features deserve comment. For example, as the strength of solvent B is decreased, the elution of later bands becomes slower, and the bands become wider and less easily detectable. Furthermore, bands may elute after the end of the elution program. In these situations, a stronger solvent B may be required to increase the final elution power of the elution program. Of course, if the last band elutes well before the end of the elution program, separation time can be saved by terminating the elution program at the time of elution of the final sample band. On the other hand, if solvent A is too

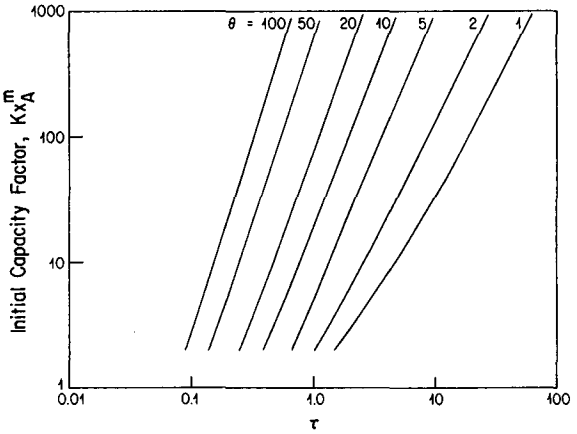

Fig. 3. Numerical results illustrating the effect of θ at $\kappa = 0.5$ and $m = -2.5$.

weak, the resolution of early eluting species may suffer. Consequently, solvents A and B must be properly chosen for the separation at hand.

Another parameter of importance in GFP is gradient steepness; *i.e.*, the rate of change of solvent composition with time. This is given by

$$\frac{dx}{d\tau} = x_A \frac{[\kappa(\theta - 1)]}{(1 + \kappa\tau)^2} \tag{17}$$

The importance of gradient steepness parallels that of the capacity factor in isocratic elution. Thus as the solvent strength is increased in isocratic elution with a concomitant decrease in the capacity factor, the resolution of a given pair of adjacent bands decreases while the sensitivity (*i.e.*, the peak height-to-width ratio) increases and analysis time decreases. Thus a compromise between adequate resolution and sensitivity exists for an intermediate solvent strength which yields k' values in the neighborhood of 2–5. As with isocratic elution, there exists a similar compromise among sensitivity, resolution, and analysis time that favors some intermediate gradient steepness. Thus, as gradient steepness increases, resolution of adjacent bands decreases while sensitivity increases and analysis time decreases.

The effect of θ at constant κ and m is summarized in Fig. 3. Note that the case $\theta = 1$ is simply isocratic flow programming. Thus, the effect of increased elution strength, as measured by θ, is illustrated. As shown, by increasing θ, the dimensionless retention time, τ, decreases for a given initial capacity factor. This is expected since an increase in θ increases the gradient steepness and hence higher concentrations of electrolyte enter the column at earlier times; this promotes the elution of the components. One can show that by increasing κ, the lines of θ are shifted to lower values of τ. Once again, higher concentrations of the eluting species reach the column at earlier times and hence, elution is promoted. Experimental results illustrating the effect of θ on the separation of OV and BSA are shown in Figs. 4–6. Note that at $\theta = 5$, the peaks are rather broad and resemble those of isocratic elution. By increasing θ, the gradient steepness increases leading to decreased retention volumes and sharper peaks. However, if θ is increased too much, the gradient steepness becomes to large and

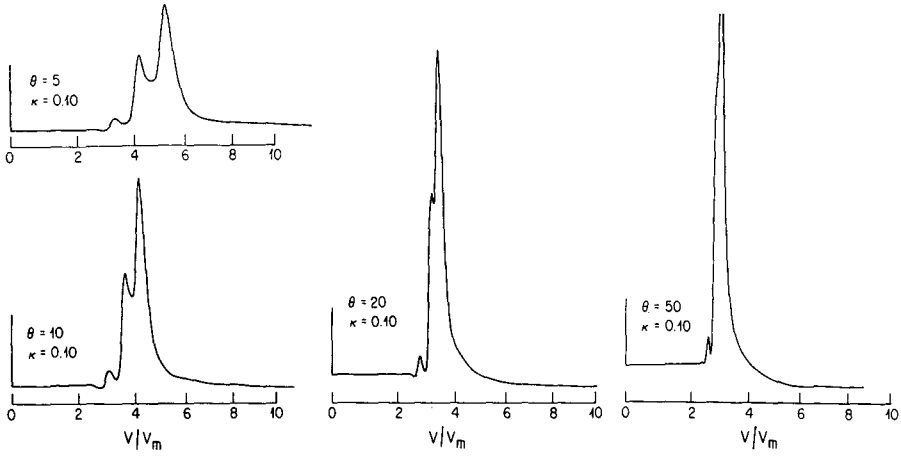

Fig. 4. Experimental results illustrating the effect of θ at $\kappa = 0.10$.

resolution suffers. Consequently, the components can no longer be adequately resolved. Thus it can be seen that a decrease in gradient steepness leads to the following changes: (i) broader bands and decreased detections sensitivity; (ii) generally improved resolution; and (iii) increased separation volumes. Finally, note that the resolution of OV and BSA is adequate under most experimental conditions and is comparable or marginally better than that of normal gradient elution under typical operating conditions as illustrated in Fig. 7. However, as previously stated, one advantage of GFP is an increase in front-end resolution due to increased column efficiency for the early eluting components. This effect will be illustrated shortly.

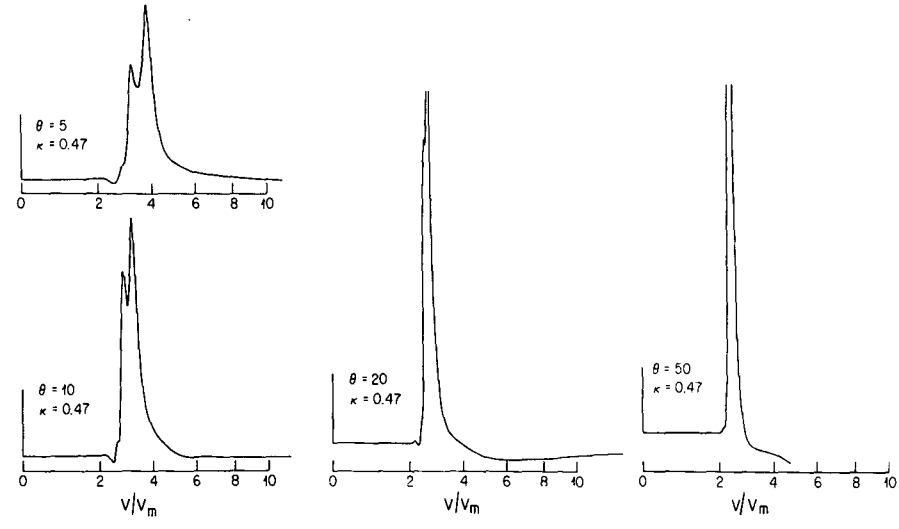

Fig. 5. Experimental results illustrating the effect of θ at $\kappa = 0.47$.

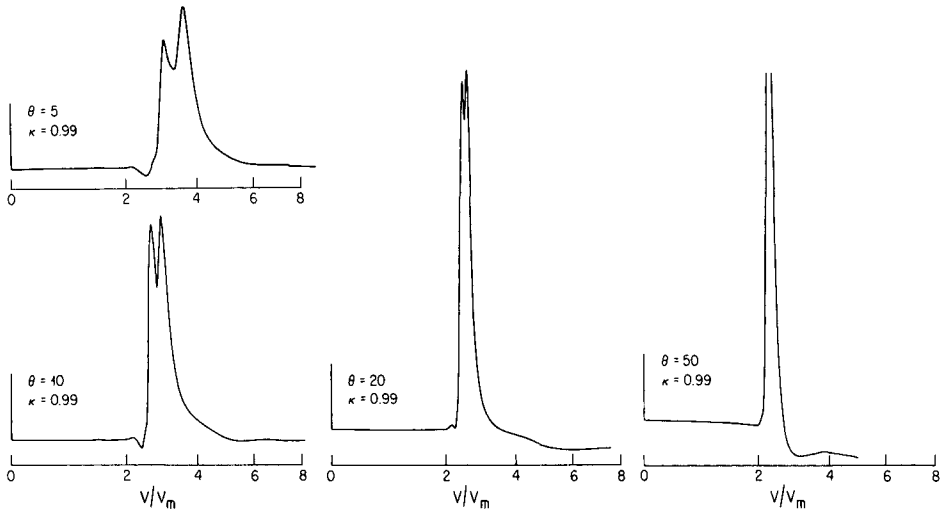

Fig. 6. Experimental results illustrating the effect of θ at $\kappa = 0.99$.

The effect of the relative increase in flow-rate as reflected through κ

The definition of κ is given by eqn. 14. Multiplication of eqns. 12 and 14 yields

$$\kappa\tau = \frac{bt}{a} \tag{18}$$

Thus κ gives an indication of the increase in the volumetric flow-rate as compared to the initial flow-rate. Note that for $\kappa\tau = 1$, pump A and pump B are delivering the same volumetric flow-rate. For $\kappa\tau < 1$, pump A delivers the bulk of the solvent to the column whereas for $\kappa\tau > 1$, pump B delivers the majority of the solvent to the column.

The effect of κ at constant m and θ on τ is summarized in Fig. 8. As illustrated, by increasing κ, the dimensionless retention time τ decreases for a given initial capacity

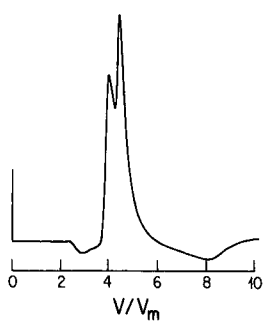

Fig. 7. Normal gradient elution of BSA and OV at pH 7.00. Elution was performed with a 30-min linear gradient from buffer alone to buffered 0.2 *M* ammonium sulfate.

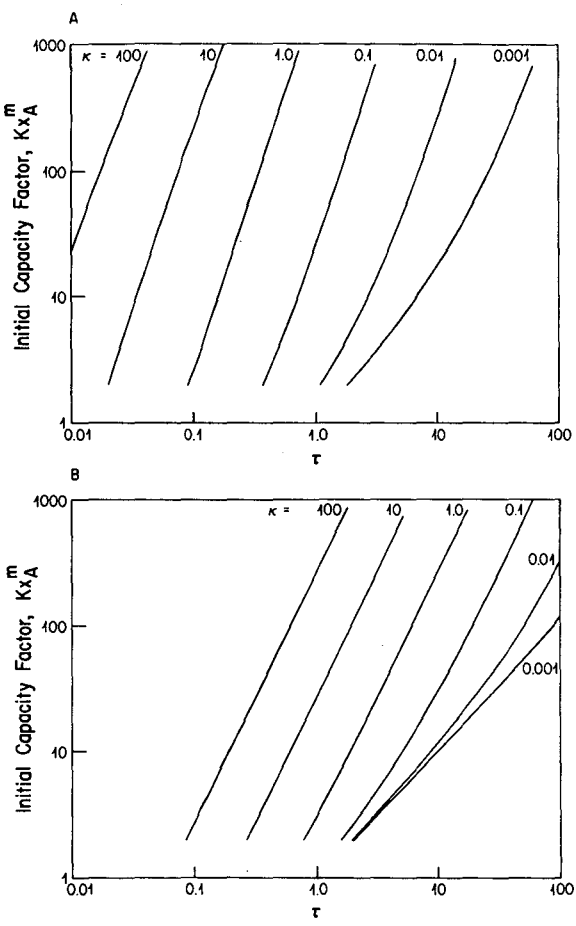

Fig. 8. Numerical results illustrating the effect of κ at (A) $\theta = 50$ and (B) $\theta = 2$. $m = -2.5$.

factor. This would be expected even under isocratic conditions due to the increase in the flow-rate; however, the effect becomes accentuated as θ increases due to an increase in the elution power of the mobile phase. Experimental results illustrating the effect of κ are shown in Figs. 9–11.

Once again, for low values of θ and κ, the chromatograms resemble those of normal elution. By increasing either θ or κ, elution is achieved by increasing the solvent strength and hence the migration of the components. Although the peaks become less broad, resolution also decreases.

As was previously stated, a driving force behind the development of GFP was in response to the poor resolution of early bands when the weakest possible solvent A is used. The proposed solution was to increase the plate number N by initially employing a low flow-rate. Thus, by increasing column efficiency, front-end resolution should be improved. This is illustrated in Fig. 12. In each case the final flow-rate is approximately the same. Consequently, $\kappa = 0.10$ represents a higher initial flow-rate than $\kappa = 0.47$ which in turn is higher than for $\kappa = 0.99$. Note that by decreasing the initial flow-rate,

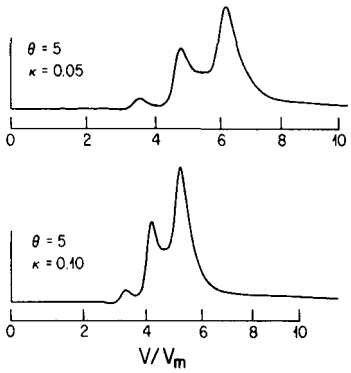

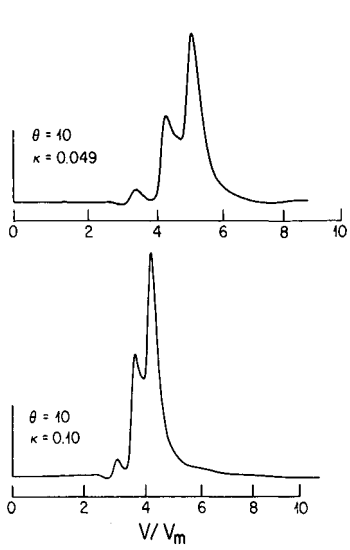

Fig. 9. Experimental results illustrating the effect of κ at $\theta = 5$.

Fig. 10. Experimental results illustrating the effect of κ at $\theta = 10$.

an improvement in resolution occurs due to increased column efficiency even for components which have observed capacity factors in the desirable range of approximately 2–5. Greater enhancement of resolution is expected for bands which are poorly retained (i.e. $k' < 2$).

Comparison between theory and experiment

Eqns. 5, 6 and 11 represent an idealized case for GFP in that they neglect the dwell volume of the apparatus. In many situations, this dwell volume V_D can be

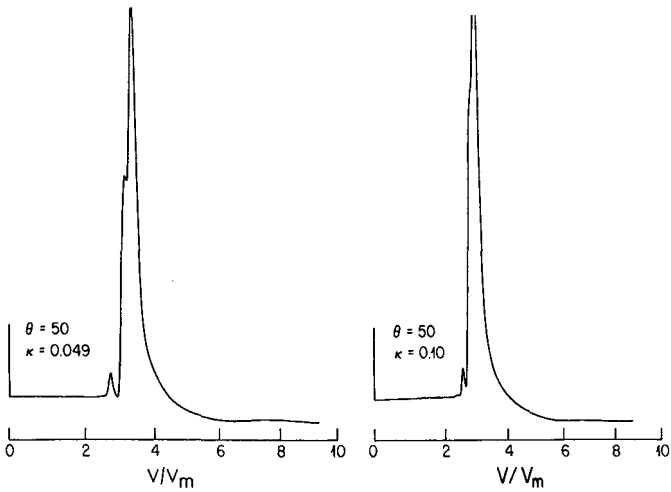

Fig. 11. Experimental results illustrating the effect of κ at $\theta = 50$.

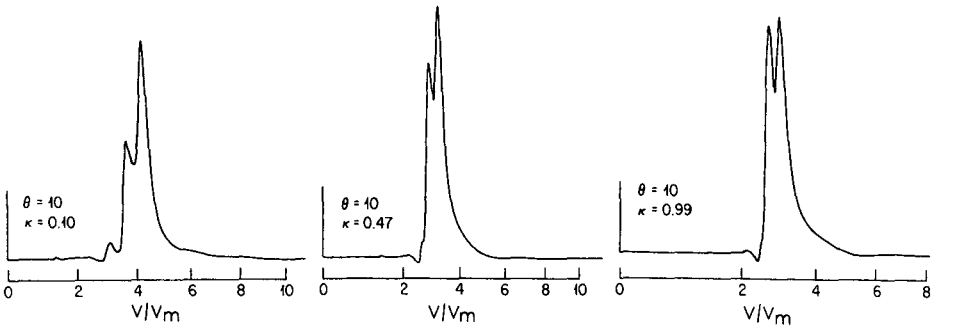

Fig. 12. Experimental results illustrating the improvement of resolution by decreasing the initial flow-rate.

significant and must be corrected for. To account for this non-ideality, the previous mathematical development is easily modified. The gradient composition now becomes

$$x = \frac{ax_A + b(t - t_D)x_B}{a + b(t - t_D)} \qquad t > t_D \tag{19}$$

$$x = x_A \qquad t \leqslant t_D \tag{20}$$

where t_D is the dwell time. The dwell time is simply the holdup time between the point where solvent mixing occurs and where the mixed solvent reaches the column inlet. Consequently, the fundamental equation for gradient elution becomes

$$\int_0^{\tau_D} (1 + \kappa\tau)d\tau + \int_{\tau_D}^{\tau_g} \frac{(1 + \kappa\tau)[1 + \kappa(\tau - \tau_D)]^m}{[1 + \kappa\theta(\tau - \tau_D)]^m} = Kx_A^m \tag{21}$$

where τ_D is the dimensionless dwell time. The first integral on the left-hand side of eqn. 21 is solved analytically whereas the second integral is solved numerically. These two integrals are then added and checked against the right-hand side of eqn. 21, which can be calculated from the parameters of Table I and then compared to the observed results. Table II summarizes the comparison between calculations employing eqn. 21 and the experimental results. The agreement is acceptable if one realizes the numerous sources of error involved. For example, the isocratic retention parameters (see Fig. 2) do not precisely fit the data. Thus, when the left-hand side of eqn. 21 is integrated numerically and checked against the calculated initial capacity factor (*i.e.* Kx_A^m), a large error in τ_g can occur due to the range of initial capacity factors (*i.e.*, Kx_A^m) which are within the confidence interval predicted by eqn. 7.

CONCLUSIONS

GFP provides a new method of attack on the general elution problem by combining the desirable features of gradient elution and flow programming. The method may prove useful when front-end resolution is poor and the weakest possible chromatographic solvent is already being employed. Experimental results with two

TABLE II

COMPARISON BETWEEN EXPERIMENTAL AND THEORETICAL RESULTS IN GFP

θ		*Observed retention time (min)*	τ_g	τ_R	*Calculated retention time (min)*
$\kappa = 0.049 \pm 0.006$; $\tau_D = 1.0$; $\tau_m = 0.98$; $V_m/a = 4.63$ min					
5.00 ± 0.33	BSA	19.8	4.43	5.41	25.0
	OV	25.3	5.14	6.12	28.3
10.0 ± 0.6	BSA	18.0	3.35	4.33	20.0
	OV	21.0	3.72	4.70	21.8
20.0 ± 1.2	BSA	15.5	2.57	3.55	16.4
	OV	17.0	2.76	3.74	17.3
50.0 ± 3.5	BSA	13.0	1.89	2.87	13.2
	OV	14.3	1.97	2.95	13.7
$\kappa = 0.47 \pm 0.04$; $\tau_D = 0.86$; $\tau_m = 0.84$; $V_m/a = 6.65$ min					
5.00 ± 0.33	BSA	14.3	1.85	2.69	17.8
	OV	16.3	1.98	2.82	18.7
10.0 ± 0.6	BSA	13.0	1.46	2.30	15.2
	OV	14.0	1.51	2.35	15.6
20.0 ± 1.2	BSA	11.8	1.22	2.06	13.7
	OV	12.3	1.25	2.09	13.9
50.0 ± 3.5	BSA	11.3	1.05	1.89	12.6
	OV	11.3	1.06	1.90	12.6
$\kappa = 0.99 \pm 0.15$; $\tau_D = 0.75$; $\tau_m = 0.73$; $V_m/a = 11.9$ min					
5.00 ± 0.33	BSA	19.5	1.36	2.09	24.8
	OV	22.3	1.44	2.17	25.8
10.0 ± 0.6	BSA	18.0	1.10	1.83	21.7
	OV	19.3	1.13	1.86	22.1
20.0 ± 1.2	BSA	16.8	0.96	1.69	20.1
	OV	17.3	0.97	1.70	20.2
50.0 ± 3.5	BSA	16.3	0.86	1.59	18.9
	OV	16.3	0.86	1.59	18.9

model proteins and an anion-exchange column illustrate the method as a function of various characteristic parameters. Resolution is good and results compare favorably to theory in view of the experimental errors involved. Improved resolution due to increased column efficiency is also demonstrated.

REFERENCES

1 L. R. Snyder, *J. Chromatogr. Sci.*, 8 (1970) 692.
2 L. R. Snyder and J. J. Kirkland, *Introduction to Modern Liquid Chromatography*, Wiley, New York, 1974, p. 38.
3 L. R. Snyder, in Cs. Horváth (Editor), *High Performance Liquid Chromatography — Advances and Perspectives*, Vol. 1, Academic Press, New York, 1980.
4 P. A. Jandera and J. Churacek, *Adv. Chromatogr. (N.Y.)*, 19 (1981) 125.
5 N. K. Boardman and S. M. Partridge, *Biochem. J.*, 59 (1955) 543.
6 W. Kopaciewicz, M. A. Rounds, J. Fausnaugh and F. F. Regnier, *J. Chromatogr.*, 266 (1983) 3.

Journal of Chromatography, 467 (1989) 15–30
Elsevier Science Publishers B.V., Amsterdam — Printed in The Netherlands

CHROM. 21 229

MULTIFACTOR SIMULTANEOUS STATISTICAL OPTIMIZATION OF THE MOBILE PHASE COMPOSITION FOR THE SEPARATION OF INORGANIC ANIONS IN REVERSED-PHASE ION-INTERACTION CHROMATOGRAPHY

Q. XIANREN* and W. BAEYENS
Department of Analytical Chemistry, Vrije Universiteit Brussel, Pleinlaan 2, 1050 Brussels (Belgium)
and
Y. MICHOTTE
Laboratory of Pharmaceutical Chemistry and Drug Analysis, Vrije Universiteit Brussel, Laarbeeklaan 103, 1090 Brussels (Belgium)
(First received October 12th, 1988; revised manuscript received December 23rd, 1988)

SUMMARY

The optimization of the analysis of a mixture of five anions with reversed-phase ion interaction chromatography has been investigated. The criteria selected were the resolution of the most critical peak pair, R_{s1} (NO_2^-–Br^-), the total analysis time which corresponds to a certain range of R_{s2} (NO_3^-–SO_4^{2-}) and the peak height of Cl^-, NO_3^- and SO_4^{2-}. The factors selected to realize the optimization were the mobile phase concentrations of tetrabutylammonium iodide and phthalate buffer, and the pH. Only a limited number of experimental data points, ordered in a central composite design, were required for the computation of the response function with a non-linear regression model. Application of this computer-aided multifactor simultaneous statistical approach resulted in a rapid optimization of the selected criteria. The computed global optimum is close to the best experimentally obtained result.

INTRODUCTION

Several approaches based on reversed-phase chromatography have been used, as an alternative to ion chromatography, to separate the common inorganic anions[1–3]. Among these, applications of ion-pair chromatography (IPC) or ion-interaction chromatography (IIC) using an octadecyl-bonded silica as a non-polar stationary phase have recently been reported[4–7]. The success of this inorganic separation technique is primarily because of the large number of variable factors that can be adjusted in the mobile phase to give improved chromatographic performance. The pH, ionic strength, the counter-ion concentration and the concentration of the hydrophobic ion-interaction or ion-pair reagent of the eluent are frequently used factors in mobile phase optimization studies[8–11]. The theoretical dependency of the capacity factor on these factors has been studied by various authors[6,12]. More detailed studies

0021-9673/89/$03.50

on the influence of various parameters on the retention behaviour have been performed by Bartha and Vigh[13,14]. Such studies provide the key to systematic optimization of IIC.

Papers concerning mobile phase optimization, an important topic for chromatographers can frequently be found in the recent literature. The aim of optimization is to achieve the maximum attainable separation of all components of a complex multi-component mixture of solutes within a minimum analysis time, and also, if possible, with the highest sensitivity for all solutes. In general, the optimization methods are based on either heavily modelled formalisms or purely empirical functions; the former are becoming cumbersome (except for fairly simple systems) as the number of parameters increases and the model grows more complex. When developing a chromatographic method, the existence of the multifactors with multicriteria to be optimized in order to achieve the best separation of a mixed sample complicates the optimization process. In addition, as discussed by some authors[9,10], optimization of chromatographic performance is especially difficult not only because of the variation in chromatographic behaviour due to the different properties of the reversed-phase materials but also because of the existence of multiple optima over the domain of mobile phase composition.

Nevertheless, many successful optimization schemes have been proposed in recent publications, such as the solvent selectivity triangle approach[15], the sequential simplex technique and the chromatographic optimization function[16,17], the overlapping resolution mapping (ORM) method[18], the "window diagram" graphic method[9,19] and recently computer-aided procedures[11,19–22]. Among these, the statistical approaches for optimization of discrete variables such as the pH and other ionic effects using a factorial design have been shown to be quite useful in specific analyses[10,16,22]. Sachok *et al.*[9] optimized the separation of a nine-component mixture of weak organic acids, bases and zwitterionic compounds using a four-level two-factor (4^2) experimental design to specify sixteen mobile phase compositions. A similar experimental design has been used by Lindberg *et al.*[10] to separate four alkaloids.

In this study, a three-factor central composite design was used for the optimization experiments. We will discuss the computer-aided multifactor statistical optimization approach and the application of a polynomial mathematical model with regard to the separation of a mixture of five inorganic anions with a reversed-phase IIC system. Computer predicted response surfaces were used to describe the combined effect of three variables or factors (ion-interaction reagent concentrations, pH, buffer concentration) on the resolutions, (R_s), of some critical peaks, and their sensitivities (peak height, h), which were the criteria selected for optimization.

EXPERIMENTAL

Apparatus and reagents

The chromatographic system consisted of a DuPont 870 HPLC pump, a Valco injection valve with 100- or 50-μl loop volume, a Partisil 10 ODS-3 RP column (250 mm × 4.6 mm I.D., Whatman) acting as a separation column and protected with a 60 mm × 2.1 mm guard column using the same packing, a Perkin-Elmer LC-21 conductivity detector and an Omniscribe B5 217-5 strip chart recorder. The separation column, guard column and detector cell were thermally isolated in a wooden box to

minimize short-term temperature variations. All separations were carried out at room temperature and a mobile phase flow-rate of 2 ml/min.

All water used was deionized and passed through a Millipore (Bedford, MA, U.S.A.) Milli-Q water purification system. Tetrabutylammonium iodide (TBAI, 98% for synthesis) was obtained from Merck, potassium hydrogenphthalate (KHP, A.R.) from R.C.B. (Belgium); all other reagents were of A.R. grade. Standard solutions (1000 ppm) of inorganic anions (chloride, nitrite, bromide, nitrate, sulphate and dichromate) were prepared by dissolving appropriate amounts of the corresponding potassium salts in pure water. These solutions were diluted daily to give the trace solutions required.

Mobile phases

The eluents used contained TBAI with KHP at pH between 4 and 6.5. The concentrations of TBAI ranged from 0.5 to 16 m*M*, and of KHP ranged from 0.5 to 2 m*M*. The pH of all mobile phases was adjusted by adding to a solution, containing a weighed amount of the salt, potassium hydroxide or acetic acid followed by a dilution to volume. These eluents were prepared daily, filtered through a 0.45-μm porosity membrane filter (Millipore HSWP 04700) and degassed before use.

Column preparation

The columns were packed in the laboratory by a slurry technique using 2-propanol as a suspending medium under a pressure of 6000–6500 p.s.i. They were washed successively with 100 ml of methanol and 60 ml water before use. Column testing was carried out with our operative mobile phase. A sample containing a mixture of chloride, nitrite, bromide, nitrate and sulphate may show capacity factors, k', between 1.3 and 7. Only columns that gave theoretical plate heights of more than 15 000 were accepted for use.

METHODS

The mobile phase optimization method we applied can be considered as a stochastic statistical procedure. The essential steps in this approach are similar to those described by Snee[23] in his optimization: (1) generation of data using a pre-planned experimental design; (2) finding a mathematical model to fit these data using statistical curve-fitting techniques and (3) examination of the response surfaces to determine the best value. This approach requires only a limited predefined number of experimental chromatograms which can be used for the construction of a model of the chromatographic system in question. The model can, in principle, accurately predict the behaviour of all solutes within the mobile phase envelope defined, without recourse to further experiments. In addition, optimum separation conditions can be inferred from the model. Since a critical problem is the fact that up to date no mathematical model exists which is able to predict the retention of the analytes and hence to describe the true response surface on the basis of solely fundamental principles, (1) the velocity field (advection and diffusion) in the separation column and (2) the binding kinetics of anions on the stationary phase, statistical optimization methods have to be used. These models are stochastic because of random uncertainties in the experimentally obtained data. For the same reason, these models cannot be

extrapolated to conditions which are beyond the scope of the experiments included in the model.

In order to improve the accuracy of the predictions achievable with the statistical model, a two level approach is adopted: (a) modification of the polynomial equations [for example instead of $y = f(x)$ ones uses $\log y = f(x)$] until a good agreement between experimental and calculated data is obtained and (b) verification of the predicted optimum by some new experiments which are planned around the location of the predicted optimum and/or extension of the variable values beyond the original domain of the factor design. The resulting data are used to improve the model and to calculate a new optimum.

Three-factor central composite experimental design

In order to investigate the effect of each variable on the separation and detection quality and their possible interaction, a three-factor central composite design which requires fifteen experiments according to Massart *et al.*[24] has been adopted as the optimization strategy. In these methods, one tries to describe the response surface in the region where the optimum is to be found using a mathematical equation. In most instances generalized polynomials are employed

$$y = b_0 + b_1x_1 + \ldots + b_nx_n + b_{11}x_1^2 + b_{12}x_1x_2 + \ldots + b_{nn}x_n^2 + \ldots \quad (1)$$

where y is the approximate response, $x_1, \ldots, x_n$ are the factors and $b_0, \ldots, b_{nn}$ are the coefficients estimating the true and unknown coefficients $\beta_0, \ldots, \beta_{nn}$. Usually, only first- or second-degree polynomials are employed, but we used a more elaborate one.

The coefficients $b_0, \ldots, b_{nn}$ are determined from a number of independent equations at least equal to the number of coefficients. If this number is m, this means that m experimental responses y_i must be determined. These are several advantages of organizing the experiments in a factorial design[25]: (i) when there are no interactions the factorial design gives the maximum efficiency in the estimation of the effects; (ii) when interactions exist, their nature being unknown, a factorial design is necessary to avoid misleading conclusions; (iii) in a factorial design the effect of a factor is estimated at several levels of the other factors, and the conclusions hold over a wide range of conditions. In particular, it is preferable to use orthogonal factorial plans. First, the factors, x_i, which have an important effect on the response have to be defined. As we mentioned earlier, the optimization of the separation of anions involves the optimization of three factors: the mobile phase buffer concentration, pH and ion-interaction reagent concentration. Then, it is convenient to scale the factors and to express the factor levels in scaled units. As a result the base point, y_0, of a factorial experiment has a scaled value of zero for each factor, and the other points can have values of $+1$, 0, -1. Next, one has to decide the kind of polynomial to be used to approximate the response surface, because it determines the number of coefficients, b_i, which have to be assessed. In our case, this number is eleven. We tested several polynomials (see below) and found that the best results were obtained with the usual second-order polynomial, see eqn. 1, extended with an eleventh term: $a_{10}x_1x_2x_3$ (see below). We can now carry out a one-, two-, three- or still higher-level factorial experiment. A three-factor, two-level design involves 8 experiments. This is not sufficient to determine the eleven coefficients, b_i, of the response surface polynomial.

A three-level factorial design involves 27 experiments which largely exceeds the requirements. A more efficient procedure is the use of a central composite design. $2n + 1$ (n being the number of factors) experiments are added to the 2^n design (two-level design), one of the additional experiments being performed at the base point and the others along the coordinate axes at a distance "a". The value of "a" making a three-factor composite design orthogonal is 1.215 (ref. 25). The resulting arrangement of experimental points (15) is shown in Fig. 1.

RESULTS AND DISCUSSION

Once the experimental design has been chosen (in our case, see discussion above, a central composite design including 15 points, which include the corners of a cube, the centre point and 6 additional points), a number of decisions have to be made in an hierarchical way before model fitting and prediction can be performed.

(1) The choice of the optimization criteria. Each optimization criterion is mathematically expressed as a response function, y, of a number of factors, x_i (see eqn. 1): y is a directly measurable parameter, for example the peak height of a given anion, or can be calculated, for example the resolution of a peak pair of anions.

The choice of the optimization criteria cannot be made on a purely theoretical basis. Some preparative experiments must indicate which anions are the most difficult to separate, which anions shows the lowest detection sensitivity and which anions determine the analysis time. In a previous work, we studied yet the influence of the mobile phase composition on the chromatographic behaviour of each anion in a mixed sample based on one factor[7] or two factors[26] at a time. We found that with most mobile phase compositions the peaks of NO_2^- and Br^- were only poorly separated, and showed the worst resolution of all peak pairs. The optimization of R_s (NO_2^-–Br^-) becomes therefore the key criterion of the global optimization. A second important criterion regarding chemical analyses is the total analysis time. Since the total elution time is related to the resolution of the last two peaks eluted (NO_3^- and SO_4^{2-}, see Fig. 2), R_s (NO_3^-–SO_4^{2-}) is used to optimize the total elution time indirectly. A third criterion of analytical interest is the sensitivity of the method. Based on these considerations, we choose in order of priority the following optimization criteria: (1) the best resolution of the most critical peak pair (NO_2^-–Br^-), (2) an optimum

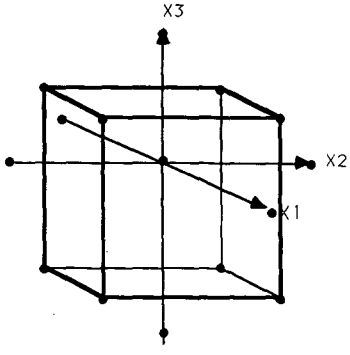

Fig. 1. Schematic representation of the three-factor central composite design.

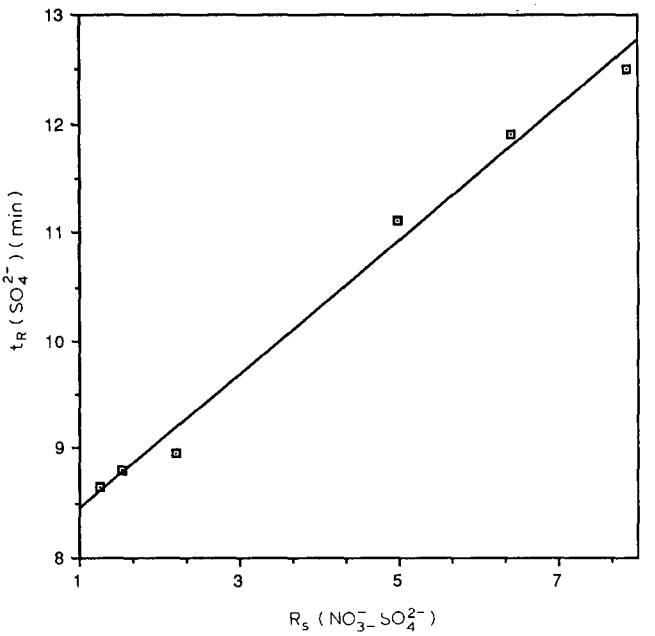

Fig. 2. Retention time dependency of the last anion peak (SO_4^{2-}) eluted from the separation column on the resolution of NO_3^-–SO_4^{2-}. [TBAI] = 8 mM, [KHP] = 1 mM, pH 5.

resolution range for the peak pair NO_3^-–SO_4^{2-}, with an under and upper limit, and (3) the best possible detection responses (peak heights in our experiments but integrated peak areas may also be used) of chloride, nitrate and sulphate.

It is clear that for other chromatographic systems, other optimization criteria and orders of priority may be chosen. For example, optimization criteria such as the "Chromatographic Response Function"[17,27], the "Relative Resolution Products"[15,28] or the "Chromatographic Optimization Function"[15] have been reported for the optimization of organic separation with mixed design. In this work, the realistic optimization criteria which can be selected based on our chromatographic experience are as follows: (a) the least acceptable resolution of the peak pair NO_2^-–Br^-, R_{s1}, is 1.35; (b) the resolution of the peak pair NO_3^-–SO_4^{2-}, R_{s2}, is restricted to the range of 1.5 to 1.8, which means that the total separation time should be less than 10 min; (c) maximum peak heights, h_i, for Cl^-, NO_3^- and SO_4^{2-}. Here no special need exists to put a restriction on h. However, if in addition to an optimum value of R_{s1} (R_{s1} exceeds 1.35) and minimum analysis time ($1.5 < R_{s2} < 1.8$) the h values exceed a given standard height, h_x, then a global optimum is found.

(2) The choice of the factors (the dependent variables x_i in eqn. 1) which will be used to optimize the selected criteria. These factors should have a major influence on the selected criterion. In a previous paper we showed that the mobile phase pH, the TBA or ion interaction reagent concentration and the buffer concentration are the variables with the largest influence on the capacity factors as well as the resolution and peak heights.

Figs. 3 and 4 which result from the data of ref. 7 show the dependency of the

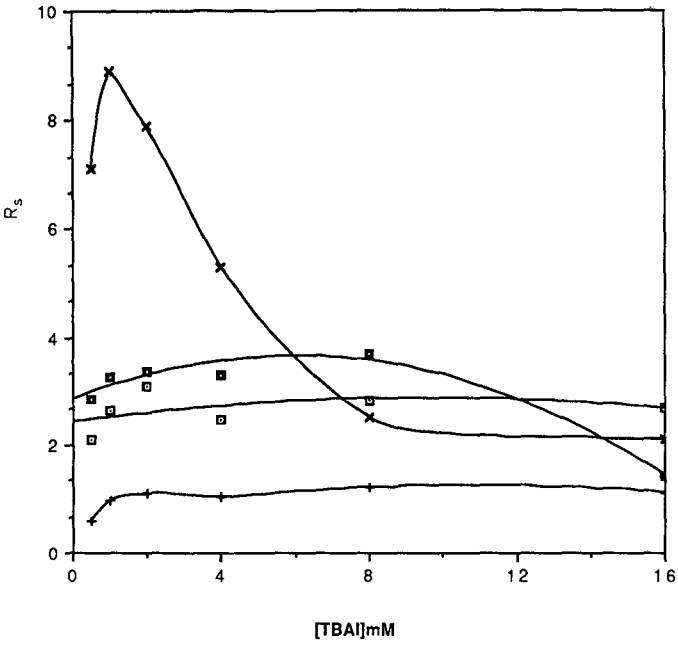

Fig. 3. Dependency of the resolution factor for several anion peak pairs on the TBAI concentration in the neat aqueous phthalate (1 m*M*) eluent (pH 5). Chromatographic conditions: flow-rate, 2 ml/min; Partisil 10 ODS-3 column; conductivity detection. (⊡) $R_s(Cl^- - NO_2^-)$; (+) $R_{s1}(NO_2^- - Br^-)$; (■) $R_s(Br^- - NO_3^-)$; (×) $R_{s2}(NO_3^- - SO_4^{2-})$.

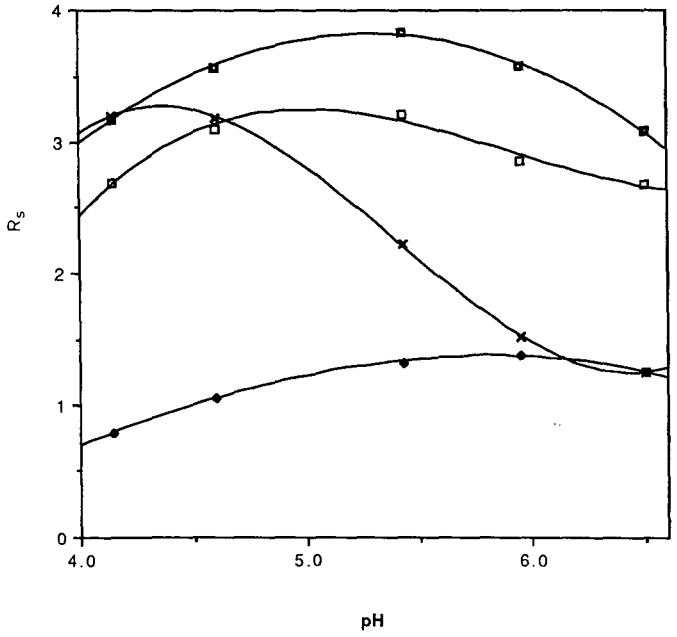

Fig. 4. Dependency of the resolution factor for several anion peak pairs on the pH with 1 m*M* KHP as the eluent. TBAI concentration: 8 m*M*. Chromatographic conditions as in Fig. 3. (□) $R_s(Cl^- - NO_2^-)$; (◆) $R_{s1}(NO_2^- - Br^-)$; (■) $R_s(Br^- - NO_3^-)$; (×) $R_{s2}(NO_3^- - SO_4^{2-})$.

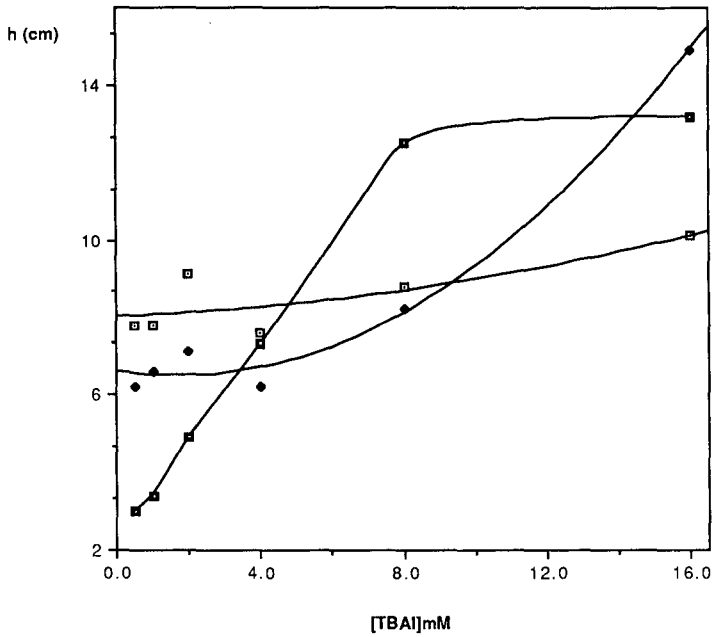

Fig. 5. Dependency of the peak height of the detected anions on the TBAI concentration in the eluent. Eluent: 1 m*M* KHP; pH 5. Chromatographic conditions as in Fig. 3. (⊡) R_1, Cl^-; (◆) R_2, NO_3^-; (■) R_3, SO_4^{2-}.

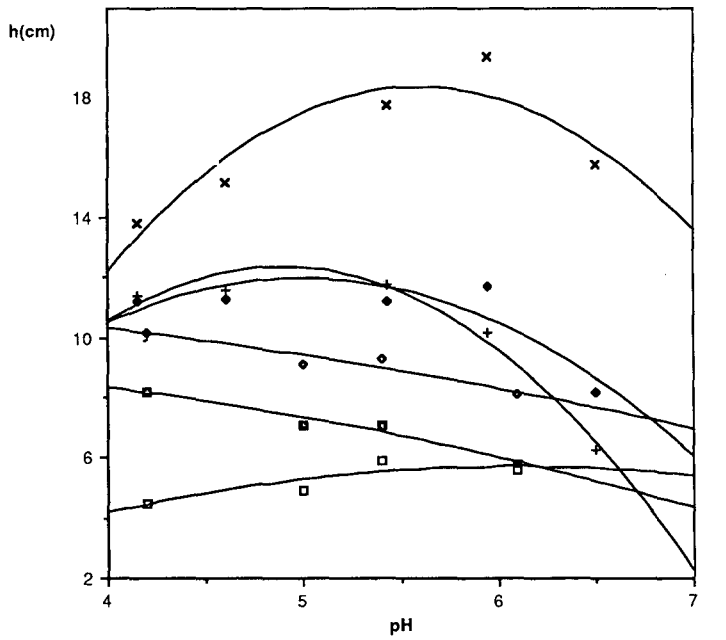

Fig. 6. Dependency of the peak height of some anions on the eluent pH. Eluent: 1 m*M* KHP; TBAI concentrations, 8 and 2 m*M*. Chromatographic conditions as in Fig. 3. (+) Cl^-, [TBA] 8 m*M*; (◆) NO_3^-, [TBA] 8 m*M*; (×) SO_4^{2-}, [TBA] 8 m*M*; (◇) Cl^-, [TBA] 2 m*M*; (■) NO_3^-, [TBA] 2 m*M*; (□) SO_4^{2-}, [TBA] 2 m*M*.

resolution, R_s, on two of the three factors chosen: [TBAI] and pH. Figs. 5 and 6 show the dependency of the peak height on [TBAI] and pH. Fig. 7 is an example of a visualized three-dimensional response surface plot[26] describing the dependency of the resolution of peak pair NO_2^-–BR^- on two variables [TBAI] and pH).

The criteria or response functions R_s and h can be expressed as a polynomial development of the three factors chosen

$$y = a_0 + a_1x_1 + a_2x_2 + a_3x_3 + a_4{x_1}^2 + a_5{x_2}^2 + a_6{x_3}^2 + a_7x_1x_2 + \\ + a_8x_1x_3 + a_9x_2x_3 + a_{10}x_1x_2x_3 \quad (2)$$

where $y = R_s$ (or h) or $\log R_s$ (or $\log h$), and $x = M$ or $\log M$, where M is the molarity or normality of a buffer salt, ion-interaction reagent or proton.

According to the optimization range of the factor space, with an appropriate computation program the response surface, y, can be described as a function of the different variables and the optimum eluent compositions can be determined. Calculating the coefficients of eqn. 2, the plotting of the response surface and the selection of the optimum mobile phase conditions were performed on the CDC computer of the VUB/ULB computing center, using programs written in Fortran 77, as well as on a Macintosh (apple) computer, using programs written in Basic. Nevertheless, all these computations are valid only within the experimental limits considered. Extrapolation may lead to serious errors.

(3) The selection of the experimental points (x_1, x_2, x_3 corresponding to the values of the selected parameters; ion-interaction reagent concentration, buffer concentration and pH) in the factor space is also a critical part of the factor planning. Here too, preparative experiments will supply the required information. Mobile phase conditions which yielded satisfactory resolutions, peak heights and analysis times are the basic candidates to serve as an experimental point in the factor space. Other experimental points result from the variability range (+ or $-\Delta x_1$, Δx_2 and Δx_3) attributed to each parameter. Most often, new experiments have to be carried out under these mobile phase conditions. However, there are some practical limits to the range of variation attributed to each of the parameters, for example the solubility of tetrabutylammonium iodide or the pH limit of the Partisil ODS-3 stationary phase. In our case, the ion-interaction reagent concentration, buffer concentration and pH

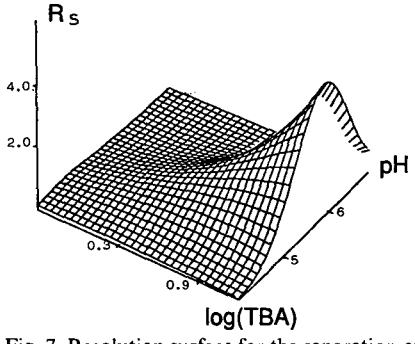

Fig. 7. Resolution surface for the separation of NO_2^- and Br^- peaks as a function of TBAI concentration (0.2–16 mM) and eluent pH (4–7). KHP concentration: 1 mM (see ref. 25).

ranged between 0.5 to 16 m*M*, 0.5 to 2 m*M* and 3.5 to 7.0, respectively. As a consequence the experimental point showing the best results cannot always be set at the centre of the central composite design.

Model fitting and prediction

In Table I, the fifteen mobile phase compositions according to the three-factor central composite design as well as the corresponding experimental resolutions and peak heights are shown. All results are the mean of three repeated experiments. To give an idea of the experimental uncertainty, ten replicate measurements at 8.0 m*M* TBAI, 1.0 m*M* KHP and pH 6.0 were carried out. The peak heights of Cl^-, NO_3^- and SO_4^{2-} showed relative errors of 4.7, 4.5 and 4.4%, respectively. The retention times of Cl^-, NO_3^- and SO_4^{2-} showed relative errors of 2.8, 1.8 and 1.7%, respectively. The experimental results in Table I were used for computer prediction of the resolution and peak height functions by polynomial fitting with eqn. 2. Predicted results were compared to the experimental values. The differences are relatively large, which is a confirmation of the too large confidence interval for the eleven polynomial coefficients of eqn. 2. In order to improve this situation, six additional experiments, selected on the basis of the results of the former optimization, were carried out. One of the advantages of a least squares regression method is that the more experimental data are available, the better the polynomial function will predict the experimental data and the smaller the confidence interval of the regression coefficients will be. The new computation confirmed that the results predicted with the 21 experimental data points are better than the results predicted with the 15 points. Differences between experimental and computed values are smaller than in the previous optimization

TABLE I

MOBILE PHASE COMPOSITIONS AND THE CORRESPONDING EXPERIMENTAL RESOLUTIONS AND PEAK HEIGHTS ACCORDING TO THE EXPERIMENTS OF THE THREE-FACTOR CENTRAL COMPOSITE DESIGN

TBAI (mM)	*KHP (mM)*	*pH*	*Experimental*		*Experimental peak height (cm)*		
			$R_s(NO_2^- - Br^-)$	$R_s(NO_3^- - SO_4^{2-})$	Cl^-	NO_3^-	SO_4^{2-}
8.0	2.0	6.0	1.11	0	11.50	3.00	6.50
8.0	2.0	4.0	0	1.12	14.00	5.50	7.20
8.0	1.0	6.0	1.35	1.52	9.90	9.20	16.20
8.0	1.0	4.0	0.73	3.34	11.30	6.80	9.0
4.0	2.0	6.0	1.00	0.97	10.00	4.50	10.20
4.0	2.0	4.0	0	2.51	13.50	5.50	5.20
4.0	1.0	6.0	1.33	3.57	8.50	4.00	7.50
4.0	1.0	4.0	0.81	7.23	14.00	5.50	5.40
8.5	1.5	5.0	0.89	1.11	13.80	5.80	8.70
3.5	1.5	5.0	0.67	5.00	9.00	3.30	2.90
6.0	2.1	5.0	0.69	1.53	8.10	2.90	4.50
6.0	0.9	5.0	0.94	4.00	12.80	6.00	10.50
6.0	1.5	6.2	1.06	0.77	11.90	5.10	9.70
6.0	1.5	4.0	0	3.76	8.20	3.80	4.00
6.0	1.5	5.0	0.64	2.67	7.30	3.30	4.10

calculation. In addition, an evaluation of different models corresponding to small changes in eqn. 2 (for example, with or without the last term $x_1x_2x_3$, of with or without the "log" form) were also carried out. As shown in Table II, the best result (smallest difference between predicted and experimental measured results) were obtained with a 21 data points prediction using the complete polynomial equation (no log form). An average deviation of 6.5% relative to the experimental results is observed. The fifteen data points prediction using the complete polynomial equation yields a larger average deviation of 14.1%. Predictions without the last term in eqn. 2 ($x_1x_2x_3$), or with the variables in the "log" form, resulted in more serious prediction errors. The results given in Table II indicate that, in the case of the three-factors optimization, with R_s or h as the response function y, the interaction term ($a_{10}x_1x_2x_3$) in eqn. 2 plays an important rôle and cannot be neglected. Similar results were also found in the prediction of the resolution $R_s(NO_3^- - SO_4^{2-})$ and the prediction of the peak heights of Cl^-, NO_3^- and SO_4^{2-} (results not shown). The 21 mobile phase composition values as well as the corresponding experimental and computer predicted resolutions and peak

TABLE II

COMPARISON BETWEEN THE EXPERIMENTALLY DETERMINED AND THE PREDICTED RESOLUTION $R_s(NO_2^- - Br^-)$ VALUES FROM 21 AND 15 EXPERIMENTAL POINTS WITH DIFFERENT MODELS

TBAI (mM)	*KHP (mM)*	*pH*	*Experimental* $R_s(NO_2^- - Br^-)$	*Predicted* $R_s(NO_2^- - Br^-)$			
				21 points simulation	*15 points simulation*	*21 points without* $x_1x_2x_3$	*21 points no* $x_1x_2x_3$ *but with log term*
8.0	2.0	6.0	1.11	1.18	1.15	5.30	4.70
8.0	2.0	4.0	0.00	0.00	0.06	2.72	0.00
8.0	1.0	6.0	1.35	1.32	1.32	3.39	1.60
8.0	1.0	4.0	0.73	0.66	0.67	2.04	0.11
4.0	2.0	6.0	1.00	0.99	1.02	3.06	0.33
4.0	2.0	4.0	0.00	0.00	0.03	1.40	0.00
4.0	1.0	6.0	1.33	0.81	1.28	1.84	0.22
4.0	1.0	4.0	0.81	0.74	0.71	1.43	0.32
8.5	1.5	5.0	0.89	0.80	0.78	3.54	0.48
3.5	1.5	5.0	0.67	0.59	0.74	1.75	0.18
6.0	2.1	5.0	0.69	0.64	0.52	3.22	0.13
6.0	0.9	5.0	0.94	0.98	1.08	2.28	1.50
6.0	1.5	6.2	1.06	1.02	0.95	3.45	0.95
6.0	1.5	4.0	0.00	0.30	0.11	1.85	0.00
6.0	1.5	5.0	0.64	0.74	0.59	2.86	0.35
6.0	0.5	6.0	1.00	1.29	1.74	2.06	0.48
4.0	1.0	5.0	1.03	0.86	1.06	1.72	1.12
2.0	1.0	4.2	0.74	0.72	1.12	1.10	0.75
1.0	1.0	5.65	0.00	0.40	1.80	0.65	0.03
1.0	2.0	4.05	0.00	0.00	0.72	0.32	0.00
0.5	1.0	5.0	0.54	0.60	1.80	0.64	0.05
Average relative deviation (%)[a]				6.50	14.06	>30	31

[a] for 17 data.

TABLE III

TWENTY-ONE MOBILE PHASE COMPOSITIONS AND THE CORRESPONDING EXPERIMENTALLY DETERMINED AND COMPUTER PREDICTED RESOLUTIONS AND PEAK HEIGHTS

TBAI (mM)	*KHP (mM)*	*pH*	$R_s(NO_2^- - Br^-)$		$R_s(NO_3^- - SO_4^{2-})$		*Peak height (cm)*					
			exptl.	*pred.*	*exptl.*	*pred.*	Cl^-		NO_3^-		SO_4^{2-}	
							exptl.	*pred.*	*explt.*	*pred.*	*exptl.*	*pred.*
8.0	2.0	6.0	1.11	1.18	0	0	11.50	11.97	3.00	3.59	6.50	6.61
8.0	2.0	4.0	0	0	1.12	1.68	14.00	12.70	5.50	4.91	7.20	6.68
8.0	1.0	6.0	1.35	1.32	1.52	2.21	9.90	10.90	9.20	7.83	16.20	13.40
8.0	1.0	4.0	0.73	0.66	3.34	3.80	11.30	11.80	6.80	6.50	9.0	8.94
4.0	2.0	6.0	1.00	0.99	0.97	1.29	10.00	9.41	4.50	4.13	10.20	9.09
4.0	2.0	4.0	0	0	2.51	2.04	13.50	11.35	5.50	4.50	5.20	3.45
4.0	1.0	6.0	1.33	0.81	3.57	3.31	8.50	7.75	4.00	3.83	7.50	11.33
4.0	1.0	4.0	0.81	0.74	7.23	6.61	14.00	12.39	5.50	6.55	5.40	5.94
8.5	1.5	5.0	0.89	0.80	1.11	1.81	13.80	10.84	5.80	5.93	8.70	7.21
3.5	1.5	5.0	0.67	0.59	5.00	3.59	9.00	8.82	3.30	4.73	2.90	5.39
6.0	2.1	5.0	0.69	0.64	1.53	1.44	8.10	10.33	2.90	3.40	4.50	5.68
6.0	0.9	5.0	0.94	0.98	4.00	4.22	12.80	9.70	6.00	5.33	10.50	9.13
6.0	1.5	6.2	1.06	1.02	0.77	0.80	11.90	10.48	5.10	4.40	9.70	9.20
6.0	1.5	4.0	0	0.30	3.76	3.16	8.20	12.16	3.80	5.14	4.00	5.34
6.0	1.5	5.0	0.64	0.74	2.67	2.55	7.30	9.99	3.30	4.46	4.10	6.42
6.0	0.5	6.0	1.00	1.29	5.11	4.61	7.40	8.78	3.40	6.00	16.10	17.65
4.0	1.0	5.0	1.03	0.86	4.98	5.29	8.80	8.94	8.20	4.89	12.50	7.79
2.0	1.0	4.2	0.74	0.72	7.86	7.51	10.20	11.06	8.20	8.23	4.50	4.21
1.0	1.0	5.65	0	0.40	5.52	5.85	4.30	5.26	4.30	4.94	11.50	8.50
1.0	2.0	4.05	0	0	2.22	2.84	7.80	9.77	6.20	7.09	3.00	5.08
0.5	1.0	5.0	0.54	0.60	7.20	7.64						
Average relative deviation (%)			6.5 (17 data)		7.0 (16 data)		10.7 (15 data)		11.5 (15 data)		13.2 (14 data)	

TABLE IV

OPTIMUM REGRESSION COEFFICIENTS OF EQN. 2 WITH 21 EXPERIMENTAL POINTS

	$R_{s1}(NO_2^- - Br^-)$	$R_{s2}(NO_3^- - SO_4^{2-})$	$h_1\ (Cl^-)$	$h_2\ (NO_3^-)$	$h_3\ (SO_4^{2-})$
a_0	3.543	32.070	69.589	48.218	30.690
a_1	−0.432	−3.812	−3.446	−6.307	−1.000
a_2	−4.060	−21.024	−13.590	−16.234	−24.550
a_3	−0.072	−1.837	−18.119	−10.022	−7.840
a_4	−0.005	0.025	−0.027	0.138	−0.019
a_5	0.283	1.141	0.047	−0.330	3.936
a_6	−0.081	−0.330	1.131	0.295	0.850
a_7	0.176	1.987	1.750	2.615	2.442
a_8	0.117	0.554	0.780	1.131	0.479
a_9	0.620	2.656	2.615	3.678	2.505
a_{10}	0.043	−0.346	−0.316	−0.625	−0.596

heights are summarized in Table III. The regression coefficients of eqn. 2 resulting from the optimization calculations with the 21 data points are presented in Table IV. The prediction error, *i.e.*, the difference, between the computed and experimental results is lower for the resolution (6.5–7.0%) than for the peak height (10.7–13.2%).

Table III indicates that the average prediction error for the resolutions $R_s(NO_2^- - Br^-)$ and $R_s(NO_3^- - SO_4^{2-})$ is about 6.5 and 7.0% (21 experimental data points). This is an acceptable magnitude. Fig. 8 shows the predicted and experimen-

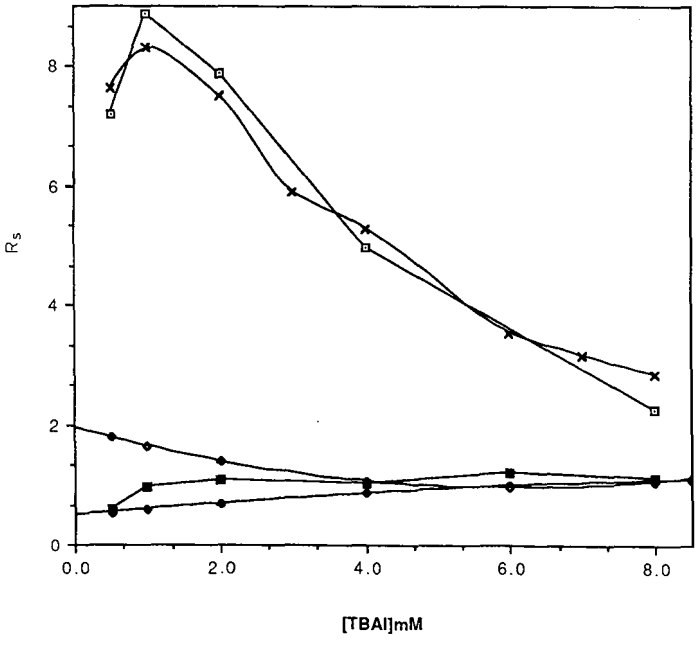

Fig. 8. Comparison between the experimental resolution factor curve and the predicted curves as a function of the TBAI concentration. KHP concentration: 1 m*M* (pH 5). (⊡) exp. R_{s2}; (◆) pred. R_{s1} (21); (×) pred. R_{s2}; (◇) pred. R_{s1} (15); (■) exp. R_{s1}.

TABLE V

OPTIMUM MOBILE PHASE COMPOSITIONS CORRESPONDING TO THE OPTIMIZATION CRITERIA OF $R_s(NO_2^- - Br^-)$, $R_s(NO_3^- - SO_4^{2-})$ AND PEAK HEIGHTS OF NO_3^- AND SO_4^{2-}

Conditions for $R_s(NO_2^- - Br^-) > 1.35$ (Computer predicted)

$R_s(NO_2^- - Br^-)$	[TBAI] (mM)	[KHP] (mM)	pH
1.37	6.0	0.5	5.0
1.36	6.5	0.5	4.5
1.41	6.5	0.5	5.0
1.41	6.5	0.5	5.5
1.37	6.5	0.5	6.0
1.37	7.0	0.5	4.5
1.44	7.0	0.5	5.0
1.47	7.0	0.5	5.5
1.45	7.0	0.5	6.0
1.40	7.0	0.5	6.5
1.38	7.5	0.5	4.5
1.47	7.5	0.5	5.0
1.52	7.5	0.5	5.5
1.53	7.5	0.5	6.0
1.50	7.5	0.5	6.5
1.35	7.5	2.0	6.5
1.38	8.0	0.5	4.5
1.50	8.0	0.5	5.0
1.57	8.0	0.5	5.5
1.39	8.0	1.0	5.5
1.38	8.0	2.0	6.5
1.38	8.5	0.5	4.5
1.52	8.5	0.5	5.0
1.37	8.5	1.0	6.0
1.46	8.5	1.0	6.5
1.36	8.5	1.5	6.5
1.40	8.5	2.0	6.5

Conditions for $R_s(NO_3^- - SO_4^{2-}) = 1.5$–$1.8$ (computer predicted)

$R_s(NO_3^- - SO_4^{2-})$	[TBAI] (mM)	[KHP] (mM)	pH
1.54	2.5	1.5	6.5
1.78	4.0	1.5	6.0
1.80	5.0	1.0	6.5
1.68	6.0	2.0	4.5
1.55	7.0	2.0	4.0
1.62	8.5	1.0	6.0

Conditions for peak height of $NO_3^- > 9.5$ cm

$h\ (NO_3^-)$	[TBAI]	[KHP]	pH
9.5	7.5	0.5	6.5
9.7	8.0	0.5	6.0
10.7	8.0	0.5	6.5
9.7	8.5	0.5	5.5
10.8	8.5	0.5	6.0
12.0	8.5	0.5	6.5

Optimum conditions for peak height of $SO_4^{2-} > 17.5$ cm

$h\ (SO_4^{2-})$	[TBAI]	[KHP]	pH
18.7	7.0	0.5	6.0
21.4	7.0	0.5	6.5
19.2	7.5	0.5	6.0
21.9	7.5	0.5	6.5
19.7	8.0	0.5	6.0
22.5	8.0	0.5	6.5
17.9	8.5	0.5	5.5
20.2	8.5	0.5	6.0
23.0	8.5	0.5	6.5

tally measured resolution curves as a function of the TBAI concentration in the eluent. The predicted $R_{s1}(NO_2^- - Br^-)$ and $R_{s2}(NO_3^- - SO_4^{2-})$ data were computed with the 21 experimental data points. Predicted curves are close to the experimental curves especially at TBAI concentrations larger than 2 m*M*. A slightly improved prediction of $R_{s1}(NO_2^- - Br^-)$ is obtained with the 21 experimental data points than with the 15 (Fig. 8).

Deviations between predicted and experimentally measured curves with respect to the peak heights of Cl^-, NO_3^- and SO_4^{2-}, however, are slightly larger. Perhaps eqn. 2 is somewhat less suited to approximate the peak heights function than it does the resolution functions.

The mobile phase optimization

Table V gives the computed resolution values of the critical peak pair $NO_2^- - Br^-$ (R_{s1}) which are higher than the resolution criterion of 1.35 as a function of the mobile phase conditions. With a step size of 0.5 m*M*, the computation was started at a TBAI concentration of 0.5 m*M* and stopped at 8.5 m*M*, but extends over the whole factor domain of buffer concentration (0.5 to 2 m*M* with a step size of 0.5 m*M*) and pH (4 to 6.5 with a step size of 0.5 pH units). The results of these predictions indicate that to satisfy the preset condition ($R_{s1} > 1.35$) for the resolution of $NO_2^- - Br^-$ the mobile phase TBAI concentration must be higher than 6 m*M*, the KHP concentration must, on the whole, not exceed 1 m*M*, and the pH must preferably be in the range of 5 to 6.5. Only a few exceptions have been observed: four points with a KHP concentration larger than 1.0 m*M* (1.5–2) but accompanied by higher pH values (6.5), and five other points with a pH value lower than 5 (4.5) and a KHP concentration below 1 m*M* (0.5 m*M*). Computed mobile phase compositions yielding $NO_3^- - SO_4^{2-}$ resolution values (R_{s2}) between 1.5 and 1.8 are also given in Table VI. Only six mobile phase compositions satisfy this requirement. On the whole, there is only one condition which meets both the adequate resolution for peak pair $NO_2^- - Br^-$ ($R_{s1} > 1.35$) and the constrained resolution value for $NO_3^- - SO_4^{2-}$ ($1.5 < R_{s2} = 1.62 < 1.8$). The corresponding values of the three variables are [TBAI] = 8.5 m*M*, [KHP] = 1 m*M* and pH 6.

As a general rule, higher TBAI concentration, higher pH and lower KHP concentration are required to obtain high peak heights for nitrate and sulphate. Optimum chloride peak heights correspond in the optimization factor domain to all TBAI and KHP concentrations but at a somewhat lower pH. The global optimum conditions, therefore, were obtained at a mobile phase composition of [TBAI] = 8 to 8.5 m*M*, [KHP] = 0.5 to 1.0 m*M* and pH 6 to 6.5. According to these values, the critical resolution value of peak pair NO_2^- and Br^- (being larger than 1.35) was guaranteed and thus a baseline separation of this peak pair was attained. At the same time an high detection response for peaks NO_3^- and SO_4^{2-} and an overall elution time within 10 min (the resolution of NO_3^- and SO_4^{2-} is in the range of 1.5 to 1.8) can also be obtained. This result coincides very well with the best result we observed experimentally (R_s of $NO_2^- - Br^-$ = 1.33 to 1.38, analysis time = 9 min and high detection response for NO_3^-, SO_4^{2-} and Cl^-) for a mobile phase composition of [TBAI] = 8 m*M*, [KHP] = 1 m*M* and pH 6.

REFERENCES

1 N. E. Skelly, *Anal. Chem.*, 54 (1982) 712–715.
2 W. E. Barber and P. W. Carr, *J. Chromatogr.*, 316 (1984) 211–215.
3 R. M. Cassidy and S. Elchuk, *Anal. Chem.*, 54 (1982) 1558–1563.
4 I. Molnár, H. Knauer and D. Wilk, *J. Chromatogr.*, 201 (1980) 225–240.
5 M. Dreux, M. Lafosse, P. Agbo-Hazoume, B. Chaabane-Doumandji, M. Gibert and Y. Levi, *J. Chromatogr.*, 354 (1986) 119–128.
6 W. E. Barber and P. W. Carr, *J. Chromatogr.*, 301 (1984) 25–38.
7 Q. Xianren and W. B. Baeyens, *J. Chromatogr.*, 456 (1988) 267–285.
8 S. N. Deming and M. L. H. Turoff, *Anal. Chem.*, 50 (1978) 546–548.
9 B. Sachok, R. C. Kong and S. N. Deming, *J. Chromatogr.*, 199 (1980) 317–325.
10 W. Lindberg, E. Johansson and K. Johansson, *J. Chromatogr.*, 211 (1981) 201–212.
11 H. A. H. Billiet, J. Vuik, J. K. Strasters and L. de Galan, *J. Chromatogr.*, 384 (1987) 153–162.
12 R. L. Smith, Z. Iskandarani and D. J. Pietzzyk, *J. Liq. Chromatogr.*, 7 (1984) 1935–1959.
13 A. Bartha and G. Vigh, *J. Chromatogr.*, 265 (1983) 171–182.
14 A. Bartha and G. Vigh, *J. Chromatogr.*, 395 (1987) 503–509.
15 J. L. Glajch, J. J. Kirkland, K. M. Squire and J. M. Minor, *J. Chromatogr.*, 199 (1980) 57–79.
16 V. Svoboda, *J. Chromatogr.*, 201 (1980) 241–252.
17 M. W. Watson and P. W. Carr, *Anal. Chem.*, 51 (1979) 1835–1842.
18 S. N. Deming and L. R. Parker, *CRC Crit. Rev. Anal. Chem.*, 7 (1978) 187–202.
19 R. J. Laub, A. Pelta and J. H. Purnell, *Anal. Chem.*, 51 (1979) 1878.
20 A. P. Goldberg, E. Nowakowska, P. E. Antle and L. R. Snyder, *J. Chromatogr.*, 316 (1984) 241–260.
21 G. D'Agostino, L. Castagnetta, F. Mitchell and M. J. O'Hare, *J. Chromatogr.*, 338 (1985) 1–23.
22 J. W. Weyland, C. H. P. Bruins and D. A. Doornbos, *J. Chromatogr. Sci.*, 22 (1984) 31–39.
23 R. D. Snee, *Chemtech.*, 9 (1979) 702–710.
24 D. L. Massart, A. Dijkstra and L. Kaufman, *Evaluation and Optimization of Laboratory Methods and Analytical Procedures*, Elsevier, Amsterdam, Oxford, New York, 1978, pp. 284–294.
25 O. L. Davies, *The Design and Analysis of Industrial Experiments*, Oliver and Boyd, London, 1967, pp. 253, 534.
26 Q. Xianren and W. Baeyens, in preparation.
27 S. L. Morgan and S. N. Deming, *J. Chromatogr.*, 112 (1975) 267–285.
28 P. J. Schoenmakers and T. Blaffert, *J. Chromatogr.*, 384 (1987) 117–133.

Journal of Chromatography, 467 (1989) 31–40
Elsevier Science Publishers B.V., Amsterdam — Printed in The Netherlands

CHROM. 21 254

INVESTIGATION OF SMALL POPULATIONS OF REACTIVE SILANOLS ON SILICA SURFACES

JACEK NAWROCKI*
Faculty of Chemistry, A. Mickiewicz University, Grunwaldzka 6, 60-780 Poznań (Poland)
DEBBIE L. MOIR
Trace Analysis Research Centre, Dalhousie University, Halifax, B3H 4J1 Nova Scotia (Canada)
and
WALENTY SZCZEPANIAK
Faculty of Chemistry, A. Mickiewicz University, Grunwaldzka 6, 60-780 Poznań (Poland)
(First received September 15th, 1988; revised manuscript received December 20th, 1988)

SUMMARY

A gas chromatographic method was used to reveal the importance of a small population of silanols on a silica surface in relation to the retention of both saturated and unsaturated hydrocarbons. The application of diethyl ketone instead of the previously applied amine as a titrant is recommended. The correlation of the surface concentration of reactive silanols with trace metal content is discussed.

INTRODUCTION

In previous papers[1–4] we showed that very small populations of active adsorption centres on silylated[1,3] and bare silica[2,4] can be responsible for a considerable part of the retention in gas chromatography (GC). The blockage of this population with amine molecules was shown to lead to a considerable improvement in column efficiency, which emphasized the importance of the silanol population on the adsorbent surface[3]. We expressed the belief that the active centres are the silanols.

Marshall and co-workers[5–7] showed that some small populations of silanols have a considerable influence on high-performance liquid chromatographic (HPLC) column efficiency. They concluded[6] that a chemically distinct group of associated silanols occur on a silica surface, and emphasized the high reactivity of the silanols.

The questions now arise of whether the sites are really silanols and why some of the silanols are more reactive than others. The silanols which occur on fully hydroxylated silica at a concentration of 8 μmol/m^2 (ref. 8) are believed to be the most important or the only adsorption sites on the silica surface under GC conditions[9,10]. Their importance in HPLC separations has also been recognized and emphasized[11,12].

It has been known for years that several kinds of silanols exist on a silica surface, namely "free" (isolated or single), "geminal" and "vicinal"[9]. These types of silanols were suspected to be associated with different retention (or reaction or adsorption) activities[9]. Snyder and Ward[13] postulated that two vicinal hydroxyl groups separated

0021-9673/89/$03.50

by an optimum distance of 3.1 Å can form a so-called reactive hydroxyl site on the silica surface. The ratio of reactive to total hydroxyls varied from 0.71 for ordinary silica to about 0.02 for pyrogenic silica of the Cab-O-Sil type. Clark-Monks and Ellis[14] found that about 10% of hydroxyls formed so-called anomalous adsorption sites on a pyrogenic silica surface. Low *et al.*[15] showed that specially prepared silica may contain on the surface really anomalous adsorption sites capable even of effecting the dissociative adsorption of hydrocarbons. It was concluded that the sites are not silanols but some structural defects of the silica skeleton. The surface concentration of the sites was determined to be 0.28 μmol/m^2 [16]. Another strange property of silica was described by Krasilnikov *et al.*[17], who found a very small number of sites (0.0001–0.0002 μmol/m^2) to adsorb oxygen, but the nature of the sites was not discussed. These few examples are outlined to show that silica may contain some sites of an unusual adsorption strength.

However, Snyder and Poppe[18] assumed that under liquid chromatographic conditions non-free silanols would not contribute to surface inhomogeneity and the silanols would have a little effect on an overall retention. The various activities of the silanols can be manifested in their different acidities and reactivities with silylating reagents. Snyder[9,13,19] suggested a higher reactivity of vicinal silanols over the isolated groups. Miller *et al.*[20] reported the possibility of the formation of a hydrogen bond between geminal silanols. For this reason the geminal silanols can belong to the group of the reactive silanols. According to Miller *et al.*[20], a silylating reagent reacts preferentially with more acidic hydroxyls and the pH of the remaining silanols increases with increase in the modifier content on the surface. The silanols were said to be unevenly distributed on the surface and grouped in the form of clusters. Earlier the alkyl radicals on the reversed-phase (RP) HPLC phases were found spectroscopically to occur in clusters on the silica surface[21,22].

A wide diversity of silica surface acidities have been reported, with pK_a values of the silanols of 1.5[23], 5–7[24], 6–8[25], 7.1 $\pm$ 0.5[26], 9.5[27] and 10[28]. One of the possible reasons for such a diversity is contamination of the silica with traces of metals. These traces were found to be responsible for the difference in adsorption activity between chromatographic-grade silica and pyrogenic silica[29,30]. On the surface of porous glasses containing appreciable amounts of boron, two acidic centres were found, one with pK_a = 5.1 and the other with pK_a = 7. Centres having pK_a = 7 were identified as silanols whereas the other sites could not be identified as B–OH because this group is much less acidic[31].

It is known, however, that an insertion of a metal impurity into the silica network should form on the surface structural Lewis sites, which cause an increase in the acidity of neighbouring silanols[32]. Theoretical *ab initio* calculations led to a similar conclusion[33]. Adsorption of amines[34,35] and of furan[36] on a silica gel surface at very low coverages (*ca.* 0.1 μmol/m^2) proceeds with much higher heats of adsorption than that at higher coverages. These high values of the heats of adsorption were connected with the presence of Al, Fe or B impurities in the silica matrix[35–37]. Silica gel containing traces of Al also has catalytic acitivity[37].

An adverse influence of traces of metals on chromatographic separations has been reported. Methods of removing the metals from GC supports have been described[38]. Verzele *et al.*[39] showed by nuclear activation analysis that chromatographic-grade silica gels may contain a variety of impurities totalling 0.1–0.3%.

Removal of trace metals was shown to improve HPLC separations[40]. The contents of trace metals in HPLC packings was briefly reviewed by Verzele[41].

Other important papers published recently are those by Köhler and co-workers[42,43] and Mauss and Engelhardt[44]. Köhler and co-workers pointed out that the undesirable adsorption of basic compounds is caused by relatively few isolated silanols with high acidity. A very small amount (*ca.* 10 nmol) of N,N-diethylaniline was found to deactivate the strongly adsorbing sites. They concluded that an unidentified concentration of bonded-phase ligand is apparently required to modify the few residual, deleterious, acidic silanol groups that remain even on a fully hydroxylated silica surface. We hope that this and our previous papers[1–4] will help to determine the surface concentration of these strongly adsorbing sites. Mauss and Engelhardt[44] also emphasized the responsibility of the acidic, isolated silanols for adsorption of basic molecules while hydroxyl-containing solutes interact mainly with vicinal hydrogen-bonded silanols.

The problem of the small, reactive population of silanols was discussed in details in a recently published review by Nawrocki and Buszewski[45].

The aim of this paper is to report the further development of the method of gas-phase titration described previously[1–4] and particularly attempts to correlate the results of the method with those obtained by neutron activation analysis and to apply compounds other than amines as the titrants. The influence of the blockage of the strongest adsorption sites on the retention of *n*-alkanes is also discussed.

EXPERIMENTAL

A GCHF 18.3 gas chromatograph (Chromatron, Berlin, G.D.R.) with a flame ionization detector was used. Argon was used as the carrier gas. Kieselgel 60 (Machery, Nagel & Co., Düren, F.R.G.), particle size 0.12–0.15 mm, extracted with 20% hydrochloric acid, was examined. Experiments on the adsorption of amines on the silica surface were carried out in stainless-steel columns (0.5 m × 4 mm I.D.). For other experiments silanized glass columns (1 m × 3 mm I.D.) were used.

n-Butylamine (BDH, Poole, U.K.) was distilled before use and methanol, acetone and diethyl ketone (all from POCh, Gliwice, Poland) were of analytical-reagent grade and were used as received. Water was doubly distilled in a quartz apparatus.

A 10-μl syringe (Hamilton, Bonaduz, Switzerland) was used for injections of amines, water, methanol, acetone and diethyl ketone and a 1-μl syringe for the injections of hydrocarbons. Usually 0.5 μl of hydrocarbon vapour was injected.

The dead volume of the column was calculated by the method of Ambrus[46] from the total retention volumes of C_5–C_9 *n*-alkanes. The specific surface area and mean pore diameter of the silica were determined by means of a Sorptomat 1700 instrument (Carlo Erba, Milan, Italy) from nitrogen adsorption data at liquid nitrogen temperature and the BET equation.

Neutron activation analysis (NAA) conditions for the silica were as follows: sample and standards were irradiated in the Dalhousie University SLOWPOKE-2 reactor (DUSR) using either an inner site for thermal neutron irradiations or the cadmium site for epithermal neutron irradiations. The reactor flux for inner sites was maintained at $5 \cdot 10^{11}$ n cm^{-2} s^{-1}. Approximately 100 mg of silica sample were used as

this allowed reproducibility while maintaining a manageable activity. Short- and medium-lived nuclides were determined by irradiating the sample in the cadmium-shielded site for 4 min, allowing them to decay for 8 min and counting for 10 min. The cadmium site was used to reduce the high activities due to ^{24}Na, ^{38}Cl and ^{28}Al. Long-lived nuclides were determined by irradiating in an inner site for 7 h, allowing a decay of approximately 3 days and counting for 12 h. The samples were counted on either a Canberra 60-cm^3 Ge(Li) detector or an Aptec planar 500-mm^2 hyperpure germanium low-energy photon detector. The detectors were coupled to a Tracor Northern TN-11 or Canberra Jupiter Series 80 multi-channel analyser, respectively. Corrections for the production of ^{28}Al due to the $^{28}Si(n, p)\ ^{28}Al$ reaction were made, and also for the production of ^{27}Mg from the $^{27}Al(n, p)\ ^{27}Mg$ reaction. Standards were prepared by spotting an appropriate amount of an atomic adsorption standard (Fisher, BDH or Alpha) on a matrix of silica gel.

RESULTS AND DISCUSSION

The silica used in all experiments is characterized in Table I. The Machery, Nagel & Co. silica purified by extraction with 20% hydrochloric acid seems to be one of the purest materials of this type compared with other silicas analysed for traces of metals by NAA[39]. It contains only calcium at a concentration of *ca.* 350 ppm, which, as will be shown later, lies in the investigated range of silanol concentrations.

Although, the principle of the gas-phase titration was described previously[4], it is outlined again in Fig. 1, which shows the main feature of the experiment. A known amount of amine is injected into a column. The retention time of amine is very long and, as it moves slowly along the column, it blocks the most active centres on the surface of the adsorbent. During the presence of amine in the column one can inject a rapidly eluting hydrocarbon, *e.g.*, benzene. The period of time elapsed from the injection of amine to the beginning of amine elution permits several injections (their number depends on the amount of amine) of benzene to be made.

The consecutive injections of benzene reveal the decrease in the retention time (or volume) of the solute. The influence of the amine on the retention time of benzene

TABLE I

CHARACTERISTIC OF THE SILICA

Characteristic[a]	*Value*	
S (m^2 g^{-1})	442	
D (nm)	7.0	
V_p (cm^3 g^{-1})	0.76	
NAA results (ppm):	Al –	Mn –
	Ca 348	Mo –
	Ce –	Na –
	Cr –	Sb 0.133
	Fe –	Sc –
	Hf 0.392	Sm 0.008
	La 16.1	Th –
	Mg 1.25	Ti 16.4

[a] S = specific surface area; D = mean pore diameter; V_p = pore volume.

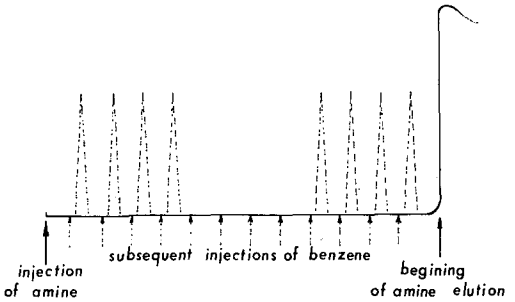

Fig. 1. Principle of the gas phase titration method.

on various adsorbents was shown previously[1–4]. Finally, before the beginning of amine elution, injection of benzene shows the shortest retention time for a given amount of amine, *i.e.*, the benzene retention reaches its final value. For various amounts of amine, various final retention times can be observed[2].

In Fig. 2 the decrease in benzene retention is plotted against the amount of amine injected. An amount of 180 μmol of amine decreases the retention of benzene by 22%. As 1:1 amine–silanol interactions can be assumed, a known amount of amine blocks a corresponding number of silanols, so it can be said that the 22% decrease in benzene retention was caused by blockage of 180 μmol of silanols. One can then further state that these blocked 180 μmol of silanols are responsible for 22% of benzene retention. As the column contained 3.185 g of silica and assuming a silanol concentration of 8 μmol m^{-2} (ref. 8), one can easily calculate the total number of silanols in the column, *viz. ca.* 11 260 μmol; 180 μmol are equal to 1.60% of all available silanols. Silanols are considered to be the main (or the only) adsorption sites on a silica surface[9,10]. Why are 1.60% of the silanols responsible for a 22% decrease in benzene retention? As was shown previously[1–4], a silica surface contains probably a small population of active centres which are much more retentive than the remaining sites. For the detection and

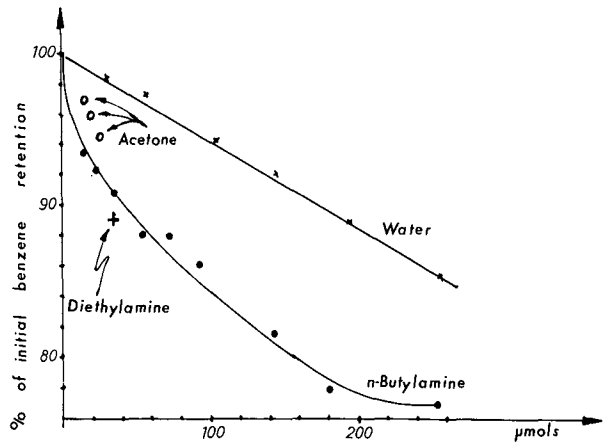

Fig. 2. Effects of various blocking reagents on retention of benzene.

quantification of the sites, blockage with an amine and subsequent examination of retention time of a rapidly eluting hydrocarbon solute can be applied.

However, the application of an amine appeared to be troublesome, particularly on bare silica surfaces because the very long retention time made the experiments very time consuming. Moreover, on some silica surfaces, the amine was chemisorbed irreversibly and even prolonged conditioning at elevated temperatures did not restore the column to its initial properties (we have to state here that for silylated surfaces an amine still seems to be the best choice). For this reason, other compounds were examined as possible blocking reagents, *viz.*, water, methanol, acetone and diethyl ketone (DEK).

Molecules of water are able to block the strongest adsorption sites on the silica surface. However, we observed a much smaller effect of water than of an amine on the retention of benzene. Some results are shown in Fig. 2. As can be seen, 180 μmol of *n*-butylamine cause a 22% decrease in the retention of benzene whereas the same amount of water decreases the retention by only 10.5%. The observed effect of a lower retentivity of benzene (or more generally of hydrocarbons) on a wet than on a dry silica surface can be considered as contradictory to the results of Hair and Hertl[10], but we think the contradiction arises because the effect seems to be the sum of two opposing phenomena: a decrease in retention as a result of blockage of the strongest adsorption sites and an increase in retention as a result of the presence of water[10]. It is likely that the former effect prevails and overall we observe a decrease in the retention of benzene.

There are two disadvantages of water as the blocking reagent. First, the retention time of water at 150°C was very short, allowing one to three injections of benzene to be made before the beginning of water elution. After 10–15 min from the injection of water the adsorbent (silica) regained its initial properties. Second, the low molecular weight of water means that 1 μl contains as much as 55 μmol (whereas with *n*-butylamine 1 μl = 10.14 μmol), which makes it difficult to investigate the smallest populations of the strongest adsorption sites.

Methanol and acetone were also tested. However, the relatively short retention times of the compounds and their high volatility make their application as blocking reagents difficult, at least at 150°C, *i.e.*, the temperature used in these experiments. Some results obtained with acetone are included in Fig. 2. Generally, neither water, methanol nor acetone should be used to replace an amine as a blocking reagent.

However, the attempt to employ DEK instead of the amine seemed to be successful. DEK is relatively non-volatile and its density and molecular weight mean that 1 μl = 9.47 μmol, which is suitable for the titration of small populations of adsorption sites.

The problem of comparing the effects of the various blocking reagents was overcome by plotting

$$\Delta V_r = \frac{\Delta V(\mathrm{cm}^3)}{A(\mu\mathrm{mol})} = \mathrm{f}(c_A)\ (\mu\mathrm{mol\ m}^{-2})$$

where ΔV is the decrease in the retention volume of benzene (or other solute), A the amount of blocking reagent, ΔV_r the relative decrease in retention volume, or in other words, the decrease in the retention of benzene caused by 1 μmol of the blocking

reagent at a given surface concentration of the reagent, and c_A the surface concentration of the blocking reagent.

In Fig. 3 the effects of *n*-butylamine and DEK on the retention of benzene are compared. The two curves lies close each other, which indicates blockage of the same adsorption sites on the silica surface. The amine curve bends at values of $c_A = 0.02$ and 0.05 μmol m^{-2} whereas the DEK curve bends at $c_A = 0.03$ μmol m^{-2}. Hence the surface concentration of the strongest adsorption sites can be determined to be 0.02–0.03 μmol m^{-2}. The linear decrease in the ΔV_r values over the range 0–0.02 (0.03) μmol m^{-2} indicates the existence of a broad range of strongly retentive silanols with decreasing strength of interaction. Assuming the total number of silanols to be 8 μmol m^{-2}, the strongly interacting population constitutes only 0.25–0.38% of the total number of the hydroxyls. Such a population can considerably influence the retention of hydrocarbon solutes. It should be emphasized that the surface concentration of the population has to be considered to be a characteristic peculiarity of the given silica and not a general property.

The dependence of the relative decrease in the retention volume of *n*-hexane on the amount of amine injected is shown in Fig. 4. The adsorption of *n*-hexane (*i.e.*, an *n*-alkane molecule belonging to the first group of the Kiselev classification[47]) is stronger on the small population of strongly interacting adsorption sites than on other sites on the surface; this was observed for both *n*-butylamine and DEK as the blocking reagent. The respective values of ΔV_r for benzene and *n*-hexane indicate that the interactions of the sites are about ten times stronger with benzene than with *n*-hexane.

NAA showed only four trace metals in ppm range: Ca, 348; La, 16.1; Ti, 16.4; and Mg, 1.25 ppm. No traces of Al, Fe and Na were detected. The latter are usually present in chromatographic-grade silica at relatively high concentrations[39]. We should emphasize the unique purity of the silica gel used here; all of the known (ref. 39 and our

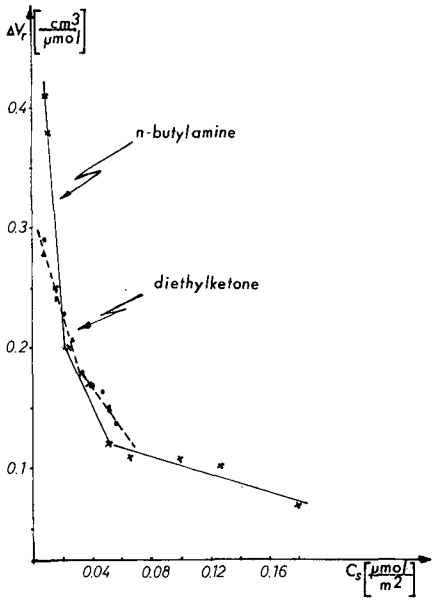

Fig. 3. Gas phase titration curves of silica gel MN. Blocking reagents: *n*-butylamine and DEK. Solute: benzene. Column temperature: 150°C.

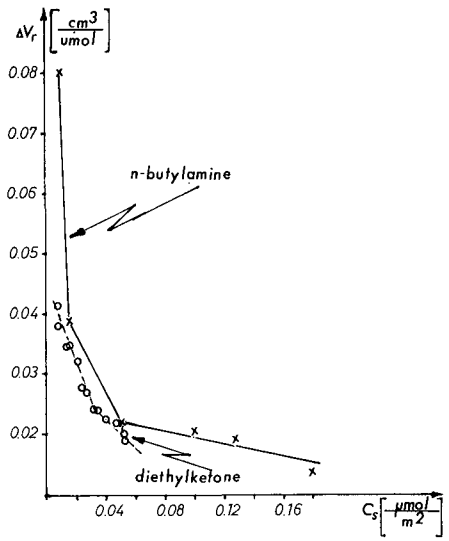

Fig. 4. Gas phase titration curves of silica gel MN. Blocking reagents: *n*-butylamine and DEK. Solute: *n*-hexane. Column temperature: 150°C.

work) silicas analysed for trace metals always contained much more impurities at higher concentrations. This unique character of the silica led us to correlate the observed Ca concentration with the "end-point" of gas-phase titration. It would be interesting to consider the results of the gas-phase titration taking into account the NAA values. Three problems can be discussed at this point: can Ca cations influence the acidity of the surface silanols?; how can the bulk concentration of Ca be recalculated as surface concentration?; and how can one compare the surface Ca concentration and the "end-points" in gas-phase titration?

The presence of Mg in the silica structure was shown[32] to produce so-called structural Lewis sites, which increased the acidity of the neighbouring silanols. The similarity of Mg and Ca allows a similar influence of Ca on the silanol acidity to be assumed. Mg inserted in the silica network can exist there in octa- or tetra-coordinated form.

The silica gel used in this work had a specific surface area of 442 $m^2 g^{-1}$. Taking into account the specific gravity of the amorphous silica (2.2 g cm^{-3})[8], we can easily calculate the average thickness of the silica skeleton, *i.e.*, *ca.* 2 nm. As the average length of Si–O bonds and the average Si–O–Si angle are well known (0.1604 nm and 130°, respectively), most of the silica walls should contain about four silicon atoms in their thickness. Other sources[48–50] report the specific gravity of the silica to be 1.9 g cm^{-3}, which would give a slightly thicker wall. We can conclude that each of the Ca atoms present in the silica network will have a surface Si atom in its vicinity. This simply means that each of the trace metal atoms can influence the acidity of the surface silanol.

Recently, Sadek *et al.*[51] also confirmed that metal impurities do not directly participate deleteriously in the chromatography of many classes of compounds, but they indirectly influence adjacent silanol groups, which causes the effect seen chromatographically.

A 348 ppm amount of Ca corresponds to 8.7 μmol of Ca per gram of SiO_2, which leads to a Ca surface concentration of 0.02 μmol m^{-2} (for La and Ti the respective values are 0.0003 and 0.0008 μmol m^{-2}). This Ca surface concentration corresponds very well with the first gas-phase titration end-point for amine titration, but for DEK the first titration end-point is observed at 0.03 μmol m^{-2}.

As one can see in Figs. 3 and 4, the strongly interacting silanols are not identical. It can be speculated that traces of metals influence the acidity of the silanols, depending on the distance between the metal and the silanol. The situation is comparable to the IR band for hydrogen-bonded silanols, the broadness of which is caused by different mutual distances between the silanols[10]. It is likely also that one trace metal atom influences the acidity of two or more silanols.

The above discussion does not prove that the existence of strongly interacting silanols is caused by the metal impurities, but the agreement between the Ca concentration and the titration end-point seems to be striking and worth further research.

ACKNOWLEDGEMENT

The authors gratefully acknowledge the substantial help of Dr. A. Chatt of the Trace Analysis Research Centre, Dalhousie University, Halifax, Canada.

REFERENCES

1 J. Nawrocki, *J. Chromatogr.*, 362 (1986) 117.
2 J. Nawrocki, *J. Chromatogr.*, 391 (1987) 266.
3 J. Nawrocki, *J. Chromatogr.*, 407 (1987) 171.
4 J. Nawrocki, *Chromatographia*, 23 (1987) 722.
5 D. B. Marshall, K. A. Stutter and C. H. Lochmüller, *J. Chromatogr. Sci.*, 22 (1984) 217.
6 D. B. Marshall, C. L. Cole and D. E. Connolly, *J. Chromatogr.*, 361 (1986) 71.
7 D. B. Marshall, C. L. Cole and A. D. Norman, *J. Chromatogr. Sci.*, 25 (1987) 262.
8 K. K. Unger, *Porous Silica*, Elsevier, Amsterdam, 1979.
9 L. R. Snyder, *Principles of Adsorption Chromatography*, Marcel Dekker, New York, 1968.
10 M. L. Hair and W. Hertl, *J. Phys. Chem.*, 73 (1969) 4269.
11 A. Nahum and Cs. Horváth, *J. Chromatogr.*, 203 (1981) 53.
12 K. E. Bij, Cs. Horváth, W. R. Melander and A. Nahum, *J. Chromatogr.*, 203 (1981) 65.
13 L. R. Snyder and J. W. Ward, *J. Phys. Chem.*, 70 (1966) 3941.
14 C. Clark-Monks and B. Ellis, *J. Colloid Interface Sci.*, 44 (1973) 37.
15 M. J. D. Low, E. McNelis and H. Mark, *J. Catal.*, 100 (1986) 328.
16 C. Morterra and M. J. D. Low, *J. Catal.*, 28 (1973) 265.
17 K. G. Krasilnikov, V. F. Kiselev and E. A. Sysoev, *Dokl. Akad. Nauk SSSR*, 116 (1957) 990.
18 L. R. Snyder and H. Poppe, *J. Chromatogr.*, 184 (1980) 363.
19 L. R. Snyder, *Sep. Sci.*, 1 (1966) 191.
20 M. L. Miller, R. W. Linton, G. E. Maciel and B. L. Hawkins, *J. Chromatogr.*, 319 (1985) 9.
21 C. H. Lochmüller, A. S. Colborn, M. L. Hunnicatt and J. M. Harris, *Anal. Chem.*, 55 (1983) 1344.
22 C. H. Lochmüller, A. S. Colborn, M. L. Hunnicatt and J. M. Harris, *J. Am. Chem. Soc.*, 106 (1984) 4077.
23 C. Walling, *J. Am. Chem. Soc.*, 72 (1950) 1164.
24 B. N. Karger, J. N. LePage and N. Tanaka, in Cs. Horváth (Editor), *High Performance Liquid Chromatography —Advances and Perspectives*, Vol. 2, Academic Press, New York, 1980, p. 133.
25 D. L. Dugger, J. H. Stanton, N. N. Irby, B. L. McConnell, W. W. Cummings and R. W. Maatman, *J. Phys. Chem.*, 68 (1964) 758.
26 M. L. Hair and W. Hertl, *J. Phys. Chem.*, 74 (1970) 91.

27 R. E. Majors, in Cs. Horváth (Editor), *High Performance Liquid Chromatography —Advances and Perspectives*, Vol. 1, Academic Press, New York, 1980, p. 78.
28 T. Bernstein, H. Ernst, D. Freude, I. Juenger, B. Standte and J. Sauer, *Z. Phys. Chem. (Leipzig)*, 262 (1981) 1123.
29 P. J. Hendra, J. R. Horder and E. J. Loader, *J. Chem. Soc. A*, (1971) 1766.
30 J. Adams and C. S. Giam, *J. Chromatogr.*, 285 (1984) 81.
31 J. Altug and M. L. Hair, *J. Phys. Chem.*, 71 (1967) 4260.
32 M. Kermarec, M. Briend-Faure and D. Delafosse, *J. Chem. Soc., Faraday Trans. I*, (1974) 2180.
33 D. Heidrich, D. Volkmann and B. Żurawski, *Chem. Phys. Lett.*, 80 (1981) 60.
34 A. V. Kiselev, B. V. Kuznetsov and S. N. Lanin, *J. Colloid Interface Sci.*, 69 (1979) 148.
35 S. G. Ash, A. V. Kiselev and B. V. Kuznetsov, *Trans. Faraday Soc.*, 67 (1971) 3118.
36 E. Robinson and R. A. Ross, *J. Chem. Soc. A*, (1970) 84.
37 P. B. West, G. L. Haller and R. L. Burwell, Jr., *J. Catal.*, 29 (1973) 486.
38 W. A. Aue, M. M. Daniewski, E. E. Picket and P. R. McCullough, *J. Chromatogr.*, 111 (1975) 37.
39 M. Verzele, M. DePotter and J. Ghysels, *J. High Resolut. Chromatogr. Chromatogr. Commun.*, 2 (1979) 151.
40 M. Verzele and C. Dewaele, *J. Chromatogr.*, 217 (1981) 399.
41 M. Verzele, *LC, Liq. Chromatogr. HPLC Mag.*, 1 (1983) 217.
42 J. Köhler, D. B. Chase, R. D. Farlee, A. J. Vega and J. J. Kirkland, *J. Chromatogr.*, 352 (1986) 275.
43 J. Köhler and J. J. Kirkland, *J. Chromatogr.*, 385 (1987) 125.
44 M. Mauss and H. Engelhardt, *J. Chromatogr.*, 371 (1986) 235.
45 J. Nawrocki and B. Buszewski, *J. Chromatogr.*, 449 (1988) 1.
46 L. Ambrus, *J. Chromatogr.*, 294 (1984) 328.
47 A. V. Kiselev and Ya. Yashin, *Gas Adsorption Chromatography*, PWN, Warsaw, 1969 (in Polish).
48 G. Berendsen and L. de Galan, *J. Liq. Chromatogr.*, 1 (1978) 403.
49 W. Strubert, *Chromatographia*, 6 (1973) 50.
50 M. Verzele, C. DeWaele and D. Duquet, *J. Chromatogr.*, 329 (1985) 351.
51 P. C. Sadek, C. J. Koester and L. D. Bowers, *J. Chromatogr. Sci.*, 25 (1987) 489.

Journal of Chromatography, 467 (1989) 41–47
Elsevier Science Publishers B.V., Amsterdam — Printed in The Netherlands

CHROM. 21 244

LIQUID CHROMATOGRAPHY ON PACKED FUSED-SILICA CAPILLARY COLUMNS WITH ELECTROCHEMICAL DETECTION

V. F. RUBAN*, A. B. BELENKII, A. Ya. GUREVICH and B. G. BELENKII
Institute of Macromolecular Compounds of the U.S.S.R., Academy of Sciences, Bolshoy, 31 Leningrad (U.S.S.R.)
(First received August 29th, 1988; revised manuscript received December 27th, 1988)

SUMMARY

A chromatographic system for reversed-phase high-performance liquid chromatography on fused-silica capillary columns [height equivalent to a theoretical plate (HETP) = $2–3d_p$; d_p = mean particle diameter] has been developed. The rate dependences of the column efficiency were investigated and the volumes for sample injection and detection were studied and optimized. An electrochemical detector with a cell volume of 1–100 nl was developed and its main characteristics were investigated. The application of this system to the high-speed ultra-sensitive chromatographic analysis of electrochemically active substances with a detection limit of a few picograms is reported.

INTRODUCTION

High-performance liquid chromatography with the application of fused-silica capillary columns of 0.2–0.4 mm I.D. packed with fine-grained sorbents exhibits advantages due to the high mass sensitivity and low consumption of the sorbent and the eluent. Columns consisting of flexible fused-silica capillaries also make it possible to attain very high efficiency (more than 100 000 plates) and high rates (more than 100 plates/s) of chromatographic separations[1–3]. The application of these columns is particularly promising in chromatographic analyses that require the exclusion of the chemical and adsorbing effects of the column material on the sample components to be separated.

In order to achieve a high efficiency of columns made of flexible fused-silica capillaries, the chromatographic system should include a sample injector and a detector measuring cell of less than 0.1 μl in volume. The most advantageous detectors for liquid chromatography on packed fused-silica columns are laser detectors with induced fluorescence[4–6]. Recently laser-induced photothermal refractometric (absorptiometric)[7,8] and electrochemical (voltamperometric) detectors have been proposed, which allow the minimization of the operating volume without substantial decreases in sensitivity and selectivity[4].

Electrochemical detection in this variant of liquid chromatography is of analytical interest because it is known that amperometric detectors with steel

0021-9673/89/$03.50

micro-columns with I.D. 1 mm[9,10] and 1.2 mm[11], glass columns of I.D. 0.7 mm[12], PTFE columns of I.D. 0.5 mm[13], glass capillary columns packed with 30-μm sorbent[14] and open glass[15] and fused-silica capillary columns[16] for the investigation of many classes of substances (phenols, catecholamines, amino acids, drugs and their metabolites, etc.) are used. The use of amperometric detectors with packed silica capillary columns of I.D. 0.35 mm has also been reported[17,18]. The latest investigations used single carbon-fibre microelectrodes of 7 μm diameter, whose size hampers their easy handling and makes the construction of a measuring cell of I.D. 50 μm difficult. The purpose of our work was to construct and investigate a chromatographic system using fused-silica capillary columns packed with fine-grained sorbents and an electrochemical detector with a measuring cell of a simple and compact design. In contrast to similar detectors that have been described[9–11,14], that proposed here permits the direct connection of the separating column and the measuring cell without the use of intermediate capillaries[17,18]. This permits the extra-column spreading to be decreased appreciably, the separation efficiency to be increased and the detection efficiency to be improved.

EXPERIMENTAL

Chromatographic system

To investigate the rate characteristics of the columns and the efficiency of the electrochemical detector and to determine the optimum injection volumes, a system was used in which the eluent was injected by a Shimadzu LC-5A high-pressure pump at a constant rate of 10–100 μl/min or at constant pressure (Fig. 1). After the Rheodyne 7410 injection valve (volume 0.5 μl) the flow is divided; the smaller part enters the fused-silica column and the larger part passes into a side-line. The degree of flow splitting is smoothly controlled with a valve located in the side-line[19]. The degree of splitting controls the eluent flow-rate in the column and the volume of the sample injected into the column (1–500 nl). The outlet of the column is connected with the cell of the electrochemical detector. The adjustment of the potential of the working electrode and the measurements of the polarization current were carried out under d.c. conditions with the aid of an OH-107 recording polarograph (Radelkis) with a time constant of 0.3 s. The eluent flow in the side-line joins that coming from the detector and enters a reservoir containing 20 ml of the initial eluent. Consequently, the

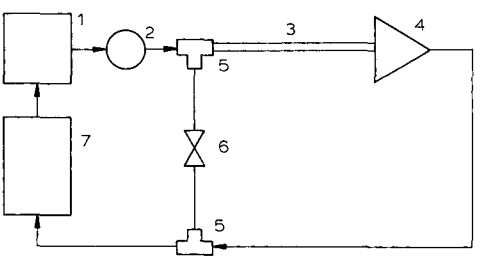

Fig. 1. Hydraulic scheme for chromatographic system: 1 = pump; 2 = injection valve; 3 = fused-silica column; 4 = electrochemical detector; 5 = T-shaped connections; 6 = valve; 7 = vessel containing the eluent.

hydraulic system becomes closed. The eluent circulates along the closed path without losses and can be repeatedly used for carrying out analyses of the same type.

With model mixtures, *i.e.*, when a sample does not contain contaminating components whose concentrations substantially exceed those of the substances under analysis, the circulation of the flow causes a drift of the zero line which is very small in comparison with the noise level. Chromatographic separation was also conducted with the use of a 30-nl injection valve (Special Design Bureau of Analytical Instruments, Academy of Sciences of the U.S.S.R.) in a non-split flow system (see Figs. 5 and 6).

Column packing

The fused-silica capillary columns (5–100 cm × 0.2–0.4 mm I.D.) were packed with Nucleosil $3C_{18}$ sorbent (Macherey, Nagel & Co.) with a particle size of 3 μm and a Separon Si-C_{18} sorbent (Lachema) with a particle size of 10 μm by a slurry packing procedure similar to that described elsewhere[20,21]. For this purpose, a sorbent suspension in methanol–isopropanol (95:5) at a concentration of 100 mg/ml was prepared, treated ultrasonically (22 kHz) for 3 min and then injected with a syringe into a stainless-steel reservoir. The suspension was displaced from this reservoir with methanol into the fused-silica capillary with the aid of a Shimadzu LC-5A pump. After the column had been packed with the sorbent, methanol was replaced with distilled water and the packed sorbent layer was stabilized for 30 min.

Electrochemical detector

The detector cell (Fig. 2) was manufactured in a variant combining the wall-jet and thin-layer types[22]. It was made of PTFE with polished operating surfaces. The upper part of the cell body (1) had openings for a fused-silica column (2) and silver chloride reference electrode (3). The flow from the column was fed to the polished surface of the glassy carbon working electrode (4). Subsequently, the electrode passed through a rectangular channel 0.1–0.2 mm in width cut in a PTFE sheet (5) 0.01–0.1 mm thick and led to a platinum or stainless-steel capillary (6) acting as the auxiliary electrode.

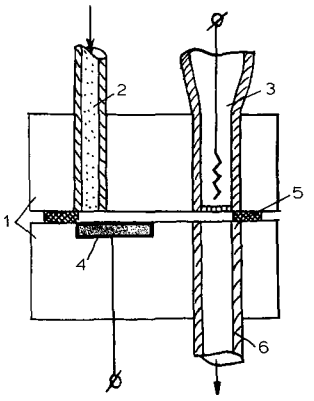

Fig. 2. Design of electrochemical detector cell: 1 = body; 2 = fused-silica column; 3 = reference electrode; 4 = working electrode; 5 = PTFE sheet; 6 = auxiliary electrode.

This construction of the electrochemical detector cell also makes it possible to carry out the recording of electrochemically active substances on two independently polarized glassy carbon (4) and platinum (6) electrodes with the appropriate scheme for the connection of the measuring instrument. The replacement of the lower part of the cell body by a similar part containing a platinum electrode instead of a glassy carbon electrode extends the possibilities of using the detector.

By changing the thickness of the PTFE sheet it is possible to vary the effective cell volume in the range 1–100 nl. In this instance the sensitivity of the electrochemical detector changes; it is considerably affected by the area of the active surface of the working electrode and is controlled by the size of the channel with the PTFE sheet.

Reagents

The eluents were prepared with doubly distilled water, acetonitrile (Chempure), phosphoric acid (specially pure), sodium perchlorate (specially pure) and EDTA (AnalaR).

RESULTS AND DISCUSSION

Efficiency of the chromatographic system

For a successful separation on a chromatographic column, it is necessary to minimize extra-column spreading. According to Kirkland *et al.*[23], when the decrease in column efficiency due to spreading in the injector does not exceed 10%, the volume dispersion of the chromatographic zone is given by

$$\sigma_s^2 = \frac{V_s^2}{12} \leqslant 0.1\ \sigma_{V_0,\mathrm{col}}^2 \tag{1}$$

where V_s is the sample volume and $\sigma_{V_0,\mathrm{col}}^2$ is the variance of the volumetric dispersion of the non-sorbed solute. For a 430 × 0.32 mm I.D. column packed with 10-μm Separon Si-C_{18}, the experimentally measured volume V_0 is 28.2 μl. The extrapolation of the dependence $N = f(V_s)$ to zero sample volume gives a maximum efficiency of $N = 8200$ plates at an flow-rate of 2.5 μl/min. In this case $\sigma_{V_0,\mathrm{col}}^2 = 0.097\ \mu\mathrm{l}^2$ and, according to eqn. 1, we should have $V_s \leqslant 0.34\ \mu$l. However, at $V_s \leqslant 0.03\ \mu$l the decrease in the efficiency of the system does not exceed 10%, as follows from the experimental results. This discrepancy between theory and experiment is due to the existence of the contributions to extra-column spreading which were not taken into account, *e.g.*, the connections of the column with the injection valve and the detector. Spreading in the cell of the electrochemical detector could be neglected because the effective volume of the cell was 1 nl.

The requirement for the miniaturization of the detector volume V_d in column chromatography[23] is expressed by the equation

$$V_d^2 \leqslant 0.16\ \sigma_{V_0,\mathrm{col}}^2 \tag{2}$$

Comparison of eqns. 1 and 2 leads to the relationship $V_d \approx 0.365 V_s$, *i.e.*, in chromatography on capillary columns the detector volume should be several nanolitres. The decrease in the column diameter and length when sorbents of grain size

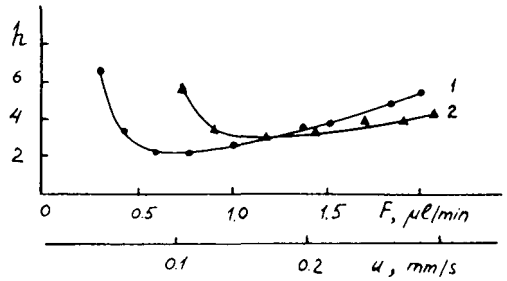

Fig. 3. Rate dependence of reduced HETP: 1, 430 × 0.32 mm I.D. column, Separon Si-C_{18} (10 μm); 2, 100 × 0.34 mm I.D. column, Nucleosil $3C_{18}$ (3 μm). Eluent, acetonitrile–water (3:7) + 0.1 *M* $NaClO_4$, 22°C; sample, hydroquinone ($k' = 0.72$); electrochemical detector, $E = +0.5$ V (Pt), $V_s = 20$ nl, $V_d = 1$ nl.

less than 10 μm are used requires a corresponding decrease in the volume of injection and the detector cell.

The rate dependence for fused-silica capillary columns shown in Fig. 3 indicates that this procedure of column packing makes it possible to attain a high efficiency. Thus, for a 10-μm sorbent at the optimum elution rate, the reduced height equivalent to a theoretical plate (HETP) is $2.1d_p$ and for a 3-μm sorbent it is $2.9d_p$, where d_p is the mean particle diameter.

Detector characterization

Electrochemical detectors used in microcolumn chromatography in which the cell volume is small and the active surface of the working electrode is a few tenths of a square millimetre usually operate under an amperometric regime[12]. The electrochemical efficiency of the detector, η, can be defined as the ratio of the number of electrons absorbed on the working electrode in the oxidation of the substance, Q_A, to that absorbed in the oxidation of the entire mass of the substance being detected, Q_K. The potential of the working electrode corresponds to the conditions of the limiting current. The value of Q_A was calculated from the surface area under the chromatographic peak and Q_K was estimated on the basis of the Faraday law.

It can be seen from Fig. 4 that the electrochemical efficiency of the detector increases with decreasing elution rate. Moreover, the greatest change in η occurs at a rate of less than 2 μl/min, whereas at the maximum rate the column efficiency of the detector is about 25%.

It is possible to determine electrochemically active substances with the aid of an amperometric detector if the linearity of the response has a relatively wide range. Hence, we investigated for phenol the dependence

$$\log I = a \log q + b \tag{3}$$

where I (nA) is the detector signal, q (pg) is the amount of phenol in the sample and a and b are constants. Processing of the experimental data by the least-squares method yields $a = 0.99 \pm 0.01$ and $b = -(1.38 \pm 0.02)$ for $\log q = 2$–5. In other words, the detector has linear characteristics over the range under investigation. The noise level in this construction does not exceed 0.12 nA. Hence, according to eqn. 3, the detection level of phenol is 6 pg.

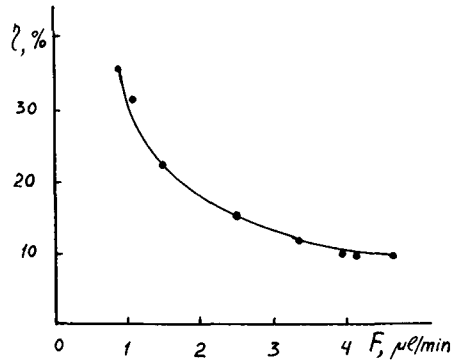

Fig. 4. Electrochemical detector efficiency *vs.* flow-rate. Column, 100 × 0.34 mm I.D., Nucleosil $3C_{18}$ (3 μm); eluent, acetonitrile–water (3:7) + 0.1 *M* $NaClO_4$, 22°C; sample, phenol, V_s = 30 nl, mass = 5 ng; electrochemical detector, E = +1.2 V (glassy carbon), V_d = 10 nl.

Analytical application

The chromatographic system was applied to the analysis of a mixture of phenol and its monosubstituted derivatives (Fig. 5). A fused-silica capillary column (100 × 0.34 mm I.D.) packed with a sorbent with a particle size of 3 μm exhibits an efficiency of more than 11 000 plates at the optimum flow-rate. The high elution rate makes it possible to separate these compounds in 6 min with a selectivity sufficient for quantitative analysis.

Fig. 6 shows the chromatographic determination of biogenic amines. The analysis time is less than 1 min. The detection limit for noradrenaline is 7 pg.

CONCLUSIONS

An electrochemical detector with a nanolitre-size cell with platinum and glassy carbon working electrodes, which is a combination of the thin-layer and wall-jet

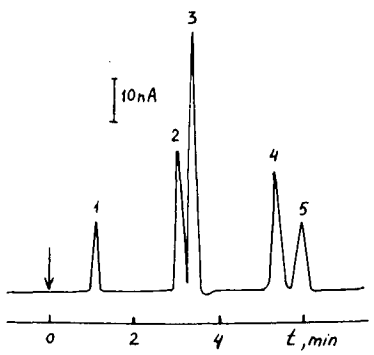

Fig. 5. Chromatography of phenol derivatives. Column, as in Fig. 4; eluent, phosphate buffer solution (pH 2.4)–acetonitrile (7:3), flow-rate 4.6 μl/min, 20°C; electrochemical detector, E = +1.5 V (Pt), V_d = 10 nl; sample volume, 30 nl. Amounts of phenol compounds, 5.75 ng of each: 1 = $NaNO_2$ (k' = 0); 2 = phenol; 3 = guaiacol; 4 = *p*-cresol; 5 = *o*-cresol.

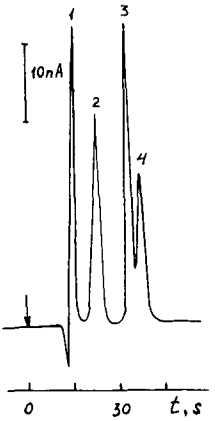

Fig. 6. High-speed analysis of catecholamines: 1 = noradrenaline (1.0 ng); 2 = adrenaline (2.0 ng); 3 = 3,4-dihydroxyphenylalanine (2.0 ng); 4 = 3,4-dihydroxythiramium (1.5 ng). Column, 60 × 0.32 mm I.D., Nucleosil $3C_{18}$ (3 μm); eluent, distilled water + 0.1 *M* $NaClO_4$ + 1 m*M* EDTA + H_3PO_4 (pH 2.0), flow-rate 11 μl/min, 20°C; sample volume, 30 nl; electrochemical detector, E = +1.5 V (Pt), V_d = 10 nl.

versions, allows the maximum use of the efficiency of silica capillary columns with an HETP of 2–3d_p. The suggested chromatographic system makes it possible to perform high-speed analyses of trace amounts of electrically active substances, especially with samples of small volume.

REFERENCES

1 P. Kucera, *J. Chromatogr.*, 198 (1980) 93.
2 C. E. Reese and R. P. W. Scott, *J. Chromatogr. Sci.*, 18 (1980) 479.
3 G. H. Knox, *J. Chromatogr. Sci.*, 18 (1980) 453.
4 R. P. W. Scott (Editor), *Liquid Chromatography Detectors*, Elsevier, Amsterdam, 1986, p. 271.
5 A. Ph. Lobazov, V. A. Mostovnikov, S. V. Nechaev, B. G. Belenkii, J. J. Kever, E. M. Korolyova and V. G. Maltsev, *J. Chromatogr.*, 365 (1986) 321.
6 M. C. Roach and M. D. Harmony, *Anal. Chem.*, 59 (1987) 411.
7 C. N. Kettler and M. J. Sepaniak, *Anal. Chem.*, 59 (1987) 1733.
8 T. O. Nolan and N. J. Dovichi, *Anal. Chem.*, 59 (1987) 2803.
9 A. Carlsson, T. Sharp, T. Zetterström and U. Ungerstedt, *J. Chromatogr.*, 368 (1986) 299.
10 A. Carlsson and K. Lundström, *J. Chromatogr.*, 350 (1985) 169.
11 E. J. Caliguri, P. Capella, L. Botarri and T. M. Mefford, *Anal. Chem.*, 57 (1985) 2423.
12 K. Šlais and O. Kouřilová, *J. Chromatogr.*, 258 (1983) 57.
13 M. Goto, Y. Koyanagi and D. Ishii, *J. Chromatogr.*, 208 (1981) 261.
14 Y. Hirata, P. T. Lin, M. Novotný and R. M. Wightman, *J. Chromatogr.*, 181 (1980) 287.
15 K. Šlais and M. Krejčí, *J. Chromatogr.*, 235 (1982) 21.
16 M. J. N. Hetem, H. A. Glaessens, P. A. Leclercq, C. K. Gramers, V. Pacakova and K. Stulik, in P, Sandra (Editor), *Proceedings of the Eighth International Symposium on Capillary Chromatography*, Vol. II, Hüthig, Heidelberg, 1987. p. 112.
17 M. Goto and K. Shimada, *Chromatographia*, 21 (1986) 631.
18 M. Goto, K. Shimada, T. Takeuchi and D. Ishii, *Anal. Sci.*, 4 (1988) 17.
19 F. J. Yang, *J. Chromatogr.*, 236 (1982) 265.
20 M. Konishi, Y. Mori and T. Amano, *Anal. Chem.*, 57 (1985) 2235.
21 J. C. Gluckman, A. Hirose, V. L. McGuffin and M. Novotny, *Chromatographia*, 17 (1983) 303.
22 W. Kemula and W. Kunter, in E. Pungor, I. Buzás and G. E. Veress (Editors), *Modern Trends in Analytical Chemistry (Analytical Chemistry Symposia Series*, Vol. 18), Elsevier, Amsterdam, 1984, p. 3.
23 J. J. Kirkland, W. W. Yau, H. J. Stoklosa and C. H. Dilks, *J. Chromatogr. Sci.*, 15 (1977) 303.

Journal of Chromatography, 467 (1989) 49–60
Elsevier Science Publishers B.V., Amsterdam — Printed in The Netherlands

CHROM. 21 252

IMPROVED EVAPORATIVE LIGHT-SCATTERING DETECTION FOR SUPERCRITICAL FLUID CHROMATOGRAPHY WITH CARBON DIOXIDE–METHANOL MOBILE PHASES

D. NIZERY, D. THIÉBAUT*, M. CAUDE and R. ROSSET
Laboratoire de Chimie Analytique, Ecole Supérieure de Physique et de Chimie de Paris, 10 Rue Vauquelin, 75005 Paris (France)
and
M. LAFOSSE and M. DREUX
Laboratoire de Chromatographie, Université d'Orléans, BP 6759, 45067 Orléans Cédex 2 (France)
(First received August 16th, 1988; revised manuscript received January 2nd, 1989)

SUMMARY

The coupling of evaporative light-scattering detection (LSD) with packed-column supercritical fluid chromatography (SFC) using a carbon dioxide–methanol mixture as the mobile phase was studied. A new column–detector interface is described which allows decompression and nebulization of the mobile phase and efficient evaporation of the methanol. In order to economize on experiments, the main parameters which influence the detector response were studied using factorial designs. Within the investigated range, the best detection conditions were deduced. The detection limit of LSD coupled with SFC was improved, permitting the sensitive analysis of solutes with no chromophoric or fluorophoric groups such as fatty acids and fatty alcohols.

INTRODUCTION

In a previous paper, we reported the use of light-scattering detection (LSD) coupled with packed-column supercritical fluid chromatography (SFC)[1]. The comparison between capillary- and packed-column SFC has already been discussed[2,3]. Obviously, packed columns exhibit higher efficiency per unit time than capillary columns and separations can be transposed directly from analytical or preparative liquid chromatography (LC) to SFC. Further, a conventional liquid chromatograph can easily be converted into a supercritical fluid chromatograph[4]. Nevertheless, in SFC, elution of polar solutes from a packed column with a carbon dioxide mobile phase often requires polar modifiers such as methanol[5,6]. Therefore, the use of a flame ionization detector is proscribed and there is a need for a universal detector when SFC is performed with polar modifiers.

In the previous paper we demonstrated the potential of LSD as a quasi-universal detection method for SFC with carbon dioxide–methanol mixtures. Further investigations were required in order to improve both the nebulization and the evap-

0021-9673/89/$03.50

oration steps before detection. In fact, difficulties arose from the cooling effect that occurred during the decompression of the mobile phase and the resulting aggregation of solutes.

Therefore, this paper describes a new interface that we constructed to enhance heat transfer and to elucidate the phenomena that occur during the decompression and modifier evaporation.

The use of factorial designs[7–9] allowed the effective study of the detector response through the variation of the main parameters affecting the detector response within a range depending on the solutes of interest.

EXPERIMENTAL

The chromatographic system, described in detail elsewhere[1,4], consisted of a Model 303 reciprocating pump (Gilson, Villiers-le-Bel, France) and a Model 8500 syringe pump (Varian, Palo Alto, CA, U.S.A.) for the carbon dioxide and the methanol, respectively, a Model 802 dynamic mixing chamber (Gilson), a heated bath for temperature control, a Rheodyne 7120 sample injector with a 4-μl injection loop and a Model DDL 10, light-scattering detector (Cunow, Clichy, France) (Fig. 1).

Pressure control was provided by a 10–20-cm length of 75-μm I.D. fused-silica tubing cemented in a 500-μm I.D. stainless-steel tube in order to hold it in the interface and to improve heat transfer between the brass holder and the fused-silica restrictor (Fig. 2).

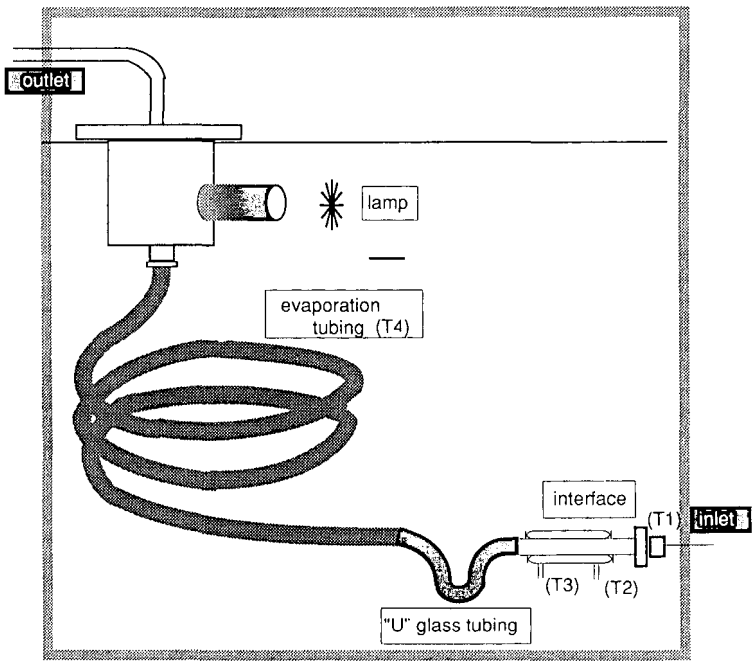

Fig. 1. Schematic diagram of the light-scattering detector. T1 = Heated restrictor holder; T2 = heating wire cemented on the glass jacket; T3 = thermoregulated glass jacket; T4 = heated evaporation tube.

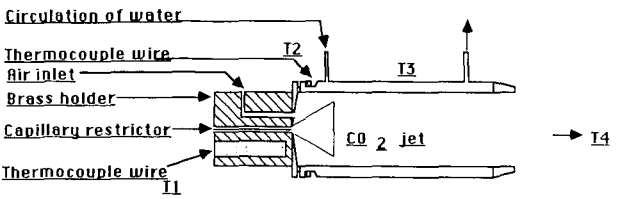

Fig. 2. Schematic diagram of the interface between the column and the light-scattering detector.

In order to reduce freezing during the expansion of the mobile phase, the outlet of the restrictor was cut with care using a special tool for optical fibre cutting (Minicut M 125-2; ATI; Courcouronnes, Evry, France).

The new device used as the interface between the column and the detector is shown in Fig. 2. The restrictor was installed in the brass part, which can be heated to 250°C through a thermocouple wire connected to an external power supply. An air supply was provided because addition of nebulization make-up gas was reported to enhance the evaporation rate[10].

Because the aerosol formation directly influences the detector response[11–13], we used a glass piece to watch nebulization and the carbon dioxide–methanol jet. To provide efficient heating during the expansion of the mobile phase, a heating wire was cemented at the top of the glass jacket where the expansion takes place. Hot water was circulated through the glass jacket to ensure modifier evaporation. The outlet of this straight glass tube was connected through a glass U-tube to the evaporation tube. The U-tube was used to collect any modifier that might condense.

Air tightness between all parts was ensured by O-ring PTFE seals. The restrictor was sealed by cementing the stainless-steel holder into the brass. Care must be taken to prevent air intake because of its water content: with bad sealing, freezing of water occurred and dry-ice appeared at the outlet of the restrictor. Consequently, solutes aggregated and the noise increased considerably. This effect was also reduced with a properly cut restrictor.

All experiments were carried out with a 15 × 0.46 cm I.D. column packed with Zorbax ODS (5–7 μm) (DuPont, Wilmington, DE, U.S.A.) or LiChrosorb RP-18 (5 μm) (Merck, Darmstadt, R.F.G.).

The responses of docosanol and palmitic acid were studied. Their properties are reported in Table I. Solutions were prepared in HPLC-grade hexane. Carbon dioxide (standard quality) was purchased from L'Air Liquide (Paris, France). Methanol (Prolabo, Paris, France) was of HPLC grade.

TABLE I

CHEMICAL PROPERTIES OF THE TEST SOLUTES

Solute	*Molecular weight (daltons)*	*Melting point (°C)*	*Boiling point (°C)*
Docosanol	326.6	71	180 (0.22 mmHg)
Palmitic acid	256.4	63	161 (1 mmHg)

RESULTS AND DISCUSSION

In our previous study[1], the interface used necessitated a high temperature of the brass holder and evaporation tubing (*ca.* 80°C) in order to evaporate the methanol succesfully before the detection of polar compounds such as carbohydrates or triglycerides. This represents a major drawback for the detection of thermolabile or volatile solutes, as they could decompose or evaporate. Therefore, in order to enhance the evaporation yield while reducing the temperature required for the evaporation of the solutes, we used a new interface (Fig. 2) which provided three different heated zones.

In addition to the temperature of the interface, it was necessary to investigate the influence of parameters that we expected would alter detector response[1] (Table II) by measuring the peak area of the test compounds. In a first step, the influence of these parameters was studied with a low content of methanol in the mobile phase (<2.4%) to define the initial conditions.

The following parameters were found to not affect the LSD response within the range studied.

Temperature of restrictor heater (T_1)

The carbon dioxide velocity was too high during the decompression step to allow effective heat exchange between the restrictor holder and the mobile phase; the calculated linear velocity of the carbon dioxide at the outlet of the restrictor equalled the speed of sound, as reported by Bally and Cramers[14]. The effect of the restrictor holder temperature on the detector response as reported previously[1] was provided by heating the inlet of evaporator tubing in close contact with the heated piece of brass.

Carbon dioxide flow-rate

The carbon dioxide flow-rates were selected because they were known to give a nearly maximum response[1]. However, as we used the same restrictor for all measurements, it was necessary to choose two close levels to avoid too much variation in the chromatographic conditions because of the dependence of density on carbon dioxide flow-rate.

TABLE II

INITIAL CONDITIONS: LEVELS OF THE STUDIED PARAMETERS

Parameter	*Level (−)*	*Level (+)*
A. Photomultiplier power supply (PM)	4	6
B. Temperature of brass holder (T_1) (°C)	35	50
C. Content of methanol (%, w/w)	1.4	2.8
D. Carbon dioxide liquid flow-rate (ml min^{-1})	5.5	6.5
E. Temperature of glass jacket (T_3) (°C)	40	50
F. Temperature of thermocouple wire (T_2) (°C)	40	62
G. Temperature of evaporation tubing (T_4) (°C)	35	50
H. Temperature of the mobile phase (T_{MP}) (°C)	40	60
I. Restrictor position in brass holder	Out	Close to the outlet

Temperature of the glass tubing (T_2, T_3)

This tubing was added to ensure fast evaporation of the modifier in order to prevent its condensation on the walls of the evaporation tubing and to compensate for the cooling effect that occurs during the expansion of the carbon dioxide. The low modifier contents in the mobile phase (<2.8% w/w) are probably the reason why this parameter had no influence during these experiments.

To achieve the maximum sensitivity, the following parameters must be considered: the restrictor outlet must be placed outside the brass holder, otherwise the detector background increases substantially; most of the modifier was evaporated in the glass jacket, hence heating of the evaporation tubing (T4) was not required otherwise the detector response would be lowered owing to partial evaporation of solutes; the power supply of the photomultiplier must be set at range 4 or 5; as Fig. 3 shows,

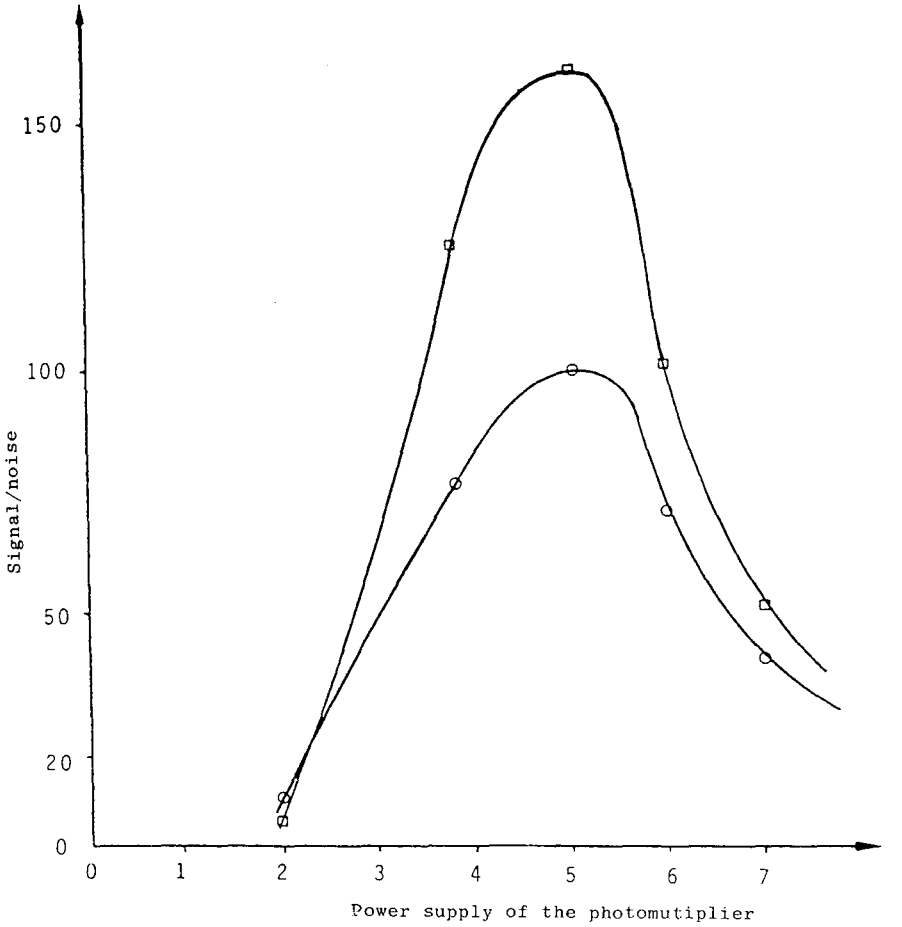

Fig. 3. Signal-to-noise ratio plotted as a function of the power supply of the photomultiplier. Column, 15 × 0.46 cm I.D. Zorbax ODS (5–7 μm); mobile phase, carbon dioxide–methanol (97:3, w/w); flow-rate, 4.5 ml min^{-1} (0°C); temperature, 30°C; column inlet pressure, 295 bar; interface, fused-silica capillary tubing (10 cm × 75 μm I.D.). Detector requirements: air, 3.7 l min^{-1} (detection cell); T_3 (glass tubing), 30°C; T_4 (evaporation tubing), 25°C. Solutes: 730 ng each of (○) docosanol and (□) palmitic acid.

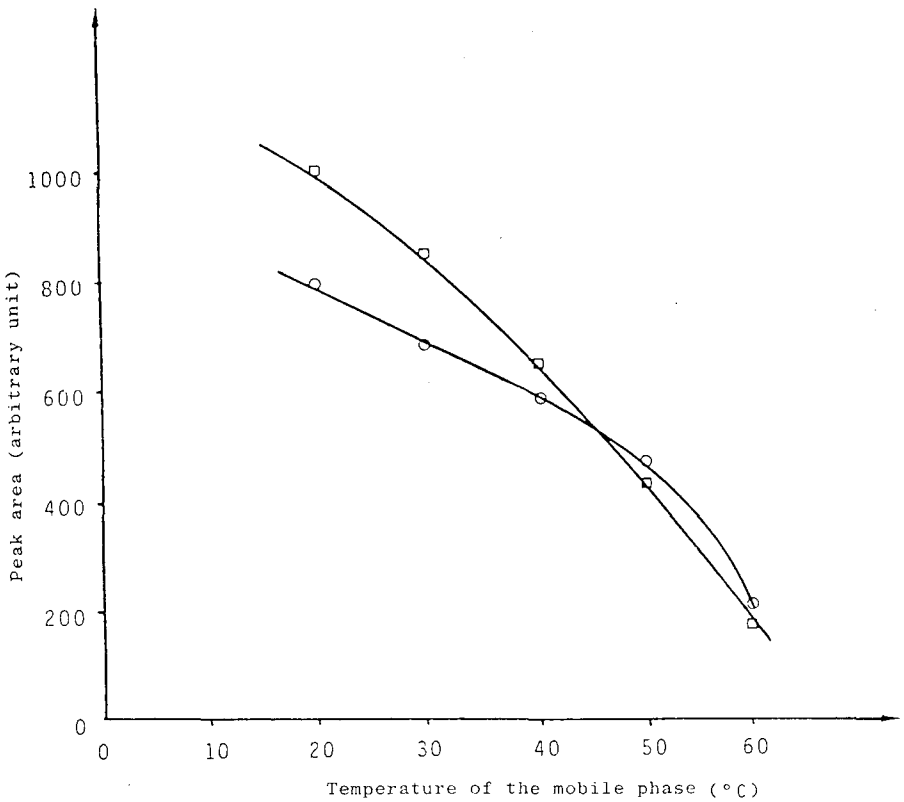

Fig. 4. Response of the light-scattering detector as a function of the temperature of the mobile phase. Column, 15 × 0.46 cm I.D., LiChrosorb Si 60 RP-18 (5 μm); mobile phase, carbon dioxide–methanol (97.2:2.8, w/w); flow-rate, 5.4 ml min^{-1}; inlet column pressure, 180 bar; interface, fused-silica capillary tubing (12 cm × 75 μm I.D.). Detector requirements as in Fig. 3. Solutes: 600 ng each of (○) docosanol and (□) palmitic acid.

the best signal-to-noise ratio was obtained at range 5.

Surprisingly, the temperature of the mobile phase was found to have a large effect on the detector response (Fig. 4). A large decrease in the detector response occurred when the temperature of the mobile phase was increased. This effect can probably be related to the relationship between the molar enthalpies of mixing (H_M^E), recently reviewed by Christensen *et al.*[15] for carbon dioxide–alkane mixtures: along isobars, small positive H_M^E below the lower critical temperature are transformed into large negative H_M^E as the temperature rises, then to large positive H_M^E near the upper critical temperature, and finally they diminish until they resemble those observed below the lower critical temperature. If similar changes in H_M^E occur during carbon dioxide–methanol mixing, as the temperature varies in the chromatograph, exothermic or endothermic effects cause increases or decreases in the temperature of the mobile phase. Consequently, a different behaviour can be expected during the chromatographic process, including the decompression step. A knowledge of H_M^E values when mixing carbon dioxide and methanol could be very useful in understanding these phenomena.

In a second step, in order to expand the potential of SFC–LSD for the analysis of polar compounds, we investigated the LSD response with mobile phases containing up to 4.8% (w/w) of methanol using a 2^5 factorial design in order to economize on experiments and to investigate the interactions between parameters.

A thorough study of factorial designs is beyond the scope of this paper, as they were only used as a tool for our purposes. We built our approach on the data published by Sado and Goupy[7], Feinberg and Ducauze[8] and Miller and Miller[9].

We assigned each parameter two levels (Table III). In the matrix of experiments, the signs indicate the level of parameters for each measurement. The effects reported in Table IV were deduced from the measurements using the matrix: the signs of the column corresponding to the parameter of interest were associated with the responses (reported in Table III) to calculate the algebraic sum of responses. Then, the sum was divided by the number of experiments to give the effect of the parameter. A significant negative or positive value indicates a decrease or an increase, respectively in the detector response, when the parameter is set to the (+) level instead of the (−) level with the level of the other parameters being fixed.

As the measurements were repeated five times, an analysis of variance was done[8]. Thus, we were able to correlate a significant effect with parameters by calculating the ratio (F) between the variance caused by the parameter (or interaction) investigated and the residual variance (Table IV). The effect was considered to be significant from Snedecor's table when $F > 7.71$.

In addition to the temperatures of the interface and the mobile phase, we also investigated the effect of air as nebulization make-up gas flowing around the restrictor outlet[10]. Other parameters were selected according to the previous conclusions.

The influence of the parameters studied is summarized in Table V as a function of the methanol content in the mobile phase. In all instances, when air was added the detector response was 2 – 5 times lower, depending on the levels of the other parameters.

For a low methanol content (2.4%), the other parameters had no effect or lowered the response when they were set to the (+) level instead of the (−) level; low temperatures of the interface and the mobile phase allow total evaporation of the mobile phase. When the temperature was increased, solute vaporization could no longer be neglected and consequently a decrease in detector response occurred.

For a high methanol content (4.8%), without air, the maximum response was determined when the temperature of the glass jacket (T_3) or the mobile phase temperature was set at the (+) level for low levels of the other parameters only. When air was added, the maximum response occurred for maximum heating of only the interface. These results are consistent with the previous conclusions. Obviously, the highest methanol content in the mobile phase requires supplementary heating. However, these results also emphasize the large effect of interactions; when another temperature was elevated in addition to T_3, the response decreased.

Finally, using these conclusions, the detection limit (signal-to-noise ratio = 3) measured with docosanol ($k' = 0.8$) and octadecanol ($k' = 1.2$) was 12 ng. Such a low value has never been reported before.

TABLE III

2^5 FACTORIAL DESIGN: MATRIX OF EXPERIMENTS, LEVELS OF PARAMETERS AND RESPONSES

Level	*Parameter*				
	T_2(°C) (temperature of thermo-couple wire)	T_3(°C) (temperature of glass jacket)	T_{MP}(°C) (temperature of the mobile phase)	CH_3OH (%) (methanol content in the mobile phase)	Air (l min^{-1}) (air flow-rate)
Level (−)	30	30	30	2.4	0
Level (+)	50	60	50	4.8	2

Experiment No.	T_2	T_3	T_{MP}	CH_3OH	Air	*Peak area of docosanol* ($\times 10^{-3}$)	*Peak area of palmitic acid* ($\times 10^{-3}$)
1	−	−	−	−	−	1130	1328
2	+	−	−	−	−	1082	1194
3	−	+	−	−	−	944	993
4	+	+	−	−	−	886	905
5	−	−	+	−	−	1237	934
6	+	−	+	−	−	770	604
7	−	+	+	−	−	683	388
8	+	+	+	−	−	746	461
9	−	−	−	+	−	84	85
10	+	−	−	+	−	204	207
11	−	+	−	+	−	1130	1111
12	+	+	−	+	−	1193	1146
13	−	−	+	+	−	1250	1320
14	+	−	+	+	−	1368	1492
15	−	+	+	+	−	824	662
16	+	+	+	+	−	826	595
17	−	−	−	−	+	269	320
18	+	−	−	−	+	260	303
19	−	+	−	−	+	267	283
20	+	+	−	−	+	229	252
21	−	−	+	−	+	260	227
22	+	−	+	−	+	197	185
23	−	+	+	−	+	190	107
24	+	+	+	−	+	190	125
25	−	−	−	+	+	274	316
26	+	−	−	+	+	355	361
27	−	+	−	+	+	508	603
28	+	+	−	+	+	352	395
29	−	−	+	+	+	182	174
30	+	−	+	+	+	183	175
31	−	+	+	+	+	205	184
32	+	+	+	+	+	234	214

TABLE IV

2^5 FACTORIAL DESIGN: CALCULATED EFFECT OF THE PARAMETERS AND CORRESPONDING *F* VALUE

Parameters	*Docosanol*		*Palmitic acid*	
	Effect	*F*	*Effect*	*F*
T_2	−11.5	7.5	−13.5	3.2
T_3	9	2.4	−20.5	11.1
T_{MP}	5	3.2	−61	70.3
CH_3OH	5	3.2	13.5	2.9
Air	−318	4762	−287.5	1544
T_2T_3	5	0.1	1.5	2.1
T_2T_{MP}	−8	0.3	4.5	4.9
T_2CH_3OH	27	8.2	21	33
T_2Air	−1.5	0	0.5	0.6
T_3T_{MP}	−106	285	−123.5	542
T_3CH_3OH	76	99.5	124	273
T_3Air	3	17.9	31.5	1
$T_{MP}CH_3OH$	55	179	98	137
T_{MP}Air	−60	15	−61	183
CH_3OHAir	32	12.1	25.5	50
$T_2T_3T_{MP}$	26	3	17.5	21.6
$T_2T_3CH_3OH$	−29	20	−32.5	39
T_2T_3Air	−16	2	−9.5	14.3
T_2T_{MP} CH_3OH	11	0.6	5	4.9
T_2T_{MP}Air	−14	1.9	9.5	12.5
T_2CH_3OHAir	−23	11.1	−25	24
$T_3T_{MP}CH_3OH$	−91	240	−113.5	374
T_3T_{MP}Air	93	193	100.5	426
T_3CH_3OHAir	−50	21.3	−34	118
$T_{MP}CH_3OH$Air	−86	293	−124	341
$T_2T_3T_{MP}CH_3OH$	−13	1.5	−9.5	8.4
$T_2T_3T_{MP}$Air	−4	0.4	4.5	1
$T_2T_3CH_3OH$Air	14	5.4	15.1	9.5
$T_2T_{MP}CH_3OH$Air	−4	0.7	6	0
$T_3T_{MP}CH_3OH$Air	91	193	113.5	322
$T_2T_3T_{MP}CH_3OH$Air	24	9.2	22.5	27.5

APPLICATIONS

Fig. 5 shows the chromatogram of docosanol and palmitic acid used as test solutes during the study of the detector response.

The coupling of SFC with LSD can be used to advantage for the analysis of fatty alcohols and fatty acids, as demonstrated in Figs. 6 and 7; such compounds are very difficult to elute from a packed column when only carbon dioxide is used as the mobile phase (*i.e.*, with flame-ionization detection[10]). One can deduce from these chromatograms that the LSD response varies as a function of volatility, for the operating conditions in Fig. 6, tetradecanol started to evaporate and consequently gave a lower signal than the other solutes; moreover, the LSD response is a function of the particle diameter in the detection cell, which is related to the concentration of the solutes in the effluent before the nebulization step[13]. Consequently, a correction

TABLE V

2^5 FACTORIAL DESIGN: EFFECT OF THE PARAMETERS AS A FUNCTION OF METHANOL CONTENT

0 = no significant effect; ↑ and ↓ = increase and decrease, respectively, in detector response.

Methanol content (%)	*Air*	*Temperature of the thermo-couple wire (T_2)*	*Temperature of the glass tubing (T_3)*	*Temperature of the mobile phase (T_{MP})*	*Temperature of the glass jacket / mobile phase*
2.4	With	0	↓	↓	↓
	Without	0	↓	↓	↓
4.8	Without	0	↑	↑	↓
	With	0	↑	↓	↓

factor was proposed in order to take into account the retention of the solutes for peak-area calculation[10]. This permitted its influence to be partially reduced but more investigations are required on the main parameters (molecular weight, volatility, refractive index, retention, etc.) that affect the LSD response. The retention dependence of the LSD response is not a major drawback as a calibration graph is required for quantitative analysis because of the non-linear relationship between the LSD response and concentration[1,11,13,16–20].

With the improved sensitivity we obtained, LSD can be regarded as a sensitive detection method for SFC when the analysis of this type of solute must be performed on packed columns.

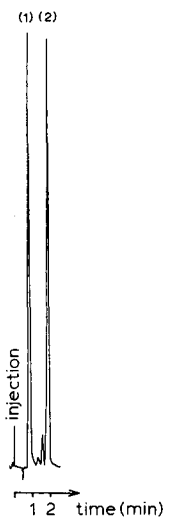

Fig. 5. SFC–LSD chromatogram of (1) palmitic acid and (2) docosanol used as test compounds for optimization. Conditions as in Fig. 3.

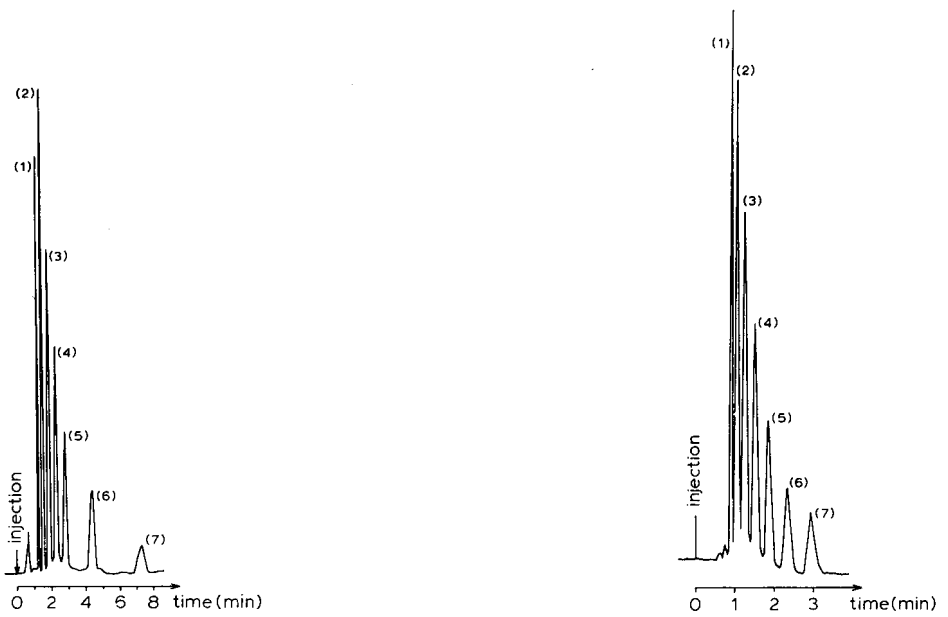

Fig. 6. SFC–LSD chromatogram of fatty alcohols. Column, 15 × 0.46 cm I.D., Zorbax ODS (5–7 μm); mobile phase, carbon dioxide–methanol (98.7:1.3, w/w); flow-rate, 5.6 ml min^{-1}; inlet column pressure, 290 bar; interface, fused-silica capillary tubing (12 cm × 75 μm I.D.). Detector requirements: air, 3.7 l min^{-1} (detection cell); T_3 (glass tubing), 30°C; T_4 (evaporation tubing), 30°C. Solutes: 1 = tetradecanol; 2 = hexadecanol; 3 = octadecanol; 4 = eicosanol; 5 = docosanol; 6 = hexacosanol; 7 = triacontanol. Amount injected, 700 ng, except tetradecanol, 1.4 μg.

Fig. 7. SFC–LSD chromatogram of fatty acids. Column, 15 × 0.46 cm I.D., Zorbax ODS (5–7 μm); mobile phase: carbon dioxide–methanol (97.6:2.4, w/w); flow-rate, 3.9 ml min^{-1}; inlet column pressure, 200 bar; interface, fused-silica capillary tubing, 12 cm × 75 μm I.D. LSD requirements: air, 3.7 l min^{-1} (detection cell); T_3 (glass tubing), 30°C; T_4 (evaporation tubing), 30°C. Solutes: 1 = lauric acid; 2 = myristic acid; 3 = palmitic acid; 4 = stearic acid; 5 = arachidic acid; 6 = docosanoic acid; 7 = tetracosanoic acid. Amount injected, 700 ng of each solute.

CONCLUSION

With the new interface design between the column and the light-scattering detector, the sensitivity of SFC-LSD was enhanced by a factor of 4 in comparison with our previous results while the temperatures of the interface and evaporation tubing were significantly reduced even with a methanol content of up to 5% in the mobile phase. Hence the gain in sensitivity is a real improvement because the risk of partial evaporation or degradation of solutes before the detection stage is also greatly reduced.

Factorial designs were used to plan and to economize on measurements. Obviously, the conclusions must be considered with care as they concern a limited range of variation of the parameters. Without further experiments, a linear relationship must be assumed between the two levels of the parameters we studied. Nevertheless, the 2^5 factorial design demonstrated their potential as we investigated interactions between parameters which were found to influence greatly the detector response. It permitted

the use of LSD under conditions such that the best sensitivity was obtained for this type of compound.

Various applications in the field of carbohydrate and triglyceride analysis are under investigation to demonstrate the potential and advantages of SFC–LSD.

ACKNOWLEDGEMENTS

We thank Mr. J. Goupy of the C.R.D. Total-France for his help during the experiments with factorial designs.

REFERENCES

1 P. Carraud, D. Thiebaut, M. Caude, R. Rosset, M. Lafosse and M. Dreux, *J. Chromatogr. Sci.*, 25 (1987) 395.
2 M. Caude and R. Rosset, *Analusis*, 14 (1986) 310.
3 P. J. Schoenmakers and F.C.C.J.G. Verhoeven, *Trends Anal. Chem.*, 6 (1987) 10.
4 P. Mourier, E. Eliot, M. Caude and R. Rosset, *Anal. Chem.*, 57 (1985) 2819.
5 J. Doehl, A. Farbrot, T. Greibrokk and B. Iversen, *J. Chromatogr.*, 392 (1987) 175.
6 J. L. Janicot, M. Caude and R. Rosset, *J. Chromatogr.*, 437 (1988) 351.
7 G. Sado and J. Goupy, *Analusis*, 14 (1986) 389.
8 M. Feinberg and C. Ducauze, *Analusis*, 8 (1980) 185.
9 J. C. Miller and J. N. Miller, *Statistics for Analytical Chemistry*, Wiley, Chichester, 2nd. ed., 1988.
10 D. Thiebaut, *Thèse*, Université P. et M. Curie, Paris, 1988.
11 J. M. Charlesworth, *Anal. Chem.*, 50 (1978) 1414.
12 T. H. Mourey and L. E. Oppenheimer, *Anal. Chem.*, 56 (1984) 2427.
13 P. A. Asmus and J. B. Landis, *J. Chromatogr.*, 316 (1984) 461.
14 R. W. Bally and C. A. Cramers, *J. High Resolut. Chromatogr. Chromatogr. Commun.*, 9 (1986) 626.
15 J. J. Christensen, R. M. Izatt and D. M. Zebolsky, *Fluid Phase Equilibria*, 38 (1987) 163.
16 A. Stolyhwo, H. Colin and G. Guiochon, *J. Chromatogr.*, 265 (1983) 1.
17 A. Stolyhwo, H. Colin, M. Martin and G. Guiochon, *J. Chromatogr.*, 288 (1984) 253.
18 L. E. Oppenheimer and T. H. Mourey, *J. Chromatogr.*, 323 (1985) 297.
19 T. H. Mourey and L. E. Oppenheimer, *Anal. Chem.*, 56 (1984) 2427.
20 L. E. Oppenheimer and T. H. Mourey, *J. Chromatogr.*, 298 (1984) 217.

Journal of Chromatography, 467 (1989) 61–74
Elsevier Science Publishers B.V., Amsterdam — Printed in The Netherlands

CHROM. 21 200

DETERMINATION OF NITROGEN COMPOUNDS BY SUPERCRITICAL FLUID CHROMATOGRAPHY USING NITROUS OXIDE AS THE MOBILE PHASE AND NITROGEN-SENSITIVE DETECTION

LENNART MATHIASSON*, JAN ÅKE JÖNSSON and LARS KARLSSON
Department of Analytical Chemistry, University of Lund, S-221 00 Lund (Sweden)
(First received September 8th, 1988; revised manuscript received December 19th, 1988)

SUMMARY

A supercritical fluid chromatography system with nitrous oxide as the mobile phase and a nitrogen sensitive gas chromatographic detector was evaluated for the determination of amines and their amide and carbamate derivatives. Special interest was focused on the detector performance. The detector sensitivity for amines was comparable with that observed when the same detector was used in gas chromatography. However, the selectivity towards hydrocarbons was 25–50 times lower, only *ca.* 200. No variation of detector sensitivity was observed for amines and their derivatives when the system pressure was varied. Methanol was found to be the best sample solvent, with a detector response more than 50 times lower than those of other solvents tested. Linear calibration graphs were obtained in the concentration range 10–1000 ppm for amide and carbamate derivatives. For free amines, however, a curvature was found below 100 ppm, at least partly depending on adsorption in the column. The precision in peak area measurements in pressure-programmed experiments at concentrations above 100 ppm was *ca.* 4%.

INTRODUCTION

The technique of using supercritical fluids, *e.g.*, carbon dioxide and nitrous oxide at high pressures, as mobile phases in combination with capillary columns with small inner diameters, is under rapid development. Several review articles discussing the merits and obstacles of supercritical fluid chromatography (SFC) as a separation technique have recently appeared[1–6].

One very interesting feature, to which special attention has been paid in this work, is that separations can be performed under conditions similar to liquid chromatography with a mobile phase of high solvating power, while ordinary gas chromatographic detectors can be employed.

Concerning the type of molecules investigated, most work has hitherto been directed towards the possibility of expanding the molecular weight range of molecules which can be separated by gas chromatography (GC). Less attention has been paid to the possibility of analyzing thermolabile substances near room temperature. Still less considered is the possibility of extending the applicability of GC to the separation of

0021-9673/89/$03.50

low concentrations of polar compounds. The concentrations of the analytes have generally been high, most often above 0.1%. In many cases the concentrations are not stated, which makes the results difficult to interpret, as adsorption effects are expected, influencing the peak shape and retention.

Investigations of polar nitrogen compounds such as amines, alkanolamines and aliphatic amides are very rare, especially those involving short-chain molecules in low concentrations. In a compilation of 335 representative chromatograms published at a recent conference[7], only about 5 chromatograms showed amines and related compounds, all using CO_2 as a carrier. Low solute concentrations were not studied in any of those five. Polar and basic compounds such as polyamines and alkanolamines are difficult or even impossible to handle at low concentrations by GC and difficult to detect with liquid chromatographic detectors. For these compounds, SFC can be a good alternative.

In this work we present an investigation concerning determinations of nitrogen compounds on columns with different polarities using nitrous oxide (N_2O) as a mobile phase and nitrogen sensitive detection. This combination has not, to our knowledge, hitherto been exploited for analysis of basic compounds. Nitrous oxide was chosen as the mobile phase instead of the most commonly used carbon dioxide, to eliminate the risk of reactions with analytes containing primary or secondary amine functions. The permanent dipole moment of nitrous oxide was also expected to give better solvation power for molecules without aromatic ring systems. A nitrogen sensitive detector was chosen instead of the more common flame ionization detector. Our hope was that the high selectivity and low detection limits obtained for nitrogen compounds with the nitrogen detector in GC with nitrogen as a carrier gas would also be obtained in SFC with nitrous oxide as the mobile phase.

EXPERIMENTAL

Equipment

The equipment is shown in Fig. 1. It consists of a pump (Model 8500; Varian, Walnut Creek, CA, U.S.A.) and a gas chromatograph (Model 3710, Varian) equipped with a thermionic, nitrogen–phosphorus detector (Model TSD, Varian). The pump was modified to work under constant pressure, as described[8]. A digital voltmeter (DVM) showed the pressure directly in bar, a digital pulse counter measured the

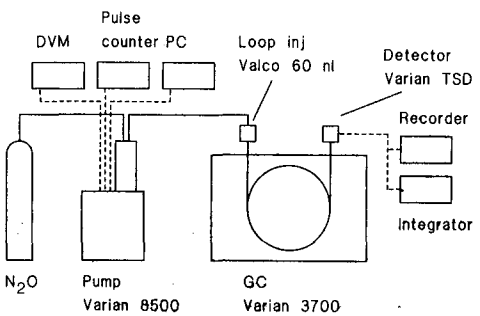

Fig. 1. Schematic diagram of the SFC equipment used in this work.

flow-rate (3600 pulses correspond to 1 ml) and a table-top computer (PC), ABC-80; Luxor, Motala, Sweden) was used for creating linear and quadratic pressure gradients. Samples were injected using a manual, 60-nl loop injector (Model CI4W; Valco, Houston, TX, U.S.A.). Chromatograms were evaluated with a digital integrator (Model 3390A; Hewlett-Packard, Palo Alto, CA, U.S.A.).

The capillary column was connected with a zero dead-volume union (Valco) to a 50-μm frit restrictor (Lee Scientific, Salt Lake City, UT, U.S.A.). The restrictor end was positioned 1–2 mm below the outlet of the detector tip and swept with a make-up gas (25 ml/min of nitrogen) entering at the detector base.

Detector settings were typically: hydrogen flow-rate 1.2 ml/min, air flow-rate 210 ml/min, bead current 3.27 A (580 scale divisions) and bias voltage 7 V. For details concerning these settings, see below. Nitrous oxide was used as the mobile phase, in some experiments modified with low concentrations of methanol. Methanol mixtures, 0.1–1%, were prepared by adding small amounts of methanol directly to the pump cylinder (volume 250 ml) before pressurization of the system with nitrous oxide from the supply cylinder.

Typical flow-rates from the pump at room temperatur and 100 bar (measured by the pulse counter) were 6 μl/min. A change of the pressure from 80 to 160 bar typically increased the flow-rate by about 35%.

Columns

The columns investigated were DB-5 (95% dimethyl–5% diphenyl polysiloxane), 10 m × 50 μm I.D., film thickness 0.2 μm (J&W Scientific, Folsom, CA, U.S.A.) and DB-17 (50% methyl–50% phenyl polysiloxane), 10 m × 50 μm I.D., film thickness 0.10 μm (J&W) and SB-octyl-50 (50% *n*-octyl-50% methyl polysiloxane), 10 m × 100 μm I.D., film thickness 0.5 μm (Lee Scientific).

Chemicals

All substances used as solutes are listed in Table I together with abbreviations. The diamines (2,4-TDA, 2,6-TDA and MDA) were obtained from Merck (Darmstadt, F.R.G.). Their carbamate derivatives (2,4-TDC, 2,6-TDC and MDC) were made by reacting the corresponding diamine with ethyl chloroformate (Sigma, St. Louis, MO, U.S.A.) according to the procedure described[9]. The amide derivatives (2,4-FTDA, 2,6-FTDA and FMDA) were prepared at the Department of Occupational Medicine (University Hospital of Lund). Tri-*n*-butylamine (p.a.), tri-*n*-decylamine (purum), tri-*n*-hexylamine (>95% by GC) and tri-*n*-pentylamine (>97% by GC) were obtained from Fluka (Buchs, Switzerland). Tri-*n*-octylamine (>95% by GC) and triethanolamine (p.a.) were obtained from Merck. Solvents used were all of highest available purity (p.a. or HPLC grade).

RESULTS AND DISCUSSION

Optimization of the detector

After initial settings of the hydrogen flow-rate, air flow-rate and bead current according to our experience of the detector performance in capillary GC, the flow-rate of the make-up gas was varied in the range 10–40 ml/min with 2,6-TDC as a test substance. Within a flow-rate range of 20–30 ml/min. the peak heights for the test

TABLE I

COMPOUNDS INVESTIGATED

Name	*Abbreviation*
Dibutyl phthalate	DBP
n-Hexadecane	
2,4-Toluenediamine	2,4-TDA
2,4-Toluenediethyldicarbamate	2,4-TDC
2,4-Toluenediamine (perfluorobutyro derivative)	2,4-FTDA
2,6-Toluenediamine	2,6-TDA
2,6-Toluenediethyldicarbamate	2.6-TDC
2,6-Toluenediamine (perfluorobutyro derivative)	2,6-FTDA
4,4'-Diaminodiphenylmethane	MDA
4,4'-Diaminodiphenylmethane (diethylcarbamate derivative)	MDC
4,4'-Diaminodiphenylmethane (perfluorobutyro derivative)	FMDA
Tri-*n*-butylamine	
Tri-*n*-pentylamine	
Tri-*n*-hexylamine	
Tri-*n*-octylamine	
Tri-*n*-decylamine	
Triethanolamine	

substance were almost equal. At 10 and 40 ml/min, the signal was about 8% lower than at 25 ml/min, the value used in further experiments.

The bead current was set at 3.27 A (580 scale divisions) after testing the bead under GC conditions. This value was chosen so that the sensitivity for nitrogen-containing compounds was high but still permitted an acceptable lifetime of the bead. A high bead temperature gives high sensitivity and selectivity but decreases the lifetime. When using this detector for GC, with nitrogen or helium as the carrier, a setting at 3.21–3.31 A (550–600 scale divisions) gives a bead lifetime which usually exceeds 6 months of continuous use. Each bead is manufactured manually and settings which give equal performance differs somewhat from bead to bead.

With a make-up flow-rate of 25 ml/min and a bead current of 3.27 A (580 scale divisions), the following parameters were varied: hydrogen flow-rate between 0.9 and 6.5 ml/min, air flow-rate between 135 and 275 ml/min and bias voltage between 6 and 9 V. Optimization was performed using the Simplex technique[10] with a test mixture of 2,6-TDC (A) and eicosane (B) in concentrations of 100 ppm and 0.2%, respectively. The maximum of the product of the sensitivity for A times the selectivity compared to B [(peak height of A)^2/(peak height of B)] was used as the criterion of maximum performance. All measurements were performed at a constant pressure (120 bar) of the supercritical fluid. The optimization procedure converged after eleven steps to the values 1.2 ml/min, 230 ml/min and 7.0 V, respectively. With these settings, a selectivity of about 200 was obtained.

The selectivity obtained here is much less than that in GC where values of 5000–10 000 are generally obtained for comparable compounds. This is probably due to the use of nitrous oxide as the carrier. The sensitivity for nitrogen compounds such as amines and carbamates is, within experimental uncertainties, the same as in GC. This means that the decrease in selectivity is due to an increase in sensitivity for hydrocarbons in the detector. Such an increase has been observed for the electron-

capture detector after doping the carrier gas with nitrous oxide[11]. In the nitrogen sensitive detector used here, ions are stated to be formed by a thermoionic process. However, the effects can be anticipated to be similar to those in an electron-capture detector. The different chemistry obtained around the bead when changing from nitrogen to nitrous oxide as the carrier is also reflected by the unexpected low value (1.2 ml/min) of the optimum hydrogen flow-rate compared to flow-rates of 2.5–4 ml/min normally used in GC.

Detector performance at varying system pressure

The detector optimization above was performed at constant pressure, *i.e.*, constant mass flow of nitrous oxide to the detector. The most important technique in SFC for obtaining good chromatographic behaviour, pressure programming, leads to a change of mobile phase flow-rate. A possible influence of the flow-rate of N_2O on the selectivity suggested by the experiments presented above might influence quantitation in pressure-programmed experiments. Experiments were therefore performed at different pressures, using a test mixture of 2,6-TDC (500 ppm), MDA (500 ppm) and dibutyl phthalate (10%) dissolved in methanol, on a DB-17 column.

The different peak shapes and retention times obtained at each pressure create a difficult task for a simple electronic integrator. In order to obtain the necessary accuracy in the peak area measurements, the cut-and-weigh method had to be applied. Fig. 2 shows the dependence of peak areas on the system pressure. Above 100 bar the peak areas of 2,6-TDC and MDA are independent of the pressure, while the peak area for dibutyl phthalate increases markedly as the pressure and thus the mass flow-rate of nitrous oxide to the detector is increased. As the system pressure increases, retention times decrease, leading to an increased mass flow-rate of analyte into the detector. To

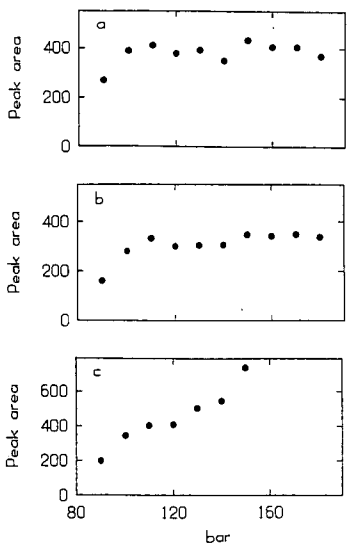

Fig. 2. Peak areas for some model substances *versus* the system pressure. (a) 2,6-TDC (500 ppm), (b) MDA (500 ppm) and (c) DBP (10%) (for abbreviations, see Table I). Sample solvent: methanol. Column: 10-m DB-17. Temperature: 130°C.

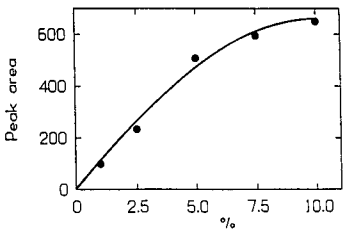

Fig. 3. Calibration curve for DBP (dibutyl phthalate). System pressure 140 bar; other chromatographic conditions as in Fig. 2.

ascertain that this effect was not responsible for the increased response for dibutyl phthalate shown in Fig. 2c, a calibration graph of peak area *versus* solute concentration was made at constant pressure. At this curve is convex due to detector overloading above 5%, as shown in Fig. 3, the effect of increased mass flow-rate of the analyte in fact leads to a decrease in the detector response. Thus, with the concentration of dibutyl phthalate used, the effect of the nitrous oxide mass flow-rate on the sensitivity is underestimated: at 140 bar, only about 70% of the real effect is observed. At lower pressures, the discrepancy is smaller.

To exclude the possibility that the oxygens in the dibutyl phthalate molecule influence the results of the experiment described above, a similar plot of peak area *versus* pressure was made with 2% *n*-hexadecane in diethyl ether on a DB-5 column. In the pressure range 90–160 bar a similar increase was observed.

The lower values of the peak areas, measured for 2,6-TDC and MDA at 90 bar, are probably due to adsorption on the column. With a reversible adsorption, which seems most likely, the decrease in peak area is an artifact in the measurements due to the difficulty in distinguishing the tail of the peak from the baseline.

At low pressure, the solvation power of nitrous oxide is relatively poor so the situation is similar to conditions in GC. In GC, with non-polar stationary phases and polar analytes, we[12] and others[13] have shown the possibility of adsorption of the analyte at the surface of the stationary phase as well as on the surface of the support material. The possibility that the low peak area at low pressures is due to poor solubility of the sample solvent in the carrier fluid, which may result in a thin film of sample solution on the walls of the injection loop, is ruled out here because of the long injection times (at least 10 s). This matter is further discussed below.

The results in Fig. 2 where the peak area increases about 2.5 times from 100 to 150 bar for dibutyl phthalate and is unchanged above 100 bar for 2,6-TDC and MDA, together with the fact that the selectivity is about 200 for these nitrogen compounds compared to dibutyl phthalate, gives information about the reactions in the detector. The results can be explained only if the increased ionization, occurring when nitrous oxide is present in the gas mixture around the detector bead, is rather non-specific. The increased ionization at the carbon chain in the nitrogen compounds will then with a selectivity of 200 contribute to an area increase of only about 1–2%, within experimental errors. This explanation is also supported by the similar results obtained for *n*-hexadecane mentioned above. Therefore it seems likely that the reactions between nitrous oxide and the compounds considered involve an attack on the carbon chain and that heteroatoms such as nitrogen and oxygen (in the phthalate) do not

contribute significantly to the ionization process induced by nitrous oxide. This is also consistent, as mentioned earlier, with the results obtained for hydrocarbons, using an electon-capture detector, doped with nitrous oxide[11]. These results also imply that quantitations of nitrogen compounds in pressure-programmed experiments will be possible without elaborate standardization procedures.

Choice of solvent

The main parameter of interest in this context is the peak height of the eluting solvent. Solvents containing nitrogen, such as acetonitrile, should obviously be avoided. Results concerning several solvents are given in Table II.

It is clear that methanol is by far the best solvent concerning detector performance, allowing determination of compounds eluting close to the solvent. The peak height of methanol normally corresponds to a concentration of less than 10 ppm of a compound such as 2,6-TDC. The reason why the signal from methanol is so low compared to other solvents is not obvious. However, many high-molecular-weight compounds, especially non-polar ones, have limited solubility in methanol. It also seems that the solubility of methanol in nitrous oxide at pressures below 100 bar is not too good. This may lead to problems of transporting the analyte from the injection loop to the column (see below). These two features should thus be considered before using methanol as a solvent.

Injection

Injection with the 60-nl loop injector was studied with 100 ppm of 2,6-TDC as a test substance with methanol as the solvent at a pressure of 90 bar on a DB-5 column. Fig. 4 shows how the peak height varies with the injection time, t_{inj}, *i.e.*, the time during which the internal sample loop is connected to the column. At 90 bar, an injection time of *ca.* 5 s is required for good reproducibility. The introduction of a sample into the column thus creates some band broadening. The mobile phase flow-rate was *ca.* 0.7 ml/h which means that during 5 s a volume of mobile phase corresponding to *ca.* 15 loop volumes has passed through the loop. Addition of ammonia (500–1500 ppm) to the test solution did not make it possible to shorten the injection time, which indicates that adsorption of the substance in the injector is not the cause of the problem. The explanation of the relatively long injection times needed is probably that a thin film of methanol, retaining a portion of the analyte, is formed at the inner walls of the injector

TABLE II

RESPONSES FOR DIFFERENT SOLVENTS

Detector: Varian TSD. System pressure: 100 bar. Temperature: 150°C. Column: 10-m DB-5.

Solvent	*Relative peak height*
Methanol	1
Diethyl ether	65
Ethanol	80
Toluene	90
Dimethyl sulphoxide	115
Diisopropyl ether	270

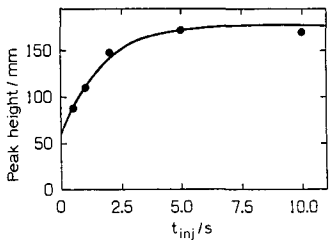

Fig. 4. Variation of peak height with injection time, t_{inj}, for 2,6-TDC (100 ppm) in methanol (for abbreviations, see Table I). System pressure: 90 bar. Column: 10-m DB-5. Temperature: 100°C.

and that this film, due to limited solubility in supercritical nitrous oxide, needs several loop volumes to be swept out. The situation is considerably improved at higher system pressures.

For very polar and very basic compounds, peak shapes may be influenced both by adsorption and by solvent solibility in the mobile phase. Peak heights become lower than expected and severe tailing occurs at lower concentrations. However, at present it is not possible to distinguish adsorption effects originating in the injector from such effects on the column.

Stationary and mobile phases

Of the columns considered, both DB-5 and DB-17 may be used for free amines as well as for the different amine derivatives. On SB-octyl-50, aromatic amines such as MDA and 2,6-TDA were not eluted in spite of the higher film thickness of this column, which otherwise was expected to minimize adsorption. Chromatograms of some test substances at two different, fairly low concentrations obtained in pressure-programmed experiments are shown in Fig. 5. For substances where the basic character of the nitrogen atom has been suppressed by derivatization, the peaks are considerably more symmetric than for the free amines. The number of theoretical plates (calculated for 2,6-TDC) was about 13 000 on both DB-17 and DB-5 columns at 150 bar and 100°C. For SB-octyl-50, plate numbers of the order of 10 000 were obtained, as expected with a thicker film and a larger column diameter. The peak shapes of the most polar solutes, the free amines (peaks 4 and 6), vary slightly with concentration, apparently due to adsorption in the chromatographic system. The observed variation of retention times of *ca.*3% over the concentration range 10–1000 ppm is consistent with the magnitude of the peak shape changes.

With proper pressure-programming conditions, even strongly basic compounds such as tertiary aliphatic amines can be chromatographed at low concentrations as shown in Fig. 6.

Ammonia was added to the solutions for controlling adsorptions on the walls of vessels and syringes according to our previous experiences[14]. Interestingly, the detector selectivity towards ammonia for the amines is only about 100, while in GC work with nitrogen as the carrier gas it is of the order of 5000–10 000.

For strongly polar and basic compounds such as triethanolamine it is obvious that adsorption will be a problem in quantification at low concentrations as illustrated in Fig. 7. Below 200 ppm, the peak tailing is severe.

Pressure programming of the mobile phase is not sufficiently efficient for

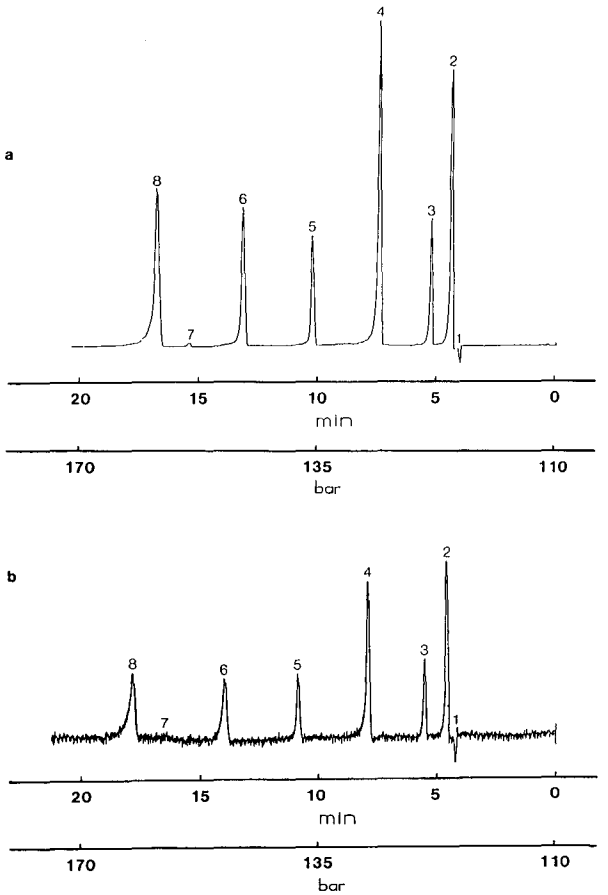

Fig. 5. Chromatograms of some model substances. Concentrations: (a) 250 ppm; $1 \cdot 10^{-11}$ A f.s.; (b) 25 ppm; $2 \cdot 10^{-12}$ A f.s. Peaks: 1 = solvent front; 2 = MDC; 3 = 2,6-FTDA; 4 = 2,6-TDA; 5 = FMDA; 6 = 2,6-TDC; 7 = impurity from MDA; 8 = MDA (for abbreviations, see Table I). Sample solvent: methanol. Injection volume: 60 nl. Pressure programme as shown. Column: 10-m DB-17. Temperature: 130°C.

improving the chromatographic performance. Another measure taken to improve the situation, namely addition of a polar modifier, methanol, to the mobile phase did not significantly improve the peak shape of triethanolamine in the methanol concentration range 0.1–0.5% but, as expected, the peak was eluted closer to the front with increasing methanol concentration. For good chromatography of basic analytes, the polar modifier should have a basic character.

Furthermore, the stability of the column may not be as good when using a mobile phase containing methanol. In such a system, with a methanol concentration of about 1% and a DB-5 column used for about 2 weeks, often above 200 bar, a drastically impaired performance was observed. Without methanol, the same column had been used at these pressures without problems for more than 2 months.

Above *ca.* 0.8% methanol, the signal from the analyte rapidly decreased. This

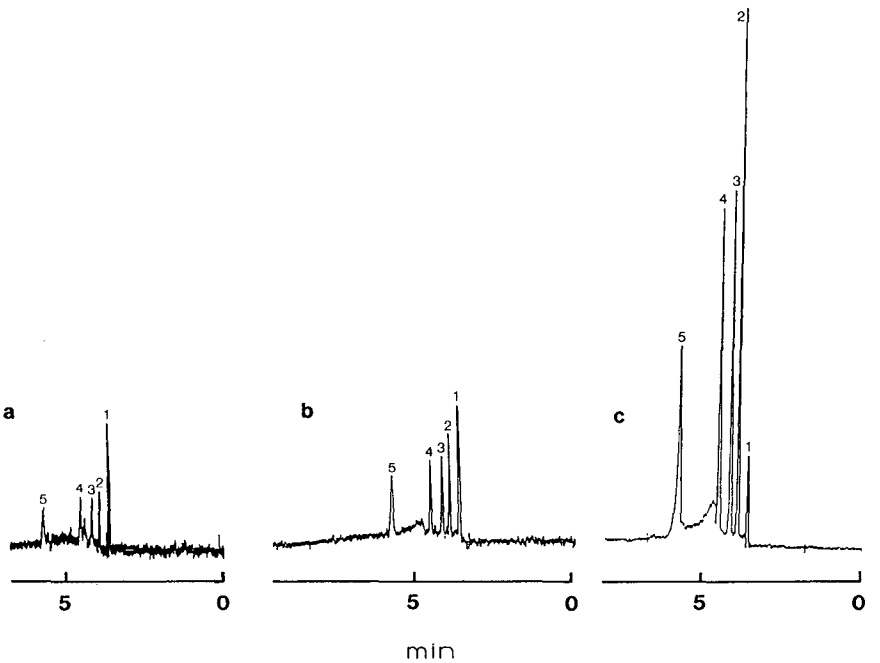

Fig. 6. Chromatograms of tertiary aliphatic amines. Concentrations: (a) 2.5 ppm; $1 \cdot 10^{-12}$ A f.s.; (b) 10 ppm; $2 \cdot 10^{-12}$ A f.s.; (c) 100 ppm; $4 \cdot 10^{-12}$ A f.s. Peaks: 1 = ammonia; 2 = tri-*n*-butylamine; 3 = tri-*n*-pentylamine; 4 = tri-*n*-hexylamine; 5 = tri-*n*-octylamine. Sample solvent: methanol with *ca.* 1000 ppm NH_3. Injection volume: 60 nl. Pressure programme: 95–130 bar, 5 bar/min. Column: 10-m DB-5. Temperature: 100°C.

behaviour is in accordance with results discussed above, where it was shown that nitrous oxide increased the detector signal for the hydrocarbon part of the molecule. With carbon dioxide as the mobile phase, the detector would most probably have tolerated an higher methanol concentration. Greibrokk *et al.*[6] used 7% methanol in carbon dioxide for the determination of 2,4-nitroaniline with nitrogen sensitive detection, and an Hewlett-Packard thermionic detector.

The combination of a polar mobile phase with a constant dipole moment, somewhat polar columns such as DB-17 and polar solutes, with possibilities for specific interactions, implies that changes in pressure and temperature are expected to give changes in resolution. This is illustrated by the observation that a change of the system pressure from 86 to 100 bar increased the resolution between 2,4-TDC and 2,6-TDC from 1.3 to 2.1 with an increase in retention time from about 10 to 15 min. At the same time, the occurrence of specific interactions makes the retention behaviour very difficult to interpret as shown by the following example: if tridecylamine is included in the sample of tertiary amines, shown in Fig. 6, a shorter retention time is obtained for this compound than for trihexylamine. Evidently, only small changes in hydrophobicity contra polarity may give large and unexpected effects. Much work remains before a deeper insight in the retention mechanisms of SFC is reached. However, recent work by Yonker and co-workers concerning the influence of temperature[15], density[16], solute concentration[17] and modifier concentration[18] on

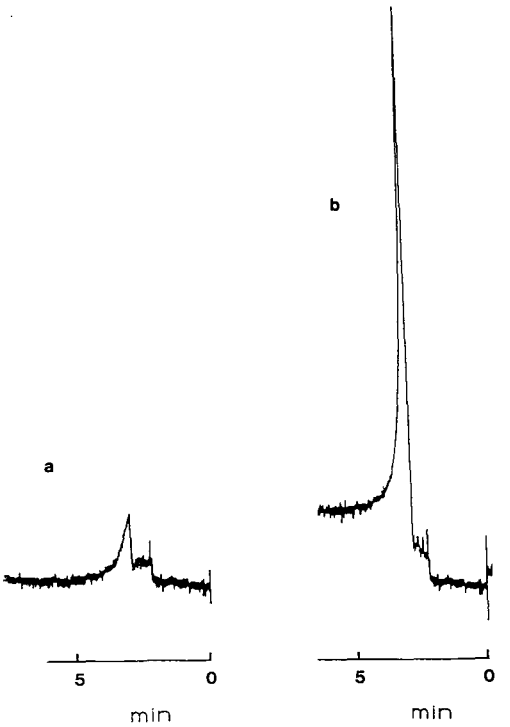

Fig. 7. Chromatograms of triethanolamine. Concentrations: (a) 100 ppm; (b) 250 ppm. Attenuation: $1 \cdot 10^{-12}$ A f.s. Sample solvent: methanol. Injection volume: 60 nl. Pressure programme: 95–160 bar, 5 bar/min. Column: 10-m DB-5. Temperature: 100°C.

retention has provided some insight in the underlying mechanisms determining the retention in SFC.

The columns investigated here are non-polar to slightly polar. The choice has been governed by our knowledge concerning capillary GC for the determination of basic nitrogen compounds as free aromatic amines and carbamates. In such systems, the best behaviour has always been obtained for relatively non-polar columns, while more polar columns, such as those based on polyethylene glycol have given adsorption problems probably due to the presence of acidic sites.

Quantitative analysis

Calibration graphs in the range of 10–1000 ppm were obtained for a mixture of four test substances: 2,6-TDA, 2,6-TDC, MDA and FMDA (see Table I) representing free amines as well as their carbamate and amide derivatives. The chromatographic conditions were as in Fig. 5. As shown in Fig. 8, the graphs seem to be virtually linear over the concentration range considered. The concentration is expressed in ppm, *i.e.*, weight units. If it is instead expressed in moles of nitrogen, the graphs for TDA and TDC will overlap, as will those of MDA and FMDA. The detector response is thus caused mainly by the nitrogen atom, and seems to be relatively independent of derivatization.

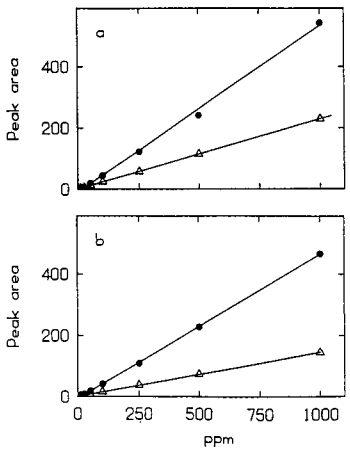

Fig. 8. Calibration graphs in pressure-programmed experiments. Peak area *versus* concentration. (a) ● = 2,6-TDA; △ = 2,6-TDC; (b) ● = MDA; △ = FMDA. (for abbreviations, see Table I). Chromatographic conditions as in Fig. 5.

The correlation coefficients were 0.9989, 0.9997, 0.99990 and 0.99991, respectively. For 2,6-TDA and MDA, negative intercepts were obtained, but the 95% confidence interval did not include the origin only in the case of MDA. The occurrence of negative intercepts indicates that other retention mechanisms, *e.g.*, adsorption may be present. In such cases the behaviour of these test solutes at low concentrations is interesting. Instead of drawing calibration lines as above, it is better to normalize the response by dividing by the solute concentration. This is illustrated in Fig. 9, where the relative response has been calculated as the normalized response divided by the normalized response at 1000 ppm.

No significant variation of the relative response with concentration was found for the two derivatives, while for the two free amines a marked decrease occurred

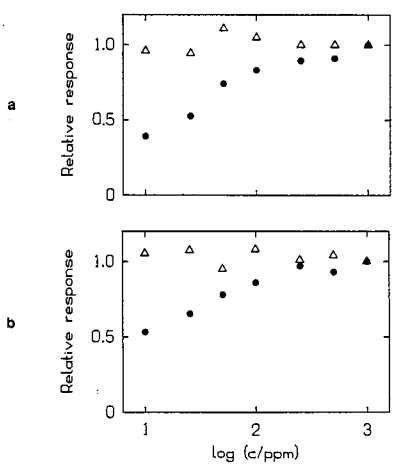

Fig. 9. Relative response as defined in the text *versus* logarithm of concentration (c). Details as in Fig. 8.

below 100 ppm. These results imply that derivatization may in many cases be advantageous. The results also show that for free amines in the low concentration range, a calibration graph should only cover a small concentration range, say one decade, to improve the accuracy in the quantitation.

The precision in peak area measurements, based on triple injections for the four test substances in the pressure-programmed experiments described above, was about equal (*ca.* 4% R.S.D.) above a concentration of 100 ppm. At low concentrations the precision was, as expected, better for the two derivatives, 2,6-TDC and FMDA. At a concentration of 25 ppm it was on average *ca.* 6%, compared to an average of *ca.* 12% for the free amines 2,6-TDA and MDA.

The precision has also been investigated at different constant pressures (110–180 bar) and temperatures (100–150°C) for 2,6-TDC at a concentration of 100 ppm. Triple injection gave in this case slightly better results, *ca.* 3% at 100°C and 110 bar, the starting pressure in the pressure-programmed experiments. The precision varied insignificantly in the investigated pressure and temperature ranges.

The precision obtained in this work, with manual direct injection of 60 nl at a solute concentration of 100 ppm, can be compared with that obtained by Richter *et al.*[19], using time-split injection introducing approximately the same sample volume (70 nl) at a concentration of 200 ppm. The solutes used in their investigation were long-chain *n*-alkanes which should behave ideally in the chromatographic system. Depending on the choice of valve, the precision varied between 2 and 4%, in agreement with our results.

CONCLUSION

We have shown that a combination of supercritical nitrous oxide as the mobile phase and a nitrogen selective detector can be used for quantitation of small, polar nitrogen compounds even at relatively low concentrations with acceptable precision. Derivatization is expected to improve the chromatographic behaviour, especially for compounds with primary or secondary amine functions.

ACKNOWLEDGEMENTS

Skilful experimental work by Anita Olsson and Per Brunmark is gratefully acknowledged. This work was supported by a grant from the Swedish Work Environment Fund.

REFERENCES

1 C. M. White and R. K. Houck, *J. H. Resolut. Chromatogr. Chromatogr. Commun.*, 9 (1986) 4.
2 M. L. Lee and K. E. Markides, *J. H. Resolut. Chromatogr. Chromatogr. Commun.*, 9 (1986) 652.
3 T. L. Chester, *J. Chromatogr. Sci.*, 24 (1986) 226.
4 M. Novotny, *J. H. Resolut. Chromatogr. Chromatogr. Commun.*, 9 (1986) 137.
5 P. J. Schoenmakers and F. C. C. J. G. Verhoeven, *Trends Anal. Chem.*, 6 (1987) 10.
6 T. Greibrokk, B. Berg, A. L. Blilie, J. Doehl, A. Farbrot and E. Lundanes, *J. Chromatogr.*, 394 (1987) 429.
7 K. E. Markides and M. L. Lee (Editors), *SFC Applications, 1988 Workshop on Supercritical Fluid Chromatography, Park City, UT*, Brigham Young University Press, Provo, UT, 1988.
8 F. J. van Lenter and L. D. Rothman, *Anal. Chem.*, 48 (1976) 1430.

9 M. Dalene, L. Mathiasson, G. Skarping, C. Sangö and J. F. Sandström, *J. Chromatogr.*, 435 (1988) 469.
10 M. S. Caceci and W. P. Cacheris, *Byte*, May (1984) 340.
11 F. C. Fehsenfeld, P. D. Goldan, M. P. Phillips and R. E. Sievers, in A. Zlatkis and C. F. Poole (Editors), *Electron Capture —Theory and Practice in Chromatography*, Elsevier, Amsterdam, 1981, pp. 69–90.
12 J. Å. Jönsson and L. Mathiasson, in J. Å. Jönsson (Editor), *Chromatographic Theory and Basic Principles*, Marcel Dekker, New York, 1987, pp. 189–243.
13 J. R. Conder, N. K. Ibrahim, G. J. Rees and G. A. Oweimreen, *J. Phys. Chem.*, 89 (1985) 2571.
14 M. Dalene, L. Mathiasson and J. Å. Jönsson, *J. Chromatogr.*, 207 (1981) 37.
15 C. R. Yonker, B. W. Wright, R. C. Petersen and R. D. Smith, *J. Phys. Chem.*, 89 (1985) 5526.
16 C. R. Yonker and R. D. Smith, *J. Chromatogr.*, 351 (1986) 211.
17 C. R. Yonker, R. W. Gale and R. D. Smith, *J. Chromatogr.*, 389 (1987) 433.
18 C. R. Yonker, D. G. McMinn, B. W. Wright and R. D. Smith, *J. Chromatogr.*, 396 (1987) 19.
19 B. E. Richter, D. E. Knowles, M. R. Andersen, N. L. Porter, E. R. Campbell and D. W. Later, *J. H. Resolut. Chromatogr. Chromatogr. Commun.*, 11 (1988) 29.

Journal of Chromatography, 467 (1989) 75–84
Elsevier Science Publishers B.V., Amsterdam — Printed in The Netherlands

CHROM. 21 228

SELECTIVE DETECTION OF VOLATILE IRON COMPOUNDS BY FLAME PHOTOMETRY[a]

XUN-YUN SUN and WALTER A. AUE*
Department of Chemistry, Dalhousie University, Halifax, NS B3H 4J3 (Canada)
(Received December 21st, 1988)

SUMMARY

Volatile iron compounds respond in the flame photometric detector with good sensitivity and selectivity. For instance, the minimum detectable amount of ferrocene (signal-to-noise ratio = 2) is $1.0 \cdot 10^{-10}$ g or $5.4 \cdot 10^{-14}$ mol/s. Its linear range spans four orders of magnitude, and it responds $1.1 \cdot 10^{3}$ times stronger on a weight basis, or $1.5 \cdot 10^{4}$ times stronger on a mol (Fe/C) basis, than dodecane. Ferrocene response, at optimized conditions of high hydrogen and low air flow-rates, is suggested to arise from the chemiluminescent emission of a few of the prominent atomic iron lines in the ultraviolet (the less sensitive response from the stoichiometric hydrogen–air flame is spectrally more complex). Hydrocarbon-type quenching is minimal, *e.g.* it takes about 4800 ppm methane in the detector atmosphere to reduce the ferrocene peak by 50%. Conditions optimal for iron strongly suppress sulphur response. Various volatile iron compounds, including the pentacarbonyl, behave similar to ferrocene.

INTRODUCTION

Ferrocene [bis(cyclopentadienyl)iron] and many of its derivatives are stable, volatile compounds. Their number is large: several volumes of *Gmelins Handbuch* are devoted exclusively to their description. They serve in a variety of roles, *e.g.* as additives to flames (antiknock compounds), as stabilizers of lubricants and polymers, as photosensitizers, etc. Some have also insecticidal properties[1]. Although many ferrocenes may merely represent the elegant answer to a non-existing problem, there does exist a need for the sensitive, selective, and individual determination of a few of them. The fact that iron is an element ubiquitous in internal and external human endeavors —besides being fairly toxic[2]— further supports the general interest in its analytical methodology.

Earlier uses of ferrocenes suggest that the method of their determination should be able to cope with matrices of a predominantly hydrocarbonaceous nature and, at the same time, allow for their speciation. As long as the ferrocenes (or other types of ferrous compounds such as carbonyls or chelates) are of the required volatility and

[a] This work is part of the doctoral thesis requirements of X.-Y. S.

0021-9673/89/$03.50

thermal stability, gas chromatography (GC) in conjunction with a selective detector appears to be the method of choice. Volatile iron compounds have been determined by GC almost from the beginning of this technique, by using non-selective detectors such as the thermal conductivity detector. This was mainly done to gauge the success of various organometallic syntheses. Ferrocene and iron pentacarbonyl, in particular, chromatograph easily and without evidence of premature decomposition. The relevant literature is well covered in several monographs[3–5].

A variety of techniques could undoubtedly be used for the sensitive and selective detection of ferrocenes after GC separation — methods such as GC–single-ion monitoring mass spectrometry (SIM-MS), GC–atomic absorption spectrometry (AAS), GC–ETV-AAS, GC–microwave-induced plasma emission spectrometry (MIP-ES), GC–direct-current plasma-ES, GC–inductively coupled plasma (ICP) atomic emission spectrometry, GC–ICP-MS, GC–atmospheric pressure ionization (API)-MS, etc. However, a conventional (*i.e.* a simple, rugged, and inexpensive) GC detector would seem preferable for most types of analysis.

One GC detector that does an excellent job on iron- (and some further metal) containing species is the hydrogen-rich flame ionization detector (HAFID)[6]. For ferrocene its minimum detectable amount is 2.1 pg, its linear range about three-and-a-half orders of magnitude, and its selectivity against hydrocarbons (tetradecane) approximately $1.9 \cdot 10^5$. Although the HAFID is, construction-wise, a relatively simple variant of the common flame ionization detector, the device is to our knowledge not available in commercial form.

Among the commercially available units, the flame photometric detector (FPD) was shown, quite some time ago, to respond to ferrocene. The minimum detectable limit was then about 2 ng and the linear range more than two orders of magnitude. However, this result was obtained in a survey of compounds containing a larger variety of hetero-elements. The detector conditions were uniform for all analytes, and the spectral features that gave rise to the various luminescences were not investigated. Besides, ferrocene was the only iron compound tested[7].

It seemed reasonable, therefore, to re-investigate and optimize the FPD's response to iron-containing organometallics —the more so because the ferrocene analogue bis(cyclopentadienyl)ruthenium could recently be determined in an amount as low as $2 \cdot 10^{-12}$ g, or just about 1 fmol/s, by a (slightly modified) FPD[8].

Also, the FPD has been used primarily for *main*-group elements in the past. Besides the two for which it was developed and for which it is best known, phosphorus and sulphur, it also responds in an analytically useful way to tin, germanium, arsenic, selenium, boron and tellurium[9,10]. Aside from the present entry ruthenium, the only *transition* element from which the FPD was known for some time to produce significant levels of luminescene, was chromium[11]. The FPD in its various forms and response modes has been reviewed in detail in a recently published book[9], and several monographs on the subject are available.

Given the dearth of information on the behaviour of volatile iron compounds in the FPD, this study was designed to optimize ferrocene response, map the spectrum of its luminescence, chromatograph additional iron compounds, establish calibration characteristics, and check for interference by hydrocarbons.

EXPERIMENTAL

All experimental work was carried out on a Shimadzu 4BMPF gas chromatograph carrying a dual-channel FPD. The 1 m × 3 mm I.D. borosilicate glass column was packed with 5% OV-101 on 45–60-mesh Chromosorb W, and used under a nitrogen flow-rate of 32 ml/min. The column temperature was usually chosen such that the respective analyte would elute at a retention time of about 2 min (*e.g.*, 130°C for ferrocene). The injection port and detector base temperatures were 200 and 170°C, respectively. A simple resistance (R)–capacitance (C) filter (R = 10 kΩ, C = 200 μF) was inserted between electrometer and stripchart recorder. Other operating conditions are noted in the text or in the legends. The FPD outlet was situated directly under an efficient exhaust duct.

For spectral purposes, one of the photomultiplier channels of the FPD was replaced by a Jarrel-Ash Model 82-415 quarter-meter monochromator with a 1180-groves/mm grating blazed for 500 nm, and 2.0- (or, when possible, 0.5-) mm slits. The photomultiplier was the same as used for directly observing the luminescence in the FPD, *i.e.* a Hamamatsu R-268 tube (bialkali, 300–650 nm, maximum response at 420 nm). Two means of introduction were used to obtain the spectra: ferrocene was either repeatedly injected in solution and the wavelength drive adjusted stepwise by hand (which obviates the recording of possible background emissions), or ferrocene was coated onto Chromosorb W, filled into an empty column, and heated to a temperature that would produce the desired, constant level of analyte in nitrogen for an automatically scannable spectrum.

For analytical purposes, and unless stated otherwise, the FPD was operated *without* the conventional quartz chimney, adjustable flame shield and interference filter. A hydrogen flow-rate of 370 ml/min and an air flow-rate of 60 ml/min plus 23 ml/min additional nitrogen were piped into the detector to form the flame. (These are the "optimized" conditions referred to later in the text.)

The input of methane —used here as a simple hydrocarbon quencher— was slowly varied by injecting pure methane into an exponential dilution flask. This flask was inserted into the hydrogen supply line (which then joins the column effluent line before entering the detector volume). The concentration of quencher or additive is calculated on a *total* (not just on a hydrogen or column) flow basis.

Thermocouple-temperature measurements were made with fine and coarse wire thermocouple units via a simple amplifier (Omega OMNI-AMP II-A). The fine-wire (0.2 mm diameter) iron–constantan thermocouple was used with and without a coat of phosphoric acid.

RESULTS AND DISCUSSION

Fig. 1 shows a graph with typical data from one of the optimization runs. Here, the amount of air, hence the temperature, is varied over a larger range. The response —*i.e.* the luminescence emitted upon introduction of ferrocene— increases steadily with the air flow. Note that "response" includes any spectral feature within the purview of the photomultiplier tube. We shall discuss this behaviour later in the context of possible excitation processes.

Unfortunately but not unexpectedly, the baseline noise also increases with in-

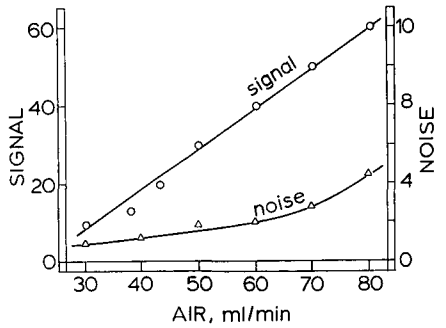

Fig. 1. Increase of signal and noise with increasing air supply. Analyte: ferrocene. Hydrogen flow-rate: 250 ml/min. No quartz chimney, no flame shield, and no optical discrimination. Other conditions as given in the experimental section.

creasing air flow-rate, *i.e.* with temperature and baseline current, and it does so in an apparently exponential fashion. This means that the signal-to-noise (S/N) ratios will reach maxima, and a few of these maxima are shown in Fig. 2. The highest S/N ratio is obtained at about 370 ml/min hydrogen and 60 ml/min air (plus 23 ml/min nitrogen added to the air supply, and 32 ml/min nitrogen coming from the column).

The optimum hydrogen flow-rate here is quite high for an FPD (*cf.* ref. 9), but the optimum air flow-rate supplies only about 7% of the oxygen that would be required for a stoichiometric flame. At these conditions, the maximum temperature measurable by the thermocouple is 570°C at the base of the flame (compare the theoretical maximum temperature of a hydrogen–air flame of 2115°C[12]. It makes little difference whether thinner or thicker wires are used, or whether the thermocouple is coated with phosphoric acid. Clearly, this result has nothing to do with *excitation* temperatures. Furthermore, such measurements are notoriously vague in *diffusion* flames. Yet, they do provide a valuable and dramatic indication of how low a level of thermal (as opposed to chemical) energy is actually available.

Other optimization strategies were pursued as well. As noted in the Experimental section, the quartz chimney and the adjustable steel flame shield were removed, with small but noticeably beneficial effects. No changes were apparent on varying the injection port and detector base temperatures between 160 and 200°C.

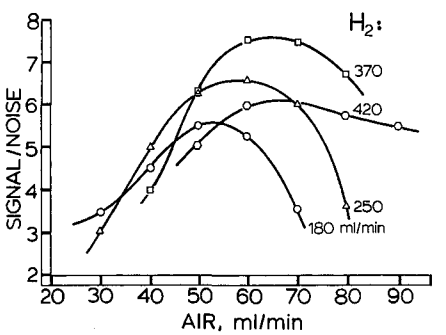

Fig. 2. Variation of the signal-to-noise ratio with varying air flow-rate, measured at four different hydrogen levels, as indicated. Other conditions as in Fig. 1.

(This suggests, *inter alia,* that no significant premature decomposition of ferrocene occurred in the chromatographic system.) Adding nitrogen to the air supply also improved performance, but larger amounts extinguished the flame.

Besides empirically optimizing the S/N ratio, analytical prudence suggests that the response spectrum be determined. This can serve to improve selectivity vis-à-vis other hetero-elements, and/or lead to better S/N ratios by the judicious use of optical filters. Also, it may on occasion yield results of general spectroscopic interest.

Fig. 3 shows a spectral scan of luminescence from a ferrocene-doped flame under conditions close to the analytical optimum. The peak width is determined by the very wide 2.0-mm slits (bandpath 6.7 nm), but that is all the low intensity and the diffuse nature of the luminescence would permit. The wavelengths of the peaks suggest that they represent some of the commonly found atomic lines. For instance, in a copper arc, the three strongest lines for transitions to the $^5D_4$ *ground* state are, in order of their intensity, 3719.94, 3859.91 and 3440.61 Å[13]. These numbers correspond, given our wide error limits, quite well to the peaks shown in Fig. 3 (373, 387 and 345 nm), although the latter might include more lines than the three cited ones. The strongest line in the copper arc is located at 3734.87 Å (from a 33 695 → 6928 cm^{-1} transition) and it may also be present here as well as become more prominent in the following spectra. Unfortunately, the inevitably low resolution does not allow us to distinguish among the several possible atomic emissions in the vicinity of 373 nm.

It seems reasonable to assume that the excitation process is chemical rather than thermal. The thermocouple temperature is fairly low (maximum 570°C for optimum flow-rates as given in the Experimental section), and other prominent lines of iron —*e.g.* the one at 3581.20 Å (34 844 → 6928 cm^{-1}), which is second-most intense in a copper arc— do not (yet) show up. The fact that the three that do result from transitions to the *ground* state, is expected: there must be an upper energy limit to the chemiluminescence. Note that 344 nm corresponds to 3.60 eV or 348 kJ/mol, and 34 844 cm^{-1} to 4.32 eV or 417 kJ/mol. A second argument in favour of a chemi-

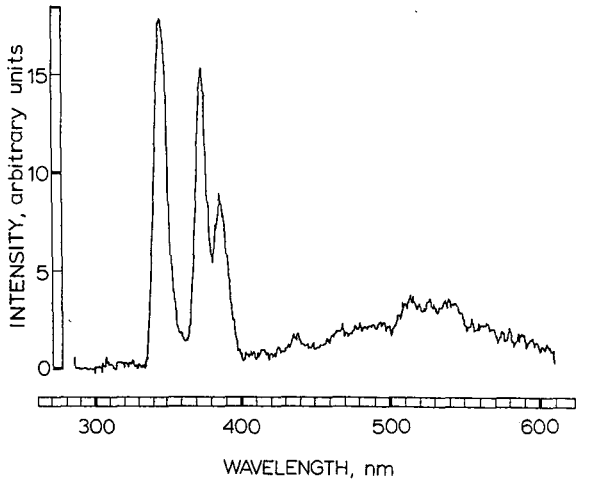

Fig. 3. Spectrum of "ferrocene", close to optimal flame conditions, but with a slightly higher air flow-rate (80 ml/min) to produce sufficient light. Slits: 2.0 mm (6.7 nm bandpath).

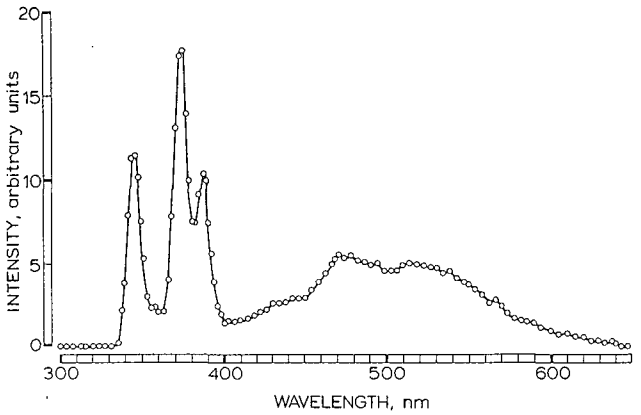

Fig. 4. Spectrum of "ferrocene", air-richer (81 ml/min) and hydrogen-poorer (260 ml/min) than at optimal conditions. Slits: 2.0 mm.

luminescent excitation process is an indirect but, in our opinion, rather strong one. If the excitation process were thermal, many other elements should respond with commensurate strength. The fact that most of the ones we tested did not, consequently suggests *non*-thermal excitation.

With slightly lower hydrogen and higher air supply rates, the spectrum changes (Fig. 4). The peak at *ca.* 373 nm has increased; this may, but need not, be due to the emergence of the above-mentioned 3734.87 Å line (whose excited state is at *ca.* 4.18 eV or 403 kJ/mol above the ground state). Also, a broad feature is starting to emerge between about 400 and 600 nm.

In the next spectrum, shown in Fig. 5, the hydrogen flow-rate has been dramatically decreased to the point that the flame is now approximately stoichiometric. The

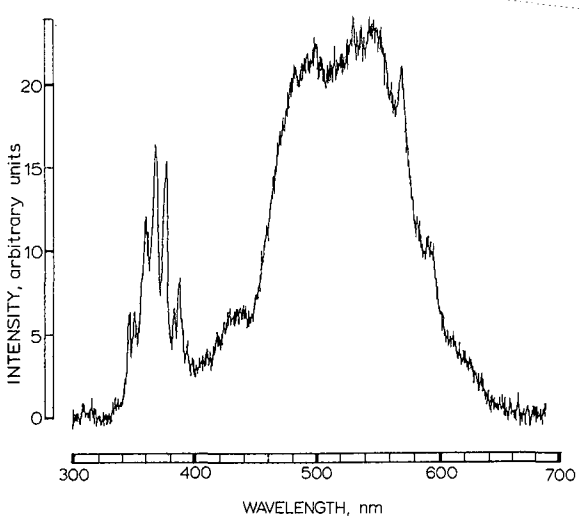

Fig. 5. Spectrum of "ferrocene", close to stoichiometric flame conditions. Hydrogen: 45.5 ml/min, air: 75 ml/min. Slits: 0.5 mm (bandpath 1.7 nm).

0.5-mm slits can be used because of the vastly increased light level. Some of the atomic lines may still be present, but they are now dwarfed by other features. In the ultraviolet, some new peaks have come up at *ca.* 359 and particularly at 367 nm; those may be related to the two groups of bands described by Gaydon as "probably FeOH. The first group lies in the region 3530–3580 Å and the second 3630–3675 Å, with a diffuse head, degraded to shorter wavelengths, at 3675 Å"[14]. Bands found in the hydrogen–air flame at *ca.* 344, 358, 383, 388 and 393 nm, and attributed[15] to FeO, may also be present; however, these may as well be due to prominent atomic lines originating from higher excited states of the iron atom[13]. The large hump between 460 and 580 nm must remain unassigned (perhaps it is even due to particle formation). The occurrence of FeH[16] and FeO[14] bands in that region cannot be ruled out; however, their contribution, if any, is not immediately apparent.

Note that Figs. 3 and 5 differ from Fig. 4 in that the former were run with a constant input of ferrocene and automatic wavelength scanning. Fig. 4, on the other hand, was determined by repeatedly injecting ferrocene while manually advancing the wavelength drive. Fig. 4 thus recorded the pure response, while emissions other than those resulting from ferrocene could have shown up in Figs. 3 and 5. However, scans of the blank flame in these cases confirmed that luminescence from the flame itself was negligible.

For analytical selectivity, the line at 344 nm or the lines at 372–374 (if they are indeed lines) would likely be the best bets for analysis with an interference filter. Another possibility may be to use a 400-nm cut-off filter, depending on what other FPD-active elements one wishes to guard against. However, the following calibration curves, with one exception as stated, have been established with no spectral discrimination whatsoever (beyond the response profile of the photomultiplier tube).

Fig. 6 shows several of such calibration curves for iron-containing analytes; plus, for purpose of comparison, one for a sulphur and two for a couple of hydrocarbon compounds.

The calibration curve for ferrocene under optimized conditions (curve 1) ends at a minimum detectable amount (S/N = 2) of 100 pg, or 10 pg/s, or 54 fmol/s. This is one order of magnitude better than found in the earlier survey[7]. The linear range spans four orders of magnitude. The selectivity against dodecane (which appears here as an alkane standard) is about $1.1 \cdot 10^3$, or $1.5 \cdot 10^4$ on an elemental (mol Fe/mol C) basis. In terms of a sensitivity ranking for the FPD, this performance places iron in the vicinity of sulphur and chromium (with only phosphorus, ruthenium, germanium and tin above it; and with arsenic, selenium, boron and tellurium clearly below it)[10].

Of course, this does not mean that sulphur would show up equally well at conditions optimized for *iron*. In particular, the absence of the quartz chimney decreases sulphur (but increases iron) response. Curve 7 shows the calibration for di-*tert.*-butyldisulphide, obtained under the same conditions as curve 1 for ferrocene. Not surprisingly, the selectivity of iron *versus* sulphur is now also much better than in the earlier study[7].

Curve 2 shows the calibration curve for ferrocene, but without the additional 23 ml/min nitrogen diluting the air supply (see the experimental section). The corresponding decrease in response is similar to that of ruthenocene[8].

Curve 3, which coincides with curve 2 over most of the graph, is that of iron pentacarbonyl. This compound is an interesting analyte in its own right, but it also

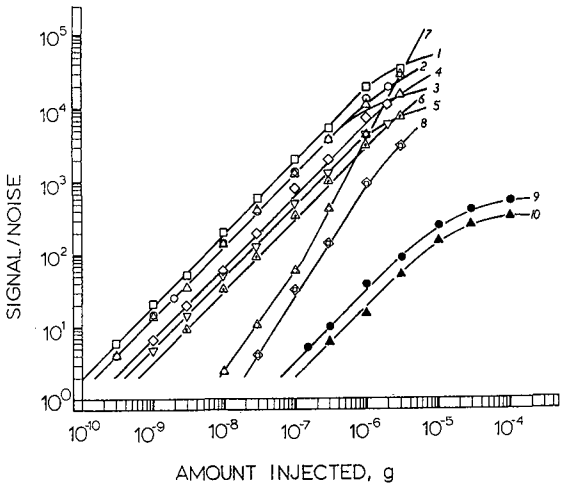

Fig. 6. Calibration curves: (1) Ferrocene at optimal conditions. Flow-rates in ml/min: hydrogen, 370; air, 60; carrier nitrogen, 32; additional nitrogen, 23. Temperatures in °C: column, 130; injection port, 200; detector base, 170. No quartz chimney. (2) Ferrocene. Conditions as in curve 1, but no additional nitrogen. (3) Iron pentacarbonyl. Conditions as in curve 1, but carrier nitrogen 11 and additional nitrogen 25 ml/min; column 35, injector 80 and detector 80°C. (4) Acetylferrocene. Conditions as in curve 1, but column temperature 180°C. (5) Ferrocene. Conditions as in curve 1, but original Shimadzu quartz chimney present. (6) Cyclooctatetraeneiron tricarbonyl. Conditions as in curve 1, but column temperature 150°C. (7) Di-*tert.*-butyldisulphide. Conditions as in curve 1, but column temperature 150°C. (8) Ferrocene. Conditions as in curve 1, but hydrogen 37 and air 83 ml/min (close to stoichiometric); 460 nm cut-on and 580 nm cut-off filter. (9) Naphthalene. Conditions as in curve 1, but column temperature 125°C. (10) Dodecane. Conditions as in curve 1, but column temperature 118°C.

demonstrates that the metallocene structure is not a necessary criterion for response. Two further iron compounds, acetylferrocene and cyclooctatetraeneiron tricarbonyl, are shown in curves 4 and 6, respectively.

Curve 5 shows the determination of ferrocene, with the original quartz tube of the Shimadzu FPD re-inserted. This is the same effect as discussed in the ruthenocene paper[8] and we still have no cogent explanation to offer for it. Analytically, of course, the removal of the conventional quartz cylinder turns out to be highly beneficial.

Curve 8 shows the calibration of ferrocene under stoichiometric flame conditions, with cut-on and cut-off filters around the big amorphous feature shown in the spectrum of Fig. 5. Note that response *per se* is higher, but that this response is analytically barren because of the concomitant high noise level.

Curves 9 and 10 are those of an aromatic and an aliphatic hydrocarbon, which have been included here to characterize the behaviour of a possible hydrocarbon sample matrix. As is well known, aromatics produce somewhat higher light levels.

In flame photometric analysis, particularly when the flame is weak and cool, quenching can seriously reduce response. The classical example of this type of interference is the diminution of S_2 luminescence by co-eluting hydrocarbons. To test for the relative importance of quenching, Fig. 7 shows the decrease in response of ferrocene and dodecane, as caused by increasing amounts of methane in the detector atmosphere. It may be worth noting that methane affects its homologue dodecane stronger than it does ferrocene.

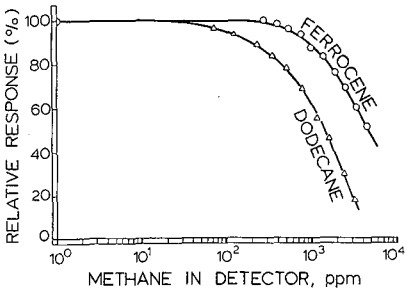

Fig. 7. Quenching of ferrocene and dodecane response by methane. Methane concentration given per total detector gas flow.

How serious is such quenching for the analyte ferrocene? It takes about $4.8 \cdot 10^3$ ppm methane in the total detector gases —corresponding to a carbon mass flow-rate of about 1 mg/min— to reduce the ferrocene peak by 50%. If methane had been doped only into the column flow, the corresponding concentration there would have been about 7%. That is far larger than any likely *continuous* input due to contamination. If, on the other hand, the same level of interfering carbon compound had eluted *as a peak* of the same retention time as ferrocene, quenching would have been observed only in the upper regions of the calibration curve. In its lower regions, the interferent would have *added* to the peak height, *i.e.* its own response would have been larger than the quenching it inflicted on the ferrocene response. The large amounts of carbon necessary to produce a 50% reduction in ferrocene peak height suggest that quenching should not present a serious problem under conventional circumstances.

Fig. 8 presents a temperature-programmed separation of six volatile iron compounds injected in 0.5–2-ng amounts. The chromatogram also shows 200 ng of a

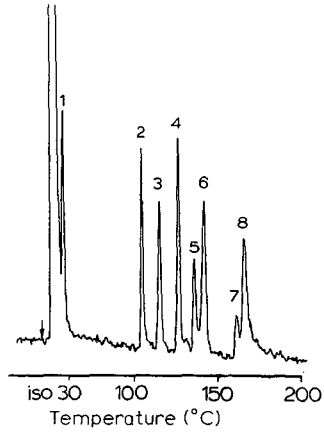

Fig. 8. Temperature-programmed chromatography at detector conditions optimal for ferrocene. Isothermal at 30°C until $Fe(CO)_5$ elutes, then 18°C/min till 100°C, then 10°C/min from 100 to 200°C. Peaks: 1 = 1 ng ironpentacarbonyl; 2 = 200 ng di-*tert.*-butyldisulphide; 3 = 800 ng dodecane; 4 = 1 ng ferrocene; 5 = 0.5 ng 1,1'-dimethylferrocene; 6 = 1 ng acetylferrocene; 7 = 0.5 ng ferrocene carboxaldehyde; 8 = 2 ng cyclooctatetraeneiron tricarbonyl.

disulphide and 800 ng of a hydrocarbon, which produce peaks of comparable size. This demonstrates graphically the point made earlier in regard to the corresponding calibration curves, *i.e.* that the normally large response of sulphur is diminished to a significant degree by choosing conditions optimal for iron compounds. Besides selectivity, the chromatogram also illustrates the sensitivity with which iron compounds respond. Given that the separation has taken place on a short, low-resolution packed column, still higher sensitivities could be expected from peaks of higher chromatographic efficiency.

ACKNOWLEDGEMENT

This study was supported by NSERC operating grant A-9604.

REFERENCES

1 *Gmelins Handbuch der Anorganischen Chemie, Vol. 14A, Ferrocen 1,* Springer, Berlin, 1974, p. 193.
2 N. Irving Sax, *Dangerous Properties of Industrial Materials,* Van Nostrand-Reinhold, New York, 5th ed, 1979.
3 G. Guiochon and C. Pommier, *Gas Chromatography in Inorganics and Organometallics,* Ann Arbor Sci. Publ., Ann Arbor, MI, 1973, p. 192.
4 P. C. Uden, in J. C. MacDonald (Editor), *Inorganic Chromatographic Analysis (Chemical Analysis,* Vol. 78), Wiley, New York, 1985, p. 263.
5 T. R. Crompton, *Comprehensive Organometallic Analysis,* Plenum, New York, 1987.
6 H. H. Hill, Jr. and W. A. Aue, *J. Chromatogr.,* 122 (1976) 515.
7 W. A. Aue and C. R. Hastings, *J. Chromatogr.,* 87 (1973) 232.
8 X.-Y. Sun and W. A. Aue, *Can. J. Chem.*, in press.
9 M. Dressler, *Selective Gas Chromatographic Detectors (Journal of Chromatography Library,* Vol. 36), Elsevier, Amsterdam, 1986, pp. 133–160.
10 C. G. Flinn and W. A. Aue, *Can. J. Spectrosc.,* 25 (1980) 141.
11 R. Ross and T. Shafik, *J. Chromatogr. Sci.,* 11 (1973) 46.
12 As cited in R. N. Kniseley, in J. A. Dean and T. C. Rains, (Editors) *Flame Emission and Atomic Absorption Spectrometry,* Vol. 1, Marcel Dekker, New York, 1969, p. 191.
13 W. F. Meggers, C. H. Corliss and B. F. Scribner, *Tables of Spectral-Line Intensities,* Part 1, NBS Monograph 145, National Bureau of Standards, U.S. Government Printing Office, Washington, DC, 2nd ed., 1975, p. 121.
14 R. W. B. Pearse and A. G. Gaydon, *The Identification of Molecular Spectra,* Chapman & Hall, London, 4th ed., 1976, p. 157
15 M. L. Parsons and P. M. McElfresh, *Flame Spectroscopy: Atlas of Spectral Lines,* IFI/Plenum, New York, 1971, p. 53.
16 P. K. Carroll and P. McCormack, *Astrophys. J.,* 177 (1972) L33.

Journal of Chromatography, 467 (1989) 85–98
Elsevier Science Publishers B.V., Amsterdam — Printed in The Netherlands

CHROM. 21 234

APPLICATION OF CAPILLARY GAS CHROMATOGRAPHY WITH MASS SELECTIVE DETECTION TO PESTICIDE RESIDUE ANALYSIS

HANS-JÜRGEN STAN
Institut für Lebensmittelchemie, Technische Universität Berlin, Gustav-Meyer-Allee 25, 1000 Berlin 65 (F.R.G.)

(First received June 10th, 1988; revised manuscript received December 29th, 1988)

SUMMARY

A random sample of 76 pesticides with good gas chromatographic properties has been collected in order to test the applicability of the mass selective detector HP MSD for pesticide residue analysis. Using a capillary column, mass spectra of good quality were produced with 10 or 20 ng of each pesticide. Seventy two compounds were not only identified at this concentration with the PBM (probability based matching) search routine in the NBS library, but also remarkably with the best fit in the corresponding hit list. Lower concentrations can be detected only with selected ion monitoring (SIM). A mixture of 18 chlorinated pesticides was added to green pepper at the 10 ppb level. All compounds were detected with SIM using special time programming in one gas chromatographic analysis. The detection sensitivity of the mass selective detector in SIM mode approaches that of established selective detectors. The reliability of the results with respect to the identity of a pesticide residue, however, is orders of magnitude better. Therefore, this detector is a valuable tool for performing confirmatory analysis.

INTRODUCTION

Multiresidue analysis of pesticides in food and environmental samples must provide reliable identification and quantitation of a large number of compounds at very low concentrations. The analysis starts with an extraction step. Coextractants from the sample matrix are eliminated or reduced using a variety of clean-up procedures[1–5].

Gas chromatography (GC) with the selective electron-capture (ECD) and nitrogen–phosphorus (NPD) detection allows the detection of contaminants at trace levels in the lower ppb[a] range in the presence of a multitude of compounds extracted from the matrix to which these detectors do not respond. The number of compounds used in agriculture for plant protection has now surpassed 400. Additionally, the input of pollutants into the environment has increased and so it is impossible to separate all

[a] Throughout this article the American billion (10^9) is meant.

0021-9673/89/$03.50

these compounds in a single analysis, even with the application of high-performance capillary columns.

Reliability of multiresidue analysis can be achieved by different approaches. One technique that I have used for a decade is effluent splitting after the capillary column to two selective detectors. Each peak is characterized by its retention time and the response factors in the different detectors. Confirmation is accomplished by applying the same technique to a second capillary column coated with a separation phase of different polarity[6]. A second approach developed in our laboratory is two-dimensional capillary GC with pneumatic switching between two columns of differing polarities. Again, it is possible to increase the information content of the chromatographic data enormously by applying effluent splitting after the first or after both columns to several detectors[7]. A third approach is the application of a more extensive clean-up. One procedure widely used in Germany divides the sample into up to six fractions, applying chromatography on a small silica gel column[8]. Many of the pesticides are separated from overlapping matrix compounds by means of this method. At the same time, the classification of pesticides according to their partition coefficients in a system of water and organic solvents of increasing polarity is a valuable independent method.

With these methods, data processing on-line by means of a minicomputer may be used as a support in identifying suspected pesticide residues by checking the data against a data base of calibrated compounds[9].

The fourth and most sophisticated approach combines high-resolution GC with mass spectrometry (GC–MS). The mass spectrometer is without doubt the most specific detector available in multiresidue analysis. The specificity is based on the fact that molecules when bombarded with electrons of particular energy under vacuum conditions fragment following strict rules. The resulting fragmentation pattern reflects the individual molecular structure in a mass spectrum that is often considered as the fingerprint of the substance. These mass spectra show such specific characteristics that it is possible to differentiate many tens of thousands of compounds. It is of great importance that these mass spectra do not depend on the instrument used for measuring them but only on the ionization conditions applied. Standardized ionization conditions can easily be reproduced. Therefore, it is possible to compile all the mass spectra recorded all over the world in libraries. Such documented spectra are used to identify unknown compounds by comparing their spectra with those well established. The formerly laborious task of comparing mass spectra is now performed with the help of computers and sophisticated software programs. Within a few seconds such a computer program can perform a search of more than 40 000 documented mass spectra and draw up a list of a few mass spectra ranked according to their strongest resemblance to the one just recorded. In this way it is possible to identify an unknown peak in a gas chromatogram without having the corresponding test substance available.

Until recent years, the mass spectrometer appeared to be an instrument of great complexity that required a lot of maintenance and technical skill when used as an analytical tool. Nevertheless, from the beginning of reliable environmental studies it was recognized as the ultimate GC detector for confirming results obtained by means of the very sensitive selective detectors. Today, with mass selective detection (MSD), a small mass spectrometer is commercially available designed as a sensitive and most specific detector for high-resolution GC. MSD offers the full capacity of any

quadrupole mass spectrometer when coupled with a gas chromatograph. However, this detector is as easy to maintain and to handle as any other GC detector.

MSD can be used in two different modes that are very useful in pesticide multiresidue analysis: cyclic scanning or selected ion monitoring (SIM). In cyclic scanning the mass spectrometer acquires a series of mass spectra continuously over the whole time the GC separation process is underway. The summation of all the ions from the ionization process results in the total ion current (TIC) trace which looks like a signal recording from any GC detector. However, each point in the gas chromatogram represents a full mass spectrum stored in a data file on the disc which can be inspected at any time on the screen. These mass spectra can be manipulated by the computer software to obtain background subtraction or averaged spectra. Mass spectra corrected in this way can now be used for library search in order to identify the substance.

In SIM the sensitivity is very much increased at the expense of information. Instead of scanning the entire spectrum over the whole mass range, only a few ions are recorded which are indicative for the compound to be searched for. The gain in sensitivity is the result of longer specific sampling times for each of the ions selected. The highest detection sensitivity achievable with a mass spectrometric detector is single ion monitoring where the instrument is adjusted to collect only ions of one defined mass.

The application of SIM requires the knowledge of the mass spectrum of the compound to be analyzed and its retention time on the capillary column used. The combined data from SIM and the exact retention time provide the optimum in detection sensitivity and reliability with respect to the identity of the analyzed pesticide residue that can be achieved today.

In this paper a study of the analysis of 76 pesticides representing a variety of chemical structures by means of GC with MSD is reported.

EXPERIMENTAL

Instrumentation

Gas chromatograph HP 5890 with a mass selective detector MSD HP 5970 and MS ChemStation HP 59970 including an HP 59973 NBS mass spectral library (NBS REVE) and a split/splitless injector for capillary columns was employed.

Gas chromatography

A fused-silica column, 25 m × 0.20 mm HP-1 (cross-linked methyl silicone gum) with film thickness 0.33 μm was used with helium as the carrier gas. Temperature settings (°C): injection port, 250; transfer line, 260. Temperature programme (°C): 1 min at 100, 30°/min to 150, held for 2 min, 3°/min to 205, 10°/min to 240, 2°/min to 260, held for 10 min. A 1-μl volume of sample was injected manually applying the hot splitless injection technique with the split closed for 1 min.

Mass spectrometric acquisition parameters

Temperature settings (°C); transfer line, 180; ion source, 175; mass analyzer, 180. Scan parameters: scanned mass range, 50–500 daltons; scan rate, 1.22 scans/s; threshold, 500. Solvent delay: 2.5 min. The voltages of the repeller, draw out, ion focus,

TABLE I

COMPILATION OF PESTICIDES USED

Retention times (t_R in min) recorded under the experimental conditions. A = Acaricide; F = fungicide; H = herbicide; I = insecticide; N = nematicide; I* = insecticide used as the internal standard. HCH = BHC = isomers of 1,2,3,4,5,6-hexachlorocyclohexane. HCB = hexachlorobenzene.

No.	*Common name*	*CAS No.*	*Mol.wt.*	*Formula*	*Use*	t_R
1	Aldrin	309-00-2	364.92	$C_{12}H_8Cl_6$	I*	23.82
2	Amidithion	919-76-6	273.31	$C_7H_{16}NO_4PS_2$	I	23.62
3	Azinphos-ethyl	2642-71-9	345.38	$C_{12}H_{16}N_3O_3PS_2$	I	38.36
4	Bromophos	2104-96-3	366.00	$C_8H_8BrCl_2O_3PS$	I	25.11
5	Bromophos-ethyl	4824-78-6	394.05	$C_{10}H_{12}BrCl_2O_3PS$	I	26.87
6	Bromopropylate	18181-80-1	428.12	$C_{17}H_{16}Br_2O_3$	I	34.19
7	Carbophenothion	786-19-6	342.87	$C_{11}H_{16}ClO_2PS_3$	I	31.14
8	Chlorfenprop-methyl	14437-17-3	233.10	$C_{10}H_{10}Cl_2O_2$	I	12.31
9	Chlorfenvinphos	470-90-6	359.58	$C_{12}H_{14}Cl_3O_4P$	I	26.15
10	Chlormephos	24934-91-6	234.70	$C_5H_{12}ClO_2PS_2$	I	8.58
11	Chloroneb	2675-77-6	207.06	$C_8H_8Cl_2O_2$	F	10.17
12	Chloropropylate	5836-10-2	339.22	$C_{17}H_{16}Cl_2O_3$	A	29.53
13	Chlorothalonil	1897-45-6	265.91	$C_8Cl_4N_2$	F	19.16
14	Chlorthal-dimethyl	1861-32-1	331.97	$C_{10}H_6Cl_4O_4$	H	24.53
15	Chlorthion	500-28-7	297.66	$C_8H_9ClNO_5PS$	I*	24.79
16	Coumaphos	56-72-4	362.77	$C_{14}H_{16}ClO_5PS$	F	41.07
34	DDD-o,p'	53-19-0	320.05	$C_{14}H_{10}Cl_4$	I	28.53
18	DDD-p,p'	72-54-8	320.05	$C_{14}H_{10}Cl_4$	I	29.96
19	DDE-o,p'	3424-82-6	318.03	$C_{14}H_8Cl_4$	I	26.92
20	DDE-p,p'	72-55-9	318.03	$C_{14}H_8Cl_4$	I	28.17
21	DDT-o,p'	789-02-6	354.49	$C_{14}H_9Cl_5$	I	30.11
22	DDT-p,p'	50-29-3	354.49	$C_{14}H_9Cl_5$	I	31.67
23	Dialifos	10311-84-9	393.85	$C_{14}H_{17}ClNO_4PS_2$	I	38.77
24	Diazinon	333-41-5	304.35	$C_{12}H_{21}N_2O_3PS$	I	18.55
25	Dichlobenil	1194-65-6	172.01	$C_7H_3Cl_2N$	H	6.93
26	Dichlofenthion	97-17-6	315.16	$C_{10}H_{13}Cl_2O_3PS$	N	20.79
27	Dichlofluanid	1085-98-9	333.23	$C_9H_{11}Cl_2FN_2O_2S_2$	F	23.54
28	Dichloran	99-30-9	207.02	$C_6H_4Cl_2N_2O_2$	F	16.17
29	Dieldrin	60-57-1	380.91	$C_{12}H_8Cl_6O$	I	28.24
30	Dimethoate	60-51-5	229.26	$C_5H_{12}NO_3PS_2$	I	16.31
31	Disulfoton	298-04-4	274.41	$C_8H_{19}O_2PS_3$	IA	18.75
32	Ditalimfos	5131-24-8	299.29	$C_{12}H_{14}NO_4PS$	F	27.42
33	Endosulfan I (alpha)	115-29-7	406.93	$C_9H_6Cl_6O_3S$	I	27.18
	Endosulfan II (beta)	115-29-7	406.93	$C_9H_6Cl_6O_3S$	I	29.74
34	Ethion	563-12-2	384.48	$C_9H_{22}O_4P_2S_4$	I	30.18
35	Ethoprophos	13194-48-4	242.34	$C_8H_{19}O_2PS_2$	IN	13.48
36	Fenchlorphos	299-84-3	321.55	$C_8H_8Cl_3O_3PS$	I	22.25
37	Fenitrothion	122-14-5	277.24	$C_9H_{12}NO_5PS$	I	23.10
38	Fensulfothion	115-90-2	308.36	$C_{11}H_{17}O_4PS_2$	IN	29.74
39	Fenthion	55-38-9	278.33	$C_{10}H_{15}O_3PS_2$	I	24.17
40	Folpet	133-07-3	296.62	$C_9H_4C_{13}NO_2S_2$	F	26.34
41	Fonofos	944-22-9	246.33	$C_{10}H_{15}OPS_2$	I	17.94
42	Formothion	2540-82-1	257.27	$C_6H_{12}NO_4PS_2$	I	20.04
43	HCB	118-74-1	284.78	C_6Cl_6	F	15.98
44	HCH-alpha	319-84-6	290.83	$C_6H_6Cl_6$	I	15.54
45	HCH-beta	319-85-7	290.83	$C_6H_6Cl_6$	I	17.06
46	HCH-delta	319-86-8	290.83	$C_6H_6Cl_6$	I	18.85
47	Heptachlor	76-44-8	373.32	$C_{10}H_5Cl_7$	I	21.76

TABLE I *(continued)*

No.	*Common name*	*CAS No.*	*Mol.wt.*	*Formula*	*Use*	t_R
48	Heptachlorepoxide-c	1024-57-3	389.32	$C_{10}H_5Cl_7O$	I	25.76
49	Heptachlorepoxide-t	1024-57-3	389.32	$C_{10}H_5Cl_7O$	I	25.94
50	Heptenophos	34783-40-9	250.62	$C_9H_{12}ClO_4P$	I	11.94
51	Lindane	58-89-9	290.83	$C_6H_6Cl_6$	I	17.45
52	Methoxychlor	72-43-5	345.66	$C_{16}H_{15}Cl_3O_2$	I	34.58
53	Mevinphos	7786-34-7	224.15	$C_7H_{13}O_6P$	I	8.28
54	Mirex	2385-85-5	545.55	$C_{10}Cl_{12}$	I*	36.90
55	Parathion	56-38-2	291.26	$C_{10}H_{14}NO_5PS$	IA	24.33
56	Parathion-methyl	298-00-0	263.21	$C_8H_{10}NO_5PS$	IA	21.36
57	Phenkapton	2275-14-1	377.31	$C_{11}H_{15}Cl_2O_2PS_3$	A	34.68
58	Phosalone	2310-17-0	367.81	$C_{12}H_{15}ClNO_4PS_2$	IA	36.23
59	Phosmet	732-11-6	317.32	$C_{11}H_{12}NO_4PS_2$	I	34.09
60	Phosphamidon	13171-21-6	299.69	$C_{10}H_{19}ClNO_5P$	IA	20.87
61	Pirimiphos-ethyl	23505-41-1	333.39	$C_{13}H_{24}N_3O_3PS$	I	25.37
62	Pirimiphos-methyl	29232-93-7	305.34	$C_{11}H_{20}N_3O_3PS$	I	23.26
63	Propachlor	1918-16-7	211.69	$C_{11}H_{14}ClNO$	H	12.92
64	Propyzamide	23950-58-5	256.13	$C_{12}H_{11}Cl_2NO$	H	17.94
65	Prothiofos	34643-46-4	345.25	$C_{11}H_{15}Cl_2O_2PS_2$	I	27.91
66	Pyrazophos	13457-18-6	373.37	$C_{14}H_{20}N_3O_5PS$	FAI	38.26
67	Quintozene	82-68-8	295.34	$C_6Cl_5NO_2$	F	17.75
68	Sulfotep	3689-24-5	322.32	$C_8H_{20}O_5P_2S_2$	I	15.01
69	Tecnazene	117-18-0	260.89	$C_6HCl_4NO_2$	F	12.79
70	Tetrachlorvinphos	22248-79-9	365.97	$C_{10}H_9Cl_4O_4P$	I	27.17
71	Tetradifon	116-29-0	356.06	$C_{12}H_6Cl_4O_2S$	A	35.68
72	Tolylfluanid	731-27-1	347.26	$C_{10}H_{13}Cl_2FN_2O_2S_2$	F	25.98
73	Triadimefon	43121-43-3	293.76	$C_{14}H_{16}ClN_3O_2$	F	24.46
74	Triazophos	24017-47-8	313.32	$C_{12}H_{16}N_3O_3PS$	IA	30.75
75	Trifluralin	1582-09-8	335.29	$C_{13}H_{16}F_3N_3O_4$	H	14.69
76	Vinclozolin	50471-44-8	286.12	$C_{12}H_9Cl_2NO_3$	F	21.37

entrance lens and X-ray and the parameters for the quadrupole mass filter were set according to the values proposed by the program AUTOTUNE, which automatically optimizes these parameters using perfluorotributylamine (PFTBA) as a calibration standard.

Materials

Pesticides were obtained as test substances from Dr. Ehrenstorfer, Augsburg, F.R.G. and Promochem, Wesel, F.R.G., with 97–99% purity. All substances were dissolved in toluene (Promochem, Nanograde).

Clean up

Food samples were analyzed using method S 19 in ref. 1. Plant material with high water content was extracted with acetone. To plant material with low water content water was added to adjust the acetone: water ratio during extraction to 2:1 (v/v). The extract was saturated with sodium chloride and diluted in dichloromethane in order to separate excess of water. The evaporation residue of the organic phase or a fat solution was cleaned up by gel permeation chromatography on Bio-Beads SX-3 polystyrene

gel, using a mixture of cyclohexane and ethyl acetate as the eluent and an automated gel permeation chromatograph. The residue-containing fraction was concentrated and fractionated on a small silica gel column into six fractions. The eluents were mixtures of toluene with hexane or increasing amounts of acetone. The fractions were evaporated, brought to volume with toluene and analyzed by capillary GC with MSD. In our laboratory, fractions 1 and 2 are collected together as one fraction containing all chlorinated pesticides.

RESULTS

In Table I the 76 pesticides included in this study are compiled. Only compounds that are known to be analyzed easily by GC are listed. Most of them show good responses to the very sensitive ECD, NPD and flame photometric detection (FPD). These pesticides represent a variety in chemical structure as well as the different applications in agricultural production.

In Fig. 1 the TIC of a mixture of chlorinated hydrocarbon insecticides is shown. The mixture contains pesticides that have been extensively used all over the world from the early days of introduction of these chemicals for plant protection around 1950. They are now banned in most western industrialized countries but, however, are still in use in many other countries. Because of their great chemical stability they persist for decades in the environment. These substances can be analyzed at trace level by means of GC using ECD but this detection method is prone to many interferences and consequently the results are not always reliable. Fig. 1 represents the separation of 10 ng of each pesticide. By means of background subtraction, mass spectra of good quality were obtained that were added to a special sub-library for pesticides. All these spectra are in good agreement with those already stored in the NBS library (NBS REVE with HP 59973B Library software) or measured in our laboratory as well as others using GC–MS instruments of both the magnetic field and the quadrupole filter type[10–16].

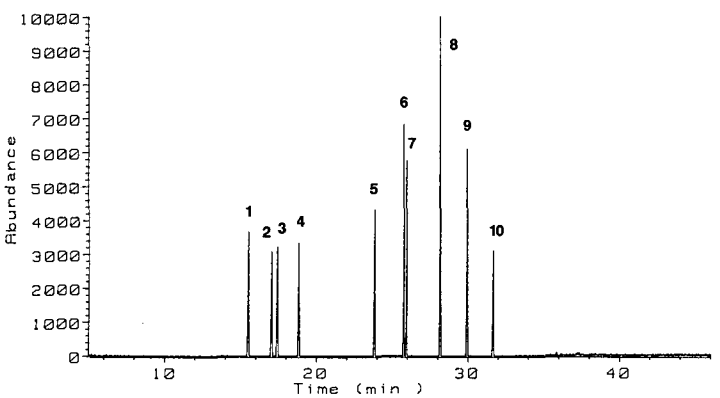

Fig. 1. TIC of chlorinated pesticides. A 10-ng amount of each of the following compounds was injected: 1 = α-HCH; 2 = β-HCH; 3 = lindane; 4 = δ-HCH; 5 = aldrin; 6 = *cis*-heptachlorepoxide; 7 = *trans*-heptachlorepoxide; 8 = p,p'-DDE; 9 = p,p'-DDD; 10 = p,p'-DDT.

In Fig. 2 the TIC of a mixture of organophosphorus pesticides is shown demonstrating the very good GC separation of all 29 compounds. Each of these peaks represents 20 ng of substance. The TIC trace gives an idea of the different yields in ionization intensities depending on the chemical structure. However, at this level of concentration, from each organophosphorus pesticide representative mass spectra were produced. In the same way, mixtures containing all the other pesticides were analyzed with the described GC–MSD method at concentration levels of 10 or 20 ng of each substance. Mass spectra of all compounds were directly (or after background subtraction) applied to a library search in the NBS library. Seventy two of the pesticides were identified correctly by means of the PBM (propability based matching) searching routine developed by McLafferty *et al.*[17–19]. The remaining four pesticides were not found because their spectra were not included in the NBS library. A compilation of the results of the library search is given in Table II. It is in fact most remarkable that all 72 compounds were not only found at concentrations of 10 or 20 ng per peak but also with the best fit. As is seen from the last row in Table II, several compounds were not indicated with their common names but with one applied by other organizations or with the chemical name according to IUPAC.

In Fig. 3 the mass spectra of the four pesticides not found in the NBS library are reported. This gives the opportunity to demonstrate the quality of spectra obtained with 10 or 20 ng of substance under the described experimental conditions that are exactly the same as applied to pesticide residue analysis.

After having entered all the mass spectra into the pesticide sub-library, preliminary measurements were performed with diluted solutions of the described pesticide mixtures. Applying the cyclic scan mode, a mixture of chlorinated pesticides containing 2 ng of each compound was analyzed as shown in Fig. 4. All 20 substances were correctly identified by means of a library search. The signal-to-noise ratio of the TIC trace indicates that a concentration of 2 ng per peak approaches the limit of detection of many pesticides with cyclic scanning.

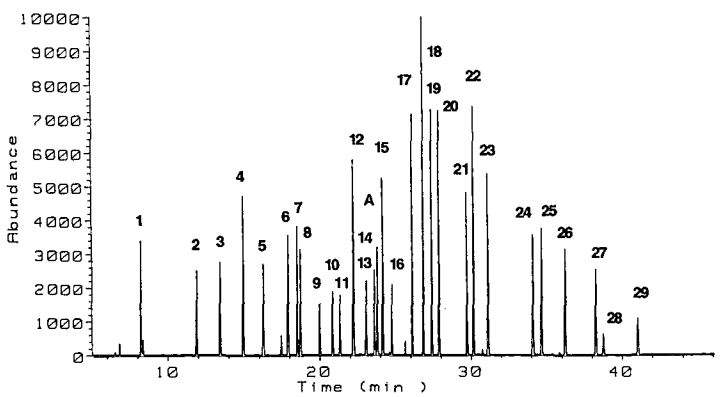

Fig. 2. TIC of organophosphate pesticides. A 20-ng amount of each of the following compounds was injected: 1 = mevinphos; 2 = heptenophos; 3 = ethoprophos; 4 = sulfotep; 5 = dimethoate; 6 = fonofos; 7 = diazinon; 8 = disulfoton; 9 = formothion; 10 = phosphamidon: 11 = parathion-methyl; 12 = fenchlorphos; 13 = fenitrothion; 14 = amidithion; 15 = fenthion; 16 = chlorthion; 17 = chlorfenvinphos; 18 = bromophos-ethyl; 19 = ditalimfos; 20 = prothiofos; 21 = fensulfothion; 22 = ethion; 23 = carbophenothion; 24 = phosmet; 25 = phenkapton; 26 = phosalone; 27 = pyrazophos; 28 = dialifos; 29 = coumaphos; A = aldrin (internal standard).

TABLE II

RESULT OF LIBRARY SEARCH WITH 76 PESTICIDES

No.	*Common name*	*CAS No.*	*Mol.wt.*	*NBS No.*	*Best fit*
1	Aldrin	309-00-2	361.875	34152	
2	Amidithion	919-76-6	273.025	26449	
3	Azinphos-ethyl	2642-71-9	345.036	33020	
4	Bromophos	2104-96-3	363.848	34387	
5	Bromophos-ethyl	4824-78-6	391.880	35899	
6	Bromopropylate	18181-80-1	425.946	37527	
7	Carbophenothion	786-19-6	341.973	32781	
8	Chlorfenprop-methyl	14437-17-3	232.005	21311	
9	Chlorfenvinphos	470-90-6	357.969	33865	
10	Chlormephos	24934-91-6	233.970	21673	
11	Chloroneb	2675-77-6	205.989	17624	Benzene, ...[b]
12	Chloropropylate	5836-10-2	338.047	32520	
13	Chlorothalonil	1897-45-6	263.881	25431	Tetrachloro[c]
14	Chlorthal-dimethyl	1861-32-1	329.901	31821	DCPA[a]
15	Chlorthion	500-28-7	296.962	28934	
16	Coumaphos	56-72-4	362.014	34155	
17	DDD-o,p'	53-19-0	317.953	30874	
18	DDD-p,p'	72-54-8	317.953	30875	1,1-Dichloro[d]
19	DDE-o,p'	3424-82-6	315.937	30697	
20	DDE-p,p'	72-55-9	315.937	30696	
21	DDT-o,p'	789-02-6	351.914	33482	
22	DDT-p,p'	50-29-3	351.914	33481	
23	Dialifos	10311-84-9	393.002	35976	Dialifor[a]
24	Diazinon	333-41-5	304.100	29598	Dimpylate[a]
25	Dichlobenil	1194-65-6	170.964	11664	Benzonitrile[e]
26	Dichlofenthion	97-17-6	313.969	30462	
27	Dichlofluanid	1085-98-9	331.961	32138	
28	Dichloran	99-30-9	205.964	17600	2,6-Dichloro[f]
29	Dieldrin	60-57-1	377.870	35144	
30	Dimethoate	60-51-5	228.999	21040	
31	Disulfoton	298-04-4	274.028	26595	
32	Ditalimfos	5131-24-8	299.037	29101	O,O-Diethyl[g]
33	Endosulfan	115-29-7	403.816	36627	
34	Ethion	563-12-2	383.987	35518	
35	Ethoprophos	13194-48-4	242.056	22777	
36	Fenchlorphos	299-84-3	319.899	31163	Ronnel[a]
37	Fenitrothion	122-14-4	277.017	26839	
38	Fensulfothion	115-90-2	308.030	29926	
39	Fenthion	55-38-9	278.019	26843	
40	Folpet	133-07-3	294.902	28695	
41	Fonofos	944-22-9	246.029	23060	
42	Formothion	2540-82-1	256.994	24582	
43	HCB	118-74-1	281.812	27405	
44	HCH-alpha	319-84-6	287.859	28091	alpha-Lindane
45	HCH-beta	319-85-7	287.859	28092	Cyclohexane[h]
46	HCH-delta	319-86-8	287.859	28093	delta-Lindane
47	Heptachlor	76-44-8	369.820	34677	
48	Heptachlorepoxide-c	1024-57-3	385.815	35535	
49	Heptachlorepoxide-t	1024-57-3	385.815	35535	
50	Heptenophos	34783-40-9			No match
51	Lindane	58-89-9	287.859	28090	

TABLE II (*continued*)

No.	*Common name*	*CAS No.*	*Mol.wt.*	*NBS No.*	*Best fit*
52	Methoxychlor	72-43-5	344.013	32941	
53	Mevinphos	7786-34-7	224.044	20347	
54	Mirex	2385-85-5	539.625	40520	
55	Parathion	56-38-2	291.032	28324	
56	Parathion-methyl	298-00-0	263.001	25275	
57	Phenkapton	2275-14-1	375.934	35055	
58	Phosalone	2310-17-0	366.986	34511	
59	Phosmet	732-11-6	316.994	30824	
60	Phosphamidon	13171-21-6	299.068	29096	
61	Pirimiphos-ethyl	23505-41-1	333.127	32142	
62	Pirimiphos-methyl	29232-93-7	305.095	29718	
63	Propachlor	1918-16-7	211.075	18300	Acetamide[i]
64	Propyzamide	23950-58-5	255.021	24288	
65	Prothiofos	34643-46-4			No match
66	Pyrazophos	13457-18-6	373.085	24935	
67	Quintozene	82-68-8	292.836	28520	Benzene ...[j]
68	Sulfotep	3689-24-5	322.022	31305	
69	Tecnazene	117-18-0	258.875	24834	Benzene ...[k]
70	Tetrachlorvinphos	22248-79-9	363.898	34285	
71	Tetradifon	116-29-0	353.883	33616	
72	Tolylfluanid	731-27-1			No match
73	Triadimefon	43121-43-3	293.092	28489	Butanone, ...[l]
74	Triazophos	24017-47-8	313.064	30419	
75	Trifluralin	1582-09-8	335.108	32328	
76	Vinclozolin	50471-44-8			No match

[a] Common name approved by organizations other than ISO or BSI.
[b] Benzene, 1,4-dichloro-2,5-methoxy.
[c] Tetrachloroisophthalonitrile.
[d] 1,1-Dichloro-2,2-bis(*p*-chlorophenyl)ethane.
[e] Benzonitrile, 2,6-dichloro.
[f] 2,6-Dichloro-4-nitroaniline.
[g] O,O-Diethylphthalimidophosphonothioate.
[h] Cyclohexane, 1,2,3,4,5,6-hexachloro.
[i] Acetamide, 2-chloro-N-(1-methylethyl)-N-phenyl.
[j] Benzene, pentachloronitro.
[k] Benzene, 1,2,4,5-tetrachloro-3-nitro.
[l] 2-Butanone, 1-(4-chlorophenoxy)-3,3-dimethyl-1-(1H-1,2,4-triazol-1-yl).

A survey of all compounds at this concentration level resulted in a correct recognition of all chlorinated pesticides, but pesticides of other structural classes were less reliably identified. Most of them would certainly not have been recognized in the presence of biological matrix compounds. Frequently, however, the presence of the individual pesticide was detected at the expected retention time in the chromatogram by extracting the indicative ions from the cyclic scan data.

The application of SIM enhances the detection sensitivity by orders of magnitude and at the same time the overlapping signals from the matrix compounds are considerably reduced. In Fig. 5 the SIM records of an analytical fraction of green pepper spiked with a mixture of chlorinated pesticides at the low concentration of 10

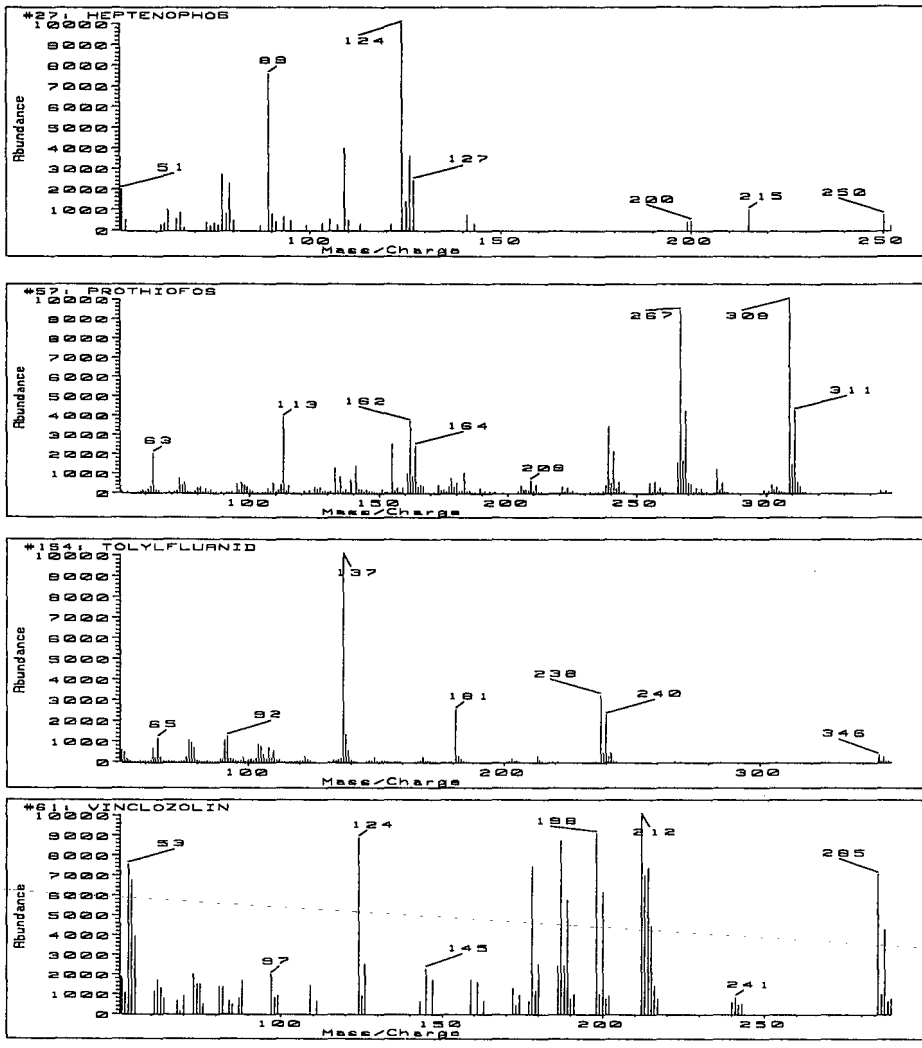

Fig. 3. Mass spectra of four pesticides not found in the NBS library. A 20-ng amount of each of heptenophos, prothiofos, tolylfluanid and vinclozolin was analyzed with GC–MS. Mass spectra after background subtraction.

ppb are presented. The injected extract volume of 1 μl contained about 50 pg of each pesticide together with the coextracted matrix compounds equivalent to 5 mg of vegetable. Highest sensitivity was achieved by selecting only a few masses in one time interval. This rule, however, was not applicable to all the time intervals. Seven masses had to be recorded in the first time interval between 15 and 20 min in order to screen simultaneously for HCB, quintozene and the HCH isomers. The SIM traces presented in Fig. 5 demonstrate that all the added chlorinated pesticides were detected in the spiked pepper sample at trace levels. At the same time the confirmation of 50 ppb endosulfan, first detected with GC–ECD in the green pepper sample, is presented.

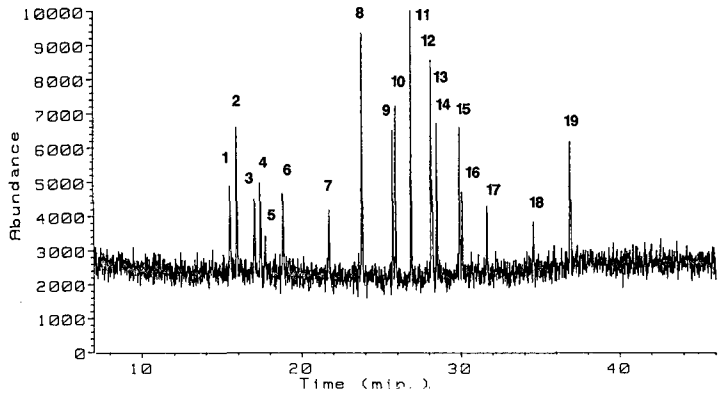

Fig. 4. Total ion chromatogram of a diluted mixture of chlorinated pesticides. A 2-ng amount of each of the following compounds was injected: 1 = α-HCH; 2 = HCB; 3 = β-HCH; 4 = lindane; 5 = quintozene; 6 = δ-HCH; 7 = heptachlor; 8 = aldrin; 9 = *cis*-heptachlorepoxide; 10 = *trans*-heptachlorepoxide; 11 = o,p'-DDE; 12 = p,p'-DDE; 13 = dieldrin; 14 = o,p'-DDD; 15 = p,p'-DDD; 16 = o,p'-DDT; 17 = p,p'-DDT; 18 = methoxychlor; 19 = mirex.

Although with GC–ECD two peaks representing endosulfan-I and endosulfan-II were detected, only endosulfan-I can be monitored with SIM at this low concentration, owing to the extensive fragmentation of endosulfan-II yielding only ions of low intensity.

DISCUSSION

The study confirmed that the combination of capillary GC with MSD can be applied to pesticide residue analysis in food samples. The MSD detector is really a mass selective GC detector that does not need the skill of maintainance that is necessary to operate a mass spectrometer. In our laboratory, MSD was much easier to handle than NPD, for instance. One of the spectacular features of GC–MS is the cyclic scan mode. After having performed a GC analysis a computer program can identify the peaks and automatically carry out a library search. The result of such a GC analysis is a list of compounds identified in an unknown sample.

The reliable recognition of 72 pesticides in the various test mixtures at amounts of 10 or 20 ng (Table II) was an impressive demonstration of the effectiveness of the PBM search routine developed by McLafferty *et al.*[17–19]. The library search was executed by an operator who did not know the composition of the pesticide mixtures. In all library searches for the 72 gas chromatographic peaks the pesticide was set into the first place (best fit) of a list of 10 compounds ranked for similarity of the sample spectrum to the over 42 000 spectra in the NBS library. This tempts one to believe that the fully automated qualitative analysis has been established at a very low concentration.

In pesticide residue analysis in food samples, however, this beautiful perspective is seldom reality. In Fig. 4 the analysis of a mixture of 2 ng of each pesticide is shown. These chlorinated pesticides were identified by an experienced analyst by means of the mass spectra after background subtraction and the retention time. Background

subtraction, however, did not yield mass spectra free of additional masses which decreases considerably the reliability of an automated library search.

When following established clean-up procedures[1,8], an amount of 2 ng of a pesticide means a concentration of 400 ppb in the food sample. Although all chlorinated pesticides were recognized at this concentration in test mixtures without interfering matrix compounds, about half of the pesticides under study did not produce mass spectra of sufficient quality. The problem mostly cannot be overcome by concentrating the sample extracts because the coextractants are enriched in the same proportion. On the other hand, for many pesticides, maximum tolerance limits are established at 10 ppb. At this concentration the identification of a pesticide by means of a full mass spectrum is expected only in a few very favourable situations with respect to the chemical structure of the compound and the coextractants from the food matrix. Therefore, pesticide residue analysis at this relevant low concentration has to rely on SIM. A good example to demonstrate the potential of this method is given in Fig. 5

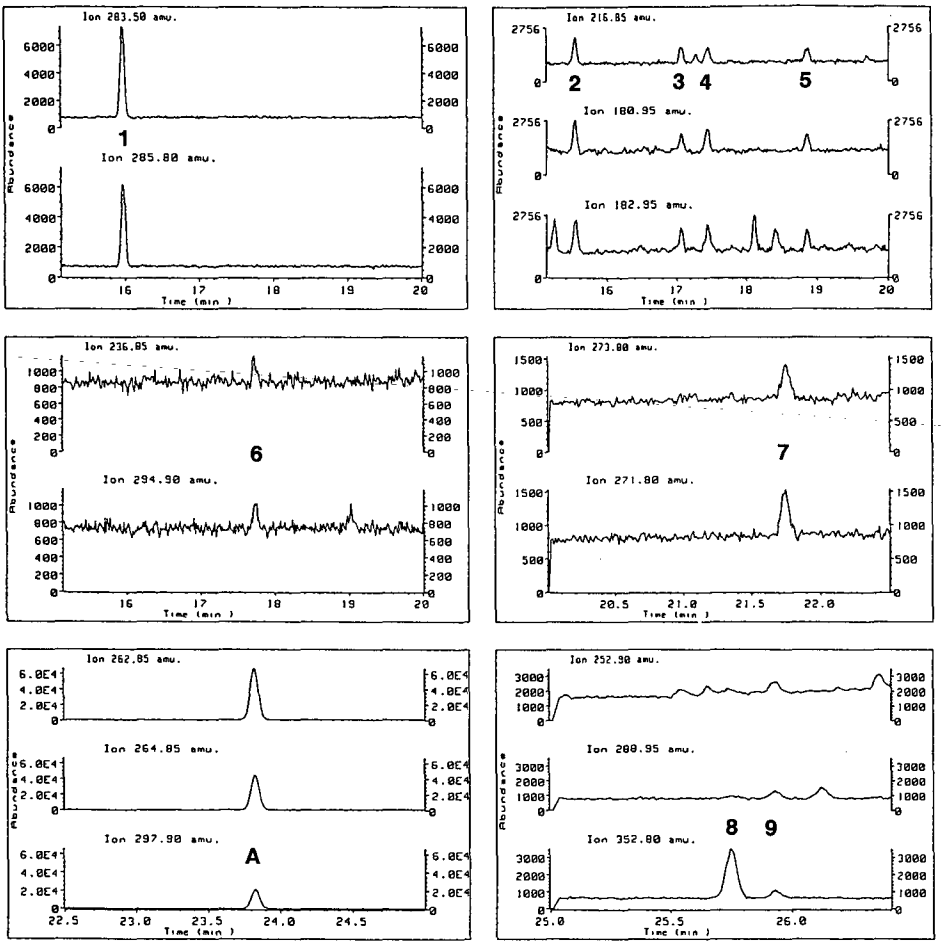

Fig. 5.

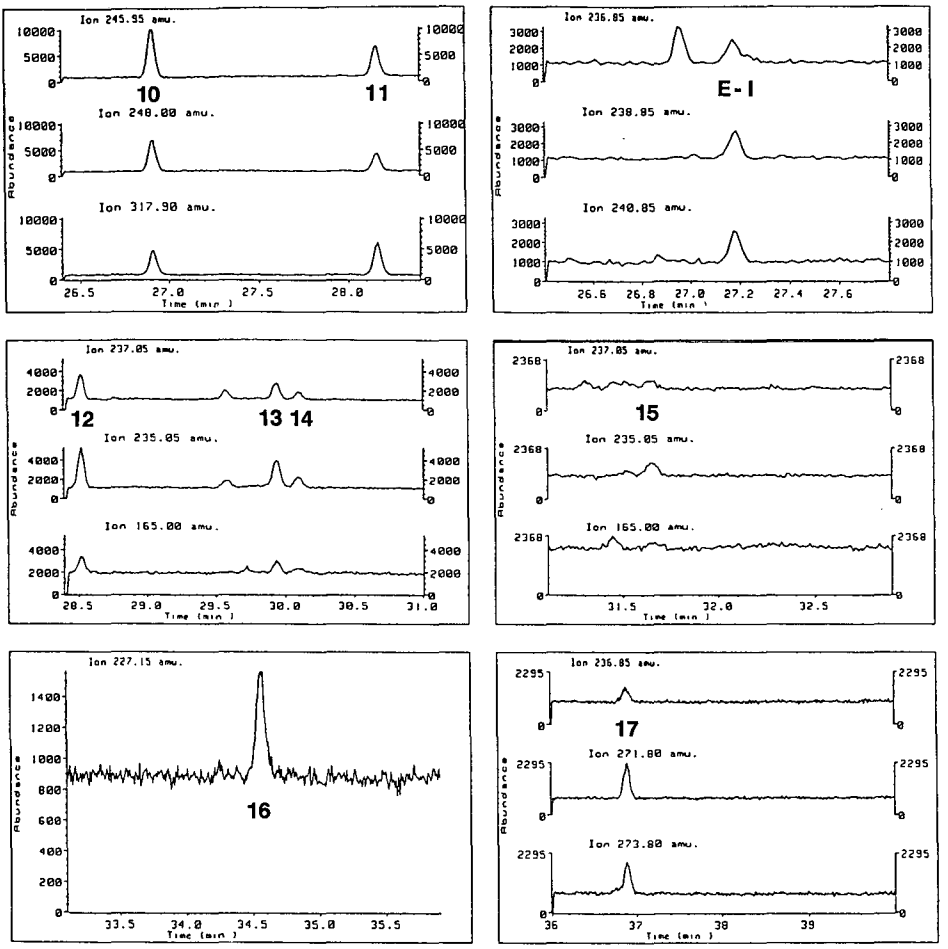

Fig. 5. SIM of chlorinated pesticides in green pepper. The food sample was spiked with 10 ppb of the following pesticides: 1 = HCB; 2 = α-HCH; 3 = β-HCH; 4 = lindane; 5 = δ-HCH; 6 = quintozene; 7 = heptachlor; 8 = *cis*-heptachlorepoxide; 9 = *trans*-heptachlorepoxide; 10 = o,p′-DDE; 11 = p,p′-DDE; 12 = o,p′-DDD; 13 = p,p′-DDD; 14 = o,p′-DDT; 15 = p,p′-DDT; 16 = methoxychlor; 17 = mirex. E-I = 50 ppb endosulfan I detected in the food sample. A = Aldrin (500 ppb) as internal standard.

where 18 chlorinated pesticides added to a vegetable sample at a concentration of 10 ppb were correctly detected. The knowledge of the retention times of the pesticides allowed the programming of time intervals with the appropriate selective ions. So it was possible to screen for all the important chlorinated pesticides in one GC analysis. The baseline of most of the ion traces was remarkably smooth. HCB forms a very stable molecular ion that produced the most intense signal of all compounds. Quintozene with only one of the six chlorine atoms substituted by the nitro group produces two ions in the higher mass region that only just formed a visible signal. It must be pointed out that the detection sensitivity for chlorinated pesticides approaches that of ECD, which has the reputation of being the most sensitive detection mode for

this compound group. One pesticide, however, can be detected far more sensitively with SIM than with ECD, namely methoxychlor which has never been traced at the 10 ppb level by ECD in our laboratory.

CONCLUSIONS

The results presented here demonstrate that capillary GC in connection with MSD allows one to detect and identify pesticide residues at concentrations which can be compared with those achieved by the other selective detectors in common use. Therefore, MSD can be highly recommended in pesticide residue analysis and in the control of other environmental pollutants for confirmatory analysis. This detector also has the potential for application to routine screening analyses.

A compilation of the mass spectra of all pesticides that can be determined with GC is considered as a prerequisite to achieve reliable results. It is recommended that they be filed in a separate sub-library with their common names. Otherwise, in routine analysis it may happen that a detected pesticide is not recognized because of its strange name when the pesticide is included in a hit list of 10 or 20 compounds in the PBM report. A few examples can be found in Table II. More important, however, is the creation of a list of all pesticides with their retention times and most suitable masses for SIM analysis.

REFERENCES

1 H.-P. Thier and H. Zeumer (Editors), *Manual of Pesticide Residue Analysis*, DFG, Dt. Forschungsgemeinschaft, Pesticides Comm., VCH, Weinheim, 1987.
2 H. A. Moye (Editor), *Analysis of Pesticide Residues. Chemical Analysis Series*, Vol. 58, Wiley, New York, 1981.
3 A. Ambrus, J. Lantos, E. Visi, I. Csatlos and L. Sarvari, *J. Assoc. Off. Anal. Chem.*, 64 (1981) 733.
4 *FDA Pesticide Analytical Manual*, Food and Drug Administration, Washington, DC, Vol. 1, 1985.
5 M. A. Luke and H. T. Masumoto, in G. Zweig and J. Sherma (Editors), *Analytical Methods for Pesticides and Plant Growth Regulators*, Vol. XV, Academic Press, Orlando, FL, 1986, p. 161.
6 H. Goebel and H.-J. Stan, *J. Chromatogr.*, 279 (1983) 523.
7 H.-J. Stan and D. Mrowetz, *J. Chromatogr.*, 279 (1983) 173.
8 W. Specht and M. Tillkes, *Fresenius' Z. Anal. Chem.*, 322 (1985) 443.
9 J. Lipinski and H.-J. Stan, *J. Chromatogr.*, 441 (1988) 213.
10 R. A. Hites, *CRC Handbook of Mass Spectra of Environmental Contaminants*, CRC Press, Boca Raton, FL, 1985.
11 T. Cairns, E. G. Siegmund and R. A. Jacobson (Editors), *Mass Spectral Data Compilation of Pesticides and Industrial Chemicals*, Food and Drug Administration, Los Angeles, CA, 1987.
12 J. N. Damico, in R. G. Waller (Editor), *Biochemical Applications of Mass Spectrometry*, Wiley, New York, 1972, p. 623.
13 S. Safe and O. Hutzinger, *Mass Spectrometry of Pesticides and Pollutants*, CRC Press, Cleveland, OH, 1973.
14 J. Freudenthal and L. G. Gramberg, *Catalogue of Mass Spectra of Pesticides*, National Institute of Public Health, Bilthoven, 1975.
15 H.-J. Stan, B. Abraham, J. Jung, M. Kellert and K. Steinland, *Fresenius' Z. Anal. Chem.*, 287 (1977) 271.
16 H.-J. Stan and G. Kellner, *Biomed. Environ. Mass Spectrom.*, in press.
17 F. W. McLafferty, R. H. Hertel and R. D. Villwock, *Org. Mass Spectrom.*, 9 (1974) 690.
18 G. M. Pensyna, R. Venkataraghavan, H. E. Dayringer and F. W. McLafferty, *Anal. Chem.*, 48 (1976) 1362.
19 In Ki Mun, D. R. Bartholomew, D. B. Stauffer and F. W. McLafferty, *Anal. Chem.*, 53 (1981) 1938.

Journal of Chromatography, 467 (1989) 99–110
Elsevier Science Publishers B.V., Amsterdam — Printed in The Netherlands

CHROM. 21 242

SYNTHESIS, GAS–LIQUID CHROMATOGRAPHIC ANALYSIS AND GAS CHROMATOGRAPHIC–MASS SPECTROMETRIC IDENTIFICATION OF NITROVANILLINS, CHLORONITROVANILLINS, NITROGUAIACOLS AND CHLORONITROGUAIACOLS

PER-ÅKE HYNNING, MIKAEL REMBERGER and ALASDAIR H. NEILSON*
Swedish Environmental Research Institute, Box 21060, S-100 31 Stockholm (Sweden)
(First received September 30th, 1988; revised manuscript received January 2nd, 1989)

SUMMARY

The synthesis of guaiacols and vanillins bearing nitro, or nitro and chloro, substituents is described. A procedure for analysis of these and other nitrophenolic compounds by gas–liquid chromatography after derivatization is given. Attention is directed to problems in the preparation and stability of the O-acetates and O-ethyl ethers due to their susceptibility to hydrolysis: the O-acetates were found to be the most suitable derivatives for quantitative analysis. Recoveries from aqueous solutions of >95% were achieved by extraction with *tert.*-butyl methyl ether or by adsorption to C_{18} Bond Elut columns. Mass spectra, electron impact and negative chemical ionization were examined and the diagnostic interpretation of the spectra is discussed.

INTRODUCTION

Kraft pulp produced by the sulphate process is generally brightened by removal of residual lignin. This is often accomplished by use of molecular chlorine, and results in the production of several hundred organochlorine compounds[1], including chloroguaiacols, chlorocatechols and chlorovanillins. On account of the potential hazard of discharging bleachery effluents into the aquatic environment[2], efforts have been directed to the use of delignification agents other than molecular chlorine.

The prenox process[3] is based upon the use of oxides of nitrogen to carry out delignification, and although the action of nitric acid on lignin was briefly noted as long ago as 1918[4], there have since been only sporadic studies on the nitration of lignin and lignin-related compounds[5,6]. By analogy with the reactions of molecular chlorine, it may be predicted that two series of reactions will occur: (i) nitration of the lignin residues with partial oxidation of the C_3 residues and formation of nitrovanillins and (ii) nitration with concomitant elimination of the C_3 residues and formation of nitroguaiacols. Subsequent chlorination of residual nitro compounds may then give rise to a range of guaiacols and vanillins containing both chloro and nitro groups. On the other hand, in contrast to reactions which take place during chlorination, dealkylation and formation of polynitrated products are probably of minor significance.

0021-9673/89/$03.50

We have developed experimental procedures for assessing the impact of industrial discharge on the aquatic environment[2]. As a prerequisite to the application of these procedures to effluents from the prenox process, we required analytical and identification procedures for all the compounds likely to be encountered, together with their potential microbial metabolites. In view of the complex range of organic compounds occurring in extracts of such samples, it is necessary either to introduce a purification step or to use derivatized samples: by choice of appropriate derivatives, purification is automatically and conveniently introduced.

In this communication, we describe: (i) the synthesis of the relevant vanillins and guaiacols containing nitro, and nitro and chloro substituents, (ii) analytical procedures for quantification which take into account certain inherent problems in extraction of these relatively water-soluble compounds from aqueous solutions and (iii) procedures for conclusive identification of all of these compounds based on mass spectrometry (MS) in electron impact (EI) and negative chemical ionization (NCI) modes.

To the best of our knowledge, none of these problems has been systematically investigated previously, though procedures for individual compounds[7,8] and mass spectra (NCI) of a restricted range of nitrophenols[9] have been published.

EXPERIMENTAL

Substrates

The chloronitrophenols were gifts from ICI, Agrochemicals Division (Jealott's Hill, U.K.); 2- and 4-nitrophenol and 4-nitrocatechol were obtained from Merck (Darmstadt, F.R.G.), 3-nitrophenol from Janssen (Beerse, Belgium) and 2,4-dinitrophenol from Serva (Heidelberg, F.R.G.). Other compounds were synthesized as described below.

Solvents and reagents

Fuming nitric acid (specific gravity 1.52), diethyl sulphate and acetic acid were obtained from Merck, *tert.*-butyl methyl ether, dimethylformamide and hexane from Burdick & Jackson (Muskegon, MI, U.S.A.), pyridine, acetyl chloride, tetramethyl- and tetrabutylammonium hydroxide, guaiacol, vanillin and veratrole from Janssen, acetic anhydride and ethyl iodide from Fluka (Buchs, Switzerland) and 2,6-dimethoxyphenol from EGA (Steinheim, F.R.G.).

Synthesis of substrates

The structures and ring position numbering of the unsubstituted compounds are given in Fig 1.

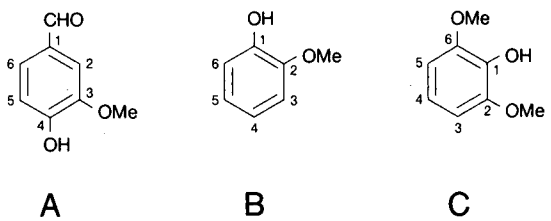

Fig. 1. Structure and ring numbering of vanillin (A), guaiacol (B) and syringol (C). Me = Methyl.

5-Nitrovanillin was prepared as follows. Vanillin (Fig. 1A) (10 g) was dissolved in acetic acid (*ca.* 30 ml), and a solution of fuming nitric acid (3 ml) in acetic acid (20 ml) slowly added with stirring. The mixture was poured into water, the product was removed by filtration, washed with water and recrystallized from acetic acid (*m/z* of the parent ion of the O-acetate $C_{10}H_9NO_6$: 239).

The compunds 2- and 6-nitrovanillin were prepared by the method of Raiford and Stoesser[10]. 2-Nitrovanillin was recrystallized from benzene, and 6-nitrovanillin from acetic acid (*m/z* of the O-acetates as for the 5-nitro isomer).

4,6-Dinitroguaiacol was prepared from guaiacol (Fig. 1B) by the procedure used for 5-nitrovanillin. The product, which was almost black, was purified by repeated recrystallization from acetic acid (*m/z* of parent ion of the O-acetate $C_9H_8N_2O_7$: 256).

3,5-Dinitroguaiacol was prepared as follows. Guaiacol was acetylated with acetic anhydride in refluxing acetic acid (1 h), the mixture poured into water and the product extracted with *tert.*-butyl methyl ether. Nitration was carried out by the procedure used for 2-nitrovanillin and, after hydrolysis with methanolic KOH, the product was recrystallized from benzene–cyclohexane (1:1) (*m/z* of the O-acetate as for the 4,6-dinitro isomer). The orientation of the nitro groups was unambiguously shown from the identity of the mass spectrum of the O-methyl ether with that of 3,5-dinitroveratrole prepared from 4,6-dinitroguaiacol (*m/z* for $C_8H_8N_2O_6$: 228).

4,5-Dinitroguaiacol was prepared from 4,5-dinitroveratrole by the method of Ehrlich and Bogert[11] and recrystallized from toluene. The parent ion of the O-acetate had *m/z* values identical to those of 3,5- and 4,6-dinitroguaiacol, whereas the mass spectrum of the O-methyl ether (veratrole) had a different gas–liquid chromatographic (GC) retention time and mass spectrum from that of 3,5-dinitroveratrole.

3,5-Dinitrosyringol was prepared from syringol (Fig. 1C) by the procedure used for 3,5-dinitroguaiacol and was recrystallized from benzene–cyclohexane (1:1) (*m/z* of the parent ion of the O-acetate $C_{10}H_{10}N_2O_8$: 286).

4-Chloro-3-nitrosyringol was prepared as follows. Syringol was chlorinated (*ca.* 1 h) in refluxing diethyl ether with sulphuryl chloride (1.1 mol), solvent removed and the product acetylated with acetic anhydride in refluxing acetic acid. Nitration and hydrolysis were carried out as for the synthesis of 3,5-dinitrosyringol to yield an oil. This was chromatographed on a column of SiO_2 (5 cm × 2 cm I.D., Merck Kieselgel 60, 70–230 mesh), the product eluted with dichloromethane and recrystallized from benzene–cyclohexane (1:1) (*m/z* of the parent ions of the O-acetate $C_{10}H_{10}ClNO_6$: 275, 277 in the ratio 3:1).

2-Nitro-5-chlorovanillin and 6-chloro-2-nitrovanillin were prepared by the method of Raiford and Lichty[12]. The former was recrystallized from acetic acid and the latter from water (*m/z* of the parent ions of the O-acetate $C_{10}H_8ClNO_6$: 273, 275 in the ratio 3:1).

4-Chloro-6-nitroguaiacol was prepared from 4-chloroguaiacol[13] by nitration in acetic acid as described for the synthesis of 5-nitrovanillin, and the product recrystallized from benzene (*m/z* of the parent ions of the O-acetate $C_9H_8ClNO_5$: 245, 247 in the ratio 3:1).

GC

Analyses were carried out with a Varian (Palo Alto, CA, U.S.A.) 3700 Model gas chromatograph equipped with a Model 8000 autosampler and an Hewlett-Packard

3390A integrator. The electron-capture detector was held at 300°C, the injector at 250°C and the following temperature programme was used: 1 min isothermal at 150°C followed by an increase at 2°C/min to 245°C. Helium was used as the carrier gas at a flow-rate of 20 cm/s with a splitting ratio of 1:25. A fused-silica capillary column, DB-5-30N, with an I.D. of 0.25 mm and a film thickness of 0.25 μm (J & W Scientific, Folsom, CA, U.S.A.) was used.

GC–MS

GC–MS analyses were carried out with a TRIO 2 mass spectrometer (VG MassLab, Altrincham, U.K.) and an Hewlett-Packard 5890A gas chromatograph equipped with a DB-5-15N fused-silica column with an I.D. of 0.25 mm and a film thickness of 0.25 μm (J & W Scientific) and using helium as the carrier gas. The gas chromatograph was operated in the splitless mode under the following conditions: injector temperature 220°C; temperature programme, 50°C for 1 min isothermal, increasing at 15°C/min to 220°C which was held for 10 min. For EI mass spectra, the operating conditions were: source temperature 200°C, emission current 210 μA and an electron energy of 40 eV. The NCI mass spectra were obtained with methane as a reagent gas, a source temperature of 150°C, an emission current of 900 μA and a electron energy of 40 eV.

Preparation and stability of derivatives

O-Acetates were prepared as follows. The nitrophenols were dissolved in *tert.*-butyl methyl ether–hexane (1:1), pyridine (50 μl) and acetic anhydride or acetyl chloride (125 μl) added. The mixture was heated at 75°C for 30 min with occasional shaking, pyridine was removed with HCl (2 ml, 0.5 *M*) and the excess of acetylating reagent hydrolysed with 4 ml water for 15 min. The organic phase was used for analysis.

The yield of the products, the optimum derivatization conditions and the stability of the derivatives were determined from the results of experiments using pure samples of the O-acetates of 2,4-dinitrophenol and 6-chloro-2-nitrovanillin. These standards were prepared by acetylation of the phenolic compounds with acetic anhydride in refluxing acetic acid (1 h), the products isolated after destroying the excess of reagent with ice–water and recrystallization from cyclohexane. Based on the optimum derivatization procedure, the stability of all the O-acetates was examined.

O-Ethyl ethers were prepared by dissolving the compounds in 1 ml each of *tert.*-butyl methyl ether–hexane (1:1) and dimethyl formamide. A solution of tetrabutylammonium hydroxide in methanol (0.8 *M*, 15 μl) was added followed by ethyl iodide (10 μl) and the mixture shaken at room temperature for 15 min. The excess of ethyl iodide was removed by reaction with pyridine (50 μl), the sample shaken with HCl (2 ml, 0.5 *M*) to remove pyridine and finally with water (2 ml) to remove dimethylformamide. The organic phase was used for analysis. Due to the extreme sensitivity of the products to hydrolysis, this method was not uniformly suitable for preparation of the O-ethers of *ortho*-nitro-substituted phenolic compounds.

Recovery procedures for water samples and their efficiency

The extraction efficiency was determined using a synthetic mixture of the compounds dissolved in water (1 or 5 ml) at concentrations of 20 and 100 μg l^{-1}.

Solvent extraction with two solvents was examined: *tert.*-butyl methyl ether–hexane (1:1) and *tert.*-butyl methyl ether alone. The samples were acidified to a pH of < 1, ascorbic acid (100 mg) added and the solutions saturated with NaCl. Extraction was carried out with the two test solvents [1.5 ml, containing 2,4,6-tribromophenol (0.4 μg ml^{-1}) as the internal standard], and twice more with solvent (1.5 ml) lacking the internal standard. The organic phases were pooled, and the volume reduced to 2 ml in a stream of nitrogen at room temperature. In order to facilitate drying of the samples before acetylation, hexane (1 ml) was added, the volume again reduced to 2 ml and the extract dried (Na_2SO_4) for at least 15 min.

Use of C_{18} adsorption was also evaluated. The acidified solution was applied to an activated Bond Elut column (Analytichem, Harbor City, CA, U.S.A.), washed with HCl (1 ml, 0.1 *M*) and the nitrophenols eluted with *tert.*-butyl methyl ether [3.5 ml containing 2,4,6-tribromophenol (0.4 μg ml^{-1}) as the internal standard]. The eluate was treated as above for direct solvent extraction.

RESULTS AND DISCUSSION

Synthesis of substrates

Different procedures were used depending on the substitution pattern of the desired products. Synthesis of 2- and 4-nitro-substituted phenolic compounds was successfully carried out with fuming nitric acid in acetic acid at ambient temperature, whereas synthesis of the 3-substituted compounds required acetylation before nitration of the solid compound which was added portionwise to fuming nitric acid at 2–4°C. The purity of the compounds after recrystallization was >98% (GC–MS).

GC analysis

Industrial effluents invariably contain a large and structurally heterogeneous range of organic compounds. Experience in the analysis both of bleachery effluents which contain several hundred structurally diverse chlorinated organic compounds[1], and samples from metabolic experiments with microorganisms which contain a variety of metabolites[2], has clearly shown the advantage, and in general the necessity, of preparing derivatives of the phenolic compounds before attempting GC analysis. Use of the O-acetates of chlorophenolic compounds has also provided good resolution of isomeric compounds[14], and in addition, a satisfactory degree of purification is thereby introduced. We were concerned with the development of comparable procedures for nitrophenolic compounds. Use of such relatively clean samples also considerably simplifies problems in GC–MS structural determination (see below).

Derivatization for GC analysis presented a number of problems, primarily due to the susceptibility of the derivatives to hydrolysis: for example, trifluoroacetylation was accomplished readily, but the derivatives were so susceptible to hydrolysis that during destruction of the excess of reagent with water they were completely hydrolysed. On the other hand, acetylation was not quantitatively accomplished with sodium acetate as the base: the use of pyridine was obligatory. Again, it was found that hydrolysis of the O-acetates presented a problem: to minimize this, pyridine must be removed from the reaction mixture immediately after derivatization. Hydrolysis of excess of acetic anhydride with sodium carbonate[15] could not be used since hydrolysis of the nitrophenol O-acetates occurred: it was found, however, that shaking with water

alone was satisfactory. Two of the more recalcitrant compounds, 2,4-dinitrophenol and 6-chloro-2-nitrovanillin, were chosen for detailed examination. The rates of acetylation of these are shown in Fig. 2. The yields of the acetylated products were virtually quantitative within 20 min, though in practice the reaction time was routinely extended to 30 min. Since the products from the acetylation of 2,4-dinitrophenol and 6-chloro-2-nitrovanillin, as well as the pure O-acetates from these, were stable in the extraction solvent maintained at room temperature for 20 h, it was judged that O-acetates could be used for quantitative analysis. All the O-acetates were stable at room temperature for at least 18 h, and, with the exception of those derived from 2-nitro-, 2-nitro-5-chloro- and 2-nitro-6-chlorovanillin, were stable for up to 66 h. At −20°C, all were stable for at least 4 days. It was therefore judged that the stability of the derivatives was sufficient for repeat GC analyses to be carried out. The relative retention times (Table I) showed clearly that adequate resolution of the substances examined can be achieved with the operating conditions used. Whereas use of the O-ethyl ethers may be a valuable complement for identification, the structural discrimination of these was significantly poorer (Table I). In addition, on account of the difficulty encountered in their preparation and their susceptibility to hydrolysis (discussed below), they were not suitable for quantitative studies.

Recovery of compounds from aqueous solutions

The solvent extractability of the compounds using *tert.*-butyl methyl ether–hexane (1:1) was low for the nitrovanillins, 6-chloro-2-nitrovanillin and 4-nitrocatechol: by use of *tert.*-butyl ether alone, however, the extractability exceeded 95% for all compounds. The C_{18} adsorption procedure provided equally quantitative recovery, and we therefore conclude that either procedure would be applicable to the recovery of a wide range of structurally diverse nitrophenolic compounds from waste-water samples.

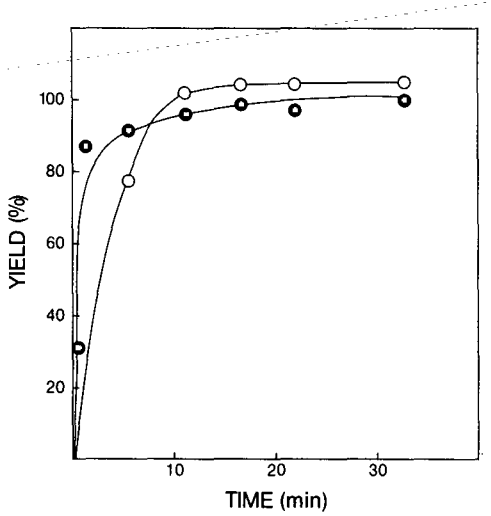

Fig. 2. Yield (%) of the O-acetates of 2,4-dinitrophenol (●) and 6-chloro-2-nitrovanillin (○) as a function of the reaction time (min) at 75°C. Yields were calculated on the basis of the pure O-acetates.

TABLE I

RETENTION TIMES AND RESPONSE FACTORS OF THE O-ACETATES OF THE NITROPHENOLS RELATIVE TO THAT OF 2,4-DINITROPHENOL, AND RELATIVE RETENTION TIMES OF THE O-ETHYL ETHERS RELATIVE TO 2,4-DINITROPHENETOLE

Substance	*O-Acetates*		*O-Ethyl ethers*
	Relative retention time	*Relative response*	*Relative retention time*
2-Nitrophenol	0.445	1.05	0.361
3-Nitrophenol	0.521	1.05	0.365
4-Nitrophenol	0.550	1.43	0.447
4-Chloro-2-nitrophenol	0.616	4.79	0.528
2-Chloro-4-nitrophenol	0.706	4.64	0.659
2,4-Dichloro-6-nitrophenol	0.759	4.30	0.534
2,4-Dinitrophenol	1.000	1.00	1.000
4-Chloro-6-nitroguaiacol	1.034	2.75	0.723
2-Nitrovanillin	1.084	2.02	0.953
4-Nitrocatechol	1.113	2.56	0.809
5-Chloro-2-nitrovanillin	1.247	4.73	0.934
5-Nitrovanillin	1.260	1.79	0.895
4-Chloro-3-nitrosyringol	1.332	2.74	0.872
6-Nitrovanillin	1.351	1.01	1.090
3,5-Dinitroguaiacol	1.400	4.87	1.141
4,6-Dinitroguaiacol	1.466	2.01	1.142
6-Chloro-2-nitrovanillin	1.636	3.87	1.455
3,5-Dinitrosyringol	1.730	8.27	1.218
4,5-Dinitroguaiacol	1.782	2.07	1.822

Recommended analytical procedure

On the basis of the above investigations, we suggest the following steps for analysis of nitrophenolic compounds in aqueous samples: (i) extraction with *tert.*-butyl methyl ether, or adsorption onto a C_{18} Bond Elut column followed by elution with *tert.*-butyl methyl ether, (ii) derivatization of the nitrophenolic compounds by pyridine-catalysed acetylation with acetic anhydride following the detailed procedures provided and (iii) using known standard compounds, quantitative GC analysis of the organic extracts using a fused-silica DB-5-30N capillary column.

GC–MS analysis

Previous mass spectrometric studies have used underivatized samples[8]. For analysis and identification of environmental samples, however, this is not an ideal procedure. Such samples are generally contaminated with a large number of compounds other than those to be analysed so that inclusion of a separation stage before analysis is highly advantageous. This is conveniently combined with derivatization of specific functional groups, and considerable effort was therefore expended in finding suitable derivatives. They should fulfil the following criteria: (i) be produced in quantitative yield, (ii) be chemically stable for at least 20 h and (iii) yield structurally informative mass spectra.

It had been hoped that alkylation would provide stable derivatives: these would

be attractive for GC–MS analysis in the EI mode since the intensity of the parent ions would be greater than from the corresponding acetates. Alkylation, however, introduced a number of serious problems to which no satisfactory general solutions were found. Use of diazoalkanes, which has been successfully used by other workers for analysis of Dinoseb[7], was suitable only for nitrophenols themselves since a complex reaction with the aldehyde group of the nitrovanillins precluded its general use[16]. Among other alkylation reagents, diethyl sulphate in aqueous solution was unsuitable since it was found that, before GC–MS analysis, the excess of reagent must be removed and this could not readily be accomplished using ammonia or alkali without hydrolysis of the alkali-sensitive O-ethyl ethers. In order to solve simultaneously the problems of extraction and derivatization, attempts were made to use extractive alkylation procedures. Use of ethyl iodide and tetrabutylammonium hydroxide in dichloromethane resulted in rapid alkylation, but simultaneous hydrolysis of the O-ethyl ether occurred so that this was an unsuitable procedure for quantitative work. On the other hand, use of tetramethylammonium hydroxide was precluded due to ineffective transfer of the ion pair to the organic phase. We therefore reluctantly concluded that the compounds for analysis must first be extracted with an organic solvent, and then alkylated in dimethylformamide using the procedure detailed in the Experimental section. Even by this procedure, however, hydrolysis sometimes occurred although usually to a minor extent: for example, ethylation of 4,5-dinitroguaiacol produced small amounts of the catechol di-O-ethyl ether and this method was generally not effective for 2- and 4-nitro-substituted phenolic substances. The rapid rate of hydrolysis of the O-ethyl ethers clearly precluded this as a quantitative method. Other potentially suitable solvents such as dimethyl sulphoxide clearly cannot be used for the nitrovanillins due to reaction between the active methylene group of the solvent and the carbonyl group.

Detailed discussion of the mass spectra is not justified but we draw attention to points of diagnostic significance. The following conclusions may be drawn from examination of the EI spectra:

(i) The parent ions of the O-acetates were weak, in contrast to the relatively strong ones produced from the O-ethyl ethers.

(ii) *ortho*-Nitrophenols produced no M − 30 ion (loss of NO) from the O-acetates and no M − 16 (loss of O) ion from the O-ethyl ethers.

(iii) For the O-acetates, the base peak was generally that corresponding to M − 42 (loss of $COCH_2$) and for the O-ethyl ethers to M − 28 (loss of C_2H_4).

(iv) Ions at M − 30 (loss of NO) were observed only from the vanillin O-ethyl ethers, and an M − 46 ion (loss of NO_2) only from 3-nitrophenol O-ethyl ether.

(v) Base peaks of low m/z (63–155) were observed for a number of O-acetates, and for some of the vanillin O-ethers.

Our decision to examine NCI mass spectra was motivated by the fact that this procedure has been recommended for analysis of nitroaromatic hydrocarbons on account of its enhanced sensitivity[17], and was used in a comprehensive study of a variety of aromatic nitro compounds including some nitrophenols[9]. Our spectra for the O-acetates and the O-ethers of 2-nitro- and 2,4-dinitrophenol correspond closely to those published in the latter study. We therefore concluded that the two studies were compatible and that the interpretations given by these authors were valid for the compounds investigated by us.

As expected, the NCI spectra were less amenable to formulation of fragmentation patterns than the EI spectra, and those of the O-acetates and O-ethyl ethers were, in general, significantly different with two important exceptions: (i) M − 15 ions (loss of CH_3) were formed both from both the O-acetates and O-ethyl ethers of 3,5-dinitroguaiacol, 4,5-dinitroguaiacol, 3,5-dinitrosyringol, and 4-chloro-3-nitrosyringol, all of which have two strongly electron-attracting groups on the ring; (ii) 2-nitrovanillins had a base peak at M − 30. On the basis of the data presented, however, we are unable to distinguish between formation of this ion by loss of NO or by reduction of the nitro to an amino group[9,18]. The spectra of the O-acetates showed the following characteristics:

(i) *ortho*-nitrophenols had no parent ions and had base peaks at M − 59 (loss of $OCO–CH_3$) or 59 ($OCO–CH_3$),

(ii) M − 46 ions (loss of NO_2) were observed only from 5-chloro-2-nitro- and 6-chloro-2-nitrovanillin, and

(iii) M − 43 ions (loss of $CO–CH_3$) were characterististic of 4-nitrophenols (except 4,6-dinitroguaiacol).

A simpler pattern was found for the O-ethyl ethers: with the exception of the 2-nitrovanillins and the substituted syringols noted above, all compounds had base peaks either at M or M − 29 (loss of C_2H_5).

Both the EI and NCI spectra of 4,5-dinitroguaiacol O-acetate and O-ethyl ether were unique in having ions corresponding to M − 16, M − 32 and M − 48: these can be attributed to successive loss of oxygen atoms from the *ortho* nitro groups with ultimate formation of an isoxadiazole ring (M − 48). A similar fragmentation pattern has been reported for the EI spectrum of 2,3-dinitrofluoranthene[19].

Examples of spectra illustrating these points, and the specific influence of molecular structure on the fragmentation patterns, are given in Figs. 3–6. We

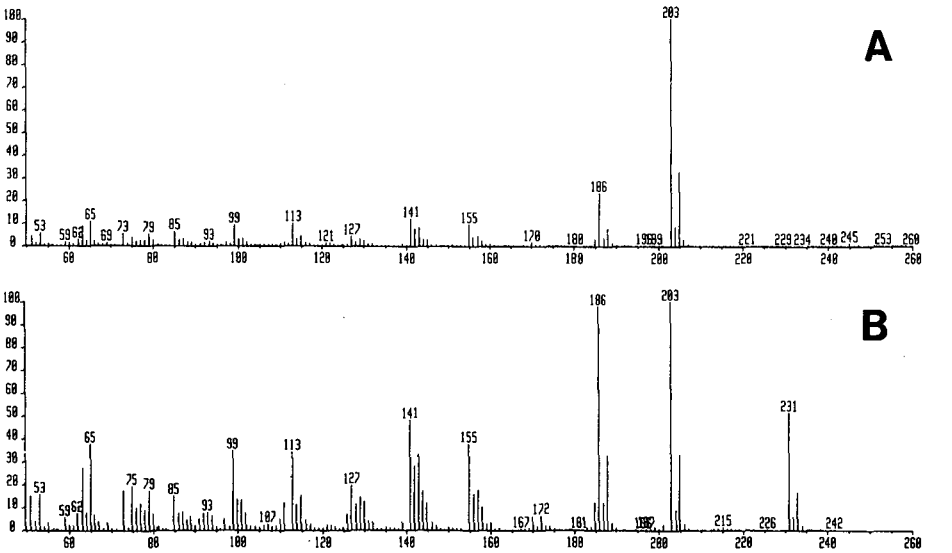

Fig. 3. Mass spectra (EI) of (A) 4-chloro-6-nitroguaiacol O-acetate and (B) 4-chloro-6-nitroguaiacol O-ethyl ether.

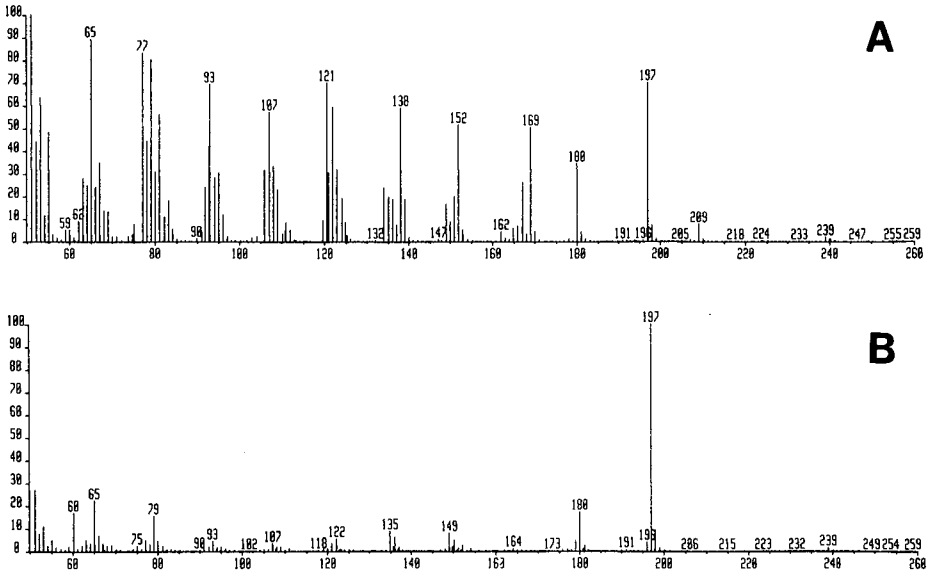

Fig. 4. Mass spectra (EI) of the O-acetates of (A) 2-nitrovanillin and (B) 5-nitrovanillin.

concluded that mass spectra provided a valuable basis for identification of the compounds examined in this study. The discrimination between isomers was clear-cut and contrasts with the situation in O-acetates of chlorophenols and chloroguaiacols. The strongly electron-withdrawing nitro group clearly played a significant rôle. Since, however, a complex array of fragmentation patterns was generally observed, this study emphasizes the need for access to reference compounds of known structure.

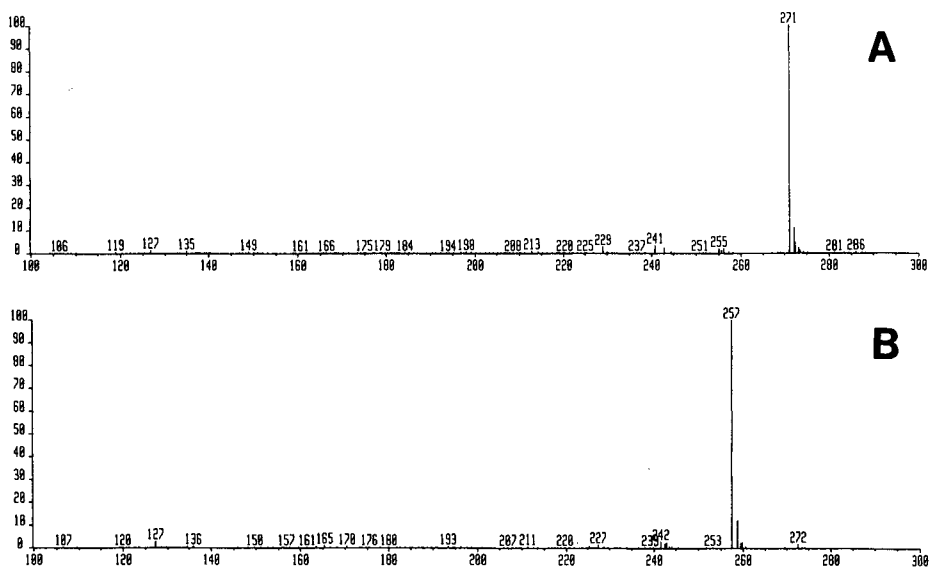

Fig. 5. Mass spectra (NCI) of (A) 3,5-dinitrosyringol O-acetate and (B) 3,5-dinitrosyringol O-ethyl ether.

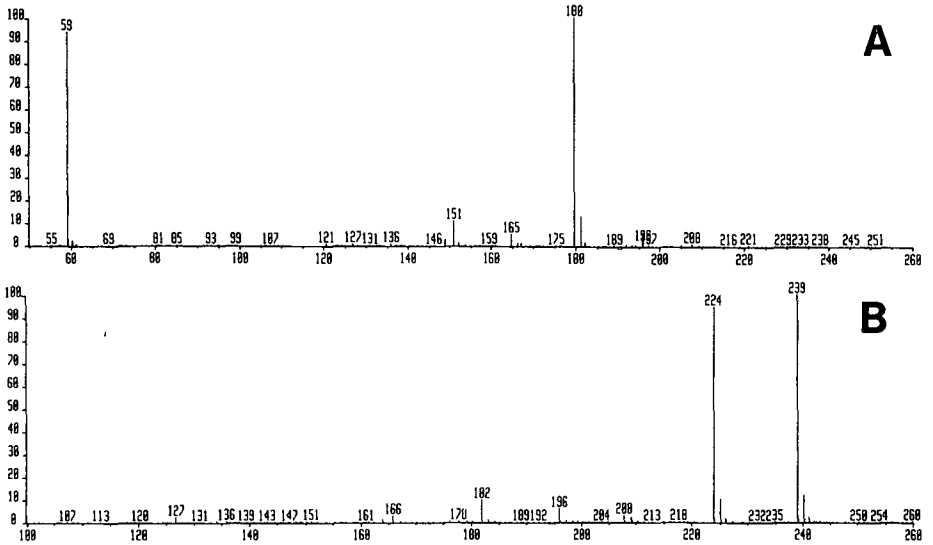

Fig. 6. Mass spectra (NCI) of the O-acetates of (A) 5-nitrovanillin and (B) 6-nitrovanillin.

General environmental significance

Nitrophenolic compounds are also of environmental significance in a wider context[20]. For example, some are employed as biocides or are used as starting material for their synthesis[21], while others may be formed by atmospheric nitration of phenolic compounds produced from aromatic hydrocarbons by reaction with hydroxyl radicals[22]: such compounds have been identified in rainwater[23] as well as in particulates collected from the atmosphere[24]. The methods developed in this study, modified as necessary, would clearly be applicable to the study of the environmental fate of these compounds also.

CONCLUSIONS

This study has provided experimental procedures for the quantitative analysis and identification of a structurally diverse range of nitrophenolic compounds in aqueous solutions. Attention is drawn to the following salient results.

(i) The susceptibility to hydrolysis of derivatives of some of the nitrophenolic compounds presented difficulties in their quantitative preparation. An optimum procedure for preparation of the O-acetates was developed, and it was shown that these derivatives were stable for at least 20 h at room temperature. Diazoethane cannot be used for preparation of the O-ethers of vanillins, and use of tetrabutylammonium hydroxide and ethyl iodide was not uniformly successful: these derivatives are not therefore suitable for quantitative analysis.

(ii) All test compounds were recovered from aqueous solutions either by extraction with *tert.*-butyl methyl ether, or by adsorption on C_{18} Bond Elut columns followed by elution with *tert.*-butyl methyl ether or, less desirably, acetone. Methanol cannot be used due to the ready formation of acetals from the nitrovanillins.

(iii) EI spectra of the O-acetates and O-ethyl ethers gave spectra displaying the expected fragmentation patterns although the parent ions of the former were usually weak, and the peak intensities of all ions were strongly dependent on the molecular structure: in particular, the EI spectra of compounds with nitro groups *ortho* to the O-acetyl or O-ethyl group were unique in failing to show M−30 and M−16 ions respectively. NCI spectra were structurally valuable even though a complex array of fragmentation patterns was found particularly for the O-acetates.

ACKNOWLEDGEMENTS

We thank the Knut and Alice Wallenberg Foundation for the provision of funds for purchase of the mass spectrometer.

REFERENCES

1 K. P. Kringstad and K. Lindström, *Environ. Sci. Technol.*, 18 (1984) 236A.
2 A.-S. Allard, M.Remberger, T. Viktor and A. H. Neilson, *Water Sci. Technol.*, 20 (1988) 131.
3 K. Abrahamsson, L. Löwendahl and O. Samuelson, *Sven. Papperstidn.*, 84 (1981) R152.
4 E. Hägglund, *Ark. Kemi Mineral. Geol.*, 7 (1918) 1.
5 K. Freudenberg and W. Dürr, *Chem Ber.*, 63 (1930) 2713.
6 C. Gustafsson and L.Andersen, *Pap. Puu*, (1955) 1.
7 S. F. Howard and G. Yip, *J. Assoc. Off. Anal. Chem.*, 54 (1971) 970.
8 T. A. Robert and A. N. Hagardorn, *J. Chromatogr.*, 276 (1983) 77.
9 E. A. Stemmier and R. A. Hites, *Biomed. Environ. Mass Spectrom.*, 14 (1987) 417.
10 L. C. Raiford and W. C. Stoesser, *J. Am. Chem. Soc.*, 50 (1928) 2556.
11 J. Ehrlich and T. Bogert, *J. Org. Chem.*, 12 (1947) 522.
12 L. C. Raiford and J. G. Lichty, *J. Am. Chem. Soc.*, 52 (1930) 4576.
13 A. H. Neilson, A.-S. Allard, P. Å. Hynning, M. Remberger and L. Landner, *Appl. Environ. Microbiol.*, 45 (1983) 774.
14 I. O. O. Korhonen and J. Knuutinen, *J. Chromatogr.*, 256 (1983) 135.
15 A.-S. Allard, M. Remberger and A. H. Neilson, *Appl. Environ. Microbiol.*, 49 (1985) 279.
16 C. D. Gutsche, in R. Adams (Editor), *Organic Reactions*, Vol. 8, Wiley, New York, 1954, p. 364.
17 T. Ramdahl and K. Urdal, *Anal. Chem.*, 54 (1982) 2256.
18 J. J. Brophy, V. Diakiw, R. J. Goldsack, D. Nelson and J. S. Shannon, *Org. Mass Spectrom.*, 14 (1979) 201.
19 T. Ramdahl, B. Zielinska, J. Arey and R. W. Kondrat, *Biomed. Environ. Mass Spectrom.*, 17 (1988) 55.
20 R. P. Schwarzenbach, R. Stiertl, B. R. Folsom and J. Zeyer, *Environ. Sci. Technol.*, 22 (1988) 83.
21 I. R. Hill and S. J. L. Wright (Editors), *Pesticide Microbiology*, Academic Press, New York, 1978.
22 R. Atkinson, J. Arey, B. Zielinska and S. M. Aschman, *Environ. Sci. Technol.*, 21 (1987) 1014.
23 C. Leuenberger, J. Czuczwa, J. Tremp and W. Giger, *Chemosphere*, 17 (1988) 511.
24 M. G. Nishioka, C. C. Howard, D. A. Contos, L. M. Bell and J. Lewtas, *Environ. Sci. Technol.*, 22 (1988) 908.

Journal of Chromatography, 467 (1989) 111–128
Elsevier Science Publishers B.V., Amsterdam — Printed in The Netherlands

CHROM. 21 274

MODIFIED ANALYTICAL TECHNIQUE FOR THE DETERMINATION OF TRACE ORGANICS IN WATER USING DYNAMIC HEADSPACE AND GAS CHROMATOGRAPHY–MASS SPECTROMETRY

ALEXANDER BIANCHI*
Exxon Chemical Co., Department of Environmental Affairs, Fawley, Southampton (U.K.)
MARK S. VARNEY
Department of Oceanography, University of Southampton, Southampton (U.K.)
and
JOHN PHILLIPS
Department of Earth Sciences, The Open University, Walton Hall, Milton Keynes (U.K.)
(First received October 3rd, 1988; revised manuscript received January 10th, 1989)

SUMMARY

In this paper we report a modified variant of the purge-and-trap gas chromatographic analysis of volatile organic carbon compounds in water. Samples collected in all-glass 1-l bottles are purged at 60°C for 1 h in an ultrapure helium gas stream using an open-loop arrangement. Volatile eluates are trapped onto selective adsorbents packed inside stainless-steel tubes connected in series. After stripping at a flow-rate of 100 ml min^{-1} for 60 min, the adsorbent tubes are disconnected, fitted with analytical desorption caps and sequentially desorbed for 10 min on a thermal desorber. The desorbed organics are trapped at −30°C on a packed cold trap prior to flash volatilisation of the volatiles across a fused-silica transfer line onto a capillary column.

The method separates over 200 organic compounds within 40 min utilising flame ionisation and ion trap detection and is capable of quantitation down to 5 ng l^{-1} per component. The results of a case study on the Solent estuary in southern England are briefly summarised.

INTRODUCTION

Over the past 10–15 years, concern over the quality of water resources has continued to intensify. The availability of clean water is fundamental to many of the activities of man both in terms of sufficiently pure domestic and unpolluted recreational supplies. Consequently, pressures continue to mount on environmental analysts to detect trace levels of many types of potentially harmful organic pollutants in lakes and estuaries. Many of these compounds arise from the use of surface and ground waters as sinks for industrial effluents and untreated sewage. In addition, a wide range of volatile organic compounds is generated by natural seasonal biogenic[1] processes and chemical reactions between man-made inputs and compounds occurring

0021-9673/89/$03.50

in nature[2]. As the complexity of environmental pollution develops, so the need for systematic and functionally complete analytical methods grows.

Dynamic non-equilibrium headspace analysis represents one of the most scientifically advanced techniques available for the detection of volatile organic micropollutants in water[3]. Recent research has restated the efficiency of the technique under stringent experimental conditions[4]. By performing analysis on a gas phase in thermodynamic equilibrium with the medium under study, it is possible to eliminate many of the disadvantages associated with preconcentration methods at low levels concentrations, *e.g.* ng l^{-1}. Consequently, unlike methods necessitating exensive preliminary procedures, dynamic headspace avoids overloading or contamination of the chromatographic column with water or high-boiling non-volatile compounds[3].

The closed-loop stripping apparatus developed by Grob and co-workers[5–8] represents one of the most powerful techniques developed for the rapid analysis of many types of organic compounds in water. The method has also been widely applied in a variety of reported studies concerning the trace analysis of organics in water samples[9–15]. However, the range of compounds that can be detected using closed-loop stripping is limited. Highly volatile components are lost within the extraction solvent peak, and moderate to highly polar species are inefficiently recovered using the method. The technique has been used to screen large numbers of compounds, but its outstanding concentration factor makes the system useful even when only a small number of compounds is of interest.

We have developed a modification of the open-loop stripping apparatus reported by Borén *et al.*[16]. Although open-loop stripping methods were initially developed by Bellar and Lichtenberg in 1974[17], the basic design continues to represent a practical and realistic alternative to closed-loop stripping. The method of stripping and trapping of analytes both in closed- and in open-loop arrangements have been reported as yielding good analytical results[4]. Whereas in a closed circuit the stripping–trapping process can be accomplished in either a conservation or an equilibration regime, conservation or pseudoequilibration modes are possible when utilising open-loop stripping. Fig. 1 illustrates the basic differences in layout. However, Borén *et al.*[16] reported an improved blank level, the minimisation of contamination by laboratory air and a minimum detection limit at least equal to that achieved by closed-loop stripping methods when using an open-loop arrangement. Drozd *et al.*[4] have stated that when working with an open arrangement, better results are obtained by conservation trapping. This observation has been confirmed by the authors' experience in developing this method.

Several purge-and-trap methods reported rely on the solvent desorption of organics adsorbed onto a charcoal filter bed[5,8,18,19]. However, this method has limitations which must be taken into account where it is applied. Problems include a strong affinity for water, which is frequently found in headspace vapour samples and affects the adsorption properties, an excessive surface activity (activated charcoal) or the presence of large numbers of active sites for polar compounds (graphitized sorbents) which makes their use limited due to irreversible adsorption or decomposition problems. Additional problems include masking of highly volatile compounds by the solvent peak, the increased potential for artefacts generated through impure solvent preparation, and thermal decomposition of unstable organic compounds where high thermal desorption temperatures have to be used. Further

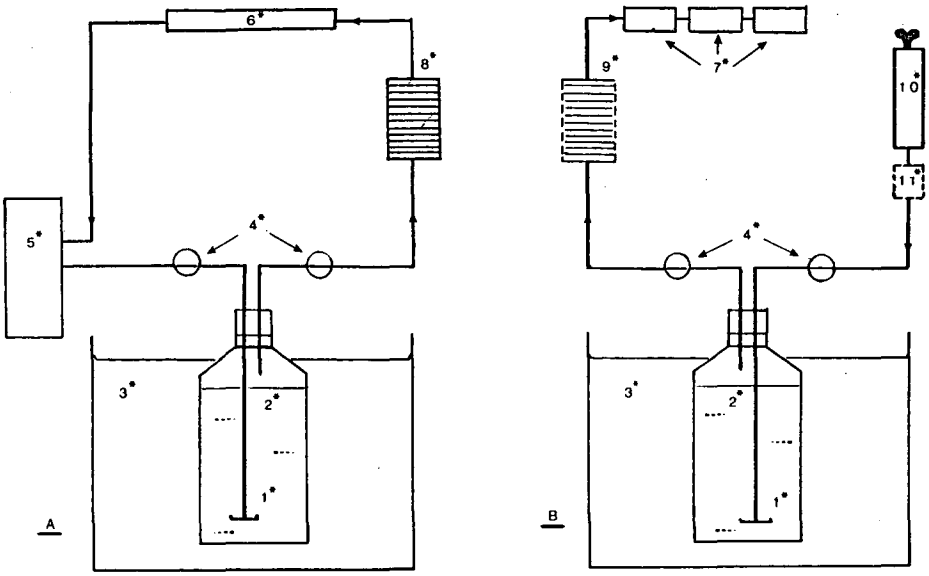

Fig. 1. Diagrammatic representation of (A) closed-loop stripping apparatus and (B) open-loop stripping apparatus. 1 = Gas sparger; 2 = water sample; 3 = thermostatically controlled water bath; 4 = glass–metal union connectors; 5 = pump; 6 = organic vapour adsorbent trap (activated charcoal); 7 = organic vapour adsorbent trap-train; 8 = tube heater unit; 9 = tube heater unit (optional); 10 = purge gas supply (ultrapure); 11 = gas filters (optional).

criticisms have been made against the use of activated charcoal, *i.e.* random variability in experimentally derived minimum detection limits and poor recovery performance at ppb[a] concentration levels[20]. However, it has been recognised that activated carbon or graphitized sorbents remain a suitable choice for exceptionally volatile compounds where porous polymers have insufficient sampling capacity and allow such compounds to break through[11], *e.g.* C_2 to C_4 species. The application of organic polymeric sorbents as alternative trapping media for headspace volatiles has increased significantly during the last decade, as they eliminate many of the drawbacks encountered using activated charcoal or graphitized sorbents. They have a low capacity for water and do not display irreversible adsorption or decomposition phenomena in general use[21]. Accordingly, there have been a number of chromatographic reviews assessing the value of polymeric substances[22–27], particularly Tenax-GC [poly(2,6-diphenyl-*p*-phenylene oxide)] and a modified, improved variant, Tenax-TA, which further minimises the generation of low-level artefacts in continuous use[28]. Nevertheless, although good analytical results have been achieved, the use of a single adsorbent has led to compromise in the retention of compounds covering a wide boiling-point range, with highly volatile compounds being poorly retained on some adsorbents, *e.g.* Tenax-TA, resulting in breakthrough and component loss[21] and higher boiling compounds being incompletely recovered from other adsorbents, *e.g.* Chromosorb Century Series. We have experimented with the application of a combination of

[a] Throughout this paper the American billion (10^9) is meant.

adsorbents in the quantitative trapping of volatile organic compounds from water, ranging from C_4 to C_{20} compounds. The modified method avoids component loss and contamination problems associated with extraction solvents and is capable of analysing either for specific groups of compounds, *e.g.* volatile organohalogens, or performing broader analyses of a wide range of volatile and semi-volatile organics found in rivers and estuaries. Used in conjunction with thermal desorption techniques, the method forms part of a high-performance, semi-automated integrated analytical system[29].

EXPERIMENTAL

Chemicals and adsorbents

Standards were prepared using analytical-grade materials (Aldrich, Wimborne, U.K.). Stock standard mixtures encompassing a range of compound classes were blended gravimetrically in all-glass vessels according to certified CONCAWE[30] and U.S. Environmental Protection Agency (EPA)[31] methods. Replicate standards containing organic compounds varying in boiling point from *n*-pentane to eicosane were made up to 1-l volumes in volumetric flasks, inverted and spiked via aluminium-coated poly(tetrafluoroethylene) (PTFE) septa with *n*-butane and 1,3-butadiene gas mixtures (Air Products Specialty Gases, Bracknell, U.K.) using gas-tight syringes.

Blank seawater volumes were prepared by solvent extracting seawater taken from a relatively unpolluted coastal site. Following extraction of solvent-extractable organics into re-distilled dichloromethane [Aldrich, high-performance liquid chromatography (HPLC)-grade, >99.99% purity after re-distillation], seawater aliquots (2 l) were purged overnight with ultrapure nitrogen (grade 5.5) at 500 ml min^{-1} to remove any further organic compounds. Secondary blank seawater was prepared by spiking AnalaR-grade distilled water (BDH, Poole, U.K.) with a heat-treated sea-salt mixture to simulate natural seawater (Instant Ocean, OH, U.S.A.) followed by nitrogen purging. Heat treatment of the sea-salt for 60 min in a clean laboratory oven held at 250°C was utilised to remove any contaminative volatile material present within the sea-salt mixture.

Seawater standards were prepared by chilling 1-l volumes of blank seawater to 4°C, followed by gravimetric addition of stock standard mixtures via hypodermic syringes (SGE, Milton Keynes, U.K.) under zero headspace. The specially made all-glass vessels (Hampshire Glassware, Southampton, U.K.) were then shaken for 10 min on a two-dimensional shaker (Turbula, Geneva, Switzerland), immediately followed by headspace extraction analysis.

The internal standards, 1-chlorohexane, 1-chlorooctane and 1-chlorodecane, were blended gravimetrically into re-distilled isopentane and stored in sealed glass flasks (10-ml volumes) under an ultrapure nitrogen blanket. Internal standards were prepared freshly each day.

Adsorbents

Tenax-TA (60–80 mesh), packed into $\frac{1}{4}$-in. O.D. pre-cleaned stainless-steel tubing was conditioned by heating at 30°C for 10 min in a stream of oxygen-free pre-filtered nitrogen at 15 ml min^{-1}. The packed tubing was then connected via

a Swagelock connection to the packed-column injector inside a gas chromatograph oven. After 10 min, the temperature was raised at 8°C min^{-1} to 350°C, held for 1 h. Maintaining the gas flow, it was cooled to 200°C and conditioned at this temperature overnight prior to packing into adsorbent tubes.

Chromosorb 106 (60–80 mesh), a non-polar resinous hard granular solid, was packed into $\frac{1}{4}$-in. stainless-steel tubing, and then heated from room temperature to 250°C at 8°C min^{-1} in a 15-ml min^{-1} flow of pre-filtered nitrogen. After 16 h at 250°C, the Chromosorb 106 was cooled and immediately packed into adsorbent tubes[32].

Spherocarb (60–80 mesh), a hard, non-friable molecular sieve, was conditioned according to the protocol for Chromosorb 106.

In Table I a summary is given of individual adsorbent physical properties. All adsorbents were supplied by Perkin-Elmer.

Sampling apparatus

The purge-and-trap stripping apparatus consisted of an all-glass 1-l bottle (nominal capacity, 1150 ml). A modified dreschel-head assembly incorporating a ground glass collar (19/24 mm) was inserted into the ground glass neck of the sample bottle (19/24 mm) and locked using a PTFE cage (Fig. 2).

Ultrapure nitrogen was metered via a metal–glass joint into a 7-mm O.D., 7-cm length of glass tubing fabricated onto the inlet of the purge head assembly. The internal glass tubing of the inlet purge head was fitted with a medium porosity frit (Grade 1) reaching to a depth of 2 cm from the base of the sample vessel. The exit flow glass tubing was lengthened to 12 cm, in order to accommodate a heated-clamp assembly capable of heating a 7-cm length of the glass tubing up to temperatures exceeding 250°C (Bastock Marketing, Oxon, U.K.). This unit, an optional addition to the apparatus, minimises the formation of condensing water droplets on the inner walls of the exit tubing.

Three adsorbent tubes, 90 mm × 5 mm I.D. [automated thermal desorber (ATD)-50 compatible, Perkin-Elmer, Beaconsfield, U.K.] of pre-cleaned stainless-steel fabrication, were packed and connected in series using standard $\frac{1}{4}$-in.–$\frac{1}{4}$-in. stainless-steel Swagelock connections and $\frac{1}{4}$-in. PTFE ferrules. The assembled tubes were located via a leaktight PTFE sealing washer into the exit point of the purge head assembly and locked using a PTFE collar. Prior to assembly, the tubes were packed

TABLE I

PHYSICAL PROPERTIES OF ADSORBENTS USED IN THE MODIFIED METHOD FOR PRE-CONCENTRATION OF TRACE VOLATILE ORGANICS

Sorbent	*Composition*	*Specific surface area (m^2/g)*	*Mean pore diameter (Å)*	*Temperature limit (°C)*
Tenax-TA (60–80 mesh)	Poly(2,6-diphenyl-*p*-phenylene oxide)	19–30	720	375
Chromosorb-106 (60–80 mesh)	Polystyrene, non-polar cross-linked resin	600–800	50	250
Spherocarb™ (60–80 mesh)	Molecular sieve, a hard, non-friable carbon	1200	15	300

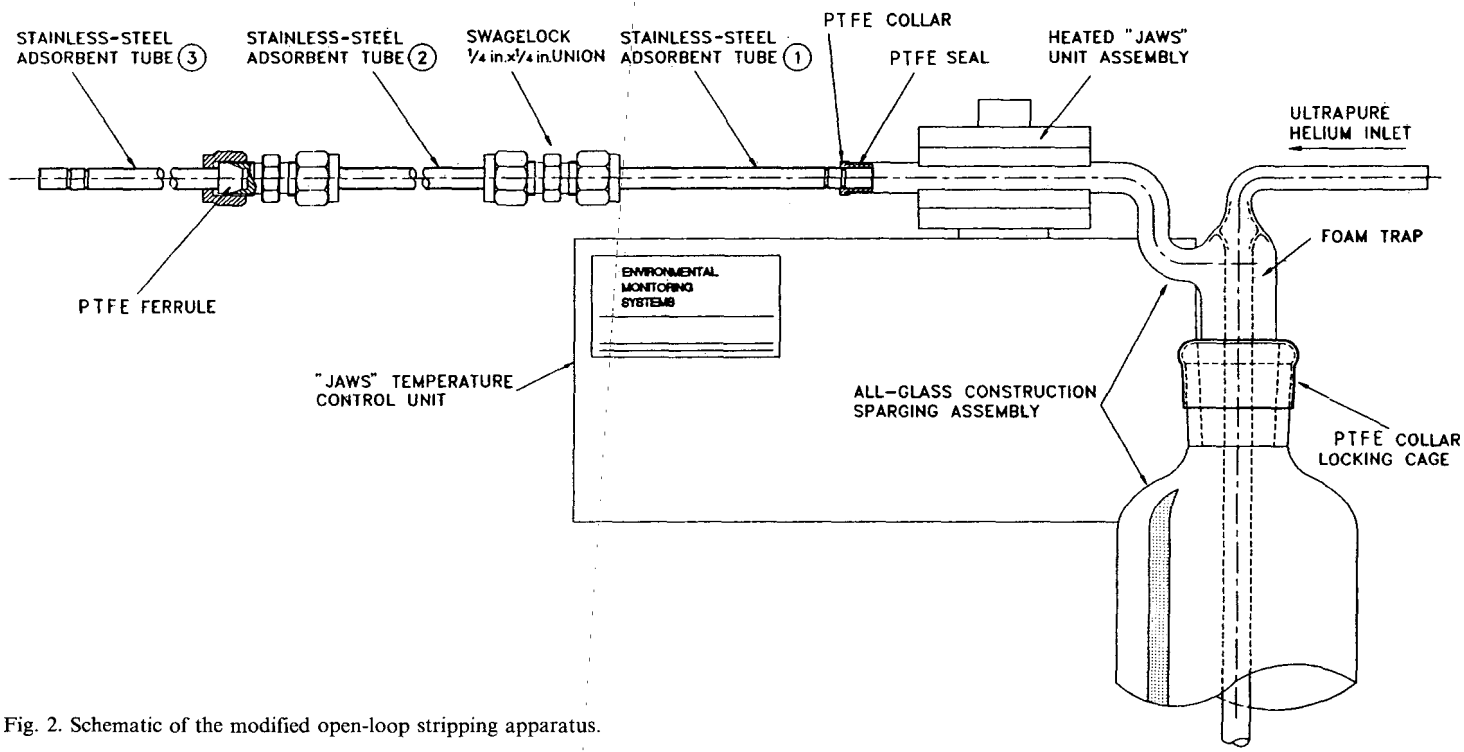

Fig. 2. Schematic of the modified open-loop stripping apparatus.

with 70 ± 5 mg of conditioned Tenax-TA (60–80 mesh), and held in place using stainless-steel gauge frits and silanised glass wool. The glass stripping vessel was then immersed into a thermostatically controlled water bath (Grant Instruments, Cambridge, U.K.) to vessel depth, allowing 15 min for thermostatic equilibrium to be attained.

Instrumentation and capillary column

An ATD-50 was connected to a Model 8310 gas chromatograph (Perkin-Elmer) via a 1-m length of deactivated fused-silica transfer line, 0.22 mm I.D., held at 150°C. The ATD-50 is a multi-functional instrument the principal role of which is for the analysis of organic vapours at very low concentrations (sub-ppm)[33]. A two-stage desorption facility is available whereby organic compounds desorbed from adsorption tubes at 150°C are re-trapped inside an electronically cooled cold trap, packed with a secondary adsorbent at temperatures down to −30°C. Retention of the sample vapours inside the cold trap therefore depends on chromatographic factors rather than condensation[33]. The trap is then heated at a rate exceeding 1000°C min^{-1} to a defined upper limit of 300°C, sending a discrete band of concentrated sample through the fused-silica transfer line to the gas chromatographic (GC) capillary column.

The gas chromatograph was fitted with a cradle-mounted, 50 m × 0.22 mm I.D. BP-1 wall coated open-tubular fused-silica capillary column, 0.5 μm film thickness (SGE). The exit point of the column was connected to a twin-hole split ferrule (Chrompack, London, U.K.) allowing 50% of the column eluent to be routed to a flame ionisation detector. The remaining 50% is swept via a second 1-m length of transfer line at 250°C into an ion trap detector–mass spectrometer[34] (Finnigan MAT, U.K.).

Analytical operating parameters. The final selected GC system conditions instituted were as follows. Carrier gas: ultrapure helium 5.5 grade (Air Products). ATD-50: cold-trap packing, 20 mg Tenax-TA; cold trap low temperature, −30°C; cold trap high temperature, 250°C; split ratio (combined), 200:1; desorption box temperature, 150°C; desorption oven temperature, 250°C; desorption time, 10 min; carrier gas pressure, 25 p.s.i.

Gas chromatograph. Detector temperature, 300°C; carrier gas flow-rate, 1 ml min^{-1}. Temperature conditions: oven temperature, 40°C; isothermal time 1, 10.5 min; ramp rate 1, 5°C min^{-1}; oven temperature 2, 95°C; isothermal time 2, 0.1 min; ramp rate 2, 15°C min^{-1}; oven temperature 3, 235°C; final hold time, 15 min.

Ion trap detector. Ionisation voltage, 70 eV; seconds/scan, 1.0; mass range, 25–250 mass units; transfer temperature, 250°C; ion source temperature, 250°C; multiplier delay, 200 s; mass defect, 100 m.m.u./100 a.m.u.; acquire time, 50 min.

Flame ionisation chromatograms were interpreted by reference to retention indices, and retention times derived from comparison with pure co-injected standard mixtures. Mass spectra were interpreted by comparison with a National Bureau of Standards and General Purpose computerised mass spectral library stored on hard Winchester disk drive (supplied by Finnigan MAT). We also utilised a library of mass spectra kept on laboratory files and co-injected standard reference spectra subsequently stored on a user-defined library within the ion trap detector computer. (Epson PC AX, 40 Mbyte)

Analytical procedure

Known aliquots of multicomponent stock standards were used to prepare fresh seawater standards on a daily basis over a range of concentration from 5 ng l^{-1} per component to 500 μg l^{-1} per component.

The effect of several key analytical variables on the analytical system were examined experimentally. A standard containing approximately 5–15 μg l^{-1} of each component was prepared, and the selective influence of stripping temperature, stripping time and flow-rate investigated.

Temperature: Standards were initially stripped at a flow-rate of 100 ml min^{-1} at 30°C over several time periods. At a strip time of 60 min (which preliminary analyses had indicated as the optimum for many low-boiling compounds), we logged recovery percentages at 10°C temperature increments up to 90°C.

Time: Standards were stripped at 7.5-, 15-, 30-, 60- and 120-min intervals at a flow-rate of 100 ml min^{-1} and 60°C.

Flow-rate: Flow-rates between 50 ml min^{-1} and 500 ml min^{-1} were experimented with in order to determine the effect of flow-rate on recovery.

The trapping efficiency of the adsorbent train was investigated by preparing three Tenax-TA tubes in series according to Bertsch *et al.*[21] and purging standards at optimised experimental parameters, *i.e.* 100 ml min^{-1}, and 60°C for 1 h. Each tube was disconnected after purging and individually thermally desorbed and analysed. The recovery (%) of each component on each tube was quantitated and logged. Repeat experiments using a fourth Tenax-TA tube in series was used in order to detect breakthrough of volatile components.

We decided to evaluate different adsorbents using the model standards in order to achieve improved selective trapping of volatile organics and minimise breakthrough[3]. We repeated the experiments using more powerful adsorbents by substituting Chromosorb 106 into the second tube, Spherocarb into the third tube and retaining Tenax-TA in the first tube. A fourth tube was double-packed containing a mixture of Tenax-TA and Chromosorb 106 (50:50) in order to detect breakthrough.

RESULTS AND DISCUSSION

The results of these basic experiments showed that temperature, stripping time and purge flow-rates all influence the recovery of organic compounds.

Although recoveries in excess of 50% were achievable for many compounds at 30°C, total recoveries increased over a broad range of compounds including alcohols and ketones as strip temperature was increased. Recoveries for a wide range of compounds, *e.g.* volatile aromatics, organochlorines and low-molecular-weight alkanes reached a maximum at 60°C. These data are presented in Table II.

The effect of varying the stripping time (at 60°C and 100 ml min^{-1} flow-rate) of a standard containing seven key compounds found in contaminated coastal seawater samples is shown in Fig. 3, and exemplifies the variation in recovery percentages we obtained as a function of time.

Flow-rates above 250 ml min^{-1} were found to generate excessive back pressure inside the purging assembly due to resistance from the purge frit, sample and adsorbent train. It was noted that differences of $< 1\%$ recovery were obtained when flow-rates between 50 and 200 ml min^{-1} were used. At 100 ml min^{-1} the vigorous dispersion of

TABLE II

RECOVERIES OF MODEL ORGANIC COMPOUNDS FROM WATER AT 30 AND 60°C

Conditions: Nitrogen flow-rate, 100 ml min^{-1}; sampling time, 60 min; water volume, 1 l.

Compound	*Molecular mass*	*Boiling point (°C)*	*Recovery (%)*	
			30°C	*60°C*
n-Pentane	72.1	35	88	103
n-Hexane	86.2	69	86	102
n-Heptane	100.2	98	86	101
n-Octane	114.2	125–127	85	101
n-Nonane	128.2	151	83	99
n-Decane	142.3	174	83	99
n-Undecane	156.3	196	82	98
n-Dodecane	170.3	216	81	97
n-Tridecane	184.4	234	80	95
n-Tetradecane	198.4	254	77	92
n-Pentadecane	212.4	270	73	89
n-Hexadecane	226.5	287	70	87
n-Heptadecane	240.48	302	66	85
3-Methyl-1,3-butadiene	68.1	34	77	95
2,2-Dimethylbutane	86.2	49.7	52	84
2,3-Dimethylbutane	86.2	57.9	50	85
2-Methylpentane	86.2	62	65	93
3-Methylpentane	86.2	64	65	93
Cyclopentane	70.1	50	73	95
2,2,4-Trimethylpentane	114.2	98	70	90
2,4,4-Trimethylpentene-2	112.2	102	77	96
2,4,4-Trimethylpentene-1	112.2	104	77	96
Benzene	84	79	93	102
Methylbenzene	92.1	111	87	101
1,3-Dimethylbenzene	106.2	139	87	100
1,2-Dimethylbenzene	106.2	144	88	99
Ethylbenzene	116.2	135	89	114
Isopropylbenzene	120.2	153	85	100
n-Propylbenzene	120.2	159	84	99
1,2,3-Trimethylbenzene	120.2	176	84	99
1,2,4-Trimethylbenzene	120.2	168	83	92
1,3,5-Trimethylbenzene	120.2	163	80	92
1,2,3,4-Tetramethylbenzene	134.2	205	79	89
1-Methyl-2-ethylbenzene	120.2		65	79
1,2-Dichlorobenzene	147	179	90	104
Dichloromethane	86.95	40	92	106
Chloroform	120.39	61	94	99.5
1,1,1-Trichloroethane	133.4	75	95	110
Trichloroethylene	131.4	86.9	95	107
Bromodichloromethane	163.8	87	93	101
Trichlorofluoromethane	137.37	23.7	100	107
Chloroethane	64.52	12.5	98	105
1,1,2-Trichlorotrifluoroethane	187.4	47	98	106

(Continued on p. 120)

TABLE II *(continued)*

Compound	*Molecular mass*	*Boiling point (°C)*	*Recovery (%)*	
			30°C	*60°C*
Dimethylsulphide	62	38	79	99
Dimethyldisulphide	94.2	109	80	97
2-Methylthiophene	98.2	113	80	96
Ethanol	46	78	59	87
Propanol-2	60	82	59	87
tert.-Butanol	75	118	58	84
n-Butanol	75	118	58	84
2-Butanol	74	98	59	85
Propanal	58	46–50	79	91
Pentanal	86.1	103	78	90
Heptanal	114.2	153	75	90
Benzaldehyde	106	179	70	91
2-Butanone	72.1	80	48	89
2-Pentanone	86.1	101	48	88
2-Heptanone	114.2	150	46	85
2-Decanone	156	211	65	72
Methyl isobutyl ketone	100	118	57	90
Naphthalene	128.2	217	60	97
Indene	116.6	182	71	100
1,3-Dimethylnaphthalene	156.2	263	57	94
1,2-Dimethylnaphthalene	156.2	266–267	58	94
2-Methylfuran	82.1	63–66	81	94
2,5-Dimethylfuran	96.1	92–94	74	93
1-Chloroheptane	134.7	159–161	92	101
1-Chlorodecane	176.7	183	93	101
1-Chlorooctane	148.68	223	94	104
2-Methylbutane	72.2	30	95	102
1,3-Butadiene	54.09	−4.5	100	103
cis-Butene-2	56.11	3.7	100	101
trans-Butene-2	56.11	1	97	101
1-Butene	56.11	−6.3	99	102

gas bubbles through the sample was achieved allowing maximum gas–sample contact without generating excessive internal pressure which could precipitate leaks.

Where Tenax-TA tubes were used in series according to the protocol of Bertsch *et al.*[21], the recovery percentages are shown in Table III. The resulting improvements in recoveries obtained by substituting the second Tenax-TA tube with Chromosorb 106 and the third Tenax-TA tube with Spherocarb are shown in Table IV.

Zero breakthrough of the standard compounds was observed from analysis of the third tube up to individual concentrations of 500 $\mu g\ l^{-1}$ per component. It was found that by utilising such progressively stronger adsorbents, with an increasing

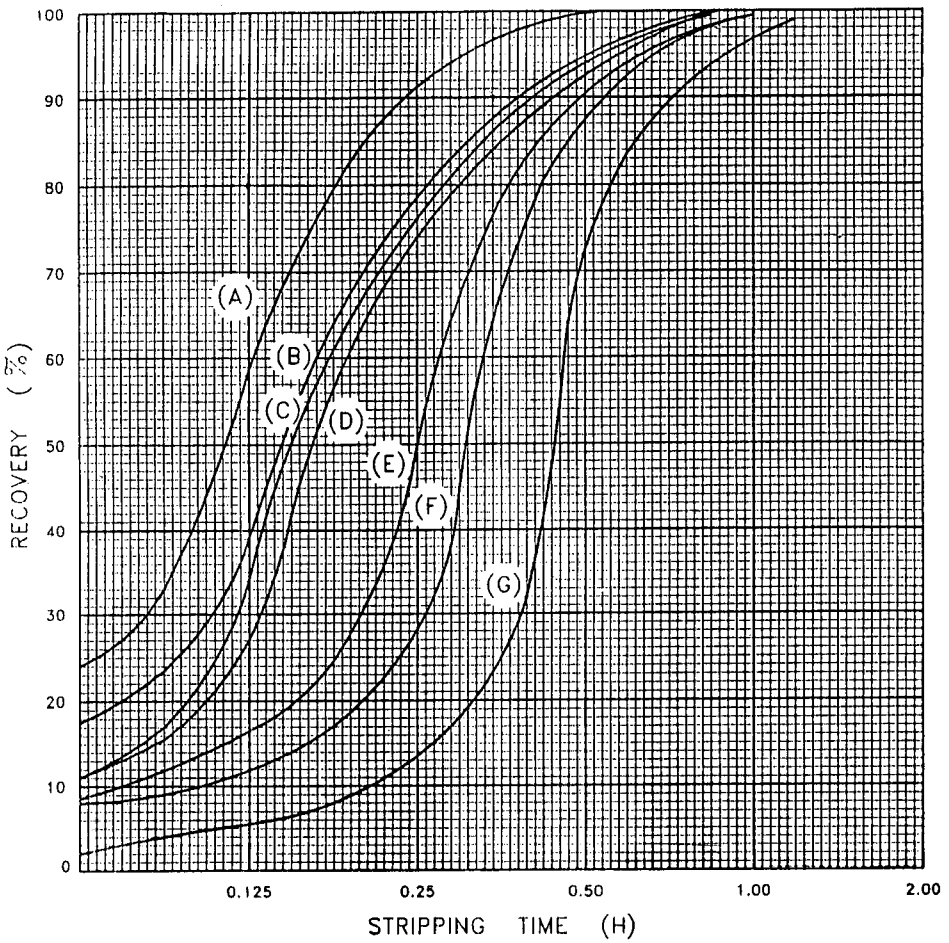

Fig. 3. Experimental effects of stripping time on the recovery of seven different compounds at 60°C and a flow-rate of 100 ml min^{-1}. (A) 1,2-Dichlorobenzene; (B) benzene; (C) methylbenzene; (D) 1,3-dimethylbenzene; (E) trichloromethane; (F) *n*-nonane; (G) naphthalene.

retention volume capacity for volatile compounds, extremely volatile compounds such as light hydrocarbons (which break through porous polymer sorbents) were efficiently retained *i.e.* on Spherocarb. Further, the comparitively poor trapping of alcohols, ketones and lighter substituted alkanes, *e.g.* 2,2-dimethylbutane, on Tenax-TA was overcome by employing Chromosorb 106, as predicted by Murray[32]. Components of higher molecular weight and boiling point were found to be efficiently retained by Tenax-TA.

The relative differences in the volatility and physicochemical properties of many organic compounds found in surface waters complex the analytical task. The results achieved by the application of a multi-sorbent trapping apparatus have yielded complete recovery of compounds varying in volatility from *n*-butane to eicosane. The combination of sorbents minimises overloading which may be encountered when

TABLE III

BREAKTHROUGH CAPACITIES OF TENAX ADSORBENT TUBES FOR VARIOUS COMPOUNDS

Conditions: Nitrogen flow-rate, 100 ml min^{-1}; sampling time, 60 min; air temperature, 20°C; tube dimensions, 90 × 5 mm I.D.; 60–80 mesh; strip temperature, 60°C.

Compound	*Recovery (%)*			
	Tenax, tube 1	*Tenax, tube 2*	*Tenax, tube 3*	*Breakthrough loss*
n-Butane	5.3	10.0	15.9	68.8
1,3-Butadiene	17.2	28.7	18.5	35.6
n-Pentane	57.8	32.9	6.6	2.7
3-Methyl-1,3-butadiene	23.9	54.5	12.7	8.9
Dichloromethane	19.1	28.3	47.6	5.0
Dimethylsulphide	84.2	12.7	2.2	0.9
tert.-Butanol	29.0	33.7	33.4	3.9
2,2-Dimethylbutane	33.7	38.5	26.1	1.7
3-Methylpentane	40.1	49.3	10.4	0.2
Trichloromethane	81.5	8.3	6.1	4.1
2-Butanone	29.3	50.8	13.6	6.3
2-Methyl-pentane-1	42.2	53.2	3.7	0.1
Benzene	85.7	10.5	3.7	0.1
Pentanal	63.2	27.5	7.5	1.8
n-Heptane	90.0	8.3	1.3	0.4
Methylbenzene	89.9	7.8	2.2	0.1
n-Octane	79.1	15.6	5.2	0.1
Chlorobenzene	68.3	24.9	6.8	–
Ethylbenzene	85.6	13.5	0.9	–
1,2-Dimethylbenzene	88.8	10.7	0.3	0.2
n-Nonane	82.5	17.3	0.2	–
n-Propylbenzene	92.7	6.9	0.4	–
Benzaldehyde	75.3	20.1	4.6	–
1,2,3-Trimethylbenzene	96.0	3.3	0.7	–
1,2,3,4-Tetramethylbenzene	96.9	3.1	–	–
Naphthalene	96.3	3.7	–	–

employing a single tube, with organic eluates, and potential interferences which may occur between the sorbates on a single tube. Indeed, if there are great differences in the sorbabilities of the trapped components, and some of the components are sorbed so strongly as to precipitate displacement of the less strongly sorbed components, the latter will be subjected to displacement rather than frontal chromatography. Components that form displacement zones during the trapping process will be pushed out of the trapping column and consequently only small amounts of such components will be recovered from the trap tube in the state of final equilibration. With conservation trapping such effects are not as significant as compared to equilibration trapping, where the components are lost for analysis. Nevertheless, with multi-sorbent trapping, any displaced components are re-trapped on the subsequent tube and therefore retained for desorption analysis. A specimen purge standard chromatogram (Tenax-TA tube) is shown in Fig. 4.

Strict adherence to method parameters was found to be essential for precise

TABLE IV

BREAKTHROUGH CAPACITIES OF TENAX, CHROMOSORB-106, AND SPHEROCARB ADSORBENT TUBES FOR VARIOUS COMPOUNDS

Conditions: Nitrogen flow-rate, 100 ml min^{-1}; sampling time, 60 min; air temperature, 20°C; tube dimensions, 90 × 5 mm I.D.; 60–80 mesh, each tube; strip temperature, 60°C.

Compound	*Recovery (%)*		
	Tenax, tube 1	*Chromosorb 106, tube 2*	*Spherocarb, tube 3*
n-Butane	6.9	39.7	53.4
1,3-Butadiene	17.7	43.3	39.0
n-Pentane	56.1	40.4	3.5
3-Methyl-1,3-butadiene	22.4	75.5	2.1
Dichloromethane	18.5	80.7	0.8
Dimethylsulphide	84.5	15.5	–
tert.-Butanol	27.4	70.7	1.9
2,2-Dimethylbutane	33.0	64.4	2.6
3-Methylpentane	40.7	58.5	0.8
Trichloromethane	80.1	19.8	0.1
2-Butanone	29.7	68.3	2.0
2-Methylpentene-1	42.0	57.8	0.2
Benzene	85.7	14.3	–
Pentanal	62.9	36.4	0.7
n-Heptane	90.4	9.6	–
Methylbenzene	90.1	9.8	0.1
n-Octane	79.5	20.5	–
Chlorobenzene	68.7	31.3	–
Ethylbenzene	85.7	14.3	–
1,2-Dimethylbenzene	88.0	12.0	–
n-Nonane	82.9	17.1	–
n-Propylbenzene	91.5	8.5	–
Benzaldehyde	75.2	24.8	0.2
1,2,3-Trimethylbenzene	96.7	3.3	–
1,2,3,4-Tetramethylbenzene	96.7	3.3	–
Naphthalene	96.1	3.9	–

operation of the method, *i.e.* temperature and strip time. The repeatability of the system method (expressed as the coefficient of variation, %) was within 2% for all components, except *n*-butane (5.8%) and 1,3-butadiene (4.9%). The optimum recovery of many environmentally important components, *e.g.* benzene, methylbenzene (toluene) and ethylbenzene (EPA-listed priority pollutants)[35] approached maximum at 60 min stripping time and 60°C strip temperature. Alcohols and ketones were less efficiently recovered, being more hydrophilic and polar. For the more volatile ketones, however, *e.g.* 2-butanone, recoveries greater than 80% were achieved.

Further increases in high-performance capillary column separation of light hydrocarbons, *i.e.* C_2, C_3 and C_4 gases, can be achieved by subjecting the Spherocarb tube (upon which the majority of light hydrocarbons are retained) to a modified sub-ambient method devised by Bianchi and Cook[36] using identical desorption parameters and chromatographic capillary column but operating the column isothermally at −35°C.

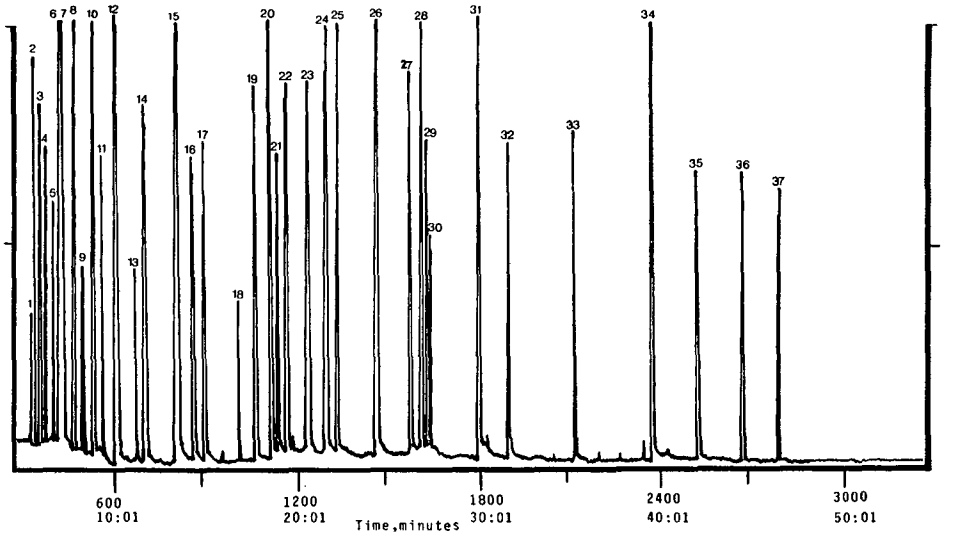

Fig. 4. Specimen purge seawater standard chromatogram obtained from Tenax-TA tube. Peaks: 1 = *n*-Pentane; 2 = 3-methyl-1,3-butadiene; 3 = dimethyldisulphide; 4 = 1,1,2-trichloro-1,2,2-trifluoroethane; 5 = 2,2-dimethylbutane; 6 = methyl *tert.*-butyl ether; 7 = 2-methylpentane; 8 = methylcyclopentane; 9 = 1,2-dichloroethane; 10 = benzene; 11 = thiofuran; 12 = *n*-heptane; 13 = 2,4,4-trimethylpentane; 14 = 1,1,2-trichloroethane; 15 = methylbenzene; 16 = hexanal; 17 = 1,2-dibromoethane; 18 = tetrachloroethylene; 19 = chlorobenzene; 20 = 1-chlorohexane; 21 = ethylbenzene; 22 = 1,3-dimethylbenzene; 23 = 1,2-dimethylbenzene; 24 = *n*-nonane; 25 = isopropylbenzene; 26 = 1,3,5-trimethylbenzene; 27 = 2-phenylbutane; 28 = 1,2,3-trimethylbenzene; 29 = indene; 30 = (+)-limonene (optically active); 31 = *n*-undecane; 32 = 1,2,3,4-tetramethylbenzene; 33 = 1-chlorodecane; 34 = *n*-tetradecane; 35 = 1,4-dimethylnaphthalene; 36 = *n*-hexadecane; 37 = *n*-heptadecane.

The modified stripping method is now routinely used in two industrial-environmental laboratories and a university laboratory. It has proved reliable in use, having been applied to the analysis of several hundred wastewater, riverine and estuarial water samples and recently for domestic water quality studies.

The Solent estuary —a case study

The Solent estuary forms a body of water separating the Isle of Wight from the submerged channel of Southampton Water on the coastline of central southern England. The sub-estuary of Southampton Water, a semi-industrialised water stretch accomodating an extensive range of activities including petrochemical processing, large-scale electric power generation and intense boating and marine operations, has become a major sink for many of the waste products associated with such activities. In addition the estuary receives wastes from water treatment plants and agricultural run-off which have recently been the topic of a separate study programme[37]. Analysing the total volatile organic content of the estuarine water presents difficulties as individual component numbers frequently in excess of 200 separate compounds have been recovered from a single sample. A specimen chromatogram from the head of the estuary is shown in Fig. 5a. (The respective purge blank chromatogram is also shown, in Fig. 5b.) Organic classes identified include alkanes, alcohols, ketones,

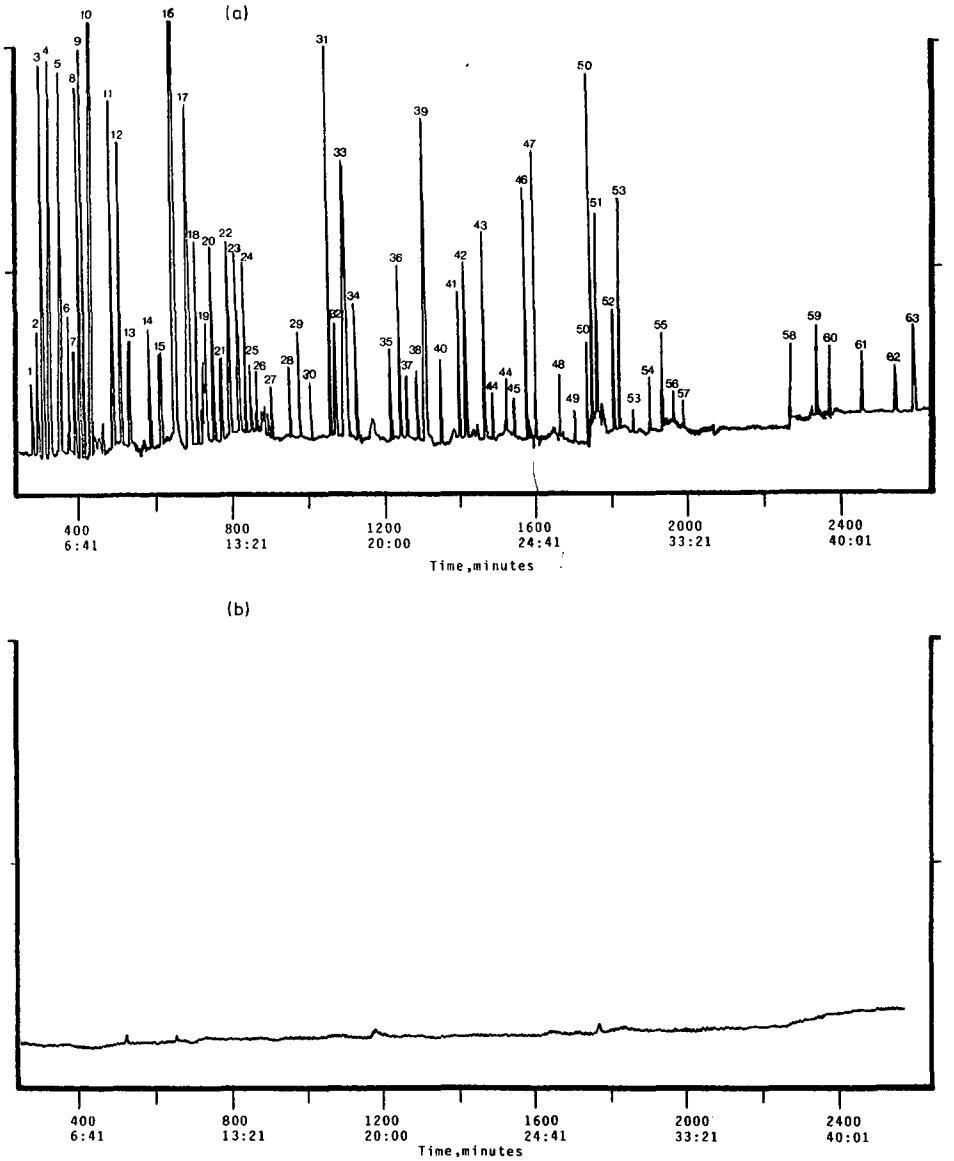

Fig. 5. (a) Specimen chromatogram of seawater sample taken at the head of the Southampton Water estuary, and (b) respective purge blank chromatogram. Peaks: 1 = *n*-Butane; 2 = propanal; 3 = *n*-pentane; 4 = 3-methyl-1,3-butadiene; 5 = dichloromethane; 6 = dimethylsulphide; 7 = 1,1,2-trichloro-1,2,2-trifluoroethane; 8 = 2,2-dimethylbutane; 9 = *n*-hexane; 10 = 2-methylpentene-1; 11 = 3-methylbutanal; 12 = benzene; 13 = cyclohexane; 14 = 2,4,4-trimethylpentane; 15 = 2,5-dimethylfuran; 16 = *n*-heptane; 17 = 2,4,4-trimethylpentene-1; 18 = 2,4,4-trimethylpentene-2; 19 = dimethyldisulphide; 20 = 2,3-dimethylpentene-1; 21 = 3-methyl-2-butenal; 22 = methylbenzene; 23 = 3,4,4-trimethylpentene-2; 24 = 3-methylthiophene; 25 = hexanal; 26 = 2,2,5-trimethylhexane; 27 = 1,2-dibromoethane; 28 = tetrachloroethylene; 29 = *n*-octane; 30 = chlorobenzene; 31 = unknown ?; 32 = 2,3,5-trimethylhexane; 33 = 2,2,3-trimethylhexane; 34 = 1-chlorohexane; 35 = ethylbenzene; 36 = 1,3-dimethylbenzene; 37 = 1,2-dimethylbenzene; 38 = *n*-nonane; 39 = isopropylbenzene; 40 = (α)-pinene; 41 = benzaldehyde; 42 = aldehyde?; 43 = 1,3,5-trimethylbenzene; 44 = 1,2,4-trimethylbenzene; 45 = *n*-decane; 46 = 1,2,3-trimethylbenzene; 47 = 3,3,5-trimethylpentane ?; 48 = 2,3-dihydroindene; 49 = (+)-limonene; 50 = indene; 51 = nonanal; 52 = *n*-undecane; 53 = 1,2,3,5-tetramethylbenzene; 54 = naphthalene; 55 = *n*-tridecane; 56 = 1-methylnaphthalene; 57 = branched alkene ?; 58 = biphenyl; 59 = dodecanal; 60 = *n*-tetradecane; 61 = 1,3-dimethylnaphthalene; 62 = 1,4-dimethylnaphthalene; 63 = aldehyde structure ?.

TABLE V

IDENTIFIED ORGANIC COMPONENTS FOUND IN DOMESTIC TAP WATER DRINKING SUPPLIES

Samples: (1) City of Southampton; (2) Marchwood (a semi-rural village, 10 km S.W. of Southampton City); (3) Dibden Purlieu (a village 17 km S.W. of Southampton City).

Substance	*Concentration ($\mu g\ l^{-1}$)*		
	Sample 1	*Sample 2*	*Sample 3*
Trichloromethane	20.01	29.73	35.07
Tetrachloromethane	0.01	0.13	0.01
Dichlorobromomethane	15.73	19.17	23.65
Chlorodibromomethane	7.94	10.00	14.72
Dichlorodibromomethane	1.11	2.56	4.69
Tribromomethane	2.45	2.99	4.00
1,1,1-Trichloroethane	0.01	0.71	1.01
Benzene	0.29	0.53	1.02
1,2,-Dichloroethane	0.05	0.42	0.04
Methylbenzene	0.57	0.99	1.73

aldehydes, furans, aromatic and alkylaromatics, organosulphides and organohalogens.

Seasonal differences are marked within the estuary, with simple aromatic compounds reaching a maximum in winter months (benzene concentrations exceeding 350 $\mu g\ l^{-1}$ during December) and a secondary short-term maximum in summer months. These are largely due to increases in the use of fossil fuels by the inhabitants of Southampton and its urban conurbations in winter and major increases in pleasure boating in the summer, respectively. There are other causes which contribute to the dynamic nature of such inputs including random pollution events and a progressively developing contribution from motor vehicles.

Halogenated hydrocarbons, *e.g.* Freons, are recovered all year round resulting from a myriad diversity of anthropogenic activities. Disturbingly, following recent concern over the effects of Freons in depletion of the ozone layer, we have found Freon-113 (1,1,2-trichloro-1,2,2-trifluoroethane) consistently at concentrations rarely below 10 $\mu g\ l^{-1}$ in both water and sediment samples. We have not yet been able to pinpoint a significant single key source and investigative work is continuing in this area.

Confirmation of the identity of many volatile Freons has been conducted by independant consulting laboratories who have also confirmed the presence of yet further higher-molecular-weight Freon species in estuarine samples.

Organic sulphur compounds, particularly dimethylsulphide, are ubiquitous in the estuary due to anaerobic decomposition of organic matter in saltmarsh muds. The dumping of untreated sewage is a second major source of organic sulphur compounds and a wide range of organosulphur species have also been found in marine sediments throughout the estuary.

However, compounds of non-anthropogenic source have been identified, including terpenoid materials. Found in midsummer and late autumn at concentra-

tions up to 100 $\mu g\ l^{-1}$, they are associated with fresh water runoff into the estuary. Isoprene (3-methyl-1,3-butadiene), a biogenically derived plant breakdown product, reaches an absolute maximum by mid-November whereas a structurally similar compound, (+)-limonene, is found in higher concentrations in midsummer, mainly produced by peak phytoplanktonic activity.

Such detailed studies have illustrated a range of natural, seasonal and pollution-related processes occurring within the water column and yield significant information on complex interactions and inter-relationships between organic compounds. The modified stripping method has also been applied to a detailed examination of potable-water supplies piped into domestic households. A number of organohalogens have been recovered from tap water samples taken from Southampton City supplies, and from villages in the semi-rural districts outside of the city which have regularly shown higher concentrations of contaminant compounds (see Table V). We believe the results show a constant bias as a result of inefficient chlorination of the water by the Water Authority or alternatively a yet unquantified function of the relationship between the piped supply network (which is known to be subject to irregular pressure distribution), and an adsorption–desorption phenomenon inside the walls of the supply pipework. As the village sampling points are in area of increased pressure, it is feasible that organochlorines are being pressure concentrated in zones immediately prior to entering dwelling houses. Research is continuing in this area and a more comprehensive report is planned for 1990.

CONCLUSION

The modified purge-and-trap thermal desorption method, developed for comparitive simplicity in use combined with low-level accuracy at sub-ppb levels should be worthy of serious consideration by the environmental chemist. A low-cost laboratory computer system has been added to the analysis to perform simultaneous integration and data handling, operated in conjunction with the ion trap detector, Available to most laboratories, modern simple benchtop personal computers can be programmed to identify and integrate assignable and non-assignable compounds from each of the three chromatograms produced from one sample. We believe that with the advent of new research projects examining the occurrence, source and fate of organic micropollutants in areas such as the North Sea and developing interests in coastal pollution, these methods have a role to play in facilitating such analytically complex tasks.

REFERENCES

1 F. Jüttner and J. J. Henatsch, *Nature (London)*, 323 (1986) 797.
2 R. Pizzie, *Ph.D. Thesis*, University of Southampton, Southampton, 1984.
3 A. J. Núñez, L. F. González and J. Janák, *J. Chromatogr.*, 300 (1984) 127.
4 J. Drozd, Z. Vodáková and J. Novák, *J. Chromatogr.*, 354 (1986) 47.
5 K. Grob, *J. Chromatogr.*, 84 (1973) 255.
6 K. Grob and G. Grob, *J. Chromatogr.*, 90 (1974) 303.
7 K. Grob, K. Grob, Jr. and G. Grob, *J. Chromatogr.*, 106 (1975) 299.
8 K. Grob and F. Zürcher, *J. Chromatogr.*, 117 (1976) 285.
9 M. M. Thomason and W. Bertsch, *J. Chromatogr.*, 279 (1983) 383.
10 J. Curvers, Th. Noy, C. Cramers and J. A. Rijks, *J. Chromatogr.*, 289 (1984) 171.

11 A. J. Núñez and H. Maarse, *Chromatographia*, 21 (1986) 44.
12 B. Brown, Senior Analytical Chemist, Wessex Water Authority, Bristol, personal communication.
13 P. M. Gschwend, O. C. Zafiriou, R. F. C. Mantoura, R. P. Schwarzenbach and R. B. Gagosian, *Environ. Sci. Technol.*, 16 (1982) 31.
14 S. G. Wakeham, J. T. Goodwin and A. C. Davies, *Can. J. Fish. Aquat. Sci.*, 40 (1983) 304.
15 R. P. Schwarzenbach, R. H. Bromund, P. M. Gschwend and O. C. Zafiriou, *Org. Geochem.*, 1 (1978) 93.
16 H. Borén, A. Grimvall and R. Sävenhed, *J. Chromatogr.*, 252 (1982) 139.
17 T. A. Bellar and J. J. Lichtenberg, *J. Am. Water Works Assoc.*, 66 (1974) 739.
18 R. D. Kleopfer and B. J. Fairless, *Environ. Sci. Technol.*, 6 (1972) 1036.
19 J. W. Swinnerton and V. J. Linnenbom, *J. Gas Chromatogr.*, 5 (1967) 570.
20 B. A. Colenutt and S. Thorburn, *Int. J. Environ. Anal. Chem.*, 7 (1975) 701.
21 W. Bertsch, E. Anderson and G. Holzer, *J. Chromatogr.*, 112 (1975) 701.
22 K. Kawata, T. Uemura, I. Kifune, Y. Tomikaga and K. Oikawa, *Bunseki Kagaku*, 8 (1982) 453.
23 K. J. Krost, E. D. Pellizzari, S. G. Walburn and S. A. Hubbard, *Anal. Chem.*, 54 (1982) 810.
24 N. R. Rakshieva, S. Wičar, J. Novák and J. Janák, *J. Chromatogr.*, 91 (1974) 59.
25 R. F. Simpson, *Chromatographia*, 12 (1979) 733.
26 R. D. Barnes, L. M. Law and A. J. MacLeod, *Analyst (London)*, 106 (1981) 412.
27 A. G. Vitenberg, B. V. Ioffe and V. N. Borisov, *Chromatographia*, 7 (1974) 610.
28 G. MacLeod and J. M. Ames, *J. Chromatogr.*, 355 (1980) 393.
29 A. Bianchi, *Int. Environ. Saf.*, 6 (3) (1988) 8.
30 *Oil Companies International Study Group for the Conservation of Clean Air and Water (ConCAWe)*, *Report No. 8/86*, ConCAWe, The Hague, 1986.
31 *Method 624-Purgeables*, U.S. Environmental Protect. Agency, Environmental Monitoring and Support Laboratory, Cincinnati, OH, July 1982.
32 K. E. Murray, *J. Chromatogr.*, 135 (1977) 49.
33 R. A. Hurrel, *Int. Environ. Safety*, June (1981) 18.
34 P. Bishop, *Proc. Anal. Div. Soc. Chem.*, 24 (1987) 368.
35 R. L. Grob (Editor), *Modern Practice of Gas Chromatography*, Wiley, 2nd ed., 1985, Ch. 10, p. 495.
36 A. Bianchi and H. A. Cook, *J. Chromatogr.*, 449 (1988) 175.
37 A. Bianchi and M. S. Varney, *Water Waste Treat*, 31, No. 9 (1988) 14.

Journal of Chromatography, 467 (1989) 129–138
Elsevier Science Publishers B.V., Amsterdam — Printed in The Netherlands

CHROM. 21 238

GAS CHROMATOGRAPHIC DETERMINATION OF METHYLPHOSPHONIC ACIDS BY METHYLATION WITH TRIMETHYLPHENYLAMMONIUM HYDROXIDE

J. Aa. TØRNES* and B. A. JOHNSEN
Norwegian Defence Research Establishment, Division for Environmental Toxicology, P.O. Box 25, N-2007 Kjeller (Norway)
(First received October 3rd, 1988; revised manuscript received December 29th, 1988)

SUMMARY

A method is described for the isolation of decomposition products of nerve agents from aqueous solutions and their determination by gas chromatography. The methylphosphonic acids were retained on an aminopropyl ion exchanger and eluted with trimethylphenylammonium hydroxide, which also acted as a methylating reagent. The procedure was applied to environmental samples in a field exercise in which samples contaminated with the nerve agents sarin and soman were exposed to the prevailing weather for periods of up to 4 weeks. The methylphosphonic acids were detected in all the samples examined.

INTRODUCTION

In connection with the verification of the use of chemical warfare agents, additional information can be obtained from the determination of the degradation products of unstable compounds such as nerve agents. Hence it is important to have methods available for the determination of such compounds. The nerve agents isopropyl methylphosphonofluoridate (sarin, GB), 1,2,2-trimethylpropyl methylphosphonofluoridate (soman, GD) and ethyl S-2-diisopropylaminoethyl methylphosphonothiolate (VX) are hydrolysed to methylphosphonic acids according to the scheme outlined in Fig 1.

The methylphosphonic acids are polar, non-volatile compounds, and should therefore be well suited for determination by high-performance liquid chromatography (HPLC)[1–3]. The problem, however, is that no sensitive detectors for compounds such as methylphosphonic acids are available. These compounds have therefore often been determined by gas chromatography (GC) with prior derivatization. The most common derivatization methods have been the formation of trimethylsilyl (TMS) ethers or *tert.*-butyldimethylsilyl (t-BDMS) ethers from the acids[4,5] or methylation with diazomethane[6,7]. Experiments carried out in our laboratory have shown that the formation of t-BDMS ethers gave poor yields, especially from methylphosphonic acids with small alkyl groups. In addition, the silyl ethers were unstable and sensitive to moisture.

0021-9673/89/$03.50

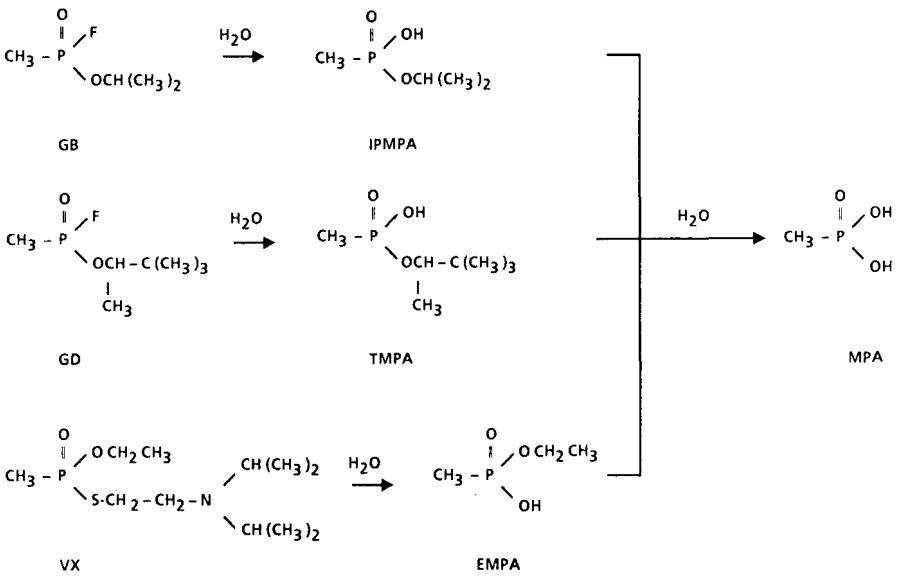

Fig. 1. Reaction scheme for hydrolysis of the nerve agents sarin (GB), soman (GD) and VX.

The use of diazomethane as a derivatization reagent gives high yields, but is not recommended because of its explosive and carcinogenic properties. Another disadvantage of diazomethane is that it is unstable and has to be prepared freshly every day.

A method that has been used for the methylation of acids that are difficult to esterify, *e.g.*, barbituric acids and sterically hindered carboxylic acids[8–13], has now been applied to the methylphosphonic acids. This method is based on formation of ion pairs of the acids with trimethylphenylammonium hydroxide (TMPAH) and subsequent methylation in the injection port of the gas chromatograph. This derivatization method is fast and gives stable methyl esters in quantitative yields from isopropyl methylphosphonic acid (IMPA), 1,2,2-trimethylpropyl methylphosphonic acid (TMPA) and methyl methyl phosphonic acid (MMPA), even from aqueous solutions of the acids.

The methylphosphonic acids have pK_a values of about 2.5 and are totally dissociated in neutral aqueous solutions. It should therefore be possible to retain the acids on anion-exchange cartridges. Hydrolysed sarin (IPMPA) and hydrolysed soman (TMPA) were applied to different sorts of anion exchangers and the results are reported in this paper.

Experiments have shown that large excess of the reagent should be used in order to obtain quantitative yields from the derivatization with TMPAH. This problem has been solved by using TMPAH as the solvent to elute the methylphosphonic acids from the ion-exchange cartridges.

EXPERIMENTAL

Sorbents and chemicals

The ion exchangers used were aminopropyl (NH_2), diethylaminopropyl (DEA) and trimethylaminopropyl (SAX) from Analytichem International. In addition, octadecylsilane (C_{18}) cartridges from the same company were used in the field experiments. All cartridges contained 100 mg of packing material.

The TMPAH derivatization reagent was a 0.1 *M* solution in methanol from Kodak. Other chemicals used were Uvasol-grade methanol and chloroform from Merck.

Isopropyl methylphosphonic acid, 1,2,2-trimethylpropyl methylphosphonic acid and methyl methylphosphonic acid were synthesized and purified (>95%) as described in the literature[14,15].

Chromatographic equipment and conditions

The analysis of the hydrolysed and derivatized nerve agents was performed on a Packard Model 438 gas chromatograph coupled to a LKB 2091 mass spectrometer. A 3-ft glass column packed with SP1200–1% H_3PO_4 liquid stationary phase on 80–100-mesh Chromosorb W AW was used for separation. The column temperature was maintained at 120°C for 2 min and then raised at 16°C/min to 170°C. The temperature of the transfer line between the gas chromatograph and the mass spectrometer was set at 250°C and the injector temperature at 300°C. The compounds were detected by selected ion monitoring (SIM) and the mass fragments used for detection were *m/z* 111 (100%) and 137 (32%) for methylated IPMPA, *m/z* 138 (100%) and 111 (86%) for methylated TMPA, *m/z* 94 (100%) for methylated MMPA and *m/z* 57 (100%) for decane. SIM curves of a mixture of IPMPA and TMPA methylated with TMPAH together with decane as internal standard are shown in Fig 2.

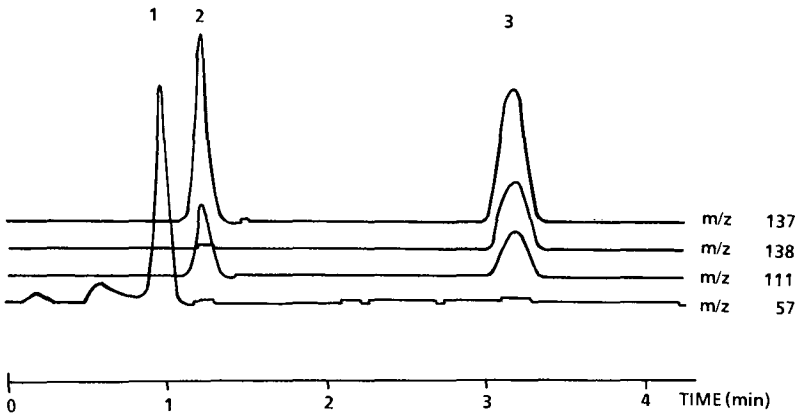

Fig. 2. SIM curves for a sample containing 10 μg/ml of IPMPA (2) and TMPA (3) methylated with TMPAH, together with decane (1) as internal standard. The chromatographic conditions are given in the text.

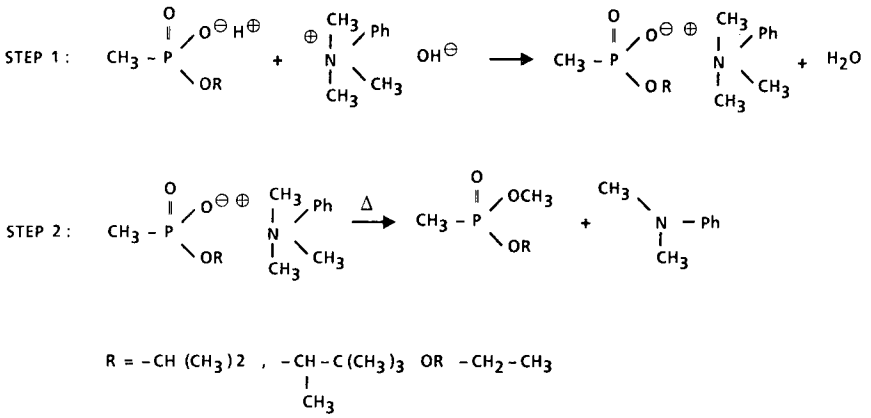

Fig. 3. Reaction scheme for methylation of methylphosphonic acids with TMPAH.

Derivatization

A derivatization method applicable to GC should be fast and non-hazardous when a large number of samples are to be handled. The methylation by TMPAH meets these requirements, and it can even be used with aqueous samples.

When a solution of methylphosphonic acids is mixed with TMPAH in methanol, the methylation of the acids takes place in the injection port of the gas chromatograph at high temperature after the injection[8–13] (Fig 3). The temperature in the injector is an important factor in obtaining the maximum yields. To find the optimum conditions, 50 μl of an aqueous solution of 1 mg/ml of IPMPA were mixed with 300 μl of 0.1 *M* TMPAH in methanol and 1 -μl aliquots of the mixture were injected on to the gas chromatograph with injector temperatures varying from 160 to 300°C. A plot of the peak area *versus* the injector temperature (Fig 4) shows that temperatures in excess of 260°C should be used. In the following experiments the injector temperature was set at 300°C.

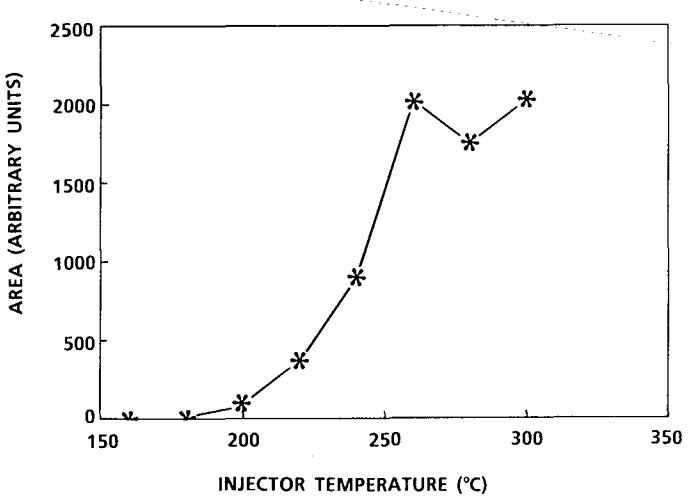

Fig. 4. Plot of the peak area *versus* injector temperature for a mixture of IPMPA and TMPAH.

Selection of ion exchangers

The ion exchanger selected for the preparation of samples containing methylphosphonic acids for GC analysis should be able to retain acids containing different alkyl chains with high effciency. In order to take full advantage of the methylating reagent TMPAH, the methylphosphonic acids should also be eluted from the selected ion exchanger with this reagent with high efficiency.

In order to find the best ion exchanger, the recoveries of hydrolysed sarin (IPMPA) and hydrolysed soman (TMPA) from different anion exchangers were investigated. Volumes of 10 ml of aqueous solutions of 1 mg of IPMPA and 1 mg of TMPA were passed through cartridges packed with NH_2, DEA or SAX ion exchangers that had previously been wetted with 0.5 ml of methanol and 2 ml of distilled water. The aqueous phases were collected in order to check the amounts of the acids not retained on the cartridges. Volumes of 50 μl of these aqueous phases were mixed with 300 μl of TMPAH in methanol and 1 μl of the mixture was injected on to the gas chromatograph; 20 μl of a 0.2% solution of decane were added to the mixture as an internal standard before injection. The methylphosphonic acids were eluted from the cartridges with 300 μl of TMPAH (pH 13.0), internal standards were added and the samples were injected into the gas chromatograph. Seven replicates were analysed for each sample, and the amounts of acids recovered from the aqueous phases and from the TMPAH eluates together with standard deviations are shown in Table I. According to these results, the NH_2 and the DEA cartridges gave the best recoveries from the eluate. The best results were obtained with the NH_2 cartridge, which was selected for further investigations.

TABLE I

RECOVERIES OF IPMPA AND TMPA FROM THE AQUEOUS PHASE AND THE ELUATE FROM DIFFERENT ION EXCHANGERS

Recoveries ± S.D. (n = 7).

Agent	*Phase*	*Recoveries from cartridges (%)*		
		NH_2	*DEA*	*SAX*
IPMPA	Aqueous phase	6±3	5±3	11±3
	Eluate	88±7	73±3	27±9
TMPA	Aqueous phase	10±5	45±19	1±1
	Eluate	75±6	62±8	4±2

Optimization of the preparation procedure

The capability of a cartridge containing 100 mg of NH_2 sorbent to retain methylphosphonic acids from various sample volumes was investigated. Volumes of 10, 50 and 100 ml of aqueous solutions of 1 mg of IPMPA and 1 mg of TMPA were passed through NH_2 cartridges, eluted with 300 μl of TMPAH and analysed as described above. The recoveries, which are given in Table II, showed a significant decrease with increasing sample volume. This decrease is probably due to inefficient retention of the methylphosphonic acids from large sample volumes, because experiments have

TABLE II

RECOVERIES OF IPMPA AND TMPA FROM NH_2 CARTRIDGES WITH DIFFERENT SAMPLE VOLUMES

Sample volume (ml)	*Recovery (%)*	
	IPMPA	*TMPA*
10	88	75
50	78	59
100	57	40

shown that the recoveries did not vary significantly with sample concentration. Therefore, if sample volumes in excess of 100 ml are to be handled, cartridges containing larger amounts of packing material should be applied.

It was expected that the recoveries of methylphosphonic acids from large sample volumes could be enhanced if lower flow-rates are used. Ion-exchange interaction is a slower process than polar and non-polar interactions and a maximum flow-rate of 5 ml/min has been suggested in the literature[16]. To verify this, 50 ml of aqueous solutions containing 1 mg of IPMPA were passed through NH_2 cartridges at different flow-rates from 1.7 to 10 ml/min. The methylphosphonic acids were eluted and analysed by GC as above. These experiments showed no significant differences in recoveries with the different flow-rates investigated.

Investigations did not show significant differences in the amounts recovered when the volume of the elution solvent was varied from 300 μl to 1 ml. However, 300 μl was considered to be the minimum amount required to elute the acids from the cartridges in a reproducible manner, and was therefore used in the following studies.

Field experiments

The procedure for the determination of hydrolysed sarin and soman was applied in a field exercise in order to evaluate the usefulness of the method. Amounts of 1 mg of sarin and soman were added to samples of 50 ml of water or about 10 g of grass, sand or soil, and the samples were exposed to the prevailing weather for periods of up to 4 weeks. The concentrations of both nerve agents and the methylphosphonic acids were measured after 1, 2 and 4 weeks. The temperature and relative humidity were recorded. The mean temperature was 15°C during the first week, 10°C during the second week and about 15°C during the third and fourth week. The relative humidity varied from about 30% during the day to about 95% during the night.

In order to determine both nerve agents and methylphosphonic acids in the same samples, C_{18} cartridges were connected with the NH_2 cartridges. The nerve agents were retained on the C_{18} cartridges on top [17,18], whereas the acids passed through and were retained on the NH_2 cartridges at the bottom.

Samples of about 10 g of grass, sand or soil were extracted with 50 ml of water by shaking for 1 min. The aqueous phases, together with the 50-ml water samples, were then filtered and passed through the cartridges which were pre-wetted with 1 ml of methanol and 5 ml of water[17,18]. The C_{18} and NH_2 cartridges were separated before the compounds were eluted. The nerve agents were eluted from the C_{18} car-

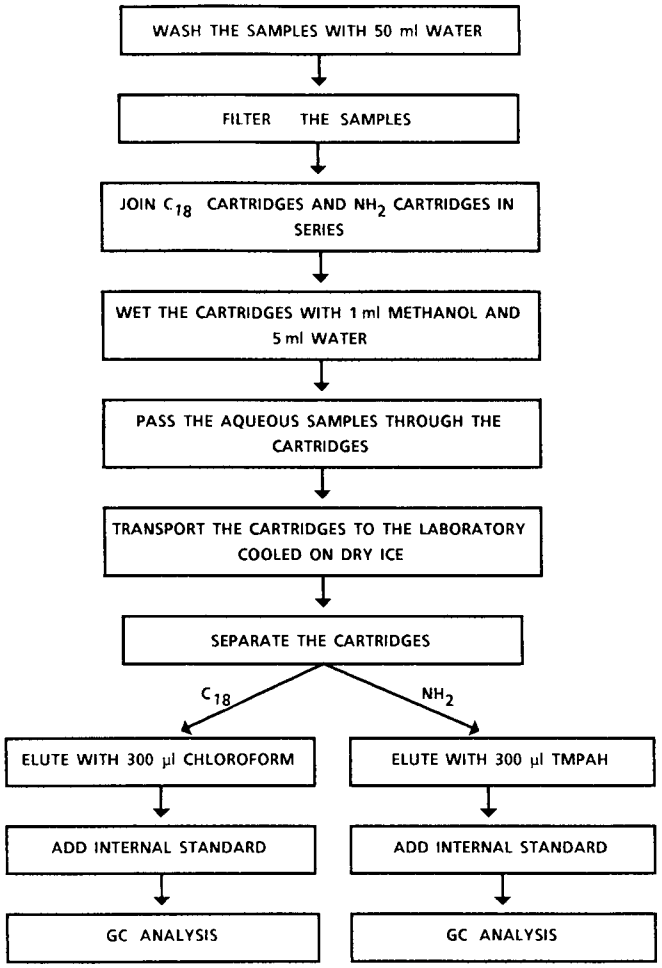

Fig. 5. Flow chart showing the procedure for the determination of nerve agents and methylphosphonic acids from environmental samples.

tridges with 300 µl of chloroform and the methylphosphonic acids were eluted from the NH_2 cartridges with 300 µl of TMPAH in methanol. Decane was added as internal standard and 1-µl samples were injected on to the gas chromatograph. The overall preparation procedure is summarized in Fig. 5.

RESULTS AND DISCUSSION

Evaluation of ion exchangers

The investigations described above showed that the NH_2 anion exchanger was the most efficient for the isolation of hydrolysed sarin (IPMPA) and hydrolysed soman (TMPA) from aqueous solutions. Cartridges containing 100 mg of NH_2 sorbent were selected for further evaluations and showed a recovery of 88% for IPMPA

and 75% for TMPA from sample volumes of 10 ml. The investigations showed further that when the sample volumes exceeded 100 ml, the recoveries decreased to below 50% and cartridges containing larger amounts of sorbent should be considered.

Although a flow-rate through the ion-exchange cartridges of 5 ml/min has been suggested[16], no significant differences in the amounts of methylphosphonic acids recovered were observed when the flow-rate was varied between 1.7 and 10 ml/min, indicating that the flow-rate is not critical.

Derivatization

Elution of the methylphosphonic acids with TMPAH and subsequent methylation in the injection port of the gas chromatograph with TMPAH as derivatization reagent were selected as the best derivatization method. The minimum amount of TMPAH required to elute the acids from the NH_2 cartridges in a reproducible manner was found to be 300 μl and was therefore used in the analysis.

Detection limits

The detection limits for hydrolysed sarin (IPMPA) and hydrolysed soman (TMPA) were established by preparing and analysing sample blanks and samples containing known amounts of the methylphosphonic acids in the same way as the real samples. The detection limits were taken as the concentrations that gave a signal-to-

TABLE III

RESULTS FROM FIELD EXPERIMENTS

Agent	*Sample*	*Amount recovered (μg) after exposure for*		
		1 week	*2 weeks*	*4 weeks*
GB	Water	80	50	0.4
	Grass	0.02	0.04	–[a]
	Sand	0.1	0.2	–
	Soil	0.08	0.08	–
GD	Water	290	90	0.1
	Grass	0.5	0.07	–
	Sand	0.1	0.2	–
	Soil	0.1	–	–
IPMPA	Water	3	2	1
	Grass	0.6	2	1
	Sand	2	1	2
	Soil	0.7	1	NA[b]
TMPA	Water	2	1	0.9
	Grass	0.3	0.8	2
	Sand	0.9	0.3	2
	Soil	0.2	0.3	NA

[a] –, Concentration below detection limit.
[b] No analysis carried out.

noise ratio of 3. The minimum amounts that could be detected in a 50-ml sample volume were 100 ng for both IPMPA and TMPA when a mass spectrometer with SIM was applied. These limits could be lowered if a capillary column was used and the eluates were concentrated prior to analysis.

Results from field experiments

The amounts of nerve agents and methylphosphonic acids recovered from the different samples after exposure to the prevailing weather for up to 4 weeks are given in Table III. The recoveries shown were calculated relative to standard samples containing known amounts of the compounds and prepared in the same way as the unknown samples. Hydrolysed soman was to some extent retained on the C_{18} cartridges, leading to reduced recoveries. This did not occur with hydrolysed sarin. More recent work showed that a better approach would be to place the NH_2 cartridge on top of the C_{18} cartridge. Sarin and soman were not retained on the NH_2 cartridge and could be collected on the C_{18} cartridge at the bottom, whereas the hydrolysed nerve agents were collected on the NH_2 cartridge.

These experiments showed that after exposure for 4 weeks under summer conditions the nerve agents could only be detected in water samples. The amounts of methylphosphonic acids were fairly constant and could easily be detected after 4 weeks in all samples. In this field experiment, only one sample was analysed for each agent in each time period and it was therefore not possible to make a statistical evaluation of the results.

CONCLUSIONS

The results from the field exercise have shown that the determination of breakdown products can be an important method when alleged use of nerve agents has to be verified under summer conditions. The hydrolysed sarin and soman were easily detected after exposure to the prevailing weather for 4 weeks, whereas sarin and soman were only found close to the detection limits after 2 weeks.

Although several methods have been proposed for the determination of hydrolysed nerve agents, the present procedure has several advantages. The sample preparation is based on the same technique as used by the Norwegian Defence Research Establishment for isolation of nerve agents[17,18]. The method does not require large amounts of equipment or chemicals, and can easily be performed by untrained personnel under field conditions. The transport of the samples to the laboratory is simple as only small cartridges have to be transported. The derivatization with TMPAH is a fast and non-hazardous technique which produces stable methyl esters in high yields. Its combined use as eluent and derivatization reagent makes TMPAH especially advantageous.

REFERENCES

1 P. C. Bossle, J. J. Martin, E. W. Sarver and H. Z. Sommer, *J. Chromatogr.*, 267 (1983) 209.
2 P. C. Bossle, D. J. Reutter and E. W. Sarver, *J. Chromatogr.*, 407 (1987) 399.
3 A. Verweij, paper presented at the *2nd. Symposium on the Chemistry and Fate of Organophosphorus Compounds, Barcelona, Spain, November 10–12, 1987.*
4 D. J. Harvey and M. G. Horning, *J. Chromatogr.*, 79 (1973) 65.

5 J. G. Purdon, J. G. Pagotto and R. K. Miller, *Report DREO-936*, Defence Research Establishment Ottawa, Ottawa, 1985.
6 A. Verweij, C. E. A. M. Degenhardt and H. L. Boter, *Chemosphere*, 3 (1979) 115.
7 A. Verweij, H. L. Boter and C. E. A. M. Degenhardt, *Science*, 204 (1979) 616.
8 E. W. Robb and J. J. Westbrook, *Anal. Chem.*, 35 (1963) 1644.
9 J. MacGee, *Clin. Chem.*, 17 (1971) 587.
10 V. Prelog and M. Piantanida, *Z. Physiol. Chem.*, 244 (1936) 56.
11 R. C. Fuson, J. Corse and E. C. Horning, *J. Am. Chem. Soc.*, 61 (1939) 1290.
12 E. Brochmann-Hanssen and T. O. Oke, *J. Pharm. Sci.*, 58 (1969) 370.
13 G. W. Stevenson, *Anal. Chem.*, 38 (1966) 1948.
14 A. M. de Roos, *Recl. Trav. Chim. Pays-Bas*, 78 (1959) 145.
15 Houben-Weyl, *Metoden der organischen Chemie — Organische Phosphorverbindungen, Teil 1*, Georg Thieme, Stuttgart, 1963, pp. 387–414.
16 *Sorbent Extraction Technology — Handbook*, Analytichem International, Harbor City, CA, 1985, p. 23.
17 B. A. Johnsen, J. A. Tørnes, T. Axelsson and P. J. Karlsen, *Handling of Samples Contaminated with Chemical Warfare Agents: Part 5, FFI/RAPPORT-86/6005*, Norwegian Defence Research Establishment, Kjeller, 1986.
18 B. A. Johnsen, J. A. Tørnes, A. M. Opstad and E. Odden, *Development of Procedures for Verification of Alleged Use of Chemical Warfare Agents: Part 6, FFI/RAPPORT-87/6010*, Norwegian Defence Research Establishment, Kjeller, 1987.

Journal of Chromatography, 467 (1989) 139–147
Elsevier Science Publishers B.V., Amsterdam — Printed in The Netherlands

CHROM. 21 247

CHROMATOGRAPHY OF TANNINS

IV[a]. SEPARATION OF LABILE OLIGOMERIC HYDROLYSABLE TANNINS AND RELATED POLYPHENOLS BY CENTRIFUGAL PARTITION CHROMATOGRAPHY

TAKASHI YOSHIDA, TSUTOMU HATANO and TAKUO OKUDA*
Faculty of Pharmaceutical Sciences, Okayama University, Tsushima, Okayama 700 (Japan)
(First received July 4th, 1988; revised manuscript received January 2nd, 1989)

SUMMARY

Using centrifugal partition chromatography for the separation and purification of oligomeric hydrolysable tannins extracted from *Heterocentron roseum*, a labile trimer, nobotanin J, which was readily decomposed into a monomer and dimer(s) on a gel column chromatographic solid support, and a more polar tetramer, nobotanin K, were efficiently purified by normal- and reversed-phase developments using the solvent system *n*-butanol–*n*-propanol–water (4:1:5, v/v/v). Licochalcone B, a polyphenol having tannin-like activity, was also separated from other components with related structures in Sinkiang licorice extract by centrifugal partition chromatography with normal-phase development using chloroform–methanol–water (7:13:8, v/v/v) as the solvent system.

INTRODUCTION

Recently found activities of tannins, such as antitumour[1–3] and antiperoxidation[4,5], which are largely dependent on the structure of the tannin, have increased the need for the isolation of each component in tannin mixtures obtained from plants, as such tannins are frequently present in foods and drinks and also in medicinal plants.

In general, the separation and purification of these tannins from plant extracts can be achieved by a combination of droplet counter-current chromatography with column chromatography over an appropriate solid support such as vinyl polymer resins, *e.g.*, Toyopearl HW-40 and MCI-gel CHP-20P, and dextran gel (Sephadex LH-20)[6], and sometimes with high-performance liquid chromatography (HPLC) on a preparative scale in the final stage of purification. However, as tannins are often present as mixtures of labile polyphenols with large molecules, which are easily adsorbed on various substances, column chromatography of tannins and related polyphenols using solid supports is often problematic owing to adsorption, and some-

[a] For Part III, see T. Hatano, T. Yoshida and T. Okuda, *J. Chromatogr.*, 435 (1988) 285.

0021-9673/89/$03.50

times hydrolysis, on the solid support. Preparative HPLC is often accompanied by sample loss and deterioration and contamination of the column.

The application of centrifugal partition chromatography to the preparative fractionation of hydrolysable tannins was reported in a previous paper[6]. This technique has the advantages over other techniques of chromatography, particularly on the preparative scale, of absence of a solid support, which causes losses of tannins by adsorption, and of a shorter development time[7]. It also has the advantage of requiring only a small volume of the developing solvent, which shortens the time of evaporation of the solvent from each fraction. The absence of a solid support is particularly favourable for the separation of tannins with large molecules, such as the oligomeric hydrolysable tannins which are often adsorbed strongly on a solid support.

However, most of the examples described in our previous paper[6] involved the separation of tannins in the crude extracts from plants into several fractions containing two or more tannins or related polyphenols, except for one example in which the normal-phase development of a fraction obtained by reversed-phase development led to further purification of each tannin. Final purification of the components in each fraction was mostly carried out by gel column chromatography.

We now present the results of the application of centrifugal partition chromatography to the purification of labile oligomeric hydrolysable tannins extracted from *Heterocentron roseum*, which are hardly purified by gel column chromatography because it is readily hydrolysed during the development. The separation of bioactive polyphenols of other types, extracted from Sinkiang licorice, by centrifugal partition chromatography is also described.

EXPERIMENTAL

Apparatus

A Model L-90 centrifugal partition chromatograph (Sanki Engineering, Nagaokakyo, Kyoto, Japan), consisting of a centrifuge with twelve column cartridges, each containing a polyfluoroethylene resin block (150 mm × 40 mm × 40 mm), was used. Each resin block has 50 holes which act as the separation columns (40 mm × 3 mm), connected to each other by fine resin tubes. The internal volume of each cartridge is *ca.* 15 ml[7]. The sample solution and the solvents were pumped into the columns, rotating at 700 rpm, with a Model CPC-LBP-II pump (Sanki). A Model CPC-UVM-I UV absorbance monitor, equipped with a cell of light path 0.2 mm (Sanki), was used at 254 nm, and fractions were collected with a Model SF-160 K fraction collector (Toyo Kagaku Sangyo, Tokyo, Japan).

Solvent

The solvent systems used were those previously found to be widely applicable for the separation and purification of tannins and related polyphenols by droplet counter-current chromatography[6] and also by centrifugal partition chromatography[6], with good efficiency and without causing hydrolysis. Solvent A was *n*-butanol–*n*-propanol–water (4:1:5, v/v/v). The lower layer was used as the stationary phase for the normal-phase development, and was pumped into the column prior to loading of the sample solution. The upper layer was used as the stationary phase for the

reversed-phase development. Solvent B was chloroform–methanol–water (7:13:8, v/v/v). The upper layer was used as the stationary phase for the normal-phase development.

Analysis of fractions

Every second or third fraction was monitored, after evaporation of the solvent, by HPLC with UV detection at 280 nm, and also with diode-array UV detection. The apparatus consisted of an LC-6A system (Shimadzu, Kyoto, Japan) equipped with a YMC A312 (ODS) column (150 × 6 mm I.D.; Yamamura-kagaku, Kyoto, Japan), an SPD-6A UV monitor (Shimadzu) and an MCPD-350PC, System II diode array detector (Otsuka Electronics, Hirakata, Osaka, Japan). The column was kept at 40°C in an oven and was eluted with the solvent system (a) 0.05 *M* H_3PO_4–0.05 *M* KH_2PO_4–ethanol–ethyl acetate (40:40:15:5, v/v), (b) acetonitrile–water–acetic acid (35:60:5, v/v/v) or (c) methanol–water–acetic acid (60:35:5, v/v/v). Normal-phase HPLC was performed on a column (150 × 4 mm I.D.) of Develosil 60-5 (high-porosity silica) (Nomura Chemical, Seto, Aichi, Japan), using hexane–methanol–tetrahydrofuran–formic acid (60:45:15:1, v/v) containing oxalic acid (500 mg in 1.2 l) as eluent.

The effluent was monitored by UV absorption at 280 nm. The purity of the isolated components was also confirmed by TLC on Kieselgel PF_{254} (Merck) developed with chloroform–water–acetic acid (155:33:12, v/v/v), and by ^1H and ^{13}C nuclear magnetic resonance (NMR) spectroscopy using a Varian VXR 500 instrument (500 MHz for ^1H and 126 MHz for ^{13}C) at the SC NMR Laboratory of Okayama University.

Preparation and fractionation of plant extracts

Fresh leaves (2.1 kg) of *Heterocentron roseum* were extracted with acetone–water (7:3, v/v) and filtered. After removal of the acetone by distillation, the aqueous solution was succesively extracted with diethyl ether, ethyl acetate and *n*-butanol saturated with water. The *n*-butanol extract (8.1 g) was chromatographed on a column (33 cm × 3 cm I.D.) of Diaion HP-20 polystyrene resin (Mitsubishi Chemical Industries, Tokyo, Japan) by stepwise elution with water with an increasing amount of methanol. The eluate with 40% methanol (3.6 g) was then rechromatographed on a column (42 cm × 2.2 cm I.D.) of Toyopearl HW-40 high-porosity vinyl polymer (coarse grade) (TOSOH, Tokyo, Japan) by stepwise elution with methanol–water (7:3, v/v; 1.4 l) → methanol–water (8:2, v/v; 4 l) → methanol–water–acetone (7:2:1, v/v/v; 1 l) → methanol–water–acetone (3:1:1, v/v/v; 0.7 l) → water–acetone (3:7, v/v; 0.5 l). Fractions of 7–10 ml were collected with a Model SF-100G fraction collector (Toyo Kagaku Sangyo) and every third fraction was monitored by UV absorption at 280 nm. The crude trimer nobotanin J (**1**) (1.1 g) was obtained from the fraction eluted with methanol–water–acetone (3:1:1, v/v/v). The 70% aqueous acetone eluate yielded a mixture of tetramers (650 mg) containing nobotanin K (**6**) as the main component (Scheme 1). The crude nobotanin J was dissolved in the lower layer of solvent system A (20 ml) and was subjected to centrifugal partition chromatography with development with the upper layer of the same solvent system (normal-phase development) at a rate of 1.0 ml/min. A portion (410 mg) of the tetramer fraction, which is more polar than the trimers, was purified by centrifugal partition chromato-

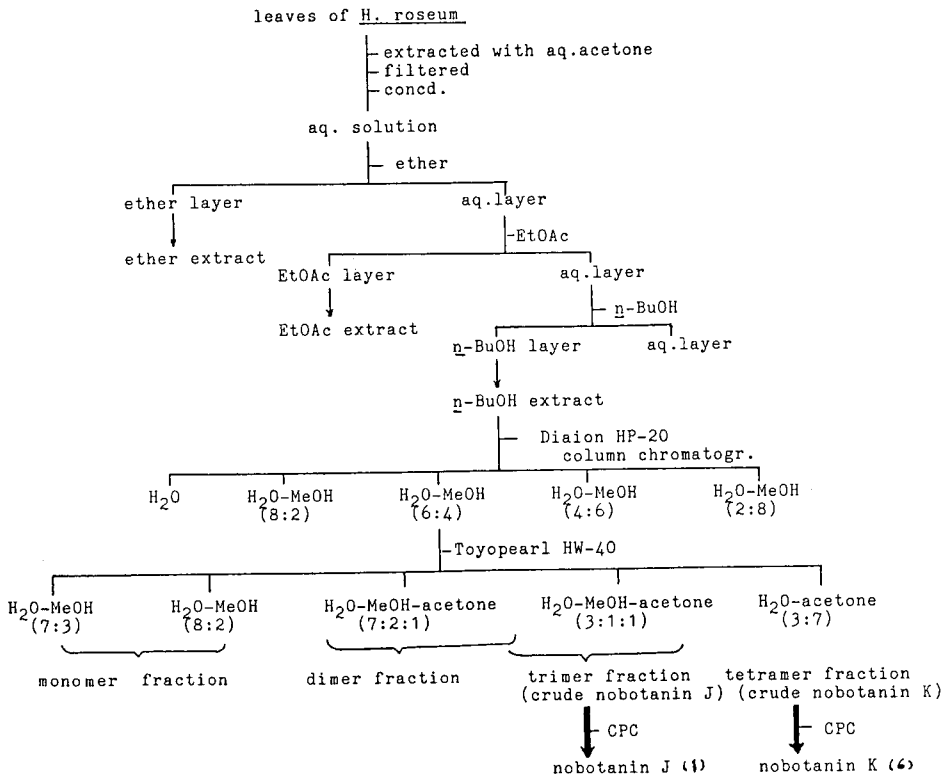

Scheme 1. MeOH = methanol, BuOH = butanol, EtOAc = ethyl acetate.

graphy with reversed-phase development with solvent system A to yield nobotanin K (**6**) (112 mg).

The aqueous acetone extract of Sinkiang licorice (licorice roots from the Sinkiang region of China) was partitioned between water and diethyl ether. The aqueous layer was further extracted with ethyl acetate and then *n*-butanol saturated with water. A portion (3 g) of the ether extract was fractionated by centrifugal partition chromatography with normal-phase development with solvent system B, collecting 10-g portions of the elute. Crude licochalcone B obtained on evaporation of fraction IV (Fig. 4) was further chromatographed over Kieselgel 60 (Merck) using chloroform–methanol (98:2, v/v) to isolate pure licochalcone B (**7**) (122 mg) and 7,4′-dihydroxyflavone (**8**) (6 mg). The eluate from fraction II (Fig. 4) was similarly subjected to a further fractionation on a Kieselgel 60 column using the same solvent, to give licochalcone A (**9**) (112 mg).

The purities of these compounds were confirmed by TLC (Kieselgel PF_{254}) and reversed-phase HPLC (solvent b or c).

RESULTS AND DISCUSSION

Separation of labile and highly polar oligomeric hydrolysable tannins

Heterocentron roseum, a tropical plant belonging to Melastomataceae, is rich in oligomeric hydrolysable tannins, including dimers, trimers and tetramers. Although five dimers (nobotanin B, F, G, H and I)[8–10] and a trimer (nobotanin E)[10] were isolated by column chromatography on a vinyl polymer resin (Toyopearl HW-40), another trimer, nobotanin J (**1**), which is more labile than the others, could not be purified even by repeated chromatography on the resin column developed with water–methanol–acetone of various proportions. Substantial contamination by monomers and dimers, which should include those produced by the partial hydrolysis of **1** on the solid support during the development, was always observed. This hydrolysis was particularly extensive when the column chromatography was carried out on Sephadex LH-20, resulting in conversion of more than 70% of nobotanin J into a mixture of a monomer and dimers, although a small amount of pure nobotanin J was isolated by this column chromatography. In order to minimize this undesirable hydrolysis during the purification procedure, application of centrifugal partition chromatography, which can be performed rapidly in the absence of the solid support, was attempted.

The crude nobotanin J (**1**) (1.1 g) (purity *ca.* 72% when calculated from peak areas in HPLC), which was obtained from column chromatography over Toyopearl HW-40 (coarse grade) (Scheme 1), was finally purified by centrifugal partition chromatography in the normal-phase mode using solvent system A, to yield nobotanin J (154 mg) composed of fraction III, as shown in Fig. 1. The nobotanin J thus obtained was pure enough to exhibit a single peak in normal- and reversed-phase HPLC, and showed ^{1}H and ^{13}C NMR peaks almost exclusively assignable to the given structure (**1**). The HPLC trace of the residue (510 mg) obtained by evaporation of fraction II still showed small peaks ascribable to **2** and **3** (88% purity for **1**). Fraction I (122 mg)

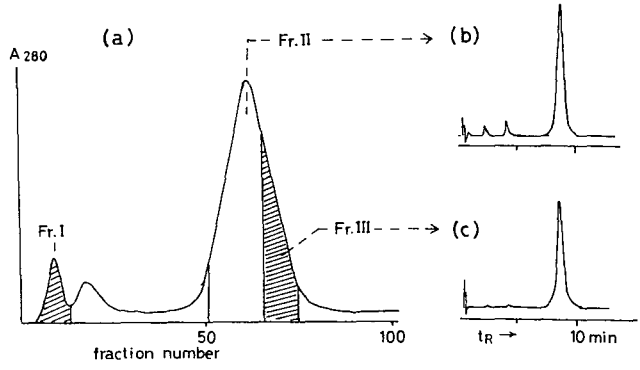

Fig. 1. Centrifugal partition chromatogram of crude nobotanin J from *n*-butanol extract of *H. roseum*, and HPLC fractions of II and III. (a) Centrifugal partition chromatogram (normal-phase development with solvent A); (b) HPLC (normal phase) of fraction II; (c) HPLC (normal phase) of fraction III. HPLC conditions: column, Develosil 60-5; solvent, hexane–methanol–tetrahydrofuran–formic acid (60:45:15:1) containing oxalic acid (500 mg in 1.2 l); detection, 280 nm; 0.04 a.u.f.s.

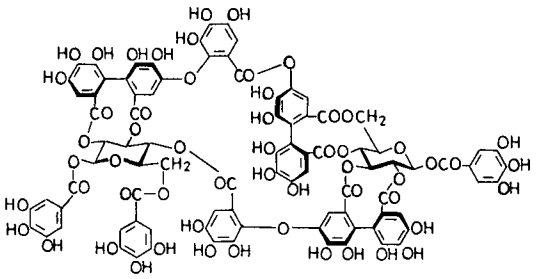

5

was found to contain a dimeric hydrolysable tannin whose structure was elucidated to be **5** (nobotanin I[10]) based on chemical and spectral evidence. The chemical lability of nobotanin J (**1**) in solution was shown by its decomposition into a mixture of a monomer, pedunculagin (**2**)[11], and a dimer (**3**), which occurred on keeping it in aqueous solution at 37°C for 22 days. Methanolysis of nobotanin J (**1**) at room temperature for 30 days similarly afforded **2** and the methyl ester (**4**) of **3** (Scheme 2).

Nobotanin K (**6**)[12], a tetrameric hydrolysable tannin, which is more polar than the trimers such as nobotanin E[10] and J (**1**), was strongly adsorbed on the solid support. Although the fraction containing **6**, which was the final eluate from column chromatography on Toyopearl HW-40, exhibited a single peak on the normal-phase HPLC, reversed-phase HPLC showed that it is contaminated by the other com-

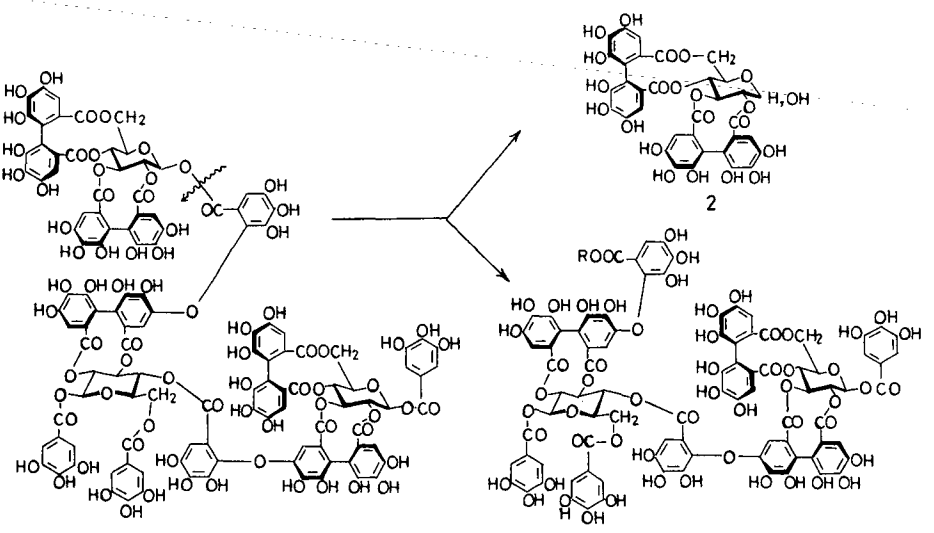

1 2 3 R=H 4 R=Me

Scheme 2.

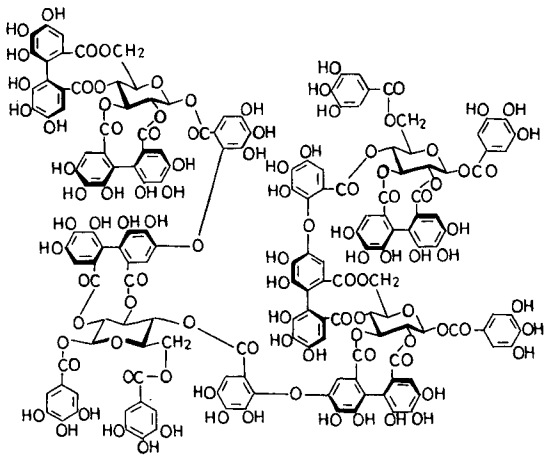

6

pounds (Fig. 2), which were shown by the NMR spectra to be tetramers with related structures. These tetramers were also efficiently separated from each other by centrifugal partition chromatography with reversed-phase development employing solvent system A. The centrifugal partition chromatogram and high-performance liquid chromatogram of each fraction are shown in Fig. 3, and nobotanin K (**6**) (112 mg) was obtained from fraction II.

Separation of bioactive polyphenols from licorice roots

We have recently found that extracts of licorice roots have tannin-like activity, as judged by the binding ability (astringency) with hemoglobin[13]. The diethyl ether extract from Sinkiang licorice which exhibited significant tannin-like activity [RAG (astringency relative to that of geraniin)[13], 0.18] was separated by centrifugal partition chromatography in the normal-phase mode using solvent system B into four fractions (I–IV), among which only fraction IV was found to show considerable

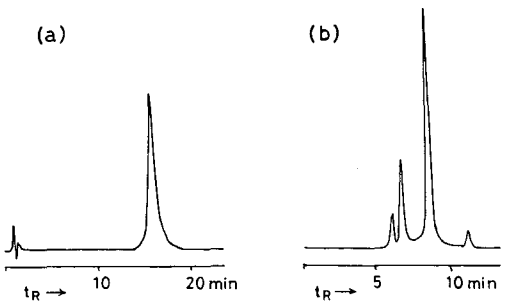

Fig. 2. HPLC of tetramer fraction obtained from column chromatography on Toyopearl HW-40 of *n*-butanol extract of *H. roseum*. (a) Normal-phase HPLC (conditions as in Fig. 1); (b) reversed-phase HPLC [column, YMC A312 (ODS); solvent A; detection, 280 nm, 0.04 a.u.f.s.].

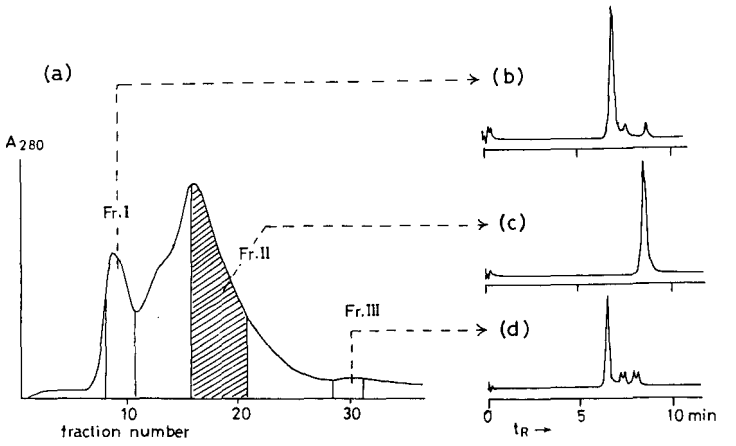

Fig. 3. Centrifugal partition chromatogram of tetramer fraction obtained from Toyopearl HW-40 of *n*-butanol extract of *H. roseum*, and reversed-phase HPLC of each fraction. (a) Centrifugal partition chromatogram (reversed-phase development with solvent A); (b) HPLC of fraction I; (c) HPLC of fraction II; (d) HPLC of fraction III. HPLC conditions as in Fig. 2.

tannic activity[13] (Fig. 4). Subsequent purification of fraction IV by column chromatography over Kieselgel 60 gave the tannin-like component **7** (RAG 0.40) and 7,4'-dihydroxyflavone (**8**), the former of which was characterized as licochalcone B[14]. Similarly licochalcone A (**9**) was obtained from fraction II. Application of centrifugal partition chromatography to the separation of the polyphenols in licorice has therefore been found to be useful in the preliminary separation of these structurally related components on a preparative scale.

Licochalcone A (**9**) and B (**7**) isolated in this way were found to show inhibitory effects on the formation of 5-HETE, 12-HETE, 5,12-diHETE, TXB_2, LTB_4 and LTC_4 in the arachidonate metabolism[15]. Licochalcone A (**9**) also showed inhibitory effects on the cytopathic activity of human immunodeficiency virus[16].

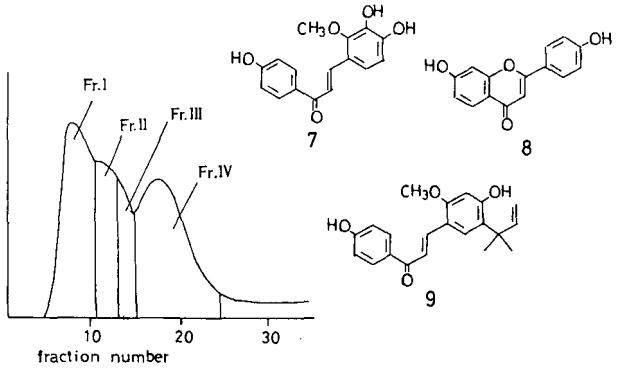

Fig. 4. Centrifugal partition chromatogram of diethyl ether extract of Sinkiang licorice (normal-phase development with solvent B).

REFERENCES

1 K. Miyamoto, N. Kishi, R. Koshiura, T. Yoshida, T. Hatano and T. Okuda, *Chem. Pharm. Bull.*, 35 (1987) 814.
2 T. Okuda, K. Mori and H. Hayatsu, *Chem. Pharm. Bull.*, 32 (1984) 3755.
3 S. Yoshizawa, T. Horiuchi, H. Fujiki, T. Yoshida, T. Okuda and T. Sugimura, *Phytother. Res..*, 1 (1987) 44.
4 T. Okuda, Y. Kimura, T. Yoshida, T. Hatano, H. Okuda and S. Arichi, *Chem. Pharm. Bull.*, 31 (1983) 1625.
5 Y. Fujita, K. Komagoe, Y. Sasaki, I. Uehara, T. Okuda and T. Yoshida, *Yakugaku Zasshi*, 107 (1987) 17.
6 T. Okuda, T. Yoshida, T. Hatano, K. Yazaki, R. Kira and Y. Ikeda, *J. Chromatogr.*, 362 (1986) 375.
7 W. Murayama, T. Kobayashi, Y. Kosuge, H. Yano, Y. Nunogaki and K. Nunogaki, *J. Chromatogr.*, 239 (1982) 643.
8 T. Yoshida, H. Ohbayashi, K. Ishihara, Y. Ohwashi, T. Shingu and T. Okuda, *Chem. Pharm. Bull.*, 34 (1986) 2676.
9 T. Yoshida, K. Haba. T. Shingu and T. Okuda, *Heterocycles*, 26 (1987) 2845.
10 T. Yoshida, K. Haba, R. Arata, T. Shingu and T. Okuda, in K. Kaneko (Editor), *Symposium papers, 29th Symposium on the Chemistry of Natural Products, Sapporo, August 1987*, Faculty of Pharmaceutical Sciences, Hokkaido University, Sapporo, p. 676.
11 T. Okuda, T. Yoshida, M. Ashida and K. Yazaki, *J. Chem. Soc., Perkin Trans. 1*, (1983) 1765.
12 T. Yoshida, K. Haba, R. Arata and T. Okuda, *Abstracts 108th Annual Meeting of the Pharmaceutical Society of Japan, April 1988, Hiroshima*, p. 339.
13 T. Okuda, K. Mori and T. Hatano, *Chem. Pharm. Bull.*, 33 (1985) 424.
15 T. Hatano, H. Kagawa, T. Yasuhara and T. Okuda, *Chem. Pharm. Bull.*, 36 (1988) 2090.
15 Y. Kimura, S. Arichi, H. Okuda, T. Hatano and T. Okuda, *J. Med. Pharm. Soc. WAKAN-YAKU*, 4 (1987) 350.
16 T. Hatano, T. Yasuhara, K. Miyamoto and T. Okuda, *Chem. Pharm. Bull.*, 36 (1988) 2286.

Journal of Chromatography, 467 (1989) 149–157
Elsevier Science Publishers B.V., Amsterdam — Printed in The Netherlands

CHROM. 21 237

COMBINED MONITORING OF UV ABSORBANCE AND FLUORESCENCE INTENSITY AS A DIAGNOSTIC CRITERION IN REVERSED-PHASE HIGH-PERFORMANCE LIQUID CHROMATOGRAPHIC SEPARATIONS OF NATURAL PHENOLIC ACIDS

J. A. DELCOUR*, C. J. A. VINKX, S. VANHAMEL and G. G. A. G. BLOCK
Laboratorium voor Toegepaste Organische Scheikunde, Katholieke Universiteit te Leuven, Kardinaal Mercierlaan 92, B-3030 Heverlee (Belgium)
(First received February 29th, 1988; revised manuscript received December 29th, 1988)

SUMMARY

Under standardized conditions, the combined monitoring of UV absorbance (A_{280}) and fluorescence intensity (I_F) at 390 or 393 nm (on excitation at 300 or 340 nm, respectively) provides a diagnostic criterion for the identification of cinnamic and benzoic acid derivatives by reversed-phase high-performance liquid chromatographic seperations of natural phenolic acids. The method can easily be used to determine the concentrations of these compounds if 3,5-dinitrobenzoic acid is applied as an internal standard. When applied to a saponified rye kernel water extract, ferulic, *p*-coumaric, sinapic, syringic and vanillic acids were shown to be present.

INTRODUCTION

Reversed-phase high-performance liquid chromatographic (HPLC) separations of natural phenolic acids are traditionally monitored by measurement of the UV absorbance of the eluate[1–8]. The retention time of these components under standardized conditions is, however, not a reliable criterion for their identification because in complex chromatograms of natural extracts many substances of similar structures occur that can yield peaks with only slightly different or even the same retention times[8]. It is therefore advisable in many instances to verify the identity of a particular peak by applying a second chromatographic technique such as thin-layer chromatography (TLC)[1,2,7–13]. The recovery of samples run on analytical reversed-phase HPLC columns in order to perform this second analysis (*e.g.*, by TLC) is, however, laborious.

As cinnamic and *o*-hydroxybenzoic acid and their derivatives display fluorescence when exposed to light of the Wood wavelength (366 nm)[14] and as this property is exploited both in the study of cereals by fluorescence microscopy[9,15–19] and in the TLC analysis of phenolic acids, we decided to establish whether or not the joint monitoring of UV absorbance and fluorescence intensity could provide an additional and simple criterion for the identification of phenolic acids in our standardized HPLC

0021-9673/89/$03.50

separation of these natural substances. To the best of our knowledge, the use of fluorescence intensity as a monitoring technique for the HPLC separations of plant phenolic acids has not been reported before. This is understandable to a certain extent, as it is necessary to find suitable combinations of excitation and emission wavelengths such that at least a considerable proportion of the studied compounds display fluorescence.

It seemed to us that the joint measurement of the UV absorbances and fluorescence intensities of the separated compounds could offer an interesting diagnostic criterion, not only to allow for a distinction between the compounds that display fluorescence under the experimental conditions and those that do not, but also between different phenolic acids characterized by varying ratios between their UV absorbance and fluorescence intensity under standardized conditions.

In this paper it is shown that different excitation and fluorescence wavelength combinations can be chosen for the identification of natural phenolic acids via the above method. It is also demonstrated that 3,5-dinitrobenzoic acid can serve as an internal standard for quantitative work. The method was applied to the chromatography of the natural phenolic acids associated with rye water solubles.

Ferulic acid was previously found to be associated with rye water soluble pentosan material[12]. It is likely that ferulic acid associated with such pentosans is important for the oxidative gelation of these materials[20,21], which have a positive effect on the breadmaking properties of rye flour[21].

EXPERIMENTAL

Instrumentation

The HPLC system consisted of the following Shimadzu equipment: an SCL-6A system controller, two LC-60 chromatography pumps and an HPLC fluorescence monitor. The UV absorbance detector, equipped with a 280-nm filter, was a Pharmacia UV-2 dual-path monitor. The chromatographic separations were performed on an Alltech ROSIL C_{18} column (250 × 4.6 mm I.D., particle size 5 μm). We used a precolumn (10 × 4.6 mm I.D.) with the same stationary phase. All samples were injected with a Rheodyne 7125 injector (installed with a 20-μl loop) as solutions in glass-distilled methanol after double filtration on Schleicher & Schüll FP 030/70 disposable 0.45-μm filter holders. The eluate from the fluorescence detector was fed directly to the UV monitor and both the UV and the fluorescence signal were registered with a Pharmacia Rec-2 two-channel recorder.

All separations were achieved under isocratic conditions. Although the gradient mode allows for faster separations, we preferred to achieve separations devoid of baseline drift, a phenomenon encountered in the gradient elution of the compounds studied here[1,2,8].

Solvents and chemicals

The elution solvent (flow-rate 1.0 ml/min) was water–methanol–acetic acid (95:15:5, v/v/v). The water was deionized and glass distilled immediately before use. Methanol was glass distilled and glacial acetic acid was purchased from Merck (GR grade). The solvent was vacuum filtered through FP-450 47 mm 0.45 μm FP Vericel membrane filters purchased from Gelman and used without further degassing.

Caffeic, ferulic, *p*-coumaric, syringic, vanillic and 3,5-dinitrobenzoic acids were purchased from Fluka and sinapic and gallic acids were obtained from Aldrich. Protocatechuic acid, *p*-hydroxybenzoic acid and salicylic acid were obtained from Sigma, UCB and Eastman Kodak, respectively. The cinnamic acid derivatives were *trans* isomers.

All compounds were injected as solutions in methanol (60 ppm), except for vanillic acid and *p*-hydroxybenzoic acid, where other concentrations in the same solvent (30 and 240 ppm, respectively) were used. When injected alone they all gave single peaks.

Isolation of rye water solubles

The rye sample was of the Danko variety (1987 harvest), grown in Limburg Province, Belgium. The sample was the same as that used in a study of the relative monosaccharide compositions in milled rye products[22].

Rye kernels were cooked in ethanol (95%) for 60 min. After removal of the solvent by filtration and drying at room temperature, the kernels were milled using a D.D.D. President Mill (Ieper, Belgium). Whole rye meal (500 g) was extracted with 2000 ml of deionized water for 4 h at room temperature with continuous mechanical stirring. After centrifugation (30 min, 2000 *g*) the extract (1650 ml) was lyophilized (yield 39.84 g).

Isolation of phenolic acids in rye water solubles

The isolation was carried out in the dark whenever possible, as free cinnamic acids can rapidly undergo *trans–cis* isomerization in daylight[10,23,24].

Lyophilized water solubles (1.00 g) were saponified in 100 ml of 0.5 *M* sodium hydroxide solution for 90 min at 60°C under a nitrogen atmosphere. The saponified mixture was neutralized with concentrated hydrochloric acid. Two volumes of ethanol (95%) were added to one volume of extract in order to precipitate the pentosan material (overnight at 6°C). The precipitate was removed by centrifugation (10 min, 2000 *g*), the residue was washed with ethanol and the washings were added to the supernatant. The ethanol was removed from this solution by vacuum evaporation at 40°C. The pH of the water phase was then adjusted to 3.0 using 2.0 *M* hydrochloric acid. The phenolic acids were subsequently extracted with ethyl acetate (3 × 100 ml). The extract was dried over anhydrous sodium sulphate and evaporated (under vacuum at 40°C) to dryness. This extract was dissolved in 2.0 ml of methanol containing the internal standard 3,5-dinitrobenzoic acid (0.1 mg/ml). It was then filtered twice as above and analysed by HPLC as described above.

Quantitative data were obtained using the relative peak heights (peak height of the compound to be analysed / peak height of 3,5-dinitrobenzoic acid) in the chromatogram (A_{280}) and the relationship between the relative peak heights and the relative concentrations for each compound.

RESULTS

The structures of the compounds studied are shown in Fig. 1 and typical examples of chromatographic separations monitored either by UV absorbance at 280 nm (A_{280}) or by the fluorescence intensities at different filter combinations (I_F) are given

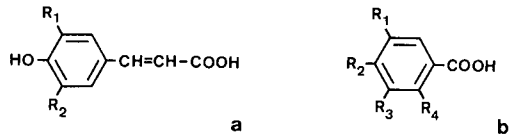

Fig. 1. Structural formulae of (a) cinnamic acid derivatives and (b) benzoic acid derivatives. (a) $R_1 = R_2 =$ H, *p*-coumaric acid; $R_1 =$ H, $R_2 =$ OH, caffeic acid; $R_1 =$ OMe, $R_2 =$ H, ferulic acid; $R_1 = R_2 =$ OMe, sinapic acid. (b) $R_1 = R_2 = R_3 =$ H, $R_4 =$ OH, salicylic acid; $R_1 = R_3 =$ OMe, $R_2 =$ OH, $R_4 =$ H, syringic acid; $R_1 =$ OMe, $R_2 =$ OH, $R_3 = R_4 =$ H, vanillic acid; $R_1 = R_3 = R_4 =$ H, $R_2 =$ OH, *p*-hydroxybenzoic acid; $R_1 = R_2 =$ OH, $R_3 = R_4 =$ H, protocatechuic acid; $R_1 = R_2 = R_3 =$ OH, $R_4 =$ H, gallic acid; $R_1 = R_3 = NO_2$, $R_2 = R_4 =$ H, 3,5-dinitrobenzoic acid.

in Fig. 2. Adequate baseline separations were obtained under the chromatographic conditions applied.

Typical retention times of the compounds and ratios between their UV absorbance and fluorescence intensities at different wavelength combinations are listed in

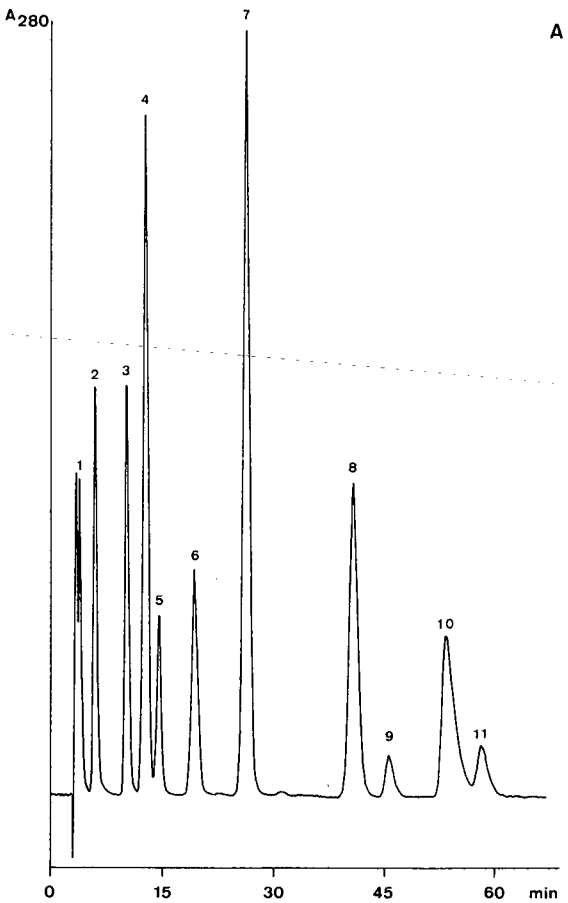

Fig. 2.

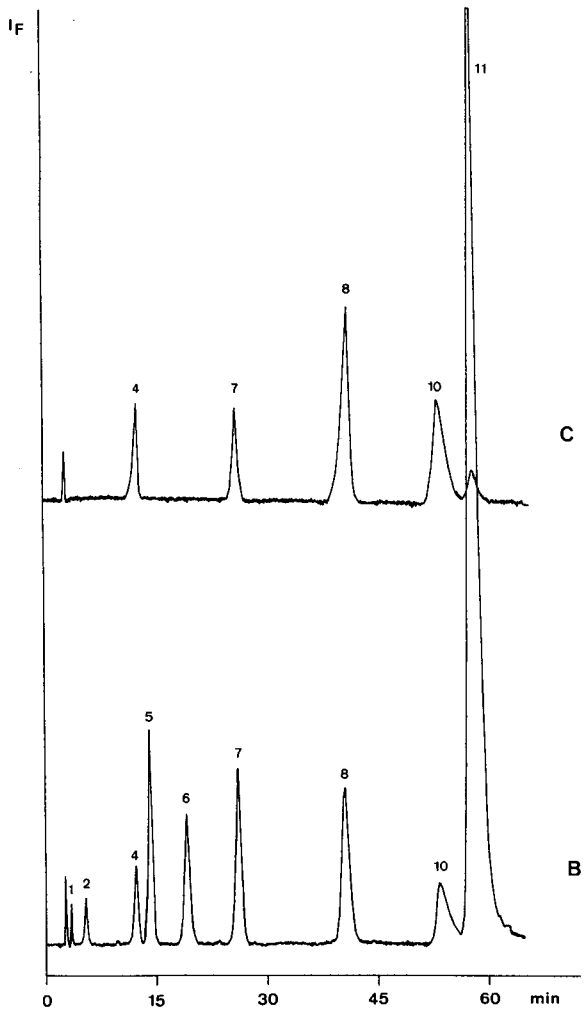

Fig. 2. HPLC separation of standard phenolic compounds on ROSIL C_{18} (250 × 4.6 mm I.D., 5 μm, with precolumn) with water–methanol–acetic acid (95:15:5, v/v/v) at 1.0 ml/min as eluent. An aliquot (20 μl) of solutions in methanol with concentrations as described in the text was chromatographed and the separations were monitored by recording (A) the A_{280} values (0.2 a.u.f.s.) or the fluorescence intensities (I_F) at (B) 390 and (C) 393 nm with excitation at 300 and 340 nm, respectively. Peaks: 1 = gallic acid; 2 = protocatechuic acid; 3 = *p*-hydroxybenzoic acid; 4 = caffeic acid; 5 = vanillic acid; 6 = syringic acid; 7 = *p*-coumaric acid; 8 = ferulic acid; 9 = 3,5-dinitrobenzoic acid; 10 = sinapic acid; 11 = salicylic acid.

Table I. These ratios are given in arbitrary units as they are based on peak heights registered under highly standardized conditions.

Of further interest is the fact that the *cis* isomers generated on UV irradation of cinnamic acid derivatives[10,23,24] do not display fluorescence under the experimental conditions applied here.

Phenolic acids associated with rye water solubles are vanillic, syringic, *p*-coumaric, ferulic and sinapic acids (Table II). This follows not only from the retention

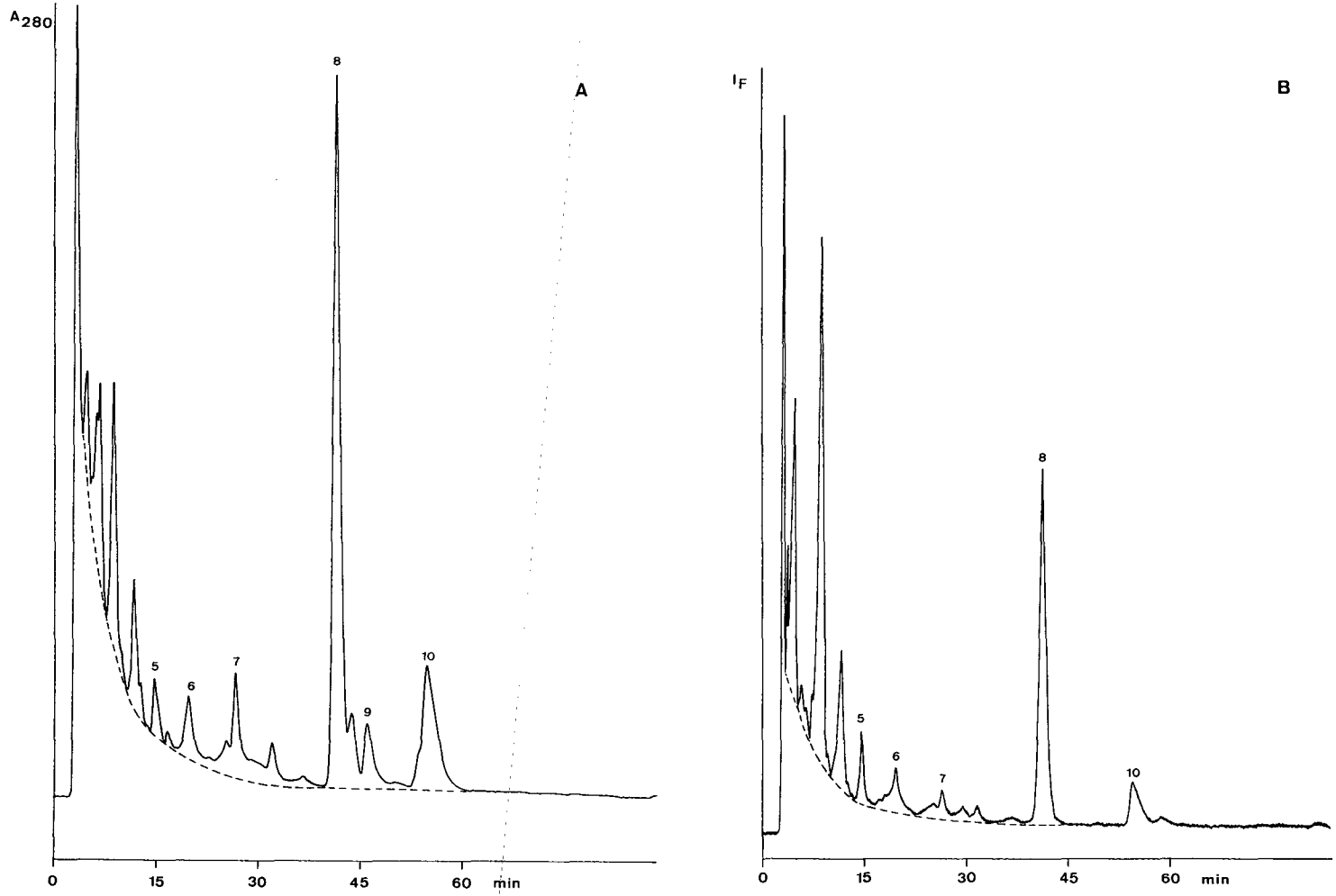

Fig. 3. HPLC separation of an ethyl acetate extract of saponified lyophilized rye water solubles, with detection of (A) the UV absorbance (A_{280}) (0.2 a.u.f.s.) and (B) the fluorescence intensity (I_F) at 390 nm with excitation at 300 nm.

TABLE I

TYPICAL RETENTION TIMES AND RATIOS (ARBITRARY UNITS) BETWEEN THE UV ABSORBANCE (A_{280}) AND THE FLUORESCENCE INTENSITIES (I_F) AT 393 AND 390 nm ON EXCITATION AT 340 AND 300 nm, RESPECTIVELY, OF DIFFERENT PHENOLIC COMPOUNDS SEPARATED AS DESCRIBED IN FIG. 2

N.f. = No fluorescence under the experimental conditions.

Compound	*Retention time (min)*	A_{280}/I_F	
		393 nm	*390 nm*
Gallic acid	4	N.f.	8.2
Protocatechuic acid	6	N.f.	8.2
p-Hydroxybenzoic acid	10	N.f.	N.f.
Caffeic acid	13	7.2	9.0
Vanillic acid	15	N.f.	0.9
Syringic acid	19.5	N.f.	1.7
p-Coumaric acid	26.5	9.4	4.3
Ferulic acid	41	1.6	2.1
3,5-Dinitrobenzoic acid	46	N.f.	N.f.
Sinapic acid	53.5	1.5	2.7
Salicylic acid	58.5	1.6	0.1

times of these compounds, but also from the ratios of the UV absorbance (280 nm) to the fluorescence intensity at 390 nm on excitation at 300 nm. With *p*-coumaric acid, the theoretical ratio (4.3) was not identical with that of the same compound observed in the natural extract (3.7). It is believed that this is mainly due to the presence of a minor component in the extract with a retention time slightly lower than that of *p*-coumaric acid. A typical chromatogram is shown in Fig. 3. The analytical data indicate that the most abundant phenolic acid is ferulic acid, as was to be expected[20,21,25]. To the best of our knowledge, the presence of these other phenolic acids in rye water solubles has not been reported before, although their occurrence in wheat, rice, oat and corn kernels is well known[25].

TABLE II

PHENOLIC ACID CONTENTS OF LYOPHILIZED RYE WATER SOLUBLES AND THE RATIOS BETWEEN THE UV ABSORBANCE (A_{280}) AND FLUORESCENCE INTENSITIES (I_F) AT 390 nm ON EXCITATION AT 300 nm, OBTAINED AS DESCRIBED IN FIG. 2

Phenolic acid	*Concentration (ppm)*	A_{280}/I_F
Vanillic acid	28	0.8
Syringic acid	26	1.5
p-Coumaric acid	21	3.7
Ferulic acid	332	2.0
Sinapic acid	18	2.8

DISCUSSION

When exposed to UV light of a particular wavelength, different fluorescent phenolic acids have different fluorescence spectra, as exhibited by differences in the wavelength and the intensity of maximum fluorescence. From this it follows that the chromatographic analysis of these phenolic acids by monitoring both the UV absorbance and the fluorescence intensity at, *e.g.* excitation and emission wavelength combinations of 300 and 390 nm or 340 and 393 nm will result in different ratios between the peak heights in the measurement of the UV absorbance and fluorescence intensity. These ratios can therefore be applied as diagnostic criteria for the identification of these phenolic compounds because we found (as was to be expected at low concentrations) that they are independent of the concentration of the chromatographed substance. In our experience gained during the identification of phenolic acids associated with rye arabinoxylans[13] and partly described here, the determination of the ratio between the peak heights of the UV absorbance and the fluorescence intensity at only one wavelenght combination suffices for the identification of unknown fluorescent phenolic acids. Further, the ratios obtained under highly standardized conditions can in many instances also be applied in order to verify whether or not a particular peak in a chromatogram results from a single substance or not.

ACKNOWLEDGEMENTS

One of us (J.A.D.) gratefully thanks the Belgian Nationaal Fonds voor Wetenschappelijk Onderzoek for a research position as "Bevoegdverklaard Navorser" and for "Krediet aan Navorsers" financial support. Helpful discussions by Professor P. Dondeyne and excellent technical assistance by Mr. Luc Van den Ende are gratefully acknowledged.

REFERENCES

1 B. Jende-Strid, *Carlsberg Res. Commun.*, 50 (1985) 1.
2 I. McMurrough, G. P. Roche and K. G. Cleary, *J. Inst. Brew.*, 90 (1984) 181.
3 L. W. Wulf and C. W. Nagel, *J. Chromatogr.*, 116 (1976) 131.
4 F. Villeneuve, G. Abravanel, M. Moutounet and G. Alibert, *J. Chromatogr.*, 234 (1982) 131.
5 D. H. Hahn, J. M. Faubion and L. W. Rooney, *Cereal Chem.*, 60 (1983) 255.
6 B. A. Charpentier and J. R. Cowles, *J. Chromatogr.*, 208 (1981) 132.
7 N. Shibuya, *Phytochemistry*, 23 (1984) 2233.
8 B. Jende-Strid, in H. F. Linskens and J. F. Jackson (Editors), *Modern Methods of Plant Analysis (New Series, Vol. 7, Beer Analysis)*, Springer, Heidelberg, 1988, p. 109.
9 M. G. Smart and T. P. O'Brien, *Aust. J. Plant Physiol.*, 6 (1979) 485.
10 R. D. Hartley and E. C. Jones, *Phytochemistry*, 15 (1976) 1157.
11 V. K. Newby, R.-M. Sablon, R. L. M. Synge, K. Vande Casteele and C. F. Van Sumere, *Phytochemistry*, 19 (1980) 651.
12 J. Schneider and H. P. Pietsch, *Nahrung*, 29 (1985) 425.
13 C. Vinkx, *Thesis Ingenieur voor de Scheikunde en de Landbouwindustrieën*, Katholieke Universiteit Leuven, 1988.
14 P. Ribéreau-Gayon, *Les Composés Phénoliques des Végétaux*, Dunod, Paris, 1968, p. 103.
15 R. G. Fulcher and S. I. Wong, in G. E. Inglett and L. Munck (Editors), *Cereals for Food and Beverages*, Academic Press, New York, 1980, p. 1.
16 R. G. Fulcher and P. J. Wood, in D. G. Bechtel (Editor), *New Frontiers in Food Microstructure*, American Association of Cereal Chemists, St. Paul, MN, 1983, p. 111.

17 C. M. McDonough, L. W. Rooney and C. F. Earp, *Food Microstruct.*, 5 (1986) 247.
18 P. J. Harris and R. D. Hartley, *Nature (London)*, 259 (1976) 508.
19 G. B. Fincher, *J. Inst. Brew.*, 82 (1976) 347.
20 T. Geissmann and H. Neukom, *Lebensm.-Wiss. Technol.*, 6 (1973) 59.
21 F. Meuser and P. Suckow, in J. M. V. Blanshard, P. J. Frazier and T. Galliard (Editors), *Chemistry and Physics of Baking. Materials, Processes, and Products*, Royal Society of Chemistry, London, 1986, p. 42.
22 J. A. Delcour, S. Vanhamel and C. De Geest, *Cereal Chem.*, 66 (1989) in press.
23 G. Kahnt, *Phytochemistry*, 6 (1967) 755.
24 R. D. Hartley and E. C. Jones, *J. Chromatogr.*, 107 (1975) 213.
25 F. Sosulski, K. Krygier and L. Hogge, *J. Agric. Food Chem.*, 30 (1982) 337.

Journal of Chromatography, 467 (1989) 159–166
Elsevier Science Publishers B.V., Amsterdam — Printed in The Netherlands

CHROM. 21 257

ANALYSIS, CHARACTERIZATION, AND PURIFICATION: REQUIREMENTS FOR TOXICOLOGICAL EVALUATION OF 1,4-DITHIANE

HAROLD C. THOMPSON, Jr.*, WILLIAM M. BLAKEMORE, DANIEL M. NESTORICK, JAMES P. FREEMAN and DWIGHT W. MILLER

Department of Health and Human Services, Food and Drug Administration, National Center for Toxicological Research, Jefferson, AR 72029 (U.S.A.)

(First received January 25th, 1988, revised manuscript received January 9th, 1989)

SUMMARY

1,4-Dithiane is an organo-sulfur chemical associated with production and storage of munitions. Toxicological evaluation of this chemical was scheduled in rats because of the paucity of such information. Prerequisite for the evaluation was the development of gas chromatographic procedures using flame ionization detection to determine the purity of the test chemical and to certify the concentration and stability of the chemical in the dosage form, sesame oil. Mass and nuclear magnetic resonance spectrometry procedures are described for assessing the structural character and purity of the test chemical. A procedure for the purification of the test chemical and data concerning its solubility in various solvents are also presented.

INTRODUCTION

1,4-Dithiane (CAS No. 505-29-3) is a groundwater contaminant at certain military installations where munitions are stored.

There is a scarcity of toxicological data in the literature for 1,4-dithiane. The oral LD_{50} in rats is reported as 3500 mg/kg in unpublished results of a range-finding study by the U.S. Army Medical Bioengineering Research and Development Laboratory. In view of the lack of toxicity data, this chemical was proposed by the Department of the Army for 90-day sub-chronic toxicological evaluation at the National Center for Toxicological Research (NCTR).

However, before such toxicological tests could be initiated, analytical procedures were required for determining the purity, structural characterization, and stability of the test chemical in the dosage form used in the animal studies. Procedures were also needed for purification of the test chemical if deleterious impurities were found and for dosage form concentration certification assays.

Experiments to determine the toxicological effect of a test chemical require that the compound be examined for the presence of impurities prior to the initiation of animal tests. The presence of excessive amounts of impurities requires that the chemical be purified to minimize or eliminate the substances that might bias the experimental results[1]. Proper control of test substances must be maintained to ensure the validity of the experiment[2].

D'Agostino and Provost[3] determined gas chromatographic (GC) retention indices of chemical warfare agents and simulants, including dithiane, using GC–flame ionization detection (FID) with several different capillary columns. Adventitious trace organics, including 1,4-dithiane, have been identified in nitramine munitions recrystallization process samples using GC–mass spectrometry (MS)[4]. Neither of these methods was totally adequate for use in our proposed work.

This paper describes GC–FID procedures (packed and capillary columns) for determination of the purity of the test chemical and its stability in sesame oil. MS and nuclear magnetic resonance (NMR) spectrometry methodologies are also presented for structural characterization and purity determinations of the test chemical. Recrystallization techniques for purification of 1,4-dithiane are also described. Data concerning the approximate solubility of 1,4-dithiane in various solvents and its stability in sesame oil are also reported.

Data obtained in these experiments allowed the 90-day sub-chronic toxicological evaluation of 1,4-dithiane in cesarean derived (CD) rats to proceed.

EXPERIMENTAL

Test chemical and solvents

The test compound 1,4-dithiane was purchased from Fairfield (Blythewood, SC, U.S.A.) and Aldrich (Milwaukee, WI, U.S.A.). Pure cold-pressed sesame oil was purchased from Hain Pure Food (Los Angeles, CA, U.S.A.). All chromatographic solvents were CP grade, residue analyzed.

Gas chromatography

Purity and dose certification assays. Purity assays were performed by GC on packed and capillary columns using conditions described in Table I. Injections on packed columns were 2 μl, and those on capillary columns were 1 μl. Injections for headspace analysis were 50 μl. Samples for purity assays were prepared at a concentration of 1 mg/ml in dichloromethane. Gavage solutions for use in toxicological tests were prepared at concentrations of 35 and 2 mg/ml in sesame seed oil. These two solutions were diluted to 1 and 0.2 mg/ml, respectively with dichloromethane for dose certification analysis by GC–FID.

Stability assays. Stability assays were performed by GC on packed columns using conditions described in Table I.

Mass spectrometry

A Finnigan (San Jose, CA, U.S.A.) Model 4023 mass spectrometer operated in the electron impact (EI) mode was used to analyze solid samples of 1,4-dithiane via a solids probe. The dry sample was placed into a glass sample cup, which was placed in the solids probe. The probe was inserted into the solids probe inlet, cooled to 0°C and the inlet was evacuated. The probe was cooled to −30°C before insertion into the mass spectrometer. Data were collected as the probe was slowly heated. The ion source temperature was 250°C and the electron energy was 70 V. Representative spectra were compared to the NIH/EPA library, which contained the mass spectrum for 1,4-dithiane.

Head space samples (100 μl) were obtained and injected via a Grob injector (splitless mode) into the GC–MS under conditions described in Table I.

TABLE I

INSTRUMENTAL CONDITIONS FOR VARIOUS ANALYSES OF 1,4-DITHIANE

	Column and temperature	*Detector temperature*[a]	*Injector temperature*	*Carrier gas and flow-rate*
GC Analysis				
Purity, dose certification, solubilities	3 ft. × 2 mm I.D. glass, 3% SP2250 on Supelcoport, 100–120 mesh; 80°C	280°C	120°C	N_2; 30 ml/min
Purity	30 m × 0.259 mm I.D. DB-1701; programmed 50–280°C at 20°C/min	300°C	programmed 50–280°C at 140°C/min	He; 1 ml/min
Purity (headspace)	15 m × 0.259 mm I.D. DB-1701; 34°C	280°C	110°C (split mode with 30:1 ratio)	He; 1 ml/min
Stability	240 cm × 4 mm I.D. glass, 10% OV-101 on Gas Chrom Q, 80–100 mesh; 150°C	270°C	160°C	He; 100 ml/min
GC–MS analysis				
Purity (headspace)	30 m × 0.259 mm I.D. DB5; programmed 40–150°C at 20°C/min		Grob splitless mode 255°C	He; 2 ml/min

[a] FID detector.

Nuclear magnetic resonance spectrometry

The 1,4-dithiane was dissolved in chloroform-d_2 (Merc Isotopes, Rahway, NJ, U.S.A.) at a concentration of 100 mg/ml for structure verification. The ^1H spectrum was obtained with a Model WM-500 NMR (Bruker Instruments, Bilerica, MA, U.S.A.) using standard acquisition parameters.

To estimate concentrations of impurities, proton NMR determinations were performed on a Model WM-500 NMR (Bruker Instruments) at room temperature in chloroform-d_2 (1 mg/ml). One transient was collected for each sample with a 78° flip angle (11.5 μs, 90° flip angle), 30K data points, 7024-Hz window, and a 20-s delay prior to pulse. The free induction decay data was treated with a 0.5-Hz line broadening prior to Fourier transformation. The spectra were analyzed for dichloromethane (singlet) and ethanol (methylene quartet and methyl triplet) by chemical shift using chloroform as a reference. Quantitation of the observed impurities was accomplished by integration of impurity resonances with respect to the 1,4-dithiane resonance.

Stability experiments

A stability study was performed to ensure that sesame oil solutions of 1,4-dithiane at the low (2 mg/ml) and high (35 mg/ml) dose levels could be stored and remain stable for the term of the study. Solutions of the chemical in sesame oil were prepared at the concentrations previously described, placed in 25 ml amber vials, sealed with Teflon™ faced septa and stored at −20°C. Triplicate vials of the high and low concentrations were assayed on days 0, 1, 2, 7, 14, 21, 28, 42, 56, and 90 after preparation, as described under *Stability assays*. Solutions were thoroughly mixed prior to taking a sample for analysis.

Purification of 1,4-dithiane

Approximately 100 g of 1,4-dithiane were dissolved in one liter of boiling absolute ethanol. After filtration the hot solution was rapidly cooled in an ice bath and the recrystallized dithiane was harvested. The recrystallized product was then allowed to air dry in a fume hood. This process was repeated several times to obtain sufficient amounts of the test chemical to perform the proposed toxicological tests.

Solubility determinations

The following are descriptions of the determination of approximate solubilities of 1,4-dithiane in the solvents listed.

Acetone, methanol and hexane. A 5-ml volume of each solvent was saturated with the test chemical. The mixture was centrifuged, a 100-μl aliquot was removed, diluted to 10 ml with dichloromethane and analyzed by GC–FID on a column containing 3% SP 2250 with GC conditions described in Table I. Quantitation was made by comparison to an appropriately diluted standard in dichloromethane.

Sesame oil. 1,4-Dithiane (100 mg) was placed in a tube and 2 ml of sesame oil were added. The mixture was sonicated causing the oil temperature to increase, which resulted in dissolution of the dithiane. Upon cooling to 25°C crystallization of a portion of the dithiane occurred. The suspension was centrifuged and a 100-μl aliquot taken and diluted to 5 ml with dichloromethane. GC–FID analysis was performed as described in the previous section.

Water. A 44-mg amount of 1,4-dithiane was placed in a tube, and 40 ml of deionized water were added. The tube was capped, vortexed for 20 min and filtered through a 0.45-μm filter. A 3-ml sample was removed and partitioned against an equal volume of dichloromethane. The dichloromethane fraction was analyzed by GC–FID as described for acetone, methanol and hexane.

DMSO and Tween 80. Amounts of 120 mg and 100 mg of dithiane were dissolved in 1 ml of DMSO and 1 ml of Tween 80, respectively, at 65°C. Upon cooling each solution to 35°C, crystallization of a portion of the dithiane occurred. Each suspension was centrifuged and a 100-μl aliquot taken and diluted to 10 ml with dichloromethane. GC–FID analysis was performed as described for acetone, methanol and hexane.

RESULTS AND DISCUSSION

When a chemical is proposed for toxicological evaluation it is imperative that preliminary experiments be performed to ensure the validity of the toxicology experiments. The chemical structure of the test compound must be verified and its purity determined. The impurities detected (if any) must be identified, if possible, to ensure that these do not bias the results of the toxicological experiment. Verification of the chemical structure of 1,4-dithiane was made using the Bruker Model WM-500 NMR. The ^1H spectrum was obtained from a solution of the chemical in chloroform-d_2 (100 mg/ml), and a singlet at 2.8 ppm[3] was observed, which matches the literature spectrum for this compound. The structure of 1,4-dithiane was also verified by EI-MS (solids probe), and the mass spectra are illustrated in Fig. 1. The library search produced 1,4-dithiane as the best match (94%), with a spectral purity of 72% indicating possible impurity ions. These impurity ions were determined to be from the

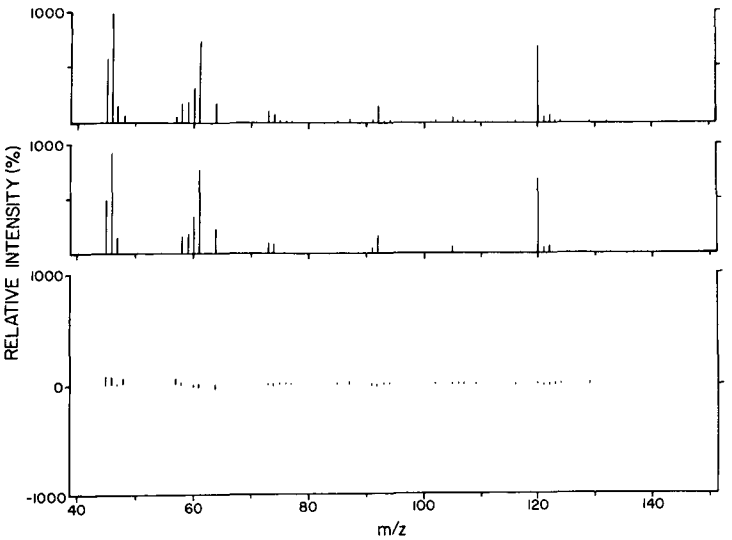

Fig. 1. Mass spectra of 1,4-dithiane. Upper is sample spectrum, middle is library spectrum for 1,4-dithiane, lower is sample spectrum subtracted from library spectrum.

Freon 12 used to cool the probe. The spectrum of the major constituent matched well with 1,4-dithiane after subtraction of the Freon 12 peaks. The isotope ratios of the M, M + 1, and M + 2 ions (*m/z* 120, 121, and 122) indicated a compound with molecular weight 120 containing two sulfur atoms, which is consistent with the 1,4-dithiane structure. The purity of the compound as received was determined by GC–FID with both packed and capillary columns. The chromatogram in Fig. 2 is the result of a

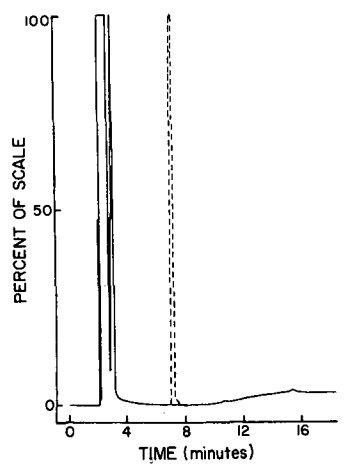

Fig. 2. Gas chromatograms of purity determination of 1,4-dithiane. Solid line is blank assay. Dotted line superimposed represents the 1,4-dithiane peak. Column, 30 m × 0.259 mm I.D. DB-1701; He carrier gas (1 ml/min); programmed from 50°C to 280°C at 20°C/min; FID detector temperature, 300°C, injection port programmed from 50°C to 280°C at 140°C/min; injection volume, 1 μl.

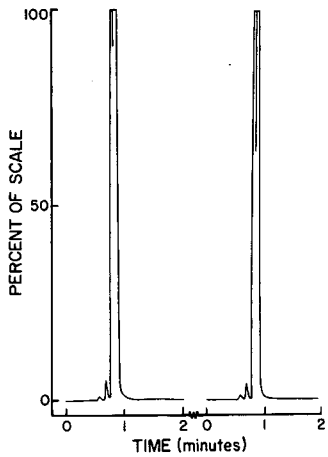

Fig. 3. Successive injections of headspace samples. Column, 30 m × 0.259 mm I.D. DB-1701; He carrier gas (1 ml/min); column and injector temperatures, 34°C, FID detector temperature, 300°C.

temperature-programmed determination on the DB-1701 capillary column. The retention time for 1,4-dithiane was 7.15 min, using conditions described in Table I. The GC–FID assays indicated that the compound was essentially pure. However, these GC conditions are not amenable to detection of more volatile impurities.

In an attempt to detect more volatile impurities in the test compound, qualitative determinations were performed by sampling the headspace above the solid compound in sealed containers with a gas tight syringe and chromatographing the samples on a DB-1701 capillary column at 34°C with FID. Fig. 3. illustrates two successive injections, which show two major volatile impurities. A headspace sample was procured in like manner for determination by GC–MS in an attempt to identify these impurities. Three peaks were observed while the column oven temperature was 40°C. One peak consisted of a single ion of *m/z* 44 and was determined to be carbon dioxide. The second peak exhibited ions at *m/z* 43, 46, and 58. This second component appeared to be acetone since its spectrum contains two of the major ions found in the standard mass spectrum of acetone (43 and 58) in the proper ratio (100:30). The presence of acetone may be from the manufacturer using this solvent in synthesis or purification schemes. The third peak had major ions at *m/z* 84,, 86, and 88 with abundances similar to those contributed by a dichloro compound. This spectrum was subjected to a library search, which produced a match with dichloromethane (95% fit). The spectra are shown in Fig. 4 along with the library spectra for dichloromethane. The concentration of dichloromethane in the test compound was estimated by NMR, as previously described in the Experimental section, to be 0.2%. Based on the techniques used, the purity of the test chemical was 99.8%. As dichloromethane is a known carcinogen, its presence in the test compound could bias any toxicological results obtained. Dichloromethane in the test chemical resulted from the manufacturer's recrystallization and purification of the product before sale. Its presence necessitated purification of the test chemical prior to the initiation of the toxicoligical experiment.

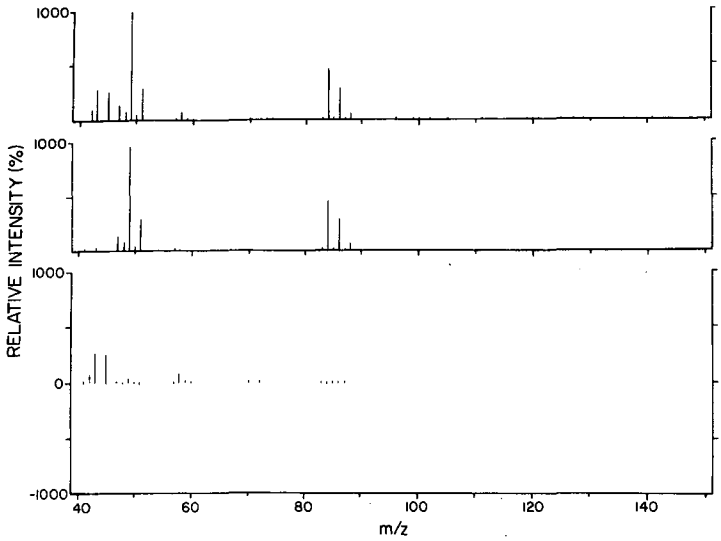

Fig. 4. Mass spectra of headspace sample. Upper is sample spectrum, middle is library spectrum for dichloromethane, lower is sample spectrum subtracted from library spectrum.

There were two obvious procedures for eliminating dichloromethane from the 1,4-dithiane — sublimation and recrystallization. Preliminary experiments were initiated to compare the efficiency of each technique. Sublimation worked well but the apparatus available was quite small and, considering the amount of compound required for this study, would have been very time-consuming and probably would have delayed the start of the experiment. It was determined that the compound could be recrystallized from absolute ethyl alcohol with a recovery of *ca.* 65%, and this method was used to purify all of the test compound. Residual ethanol in the recrystallized chemical was estimated by NMR, as described in the experimental section, to be *ca.* 0.5% and was deemed acceptable. The purity of the recrystallized product was 99.5% based on the NMR techniques used and contained no detectable dichloromethane. Samples of recrystallized and sublimed dithiane gave identical responses

TABLE II

APPROXIMATE SOLUBILITIES OF 1,4-DITHIANE IN VARIOUS SOLVENTS

Solvent	*Solubility (mg/ml)*
Sesame oil	40[a]
DMSO	98[b]
Tween 80	99[b]
Acetone	79[a]
Methanol	21[a]
Hexane	17[a]
Water	0.6[a]

[a] At 25°C.
[b] At 35°C.

TABLE III

STABILITY OF 1,4-DITHIANE IN SESAME OIL
Mean and standard deviation of triplicate assays.

Day	*Low concentration 2 mg/ml*	*High concentration 35 mg/ml*
0	1.77 ± 0.01	32.7 ± 0.94
1	1.68 ± 0.04	33.4 ± 1.36
2	1.64 ± 0.04	33.0 ± 1.23
7	1.62 ± 0.03	33.6 ± 0.40
14	1.63 ± 0.10	33.0 ± 0.59
21	1.64 ± 0.04	33.8 ± 0.58
28	1.67 ± 0.03	32.7 ± 0.77
42	1.59 ± 0.08	34.3 ± 1.01
56	1.77 ± 0.07	33.0 ± 0.75
90	1.81 ± 0.06	34.4 ± 0.86

when analyzed by GC–FID. Triplicate injections of each purified sample indicated a purity of 100 ± 1%. These data along with NMR and MS data indicate that the dithiane was essentially pure with the exception of the 0.5% ethanol.

The lack of information in the literature on 1,4-dithiane required experiments be performed to determine a suitable medium in which to administer the chemical to test animals. Due to the volatility and stench of the chemical, it was unlikely that it could be administered in feed. Initial experiments, however, showed that the animals would eat feed mixed with the compound. Unfortunately, even after pelletizing the mixed feed, stabilities of the chemical at the concentrations proposed for the study were not adequate. In an attempt to find a suitable solvent for use as a possible vehicle for delivery of the test chemical to the test animals by gavage, the approximate solubility of 1,4-dithiane in several solvents was determined. Table II lists the solubilities. Sesame oil provided adequate solubility to allow solutions of desired concentration to be prepared for dosing test animals in the proposed toxicological tests and was chosen over other solvents listed. Solutions of 1,4-dithiane in sesame oil at 2 and 35 mg/ml were prepared and subjected to a 90-day stability experiment at −20°C as previously described. The results of that experiment are presented in Table III, which demonstrate that the test chemical is stable in sesame oil stored at −20°C for 90 days.

With information developed in this study, it was then possible to prepare an experimental protocol for conducting the 90-day sub-chronic toxicological evaluation of 1,4-dithiane in rats.

ACKNOWLEDGEMENT

The authors thank Ms. Lyle Davis for typing the manuscript.

REFERENCES

1 M. C. Bowman, *J. Assoc. Off. Anal. Chem.*, 61 (1978) 1253–1262.
2 M. C. Bowman, *Clin. Toxicol.*, 15 (1979) 583–595.
3 P. A. D'Agostino and L. R. Provost, *J. Chromatogr.*, 331 (1985) 47–54.
4 E. P. Burrows and E. E. Brueggemann, *J. Chromatogr.*, 329 (1985) 285–289.

Journal of Chromatography, 467 (1989) 167–176
Elsevier Science Publishers B.V., Amsterdam — Printed in The Netherlands

CHROM. 21 232

ISOLATION, CHARACTERIZATION AND DETERMINATION OF TRACE ORGANIC IMPURITIES IN FD&C RED NO. 40[a]

NAOMI RICHFIELD-FRATZ*, WILLIAM M. BACZYNSKYJ, GEORGE C. MILLER and JOHN E. BAILEY, Jr.
Division of Colors and Cosmetics, Food and Drug Administration, Washington, DC 20204 (U.S.A.)
(Received December 6th, 1988)

SUMMARY

The unsulfonated aromatic amine 4-nitro-*p*-cresidine (2-methoxy-5-methyl-4-nitrobenzenamine) was identified as an impurity in the regulated color additive FD&C Red. No. 40. The compound was isolated from the water-soluble color by extraction with chloroform, followed by transfer of the free amines to acid solution and subsequent separation by reversed-phase high-performance liquid chromatography. The 4-nitro-*p*-cresidine was collected and then identified by gas chromatography–mass spectrometry. The levels of 4-nitro-*p*-cresidine as well as *p*-cresidine and aniline were determined in commercial batches of FD&C Red. No. 40.

INTRODUCTION

FD&C Red No. 40 is a synthetic water-soluble color that is permitted in the U.S.A. for coloring foods, drugs and cosmetics[1]. A sample from each manufactured batch of the color additive must be submitted to the Food and Drug Administration (FDA) (Washington, DC, U.S.A.) for chemical analysis to certify that the composition of the batch conforms with the chemical specifications published in the *Code of Federal Regulations*[1].

FD&C Red No. 40 is synthesized by coupling diazotized *p*-cresidine sulfonic acid (4-amino-5-methoxy-2-methylbenzenesulfonic acid) with Schaeffer's salt (the sodium salt of 6-hydroxy-2-naphthalenesulfonic acid) as shown in Fig. 1A. Because of impurities in the reactants and side reactions which occur during the manufacture of FD&C Red No. 40, the commercially prepared color is rarely pure. Included in the possible impurities that may contaminate color additives such as FD&C Red No. 40 are unsulfonated aromatic amines arising as unreacted compounds from the manufacturing intermediates. Many unsulfonated aromatic amines, including *p*-cresidine, the most likely amine contaminant of FD&C Red No. 40, have been associated with carcinogenic effects in man and/or animal[2].

[a] Presented in part at a Poster Session of the *Annual International Meeting of the Association of Official Analytical Chemists, September 14–17, 1987, San Francisco, CA, U.S.A.*

0021-9673/89/$03.50

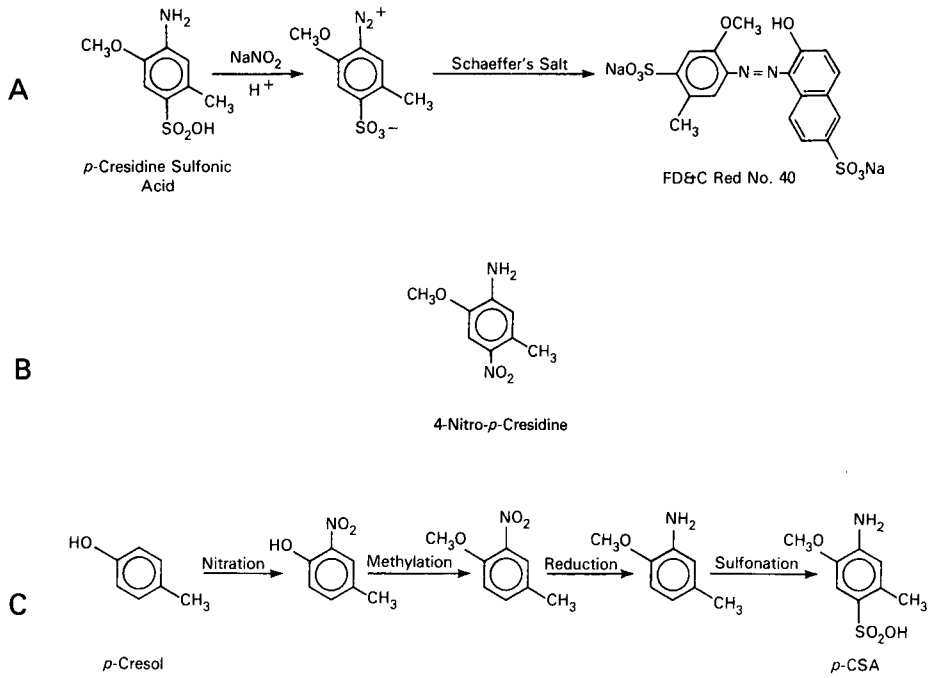

Fig. 1. (A) Manufacturing procedure for synthesis of FD&C Red No. 40. (B) 4-Nitro-*p*-cresidine. (C) Manufacturing procedure for synthesis of *p*-cresidine sulfonic acid.

Our laboratory has reported the development of methodology for the determination of trace levels of unsulfonated aromatic amines in several water-soluble color additives, including FD&C Red No. 40[3–6]. The previous report on FD&C Red No. 40 described the determination of *p*-cresidine and aniline at the ppb[a] level and included the results of a survey that measured the amounts of these impurities in color samples from certified batches. We observed that all the samples analyzed in the survey contained an extractable aromatic amine of unknown identity which, on the basis of instrument response, appeared to be present at much higher levels than the expected impurity (*p*-cresidine).

The work reported here covers the isolation and characterization of this impurity and its identification as 4-nitro-*p*-cresidine (2-methoxy-5-methyl-4-nitrobenzenamine). The impurity was extracted from FD&C Red No. 40, the extract was fractionated by high-performance liquid chromatography (HPLC), and the isolated material was identified by gas chromatography–mass spectrometry (GC–MS). Also described is the determination of 4-nitro-*p*-cresidine, *p*-cresidine and aniline in certified batches of FD&C Red No. 40, by the methodology described in ref. 6.

[a] Throughout this article the American billion (10^9) is meant.

EXPERIMENTAL

Apparatus

HPLC chromatographic system. A Perkin-Elmer (Norwalk, CT, U.S.A.) Series 4 liquid chromatograph was used with a Perkin-Elmer ISS-100 Intelligent Sampling System and a Waters Assoc. (Milford, MA, U.S.A.) Model 440 dual-channel absorbance detector with 254- and 365-nm filters. A Perkin-Elmer Chromatographics 2 data system (including a Model 3600 data station and a Model 660 graphics printer) was connected to the 2-V output of both detector channels. The output signal corresponded to actual absorbance. Both the 254- and 365-nm chromatograms were recorded at 32 mV (0.032 a.u.f.s.). The data system was programmed to simultaneously plot both detector signals.

HPLC column. A Bio-Sil (5 μm) C_{18} column, 250 mm $\times$ 4 mm I.D., was obtained from Bio-Rad (Richmond, CA, U.S.A.).

Extraction columns. Extrelut QE disposable columns, 15 cm $\times$ 4 cm I.D. (EM Science, Gibbstown, NJ, U.S.A.), were used for liquid–liquid extractions.

Gas chromatograph–mass spectrometer. A Hewlett-Packard (Palo Alto, CA, U.S.A.) Model 5970 mass-selective detector with a Model 236 work station was coupled to a Hewlett-Packard Model 5880 gas chromatograph.

GC column. An HP-5 (Hewlett-Packard) capillary column coated with a cross-linked 5% phenyl methyl silicone stationary phase (25 m $\times$ 0.31 mm I.D., 0.52-μm film thickness) was employed.

Reagents

All organic solvents were glass distilled (J. T. Baker, Phillipsburg, NJ, U.S.A., or EM Science). All other chemicals were reagent grade. Water was purified by using a Milli-Q water purification system (Millipore, Bedford, MA, U.S.A.).

HPLC eluents. Eluent A was Milli-Q-purified water and eluent B was methanol.

Standard stock solutions. (i) A 102.1-mg portion of analytical-reagent-grade aniline (Mallinkrodt, St. Louis, MO, U.S.A.) was dissolved in 100 ml of methanol. The purity was established from the absorbance of diluted aliquots in water (1-cm cell) at 229 nm (molar absorptivity of aniline in water = 7900[7]). (ii) A 17.0-mg portion of 4-nitro-*p*-cresidine (Pfaltz and Bauer, Westbury, CT, U.S.A.) was dissolved in 100 ml of methanol. (iii) A 21.7-mg portion of *p*-cresidine (Eastman, Rochester, NY, U.S.A.) was dissolved in 100 ml of 95% ethanol. The purities of (ii) and (iii) were established by elemental analysis. Fresh dilutions in water were prepared from the stock solutions before calibration analyses were performed.

Extraction

A 5-g ($\pm$0.01 g) test portion of color (Sample E in Table I) was weighed into a beaker and dissolved in approximately 35 ml of warm water containing three drops of 1 *M* sodium hydroxide. The dissolved color was poured onto a dry Extrelut QE column that had been tamped to remove any void spaces. The beaker was rinsed several times with water and the rinsings were poured onto the column. No more than a total of 50 ml of aqueous solution was applied to the column.

After the aqueous solution was allowed to drain into the column for 5 min, a 25-ml portion of chloroform was poured onto the top of the column and a 200-ml

TABLE I

DETERMINATION OF *p*-CRESIDINE, 4-NITRO-*p*-CRESIDINE AND ANILINE IN COMMERCIAL FD&C RED NO. 40 WITH QUANTITATION AT TWO WAVELENGTHS

Sample	*p-Cresidine (ppb)*		*Nitro-p-cresidine (ppb)*		*Aniline*[a] *(ppb)*	
	254 nm	*546 nm*	*254 nm*	*546 nm*	*254 nm*	*436 nm*
A[b,c]	203	203	675	678	125	123
B[c]	24	24	163	166	381	384
C	109	113	626	622	–	–
D	444	445	236	235	7	12
E	146	146	7487	7564	5	8
F	917	923	614	610	27	28
G	60	66	2215	2212	–	–
H	20	13	2192	2195	–	–
I	15	10	960	962	10	12
J	153	153	320	320	22	24
K	13	8	263	263	–	–
L	8	6	1129	1128	–	–
M	7	5	511	512	–	–
N	7	7	773	763	–	–
O	6	6	677	680	–	–
P	14	14	794	790	–	–
Q	260	265	515	518	–	–
R	19	19	871	870	–	–
S	15	16	1159	1164	2	4
T	144	146	387	389	–	–
U	14	12	263	265	–	–
V	4	4	840	838	–	–
W	110	109	228	228	57	62
X	12	12	165	166	5	7
Y	67	71	463	465	–	–
Z	12	9	1860	1850	–	–
AA	8	8	2034	2028	6	6
BB	121	121	523	526	83	84
Average	105	105	1034	1036	26	27

[a] Aniline was determined by using pyrazolone-T as the coupling agent instead of R-salt. Only FD&C Red No. 40 samples which had significant responses for aniline coupled to R-salt at both detection wavelengths were reanalyzed using pyrazolone-T. For each dash, a value of zero was used in the calculation of the average.

[b] The *p*-cresidine and 4-nitro-*p*-cresidine results for samples A–G are averages of multiple determinations. See Table III for details.

[c] Pharmacology samples.

round-bottom flask was placed under the column. A second 25-ml portion of chloroform was added after the first portion had drained into the column. After a 3- to 5-min wait, two more 25-ml portions were added to the column to make a total of 100 ml of chloroform. A 5-ml portion of 0.005 *M* sulfuric acid was added to the chloroform extract collected in the 200-ml round-bottom flask, and the chloroform was removed under aspirator vacuum (*ca.* 11 mmHg) on a rotary evaporator (45°C). Care was taken to ensure that no chloroform droplets remained in the aqueous layer and that the flask was removed from the vacuum as soon as all of the chloroform was gone. Residual chloroform vapors were gently driven from the flask with a 2-min nitrogen purge.

HPLC analysis and isolation of 4-nitro-p-cresidine

The HPLC column was equilibrated with 100% eluent A for 10 min at a flow-rate of 1 ml/min. The pH of the aqueous solution containing the extracted amines was adjusted to between 2 and 3 by adding 1 ml of a 1.5% (w/v) solution of sodium dihydrogenphosphate. A 1- to 2-ml portion of the aqueous solution was transferred to an autosampler vial by using a Pasteur pipet. At the end of the equilibration the autosampler was programmed to inject 200 μl onto the column and to initiate a linear gradient from 0 to 50% eluent B in 2 min, followed by 50–100% eluent B in 10 min. At the completion of the gradient, the column was flushed with 100% eluent B for 5 min, and the column was equilibrated with 100% eluent A to begin the next analysis.

During the gradient analysis, the absorbance display on the 365-nm detector was monitored as the retention time of the compound of interest approached. When the absorbance value began to increase, a 4-ml vial was placed at the detector outlet port tube, and the eluting solvent was collected until the absorbance value was back to the baseline reading. Fourteen injections were made and the 4-nitro-*p*-cresidine was collected each time in the same manner.

The combined isolated amine solution was transferred to a 50-ml round-bottom flask. The methanol was removed under aspirator vacuum (*ca.* 11 mmHg) at 45°C until only about 1 ml of solution remained. A 5-ml portion of water and one drop of 1 *M* sodium hydroxide were added to the flask. The contents of the flask were transferred to a 30-ml separatory funnel for extraction with three 5-ml portions of chloroform. The chloroform extract was saved for GC–MS analysis.

GC–MS analysis

A multilevel program was used to control the oven temperature of the gas chromatograph initially set at 30°C for 1 min; the oven was heated to 120°C at 30°/min and then to a final temperature of 265°C at 8°/min. The injector temperature was 220°C. Helium was used as the carrier gas with a linear velocity of 40 cm/s (measured at final temperature). The column head pressure was 13 p.s.i. The injection volume was 1 μl in the splitless mode. The mass detector was operated in the electron ionization mode at an electron energy of 70 eV, scanning over a mass range of 40–550 daltons.

Determination of aromatic amines in FD&C Red No. 40

The experimental conditions for the determination of aromatic amines in FD&C Red No. 40 were the same as described previously[6]. The standard stock solutions prepared for 4-nitro-*p*-cresidine, *p*-cresidine and aniline calibration are described above.

Samples for the analytical survey described here were selected to reflect the volume of color produced by the various manufacturers. Almost 70% of the samples represented two major producers of FD&C Red No. 40. The other manufacturers were represented by at least one batch of color. Included in the survey were two FD&C Red No. 40 pharmacology samples. These batches were used in conducting the animal feeding studies used by FDA to establish the safety of the color additive. Excluding the pharmacology samples, all the survey samples were certified between 1983 and 1987.

RESULTS AND DISCUSSION

Isolation and identification of 4-nitro-p-cresidine

p-Cresidine, an impurity in the FD&C Red No. 40 intermediate *p*-cresidine sulfonic acid (*p*-CSA), had been considered the most likely unsulfonated aromatic amine in commercial batches of the color additive. However, the determination of *p*-cresidine in a previous survey of FD&C Red No. 40 samples showed that *p*-cresidine was in most cases a minor impurity and that other unsulfonated aromatic amines were present at much higher levels[6]. A major impurity present in nearly all samples analyzed was isolated and identified as 4-nitro-*p*-cresidine (Fig. 1B). The manufacturing procedure for the synthesis of *p*-CSA is presented in Fig. 1C. The presence of 4-nitro-*p*-cresidine in the intermediate may occur if reaction conditions allow nitration at both the 1- and 4-positions on the ring, thereby blocking sulfonation in the 4-position.

An FD&C Red No. 40 sample containing the highest amount of the unidentified material was selected for the preparative work. This batch (sample E in Table I) was estimated to contain 7 ppm of the material (calculated as *p*-cresidine). The chloroform extract of this sample was yellow, whereas the extracts of the majority of FD&C Red No. 40 samples were colorless. It was speculated that the unidentified amine imparted the yellow color; therefore, a 365-nm filter was used for HPLC detection.

An HPLC chromatogram of the acid extract of sample E (Fig. 2) shows one major component eluting at about 11 min. In order to isolate sufficient quantities of this material for identification, repeated injections of the extract were made onto the HPLC column, and the fractions corresponding to the impurity were collected. The material thus isolated was extracted back into chloroform for identification by GC–MS.

The total-ion current profile and the mass spectrum obtained from GC–MS analysis of the isolated material are shown in Fig. 3B. The evaluation of this mass spectrum and the molecular weight of the isolate suggested that the material was 4-nitro-*p*-cresidine. GC–MS analysis of authentic 4-nitro-*p*-cresidine (Fig 3A) yielded an ion fragmentation pattern identical to that obtained for the isolated compound, thus confirming the identification.

To confirm that the 4-nitro-*p*-cresidine collected from sample E corresponded to the unidentified amine coupling product for that sample, a portion of the isolated

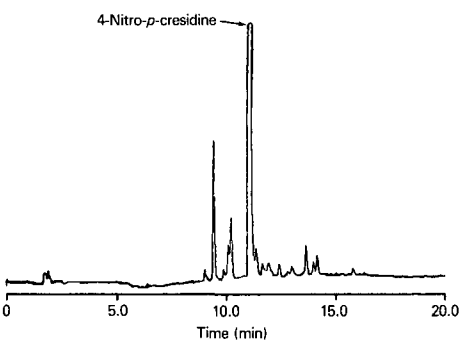

Fig. 2. HPLC chromatogram of an FD&C Red No. 40 acid extract. Detection at 365 nm (0.032 a.u.f.s.).

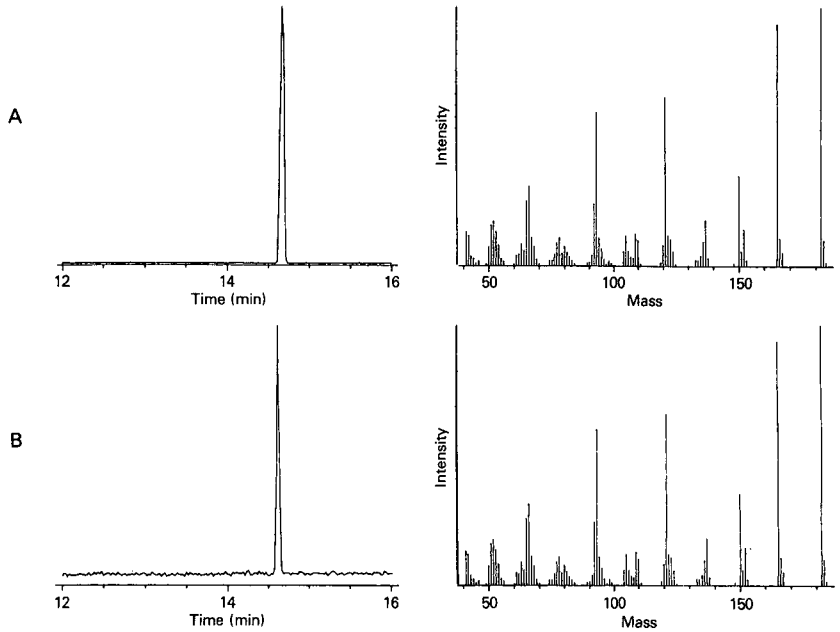

Fig. 3. (A) Total-ion current profile and mass spectrum of 4-nitro-*p*-cresidine standard. (B) Total-ion current profile and mass spectrum of 4-nitro-*p*-cresidine isolated from FD&C Red No. 40.

material was diazotized and coupled to the disodium salt of 3-hydroxy-2,7-naphthalenedisulfonic acid (R-salt) and analyzed by HPLC under the conditions described in ref. 6. The retention times and peak area ratios of the isolated 4-nitro-*p*-cresidine coupled to R-salt and the unknown amine coupling product matched exactly. In addition, a portion of the 4-nitro-*p*-cresidine standard was diazotized, coupled to R-salt and chromatographed under the conditions described in ref. 6. The retention times and peak area ratios for the derivatives of the authentic material were identical.

Determination of amines

The levels of 4-nitro-*p*-cresidine as well as *p*-cresidine and aniline in certified FD&C Red No. 40 samples were quantitated by using the procedure described in ref. 6. HPLC calibration data were obtained by using the external standard method. The liquid chromatograph was calibrated in the presence of the color to compensate for any matrix effects that might alter the extraction of the aromatic amines from a test solution. For the calibration analyses, separate weighings of color were spiked at several levels with the aromatic amines of interest. The FD&C Red No. 40 used for calibration contained small amounts of the analytes. The peak areas obtained for the unfortified color sample were subtracted from the calibration responses.

The calibration data were evaluated statistically to calculate the regression equation and to evaluate the performance of the method[8]. Summaries of the statistical evaluations of the calibration data for *p*-cresidine and 4-nitro-*p*-cresidine collected over a 2.5-month period are presented in Table II. The calibration data for 4-nitro-*p*-cresidine are excellent and reflect the relatively high concentration levels

TABLE II

STATISTICAL EVALUATION OF CALIBRATION DATA FOR DETERMINATION OF *p*-CRESIDINE, 4-NITRO-*p*-CRESIDINE AND ANILINE IN FD&C RED NO. 40

Amine	n^a	*Calibration range (ppb)*	*Wavelength (nm)*	r^b	$X_{LD}{}^c$ *(ppb)*	*C.V.*[d] *(%)*
p-Cresidine[e]	4	4–42	546	0.9929	4	13
			254	0.9892	5	17
	5	104–417	546	0.9886	42	13
			254	0.9874	45	13
4-Nitro-*p*-cresidine	10	102–5100	546	0.9985	74	7
			254	0.9986	71	6
Aniline[f]	4	5–163	436	0.9995	4	4
			254	0.9994	5	4

[a] Number of calibration points.

[b] Correlation coefficient (serves as a crude indicator of possible non-linearity but is not the parameter of choice for measuring linearity).

[c] Limit of determination at the 95% confidence level.

[d] Coefficient of variation.

[e] The best statistical fit for *p*-cresidine was obtained when the data were divided into sets of high and low range.

[f] Pyrazolone-T was used as the coupling agent instead of R-salt.

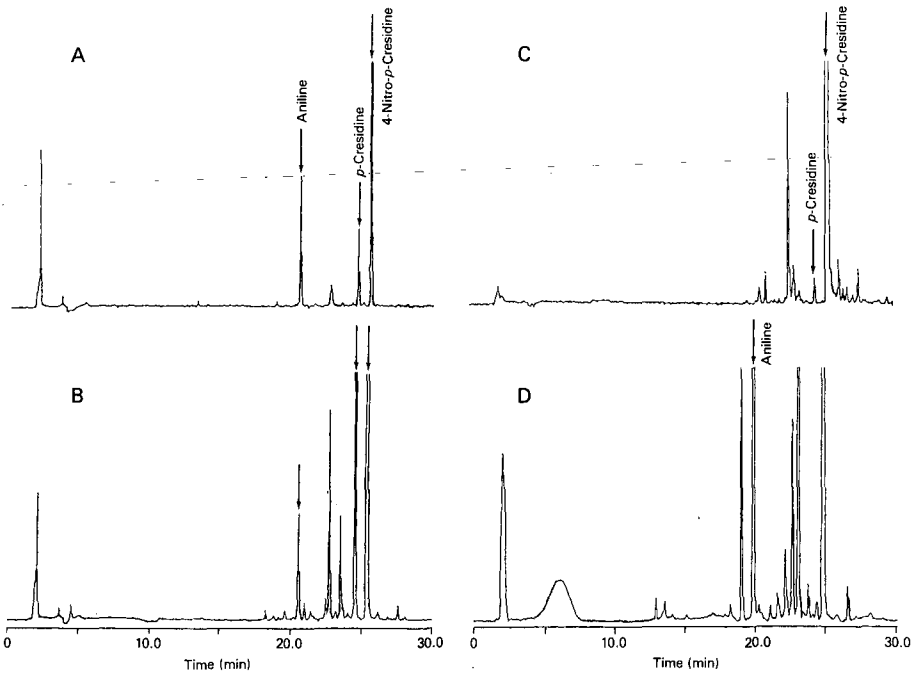

Fig. 4. HPLC chromatograms from analysis of samples of commercial FD&C Red No. 40 by the procedure described in ref. 6. (A) sample B; (B) sample A; (C) sample Z; (D) sample A. Chromatograms A, B and C represent R-salt coupling products. Chromatogram D represents pyrazolone-T coupling products. Detection (A, B, C) at 546 nm; (D) at 436 nm (0.016 a.u.f.s.).

used for 4-nitro-*p*-cresidine. For *p*-cresidine the best statistical fit was obtained when the data were divided into sets of high and low range. Depending on the peak area, the levels of *p*-cresidine in commercial FD&C Red No. 40 were calculated by using either the high or low calibration sets. The calibration data for aniline, collected in one day, were obtained by using pyrazolone-T as the coupling agent instead of R-salt. The wavelengths of measurement were 254 and 436 nm. The 546-nm filter was replaced

TABLE III

MULTIPLE ANALYSES OF COMMERCIAL FD&C RED NO. 40 FOR *p*-CRESIDINE AND 4-NITRO-*p*-CRESIDINE WITH QUANTITATION AT 254 AND 546 nm

Sample	*p-Cresidine (ppb)*		*4-Nitro-p-cresidine (ppb)*	
	254 nm	*546 nm*	*254 nm*	*546 nm*
A[a]	217	220	708	713
	188	187	641	644
Average	203	203	675	678
C.V. (%)	10	12	7	7
B[b]	24	24	178	182
	20	22	153	156
	27	25	158	160
Average	24	24	163	166
C.V. (%)	13	8	8	9
C[c]	112	114	654	645
	106	111	597	598
Average	109	113	626	622
C.V. (%)	4	2	6	5
D[a]	460	458	250	252
	452	454	242	236
	428	430	229	227
	437	436	223	225
Average	444	445	236	235
C.V. (%)	3	3	5	5
E[b]	145	142	7448	7534
	148	150	7526	7595
Average	146	146	7487	7564
C.V. (%)	1	4	1	1
F[b]	1086	1095	657	656
	1042	1053	621	626
	622	621	564	547
Average	917	923	614	610
C.V. (%)	28	28	8	9
G[b]	69	76	2199	2192
	50	53	2202	2201
	61	67	2244	2244
Average	60	66	2215	2212
C.V. (%)	16	18	1	1

[a] Analyzed over a 9-week period.
[b] Analyzed over a 6-week period.
[c] Analyzed over a 4-week period.

because 436 nm is closer to the absorption maximum for the aniline–pyrazolone-T coupling product.

A total of 28 certified samples of FD&C Red No. 40 were surveyed for 4-nitro-*p*-cresidine, *p*-cresidine and aniline. The results of the analyses of the color additive are presented in Table I. Representative chromatograms obtained from the analysis of four survey samples are shown in Fig. 4.

4-Nitro-*p*-cresidine was found in all 28 of the samples surveyed at an average level of 1035 ppb with a range of 165 to 7526 ppb. *p*-Cresidine was found in all the samples at an average level of 105 ppb with a range of 4 to 920 ppb.

HPLC responses for aniline were observed for many samples; however, there usually was poor agreement between the results for the two different wavelengths, suggesting an interfering coeluting compound. In order to resolve the interference, pyrazolone-T was used as an alternative coupling agent in place of R-salt to change the chromatographic properties of the coupling products. The samples that had measurable aniline responses with R-salt coupling were reanalyzed after pyrazolone-T was used as the coupling agent. Aniline was found at an average level of 26 ppb with a range of 0 to 383 ppb. The FD&C Red No. 40 batches that were not reanalyzed after pyrazolone-T coupling were reported as having no aniline present.

The repeatability of the amines determination was tested by performing multiple analyses (R-salt coupling) on several samples of FD&C Red No. 40 (Table III). The calculated % coefficient of variation (C.V.) values for 4-nitro-*p*-cresidine were all below 10%, indicating good repeatability at the levels tested. Although the C.V. values for *p*-cresidine were higher than those for 4-nitro-*p*-cresidine, they were comparable with values found previously[6].

CONCLUSIONS

4-Nitro-*p*-cresidine has been isolated and identified as a trace-level impurity in FD&C Red No. 40 by using preparative HPLC and GC–MS. The levels of 4-nitro-*p*-cresidine as well as those of *p*-cresidine and aniline were determined in commercial batches of the color additive. The method employed allows quantitation of these aromatic amines at levels greater than or equal to 5 ppb. Good repeatability of the method has been demonstrated.

REFERENCES

1 *Code of Federal Regulations*, Title 21, Part 74, U.S. Government Printing Office, Washington, DC, 1987.
2 *Third Annual Report on Carcinogens*, Public Health Service, U.S. Department of Health and Human Services, Washington, DC, 1983.
3 J. E. Bailey, Jr., *Anal. Chem.*, 57 (1985) 189–196.
4 J. E. Bailey, Jr. and C. J. Bailey, *Talanta*, 32 (1985) 875–882.
5 N. Richfield-Fratz, J. E. Bailey, Jr. and C. J. Bailey, *J. Chromatogr.*, 331 (1985) 109–123.
6 N. Richfield-Fratz and J. E. Bailey, Jr., *J. Chromatogr.*, 405 (1987) 283–294.
7 J. E. Bailey and R. J. Calvey, *J. Assoc. Off. Anal. Chem.*, 58 (1975) 1087–1128.
8 C. J. Bailey, E. A. Cox and J. A. Springer, *J. Assoc. Off. Anal. Chem.*, 61 (1978) 1404–1414.

Journal of Chromatography, 467 (1989) 177–184
Elsevier Science Publishers B.V., Amsterdam — Printed in The Netherlands

CHROM. 21 248

DETERMINATION OF DIISOBUTYL- AND DIISOPROPYLNAPHTHALENESULPHONATES IN PESTICIDE WETTABLE POWDERS AND DISPERSIBLE GRANULES BY HIGH-PERFORMANCE LIQUID CHROMATOGRAPHY

R. H. SCHREUDER*, A. MARTIJN and C. VAN DE KRAATS
Plant Protection Service, P.O. Box 9102, 6700 HC Wageningen (The Netherlands)
(First received October 26th, 1988; revised manuscript received January 4th, 1989)

SUMMARY

Methods are presented for determining diisobutyl and diisopropylnaphthalenesulphonates in pesticides formulated as wettable powders or water dispersible granules. The dispersing agents were concentrated on anion-exchange cartridges and after removal of interfering substances eluted with methanol containing 5% hydrochloric acid. The various isomers were separated by reversed-phase high-performance liquid chromatography on an octyl-modified column using a water–methanol gradient or on a cyanoalkyl-modified column with water–methanol. Quantitative results were obtained by comparing the peaks with those of the standard technical material. Various groups of peaks were identified as mono-, di- and triisobutylnaphthalenesulphonates respectively.

INTRODUCTION

Besides lignosulphonates and synthetic sulphonated polymers, salts of diisobutyl and diisopropylnaphthalenesulphonic acid (DBNS and DPNS) are frequently used as dispersing agents in powder and granular pesticide formulations at levels of 1–4%. Although DBNS and DPNS have been used for a considerable time, little is known about the analysis of these compounds. Given their physical and physicochemical properties, one would expect that DBNS and DPNS can be determined by the two-phase titration technique, or spectrophotometrically[1,2]. Methods based on those principles however have little specificity. As it has been shown[3] that related compounds, such as calcium dodecylbenzenesulphonates (CaDBS), can succesfully be determined by high-performance liquid chromatography (HPLC), it was obvious to choose a similar approach for the determination of DBNS and DPNS. DBNS and DPNS are produced by alkylation and subsequent sulphonation of naphthalene yielding a complex mixture of positional isomers of mono-, di- and trialkylnaphthalenesulphonates. So, the method for CaDBS cannot be used without modifications. As in addition that method was developed for determining dodecylbenzenesulphonates in the presence of ethoxylated alkylphenols in liquid samples and as wettable

0021-9673/89/$03.50

powders also may contain other sulphonated material, the clean-up procedure in particular had to be changed.

This paper describes procedures for determining DBNS and DPNS in wettable powders and water dispersible granules. The compounds were isolated by the solid phase extraction technique and subsequently determined by HPLC using octyl- and cyano-modified columns.

EXPERIMENTAL

Apparatus

The HPLC system consisted of two high-pressure pumps (Model 9208), a solvent programmer (Model 9224), an autosampler (Model 9209) with a 20-μl injection volume, all from Kipp Analytica (Delft, The Netherlands), a Pye-Unicam PU 4020 variable-wavelength detector (Philips, Eindhoven, The Netherlands) and an Hewlett-Packard 3390 electronic integrator. Columns, stainless steel, 250 mm × 4.6 mm I.D., packed with either LiChrosorb 10 RP-8 or Polygosil 60 DCN 10, were obtained from Chrompack (Middelburg, The Netherlands). The columns were protected by guard columns, 4 mm × 4 mm I.D., packed with LiChrosorb 100 RP-8 (Lichro Cart, Cat. No. 15727, Merck) and 75 mm × 2 mm I.D. packed with polar bound phase material (40 μm) respectively. Solid phase extraction cartridges filled with either aminoalkyl-modified silica (Sep-Pak, Art. No. 10830) or a quaternary amine anion exchanger (Sep-Pak QMA Art. No. 10835) were obtained from Waters Associates (Etten-Leur, The Netherlands). The cartridges fitted onto 20-ml Luer-LOK syringes.

Reagents

Methanol (HPLC quality) was obtained from Rathburn. Analytical quality 85% phosphoric acid, 37% hydrochloric acid and 25% ammonia were obtained from J. T. Baker (Deventer, The Netherlands). Demineralized water was purified to HPLC quality using a Milli-Q filtration system (Millipore). Sodium alkylnaphthalenesulphonate samples were technical materials obtained from Bayer Nederland, Chemie Linz, Hoechst Holland and Ligtermoet Chemie.

Samples

The samples investigated were all water dispersible powders or granules, taken from the Dutch market, and contained one or two of the following active ingredients: captan, chloridazon, lenacil, metamitron, methabenzthiazuron, metobromuron, metribuzin, pyridate, terbutryn, thiophanate-methyl, tolylfluanide and vinclozolin.

Standard solutions

Standards were prepared by dissolving 50 mg technical sodium salt of DBNS or of DPNS in 100.0 ml water. From these solutions 10 ml were pipetted into 50-ml volumetric flasks. To create the same conditions as for the samples, 25 ml methanol with 5% hydrochloric acid (37%) were added. The solutions were neutralized with about 2 ml 25% ammonia (pH 7 to 9), cooled to room temperature and made up to the mark with water.

Isolation of DBNS and DPNS from samples

About 1 g of the powder formulation was weighed into a 100-ml conical flask. By pipette, 50.0 ml sodium hydroxide (c = 0.01 mol/l) were added, the mixture was shaken for 30 min and then placed in an ultrasonic bath for an additional 5 min. The suspension was transferred to a centrifuge-tube and centrifuged at about 1500 g for 15 min. The supernatant was filtered through a 0.45-μm filter. With a syringe, exactly 2 ml of the clear solution were pressed slowly into a Sep-Pak QMA cartridge that had been washed with concecutively 5 ml methanol + 5% hydrochloric acid and 10 ml water. The syringe was washed two times with 1-ml portions of water and the washings were pressed through the cartridge. The liquid eluting from the cartridge was discarded. Non-ionic material was then removed from the cartridge with consecutively 5 ml water and 6 ml methanol–water (4 : 1, v/v). The anionic compounds were eluted with 5 ml methanol containing 5% hydrochloric acid, and collected in a 10-ml volumetric flask. The solution was neutralized with ± 0.4 ml 25% ammonia (pH 7 to 9), mixed with 3 ml water, cooled to room temperature and made up to the mark with water.

Chromatographic system 1 (gradient elution)

Aliquots (20 μl) of the sample and standard solutions were injected into the RP-8 column. At a flow-rate of 1 ml/min, a gradient was applied using the following eluents: A = methanol–water (35 : 65, v/v) acidified to pH 2.75 with phosphoric acid, containing a little acetone (100 μl/l) to compensate for the absorbance difference with eluent B; B = methanol–water (80 : 20, v/v) acidified to pH 3.00 with phosphoric acid. The following gradient profile was used: time 0 to 11 min, linear increase from 20 to 80% B; 11 to 16 min, linear increase from 80 to 90% B; 16 to 18 min, 90% B; 18 to 22 min, linear decrease from 90 to 20% B. The column oven temperature was 40°C and the detection took place at 290 nm.

Chromatographic system 2

Aliquots (20 μl) of the sample solution were injected onto the CN modified column. The components were separated by eluting with methanol–water (4 : 6, v/v) acidified to pH 2.75 with phosphoric acid. The flow-rate was set at 1.0 ml/min, the oven temperature was regulated such (usually between 35 and 40°C) that the last peak was eluted between 9 and 10 min. The absorption was measured at 235 nm. Peak areas were determined by electronic integration and compared with those of the standard solutions (0.1 g/l DBNS or DPNS) obtained under the same chromatographic conditions.

Isolation of fractions and identifications by mass spectrometry (MS)

Portions (20 μl) of a solution (100 g/l) of the diisobutylnaphthalenesulphonate that was also used as standard (sample a, Table I) were injected 18 times onto the RP-8 column. At a column oven temperature of 40°C, and a flow-rate of 1 ml/min, a linear gradient, 25 to 95% solvent D in 30 min, was applied [solvent C = methanol–water (35 : 65, v/v); solvent D = methanol–water (80 : 20, v/v), both acidified to pH 2.5 with hydrochloric acid]. The fractions corresponding to peaks eluted at 5.6, 6.0, 12.2, 12.8 and 16.7 min were collected (fractions 1 to 5 respectively). Each fraction was analyzed separately by chromatographic system 1.

RESULTS AND DISCUSSION

Pesticides formulated as wettable powders contain, apart from inorganic material, a mixture of polar and non-polar compounds. The active material usually belongs to the non-polar category and the dispersing agents such as DBNS and DPNS are ionic in character. Originally it was thought that the solubility of most active ingredients was low enough to remove them by a simple aqueous extraction. The interferences that were observed during subsequent chromatography required however that an additional clean-up step be carried out. Aminoalkyl-modified silica gel solid state extraction cartridges, used succesfully in a previous study[3] dealing with the analysis of calcium dodecylbenzenesulphonates in emulsifiable concentrates, retained the naphthalenesulphonates only partly. Better adsorption was obtained with anion-exchange cartridges of the Sep-Pak QMA type. The binding of the naphthalenesulphonates was rather strong; 10 ml of a saturated aqueous ammonium chloride solution did not remove them from the cartridge. A solution of 5% hydrochloric acid in methanol did however elute them (5 ml), whereas the less polar and non-polar compounds were removed by a preceding elution with 5 ml water and 6 ml of water–methanol (2:8, v/v). During the preliminary stage of the present study we tried to separate the individual components of DBNS and DPNS by the procedure used previously[3] for the analysis of calcium dodecylbenzenesulphonate (CaDBS). With this system, which uses a reversed-phase (C_8) column and water–methanol with 0.02 mol/l tetramethylammonium bromide (TMAB) as the eluent, separation of the various DBNS and DPNS components was achieved, although it was not optimal. The results indicated that the DBNS and DPNS components exhibited quite a range of polarities. A gradient system without TMAB and acidified methanol as the modifier gave the best separations.

For routine analyses, chromatographic system 2 was developed. Better quantitative results were obtained because no solvent gradient was applied and the absorbance maximum at 235 nm was used for detection. The analysis time was reduced from 25 to 15 min. Although the resolution was considerably less than for system 1, still three clusters of peaks were observed (Fig. 2), which were sufficient to identify products of different origines.

The possibility of a fluorimetric detection was considered, but UV detection was chosen, because it was assumed that the UV response of the various isomers would differ less than the fluorimetric response and because no pure standards were available.

None of the DBNS and DPNS isomers was available commercially so that the peaks could not be identified. To have at least some information about the identity of the peaks, a number of DBNS fractions was isolated and subjected to MS, to establish which peaks were produced by the mono-, di- and tributylnaphthalenesulphonates respectively. Each fraction produced one major peak when chromatographed in system 1. Fractions 1 and 2, corresponding to peaks eluted at 5.6 and 6.0 min respectively in system 1, both proved to be monobutylnaphthalenesulphonates (M = 278). Fractions 3 and 4, corresponding to peaks eluted at 12.2 and 12.8 min respectively, were dibutylnaphthalenesulphonates (M = 334) and fraction 5 (peak at 16.7 min) was a tributylnaphthalenesulphonate (M = 390). The presence of M−29 signals in the mass spectrograms, suggesting a loss of a C_2H_5 group, confirms the presence of the isobutyl groups[4].

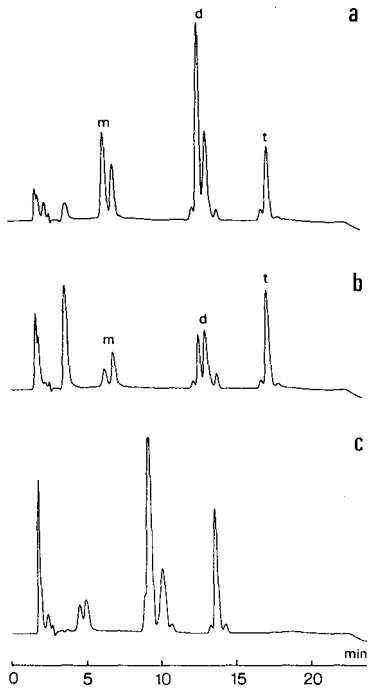

Fig. 1. Typical chromatograms obtained with HPLC system 1 of technical DBNS (a and b) and DPNS (c); m = monoisobutyl-, d = diisobutyl-, and t = triisobutylnaphthalenesulphonate. For conditions see text.

The isomeric composition of the technical DBNS can differ considerably, depending on the source of the material, as is shown in Fig. 1. In Table I the relative contents of the technical materials are given, based on the two chromatographic methods. Sample a was taken as the standard material and was also used as reference material for the determination of the content in the formulation. The calculation of the content was carried out using the areas of the three clusters of peaks, rather than the areas of the individual peaks, in order to prevent too large integration errors caused by incompletely resolved peaks and to compensate for the greatly varying ratios of the peak areas of the various technical materials. All minor peaks, in partic-

TABLE I

COMPARISON OF TWO-PHASE TITRIMETRIC AND CHROMATOGRAPHIC DETERMINATIONS OF TECHNICAL DBNS SAMPLES (%)

Sample	*Titration*	*HPLC system 1*	*HPLC system 2*
a	62.5	100[a]	100[a]
b	60.2	76	75
c	55.9	106	109
d	56.4	89	89
e	66.1	102	91

[a] Used as a standard and set at 100%.

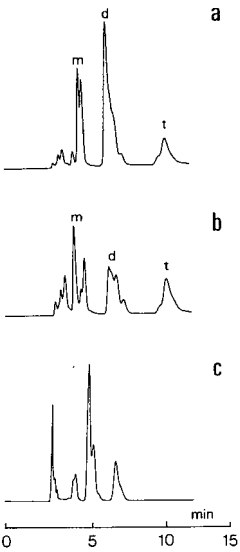

Fig. 2. Typical chromatograms obtained with HPLC system 2 of technical DBNS (a and b) and DPNS (c). Other details as in Fig. 1.

ular those eluted before 3.5 min, were neglected. An equal molecular absorbance of all the components was assumed. In the case of DPNS only one sample of the technical material was available. This was taken as the standard for the determination of the content in the formulation. The content of alkylnaphthalenesulphonate in the technical samples was also determined by the two-phase titration technique. The

TABLE II

RESULTS OF DBNS AND DPNS DETERMINATIONS IN WETTABLE POWDERS

Sample	*Nominal content (%)*	*HPLC system 1*		*HPLC system 2*	
		Found content (%)	*Recovery (%) of added*	*Found content (%)*	*Recovery (%) of added*
1[a]	1.5	1.1	93	1.0	93
2	1.6	2.0	92	2.1	102
3[a]	1.5	–	–	1.7	99
4	1.0	1.0	100	1.0	92
5[a]	2.0	2.3	90	1.8	98
6	3.0	1.6	87	1.3	99
7	3.0	2.5	104	1.6	96
8	2.0	1.8	102	1.9	108
9[a]	2.0	2.4	100	2.5	101
10	2.0	2.2	93	2.2	96
11[b]	2.0	2.2	96	2.3	100

[a] Calculation based on only two clusters of peaks. For other conditions, see text.
[b] Sample with DPNS.

contents are rather low but this is not surprising when one realizes that the materials investigated are impure reaction products which may contain considerable amounts of water soluble inorganic material and non-ionic impurities. The chromatographic determination gives the expected higher values due to the fact that one of the technical materials is used as the standard. The linearity of the response was checked by injecting increasing amounts of the standard material (r = 1.000, n = 5). The extraction procedure was checked by applying the whole procedure to the standard material. Average recoveries were 98.9% (n = 5; R.S.D. = 0.94%) for chromatographic system 1 and 100.6% (n = 5; R.S.D. = 1.5%) for system 2.

The DBNS or DPNS contents of eleven wettable powders containing different active ingredients were determined with both methods. Only one sample contained DPNS. For the DBNS containing samples technical material a was used as a standard.

In each case the recovery of the procedure was determined also by adding exactly 10 mg of the standard to the sample. The results of averages of duplicate determinations are given in Table II. Figs. 3 and 4 give the corresponding chromatographic traces. In a number of instances, interferences by compounds of unknown origin were observed. It is known that wettable powders sometimes contain several dispersing agents of different natures. The interferences were not caused by the much used lignosulphonates. Experiments have shown that lignosulphonates have retention times shorter than 3.5 min in both chromatographic systems. When interferences were observed, the affected cluster of peaks was excluded from the calculation. The deliberate choice of the standard might explain the fact that for some formulations there is a great discrepancy between the found and the declared contents. It may be that in those cases the material used for the manufacture of the formulation has a DBNS or DPNS content that differed considerably from that of the standard materi-

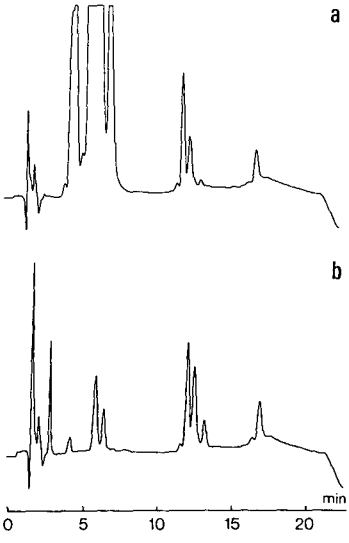

Fig. 3. Typical chromatograms of samples obtained with HPLC system 1, (a) with and (b) without interference. Compare with Fig. 1.

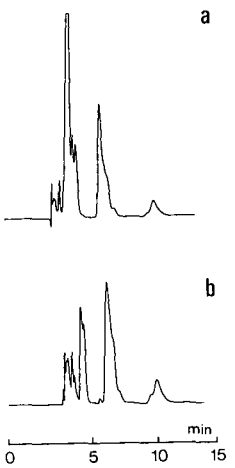

Fig. 4. Typical chromatograms of samples obtained with HPLC system 2, (a) with and (b) without interference. Compare with Fig. 2.

al used in this study. It was not known which of the technical DBNSs were present in which formulation.

CONCLUSION

High-performance liquid chromatography is a useful tool for analyzing DBNS and DPNS in pesticide formulations such as wettable powders and water dispersible granules. The exact quantitation of products of unknown origins remains a problem due to the complex nature of the material, the lack of proper standards and the widely varying ratios of the various components. The recoveries show that when proper standards are present the methods will give reasonable results. Interferences from other sulphonated materials seem to be minor.

ACKNOWLEDGEMENTS

We are grateful to Mr. C. J. Teunis of the Department of Organic Chemistry of the Agricultural University, Wageningen, The Netherlands for obtaining the mass spectra.

REFERENCES

1 M. J. Rosen and H. A. Goldsmith, *Systematic Analysis of Surface-active Agents*, Wiley-Interscience, New York, 2nd ed., 1972, pp. 230, 427.
2 G. F. Longman, *The Analysis of Detergent Products*, Wiley-Interscience, London, 1975, pp. 195, 234.
3 R. H. Schreuder and A. Martijn, *J. Chromatogr.*, 435 (1988) 73.
4 H. Budzikiewicz, C. Djerassi and D. H. Williams, *Mass Spectrometry of Organic Compounds*, Holden-Day, San Francisco, CA, 1967, p. 49.

Journal of Chromatography, 467 (1989) 185–193
Elsevier Science Publishers B.V., Amsterdam — Printed in The Netherlands

CHROM. 21 233

CHEMICAL REACTION DETECTION OF CATECHINS AND PROANTHOCYANIDINS WITH 4-DIMETHYLAMINOCINNAMALDEHYDE

D. TREUTTER
Institut für Pflanzenbau, Lehrstuhl für Obstbau, Technische Universität München, 8050 Freising-Weihenstephan (F.R.G.)
(Received December 21st, 1988)

SUMMARY

An high-performance liquid chromatographic method with post-column derivatization is described which allows the specific detection of catechins and proanthocyanidins in crude extracts from plants and beverages. In the presence of concentrated sulphuric acid, 4-dimethylaminocinnamaldehyde can be employed as a selective reagent. The advantage of the reagent is that its condensation products with flavanols show maximum absorbance at about 640 nm. Other phenols, indoles and terpenes give reaction products with different absorbances or react very weakly. A 200–40 000 fold sensitivity was found for (−)-epicatechin as compared to other phenols and substituted indoles. Concerning the terpenes, this factor ranges from 4000 (for the aromatic thymol) to $2 \cdot 10^6$.

INTRODUCTION

Catechins and their oligomeric forms, namely the proanthocyanidins (condensed tannins), are an heterogeneous group of secondary compounds[1,2] which are widespread in the plant kingdom[3–5]. The astringency of these flavanols is well known in fruits[6–8]. The content of catechins is an important factor in determining the quality of juices[9] and wines[10–12]. The oligomeric proanthocyanidins play a rôle in the durability of beers[13–15]. All the above mentioned observations are related to the ability of flavanols to precipitate proteins[16]. This precipitation reaction is probably also responsible for the participation of catechins in plant defence mechanisms[17,18].

For these reasons it is often necessary to know the composition of the various catechins and condensed tannins in plant tissues and to monitor their structural variation during beverage processing[19–23] or during the wound response of plants[24,25]. In the latter case, oxidation processes often lead to oligomerization and polymerization[1] and diseased plant tissues sometimes show an enhanced synthesis of flavanols[26].

The analytical method normally used to estimate the amount of catechin and its derivatives is the colorimetric measurement of their total content after reaction with aromatic aldehydes[27–29] in a test-tube. The qualitative pattern of these phenols can be determined by thin-layer chromatography using the known aromatic aldehydes[30–32]

0021-9673/89/$03.50

or the trinitrophenol–potassium hydroxide reagent[33] for visualization. However, the quantification of each compound normally requires its purification from other phenolic compounds. A prepurification has been carried out by several authors[34,35]. In high-performance liquid chromatographic (HPLC) analysis of flavanols extracted from plants, which are rich in phenols, the main problem is the rather low molar extinction of catechins as compared to phenolic acids. The cinnamic acids also show similar retention behaviours and often occur in plants in a more concentrated form than the flavanols. Lea[36] solved this problem using a pH-shift technique during the HPLC separation of apple juices. A chemical reaction detection of flavanols by using 4-dimethylaminocinnamaldehyde (DMACA) after their preparative separation on a Sephadex column has been described by McMurrough and McDowell[37] and McMurrough[38].

This paper deals with the post-column derivatization of catechins and proanthocyanidins for their selective detection following analytical HPLC separation of crude plant extracts and beverages.

EXPERIMENTAL

The HPLC equipment consisted of two pumps T-414 (Kontron) and the gradient programmer 205 (Kontron). The column (250 mm × 4 mm I.D.) was prepacked with Shandon Hypersil ODS, 3 μm. The solvents were 5% acetic acid (A) and methanol (B).

Gradient range: 0–5 min, isocratic, 5% B in A; 5–10 min, 5–10% B in A; 15–25 min, 10–15% B in A; 25–35 min, isocratic, 15% B in A; 35–37 min, 15–20% B in A; 37–45 min, isocratic, 20% B in A; 45–55 min, 20–30% B in A; 55–70 min, 30–45% B in A; 70–90 min, 45–90% B in A.

Because of the corrosive reagent, an inert HPLC pump (Gynkotek, F.R.G.) was used. It was equipped with titanium pump heads. Capillaries and screws were both made of PTFE. The reactor was a knitted PTFE capillary (9 m × 0.5 mm I.D.) as described by Engelhardt and Klinkner[39]. The substrate–reagent mixing was performed by a simple T-connection (titanium). The compounds were detected with an inert UV–VIS detector (Gynkotek, F.R.G.).

The estimation of the absorbance maximum and the wavelength ratio (640:620 nm) was performed with a Beckman Model 24 spectrophotometer.

RESULTS AND DISCUSSION

Application possibilities of aldehyde reagents

The reactivity of aldehydes in solutions containing strong mineral acids as well as the colour reactions of aromatic aldehyde have long been used to detect many different substances. Unsaturated compounds such as phenols[40–46], pyrroles and indoles[41,44] as well as some terpenes[42,43,45,47,48] were reported to react with aldehydes. Additionally, aliphatics, *i.e.*, alcohols, ketones may be converted into olefins under the influence of mineral acids and may then be sensitive to the aldehyde reaction[43,47,49].

In spite of these findings, colour reactions of aromatic aldehydes have often been employed specifically, such as for flavanols[29,38,45,50–57] or for indoles[58–61].

TABLE I

ABSORBANCE OF THE CONDENSATION PRODUCTS OF DMACA WITH (−)-EPICATECHIN IN THE PRESENCE OF VARIOUS ALCOHOLS

Concentration of sulphuric acid was 1.5 *M* in the corresponding alcohol.

Alcohol	*Wavelength of maximum absorbance (nm)*
Methanol	632
Ethanol	636
Propanol	638
Butanol	640

Mode of action

Principally, when dissolved in strong acids, aldehydes become electrophilic and therefore very reactive. The reaction mechanism with formaldehyde and phenols has been clarified by Finn and James[62] and by Hillis and Urbach[63]. However, such aromatic aldehydes, which are substituted, show a reduced reactivity, as compared to formaldehyde, because of the possible delocalization of the positive charge[64,65]. This requires an activated aromatic ring of the substrate, *i.e.*, of the phloroglucinol type in order to obtain optimum condensation reaction with phenols.

DMACA has the advantage that its reaction product with catechin shows an absorbance maximum between 632 and 640 nm depending on the solvent (Table I). Other aldehydes, commonly used, lead to absorption at a shorter wavelength (Table II), so that anthocyanidins or other substances which yield a red colour in the presence of acid may interfere. Moreover, the molar extinction of the products yielded with DMACA is about 1000 times higher than that with 4-dimethylaminobenzaldehyde[51].

Optimization of the derivatization system

As shown by several authors[51,60], the reaction with DMACA depends on the concentration of acid and alcohol. Since in the HPLC separation of flavanols a gradient system is necessary, the reaction conditions change during an experiment. Methanol both accelerates the reaction and increases the extinction value. However, after reaching the maximum absorbance, the extinction declined, which may be

TABLE II

ABSORBANCE OF THE CONDENSATION PRODUCTS OF VARIOUS ALDEHYDES WITH (−)-EPICATECHIN IN THE PRESENCE OF 0.075 *M* SULPHURIC ACID IN METHANOL

Aldehyde	*Wavelength of maximum absorbance (nm)*
Anisaldehyde	455
Vanillin	490
4-Dimethylaminobenzaldehyde	510
Syringaldehyde	515
4-Dimethylaminocinnamaldehyde	632

explained by a superimposed decomposition of the condensation product. The latter is also influenced by the acid and the alcohol concentration (Fig. 1). Water, acetonitrile and acetone inhibit the formation of the coloured product (Fig. 2).

In order to obtain a good sensitivity, 1% DMACA in 1.5 *M* methanolic sulphuric acid was used. The length of the knitted capillary reactor was 9 m, resulting in a reaction time of 90 s.

Selectivity and sensitivity

The use of the DMACA reagent for the specific detection of catechins demands knowledge of the relative sensitivity of other substances which are also known to give coloured products with aromatic aldehydes.

For this purpose the method of flow injection analysis[39] was used. Except for omission of the column, the system was the same as that described for the separation procedure. The solvent normally consisted of 40% methanol in 1% aqueous acetic acid. Only for some phenols and terpenes, butanol–methanol (1:5, v/v) was used as the solvent and the reagent was dissolved in butanol (containing 1.5 *M* sulphuric acid) to prevent demixing. For each compound a calibration graph was constructed to estimate the relative sensitivity.

Possible interference with catechins was shown to depend on the activation of the phenol group which determines the sensitivity towards the reagent. For this reason,

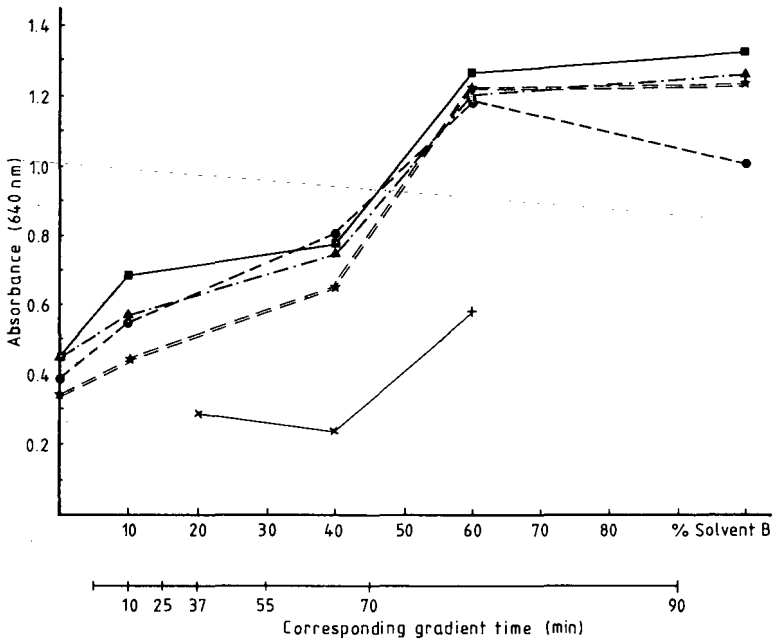

Fig. 1. Influence of the solvent composition and the reaction conditions (concentration of sulphuric acid in the 1% DMACA reagent; reaction time) on the detection sensitivity (640 nm) for (−)-epicatechin. Each data point represents the mean of four injections during flow injection analysis without the column. The injected flavanol was dissolved in that solvent which corresponded to the flow condition used at each point. (■) 0.65 *M*, 90 s; (▲) 1.15 *M*, 120 s; (●) 1.65 *M*, 60 s; (★) 5.30 *M*, 90 s; (×) 2.55 *M*, 90 s.

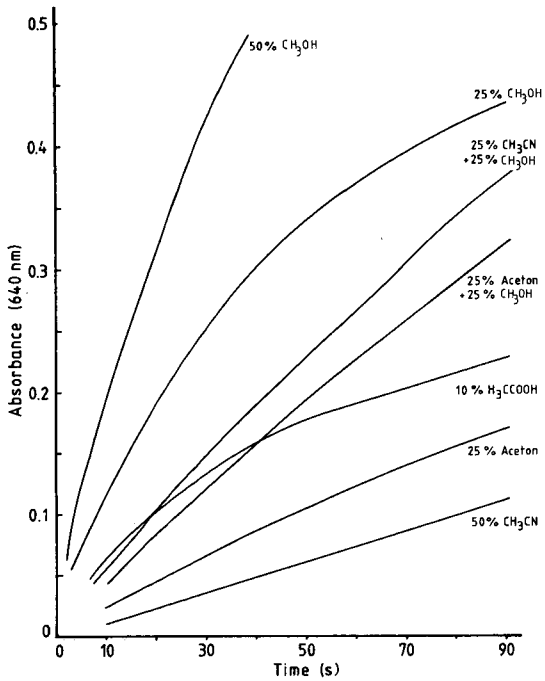

Fig. 2. Influence of the solvent on the reaction kinetics of DMACA (0.5%) with (+)-catechin (10 μg/ml) in the presence of 0.75 *M* H_2SO_4. The solvent was made up to 100% with water.

flavonoids with a carbonyl function at C4, *i.e.*, naringenin show a rather weak reaction (Table III) as already shown by Sarkar and Howarth[54]. The high sensitivity of indole was diminished by substitution at the pyrrole ring, *cf.*, tryptamine. Additionally, the relative sensitivity was affected by chromophoric groups and their binding sites.

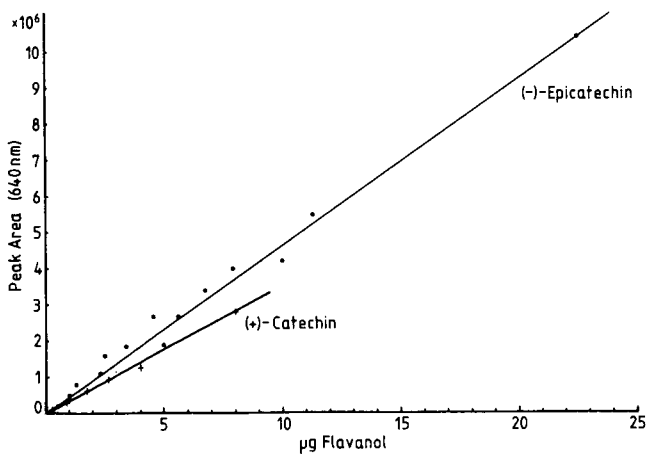

Fig. 3. Calibration graphs for (+)-catechin and (−)-epicatechin. Detection after chemical reaction with DMACA (1% in 1.5 *M* methanolic suphuric acid); for separation conditions see Experimental.

TABLE III

RELATIVE SENSITIVITY OF THE DMACA REAGENT TOWARDS VARIOUS SUBSTRATES

Flow injection conditions: solvent, 40% aqueous methanol; flow-rate 0.6 ml/min; reagent, 1% DMACA in 1.5 *M* sulphuric acid in methanol, flow-rate 0.6 ml/min.

Common name	*Structural name*	*Amount resulting in a peak of 0.04 a.u. at 640 nm (μM)*	*Relative sensitivity*[a]	*Absorbance maximum*	*Ratio 640/620 nm*
(−)-Epicatechin	3,3′,4′,5,7-Flavanpentol	$0.2 \cdot 10^{-3}$	1000 000	632	1.15
Indole		$0.4 \cdot 10^{-3}$	500 000	620	0.71
Orcinol	3,5-Dihydroxytoluol	$26 \cdot 10^{-3}$	7692	628	0.90
Phloroglucinol	1,3,5-Trihydroxybenzol	$35 \cdot 10^{-3}$	5714	618	0.51
Tryptamine	3-(2-Aminoethyl)indole	$38 \cdot 10^{-3}$	5263	576	0.72
Resorcinol	1,3-Dihydroxybenzol	$51 \cdot 10^{-3}$	3921	628	0.96
Pyrogallol	1,2,3-Trihydroxybenzol	$58 \cdot 10^{-3}$	3448	630	0.97
Catechol	1,2-Dihydroxybenzol	$60 \cdot 10^{-3}$	3333	617	0.42
Serotonine	5-Hydroxytryptamine	$160 \cdot 10^{-3}$	1250	594	0.67
Thymol[b]	2-Isopropyl-5-methylphenol	$800 \cdot 10^{-3}$	250	636	1.22
Naringenin	4′,5,7-Trihydroxyflavanone	1.8	111	570, 614	0.47
Naringin	Naringenin-7-glucosidorhamnoside	8.5	24	626	0.89
Terpinene[b]	1,3-*p*-Menthadiene	27	7.4	595	0.91
Citral[b]	3,7-Dimethyl-2,6-octadienal	54	3.7	575	0.76
Linalool	3,7-Dimethyl-1,6-octadien-3-ol	61	3.3	604	0.32
Camphene[b]	2,2-Dimethyl-3-methylenebicyclo[2.2.1]heptane	62	3.2	510	0.50
Geraniol[b]	*trans*-3,7-Dimethyl-2,6-octadienol	110	1.8	595	0.73
Guaiacol	*o*-Methylphenol	178	1.1	504	0.76
D-Limonene[b]	1,8(9)-*p*-Menthadiene	215	0.9	594	0.64
Menthol[b]	1-Methyl-4-isopropylcyclohexan-3-ol	384	0.5	600	0.53

[a] Calculated from the values in column 3 of the table as [epicatechin (μM)]/[other compound (μM)] · 10^6.

[b] Use of a butanol-containing solvent and reagent, to prevent demixing.

Another factor, which plays an important rôle in analyzing plant extracts, is the volatility of some compounds. During the concentration procedure with an evaporator, volatile substances such as indole and some terpenes disappear and do not disturb the catechin detection further. If any uncertainty about the catechin nature of a peak remains, an absorbance ratio between 640 and 620 nm for instance (Table III) may be helpful.

All these facts summarized in Table III led to the conclusion that the DMACA reagent described can be used for specific chemical reaction detection of catechin and oligomeric proanthocyanidins. It has been shown that the detector responded linearly to the signal (Fig. 3). For epicatechin the detection limit was 2.5 ng with a signal-to-noise ratio of 2.

Fig. 4 shows the separation and selective detection of the catechins and proanthocyanidins extracted from a chinese tea which is known to be rich in flavanols[66,67]. In Fig. 5 two chromatograms of the phenols of a bottled beer are compared with the detection at 280 nm (upper part) and 640 nm after chemical

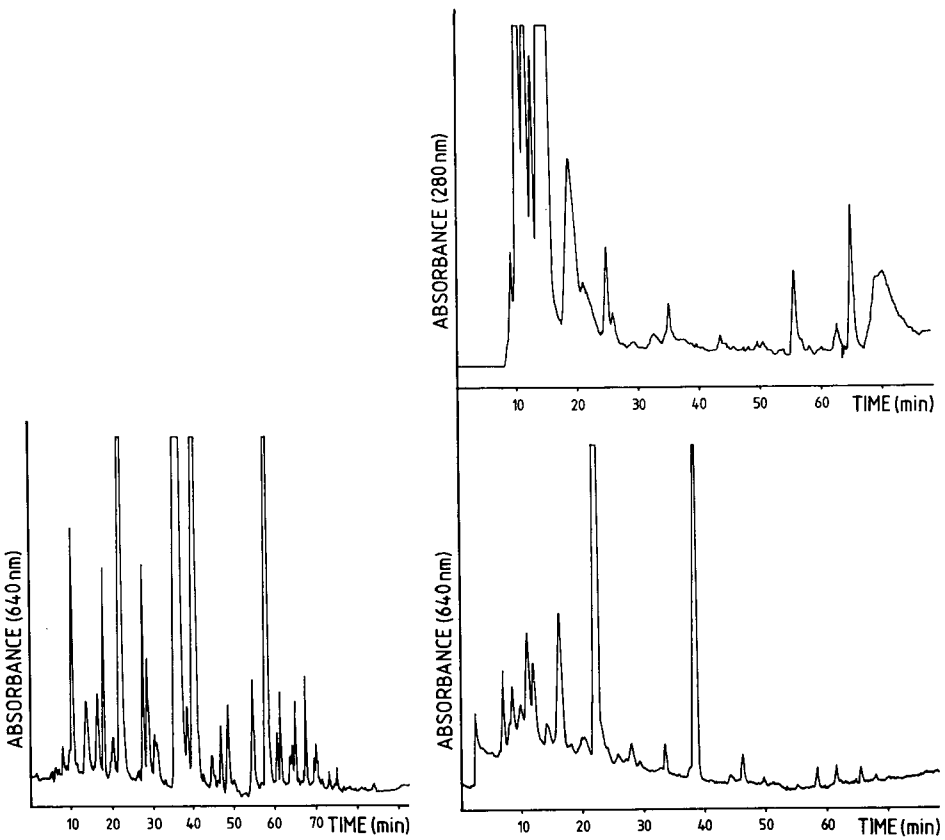

Fig. 4. HPLC separation and chemical reaction detection with DMACA of a phenolic extract from 1.5 mg dry chinese tea (*Camellia sinensis*).

Fig. 5. HPLC separation of the phenolic compounds of 0.5 ml bottled beer (concentrated to 10 μl) with detection at 280 nm (above) and after chemical reaction with DMACA at 640 nm (below).

reaction with DMACA. The UV-absorbance spectra of the main peaks of the 280-nm chromatogram (measured with a diode array detector) showed a maximum between 260 and 270 nm. From this one can conclude that the main peaks with short retention times are structurally not related to flavanols and that they overlap the catechins and proanthocyanidins. The latter were visualized with DMACA, resulting in the lower chromatogram (Fig. 5).

ACKNOWLEDGEMENTS

The author thanks Professor Dr. W. Feucht, who initiated this work, as well as Ing. agr. A. Yuri for valuable discussions. This paper is dedicated to Professor Dr. W. Feucht on the occasion of his 60th birthday.

REFERENCES

1 K. Freudenberg and K. Weinges, in T. A. Geissman (Editor), *The Chemistry of Phenolic Compounds*, Pergamon, Oxford, 1962, p. 197.
2 E. Haslam, *Chemistry of Vegetable Tannins*, Academic Press, London, 1966.
3 K. Weinges, *Phytochemistry*, 3 (1964) 263.
4 R. S. Thompson, D. Jacques, E. Haslam and R. J. N. Tanner, *J. Chem. Soc. Perkin Trans. I*, (1972) 1387.
5 L. Y. Foo and L. J. Porter, *Phytochemistry*, 19 (1980) 1747.
6 M. A. Joslyn and J. L. Goldstein, *Wallerstein Commun.*, 28 (1965) 143.
7 J. R. Ramirez-Martinez, A. Levi, H. Padua and A. Bakal, *J. Food Sci.*, 42 (1977) 1201.
8 A. G. H. Lea and G. M. Arnold, *J. Sci. Food Agric.*, 29 (1978) 478.
9 A. G. H. Lea, *J. Sci. Food Agric.*, 29 (1978) 471.
10 L. Jurd, *Am. J. Enol. Vitic.*, 20 (1969) 191.
11 A. G. H. Lea, P. Bridle, C. F. Timberlake and V. L. Singleton, *Am. J. Enol. Vitic.*, 30 (1979) 289.
12 M. Bourzeix, M. Clarens and N. Heredia, *Bull. Liaison Groupe Polyphenols*, 13 (1986) 403.
13 P. Mulkay and J. Jerumanis, *Cerevisia*, 8 (1983) 29.
14 J. A. Delcour and G. M. Tuytens, *J. Inst. Brew.*, 90 (1984) 153.
15 I. McMurrough, G. P. Hennigan and M. J. Loughrey, *J. Inst. Brew.*, 89 (1983) 15.
16 E. Haslam, T. H. Lilley and T. Ozawa, *Bull. Liaison Groupe Polyphenols*, 13 (1986) 352.
17 J. E. Beart, T. H. Lilley and E. Haslam, *Phytochemistry*, 24 (1985) 33.
18 G. Hill, F. Stellwaag-Kittler, G. Huth and E. Schlösser, *Phytopath. Z.*, 102 (1981) 102.
19 W. G. Berger and K. Herrmann, *Z. Lebensm.-Unters.-Forsch.*, 146 (1971) 266.
20 L. Narziss and H. Kessler, *Brauwissenschaft*, 24 (1971) 14.
21 A. G. H. Lea and C. F. Timberlake, *J. Sci. Food Agric.*, 29 (1978) 484.
22 J. Jerumanis, *Proc. Eur. Brew. Conv., Berlin*, (1979) 309.
23 F. Drawert, G. Leupold and V. Lessing, *Brauwissenschaft*, 30 (1977) 13.
24 W. Feucht, P. P. S. Schmid and E. Christ, *J. Plant Physiol.*, 125 (1986) 1.
25 W. Feucht, P. P. S. Schmid and E. Christ, *Obst Weinbau*, 22 (1985) 249.
26 M. E. Mace, A. A. Bell and R. D. Stipanovic, *Physiol. Plant Pathol.*, 13 (1978) 143.
27 T. Swain and W. E. Hillis, *J. Sci. Food Agric.*, 10 (1959) 63.
28 T. Swain and J. L. Goldstein, in J. B. Pridham (Editor), *Methods in Polyphenol Chemistry*, Pergamon, Oxford, 1964, p. 131.
29 J. A. Delcour and D. J. De Varebeke, *J. Inst. Brew.*, 91 (1985) 37.
30 H. Friedrich and H. Wiedemeyer, *Planta Med.*, 30 (1976) 223.
31 E. Haslam, *Phytochemistry*, 16 (1977) 1625.
32 H. A. Stafford and H. H. Lester, *Plant Physiol.*, 66 (1980) 1085.
33 A. S. L. Tirimanna and K. P. W. C. Perera, *J. Chromatogr.*, 58 (1971) 302.
34 H. A. Stafford and H. H. Lester, *Plant Physiol.*, 68 (1981) 1035.
35 A. W. Jaworski and C. Y. Lee, *J. Agric. Food Chem.*, 35 (1987) 257.
36 A. G. H. Lea, *J. Chromatogr.*, 238 (1982) 253.
37 I. McMurrough and J. McDowell, *Anal. Biochem.*, 91 (1978) 92.

38 I. McMurrough, *Proc. Eur. Brew. Conv., Berlin*, (1979) 321.
39 H. Engelhardt and R. Klinkner, *Fresenius' Z. Anal. Chem.*, 319 (1984) 277.
40 C. Hartwich and M. Winckel, *Arch. Pharm. (Weinheim Ger.)*, (1904) 462.
41 O. Lindt, *Z. Wiss. Mikroskopie Technik*, 2 (1885) 495.
42 T. von Fellenberg, *Chem.-Zt.*, 88 (1910) 791.
43 T. von Fellenberg, *Mitt. Lebensm. Hyg.*, 1 (1910) 311.
44 M. M. Raciborski, *Anz. Akad. Wiss. Krakow*, (1906) 553.
45 M. Joachimowitz, *Biochem. Z.*, 82 (1917) 324.
46 J. Kolsek and M. Perpar, *Fresenius' Z. Anal. Chem.*, 167 (1958) 161.
47 L. Rosenthaler, *Fresenius' Z. Anal. Chem.*, 44 (1905) 292.
48 L. Ekkert, *Pharm. Zentralhalle*, 68 (1927) 577.
49 L. Ekkert, *Pharm. Zentralhalle*, 69 (1928) 289.
50 T. Swain and W. E. Hillis, *J. Sci. Food Agric.*, 10 (1959) 63.
51 M. Thies and R. Fischer, *Mikrochim. Acta*, (1971) 9.
52 M. E. Mace and C. R. Howell, *Can. J. Bot.*, 52 (1974) 2423.
53 R. O. Gardner, *Stain Technol.*, 50 (1975) 315.
54 S. K. Sarkar and R. E. Howarth, *J. Agric. Food Chem.*, 24 (1976) 317.
55 W. Feucht and P. P. S. Schmid, *Gartenbauwiss.*, 48 (1983) 119.
56 M. L. Price, S. Van Scoyoc and L. G. Butler, *J. Agric. Food Chem.*, 26 (1978) 1214.
57 J. A. Delcour, in H. F. Linskens and J. F. Jackson (Editors), *Beer Analysis*, Springer, Berlin, 1988, p. 225.
58 F. C. Happold and L. Hoyle, *Biochem. J.*, 28 (1934) 1171.
59 J. Harley-Mason and A. A. P. G. Archer, *Biochem. J.*, 69 (1958) 60.
60 J. M. Turner, *Biochem. J.*, 78 (1961) 790.
61 H. Engelhardt and U. D. Neue, *Chromatographia*, 15 (1982) 403.
62 S. R. Finn and J. W. James, *J. Appl. Chem.*, 6 (1956) 466.
63 W. E. Hillis and G. Urbach, *J. Appl. Chem.*, 9 (1959) 474.
64 P. Ribereau-Gayon, *Plant Phenolics*, Oliver & Boyd, Edinburg, 1972.
65 H. Geiger, in C. F. Van Sumere and P. J. Lea (Editors), *The Biochemistry of Plant Phenolics*, Clarendon, Oxford, 1985, p. 45.
66 A. G. Brown, W. B. Eyton, A. Holmes and W. D. Ollis, *Phytochemistry*, 8 (1969) 2333.
67 A. C. Hoefler and P. Coggon, *J. Chromatogr.*, 129 (1976) 460.

Journal of Chromatography, 467 (1989) 195–208
Elsevier Science Publishers B.V., Amsterdam — Printed in The Netherlands

CHROM. 21 260

SEPARATION OF NICKEL(II) ALKYLPORPHYRINS BY REVERSED-PHASE HIGH-PERFORMANCE LIQUID CHROMATOGRAPHY

METHODOLOGY AND APPLICATION

CHRISTOPHER J. BOREHAM*
Division of Continental Geology, Bureau of Mineral Resources, Geology and Geophysics, P.O. Box 378, Canberra, 2601 (Australia)
and
CHRISTOPHER J. R. FOOKES
CSIRO, Division of Fuel Technology, Private Mail Bag 7, Menai, NSW 2234 (Australia)
(Received December 29th, 1988)

SUMMARY

Reversed-phase, high-performance liquid chromatography (HPLC) on 4 μm C_{18}-bonded silica has been used to study the elution–structure relationships in a standard set of nickel(II) porphyrins. Nickel(II) etioporphyrins (NiEtio) (C_{27}–C_{32}) were completely separated from later eluting nickel(II)desoxophylloerythroetioporphyrin (NiDPEP) (C_{30}–C_{33}). Structural isomers with a single cycloalkano ring elute before their NiDPEP counterparts unlike species with more than one ring. Within a pseudohomologous series the elution order is t_R β-hydrogen < t_R β-ethyl < t_R β-methyl = t_R β-propyl. Separation of positional isomers is readily achieved. For the NiDPEP series where the site of isomerism is between rings A, B and D, the elution order is t_R ring A < t_R ring B < t_R ring D. Within the NiEtio series t_R ring A ≤ t_R ring C. Nickel(II) alkyl porphyrins of sedimentary origin can be successfully analysed by reversed-phase HPLC. Structural types and individual members can be identified through a combination of retention times, coinjections and absorbance-ratio recording. In doing so the distributions of the structural types can be determined. There is good agreement between this HPLC approach and the assessment of the relative proportions of various structural groups by mass spectrometry.

INTRODUCTION

Petroporphyrins, most likely the fossil biomarkers derived from precursor chlorophylls[1–7] have been used in organic geochemistry as maturation indicators[8–10] and in reconstructing depositional environments[11]. Using their carbon isotopic values in conjunction with isotopic values on coexisting organic matter, various types of secondary processes within sediments which modified the primary photosynthetic organic matter can be determined[12]. These applications usually require a detailed

analysis/isolation of petroporphyrins in order to obtain pure fractions or individual species. High-performance liquid chromatography (HPLC) has been the major analytical technique used in this endeavour.

Metalloporphyrins found in sediments and petroleum are dominated by two metals, nickel(II) (Ni) and vanadium(IV) (as vanadyl, VO)[7]. Usually the metal ion is removed by strong acids and the recovered free-base alkylporphyrins have been analysed by normal-phase high-resolution HPLC on 3-μm or 5-μm silica supports[13,15–17]. In this way, identical HPLC conditions are used to analyse porphyrins chelated to a variety of metals. The separations can utilise polarity as well as basicity differences between the various structural types. However some decomposition of the porphyrin (25% or greater)[18,19] occurs in the strong acid and there is the possibility of preferential loss of different structural types.

Recently, the vanadyl alkylporphyrins have been analysed directly under high-resolution reversed-phase HPLC[18,20] (3-μm C_{18} bonded phase). By comparison, Ni porphyrins are reported to suffer poor resolution and relatively long retention times under similar reversed-phase conditions[16]. Nevertheless, analysis of Ni porphyrins by reversed-phase HPLC has led to the isolation of many compounds with novel structures[2–4,21–24].

The present study reports on the high-resolution reversed-phase HPLC analysis of Ni alkyl porphyrins covering a wide range of structural types. Retention time behaviour is addressed in terms of various substituent characteristics including pseudohomologous series, exocyclic ring size and number, and structural and positional isomerism. Retention time in combination with coinjections and absorbance-ratio recording is used to identify the distribution and relative abundances of structural types in nickel porphyrins of sedimentary origin.

EXPERIMENTAL

Nickel porphyrin standards

Fig. 1 lists the structural types (**1**–**10**) and members within each structure examined in this study.

Ten authentic samples of free-base porphyrins were generously supplied by Prof. P. Clezy. Nickel(II) was inserted using a published method[22] by adding excess $Ni(acac)_2$ (50:1) to a solution of free-base porphyrin in benzene (1 mg/ml) and refluxing under argon for 5–6 h. In this way, **1b**–**1i**, **3a** and **7** were obtained.

The remaining Ni porphyrins were isolated from geological samples using thin-layer chromatography and semi-preparative HPLC (see below). The Ni porphyrins with known structures **1a**–**1i**, **2a**–**2c**, **2e** and **2f**, **2h**, **3b** and **3c**, **4d**, **5a** and **5b**, **6**, **8a** and **8b**, and **10** were characterised by ^{1}H NMR (400 MHz) by comparison with literature chemical shifts[2–4,22–26]. Sample **1k** is a complex mixture, while structures of the novel Ni porphyrins **2d**, **2g**, **4a**–**4c** and **9a** and **9b** are only tentative at present. Chemical shifts, decoupling and limited nuclear Overhauser effect (NOE) experiments firmly established the "lower halves" of the seven structures, but sample limitations have so far prevented the extensive NOE studies required to determine the positions of the substituents in rings A and B.

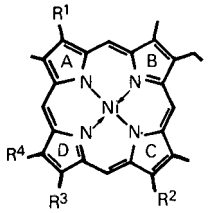

1a: $R^4 = CH_3$, $R^{1-3} = CH_2\ CH_3$ (C_{32})
1b: $R^3 = CH_3$, $R^{1,2,4} = CH_2\ CH_3$ (C_{32})
1c: $R^{1,4} = CH_3$, $R^{2,3} = CH_2\ CH_3$ (C_{31})
1d: $R^{2,4} = CH_3$, $R^{1,3} = CH_2\ CH_3$ (C_{31})
1e: $R^{1,2,4} = CH_3$, $R^3 = CH_2\ CH_3$ (C_{30})
1f: $R^1 = H$, $R^4 = CH_3$, $R^{2,3} = CH_2\ CH_3$ (C_{30})
1g: $R^2 = H$, $R^4 = CH_3$, $R^{1,3} = CH_2\ CH_3$ (C_{30})
1h: $R^1 = H$, $R^{2,4} = CH_3$, $R^3 = CH_2\ CH_3$ (C_{29})
1i: $R^2 = H$, $R^{1,4} = CH_3$, $R^3 = CH_2\ CH_3$ (C_{29})
1j: $R^{1,2} = H$, $R^4 = CH_3$, $R^3 = CH_2\ CH_3$ (C_{28})
1k: Unknown mixture of C_{27} Ni Etio

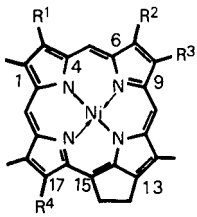

2a: $R^2 = CH_3$, $R^{1,3} = CH_2\ CH_3$, $R^4 = CH_2\ CH_2\ CH_3$ (C_{33})
2b: $R^2 = CH_3$, $R^{1,3,4} = CH_2\ CH_3$ (C_{32})
2c: $R^{1,2} = CH_3$, $R^{3,4} = CH_2\ CH_3$ (C_{31})
2d: $R^{2,3} = CH_3$, $R^{1,4} = CH_2\ CH_3$ (C_{31})
2e: $R^2 = H$, $R^{1,3,4} = CH_2\ CH_3$ (C_{31})
2f: $R^1 = H$, $R^2 = CH_3$, $R^{3,4} = CH_2\ CH_3$ (C_{30})
2g: $R^3 = H$, $R^2 = CH_3$, $R^{1,4} = CH_2\ CH_3$ (C_{30})
or $R^2 = H$, $R^3 = CH_3$, $R^{1,4} = CH_2\ CH_3$ (C_{30})
2h: $R^4 = H$, $R^2 = CH_3$, $R^{1,3} = CH_2\ CH_3$ (C_{30})

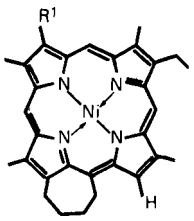

3a: $R^1 = CH_2\ CH_3$ (C_{32})
3b: $R^1 = CH_3$ (C_{31})
3c: $R^1 = H$ (C_{30})

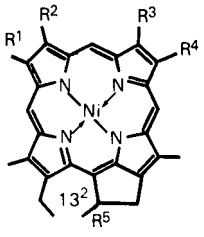

4a: $R^{1,2,3,4}$ 2 x CH_3, 2 x $CH_2\ CH_3$, $R^5 = CH_3$ (C_{33})
4b: $R^{1,2,3,4}$ 3 x CH_3, $CH_2\ CH_3$, $R^5 = CH_3$ (C_{32})
4c: $R^{1,2,3,4}$ H, 2 x CH_3, $CH_2\ CH_3$, $R^5 = CH_3$ (C_{31})
4d: $R^{1,3} = CH_3$, $R^{2,4} = CH_2\ CH_3$, $R^5 = OH$ (C_{32})

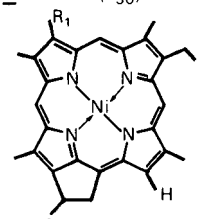

5a: $R^1 = CH_2\ CH_3$ (C_{31})
5b: $R^1 = H$ (C_{29})

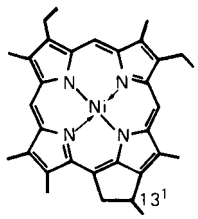

6: (C_{33})

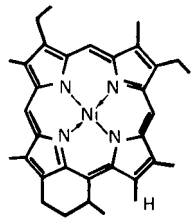

7: (C_{32})

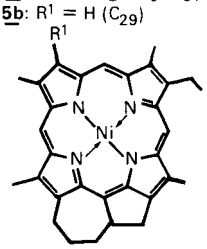

8a: $R^1 = CH_2\ CH_3$ (C_{33})
8b: $R^1 = CH_3$ (C_{32})

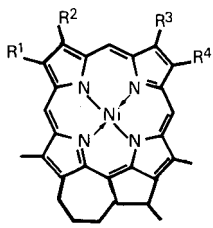

9a: $R^{1,2,3,4}$ 2 x CH_3, 2 x $CH_2\ CH_3$ (C_{34})
9b: $R^{1,2,3,4}$ 3 x CH_3, $CH_2\ CH_3$ (C_{33})

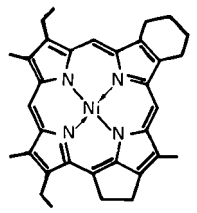

10: (C_{33})

Fig. 1. Structures of standard nickel(II) porphyrins.

Total Ni porphyrins

The total Ni porphyrins from rock extracts and petroleum were separated on silica gel (Merck 40 70–230 mesh) using a progressive solvent gradient from light petroleum (40–60 b.p.) to dichloromethane through a series of three column volume additions of 10, 20, 30, 50, and 70% light petroleum in dichloromethane mixtures; the Ni porphyrins were eluted within the 20–30% additions. This fraction (typically 2–10% in Ni porphyrin) was purified by semi-preparative HPLC and the fraction eluting from the least retained **1j** to the last eluting **10** was collected for detailed analysis by analytical HPLC.

HPLC analyses

Chromatographic separations were performed using Waters equipment: three pumps (two 510 and a 590 series) were programmed through a 680 gradient controller, a U6K injector and a 490 multi-wavelength UV–VIS detector. Synchronous dual-channel detector output [channel 1: ratio recording (the analog output is the ratio of the absorbance at 400 nm to the absorbance at 550 nm), channel 2: absorbance at 400 nm] was interfaced through a 18-bit high-resolution A/D board to the DAPA chromatographic software. Solvents used were pump A: methanol–pyridine (0.2% pyridine); pump B: acetonitrile–pyridine (0.2% pyridine); and pump C: chloroform. Pyridine was freshly distilled before use and all other solvents were HPLC grade and used without further purification. Solvents were kept under a positive helium pressure (Waters eluent stabilization system) during analysis.

Analytical method

Analyses were performed using a precolumn (Guard-Pak μBondapak C_{18}; Waters) and two columns (Nova Pak C_{18} 4 μm, each 150 × 3.9 mm I.D.; Waters) connected in series. Isocratic operation at 1.0 ml/min using methanol–pyridine (0.2% pyridine) gave a back-pressure of 1600 p.s.i. Another column that was tested used Hypersil ODS C_{18} 3 μm. In this case there was no advantage in going to the smaller particle size. Gradient operation employed the program: 0–35 min, 100% A, 1.0 ml/min; linear gradient from 35–65 min, 100% A to 85% A + 15% B, 1.0 ml/min; hold for 5 min.; linear gradient from 70–85 min, 85% A + 15% B to 100% B, 1.0 ml/min to 1.5 ml/min. This was followed by a reconditioning cycle involving a 5 min chloroform wash. Cycle time was two hours.

Semi-preparative method

The semi-preparative separations were performed on a precolumn, two 100 × 8 mm I.D. Nova Pak C_{18} Radial-Pak cartridges and a 300 × 7.8 mm I.D. μBondapak stainless-steel column connected in series. In this case pyridine was not added and the linear solvent program was 0–50 min, 70% A + 30% B to 100% B, 3.0 ml/min and held in acetonitrile mobile phase for a further 25 min. Subsequent washing and reconditioning resulted in a cycle time of 2 h. Back pressures were in the range 900–1600 p.s.i. With this column combination up to 200 μg of total Ni porphyrin could be analysed without overloading.

Mass spectra

Mass spectra were recorded using a VG70E mass spectrometer and VG11/250

data system in the full scan mode (50–650 a.m.u., 2 s scan time). Operating conditions were: electron energy 16 eV, filament current 200 μA, ion source 250°C. Samples (1–2 μg Ni porphyrin) were placed in the direct insertion probe which was temperature programmed. Typically, the probe was rapidly heated from ambient to 150°C and held there until the total ion current decayed to a stable value. The temperature was then programmed to 300°C at 20°C/min. An average spectrum was obtained from the sum of the scans between the first and last detected Ni porphyrins.

RESULTS AND DISCUSSION

Choice of HPLC conditions

Previous reports on the separation of Ni porphyrins under reversed-phase conditions, usually in connection with isolation of single species, have involved the use of a variety of solvents. Most common has been methanol while acetonitrile, ethanol and chloroform have been used in varying concentrations[2–4,21–24].

Preliminary examination in this work using either methanol or acetonitrile resulted in asymmetrical peaks with significant tailing. Considerably shorter elution times occurred with an acetonitrile mobile phase. With the addition of a small percentage (0.2%) of pyridine to the mobile phase, retention times were little affected however a more symmetrical peak shape occurred resulting in an overall two fold increase in column efficiency (32 000 plates/m for **1a**, Fig. 1; this can be compared with 33 000–104 000 plates/m for the HPLC analysis of free-base porphyrins with similar particle size supports[16]). It had been reported that improvements occurred with pyridine addition in the normal-phase HPLC separation of free-base porphyrins[16]. A decrease in porphyrin aggregation and competition for the active sites on the stationary phase had been invoked to explain this improvement.

Separation between and within pseudohomologous series

Elution positions of 35 fully or partially characterised Ni porphyrins were examined and their structures are shown in Fig. 1. In general, the retention times (t_R) for Ni porphyrins with fully alkylated β-substituents which have the five-membered exocyclic alkano ring [nickel(II) desoxophylloerythroetioporphyrin (NiDPEP) series, **2**] are longer than for those without a ring [nickel(II) etioporphyrin (NiEtio) series, **1**]. A similar order was found for free-base porphyrins under normal-phase conditions[17], while the presence of an exocyclic ring had little effect on the elution order for vanadyl porphyrins examined using reversed-phase HPLC[18]. Addition of a methyl substituent to a five-membered exocyclic ring (**4a–4c**, **6**) decreases the retention time while increasing exocyclic alkano ring number increases t_R. The component with two isolated rings (**10**, t_R = 108 min) has a longer retention time than for the species with two fused rings (**8a**, **8b**, **9a** and **9b**, Fig. 2c). This is probably due to a greater interaction between the hydrophobic bonded phase and separated ring systems.

Within a pseudohomologous series, the effect of decreasing the molecular weight through the loss of one methyl group from a β-propyl to a β-ethyl substituent is to decrease the retention time [t_R **2b** < t_R **2a** (not shown, but **2a** coelutes with **2c**, Fig. 2b)]. Presumably the decrease in porphyrin side-chain length results in less interaction with the long aliphatic C_{18} bonded phase. The opposite occurs for a methyl loss involving a β-ethyl to a β-methyl. Here the methyl-substituted member elutes after the higher-

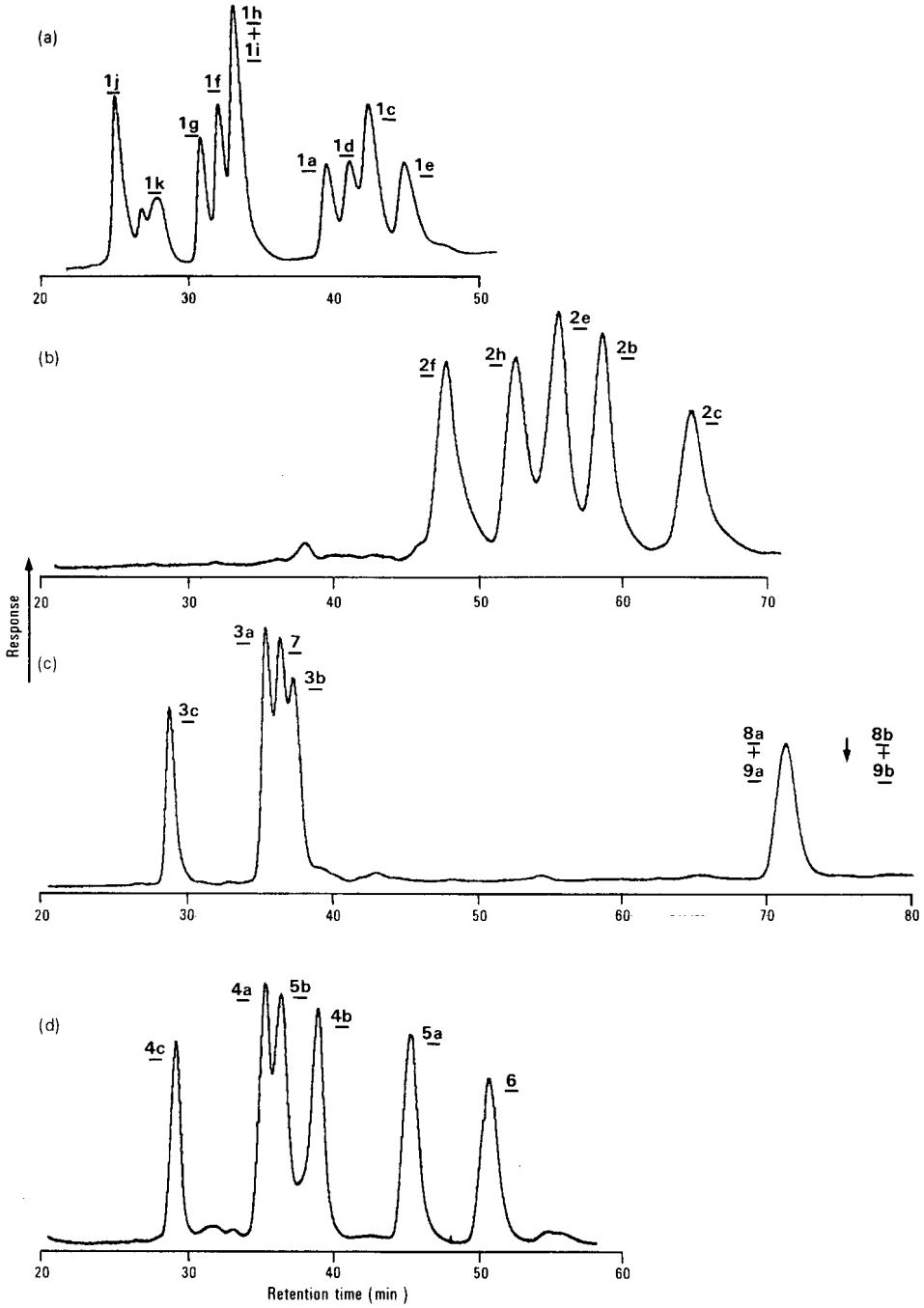

Fig. 2. HPLC traces of synthetic mixtures of standard nickel(II) porphyrins.

carbon-numbered component. Hence t_R **1c** and **1d** > t_R **1a** (Fig. 2a); t_R **2c** and **2d** > t_R **2b** (Fig. 2b); t_R **3b** > t_R **3a** (Fig. 2c); t_R **4b** > t_R **4a** (Fig. 2b); t_R **8b** > t_R **8a** (Fig. 2c); t_R **9b** > t_R **9a** (Fig. 2c). This characteristic elution order is similar to normal-phase HPLC of free-base porphyrins[17]. In the latter the increased retention is governed by the increased polarity of the methyl over the ethyl pseudohomologue. However this cannot be the sole effect which determines retention under reversed-phase HPLC for these Ni porphyrins.

The loss of an additional methyl group gives rise to either a fully alkylated component (2 ethyl groups → 2 methyl groups) or to a β-hydrogen substituent (ethyl → methyl → H). The former results in further retention (t_R **1e** > t_R **1c** and **1d**, Fig. 2a). In the latter, the β-hydrogen member elutes well before the fully alkylated pseudohomologues (again the similarity with free-base porphyrins). Thus within the four pseudohomologous series **1a**, **1c** and **1f**, **2b**, **2c** and **2f**, **3a–3c**, and **4a–4c**, the member with the β-hydrogen substituent is the least strongly retained followed by the ethyl then the methyl pseudohomologues (Fig. 2a, b, c and d, respectively). For the pseudohomologous series **1f**, **1h** and **1j** the highest-molecular-weight member already has a β-hydrogen while **1j** with two β-hydrogens is the least retained of all the Ni alkylporphyrins studied in this work. An increase in basicity of the alkano-substituted free-base porphyrin (due to their electron-donating effect[27]) was responsible for the greater retention over the β-hydrogen component[17]. With the metalloporphyrins, protonation of the pyrrole nitrogens is unlikely to occur from any residual silanol groups. If this occurred some decomposition of the porphyrin would probably result. Hence the retention of the alkano pseudohomologue may, in part, be the result of an increased electron density in the delocalised porphyrin ring system interacting with the hydrophobic bonded phase.

Addition of a polar hydroxo-group to the five-membered exocyclic ring involves a dramatic decrease in retention time; **4d** elutes at 10 min well before any Ni alkylporphyrin. Here polarity has an overriding influence on retention behaviour.

Structural isomers

For components with the same molecular weight and carbon number, the isomer with a β-hydrogen substituent has a shorter elution time than the fully alkylated counterpart. Thus the two β-hydrogen C_{30} NiEtio (**1f** and **1g**) elute well before the fully alkylated isomer, **1e**. The same elution order occurs for the C_{30} NiDPEP isomers (t_R **2e** < t_R **2c** and **2d**). The two C_{32} components with a β-hydrogen, the methyl-substituted six-membered ring (**7**) and the seven-membered ring (**3a**), also elute before the fully alkylated five-membered ring C_{32} NiDPEP (**2b**). Also **3a** has a slightly shorter t_R than **7**. Of interest are the relative t_R values of the novel porphyrins with methyl-substituted five-membered rings (**4**, **5** and **6**) and their NiDPEP counterparts (**2**). For the isomers with β-hydrogens, the elution order is t_R **4b** < t_R **5a** < t_R **2e**, even though the presence of a β-methyl group in **4b** compared with a β-ethyl substituent in the other two would help in its retention (see previous heading). The fully alkylated isomers with the methyl-substituted five-membered ring C_{32} (**4b**) and C_{33} (**4a** and **6**), elute well before their respective C_{32}NiDPEP (**2b**) and C_{33}NiDPEP (**2a**) isomers.

Positional isomers

In most cases, positional isomers can be resolved by reversed-phase HPLC. For

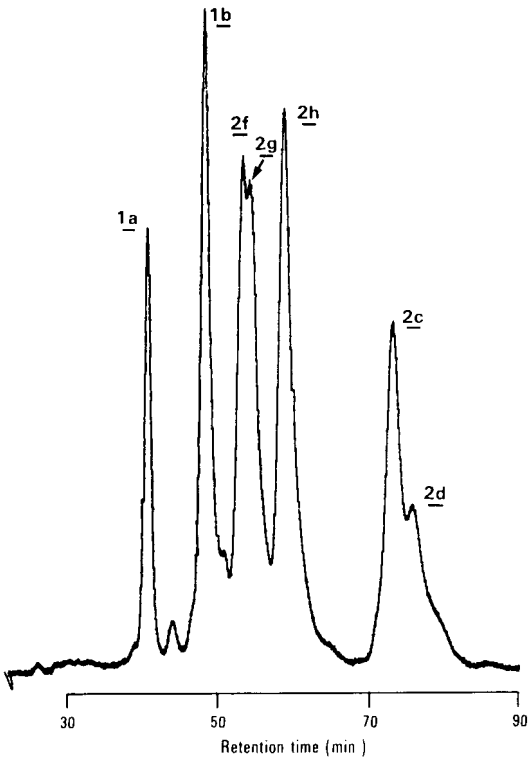

Fig. 3. HPLC trace of various positional isomers of standard nickel(II) porphyrins.

example, there is complete separation of Ni etioporphyrin III (**1a**) and Ni etioporphyrin I (**1b**) (Fig. 3). Other positional isomers which show baseline resolution are the ring A-β-hydrogen NiC_{30}DPEP (**2f**) from the ring D-β-hydrogen NiC_{30}DPEP (**2h**) (Figs. 2b and 3) and the 13(2)-methyl-substituted (13,15-ethano-) five-membered ring C_{31} species (**4c**) from the 15(2)-methyl-substituted (15,17-ethano-) five-membered ring C_{31} isomer (**5a**) (Fig. 2d). Partial separation occurs between: ring A-methyl and ring C-methyl NiC_{31}Etio (**1c** and **1d**, Fig. 1a) and likewise their respective β-hydrogen C_{30} pseudohomologues (**1f** and **1g**, Fig. 1a); ring A-methyl and ring B-methyl NiC_{31}DPEP (**2c** and **2d**, Fig. 3); ring A-β-hydrogen and ring B-β-hydrogen NiC_{30}DPEP (**2f** and **2g**, Fig. 3). The two NiC_{29}Etio positional isomers (**1h** and **1i**, Fig. 1a) coelute.

These preliminary results suggest that for Ni porphyrins of the DPEP type (**2**), the elution order for positional isomers is t_R ring A $<$ t_R ring B $<$ t_R ring D while for the NiEtio porphyrins (**1**) the order is t_R ring A $\leqslant$ t_R ring C. It is interesting to look at the two C_{33} isomers which have methyl-substituted five-membered rings. For isomer **4a** the methyl group is attached to the 13(2) carbon while for **6** it is bound to the 13(1) carbon. The shorter t_R for **4a** probably results from less effective interaction with the bonded stationary phase due to steric hindrance between the methyl group and the adjacent ring D ethyl group.

Application

Fig. 4a shows the HPLC trace under isocratic conditions of a synthetic mixture obtained on combining the mixtures in Fig. 2a–d. Severe overlap is evident in parts of the chromatogram making assignments difficult. Using the gradient program, elution times have been considerably reduced (*e.g.* **10** elutes in 80 min *cf.* 108 min previously) while elution orders remain the same (Fig. 4c *cf.* Fig. 4a).

The values for the ratio of the absorbance at 400 nm to the absorbance at 550 nm is given in Table I for all the standard Ni porphyrins. It covers a wide range from 1.4 for **1** to 9.5 for Ni butano-porphyrin **3** although it is slightly solvent dependent. For a pure single compound the absorbance-ratio plot should be a constant value over the elution profile of the peak. In Fig. 4b the ratio plot overlies the absorbance trace (Fig. 4c) and maintains a uniform value over the bulk of the peak. The slight variation in the ratio

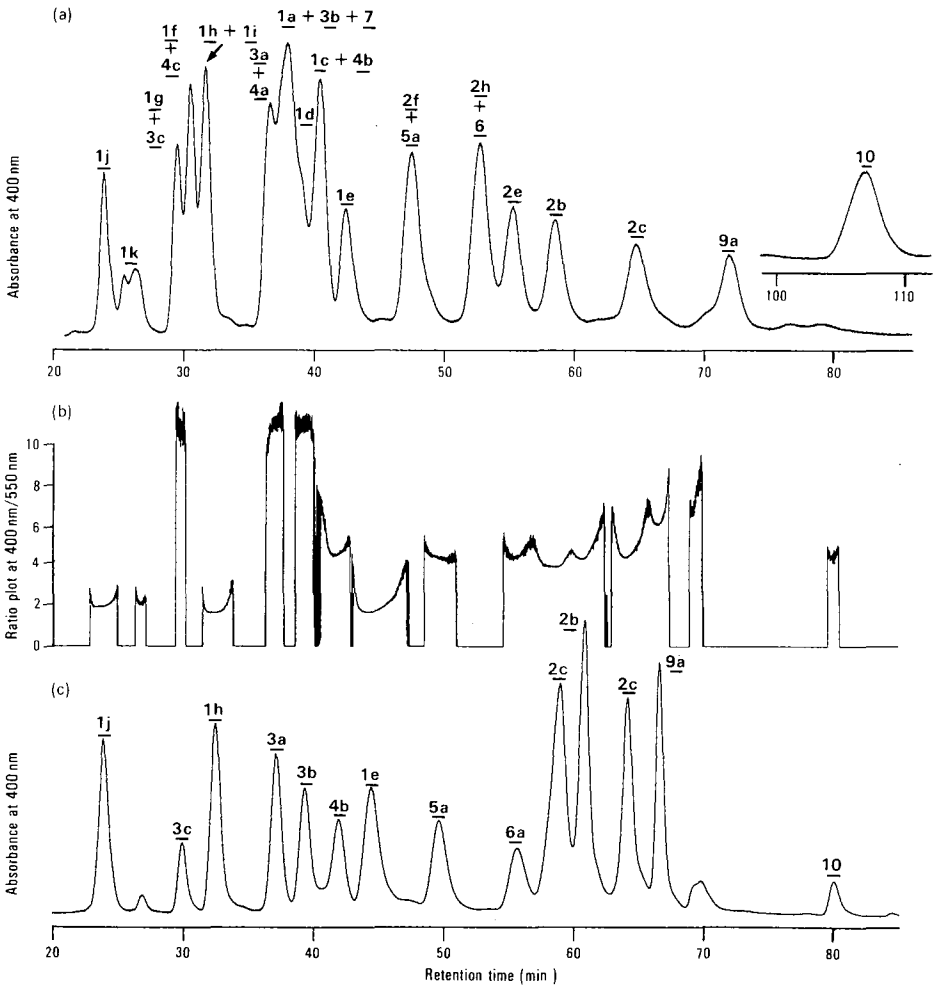

Fig. 4. HPLC traces of standard nickel(II) porphyrin mixtures. (a) Isocratic (methanol–0.2% pyridine), (b) ratio plot corresponding to absorbance plot in (c), (c) gradient program (see Experimental).

value over the total peak might be due to some impurities. A more likely explanation is that changes in porphyrin aggregation over the peak profile cause slight perturbations in the absorbance spectrum, hence ratio trace.

This dual detection approach (absorbance and absorbance-ratio monitoring) is therefore invaluable in deconvoluting coeluting or closely eluting components under the HPLC conditions used here. In a total Ni porphyrin fraction of sedimentary origin, the diverse array of structural types usually means coelutions are inevitable. Fig. 5 depicts the absorbance and ratio traces of non-polar Ni alkylporphyrins from two immature shales —the marine Julia Creek oil shale (Fig. 5a, 1401) and the lacustrine Messel oil shale (Fig. 5b, 4208). Ni porphyrins from both sediments have been extensively studied and numerous single species isolated[2–4,28,29].

The two major peaks eluting in the "Etio region" of the chromatogram for the Julia Creek sample were identified as the Ni butano porphyrins **3a** and **3b** on the basis of their retention times and high absorbance-ratio values. The slightly lower ratio observed here (Fig. 5a) than for the pure butano standards (Fig. 4b) results from minor contributions from coeluting porphyrins which have a much lower absorbance-ratio (Fig. 4a and Table I). The major component in the Messel sample was identified as the methyl-substituted (15,17 ethano-) five-membered ring porphyrin, **5a**. Although the β-hydrogen C_{30}NiDPEP (**2f**) coelutes with **5a** (Fig. 4a), the latter complex has a slightly higher absorbance-ratio (Table I). This species, first isolated as the major component in the Messel shale, is thought to be derived from chlorophyll c[24].

In order to establish relative abundances of the various structural types, the relative values for the extinction coefficients must be known at the monitoring wavelength (*i.e.* 400 nm). The Soret maxima (λ_{max}) for the standard Ni porphyrins ranges from 392 nm (**1**) to 400 nm (**3**) and is uniform within structural types. Absolute extinction coefficients (ε_{max}) have been determined for all the structural types at λ_{max} and all lie within the range 180 000–220 000 (ref. 30). The close similarity in extinction coefficients is further confirmed as follows; relative concentrations of standard mixtures of **1d**, **2b**, **3a** and **3b** were estimated from the visible spectrum using the same ε_{max} and agree to within 10% those obtained from molecular ion abundances. Hence the normalising factor for the relevant structural type relative to **3** is equal to (ε_{max} structural type/ε_{max} for **3**) × (absorbance at λ_{max}/absorbance at λ_{400}). Thus the

TABLE I

VALUE FOR THE RATIO OF ABSORBANCE AT 400 nm TO ABSORBANCE AT 550 nm (IN METHANOL–0.2% PYRIDINE)

Ni por.	*Ratio*	*Ni por.*	*Ratio*	*Ni por.*	*Ratio*	*Ni por.*	*Ratio*
1a	1.48	**1j**	1.79	**2h**	3.60	**5b**	3.87
1b	1.41	**1k**	1.76	**3a**	9.45	**6**	3.47
1c	1.42	**2a**	3.35	**3b**	9.45	**7**	4.63
1d	1.43	**2b**	3.35	**3c**	9.20	**8a**	4.60
1e	1.43	**2c**	3.28	**4a**	3.80	**8b**	4.50
1f	1.54	**2d**	3.25	**4b**	3.73	**9a**	5.00
1q	1.55	**2e**	3.30	**4c**	3.45	**9b**	4.93
1h	1.50	**2f**	3.33	**4d**	2.10	**10**	3.20
1i	1.46	**2g**	3.35	**5a**	3.73		

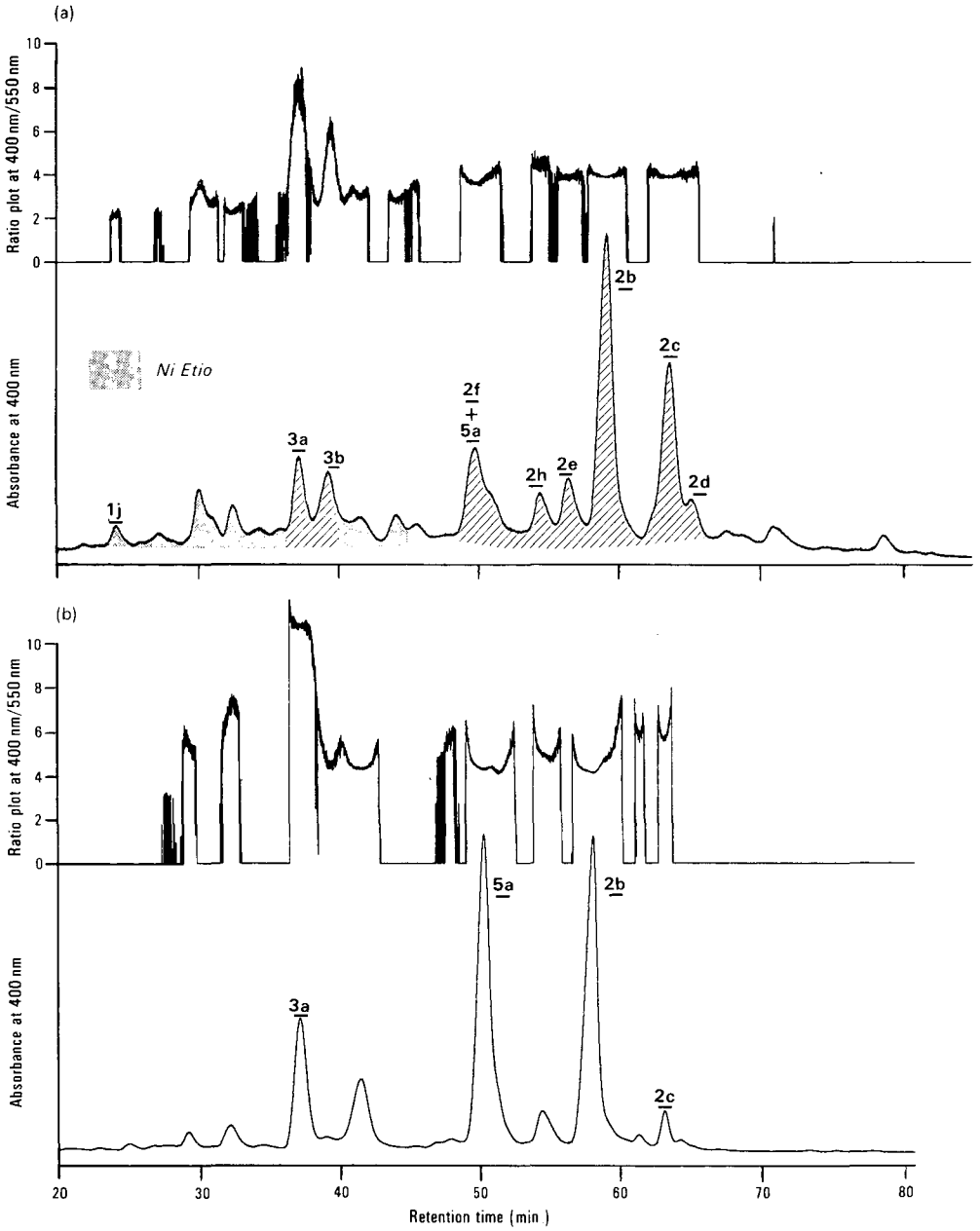

Fig. 5. HPLC traces of total nickel(II) porphyrins from (a) Julia Creek oil shale (1401), (b) Messel oil shale (4208).

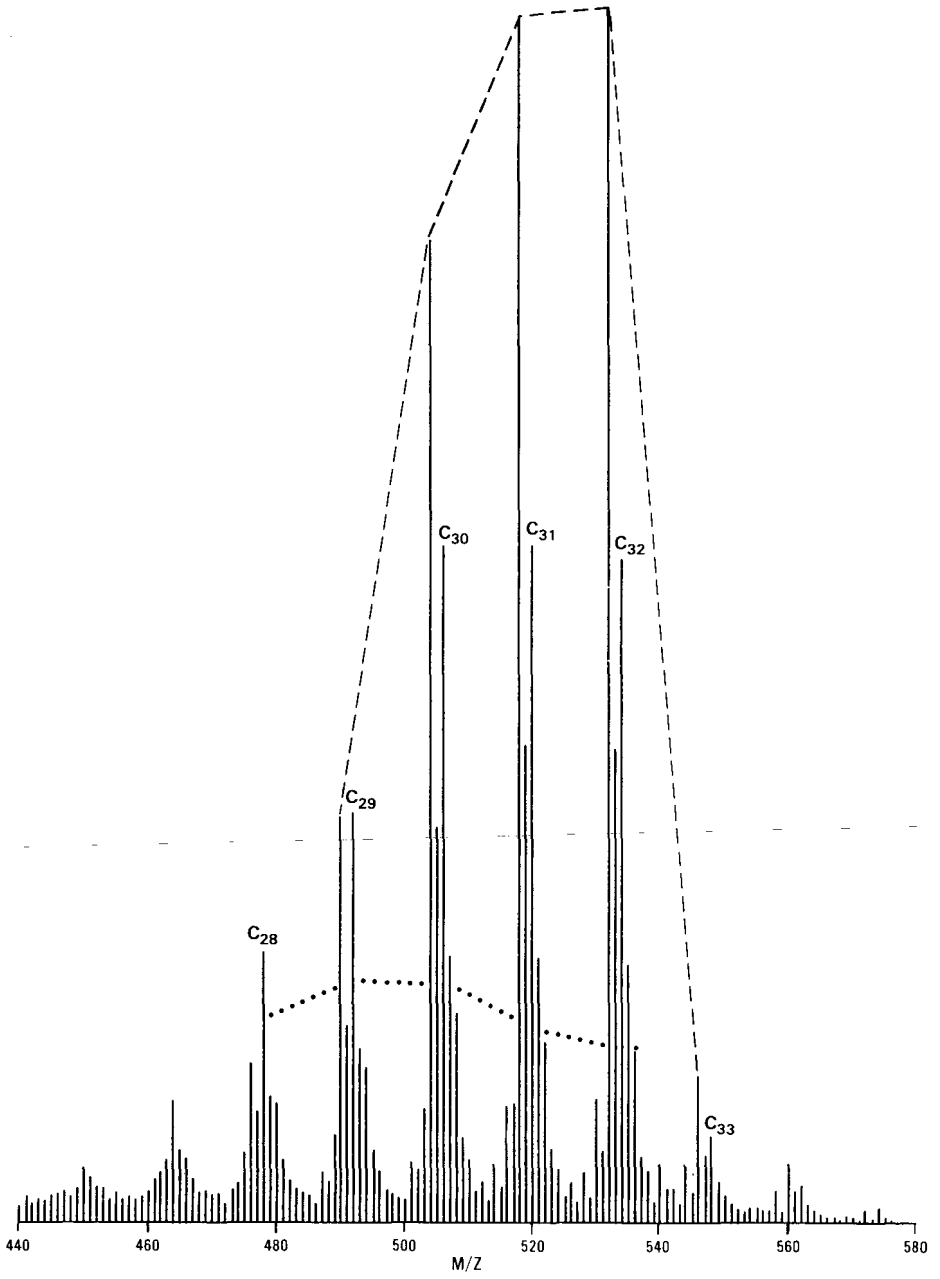

Fig. 6. Low voltage (16 eV) mass spectrum of the nickel(II) porphyrins from Julia Creek oil shale. (– – –) Monoexocyclic ring ^{58}Ni porphyrin; (.....) ^{58}NiEtio.

integrated areas are multiplied by this normalising factor and for **1**, **2**, **3**, **4**, **5**, **6**, **7**, **8**, **9** and **10** this value is equal to 1.91, 1.41, 1.0, 1.25, 1.29, 1.33, 1.09, 1.26, 1.21 and 1.30, respectively.

As an example, this approach was applied to the analysis of the Ni porphyrins in the Julia Creek sample. The integrated areas of the C_{28}–C_{32} NiEtio porphyrins (Fig. 5a) were summed and normalised as were those for the butano and DPEP series (other single exocyclic structures were very minor in comparison). The percentage of the NiEtio porphyrins was 20.6%. A complementary method which can give similar information is mass spectrometry. Here structural types can only be differentiated on the basis of the number of exocyclic rings because these give rise to molecular ions separated in steps of two daltons. After correction for the isotopic contribution from ^{13}C, ^{2}H and $^{60}Ni^{31}$ (molecular ion of a ^{60}Ni porphyrin with a single exocyclic ring is the same nominal mass number as the idential carbon numbered ^{58}NiEtio porphyrin), the percentage of C_{28}–C_{32} NiEtio porphyrins to C_{29}–C_{33} Ni porphyrins with one exocyclic ring was 19.5% (Fig. 6). This close agreement between the two unrelated techniques clearly demonstrates that reversed-phase HPLC of Ni porphyrins is a viable technique for determining the relative distribution of various structural types.

CONCLUSIONS

(1) Reversed-phase HPLC on 4-μm C_{18} bonded silica can be successfully used to separate nickel(II) alkylporphyrins covering a variety of structural types. Although the efficiency (plates/m) is less than that obtained for free-base porphyrins using similar particle-size stationary phases, good resolution is obtained in mostly acceptable elution times.

(2) The NiEtio porphyrins (C_{27}–C_{32}) are completely separated from the NiDPEP series (C_{30}–C_{33}).

(3) Within a pseudohomologous series, the elution order is t_R β-hydrogen $< t_R$ β-ethyl $< t_R$ β-methyl. For the cycloalkanoporphyrins with one isolated ring, the structural isomers of the DPEP type have the longest elution times. The addition of a second alkano ring system leads to further retention in which two isolated rings are retained longer than for two fused rings. Separation of positional isomers can be achieved and for the NiDPEP isomers t_R ring A $< t_R$ ring B $< t_R$ ring D, while for the NiEtio isomers t_R ring A $\leqslant t_R$ ring C.

(4) The combination of retention time, coinjection of authentic standards and absorbance-ratio recording is a powerful technique in the identification of Ni porphyrins with different structural types and individual members within each type.

(5) Reversed-phase HPLC of Ni porphyrins can be used to obtain reliable information on the relative abundances of various structural types without the need for demetallation.

ACKNOWLEDGEMENTS

We thank Mr. Algis Juodvalkis for his technical assistance and Prof. Peter Clezy for synthetic free-base porphyrins. C.J.B. publishes with the permission of the Director, Bureau of Mineral Resources, Geology and Geophysics.

REFERENCES

1 J. M. E. Quirke, G. Eglinton and J. R. Maxwell, *J. Am. Chem. Soc.*, 101 (1978) 7693.
2 C. J. R. Fookes, *J. Chem. Soc., Chem. Commun.*, (1983) 1472.
3 C. J. R. Fookes, *J. Chem. Soc., Chem. Commun.*, (1983) 1474.
4 C. J. R. Fookes, *J. Chem. Soc., Chem. Commun.*, (1985) 706.
5 A. Ekstrom, C. J. R. Fookes, T. Hambley, H. J. Loeh, S. A. Miller and J. C. Taylor, *Nature (London)*, 206 (1983) 173.
6 M. I. Chicarelli, S. Kaur and J. R. Maxwell, in R. H. Filby and J. F. Branthaver (Editors), *Metal Complexes in Fossil Fuels (ACS Symp Series* 344), Washington, DC, 1987, pp. 41–67.
7 E. W. Baker and J. W. Louda, in R. B. Johns (Editor), *Biological Markers in the Sedimentary Record*, Elsevier, New York, 1986, pp. 124–225.
8 A. J. G. Barwise and P. J. D. Park, in M. Bjorøy (Editor), *Advances in Organic Geochemistry, 1981*, Wiley, London, 1983, pp. 668–674.
9 J. Shi, A. S. Mackenzie, R. Alexander, G. Eglinton, A. P. Gower, G. A. Wolff and J. R. Maxwell, *Chem. Geol.*, 35 (1982) 1.
10 A. J. G. Barwise, in R. H. Filby and J. F. Branthaver (Editors), *Metal Complexes in Fossil Fuels (ACS Symp. Series* 344), Washington, DC, 1987, pp. 100–109.
11 J. Moldowan, P. Sundararaman and M. Schoell, *Org. Geochem.*, 10 (1986) 915.
12 R. Takigiku, *Ph.D. Thesis*, Indiana University, Bloomington, IN, 1987.
13 S. K. Hajibrahim, P. J. C. Tibbetts, C. D. Watts, J. R. Watts, G. Eglinton, H. Colin and G. Guiochon, *Anal. Chem.*, 50 (1978) 549.
14 J. M. E. Quirke, in R. H. Filby and J. F. Branthaver (Editors), *Metal Complexes in Fossil Fuels (ACS Symp. Series* 344), Washington, DC, 1987, pp. 308–337 and references therein.
15 A. S. MacKenzie, J. M. E. Quirke and J. R. Maxwell, in A. G. Douglas and J. R. Maxwell (Editors), *Advances in Organic Geochemistry, 1979*, Pergamon Press, Oxford, 1980, pp. 239–248.
16 A. J. G. Barwise, R. P. Evershed, G. A. Wolff, G. Eglinton and J. R. Maxwell, *J. Chromatogr.*, 368 (1986) 1.
17 M. I. Chicarelli, G. A. Wolff and J. R. Maxwell, *J. Chromatogr.*, 368 (1986) 11.
18 P. Sundararaman, *Anal. Chem.*, 57 (1985) 2204.
19 C. J. Boreham, unpublished results.
20 P. Sundararaman, W. R. Biggs, J. C. Reynolds and J. C. Petzer, *Geochim. Cosmochim. Acta.*, 52 (1988) 2337.
21 R. Ocampo, H. J. Callot and P. Albrecht, *J. Chem. Soc., Chem. Commun.*, (1985) 198.
22 J. Verne-Mismer, R. Ocampo, H. J. Callot and P. Albrecht, *Tetrahedron Lett.*, 27 (1986) 5257.
23 J. Verne-Mismer, R. Ocampo, H. J. Callot and P. Albrecht, *J. Chem. Soc., Chem. Commun.*, (1987) 1581.
24 R. Ocampo, H. J. Callot and P. Albrecht, *Tetrahedron*, 40 (1984) 4033.
25 J. Krane, T. Skjetne, N. Telnaes, M. Bjorøy, L. Schol and H. Solli, *Org. Geochem.*, 6 (1984) 193.
26 P. S. Clezy, C. J. R. Fookes and J. K. Prasher, *Aust. J. Chem.*, submitted for publication.
27 P. Hambright, in K. Smith (Editor), *Porphyrins and Metalloporphyrins*, Elsevier, Amsterdam, 1976, pp. 236–278.
28 C. J. Boreham and T. G. Powell, *Org. Geochem.*, 11 (1987) 433.
29 R. Ocampo, H. J. Callot and P. Albrecht, in R. H. Filby and J. F. Branthaver (Editors), *Metal Complexes in Fossil Fuels (ACS Symp. Series* 344), Washington, DC, 1987, pp. 68–73.
30 B. N. Popp, J. M. Hayes and C. J. Boreham, *Org. Geochem.*, submitted for publication.
31 J. W. Louda and E. W. Baker, in R. S. Yeats, B. U. Hag *et al.*, *Initial Reports of the Deep Sea Drilling Project, Vol. LXIII*, U.S. Government Printing Office, Washington, DC, 1981, pp. 785–817.

Journal of Chromatography, 467 (1989) 209–216
Elsevier Science Publishers B.V., Amsterdam — Printed in The Netherlands

CHROM. 21 210

REACTION OF *o*-PHTHALALDEHYDE WITH AMINO ACIDS AND GLUTATHIONE

APPLICATION TO HIGH-PERFORMANCE LIQUID CHROMATOGRAPHY DETERMINATION

GILLES MORINEAU, MICHEL AZOULAY and FRANÇOIS FRAPPIER*
UA-CNRS 484, Faculté de Pharmacie, 4 Avenue de l'Observatoire, 75270 Paris Cedex 06 (France)
(First received September 26th, 1988; revised manuscript received December 9th, 1988)

SUMMARY

Experimental conditions were found for the preparation of stable fluorescent adducts of *o*-phthalaldehyde with glutathione and its metabolites: glutamine, glutamic and aspartic acids, γ-glutamylglutamine and γ-glutamylglutamylglutamine. The structure of the glutathione isoindole derivative obtained was confirmed by NMR studies. The procedure was applied to reversed-phase high-performance liquid chromatographic separation of the previous compounds. The method was extended to glutathione and "total glutathione" determinations.

INTRODUCTION

Recent studies showed that glutamine and glutathione (GSH) metabolism may play an important rôle in the biochemistry of antimalaria[1,2] and anticancer[3] drugs. GSH regulation in normal cells after cytotoxic insult will be very useful in determining therapeutic research. One of the factors which regulate the GSH level in the cell is the availability of the precursor amino acids glutamate and glutamine[4]. In this context, studies carried out in our laboratory called for a specific and sensitive analytical method for characterizing and evaluating GSH in the presence of glutamate, glutamine and their metabolites aspartate and peptides γ-glutamylglutamine and γ-glutamylglutamylglutamine.

High-performance liquid chromatography (HPLC) with fluorescence detection is probably one of the more suitable means for the analysis of biological material since it provides both efficient separation and selective detection. Therefore, we searched for a reaction suitable for precolumn derivatization of thiol and amino acids and isocratic elution which is recommended for precise quantitation and routine analysis.

The reaction of *o*-phthalaldehyde (OPT) and 2-mercaptoethanol (2ME), introduced by Roth[5] for fluorometric detection of α-amino acids, was applied to reversed-phase HPLC with postcolumn[6] and precolumn[7] derivatization. On other hand, OPT was used as a reagent for a fluorometric assay[8,9], and the determination of

0021-9673/89/$03.50

thiols by HPLC with postcolumn derivatization (with OPT and taurine) was reported[10]. In this paper, we demonstrate that GSH and amino acids can be separated using the same precolumn derivatizing procedure and the technique is extended to GSH and "total GSH" determinations.

The mechanism of the reaction of OPT and thiol with primary amines was studied by Simons and Johnson[11]. In this work the structure of the isoindole derivative of GSH obtained is confirmed by NMR spectroscopy.

EXPERIMENTAL

Apparatus

Chromatographic experiments were carried out using Kontron LC14 pumps in combination with a single-valve injector (Model 7125, Rheodyne) and a Kratos Fluoromat FS 950 fluorimeter. (The excitation filter had maximum transmittance at 360 nm and the emission filter a cut-off value at 410 nm.) All separations were monitored on a LiChrosorb RP-18 column (7 μm, 250 mm × 4 mm) (Merck). A low-capacity guard column (Chrompack RP, 10 mm × 3 mm) was connected between the injector and the column. The flow-rate was 1 ml/min.

^{1}H NMR spectra at 270 MHz were obtained on a Brucker HX 270 in ^2H_2O. Chemical shifts are expressed in ppm with the following notations indicating the multiplicity of the signal: s = singlet; d = doublet; t = triplet; q = quartet; m = multiplet. The coupling constants are expressed as J values in Hertz. Two-dimensional correlation spectroscopy yields the connectivities between spins through the scalar couplings. The basic two-pulse Jeener sequence was used[12].

Mass spectra (DCI/NH_3, DCI is desorption chemical conisation) were recorded on a Nermag X1010.

Chemicals and reagents

Chemicals, solvents and reagents were of the highest purity grade available (Prolabo). Water used for the eluent preparation was distilled twice. L-Glutamyl-glutamine and OPT were from Sigma, L-glutamic, L-aspartic acids and glutamine from Janssen, L-glutamyl peptides from Bachem.

Derivatization reagent

The derivatization reagent was obtained by mixing 1 ml of 80 mM OPT solution (54 mg dissolved in 0.5 ml methanol, volume adjusted to 5 ml with 0.1 M NaOH) and 1 ml of 98 mM 2ME solution (35 μl in 5 ml of 0.1 M NaOH).

Standard solutions

Amino acids and peptides were dissolved to 10 mM in water, except for GSH which was dissolved in 0.035 M perchloric acid (pH 1.5) to prevent formation of glutathione disulphide[13].

Derivatization procedure

Aliquots of 50 μl of standard solutions were added to 50 μl derivatization reagent and the final volume was adjusted to 150 μl. After vortexing for 10 s, the mixture was incubated for 2 min and 25 μl were injected for HPLC.

For GSH estimation, 30 μl of standard solution were treated by 50 μl of 40 mM OPT and the final volume adjusted to 150 μl with 0.1 M NaOH.

For total glutathione, an aliquot of the standard solution was preincubated for 2 min with 25 μl of 98 m*M* 2ME and then treated with 25 μl of 80 m*M* OPT.

For UV and fluorescence determinations, amino acids and peptides were treated with a 2000-fold excess of the derivatization reagent prepared in 0.05 *M* borate buffer (pH 12).

For NMR and mass spectra, the samples were prepared as follows: to 4 ml of 10 m*M* GSH or amino acid solution in water were added 0.5 ml of 80 m*M* OPT and 0.4 ml of 98 m*M* of 2ME. After stirring for 30 min at 0°C, the mixture was lyophilized. An aliquot of the product obtained was dissolved in ^2H_2O just before measurement.

Glutamate adduct, **2a.** UV (ethanol): λ_{max} 232, 260 (sh), 338 nm ($\varepsilon = 5.0 \cdot 10^3$ l mol^{-1} cm^{-1}). Fluorescence (borate buffer pH 8 or 12): λ_{ex} 345 nm, λ_{em} 450 nm. ^{1}H NMR: δ 1.92, m, 2H ($2H_{10}$); 2.32, m, 1H (H_9); 2.52, m, 1H (H'_9); 2.65, t, J=6, 2H ($2H_{14}$); 3.45, t, J = 6, 2H ($2H_{13}$); 5.45, dd, J = 10, J' = 4, 1H (H_8); 7.0, m, 2H (H_5, H_6); 7.5, s, 1H (H_3); 7.62, m, 1H (H_4, H_7).

Aspartate adduct, **2b.** UV (ethanol): λ_{max} 231, 260 (sh), 338 nm ($\varepsilon = 3.3 \cdot 10^3$ l mol^{-1} cm^{-1}). Fluorescence (0.05 *M* borate, pH 8 or 12): λ_{ex} 345 nm, λ_{em} 450 nm. ^{1}H NMR: δ 2.7, m, 2H ($2H_{14}$); 3.02, m, 2H ($2H_9$); 3.45, t, J = 6, 2H ($2H_{13}$); 5.8, dd, J = 10, J' = 4, 1H (H_8); 6.95, m, 2H (H_5, H_6); 7.45. s, 1H (H_3); 7.6, m, 2H (H_4, H_7).

Glutathione adduct, **3.** UV (ethanol): λ_{max} 231, 265 (sh), 340 nm ($\varepsilon = 2.7 \cdot 10^3$ l mol^{-1} cm^{-1}). Fluorescence (borate buffer pH 8 or 12): λ_{ex} 355 nm, λ_{em} 430 nm. ^{1}H NMR: δ 1.9, m, 1H (H_{10}); 2.36–2.6, m, 3H (H_{10}, $2H_9$); 2.87, dd, J = 15, J' = 12, 1H (H_{14}); 3.2, dd, J = 15, J' = 3.5, 1H (H_{13}); 3.52, q, J = 17, 2H ($2H_{17}$); 4.77, dd, J = 12, J' = 3, 1H (H_{13}); 5.4, dd, J = 13, J' = 5, 1H (H_8); 7.0, m, 2H (H_5, H_6); 7.5, s, 1H (H_3); 7.6, m, 2H (H_4, H_7). Mass spectrum (DCI/NH_3, *m/z* and relative intensity): 406 (M+1, 9); 392(6), 362(5), 180(14), 152(19), 134(37), 118(27), 101(20), 78(27), 70(100).

Glutathione. ^{1}H NMR (^2H_2O): δ 2.0, m, 2H ($2H_{10}$); 2.37, m, 2H ($2H_9$); 2.77, dd, 1H (H_{14}); 3.11, dd, 1H (H'_{14}); 3.63, t, 1H (H_8); 3.77, s, 2H ($2H_{17}$); 4.55, m, 1H (H_{13}).

RESULTS

OPT in the presence of 2ME has been reported to react with primary amines and amino acids to give fluorescent 1-alkylthio-2-alkyl substituted isoindoles[11]. The parameters which affect the fluorescence properties of isoindole have been examined[14]. Using borate buffer (pH 9.5), the procedure was applied to precolumn derivatization of amino acids and to the separation of isoindole derivatives by reversed-phase HPLC[7].

On other hand, OPT was reported to react with thiols, and glutathione was assayed by the reaction with excess of OPT at room temperature in pH 8 buffer[8]. Fluorometric determination of thiols by anion-exchange chromatography with postcolumn derivatization with OPT and taurine at pH 10 was described[10].

Structure of fluorescent adducts

The structure of the fluorescent product obtained in the reaction of OPT and a thiol with primary amine has been determined[11]. Compared to the results cited above, the UV, fluorescence and ^{1}H NMR spectral data (*cf.*, Experimental section) obtained from the isolated OPT and 2ME adducts of glutamate and aspartate established the isoindole ring structures **2a** and **2b** (Fig. 1).

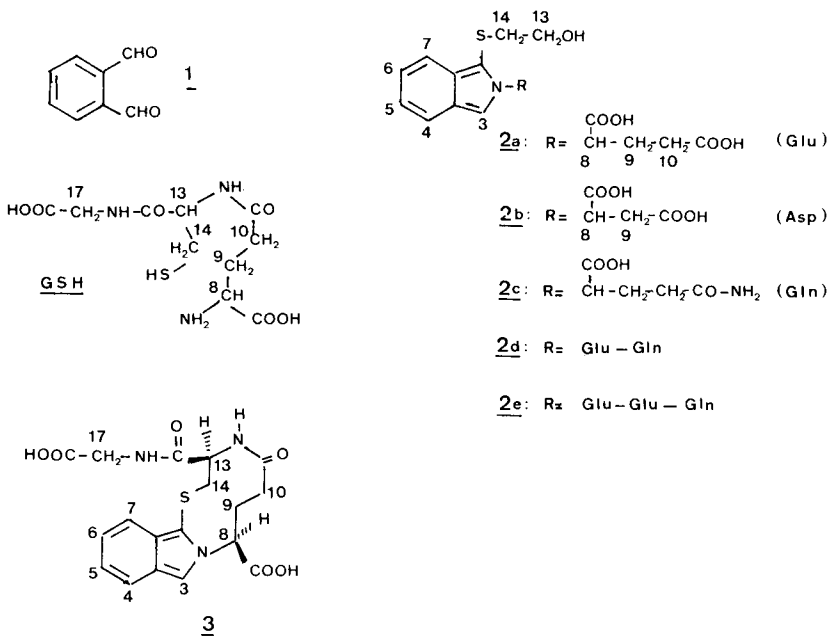

Fig. 1. Structure of *o*-phthalaldehyde (OPT) (**1**), amino acids (**2**) and glutathione (**3**) derivatives.

The similarity of the reaction conditions and the spectral properties of the product formed to those of the isoindoles suggests that the fluorescent OPT-GSH derivative is an isoindole where GSH supplies the thiol and amine functional groups[14]. We succeeded in isolating this compound and confirmed on the basis of spectroscopic data the structure **3**. The fluorescence (λ_{ex} 345 nm, λ_{em} 450 nm) and UV spectra (λ_{max} 231, 340 nm) were characteristic of the isoindole ring system[11]. Support for this structure was provided by ^{1}H NMR studies: the aromatic region displayed a 2:1:2 proton pattern as previously reported[11]: peaks at δ 7.62 (m, 2H); 7.5 (s, 1H), 7.0 (m, 2H). The signals corresponding to the protons of alkyl substituents were assigned by comparison with the spectrum of GSH (see Experimental section). The deshielding of the H_8 of glutamate observed (δ 5.4, dd) can be attributed to the aromatic ring current in the isoindole[11].

To obtain complete information about chemical shifts and proton–proton coupling, a two-dimensional correlation spectroscopy (COSY) experiment was done (Fig. 2). This confirmed the assignment of the various signals, the coupling between protons H_8 and H_9 of glutamate (δ 2.36–2.60, m, 2H) and the inequivalence of the two protons H_{17},H_{17}', of glycine (δ 3.52, q).

Furthermore, the structure was confirmed by the CI mass spectrum of **3** which showed peak at m/z = 406 corresponding to the molecular weight (M+1). Complementary studies will be necessary to determine the structure of the fragment ions observed.

Determination of conditions for fluorescence derivatization

As previously described[14], the initial fluorescence intensity of the amino

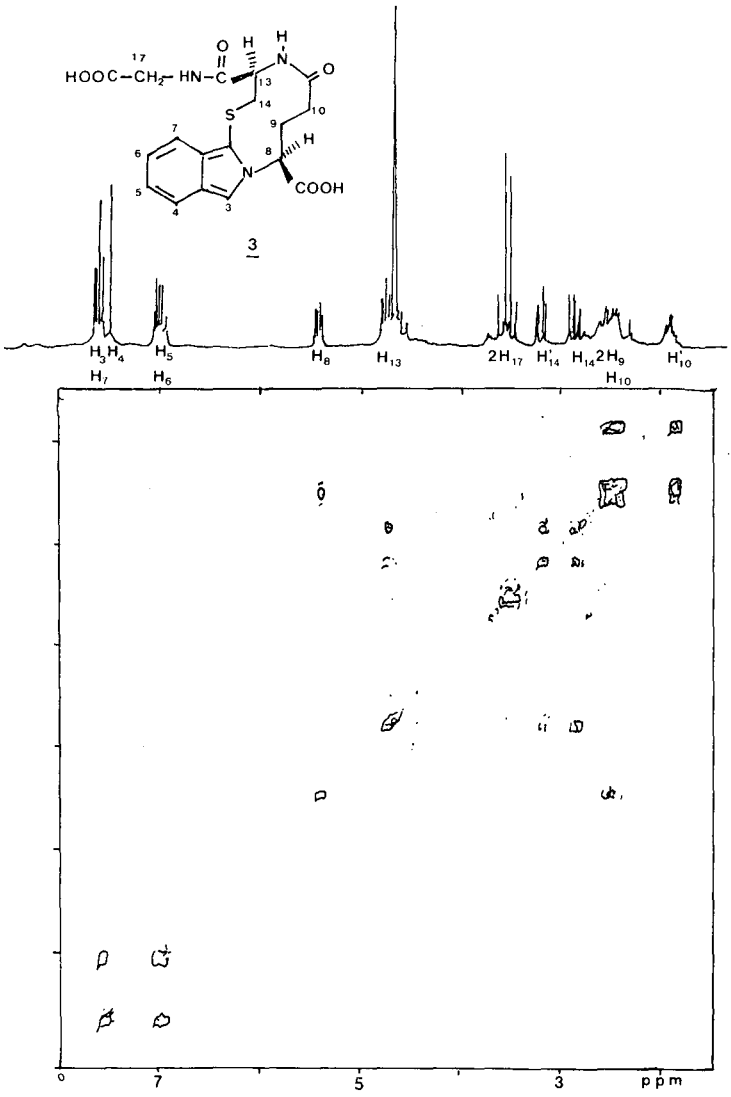

Fig. 2. Two-dimensional correlation spectrum for the OPT glutathione derivative in ^2H_2O. See Experimental section for detailed ^1H NMR data.

acid-OPT adduct **2** is relatively pH insensitive. However, the stability of these products is pH dependent: at pH 12, **2** was stable up to 30 min, but at pH 8 a 20–30% decrease of the fluorescence intensity was observed. In contrast, the stability of the GSH adduct, **3**, was unaffected by pH: the fluorescence intensity remained quite constant, for more than 30 min, either at pH 8 or 12. So, we chose to carry out the derivatization reaction at pH 12.

Addition of 1 equiv. of amino acid or peptide to an equimolar amount of OPT and 2ME yielded quantitatively, after 10 min, the adduct. In the presence of a 200-fold excess of the reagent the reaction was complete instantaneously (< 1 min). Using these

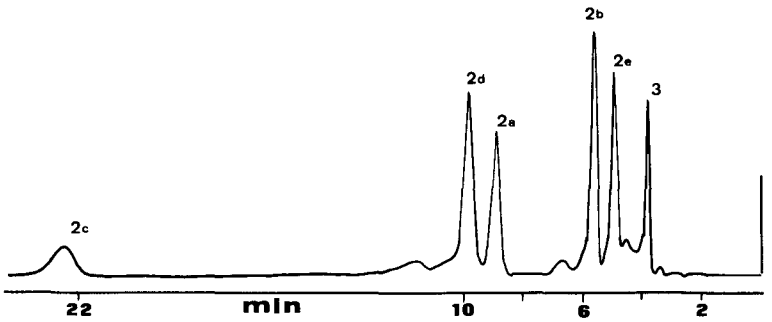

Fig. 3. Chromatogram showing the separation of glutathione (**3**), γ-glu-glh-gln (**2e**), aspartate (**2b**), glutamate (**2a**), γ-glu-gln (**2d**) and glutamine (**2c**). See Experimental section for column and mobile phase conditions.

conditions, we checked that the fluorescence response of the glutamic acid derivative was linear up to 20 μM, and unaffected by GSH. The fluorescence intensity due to the isoindole structure of the GSH derivative is not affected by 2ME.

So, the following experimental conditions for derivatization were chosen: in a final volume of 150 μl, mixed solutions of amino acids, peptides and GSH were added to 50 μl of 0.1 M NaOH containing 40 mM OPT and 50 mM 2ME. The mixture was vortexed (10 s) and, after 2 min, used for HPLC analysis.

Optimization of separation

Derivatized amino acids and peptides **2**, **3** were separated on a reversed-phase column using an isocratic system of acetonitrile and sodium acetate solution.

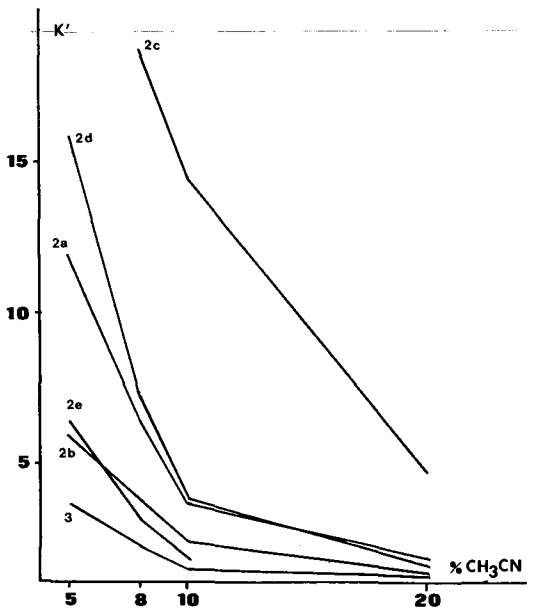

Fig. 4. The effect of the acetonitrile concentration on the capacity factors. The mobile phase contains various levels of acetonitrile in 0.3 M sodium acetate, pH 7.4. Compound numbers as in Fig. 1.

Optimization of the separation was obtained after studying the effect of the nature and the concentration of the ionic medium, the pH and the acetonitrile concentration. The mobile phase conditions leading to the best separation (Fig. 3) were: 0.3 *M* sodium acetate (pH 7.4) containing 8% acetonitrile. The criteria were the resolution, stability of the fluorescence intensity and the analysis speed. As shown in Fig. 4, the capacity factors of all derivatives decreased with acetonitrile concentration, and a change in the acetonitrile percentage in the mobile phase can be advantageous for studying a mixture without glutamine.

Glutathione estimation

The technique described has been applied to the estimation of GSH. The isoindole derivative of GSH was obtained after OPT treatment of standard solutions prepared in perchloric acid to prevent oxidation of GSH to disulphide (GSSG). The calibration graph, defined by a least squares linear regression of standard concentrations *versus* the peak height, was linear over the range 5–250 p*M* (correlation coefficient 0.999, slope 0.2522, *y* intercept −0.0253). The detection limit was estimated to be 0.1 p*M* using a signal-to-noise ratio of 5. The repeatability of fluorescence intensity was evaluated by injecting consecutively seven times a standard solution containing 165 p*M* of GSH: the coefficient of variation obtained was 0.040.

The method has been extended to the evaluation of "total glutathione" comprising GSH and GSSG. 2ME was added to a test solution of GSSG, which was rapidly and totally converted into GSH. After 2 min, OPT was added and the derivative obtained subjected to HPLC analysis: a fluorescence intensity corresponding to 2 equivalents of GSH was observed.

GSSG reduction by 2ME and derivatization by OPT gave a linear response in the HPLC analysis over a range of 2.5 to 37.5 p*M* (correlation coefficient 0.999, slope 0.2474, *y* intercept 0.013). The two lines corresponding to GSH and GSSG [expressed as 2(GSH)] estimations are identical.

DISCUSSION

Our data demonstrate that GSH, amino acids (glutamic, aspartic acids, glutamine) and peptides (γ-glutamylglutamine and γ-glutamylglutamylglutamine) can be separated by reversed-phase HPLC using the same precolumn derivatizing procedure. This technique may be extended to the separation of GSH and other amino acids, for example the precursors cysteine, glycine and the intermediate biosynthetic dipeptide, γ-glutamylcysteine.

In cells, oxidation of GSH leads to the formation of GSSG and intracellular GSH is maintained in the reduced state by GSSG reductase linked to the NADPH–NADP system. The method described is applicable to the estimation of GSH and "total glutathione" comprising GSH and GSSG. The sensitivity (0.1 p*M* detected) allows the detection of picomole quantities of GSH.

Furthermore using two successive determinations, the first one after preincubation of the sample in the presence of 2ME and the second one after treatment with a mixture of 2ME and OPT, it is possible to evaluate the glutathione present as GSSG according to:

$$(\text{GSSG}) = \frac{(\text{total glutathione}) - (\text{GSH})}{2}$$

REFERENCES

1 Y. Zhang, E. Hempelmann and R. Heiner Schirmer, *Biochem. Pharmacol.*, 37 (1988) 855–860.
2 B. C. Elford, *Parasitology Today*, 2 (1986) 309–312.
3 C. R. Wolf, A. D. Lewis, J. Carmichael, D. J. Adams, S. G. Allan and D. J. Ansell, *Biochem. Soc. Trans.*, 15 (1987) 728–730.
4 S. Bannai and N. Tateishi, *J. Membrane Biol.* 89 (1986) 1–8.
5 M. Roth, *Anal. Chem.*, 43 (1971) 880–882.
6 J. R. Benson and P. E. Hare, *Proc. Natl. Acad. Sci. U.S.A.*, 72 (1975) 619–622.
7 P. Lindroth and K. Mopper, *Anal. Chem.*, 51 (1979) 1667–1674.
8 V. H. Cohn and J. Lyle, *Anal. Biochem.*, 14 (1966) 434–440.
9 P J. Hissin and R. Hilf, *Anal. Biochem.*, 74 (1976) 214–226.
10 H. Nakamura and Z. Tamura, *Anal. Chem.*, 53 (1981) 2190–2193.
11 S. S. Simons and D. F. Johnson, *J. Org. Chem.*, 43 (1978) 2886–2891.
12 J. Jeener, *Ampere International Summer School II, Basko Pelje*, 1971.
13 T. P. M. Akerboom and H. Sies, *Methods Enzymol.*, 77 (1981) 373–382.
14 S. S. Simons and D. F. Johnson, *Anal. Biochem.*, 90 (1978) 705–725.

Journal of Chromatography, 467 (1989) 217–226
Elsevier Science Publishers B.V., Amsterdam — Printed in The Netherlands

CHROM. 21 225

SIZE-EXCLUSION CHROMATOGRAPHY OF DNA RESTRICTION FRAGMENTS

FRAGMENT LENGTH DETERMINATIONS AND A COMPARISON WITH THE BEHAVIOUR OF PROTEINS IN SIZE-EXCLUSION CHROMATOGRAPHY

HANS ELLEGREN*,[a] and TORGNY LÅÅS
Pharmacia LKB Biotechnology, S-751 82 Uppsala (Sweden)
(First received September 9th, 1988; revised manuscript received December 23rd, 1988)

SUMMARY

Size-exclusion chromatography of double-stranded DNA restriction fragments on Superose 6® is shown to be an accurate method for chain length determination of unknown DNA. Ionic interaction was observed between DNA and the gel matrix but was easily prevented by the addition of 0.15–0.2 *M* sodium chloride to the eluent. Compared to protein, the selectivity curve of DNA fragments was found to be steeper reflecting the different chromatographic behaviour of rod-like and globular molecules. The relationships between the selectivity curves of DNA and protein were similar on Superose 6 and on Sephacryl® S-500.

INTRODUCTION

Size-exclusion chromatography (SEC) or gel filtration (SEC in aqueous phase) of DNA is widely used in molecular biology laboratories both in low-pressure[1–4] and in high-pressure liquid chromatographic systems[5–7]. Although generally offering lower resolution than ion exchange (IEC) and reversed-phase chromatography (RPC), SEC offers other advantages: easy instrumentation, isocratic elution, great freedom of buffer choice and elution in strict order of size. Up to now, applications of SEC in DNA research include the purification of, *e.g.*, vectors and linkers[8,9], restriction fragments[7,10–13], plasmids[4,14], RNA–DNA hybrids[15] and mitochondrial DNA[16]. The general use of SEC and other chromatographic techniques in molecular biology has been reviewed several times[17–24].

Due to the fact that DNA fragments in SEC are eluted in a strict order according to size, we have investigated the potential of SEC for DNA size determinations on Superose 6®, an agarose-based matrix. Since size determination requires constant and ideal size exclusion conditions, the effect of ionic strength was evaluated. We also

[a] Present address: Department of Animal Breeding and Genetics, Swedish University of Agricultural Sciences, Biomedical Centre, Box 596, S-751 24 Uppsala, Sweden.

0021-9673/89/$03.50

wanted to explore in some detail the elution behaviour of DNA during SEC. To be able to discriminate between solute effects and support effects we chose two chromatography media (Superose 6 and Sephacryl® S-500) with similar overall separation properties but with completely different chemical compositions. We compared the elution behaviour of proteins and DNA on the two gels.

EXPERIMENTAL

DNA preparation

pBR 322 DNA and restriction endonucleases HaeIII and HinfI were supplied by Pharmacia LKB Biotechnology (unless otherwise stated, all chemicals and equipment were from this source). DNA was digested essentially according to the supplier's instruction (50 m*M* Tris–HCl pH 7.6 with 10 m*M* $MgSO_4$ and 1 m*M* dithiothreitol at 37°C for 3 h using a ratio of three units of endonuclease to 1 μg DNA). The mixture obtained by the HaeIII digestion contained fragments of 587, 540, 504, 458, 434, 267, 234, 213, 192, 184, 124, 123, 104, 89, 80, 64, 57, 51, 21, 18, 11 and 7 base pairs (bps). The HinfI digestion yielded fragments of 1631, 517, 506, 396, 344, 298, 221, 220, 154 and 75 bps.

The fragments were separated on Mono Q™ HR 5/5 (column dimensions 50 mm × 5 mm) anion-exchange media. Twentyseven out of the 32 fragments were purified to baseline separation with a linear gradient from 0.65 (buffer A) to 0.78 *M* (buffer B) salt (gradient slope 6.5 m*M* NaCl per ml buffer in 20 m*M* Tris–HCl pH 7.6)[25]. DNA fractions were precipitated with ethanol and analysed for purity by polyacrylamide gradient gel electrophoresis.

Chromatography

Separations were performed with a complete fast protein liquid chromatography (FPLC)® system (Pump P500, liquid chromatography controller LCC 500, UV monitor UV-M, recorder REC-482 and fraction collector Frac 100) with detection at 254 and 280 nm for DNA and proteins respectively. Size-exclusion chromatography was carried out on Superose 6 with 106 mm × 10 mm or 300 mm × 10 mm (prepacked Superose 6 HR 10/30) columns and on Sephacryl S-500 Superfine with a 89 mm × 10 mm column. Superose 6 consists of 13-μm particles derived from 6% cross-linked agarose[26,27], while Sephacryl is allyl dextran covalently cross-linked with N,N′-methylenebisacrylamide. The standard eluent was 20 m*M* Tris–HCl pH 7.6 containing 0.15 *M* sodium chloride.

Purified DNA restriction fragments (0.2–1.0 μg/ml) were typically chromatographed two or three at a time, at ambient temperature (*ca.* 24°C) with a flow-rate of 0.35 ml/min and a sample volume of 100 μl. The same conditions were used for protein (3 mg/ml) separations. The molecular weights of the proteins were in the range of 6500 to 669 000 (Pharmacia LMW and HMW calibration kits and from Sigma). When studying the effect of the ionic strength on the elution volume, the salt concentration was varied between 0 and 5 *M*.

Partition in the size-exclusion bed is expressed by the K_{av} value of a solute[28]

$$K_{av} = V_e - V_o/V_c - V_o \quad (1)$$

where V_e is the elution volume, V_0 is the void volume and V_c is the geometrical column volume. The void volume was measured with Blue Dextran 2000 for Superose 6 and with large bacteria (*Serratia*) for Sephacryl S-500.

RESULTS AND DISCUSSION

General chromatographic behaviour on Superose 6

Of the fragments studied only the largest (1631 bps) fragment was eluted in the void volume. From the calibration graph given in Fig. 1 the exclusion limit can be estimated to be $\approx$ 600 bps. A typical chromatogram is shown in Fig. 2.

One of the purposes of this study was to evaluate the suitability of the gel for molecular weight determinations of DNA restriction fragments. In an ideal gel filtration process the solute should not interact with the gel matrix. As an agarose-based medium, Superose 6 inherently contains small amounts of sulphate esters and carboxylic groups. In principle, there are two main types of possible interactions between a slightly charged solute and an agarose matrix. At low ionic strength, repulsive (in the case of negatively charged molecules such as DNA) or attractive (positively charged molecules) ionic forces may lead to decreased or to increased elution volumes, respectively. At high ionic strength the hydrophobic interaction increases and may be strong enough to cause delayed elution. In addition, the ionic strength may affect the size and shape of the solute.

To investigate the effect of ionic interactions we determined K_{av} values of DNA at different ionic strengths. At low ionic strengths the elution volumes decreased (lower K_{av} values) as predicted (Fig. 3). To avoid ionic interactions the addition of 0.15–0.20 *M* sodium chloride to the buffer solution seems appropriate. At higher ionic strengths the elution volumes tend to become more constant, an observation in agreement with studies made on other types of resins, *e.g.*, silica-based media[5]. This indicates that the hydrophobic interaction between DNA fragments and different matrices is very low even at an high ionic strength. The absence of marked hydrophobic interaction can be explained by the extremely hydrophilic nature of the DNA fragments since they are strong polyanions with a thick hydration shell protecting them from hydrophobic contacts with the gel[24].

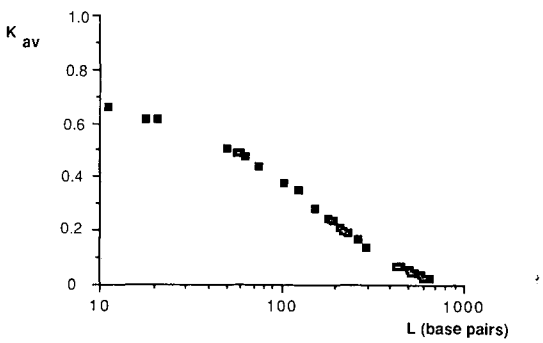

Fig. 1. Selectivity curve derived from SEC of DNA restriction fragments on Superose 6. DNA fragments were derived from a HaeIII/pBR 322 digest (and purified on a Mono Q anion-exchange column) and gel filtration was performed on a 106 mm × 10 mm column with 0.02 *M* Tris–HCl pH 7.6 containing 0.15 *M* sodium chloride as the eluent.

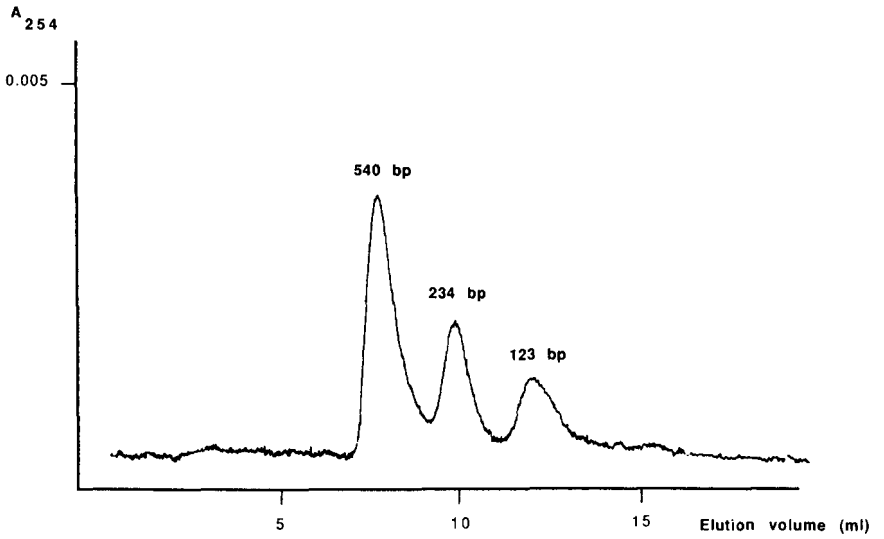

Fig. 2. Size-exclusion chromatography of three DNA restriction fragments on Superose 6. Conditions as described in Fig. 1.

Calibration graphs

When the logarithm of fragment length in base pairs was plotted against K_{av} for each purified fragment in the pBR 322/HaeIII digest a sigmoidal curve was obtained (Fig. 1). In the range of 60 to 450 base pairs the relationship was approximately linear. Using regression analysis in this linear region (K_{av} 0.05–0.5), the fragment length can be expressed as a function of K_{av}:

$$L = 2.7623 - 1.9861\ K_{av} \quad (2)$$

where L is the DNA fragment length as expressed by the logarithm of the number of base pairs and K_{av} is defined as in eqn. 1.

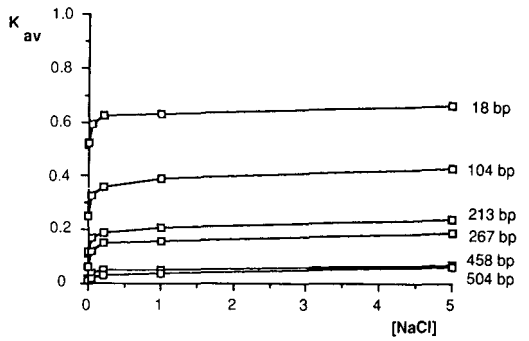

Fig. 3. Relationship between K_{av} and the amount of sodium chloride (M) added in the eluent (0.02 M Tris–HCl pH 7.6) in SEC of six DNA restriction fragments on Superose 6.

Interestingly, nearly every point in the calibation plot made a perfect fit to the line given by eqn. 2 ($r = 0.998$). This suggests SEC as a more accurate method for determination of the length of restriction fragments than IEC and RPC where the elution position is influenced by the base composition of the DNA[24,29,30]. To test the accuracy by which such determinations can be performed, we chromatographed another set of fragments originating from the pBR 322/HinfI digest. The K_{av} values for fragments of suitable lengths were applied to eqn.1 and the results are shown in Table I. It can be concluded that for the 75, 154, 220/221 and the 298 bp fragments, the estimated lengths differed by less than 4% from the true length.

Given this accuracy, it is obvious that gel filtration may be a useful alternative to gel electrophoresis for fragment length determinations. In fact, chromatography has some distinct advantages as compared to electrophoresis:

(1) Once the column is calibrated there is no further need for molecular weight markers.

(2) Accurate fragment length determinations can be completed within 30 min.

(3) While the base composition has been demonstrated to influence the migration velocity of DNA in gel electrophoresis[31], there is no demonstrable effect in SEC.

(4) Preparative SEC is a very harmless method while agarose electrophoresis has a serious drawback for preparative purposes in that the purified DNA is often contaminated with agarose impurities having enzyme-inhibiting properties.

It should be noted that the restriction fragments we used represented both fragments with blunt ends (the HaeIII digest) and fragments with 5′ overhang (the HinfI digest). In the molecular size range studied, this difference did not affect the chromatographic behaviour in contrast to the behaviour in RPC[32].

There are several reports of unexpected delayed elution of A/T-rich DNA fragments in IEC and RPC[24,29,30,33]. Two explanations have been suggested: (1) A/T-rich regions are less rigid (anomalous bending) and can therefore make more intimate contact with the matrix strengthening the interaction[24], and (2) the binding of counter ions depends on the bases[33]. Hypothesis 1 suggests that the hydrodynamic radius and hence K_{av} should depend on the base composition. When analysing the A/T

TABLE I

CHAIN LENGTH DETERMINATION OF DNA RESTRICTION FRAGMENTS ON A CALIBRATED SUPEROSE 6 COLUMN

The column was calibrated with DNA fragments originating from a HaeIII/pBR 322 digest. In the linear part of the selectivity curve derived with these fragments, the relationship between,the fragment length and K_{av} was as in eqn. 2. Applying K_{av} data from a HinfI/pBR 322 digest to this relationship, fragment length estimates were obtained.

Actual length (bps)	*Estimate (bps)*
75	77
154	157
220/221	230
298	309
506	452
517	471

content of the fragments used in this study we did not observe any tendency for A/T-rich fragments to differ from expected K_{av} values, *i.e.*, fall outside the selectivity curve. Either the hypothesis is wrong or the effect of the different stiffness on interaction in IEC and RPC is greater than its effect in SEC since it is manifested through different mechanisms.

Evaluation of DNA and protein selectivity curves

In Fig. 4 the K_{av} values for both DNA fragments and proteins derived from Superose 6 have been plotted against the logarithm of the molecular weight. The molecular weights of the DNA fragments were calculated with an average value of 660 daltons per base pair. Examining Fig. 4, there are two features that differentiate the selectivity curves for the two types of macromolecules. First, the selectivity curve for the DNA fragments is much steeper than the curve established with standard proteins (the slopes of the DNA and the protein selectivity curves are -0.50 and -0.16 respectively). Secondly, while the selectivity curve for protein is linear up to a K_{av} value of 0.8, the shape of the selectivity curve for DNA fragments bends at a K_{av} value of approximately 0.5. We suggest that, at least partly, both these differences can be explained by the structures of the two macromolecules, proteins being roughly globular and larger DNA fragments being rod-like molecules. We will discuss the two differences separately.

Slope of the selectivity curves. It is well known that retention in SEC is strongly dependent on the shape of the solute as well as the size (see for example, refs. 28, 34 and 35). It has been demonstrated that the parameter governing the retention in SEC is the hydrodynamic volume of the solute. The molecular weight of a solute is related to the radius of gyration

$$R_g = kM^a \tag{3}$$

with $a = 1$ for rods, *ca.* 0.5 for flexible coils and 0.3 for spheres[36]. From this equation it follows that the gyration radius, R_g, (and the hydrodynamic volume) increases more rapidly with mass for rods (DNA) than for spheres (proteins). It can therefore be predicted to obtain a steeper selectivity curve for rod-like DNA than for proteins[28,36], in fact exactly as observed (Fig. 4).

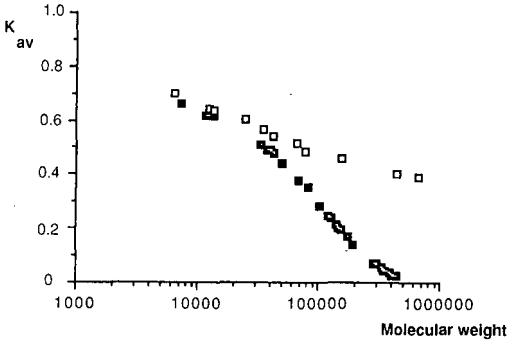

Fig. 4. Selectivity curve derived from SEC of DNA restriction fragments (■) and standard proteins (□) on Superose 6. Conditions as described in Fig. 1.

In practice this means that, with SEC, molecular weight (MW) values can be more accurately determined for DNA than for proteins since a small change in the molecular weight of DNA has a greater effect on the elution volume (K_{av}).

Shape of the selectivity curves. The linear region of the selectivity curve for DNA extends only between K_{av} of 0.1 and 0.5, in contrast to the curve for proteins which is linear at least from $K_{av} = 0.1$ to 0.8. We suggest that this relatively short linear region of the DNA curve also reflects the shape of the DNA molecules. Double-stranded DNA has a diameter of 20 Å with each base pair adding 3.4 Å in length. $K_{av} = 0.5$ where the bending of the DNA curve begins, corresponds to a molecular weight of *ca.* 12000 or 18 base pairs. This molecule has the dimensions 20 × 60 Å, that is an axial ratio of 1 to 3. Obviously such a molecule is no longer a perfect rod and still smaller DNA fragments will be even closer to a spherical form. Consequently and according to the above discussion, the slope of the part of the selectivity curve for small DNA fragments will differ from the part for longer fragments. This should explain why the slopes of the selectivity curves for DNA and proteins tend to merge in the low-molecular-weight range.

On the other hand, fragments longer than the persistence length (for DNA, approximately 150 bps) will behave more and more like flexible coils. According to eqn. 3 the slope of a selectivity curve for very large DNA molecules should therefore approach a value intermediate between that of proteins and that of moderately sized, rod-like DNA molecules. Unfortunately the separation range of Superose 6 is too small for this phenomenon to be seen.

Relationship between selectivity curves for DNA and proteins

On the basis of the parameter K_{av} we have calculated the empirical relationship between the selectivity curve for proteins and the linear part of the selectivity curve for DNA fragments on Superose 6. In this way the molecular weight of a DNA fragment, MW_{DNA}, can be expressed as a function of a protein molecular weight

$$MW_{DNA} = 101.2\ MW_{prot}^{0.495} \quad (4)$$

and the protein molecular weight, MW_{prot}, is then the molecular weight giving the same K_{av} value as a DNA fragment. This relationship should be useful for molecular weight estimates of DNA fragments on Superose 6 columns calibrated with proteins.

Comparison of Superose 6 and Sephacryl S-500

To investigate whether the relationship between the separation behaviour of DNA and proteins (as expressed in eqn. 4) is specific for the separation media, we separated suitable test proteins and DNA fragments also on Sephacryl S-500 (Fig. 5). Disregarding the fact that the fractionation ranges do not overlap exactly, it is obvious that the general picture is the same.

To test the applicability of eqn. 4 on Sephacryl S-500, the elution positions of some of the proteins in Fig. 5 were taken as elution positions for hypothetical DNA fragments given molecular weights calculated with eqn. 4. The resulting K_{av} values were plotted together with the experimentally determined values of the real DNA fragments (Fig. 6). The values calculated by eqn. 4, which was derived using Superose 6, agree very well with the experimental results on Sephacryl S-500. Hence these results indicate that the relationship between the separations of DNA fragments and proteins

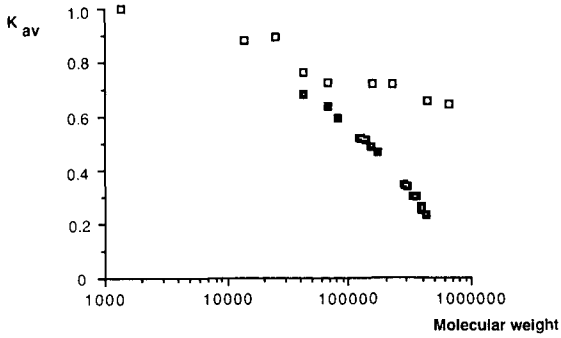

Fig. 5. Selectivity curve derived from SEC of DNA restriction fragments (■) and standard proteins (□) on Sephacryl S-500. Column dimensions: 89 mm × 10 mm. Other conditions as described in Fig. 1.

is governed by the properties of the solutes rather than by the chromatographic support. It should be emphasized, however, that eqn. 4 is applicable only in the region where DNA can be regarded as rods.

CONCLUSIONS

We have found that at low ionic strengths the elution volumes of DNA fragments on Superose 6 decrease. This indicates repulsion between the slightly negatively charged matrix and the DNA. To suppress ionic interaction, 0.15–0.20 *M* sodium chloride should be added to the buffer. Hydrophobic interactions seem to play little rôle in SEC of DNA on this support. Up to 5 *M* sodium chloride was added without significant effect on the elution behaviour. It is also shown that fragment length determinations can accurately be performed on Superose 6.

Furthermore, we have found that there is a span in molecular size where a linear relationship exists between K_{av} and log molecular weight of the DNA. It is suggested that this span reflects the size region where DNA fragments can be regarded as perfect rods. A less steep slope of the selectivity curve was observed in the low-molecular-

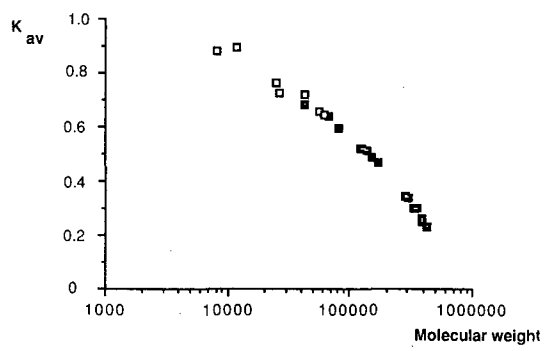

Fig. 6. Selectivity curve derived from SEC of DNA restriction fragments (■) on Sephacryl S-500. White dots (□) indicate transformed protein values according to the empirical relationship between proteins and DNA fragments established on Superose 6 and given in eqn. 4. For further details about this relationship, see text. Conditions as described in Figs. 1 and 4.

weight region where the hydrodynamic behaviour of shorter fragment approaches that of spheres. Consequently, the slope of this part of the DNA selectivity curve was similar to that of the protein selectivity curve.

An empirical relationship (eqn. 4) was derived that relates K_{av} for DNA and proteins on gel filtration media. Columns for fragment length determinations can therefore be calibrated with protein standards.

ACKNOWLEDGEMENTS

We thank Bengt Österlund for linguistic revision and Lars Hagel for valuable comments.

REFERENCES

1 A.I. Suominen, M. T. Karp and P. I. Mäntsälä, *Biochem. Int.*, 8 (1984) 209–215.
2 G. Sofer, C. Seitz and M. Lasky, *Am. Biotech. Lab.*, 2 (1984) 38–40.
3 M. Gottlieb, M. Chavko and L. Pivec, *Biologia*, 39 (1984) 807–812.
4 J. Gomez-Marques, M. Freire and F. Segade, *Gene*, 54 (1987) 255–259.
5 Y. Kato, M. Sasaki, T. Hashimoto, T. Murotsu, S. Fukushige and K. Matsubara, *J. Chromatogr.*, 266 (1983) 341–349.
6 Y. Kato, Y. Yamasaki, T. Hashimoto, T. Murotsu, S. Fukushige and K. Matsubara, *J. Chromatogr.*, 320 (1985) 440–444.
7 J.-M. Schmitter, Y. Mechulam, G. Fayat and M. Anselme, *J. Chromatogr.*, 378 (1986) 462–466.
8 M. E. Himmel, P. J. Perna and M. W. McDonell, *J. Chromatogr.*, 240 (1982) 155–163.
9 R. Dornburg, P.Földi and P. H. Hofschneider, *J. Chromatogr.*, 296 (1984) 379–385.
10 Y. Kato, M. Sasaki, T. Hashimoto, T. Murotsu, S. Fukushige and K. Matsubara, *J. Biochem.*, (Tokyo), 95 (1984) 83–86.
11 J. Kruppa, L. Graeve, A. Bauche and P. Földi, *LC · GC, Liq. Chromatogr. Gas Chromatogr. Mag.*, 2 (1984) 848–853.
12 R. Dornburg, J. Kruppa and P. Földi, *LC · GC, Liq. Chromatogr. Gas Chromatogr. Mag.*, 4 (1986) 22–29.
13 B. E. Boyes, D. G. Walker and P. L. McGeer, *Anal. Biochem.*, 170 (1988) 127–134.
14 N. Moreau, X. Tabary and F. Le Goffic, *Anal. Biochem.*, 166 (1987) 188–193.
15 H. Persson, M. Perricaudet, A. Tolun, L. Philipson and U. Pettersson, *J. Biol. Chem.*, 254 (1979) 7999–8003.
16 B. Chatterjee, B. Rao and G. R. Koteswara, *Indian J. Biochem. Biophys.*, 21 (1984) 378–380.
17 R. D. Wells, *J. Chromatogr.*, 336 (1984) 3–14.
18 R. C. Simpson, in P. R. Brown (Editor), *HPLC in Nucleic Acid Research*, Marcel Dekker, New York, 1984, pp. 181–193.
19 J. A. Thompson, *BioChromatography*, 1 (1986) 16–19.
20 G. Zon and J. A. Thompson, *BioChromatography*, 1 (1986) 22–31.
21 J. A. Thompson, *BioChromatography*, 1 (1986) 68–80.
22 J. A. Thompson, *BioChromatography*, 2 (1987) 4–18.
23 J. A. Thompson, *BioChromatography*, 2 (1987) 68–79.
24 R. Hecker and D. Riesner, *J. Chromatogr.*, 418 (1987) 97–114.
25 E. Westman, S. Eriksson, T. Låås, P-Å. Pernemalm and S-E. Sköld, *Anal. Biochem.*, 166 (1987) 158–171.
26 L. Hagel and T. Andersson, *J. Chromatogr.*, 285 (1984) 295–306.
27 T. Andersson, M. Carlson, L. Hagel, P-Å. Pernemalm and J.-C. Jansson, *J. Chromatogr.*, 326 (1985) 33–44.
28 L. Hagel, in L. Ryden and J-C. Jansson (Editors), *High Resolution Protein Purification*, Verlag Chemie, Deerfield Beach. FL. 1988, Ch. 3.
29 R. K. Patient, S. C. Hardies, R. B. Inman and J. E. Larsson, *Fed. Proc. Fed. Am. Soc. Exp. Biol.*, 37 (1978) 1499.
30 R. K. Patient, S. C. Hardies and R. D. Wells, *J. Biol. Chem.*, 254 (1979) 5548–5554.

31 N. C. Stellwagen, *Biochemistry*, 22 (1983) 6186–6193.
32 S. C. Hardies and R. D. Wells, *Proc. Natl. Acad. Sci. U.S.A.*, 73 (1976) 3117–3121.
33 W. Müller, *Eur. J. Biochem.*, 155 (1986) 203–212.
34 M. Potschka, *Anal. Biochem.*, 162 (1987) 47–64.
35 M. le Maire, A. Ghazi, J. V. Moller and L. P. Aggerbeck, *Biochem J.*, 243 (1987) 399–404.
36 W. W. Yau and D. D. Bly, *ACS Symp. Ser.*, (1980) 197.

Journal of Chromatography, 467 (1989) 227–235
Elsevier Science Publishers B.V., Amsterdam — Printed in The Netherlands

CHROM. 21 249

HEADSPACE GAS CHROMATOGRAPHY OF STIMULANTS IN URINE BY IN-COLUMN TRIFLUOROACETYL DERIVATIZATION METHOD

HITOSHI TSUCHIHASHI*, KUNIO NAKAJIMA and MAYUMI NISHIKAWA
Forensic Science Laboratory, Osaka Prefectural Police Head Quarters, 9, Otemaeno-cho, Higashi-ku, Osaka 540 (Japan)
and
KOICHI SHIOMI and SEIJI TAKAHASHI
Analytical Applications Laboratory, Shimadzu Corporation, Nishinokyo, Kuwabara-cho, Nakagyo-ku, Kyoto 604 (Japan)
(First received July 6th, 1988; revised manuscript received January 2nd, 1989)

SUMMARY

The analysis of stimulants in urine using a headspace gas chromatography system equipped with an in-column sample trifluoroacetylation unit was investigated. A 5-ml aliquot of urine containing stimulants was pipetted into a 20-ml autosampler vial together with 3.5 g of potassium carbonate. The vial was sealed and heated for 20 min at 80°C, then 0.8 ml of the headspace gas and N-methylbis(trifluoroacetamide) gas were injected simultaneously into the gas chromatograph equipped with a flame ionization detector and a fused-silica capillary column (DB-1, 30 m × 0.32 mm I.D., film thickness 0.25 μm), with a gas-tight syringe. Calibration graphs prepared by the absolute calibration curve method showed good linearity over the concentration range of 0.04 to 50 μg/ml for methamphetamine hydrochloride and amphetamine sulphate. The detection limits were 0.03 μg/ml for both of these compounds.

INTRODUCTION

In recent years, for clarifying methamphetamine use, the number of urine samples obtained from methamphetamine abusers has increased strikingly. For this reason, an automated, rapid and accurate method was required.

We have previously reported an automated analysis method for stimulants in urine, using the technique of headspace gas chromatography (HSGC)[1]. This technique requires no sample pretreatment such as liquid–liquid extraction of the target compounds. An urine sample is placed in a vial, made alkaline and subjected to HSGC. Compared with the conventional GC method which utilizes solvent extraction, this technique provides a more rapid analysis and higher sensitivity. The principal advantage was that the column was not contaminated at all by the urine components.

It was thought that the on-line connection of a mass spectrometer in HSGC would provide more reliable qualitative information, but the stimulants detected as free bases did not give any molecular ions (M^+) in electron-impact (EI) ionization mass spectrometry, only low-molecular-weight fragment ions produced by fragmen-

0021-9673/89/$03.50

tation at the β-position[2]. Our presumption was that derivatization with trifluoroacetyl (TFA) would provide higher detection sensitivity because of the higher vapour pressures of the derivatives[3–5].

In this report, a newly developed system which ensures higher sensitivity and selectivity is presented. An inlet device to introduce the TFA derivatizing reagent was attached to the injection port of the gas chromatograph. N-Methylbis(trifluoroacetamide) (MBTFA)[6], which is a moderate TFA derivatizing reagent for amines and phenols, was used for derivatization. The stimulants in the form of free bases were introduced by the headspace method, derivatized in the capillary column, chromatographed and detected as TFA derivatives.

One noteworthy advantage of this method is that the operator is not required to handle organic solvents or urine samples for pretreatment.

EXPERIMENTAL

Materials

Methamphetamine hydrochloride and amphetamine sulphate were obtained from Dainippon (Osaka, Japan) and Takeda (Osaka, Japan), respectively. MBTFA was obtained from Wako (Osaka, Japan). Other reagents were of analytical grade.

A glass vial (20 ml), poly(tetrafluoroethylene) (PTFE) septum and aluminium vial cap were obtained from Maruemu (Osaka, Japan).

The standard sample solutions, 0.01–200 μg/ml, were prepared by adding the salts of methamphetamine hydrochloride and amphetamine sulphate to urine samples obtained from healthy volunteers who had not taken any drugs. The MBTFA reagent was used without dilution.

Instrumentation

GC was carried out on a Shimadzu GC-9A gas chromatograph equipped with a CLH-702 split type sample injector, a flame ionization detector, a TFA derivatizing device, an HSS-2A headspace sampler and a C-R3A Chromatopac data processor. The column used was a DB-1 (J&W Scientific) fused-silica capillary column, 30 m × 0.32 mm I.D., film thickness 0.25 μm. The injection and detector temperatures were both 260°C, and the column temperature was 130°C. The linear velocity of the carrier gas (nitrogen) was 50 cm/s.The sample heating temperature was 80°C, the sample heating time was 20 min and the gas-tight syringe temperature was 130°C.

Adaptation of headspace sampler

The HSS-2A permitted automatic sampling and headspace gas injection of up to 40 samples placed on the carousel.

The gas-tight syringe was rinsed with purge gas (nitrogen) at temperatures of 40–150°C. This method of syringe washing was not satisfactory for the analysis of stimulant amines having high boiling points, and therefore the syringe was washed as follows: a vial containing water was placed between sample vials and heated to 80°C by the vial heating block; the syringe was washed five times with hot water and completely dried by pumping 15 times with purge gas. The syringe temperature was set at 130°C.

Device for in-column TFA derivatization

Fig. 1. shows the construction of the device for TFA derivatization. A 1-ml volume of MBTFA solution was placed in a 10-ml consolidated glass vial and nitrogen introduced into the solution at a rate of 20 ml/min. The MBTFA gas evaporated was introduced into the 1-ml sample loop connected to the six-way valve set at the position shown by the dotted line. Just after the headspace gas was introduced, the six-way valve was switched to the position indicated by the solid line. Thus, the stimulants were derivatized on the column.

Method of analysis

An urine sample (5 ml) was placed in a vial and 3.5 g of potassium carbonate were added. The vial was sealed with a septum (PTFE) and an aluminium cap, and placed on the carousel. (All the above operations were carried out manually.) Then the operational sequence of the HSS-2A was started. The carousel rotated and the sample vial was placed into the vial heating block. The vial was kept at 80°C for 20 min, until the vapour pressure in it had equilibrated. A 0.8-ml volume of the headspace gas was taken by the gas-tight syringe and injected for GC. The six-way valve of the TFA derivatizing device was switched to inject the MBTFA reagent.

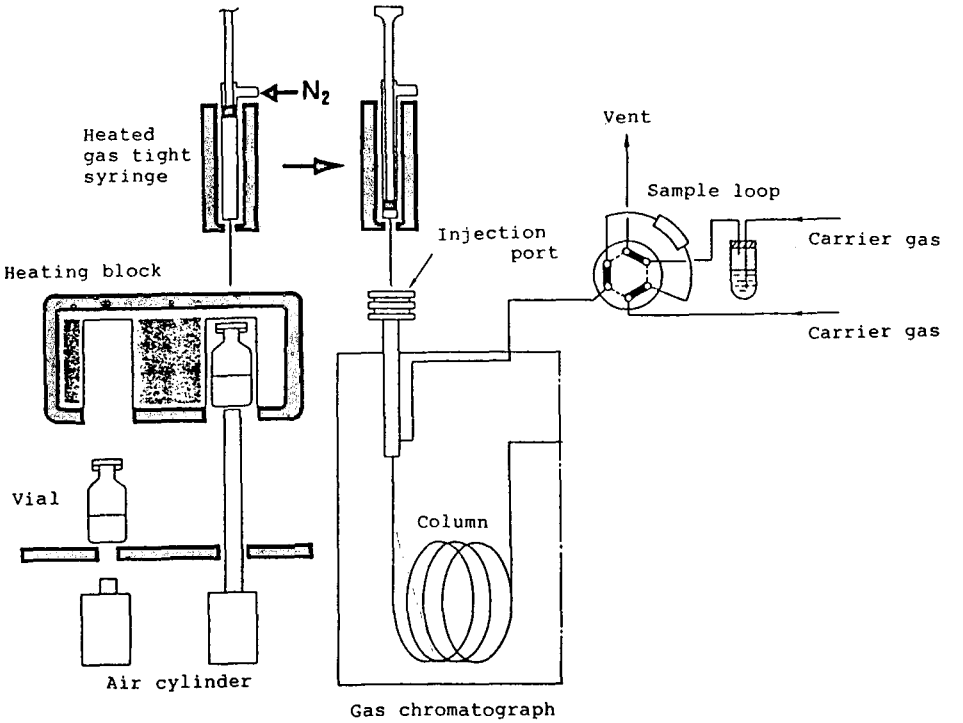

Fig. 1. Flow diagram of the in-column TFA derivatization HSGC system.

RESULTS AND DISCUSSION

Sample heating temperature and time

A 5-ml aliquot of each standard 10 μg/ml aqueous solution containing methamphetamine hydrochloride, amphetamine sulphate and 3.5 g of potassium carbonate was placed in a sample vial. The sample vials were heated for 20 min at 40, 50, 60, 80 or 90°C in the vial heating block, and 0.8 ml of the headspace gas were taken and injected for GC together with the TFA derivatizing reagent. The amounts of methamphetamine and amphetamine were related to the peak areas by means of the C-R3A data processor.

The results showed that a higher sample heating temperature gave a larger peak area. The peak area became constant at temperatures in the rang 80–90°C. In subsequent experiments, therefore, the sample heating temperature (vial heating block temperature) was set at 80°C.

The influence of the sample heating time was similarly examined and a constant value of 20 min at 80°C was found to be optimum.

Injection volume of MBTFA reagent

The volume of the MBTFA solution for effective derivatization was investigated using sample loops of different sizes. A 5-ml volume of the standard solution, containing 20 μg/ml of methamphetamine hydrochloride and amphetamine sulphate and 3.5 g of potassium carbonate was placed in a vial, and the vial was sealed and kept at 80°C for 20 min. Derivatization HSGC was carried out using sample loops of 1, 2 and 5 ml in volume. Use of the 1-ml sample loop for methamphetamine hydrochloride and amphetamine sulphate gave only the peak of the derivative and no peaks due to stimulants in their free basic states.

Addition of sodium hydroxide

In this method, an urine sample was made alkaline in the vial and the released gases of the stimulants were chromatographed after TFA derivatization. In our previous study[1], sodium hydroxide was used for alkalization and potassium carbonate for salting out. Since a certain amount of potassium carbonate can alkalize samples and, at the same time, serve as a salting-out agent, the addition of sodium hydroxide was considered unnecessary.

The effect of the addition of sodium hydroxide was investigated using standard solutions of 1, 5, 10 and 50 μg/ml, to 5 ml of which (1) 3.5 g of only potassium carbonate were added, and (2) 3.5 g of potassium carbonate and 0.5 ml of a 10% solution of sodium hydroxide were added. These samples were analyzed by HSGC after TFA derivatization. The addition of sodium hydroxide had no significant effect on the peak areas. In subsequent experiments, only potassium carbonate was added to urine samples.

Addition of potassium carbonate

The amount of potassium carbonate added was investigated. The technique of HSGC was generally applied to analyses of volatile components because heating in sample vials might not satisfactorily evaporate stimulant components which have high boiling points. It was investigated whether the evaporation efficiency can be enhanced by the salting-out effect employing potassium carbonate.

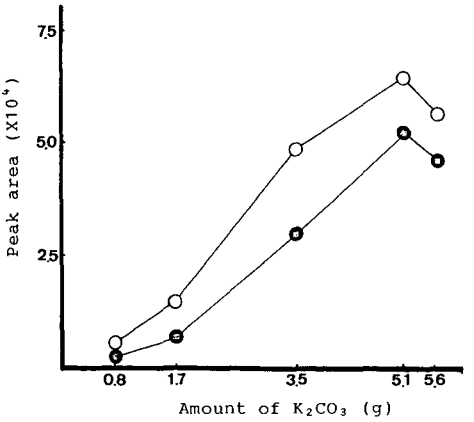

Fig. 2. Effect of potassium carbonate addition to the sample solution: ● = amphetamine; ○ = methamphetamine. Each point respresents the mean of three experimental values.

A 5-ml aliquot of each of standard 10 μg/ml aqueous solution of methamphetamine hydrochloride and amphetamine sulphate was placed into a sample vial: to each of them was added, respectively, 0.8, 1.7, 3.5, 5.1 and 5.6 g of potassium carbonate. The vials were allowed to stand at 80°C for 20 min, and the headspace gases were chromatographed after TFA derivatization. The results shown in Fig. 2 indicate significant increases in response or peak area over the range of salt added. A saturation point was reached when 5.6 g had been added, after which the sensitivity for both methamphetamine and amphetamine decreased. The appropriate amount of potassium carbonate was concluded to be *ca.* 3.5 g, the dissolution time and other factors remaining constant.

Sample volume

In HSGC the concentrations of the components in the gas phase are determined by their concentrations in the liquid phase, and do not depend on the volume of the solution[7]. In our method, however, since the salting out effect of potassium carbonate is utilized, the influence of the sample volume was investigated. Into 20-ml sample vials, 2.5, 5.0, 7.5 and 10 ml of standard 10 μg/ml aqueous solutions of methamphetamine hydrochloride and amphetamine sulphate were placed. To each of these, 0.7 g potassium carbonate were added per ml (which corresponds to 3.5 g per 5 ml of sample solution, when employing the standard volume in our method); the vials were sealed and allowed to stand at 80°C for 20 min, and the contents derivatized. The results are shown in Fig. 3. The peak areas for methamphetamine and amphetamine increase in proportion to the sample volume. A suitable sample volume was 5 ml, by consideration of the sample volumes required for other methods of analysis. The same investigation was repeated with no potassium carbonate added, and the solution made alkaline with 0.5 ml of 10% sodium hydroxide. The vials were then sealed and allowed to stand at 80°C for 20 min. The headspace gases were chromatographed after derivatization. There was no change in peak areas attributable to the change in sample volume. This shows that the addition of potassium carbonate results in vaporization of most stimulants in the solution and does not give gas–liquid equilibrium as is always the case in headspace analysis.

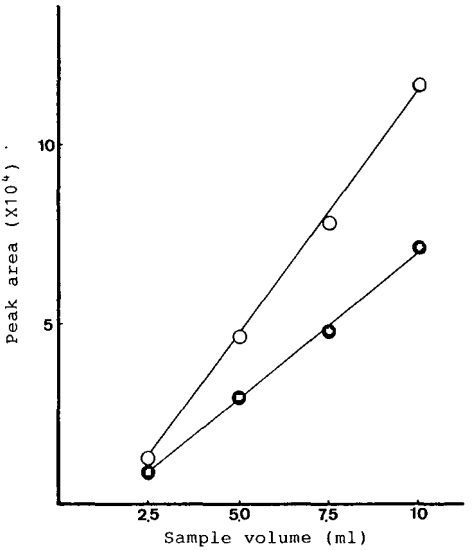

Fig. 3. Effect of sample volume: ● = amphetamine; ○ = methamphetamine. Each point represents the mean of three experimental values.

Calibration graph

Aliquots of 5 ml of standard solutions of methamphetamine hydrochloride and amphetamine sulphate were added to 5 ml of urine to give drug solutions in the concentration range of 0.01–100 μg/ml. To each of these, 3.5 g of potassium carbonate were added. Each solution was heated at 80°C for 20 min. The headspace gases were analyzed by HSGC after TFA derivatization. The calibration graphs were constructed using the absolute calibration curve method. They were linear within the concentration range from 0.04 to 50 μg/ml. Fig. 4 shows calibration graphs for methamphetamine hydrochloride and amphetamine sulphate. The detection limit is 0.03 μg/ml for both of these compounds. The detection limit in HSGC of non-derivatized stimulants is 0.07 μg/ml for both methamphetamine and amphetamine[1]. The coefficient of variation obtained for eleven replicate analyses of the standard 10 μg/ml solution was 2.36% for methamphetamine and 2.38% for amphetamine.

Deterioration of urine sample

The deterioration of the urine sample was investigated before the addition of potassium carbonate.

Standard 20 μg/ml aqueous solutions of methamphetamine hydrochloride and amphetamine sulphate were allowed to stand at room temperature for 1, 5, 10 and 20 days. Then, to 5 ml of each of these solutions were added 3.5 g of potassium carbonate and the headspace gas was chromatographed after being TFA derivatized. The results are shown in Fig. 5. No change in concentration of methamphetamine or amphetamine was observed in the samples that were allowed to stand for up to 5 days. In the case of samples allowed to stand for 10 days, the concentrations of both methamphetamine and amphetamine decreased to 96% of the initial concentrations, and in the case of 15-days-old samples the methamphetamine decreased to 86% and the

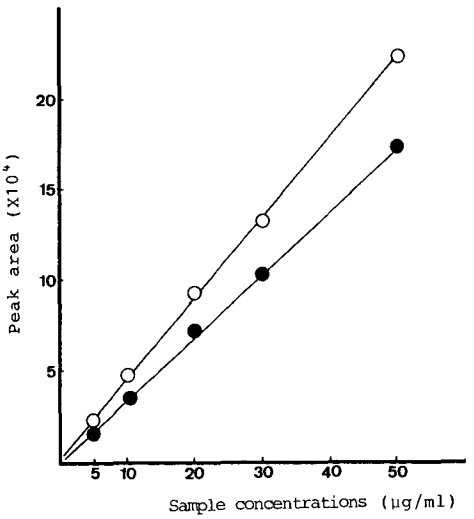

Fig. 4. Calibration graphs for amphetamine (●) and methamphetamine(○). The coefficient of variation for the 10 μg/ml sample was 2.36% for methamphetamine and 2.38% for amphetamine ($n=11$).

amphetamine to 94%. In the case of 20-days-old samples, the methamphetamine decreased to 70% and the amphetamine to 86%. It is recommended, therefore, to analyze urine samples before they deteriorate or to keep them in a refrigerator.

The analysis of deteriorated blank urine samples gave no interference peaks having retention times close to those of stimulants or similar compounds.

Comparison with solvent extraction GC method

The data obtained by the present method were compared with those obtained by the GC method in which the target compounds were extracted with organic solvents. The urine samples were taken from five suspects. In the present method, 3.5 g of

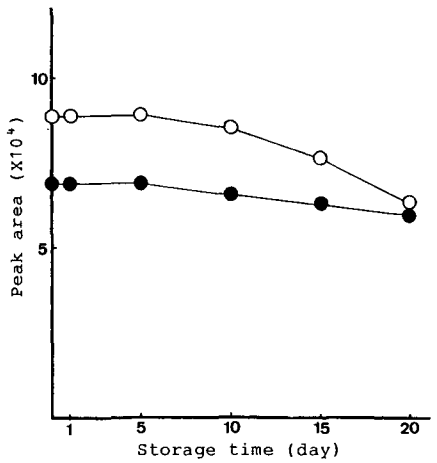

Fig. 5. Stability of amphetamine (●) and methamphetamine (○) in solution. Each point represents the mean of three experimental values.

TABLE I

COMPARISON OF GC AND HSGC FOR AMPHETAMINE AND METHAMPHETAMINE DETERMINATION IN URINE

GC method: 3 ml of urine were alkalized with ammonia and extracted with chloroform. HSGC method: 5 ml of urine and 3.5 g of K_2CO_3 were placed in a 20-ml vial. The solution was allowed to stand at 80°C for 20 min. TFA derivatized and analyzed by HSGC. Values given in μg/ml.

No.	*Amphetamine*		*Methamphetamine*	
	GC	*HSGC*	*GC*	*HSGC*
1	0.5	0.46	2.77	2.49
2	2.16	2.27	6.74	6.38
3	1.36	1.39	14.09	14.65
4	1.97	2.05	14.57	15.01
5	4.97	5.21	39.51	42.73

$r = 0.999$ ($p < 0.01$)

potassium carbonate were added to 5 ml of urine sample and the headspace gas was chromatographed after TFA derivatization. In the GC method, 3 ml of urine sample were alkalized with ammonia, and the target compounds were extracted into 1 ml of chloroform. The quantitation was carried out using the predetermined calibration graphs. Table I shows the corresponding data.

The correlation coefficient between the quantitative data of methamphetamine and amphetamine obtained by the two methods was 0.999 ($p < 0.01$). The values given by the two methods are in good agreement. Fig. 6 shows a typical gas chromatogram of a suspect urine sample.

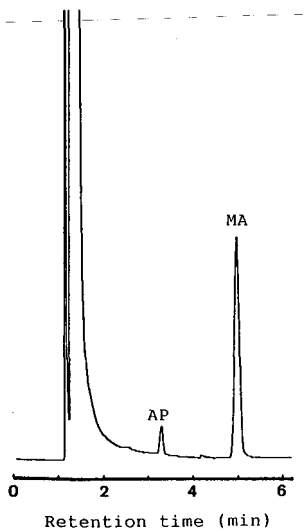

Fig. 6. Headspace gas chromatogram of trifluoroacetylated amphetamine (AP) and methamphetamine (MA) in urine. GC conditions: DB-1 fused-silica capillary column, 30 m × 0.32 mm I.D., film thickness 0.25 μm; injection temperature 260°C, column temperature 130°C. Sample: 5 ml of urine + 3.5 g of K_2CO_3 at 80°C for 20 min.

TABLE II

COMPARISON OF VARIOUS SCREENING METHODS FOR METHAMPHETAMINE IN URINE

− = Negative; + = positive. TBPE method: TBPE was added to 5 ml of urine. Simon's method: 5 ml of urine were alkalized with ammonia, and extracted with chloroform–isopropanol mixture. GC–MS method: 5 ml of urine were alkalized with ammonia, extracted with chloroform–isopropanol mixture and PFP derivatized. Present method: 5 ml of urine and 3.5 g of K_2CO_3 were placed in a 20-ml vial; the solution was allowed to stand at 80°C for 20 min, TFA derivatized and analyzed by HSGC.

TBPE method	*Simon's reagent*	*GC–MS*	*Present method*	*Number of specimens*
+	+	+	+	28
+	−	−	−	8
−	−	+	+	6
−	−	−	−	8

Comparison with conventional method of analysis

In Japan, urinary stimulants are determined in the following manner: screening test by the tetrabromophenolphthalein ethyl ester (TBPE) method, extraction of stimulants into solvent, Simon's reaction[8] and then determination by infrared spectrophotometry or gas chromatography–mass spectrometry (GC–MS). The reliability of the present method was investigated in the following way: Fifty suspect urine samples were (1) screened by the TBPE method, (2) alkalized with ammonia, subjected to extraction with chloroform–isopropanol (3:1, v/v), the solvent removed and the residue subjected to Simon's reaction; (3) some part of the sample was treated as described in (2) and derivatized with pentafluoropropionyl (PFP), and then the derivative was analyzed by GC–MS. The results were compared with those given by the present method (Table II). The sample size was 5 ml for both methods.

The present method and the GC–MS method gave the same results for 50 samples out of 50 (100% agreement), the screening method (TBPE method) and the GC–MS method for 36 samples (70% agreement) and Simon's method and the GC–MS method for 44 samples (88% agreement). These data show the high reliability of the present method.

REFERENCES

1 H. Tsuchihashi, K. Nakajima, H. Ono, A. Matsushita and M. Nishikawa, *Eisei Kagaku*, 34 (1988) 146.
2 A. S. Curry, G. Hurst, N. R. Kent and H. Powell, *Nature (London)*, 195 (1962) 603.
3 K. Kamei, M. Murata, K. Ishii, M. Namekata and A. Momose, *Chem. Pharm. Bull.*, 21 (1973) 1996.
4 R. T. Coutts, R. Dawe, G. R. Jones, S.-F. Liu and K. K. Midha, *J. Chromatogr.*, 190 (1980) 53.
5 R. B. Bruce and W. R. Maynard, *Anal. Chem.*, 41 (1969) 977.
6 T. A. Brettell, *J. Chromatogr.*, 257 (1983) 45.
7 B. Kolb, *J. Chromatogr.*, 122 (1976) 553.
8 F. Feigl, *Spot Tests in Organic Analysis*, Elsevier, Amsterdam, 7th ed., 1956, p. 251.

Journal of Chromatography, 467 (1989) 237–247
Elsevier Science Publishers B.V., Amsterdam — Printed in The Netherlands

CHROM. 21 235

SIMULTANEOUS HIGH-PERFORMANCE LIQUID CHROMATOGRAPHIC DETERMINATION OF CATECHOLAMINE-RELATED COMPOUNDS BY POST-COLUMN DERIVATIZATION INVOLVING COULOMETRIC OXIDATION FOLLOWED BY FLUORESCENCE REACTION

HITOSHI NOHTA, ETSUKO YAMAGUCHI and YOSUKE OHKURA*
Faculty of Pharmaceutical Sciences, Kyushu University 62, Maidashi, Higashi-ku, Fukuoka 812 (Japan)
and
HIDEO WATANABE
Scientific Instrument Division, Tosoh Corporation, Hayakawa, Ayase, Kanagawa 252 (Japan)
(First received October 18th, 1988; revised manuscript received December 27th, 1988)

SUMMARY

A highly selective and sensitive high-performance liquid chromatographic method for the determination of catecholamines (norepinephrine, epinephrine and dopamine) and related compounds (L-DOPA, normetanephrine, metanephrine, 3-methoxytyramine, 3,4-dihydroxymandelic acid, 3,4-dihydroxyphenylacetic acid, homovanillic acid, vanillylmandelic acid, 3,4-dihydroxyphenylethylene glycol, 4-hydroxy-3-methoxyphenylethylene glycol and 4-hydroxy-3-methoxyphenylethanol) with a post-column technique involving coulometric oxidation followed by fluorescence derivatization is described. These compounds, 3,4-dihydroxybenzylamine and ferulic acid are separated within 35 min by ion-pair reversed-phase chromatography using acidic buffers (pH 3.1) with methanol–acetonitrile (3:2, v/v) gradient elution, and then oxidized by a commercial coulometric detector to the corresponding *o*-quinones, which are converted into fluorescent derivatives by reaction with 1,2-diphenylethylenediamine. The detection limits (signal-to-noise ratio = 3) on-column are 1.5–4 pmol for the two mandelic acids, 600 fmol for L-DOPA and 20–70 fmol for the others.

INTRODUCTION

The determination of catecholamine (CA)-related compounds (for abbreviations, see Table I) can afford much information on the sympathetic nerve functions and therefore it is useful in clinical and pharmacological studies (for reviews, see refs. 1–3). Many methods have been proposed, but only high-performance liquid chromatography (HPLC) with electrochemical detection (ED) permits the simultaneous determination of CA-related compounds[4–17].

We have developed an HPLC method for the simultaneous determination of CA-related compounds based on post-column derivatization involving electrochem-

0021-9673/89/$03.50

TABLE I

CATECHOLAMINE-RELATED COMPOUNDS AND THEIR ABBREVIATIONS

Compound	*Abbrevation*
Amino compounds:	
Norepinephrine[a] }	NE
Epineprine[a] } catecholamines	E
Dopamine[a] }	DA
Normetanephrine[b]	NM
Metanephrine[b]	M
3-Methoxytyramine[b]	3MT
L-DOPA[a]	L-DOPA
Acidic compounds:	
3,4-Dihydroxymandelic acid[a]	DOMA
3,4-Dihydroxyphenylacetic acid[a]	DOPAC
Vanillylmandelic acid[b]	VMA
Homovanillic acid[b]	HVA
Alcoholic compounds:	
3,4-Dihydroxyphenylethylene glycol[a]	DOPEG
4-Hydroxy-3-methoxyphenylethylene glycol[b]	MOPEG
4-Hydroxy-3-methoxyphenylethanol[b]	MOPET

[a] Catechol compounds.
[b] 4-Hydroxy-3-methoxyphenyl compounds.

ical oxidation followed by fluorescence reaction (Fig. 1). The CA-related compounds are separated by ion-pair reversed-phase chromatography with gradient elution using an acidic buffer and a buffer containing methanol and acetonitrile, and then electrochemically oxidized to the respective *o*-quinones by a coulometric technique. The *o*-quinones are converted into fluorescent derivatives with *meso*-1,2-diphenylethylenediamine (DPE)[18], a fluorogenic reagent for catechol compounds that has previously been applied to pre-column fluorescence derivatization HPLC for the determination of three CAs in plasma[19], platelets[20], erythrocytes[20] and urine[21,22]. 3,4-Dihydroxybenzylamine (DHBA) and 4-hydroxy-3-methoxycinnamic acid (ferulic acid) were also subjected to the investigation because they should be useful as internal standards when CA-related compounds are measured in biological samples.

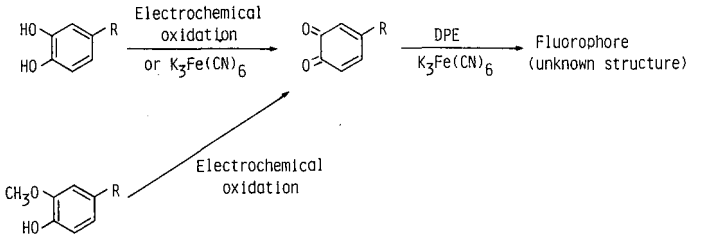

Fig. 1. Fluorescence derivatization of catechol and 4-hydroxy-3-methoxyphenyl compounds with DPE.

EXPERIMENTAL

Reagents, solutions and apparatus

NE hydrogentartrate and DA hydrochloride were purchased from Wako (Osaka, Japan), NM hydrochloride, M hydrochloride, DOMA, VMA and HVA from Nacalai Tesque (Kyoto, Japan), E hydrogentartrate, 3MT hydrochloride and L-DOPA from Sigma (St.Louis, MO, U.S.A.) and DHBA hydrochloride, DOPAC, DOPEG, MOPEG piperazine salt and MOPET from Aldrich (Milwaukee, WI, U.S.A.). Ferulic acid was obtained from Wako and recrystallized twice from water. Their standard solutions were prepared in 50 m*M* hydrochloric acid and stored at −20°C. Highly purified glycine for electrophoresis and sodium hexanesulphonate were purchased from Nacalai Tesque. All other chemicals were of analytical-reagent grade. Deionized, distilled water was used. DPE was synthesized by the method of Irving and Parkins[23] with minor modifications[18]. Dopamine 3- and 4-O-sulphates were prepared according to the method of Jenner and Rose[24].

Uncorrected fluorescence spectra were measured with a Hitachi MPF-4 spectrofluorimeter using semimicro quartz cells (10 mm width parallel to the excitation beam, 3 mm width parallel to the emission beam; 1 ml).

HPLC system and conditions

Fig. 2 shows a schematic diagram of the HPLC system. A Hitachi Model 655A-12 liquid chromatograph and a Model 655-66 controller were used for gradient elution. The HPLC column (150 × 4.6 mm I.D.) contained 5-μm TSK-gel ODS-80TM (Tosoh, Tokyo, Japan). The column temperature was ambient. A Hitachi 655A coulometric monitor was employed for the electrochemical oxidation of CA-related compounds. A Hitachi F1000 spectrofluorimeter fitted with a 20-μl flow cell was used.

The mobile phase consisted of two eluents, an aqueous solution containing 60 m*M* citric acid, 32 m*M* disodium hydrogenphosphate, 1.7 m*M* sodium hexanesulphonate as ion-pairing reagent and 0.1 m*M* disodium EDTA (pH 3.1, eluent A) and

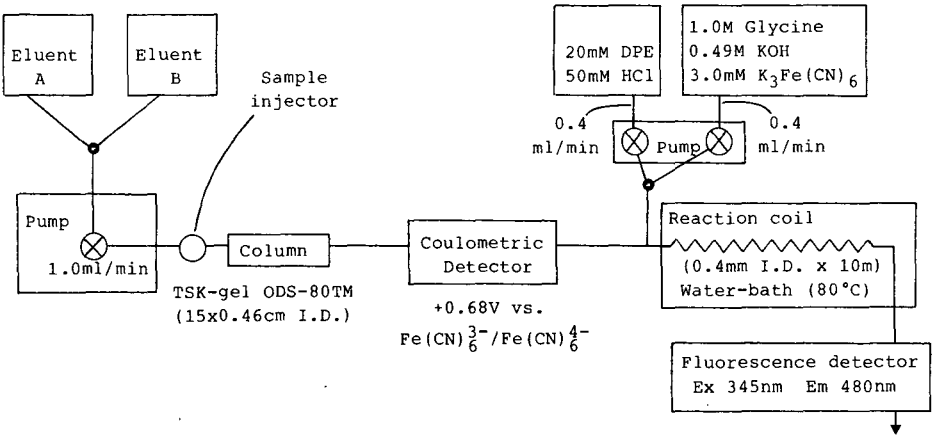

Fig. 2. Schematic diagram of post-column derivatization HPLC of catecholamine-related compounds. Ex = Exitation wavelength; Em = emission wavelength.

an aqueous solution containing 20% methanol–acetonitrile (3:2, v/v) as an organic modifier (pH 3.1, eluent B). Gradient elution using eluents A and B [0–20% (v/v) of the organic modifier] was applied for the separation, as shown in Fig. 3. The flow-rate was 1.0 ml/min. After a single run, eluent A (organic modifier concentration 0%) was passed through the column for 20 min to establish complete equilibrium for the subsequent sample injection.

The eluate from the column was introduced into the coulometric detector to oxidize catechol and 4-hydroxy-3-methoxyphenyl compounds to *o*-quinones (Fig. 1). The applied oxidation potential was the potential difference between the working and reference electrodes in the coulometric detector, and a potential of +0.68 V was usually used. Both electrodes were made of carbon cloth. The electrolyte for the reference electrode was an equimolar (200 m*M*) mixture of potassium hexacyanoferrates (II and III) containing potassium nitrate and potassium hydroxide (200 m*M* each), and the reference electrode also served as a counter electrode.

The effluent from the coulometric detector was then mixed with a stream of a mixture of two reagent solutions, 20 m*M* DPE in 50 m*M* hydrochloric acid and an aqueous solution of 1 *M* glycine – 0.49 *M* potassium hydroxide – 3 m*M* potassium hexacyanoferrate (III). Both reagent solutions delivered at a flow-rate of 0.4 ml/min by an SSP DM2M-1026 pump (Sanuki Kogyo, Tokyo, Japan). The fluorescence derivatization reaction was performed in a reaction coil (Tough tubing, 10 m × 0.47 mm I.D.; Gasukuro Kogyo, Tokyo, Japan) immersed in a water-bath (80°C). The resulting fluorescence was monitored at 480 nm with an excitation wavelength of 345 nm.

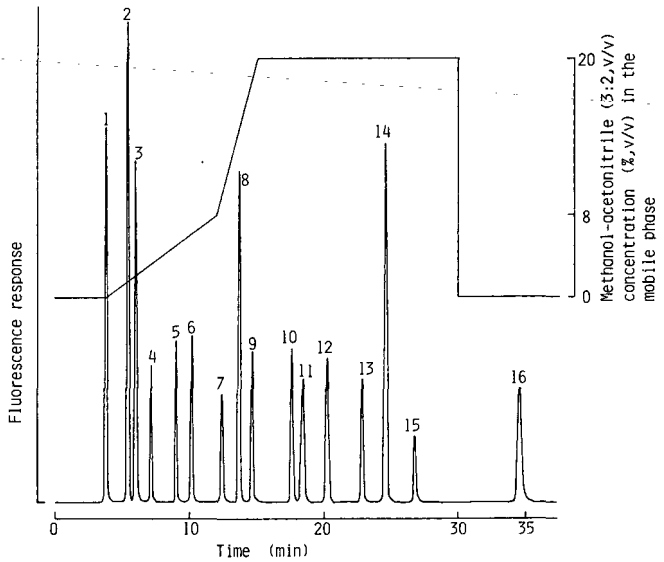

Fig. 3. Chromatogram of a standard mixture of catecholamine-related compounds. Peaks: 1 = DOMA; 2 = DOPEG; 3 = NE; 4 = VMA; 5 = L-DOPA; 6 = E; 7 = DHBA (internal standard); 8 = MOPEG; 9 = NM; 10 = DA; 11 = M; 12 = DOPAC; 13 = 3MT; 14 = MOPET; 15 = HVA; 16 = ferulic acid. Amounts (on-column): VMA and HVA, 500 pmol; L-DOPA and ferulic acid, 100 pmol; others, 10 pmol.

RESULTS AND DISCUSSION

Fig. 3 shows the chromatogram of a standard mixture of fourteen CA-related compounds, DHBA and ferulic acid. These compounds could be separated within 35 min under the recommended conditions. Table II shows the retention times and relative peak heights for the CA-related compounds and the fluorescence excitation and emission spectra of the corresponding eluates from the fluorescence detector. The fluorescence excitation and emission maxima are around 340 and 475 nm, respectively. With the present HPLC system, the fluorescence was monitored at 480 nm emission with excitation at 345 nm for the highly sensitive determination of CAs, the concentrations of which in biological samples are the lowest of CA-related compounds.

Chromatographic separation

The investigations of the HPLC separation were mainly carried out by monitoring the oxidation current in the coulometric detector. The proposed HPLC method permitted the complete separation of fourteen CA-related compounds, DHBA and ferulic acid with a linear gradient using a citrate–phosphate buffer and the buffer containing methanol–acetonitrile (3:2, v/v) (Fig. 3). Methanol, acetonitrile, ethanol

TABLE II

RETENTION TIMES, FLUORESCENCE EXCITATION AND EMISSION MAXIMA AND RELATIVE PEAK HEIGHTS OF THE DPE DERIVATIVES

Portions (50 μl) of 5 nmol/ml CA-related compounds, DHBA, ferulic acid and dopamine 3- and 4-O-sulphates were injected into the chromatograph.

Compound	*Retention time (min)*	*Excitation maximum (nm)*	*Emission maximum (nm)*	*Relative peak height*[a]
NE	6.1	340	480	100
E	10.2	350	495	49
DA	17.7	345	475	45
NM	14.7	340	480	44
M	18.5	350	495	36
3MT	22.9	345	475	42
L-DOPA	9.1	340	470	4.7
DOMA	3.8	340	480	2.2
DOPAC	20.3	340	470	42
VMA	7.2	340	480	0.8
HVA	26.8	340	470	19
DOPEG	5.5	340	475	141
MOPEG	13.7	340	475	97
MOPET	24.7	340	475	105
DHBA	12.5	345	480	31
Ferulic acid	34.7	365	500	3.3
Dopamine 3-O-sulphate	8.1	345	475	48
Dopamine 4-O-sulphate	7.9	345	475	51

[a] The peak height for NE was taken as 100.

and their mixtures were examined as organic modifiers in gradient elution; a mixture of methanol and acetonitrile (2:3, v/v) gave the most satisfactory separation.

The CA-related compounds contain an amino, carboxyl or alcoholic moiety (Table I). For the simultaneous separation of such compounds, ion-pair reversed-phase HPLC is the most suitable technique.

As catechol compounds are fairly stable in acidic media, an acidic buffer, consisting of a mixture of citric acid and disodium hydrogenphosphate (pH 3.1), was used as the mobile phase. However, the amino compounds were all in cationic form in this buffer and were not retained well on the reversed-phase HPLC column. By adding an anionic ion-pairing reagent, the amino compounds were retained on the column and thus the simultaneous separation of the CA-related compounds was achieved. As ion-pairing reagents, benzenesulphonate, pentanesulphonate, hexanesulphonate, heptanesulphonate, octanesulphonate, octanesulphate and lauryl sulphate (all sodium salts) were examined. Although these reagents resulted in longer retention times for the amino compounds in that order, the HPLC column could not be equilibrated with octanesulphonate, octanesulphate and lauryl sulphate, even after passing the mobile phase containing one of them through it for 3 h at a flow-rate of 1.0 ml/min. Therefore, hexanesulphonate was selected as the optimum reagent; with increasing concentration of the sulphonate, the retention times for the amino compounds became longer; 1.7 m*M* was used for rapid and complete separation. Hexanesulphonate did not affect the retention times of the acidic and alcoholic compounds. The pH of the mobile phase, which was adjusted by using citric acid – disodium hydrogenphosphate buffer, citrate buffer or perchlorate buffer, affected the retention times of the acidic compounds in the pH range 2.5–5.0; higher pHs made the retention times shorter. Citric acid – disodium hydrogenphosphate buffer of pH 3.1 afforded a complete separation of the CA-related compounds. The concentrations of citric acid and the phosphate in the mobile phase affected the retention times of the amino compounds and the efficiency of the coulometric oxidation. With increasing concentrations of the acid and the phosphate, the retention times decreased. A constant and stable efficiency of the oxidation in the coulometric cell was obtained with 20 m*M* citric acid – 10 m*M* disodium hydrogenphosphate buffer or more concentrated buffers; a 60 m*M* citric acid – 32 m*M* phosphate buffer is recommended. EDTA was added to the mobile phase to protect the coulometric cell and the HPLC column from adhesion of metal ions.

Coulometric oxidation

In the reaction of DPE with catechol compounds[18,19], it is presumed that catechol compounds are converted into *o*-quinones in the first stage by hexacyanoferrate (III) and then react with DPE to produce fluorescence, because catechol compounds are readily and rapidly oxidized into *o*-quinones by oxidizing reagents such as oxygen, potassium hexacyanoferrate(III) and iodine. Therefore, 4-hydroxy-3-methoxyphenyl compounds also have the possibility of reacting with DPE after conversion to the respective *o*-quinone compounds by electrochemical oxidation (Fig. 1). Based on this assumption, an electrochemical detector was incorporated in the post-column derivatization HPLC of the CA-related compounds. Two types of electrochemical detectors, amperometric and coulometric, have been utilized in the HPLC analysis of CAs and their metabolites. In the present method, quantitative oxidation of 4-hy-

droxy-3-methoxyphenyl compounds to *o*-quinones is required and hence a coulometric detector was employed.

Fig. 4 shows hydrodynamic voltammograms of the CA-related compounds and dopamine 3-O-sulphate in this HPLC system; their half-wave potentials obtained from the voltammograms varied, depending on the compounds (Table III). The potentials of 4-hydroxy-3-methoxyphenyl compounds were higher than those of the catechol compounds by 0.2–0.3 V. In this system, a potential of +0.68 V was tentatively selected for complete oxidation and reproducible results.

The fluorescence peak heights for 4-hydroxy-3-methoxyphenyl compounds were proportional to the respective responses in the coulometric detector with changing applied potential in the range 0.2–0.68 V. However, those of catechol compounds were independent of the applied potential. When an amperometric detector (Yanagimoto VDM 101) was used in place of the coulometric detector, the resulting fluorescence peak heights for 4-hydroxy-3-methoxyphenyl compounds were 2% or less of those obtained with the coulometric detector.

When the eluate for M was applied in the reversed-phase mode used in the pre-column derivatization HPLC of CAs[19], it gave the same chromatogram as that obtained for its demethylated compound, E, and the same was found with the other pairs of CA-related compounds (NE with NM, DA with 3MT, DOMA with VMA, DOPAC with HVA and DOPEG with MOPEG). The eluates from the fluorescence detector corresponding to the catechol compounds showed the same fluorescence excitation and emission maxima as those for the respective 3-O-methylated (3-methoxy-4-hydroxyphenyl) compounds (Table II).

The above observations strongly support the presumption that 4-hydroxy-3-methoxyphenyl compounds are oxidatively demethylated to *o*-quinones by coulometric oxidation and then react with DPE to produce fluorescence (Fig. 1).

In fact, the eluate for each CA-related compound gave multiple (1–4) peaks in addition to the DPE derivative peak when it was subjected to reversed-phase HPLC, although a single peak was always obtained for each CA in the pre-column deri-

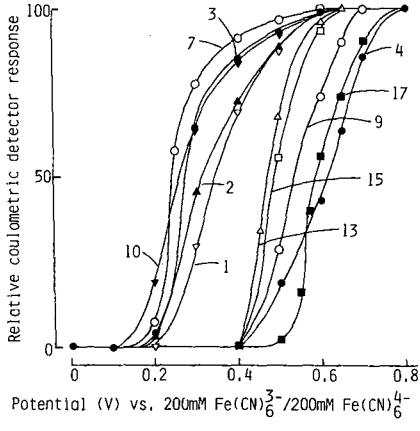

Fig. 4. Hydrodynamic voltammograms for catecholamine-related compounds. Peaks and amounts as in Fig. 3; 17, dopamine 3-O-sulphate and 10 pmol on-column. For the relative coulometric detector response, the oxidative current at 0.8 V for each compound was taken as 100.

HALF-WAVE POTENTIALS [V, *vs.* 200 m*M* Fe $(CN)_6^{3-}$/200 m*M* Fe $(CN)_6^{4-}$] OF CATECHOLAMINE-RELATED COMPOUNDS, DHBA, FERULIC ACID AND DOPAMINE 3- AND 4-O-SULPHATES IN THE PRESENT HPLC CONDITIONS

Catechol compound	*Half-wave potential*	*3-Methoxy-4-hydroxyphenyl compound*	*Half-wave potential*
NE	0.27	NM	0.54
E	0.29	M	0.54
DA	0.26	3MT	0.48
L-DOPA	0.28	VMA	0.63
DOMA	0.35	HVA	0.48
DOPAC	0.28	MOPEG	0.49
DOPEG	0.32	MOPET	0.48
DHBA	0.23	Ferulic acid	0.49
Dopamine 3- and 4-O-sulphates			0.58

vatization HPLC[19]. This may be due to by-product(s) and/or degradation product(s) formed under the present derivatization conditions, where the reaction temperature (80°C) was much higher than that in the pre-column derivatization (37°C).

All catechol O-sulphate compounds are probably oxidized electrochemically to *o*-quinones and their half-wave potentials are suspected to be higher than those of catechol and 4-hydroxy-3-methoxyphenyl compounds, because dopamine 3- and 4-O-sulphates gave fluorescence peaks under the present HPLC conditions, both the effluents from the fluorescence detector showed the same fluorescence spectra as those for DA and 3MT (Table II) and the potentials of dopamine 3-O-sulphate, 3MT and DA increased in that order (Table III). Therefore, a chromatographic separation or a decrease in the applied potentials in the coulometric detector may be required for the determination of the CA-related compounds in biological samples containing catechol O-sulphate compounds.

Fluorescence derivatization reaction

In the manual spectrofluorimetric[18] and the pre-column HPLC[19–22] methods for the determination of CAs, glycine and a water-miscible organic solvent, respectively, were employed as accelerators of the DPE reaction. In the present system, the post-column derivatization reaction was promoted most effectively by the addition of glycine. The peak heights for the CA-related compounds increased with increasing glycine concentration up to 1.2 *M*; 1.0 *M* was selected. The peak heights also increased with increasing DPE concentration up to 25 m*M*, but at concentrations higher than 15 m*M*, they increased only slightly; 20 m*M* was therefore used. The optimum pH for the post-column derivatization reaction was 7.5–8.0 for all the CA-related compounds tested, and could be adjusted with potassium hydroxide in the reagent solution; pH 7.8 was selected as the optimum value.

The temperature in the fluorescence derivatization reaction affected the peak heights. On increasing the temperature, the peak height for MOPET increased and that for L-DOPA decreased only slightly. All the other CA-related compounds gave almost maximum peak heights at 70–80°C; 80°C was therefore selected as the optimum.

The concentration of potassium hexacyanoferrate(III) affected the peak heights (Fig. 5). Almost maximum peak heights were achieved at concentrations in the reagent solution ranging from 2 to 3 m*M* and a concentration higher than 5 m*M* caused a decrease in fluorescent peak heights, probably owing to the inner filter effect by hexacyanoferrate(III) and/or oxidative degradation of the fluorescent products, except that the peak height for MN increased only slightly on increasing the oxidant concentration even higher than 3 m*M*; 3 m*M* was selected as the optimum concentration.

Calibration graphs, detection limits and precision of the method

The calibration graphs were linear in the range (pmol per 50-μl injection volume) 5–1000 for DOMA, VMA and ferulic acid, 0.5–200 for L-DOPA and 0.1–100 for the other CA-related compounds and DHBA. The detection limits for the CA-related compounds, DHBA and ferulic acid and the precision of the method (repeatability) ($n=5$) are shown in Table IV.

Selectivity of the method

Biologically important substances having neither a catechol nor a 4-hydroxy-3-methoxyphenyl moiety did not fluoresce when they were injected directly into the post-column reaction system in an amount of 1.0 nmol per 50-μl injection volume. The compounds tested were seventeen different L-α-amino acids, tyramine, histamine, serotonin, octopamine, creatine, creatinine, uric acid, putrescine, spermidine, spermine, acetone, formaldehyde, acetaldehyde, *p*-hydroxybenzaldehyde, lactic acid, pyruvic acid, α-ketoglutaric acid, phenylpyruvic acid, oxalic acid, acetic acid, D-glucose,

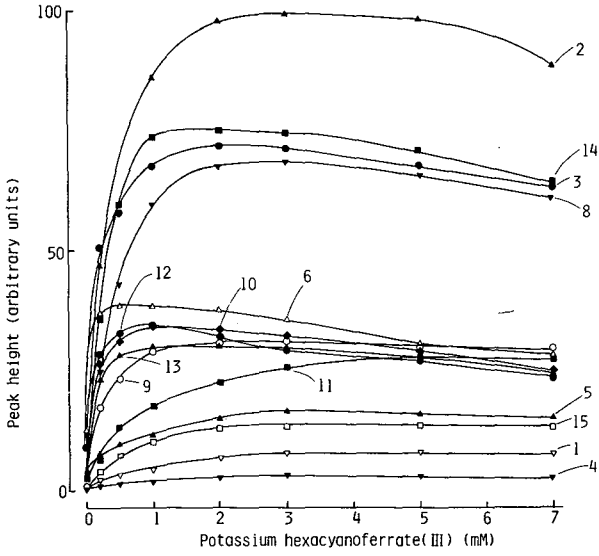

Fig. 5. Effect of potassium hexacyanoferrate(III) concentration in the reagent solution on the peak height. Portions (50 μl) of the same standard mixture as in Fig. 3 were subjected to HPLC. Peaks as in Fig. 3. Amounts (on-column); L-DOPA, DOMA and VMA, 50 pmol; others, 10 pmol.

TABLE IV

DETECTION LIMITS (SIGNAL-TO-NOISE RATIO = 3) FOR CATECHOLAMINE-RELATED COMPOUNDS, DHBA AND FERULIC ACID AND RELATIVE STANDARD DEVIATIONS (R.S.D.) OF THE PRESENT METHOD

Compound	*Detection limit (fmol on-column)*	*R.D.S.*[a] *(%)*
NE	30	0.9
E	60	2.2
DA	60	1.8
NM	60	2.1
M	60	1.5
3MT	70	1.1
L-DOPA	600	1.6
DOMA	1400	2.0
DOPAC	70	1.5
VMA	3900	1.6
HVA	120	1.7
DOPEG	20	1.2
MOPEG	30	0.7
MOPET	30	1.3
DHBA	70	1.3
Ferulic acid	900	1.8

[a] Portions (50 μl) of the same standard mixture as in Fig. 3 were subjected to HPLC.

D-fructose, D-galactose, D-ribose, D-glucosamine, maltose, sucrose, L-ascorbic acid, uracil, thymine, cytosine, adenine, guanine, cholesterol and cortisone. This suggests that the proposed method is selective for catechol and 4-hydroxy-3-methoxyphenyl compounds.

CONCLUSION

The highly selective and sensitive reaction of catechol compounds with DPE was successfully applied to the post-column derivatization of CA-related compounds, including 4-hydroxy-3-methoxyphenyl compounds, by introducing a coulometric oxidation technique. This HPLC method is comparable in terms of sensitivity to the HPLC–ED methods reported so far[4–17], and is has a higher selectivity, attributable to the highly selective fluorescence reaction. However, the sensitivity of the proposed method is lower than that of pre-column derivatization HPLC[19–22], which allows three CAs to be determined. The method should be applicable to the simultaneous determination of CA-related compounds in biological samples.

REFERENCES

1 I. J. Kopin, *Pharmacol. Rev.*, 37 (1985) 333.
2 S. W. Dziedzic, L. M. Dziedzic and S. E. Gitlow, in A. M. Krstulović (Editor), *Quantitative Analysis of Catecholamines and Related Compounds*, Ellis Horwood, Chichester, 1986, pp. 13–23.
3 B. Kågedal and D. S. Goldstein, *J. Chromatogr.*, 429 (1988) 177.
4 J. Wagner, P. Vitali, M. G. Palfreyman, M. Zraika and S. Huot, *J. Neurochem.*, 38 (1982) 1241.
5 G. S. Mayer and R. E. Shoup, *J. Chromatogr.*, 255 (1983) 533.

6 R. B. Taylor, R. Reid, K. E. Kendle, C. Geddes and P. F. Curle, *J. Chromatogr.*, 277 (1983) 101.
7 B. H. C. Westrink, *J. Liq. Chromatogr.*, 6 (1983) 2337.
8 W. A. Hunt and T. K. Dalton, *Anal. Biochem.*, 135 (1983) 269.
9 P. Kontur, R. Dawson and A. Monjan, *J. Neurosci. Methods*, 11 (1984) 5.
10 S. M. Lasley, I. A. Michaelson, R. D. Greenland and P. M. McGinnis, *J. Chromatogr.*, 305 (1984) 27.
11 M. Warnhoff, *J. Chromatogr.*, 307 (1984) 271.
12 Y. Oka, K. Kojima, A. Togari, T. Nagatsu and B. Kiss, *J. Chromatogr.*, 308 (1984) 43.
13 G. Achilli, C. Perego and F. Ponzio, *Anal. Biochem.*, 148 (1985) 1.
14 C. A. Seyfried, G. Adam and T. Greve, *Biomed. Chromatogr.*, 1 (1986) 78.
15 C. Kim, M. B. Speisky and S. N. Kharouba, *J. Chromatogr.*, 386 (1987) 25.
16 P. Wester, J. Gottfries, K. Johansson, F. Klintebäck and B. Winblad, *J. Chromatogr.*, 415 (1987) 261.
17 P. Herregodts, Y. Michotte and G. Ebinger, *J. Chromatogr.*, 421 (1987) 51.
18 H. Nohta, A. Mitsui and Y. Ohkura, *Anal. Chim. Acta*, 165 (1984) 171.
19 A. Mitsui, H. Nohta and Y. Ohkura, *J. Chromatogr.*, 344 (1985) 61.
20 H. Nohta, A. Mitsui, Y. Umegae and Y. Ohkura, *Anal. Sci.*, 2 (1986) 303.
21 H. Nohta, A. Mitsui and Y. Ohkura, *Bunseki Kagaku*, 33 (1984) E263.
22 H. Nohta, A. Mitsui and Y. Ohkura, *J. Chromatogr.*, 380 (1986) 229.
23 M. N. H. Irving and R. M. Parkins, *J. Inorg. Chem.*, 27 (1965) 271.
24 W. N. Jenner and F. A. Rose, *Biochem. J.*, 135 (1973) 109.

Journal of Chromatography, 467 (1989) 249–258
Elsevier Science Publishers B.V., Amsterdam — Printed in The Netherlands

CHROM. 21 243

LIQUID CHROMATOGRAPHIC DETERMINATION OF MORPHOLINE AND ITS THERMAL BREAKDOWN PRODUCTS IN STEAM–WATER CYCLES AT NUCLEAR POWER PLANTS

CLAUDE LAMARRE*, ROLAND GILBERT and ANDRÉ GENDRON
IREQ (Institut de Recherche d'Hydro-Québec), 1800 Montée Sainte-Julie, Varennes, Québec JOL 2PO (Canada)
(First received October 24th, 1988; revised manuscript December 27th, 1988)

SUMMARY

Morpholine and its amine breakdown products in aqueous samples were derivatized with dabsyl chloride in the presence of sodium bicarbonate and the resulting precolumn derivatives determined by high-performance liquid chromatography with visible detection at 456 nm. The analytical column was a μBondapak C_{18} reversed-phase device. The breakdown products were determined in the concentration range of 0.25–10 μg/ml in water, with a relative standard deviation of 0.38–7.08%. The amine detection limits were 0.01–0.03 μg/ml for 20-μl injections. Chromatographic analysis of 100-ml grab samples after acidification and concentration demonstrates the success of this technique for determining the quantity (ng/ml) of ammonia, methylamine, ethylamine, ethanolamine and 2-(2-aminoethoxy)ethanol in the thermal cycle at Gentilly 2 nuclear power plant. The recovery for the complete assay procedure varied between 92.0 and 106.0% depending on the product studied.

INTRODUCTION

Morpholine (6–14 μg/ml) is added to the thermal cycle of Hydro-Québec's Gentilly 2 nuclear generating station (CANDU-PHW 600 design) to keep the pH between 9 and 10 in order to counteract the corrosive action of any carbon dioxide present in the system. Recent laboratory investigations have shown that morpholine decomposes at temperatures and pressures close to the operating conditions at Gentilly 2 (260°C and 4.55 MPa) to give ammonia, methylamine, ethylamine, ethanolamine, 2-(2-aminoethoxy)ethanol and some organic acids[1]. These substances may themselves corrode the system components or thermally break down into corrosive organic or inorganic by-products, which may lead to premature equipment failure. Sensitive methods are needed to analyse morpholine breakdown products from operating steam–water systems in order to determine their contribution to the organic contaminants and investigate their corrosiveness for construction materials.

The methods generally used for determining ammonia and aliphatic amines in water samples include gas chromatography[2], continuous-flow fluorometric tech-

0021-9673/89/$03.50

niques[3], ion-exchange separation techniques[4,5] and high-performance liquid chromatography (HPLC). The HPLC techniques described in the literature involve precolumn derivatization with *m*-toluoyl chloride[6], 4-dimethylaminoazobenzene-4'-sulphonyl choride (dabsyl chloride)[7,8], 7-chloro-4-nitrobenzo-2-oxa-1,3-diazole[9], 5-dimethylaminonaphthalene-1-sulphonyl chloride (Dns chloride)[10] or acetylacetone[11] in conjection with either fluorescence, UV–VIS or Raman spectroscopic detection. These techniques were developed specifically to solve analytical problems in the field of biomedical and environmental studies, and none was designed to determine simultaneously ammonia, methylamine, ethylamine, ethanolamine, 2-(2-aminoethoxy)ethanol and morpholine as needed for this particular application.

This work presents a method based on reversed-phase HPLC for separating and quantifying the amines present in the thermal cycle of a nuclear plant via the formation of dabsylated derivatives. It allows the amount (ng/ml or ppb) of amines in water samples to be determined following concentration by evaporation. Amine levels in samples collected at Gentilly 2 are reported.

EXPERIMENTAL

Apparatus

The HPLC studies were performed with a Series 5500 chromatographic system (Varian, Walnut Creek, CA, U.S.A.) equipped with a 20-μl loop injection valve (Model 7126; Rheodyne, Cotati, CA, U.S.A.) and an ultraviolet–visible detector (Model UV-200, Varian) with a cell capacity of 4.5 μl. The detector was set at 456 nm. A μBondapak C_{18} column (30 cm × 3.9 mm I.D., 10 μm; Waters Assoc., Milford, MA, U.S.A.) was used and held at a steady temperature of 30°C. The mobile phase, consisting of a water–ethanol mixture, was pumped at 1.0 ml/min by using gradients. The chromatograms were recorded and integrated on a Varian Model DS 651, Vista Series.

Reagents and solvents

The dabsyl chloride of HPLC grade was obtained from Regis Chemical (Morton Grove, IL, U.S.A.). The sodium bicarbonate, hydrochloric acid and amine used as standards were ACS grade, while the acetone and ethanol were HPLC grade from Anachemia (Montréal, Canada); the ethanol contained 5% (v/v) isopropanol. The water used to prepare the standard solutions was purified by means of a Milli-Q filter system (Millipore, Bedford, MA, U.S.A.) and filtered over a 0.45-μm Millipore membrane for preparation of the chromatographic eluents. The Gentilly 2 samples were collected in polyethylene bottles and stored at 4 to 10°C for a maximum of 2 days before analysis.

Dabsylation procedure for standard solutions

The dabsylation procedure was a modification of that of Lin and Lin Shiau[12]. A 1.0-ml volume of an amine standard solution (0.25–300 μg/ml water) was mixed with 4.0 ml of dabsyl chloride (1.25 mg/ml acetone) and 0.6 ml of an aqueous solution of sodium bicarbonate (25 mg/ml). This mixture was allowed to stand in the dark at ambient temperature for 1 h prior to injecting 20-μl aliquots on the HPLC column (final pH of 9.4).

Dabsylation procedure for steam–water cycle samples

The pH of 100-ml samples was adjusted to 4.0 by a 0.01 *M* hydrochloric acid solution. The acidified samples were concentrated by gently boiling them in a beaker covered with a ribbed watch-glass, and stirring with a magnetic stirrer until the volume was reduced to 2.5 ml, giving a concentration factor in the range of 40. The amines contained in this concentrated solution were subsequently dabsylated as described above.

RESULTS AND DISCUSSION

Spectrophotometric properties

The poor ultraviolet absorptivity of morpholine and its decomposition products calls for precolumn derivatization for trace determination by HPLC. Dabsyl chloride has proven to be a good practical derivatizing agent for amines[7]. The reaction consists in condensing the amine with dabsyl chloride at pH 9.4 and analysing the chromophoric dabsylamides by detection in the visible region. The reaction is described by the following equation:

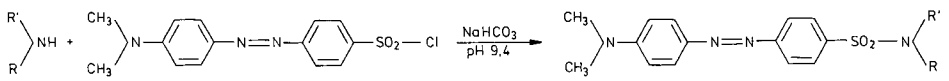

Amine Dabsyl chloride Dabsylamide

The UV–VIS spectra of the dabsylated morpholine and its decomposition products in the range of 300–600 nm were recorded on a Philips PU 8820 UV–VIS spectrophotometer. Table I lists the absorption maxima, λ_{max}, and molar extinction coefficients of these derivatives. Since the absorption maxima occurred at 453.0–458.5 nm, the derivatives were detected at 456 nm in the HPLC analysis. The extinction coefficients of the derivatives were between 6580 and 6930 l mol^{-1} cm^{-1}, showing that a reasonable sensitivity was attained.

Chromatographic separation

Optimum separations of the dabsylamides were obtained on a μBondapak C_{18} column when a gradient elution of the mobile phase was used (this gradient is defined in Table II). These experimental conditions produced the chromatogram of Fig. 1 when a mixture of 10 μg/ml of each dabsylated amine was injected. The elution peaks at 2.8 and 5.3 min are due to the dabsyl chloride and its acid form respectively, whereas the peak at 12.3 min was not identified in the present study. The dabsylamides were eluted between 22 and 29 min; their retention times are reported in Table III. The same-day relative standard deviation of the retention times was less than 0.54%, which indicates an excellent reproducibility in the separation. The chromatogram shows an excellent resolution for the dabsylated ammonia and methylamine, whereas partial separation is noted for dabsylated ethanolamine and 2-(2-aminoethoxy)ethanol as well as for dabsylated ethylamine and morpholine. The stability of the dabsylamides was determined by measuring the signal at 456 nm for different reaction times. Table IV shows that the absorbance for each derivative reached a maximum value in 1 h and

TABLE I

ABSORPTION MAXIMA AND MOLAR EXTINCTION COEFFICIENTS FOR DABSYLATED AMINES

Amine	λ_{max} *(nm)*	ε_{456}[a] *(l mol^{-1} cm^{-1})*	*Ethanol–water*[b] *(%, v/v)*
Ammonia	455.5	6580	60–40
Ethanolamine	456.0	6700	60–40
2-(2-Aminoethoxy)ethanol	455.5	6760	60–40
Methylamine	458.5	6600	63–37
Ethylamine	453.0	6880	70–30
Morpholine	458.5	6930	73–27

[a] Calculated from the chromatographic peaks of dabsylated amines according to the equation proposed by Nishikawa[11]

$$\varepsilon_{456} = (A/L)(WR/M)$$

where A is the absorption at peak height, L the path length of the detector cell (0.4 cm), M the amount of amine injected (mol), W the peak width at half-height (min) and R the flow-rate of the mobile phase (0.001 l/min). Based on standard solutions of 10 μg/ml of amines.

[b] Solvent composition used to study the UV–VIS spectra, corresponding to the gradient at the moment each peak is eluted.

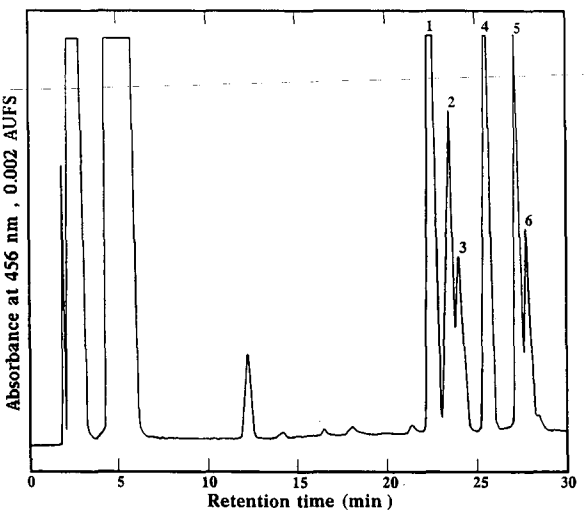

Fig. 1. Chromatogram of an HPLC separation of the dabsyl derivatives of (1) ammonia, (2) ethanolamine, (3) 2-(2-aminoethoxy)ethanol, (4) methylamine, (5) ethylamine and (6) morpholine. A 20-μl amount of an amine mixture (10 μg/ml solution of each amine) was injected. Chromatographic conditions as described in the Experimental section.

TABLE II
GRADIENT ELUTION OF THE MOBILE PHASE
Flow-rate 1.0 ml/min.

Operation	*Time (min)*	*Water–ethanol (%, v/v)*	*Pressure (atm)*	*Elution conditions*
Initial	0	75:25	160	–
Run	0–21	40:60	210	Linear
Hold	21–25	40:60	210	Isocratic
Run	25–35	0:100	180	Linear
Reverse	35–38	75:25	160	Linear
Conditioning	38–50	75:25	160	Isocratic

TABLE III
RETENTION TIMES OF DABSYLATED AMINES

Amine	*Retention time (min), mean[a] ± S.D.*	*R.S.D. (%)*
Ammonia	22.31 ± 0.12	0.54
Ethanolamine	23.23 ± 0.08	0.34
2(2-Aminoethoxy)ethanol	23.89 ± 0.11	0.46
Methylamine	25.61 ± 0.09	0.35
Ethylamine	27.71 ± 0.12	0.43
Morpholine	28.28 ± 0.13	0.46

[a] Average of 30 replicates.

TABLE IV
STABILITY OF DABSYLATED AMINES

Amine[a]	*UV–VIS[b] detector response (456 nm) versus time (h)*							
	0.5	*1*	*3*	*6*	*24*	*48*	*72*	*96*
Ammonia	6.88	8.12	8.05	8.17	8.13	8.08	8.10	8.10
Ethanolamine	2.54	2.33	2.53	2.40	2.48	2.48	2.49	2.48
2-(2-Aminoethoxy)ethanol	1.67	1.91	1.98	2.00	1.98	2.09	1.89	1.89
Methylamine	4.75	4.92	4.75	4.58	4.58	4.62	4.76	4.78
Ethylamine	3.30	3.14	3.24	3.78	3.24	3.39	3.24	3.24
Morpholine	1.53	1.54	1.51	1.50	1.49	1.60	1.53	1.52

[a] Solutions of 10 μg/ml of amine used.
[b] Peak area for a 20-μl injection expressed in $\mu V\ s \cdot 10^5$.

remained constant at least for 96 h when the reaction mixture was stored in the dark at ambient temperature. Consequently, the reaction time of the dabsylation was set at 1 h.

Quantitative response of the method

Table V reports the detection limits, analytical precision and calibration data for the dabsylated amines. The sensitivity achieved is 0.01 μg/ml for ethanolamine, 0.02

TABLE V
DETECTION LIMITS, ANALYTICAL PRECISION AND CALIBRATION DATA FOR DABSYLATED AMINES

Amine	*DL*[a] *(μg/ml)*	*QL*[b] *(μg/ml)*	*Analytical precision*			*Regression line and correlation coefficients*[e]
			Amount of amine[c] *(μg/ml)*	*Response at 456 nm*[d] *mean ± S.D.*	*R.S.D. (%)*	
Ammonia	0.03	0.15	0.25	4.64 ± 0.27	5.82	$y = 80680x + 25456$
			0.50	6.62 ± 0.16	2.41	$r = 0.9999$
			1.00	10.34 ± 0.11	1.06	
			2.50	22.92 ± 0.28	1.22	
			5.00	42.84 ± 0.75	1.75	
			10.00	83.22 ± 0.47	0.56	
Ethanolamine	0.01	0.05	0.25	0.64 ± 0.016	2.50	$y = 23790x - 515$
			0.50	1.13 ± 0.016	1.42	$r = 0.9999$
			1.00	2.38 ± 0.017	0.72	
			2.50	5.70 ± 0.22	3.86	
			5.00	11.86 ± 0.18	1.51	
			10.00	23.77 ± 0.30	1.26	
2-(2-Aminoethoxy)ethanol	0.03	0.15	0.25	0.59 ± 0.04	6.77	$y = 19848x + 1643$
			0.50	1.18 ± 0.07	5.93	$r = 0.9996$
			1.00	2.27 ± 0.12	5.28	
			2.50	4.85 ± 0.29	5.97	
			5.00	10.39 ± 0.30	2.88	
			10.00	19.92 ± 0.52	2.61	

Methylamine	0.02	0.10	0.25	3.14 ± 0.08	2.54	$y = 44807x + 18484$
			0.50	4.09 ± 0.17	4.15	$r = 0.9996$
			1.00	6.32 ± 0.22	3.48	
			2.50	12.34 ± 0.45	3.65	
			5.00	24.99 ± 1.15	4.60	
			10.00	46.46 ± 0.54	1.16	
Ethylamine	0.03	0.15	0.25	1.13 ± 0.08	7.08	$y = 31528x + 2793$
			0.50	2.00 ± 0.10	5.00	$r = 0.9999$
			1.00	3.26 ± 0.08	2.45	
			2.50	8.23 ± 0.14	1.70	
			5.00	15.86 ± 0.42	2.65	
			10.00	31.90 ± 0.12	0.38	
Morpholine	0.03	0.15	5	7.66 ± 0.51	6.65	$y = 6.62x^2 + 15345x - 26040$
			10	15.30 ± 0.72	4.70	$r = 0.999$
			25	33.74 ± 1.31	3.88	
			50	71.30 ± 2.83	3.96	
			100	150.46 ± 5.38	3.57	
			125	211.15 ± 3.46	1.64	
			150	241.50 ± 2.58	1.07	
			175	284.90 ± 2.35	2.58	
			300	516.95 ± 9.83	1.90	

[a] Detection limit.
[b] Quantification limit (QL = 5 DL).
[c] Amine concentration in aqueous sample prior to dabsylation.
[d] Peak area in $\mu V\ s \cdot 10^4$ (average of five replicates).
[e] Number of points: 5.

μg/ml for methylamine and 0.03 μg/ml for ammonia, 2-(2-aminoethoxy)ethanol, ethylamine and morpholine in water samples. These detection limits were estimated with a 95% confidence interval using the statistical approach proposed by McAinsh *et al.* [13]. The dabsylated amines were determined with 0.38–7.1% relative standard deviation in the range of 0.25–10 μg/l, except for morpholine whose concentration varied from 5 to 300 μg/l. An high degree of precision is achieved whatever the amount and nature of the amine involved. The linearity in the response of the UV–VIS detector (peak area) as a function of the amine concentration, expressed by the correlation coefficients, is reported in Table V. Coefficients of over 0.9996 were obtained for the breakdown products, indicating an excellent linearity in calibration. However, dabsylated morpholine shows a second-degree polynomial regression whose characteristics are given in Table V.

HPLC analysis of dabsylated samples of purified water with no amines added revealed the presence of two interference peaks whose elution times correspond to those of dabsylated ammonia and methylamine. The peak areas are constant (ten different preparations) and equivalent to the values caculated for the *y*-intercept of the calibration graphs for dabsylated ammonia and methylamine. The sodium bicarbonate used in the preparation of the derivatives was identified as the source of contamination but in no way does it affect the analytical precision of the method.

Analysis of real samples

The HPLC method was applied to samples collected at Gentilly 2 which revealed the presence of morpholine in the range of 6–14 μg/ml and very small amounts of decomposition products which could not be quantified with the required precision. The samples were then acidified and concentrated by evaporation following the second

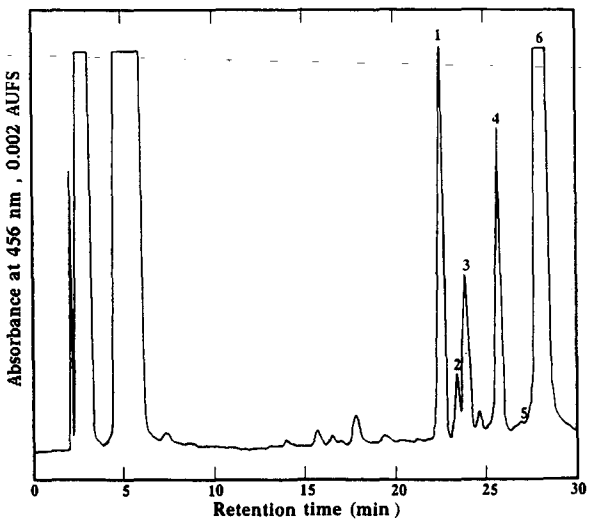

Fig. 2. Typical chromatogram of an HPLC separation of the dabsyl derivatives of morpholine and its amine breakdown products in a sample collected at Gentilly 2 (main steam sample). For peak identification and corresponding concentration, see Fig. 1 and Table VI, respectively. Chromatographic conditions as described in the Experimental section.

TABLE VI
ANALYSIS OF MORPHOLINE AND ITS AMINE BREAKDOWN PRODUCTS IN A GRAB SAMPLE COLLECTED AT GENTILLY 2 AFTER CONCENTRATION AND DABSYLATION

Amine	*Amount (ng/ml)*
Ammonia	28.9
Ethanolamine	20.6
2-(2-Aminoethoxy)ethanol	85.2
Methylamine	54.0
Ethylamine	5.2
Morpholine	6260

TABLE VII
ANALYSIS OF A STANDARD SOLUTION OF AMINES FOLLOWING CONCENTRATION OF THE AQUEOUS SOLUTION BY EVAPORATION

Amine	*Amount (ng/ml)*		*Recovery (%)*	*R.S.D. (%)*
	Added	*Found*[a]		
Ammonia	30	29.8	99.3	1.9
Ethanolamine	20	21.2	106.0	4.3
2-(2-Aminoethoxy)ethanol	85	82.6	96.0	2.6
Methylamine	54	51.1	94.6	3.6
Ethylamine	5	5.4	92.0	8.0
Morpholine	8300	8000	96.4	0.7

[a] Average of five replicates.

procedure described in the Experimental section. The representative chromatographic results illustrated in Fig. 2 and reported in Table VI show that morpholine decomposition products are present in the thermal cycle at Gentilly 2 in quantities of several ng/ml. Elution of low amounts of dabsylated ethylamine beside high amounts of dabsylated morpholine limits the ethylamine determination accuracy to 70%.

The risk of losing amines during the evaporation step, despite the acidification of the sample, was assessed. The results in Table VII reveal that the amounts of amines found after concentration are very similar to those in the initial sample. The recovery percentages were over 92%, with relative standard deviations of 0.7 to 8.0%. For this evaluation, the amines investigated were added to the water samples in proportions close to those determined in real samples (Table VI).

CONCLUSION

The analytical method developed during this research has proven to be a viable procedure for determining trace amounts of amine breakdown products of morpholine and is being used to monitor these compounds in steam–water cycles of nuclear and thermal power plants.

ACKNOWLEDGEMENTS

The authors are indebted to the personnel of the chemical laboratory at Gentilly 2 for their contribution to the success of this research project. Thanks also go to Lesley Kelley-Régnier for her assistance in the preparation of the manuscript.

REFERENCES

1 R. Gilbert and C. Lamarre, *Can. J. Chem. Eng.*, (1989) in press.
2 K. Kuwata, E. Akiyama, Y. Yamazaki, H. Yamazaki, Y. Kuge and Y. Kiso, *Anal. Chem.*, 55 (1983) 2199.
3 T. Aoki, S. Uemura and M. Munemori, *Anal. Chem.*, 55 (1983) 1620.
4 R. Gilbert and R. Rioux, *Anal. Chem.*, 56 (1984) 106.
5 S.P. Bag, *Talanta*, 32 (1985) 779.
6 E. C. M. Chen and R. A. Farquharson, *J. Chromatogr.*, 178 (1979) 358.
7 J. K. Lin and C. C. Lai, *Anal. Chem.*, 52 (1980) 630.
8 H. Koizumi and Y. Suzuki, *J. High Resolut. Chromatogr. Chromatogr. Commun.*, 10 (1987) 173.
9 G. M. Murray and M. J. Sepaniak, *J. Liq. Chromatogr.*, 6 (1983) 931.
10 A. R. Hayman, D. O. Gray and S. V. Evans, *J. Chromatogr.*, 325 (1985) 462.
11 Y. Nishikawa, *J. Chromatogr.*, 392 (1987) 349.
12 J. K. Lin and S.-Y. Lin Shiau, *J. Chinese Biochem. Soc.*, 12 (1983) 47.
13 J. McAinsh, R. A. Ferguson and B. F. Holmes, in E. Reid (Editor), *Trace Organic Sample Handling*, Vol. 10, Wiley, New York, 1981, p. 311.

Journal of Chromatography, 467 (1989) 259–266
Elsevier Science Publishers B.V., Amsterdam — Printed in The Netherlands

CHROM. 21 196

HIGH-PERFORMANCE LIQUID CHROMATOGRAPHY OF GENTIAN VIOLET, ITS DEMETHYLATED METABOLITES, LEUCOGENTIAN VIOLET AND METHYLENE BLUE WITH ELECTROCHEMICAL DETECTION

JOSE E. ROYBAL*, ROBERT K. MUNNS, JEFFREY A. HURLBUT and WILBERT SHIMODA
Animal Drug Research Center, Food and Drug Administration, Denver, CO 80225-0087 (U.S.A.)
(First received July 18th, 1988; revised manuscript received December 19th, 1988)

SUMMARY

High-performance liquid chromatographic conditions are reported for the electrochemical detection (ED) of Gentian Violet, its demethylated metabolites, Leucogentian Violet and Methylene Blue. Gentian Violet, its demethylated metabolites and Leucogentian Violet were separated within 14 min on a cyano column eluted isocratically with methanol–buffer (60:40) as the mobile phase. ED responses for Gentian Violet, Leucogentian Violet and Methylene Blue were linear over the ranges 0.54–6.75, 0.50–25.2, and 5.7–285 ng, respectively. Under these conditions, the compounds were eluted in the following order: Leucogentian Violet, N″-2-tetramethylpararosaniline chloride, N′-1-tetramethylpararosaniline chloride, pentamethylpararosaniline chloride and Gentian Violet. Methylene Blue and Gentian Violet had essentially the same retention time under these parameters. The detection limit for Gentian Violet, its demethylated metabolites and Leucogentian Violet was determined to be 0.1 pmol. A detection limit of 3 pmol was established for Methylene Blue. Detector response, elution, separation, linearity and sensitivity of detection are discussed.

INTRODUCTION

Marketed in 1951, Gentian Violet (GV) (hexamethyl pararosaniline chloride, CAS 548-62-9), also known as Crystal Violet (Colour Index No. 42555) (Fig. 1), has been used as an agent in poultry feeds to inhibit mold and fungal growth. It has also been used to control fungal and intestinal parasites in humans and for other antimicrobial purposes in veterinary medicine.

A point of clarification should be made regarding terminology. Although "Gentian Violet" and "Crystal Violet" are used interchangeably, some distinctions should be mentioned. Crystal Violet is the pure hexamethylpararosaniline chloride, $C_{25}H_{30}ClN_3$. Methyl Violet refers to pentamethylpararosaniline chloride (PENTA). GV, commonly used as an antiseptic, is the commercial product, which is a mixture of Crystal Violet and Methyl Violet that may also contain some tetramethylpararosaniline chloride. The requirement of the *U.S. Pharmacopeia XXI* (USP XXI) for GV is

0021-9673/89/$03.50

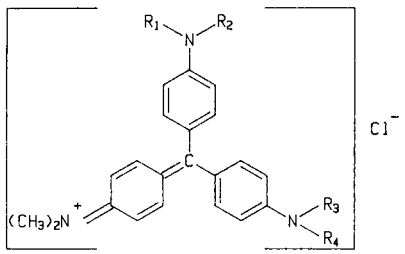

-methylpararosaniline chloride

	R_1	R_2	R_3	R_4
Hexa	CH_3	CH_3	CH_3	CH_3
Penta	CH_3	CH_3	CH_3	H
N'-1 tetra	CH_3	CH_3	H	H
N''-2 tetra	CH_3	H	CH_3	H

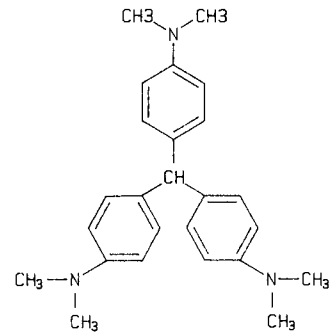

Leucogentian Violet
(Leuco Crystal Violet)
CAS 603-48-5

Fig. 1. Structures of Gentian Violet, its demethylated metabolites and Leucogentian Violet.

that it shall not contain less than 96% Crystal Violet[1]. The USP reference standard for GV was used for all the work reported here.

GV belongs to a class of compounds which have been recognized as animal carcinogens, the triphenylmethane dyes[2]. McDonald *et al.*[3] reported that demethylation of GV occurred in the uninduced liver microsomes of several species examined. The metabolic pattern was found to be similar for mouse, rat, hamster, guinea pig and chicken, regardless of sex. The major demethylated metabolites were PENTA and two isomers, N,N,N′,N′-tetramethylpararosaniline chloride (N′-1-TETRA) and N,N,N′,N″-tetramethylpararosaniline chloride (N″-2-TETRA) (Fig. 1). Intestinal microflora, under anaerobic conditions, are also capable of metabolizing GV; they reduce GV to its leuco derivative (Fig. 1)[4]. According to the National Center for Toxicological Research[5], "This leuco derivative is then structurally similar to the classical aromatic amine carcinogens.".

Methylene Blue (MB) [3,7-bis(dimethylamino)phenothiazin-5-ium chloride, CAS 61-73-4] (Fig. 2), also known as Basic Blue 9 (Colour Index No. 520125) is classified for veterinary use as an antiseptic and disinfectant and as an antidote for cyanide and nitrate poisoning. The Food and Drug Administration/Food Safety and Inspection Service Animal Drug Methodology Task Force expressed concern that MB is considered a mutagen[6–8].

A growing concern over the carcinogenicity of GV, its demethylated metabolites and Leucogentian Violet (LGV) and the mutagenicity of MB necessitates the development of methods to monitor these residues in tissues of food-producing animals. Two criteria of any good residue method are sensitivity and specificity.

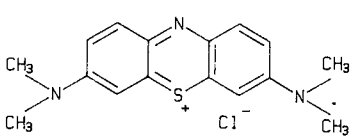

Fig. 2. Structure of Methylene Blue.

Because GV, its demethylated metabolites and MB are all highly colored compounds, detection in the visible range has been the method of choice[9–15]. However, working in the visible range does not provide the sensitivity required for trace/residue analysis (< 1 ppm). The leuco form of GV is not a colored species and gives very poor response in the visible region. As the UV absorptivity of GV, its demethylated metabolites and MB is low, simultaneous determination of all the above compounds using absorption detection is not possible.

This paper describes the development of a high-performance liquid chromatographic (HPLC) system using electrochemical detection (ED) for the simultaneous determination of LGV, GV and its demethylated metabolites. The response and chromatographic behavior of MB are also discussed.

EXPERIMENTAL

Chromatographic system

The HPLC system used in this study was modular in design. The system consisted of a Waters Assoc. (Milford, MA, U.S.A.) dual pump (Models 590 and 510) with a Waters automatic gradient control unit (Model 680) and a Waters universal liquid chromatograph injector (Model U6K). An Alltech Assoc. (Deerfield, IL, U.S.A.) CN reversed-phase, 250 × 4.6 mm I.D., 5-μm column (Stock No. 60138) was used to separate the methylpararosaniline compounds. The mobile phase was methanol–0.1 *M* sodium acetate (60:40) with the pH adjusted to 4.5 with aldehyde-free glacial acetic acid; it also contained 50 mg EDTA disodium salt per liter to help reduce background current and drift. The mobile phase flow-rate was maintained at 0.8 ml/min through the analytical column, which was operated at ambient temperature. The injection volume varied from 5 to 25 μl, depending on the level of analyte.

A Bioanalytical Systems (W. Lafayette, IN, U.S.A.) single channel LC-4B amperometric detector was used for ED determination. The detector cell consisted of a glassy carbon working electrode with a TG-2M thin-layer cell gasket. For this particular work the potential was varied from larger to smaller potentials as the need arose. The reference electrode was Ag/AgCl. The normal operating current range was set at 5 nA for full-scale deflection (f.s.d.).

Reagents and materials

All solvents were distilled-in-glass (Burdick & Jackson Labs., Muskegon, MI, U.S.A.). The glacial acetic acid was ACS grade, aldehyde-free (J. T. Baker, Phillipsburg, NJ, U.S.A.). Water for HPLC was deionized, 18 MΩ, glass-distilled. All solvents used in the HPLC system were filtered through a 0.5-μm Fluoropore filter (No. FHLP 04700, Millipore, Bedford, MA, U.S.A.).

Standard stock solutions of GV, N′-1-TETRA and N″-2-TETRA were prepared in 95% ethanol. Standard stock solutions of LGV, PENTA and MB were prepared in methanol. All subsequent dilutions of standard stock solutions were prepared with methanol.

RESULTS AND DISCUSSION

The initial HPLC was performed by using parameters similar to those reported by Rushing and Bowman[2], which consisted of a Nova-Pak, 150 × 3.9 mm I.D., 5-μm

RP-C_{18} column and a mobile phase of methanol–buffer (85:15) (buffer = 0.01 *M* KH_2PO_4, adjusted to pH 3 with 0.33 *M* H_3PO_4), at a flow-rate of 1 ml/min. The effluent was monitored at 588 nm. This system gave an elution order, in increasing elution time, of N′-1-TETRA, N″-2-TETRA, PENTA and GV. LGV had the longest elution time but had to be monitored at 280 nm.

To apply ED to the chromatographic system described above, a tee was added at the outlet of the HPLC column and a make-up mobile phase was introduced at this junction. The make-up mobile phase was methanol–buffer (20:80) introduced at 0.5 ml/min. The resultant composition of the mixture through the electrochemical detector was methanol–buffer (60:40). Introduction of the make-up solvent was necessary to allow the electrode reaction to occur. A practical guideline was to maintain a minimum concentration of 35% electrolyte solution to convey charge through the ED cell. A modifier (*e.g.*, methanol, acetonitrile, etc.) impedes the charge.

Although this composition gave a good signal (ED response), mixing of the solvents at the tee generated gas which created spiking at the recorder output. After several unsuccessful attempts to remove the gas from the line, a cyano column was used. Higher polarity of this stationary phase allowed for the elution of the compounds at lower modifier content.

Both methanol and acetonitrile were evaluated as modifiers in the HPLC system (Table I). Acetonitrile gave better separation of LGV from the other compounds (GV, PENTA, N′-1-TETRA, N″-2-TETRA, MB) (Fig. 3). Acetonitrile increased the response factor, and therefore the sensitivity, by a factor of 3–8 over that of methanol. The operating column pressure was approximately 1300 p.s.i. with acetonitrile. The column pressure with methanol was approximately 2500 p.s.i. Methanol, on the other hand, resolved not only the LGV from the other compounds but also the N′-1-TETRA from the N″-2-TETRA isomer (Fig. 4).

The main reasons for selecting methanol as the modifier for our system were that it allowed slightly longer retention times for LGV and it resolved the two tetramethyl isomers. For the detection of MB, acetonitrile was preferred because of the increase in sensitivity.

TABLE I

EVALUATION OF METHANOL AND ACETONITRILE AS MODIFIERS

Abbreviations: t_R = retention time; RRT = relative retention time with respect to LGV; RF = response factor; ND = not determined; GV = Gentian Violet; PENTA = pentamethylpararosaniline chloride; N′-1-TETRA = N,N,N′,N′-tetramethylpararosaniline chloride; N″-2-TETRA = N,N,N′,N″-tetramethylpararosaniline chloride; LGV = Leucogentian Violet; MB = Methylene Blue.

Compound	*Methanol*			*Acetonitrile*		
	t_R *(min)*	*RRT*	*RF (nA/ng)*	t_R *(min)*	*RRT*	*RF (nA/ng)*
GV	11.2	1.44	0.59	12.6	2.25	2.21
PENTA	9.8	1.26	ND	11.8	2.11	ND
N′-1-TETRA	9.2	1.18	ND	11.2	2.00	ND
N″-2-TETRA	8.6	1.10	ND	11.0	1.96	ND
LGV	7.8	1.00	1.14	5.6	1.00	6.50
MB	11.2	1.44	0.036	12.0	2.14	0.291

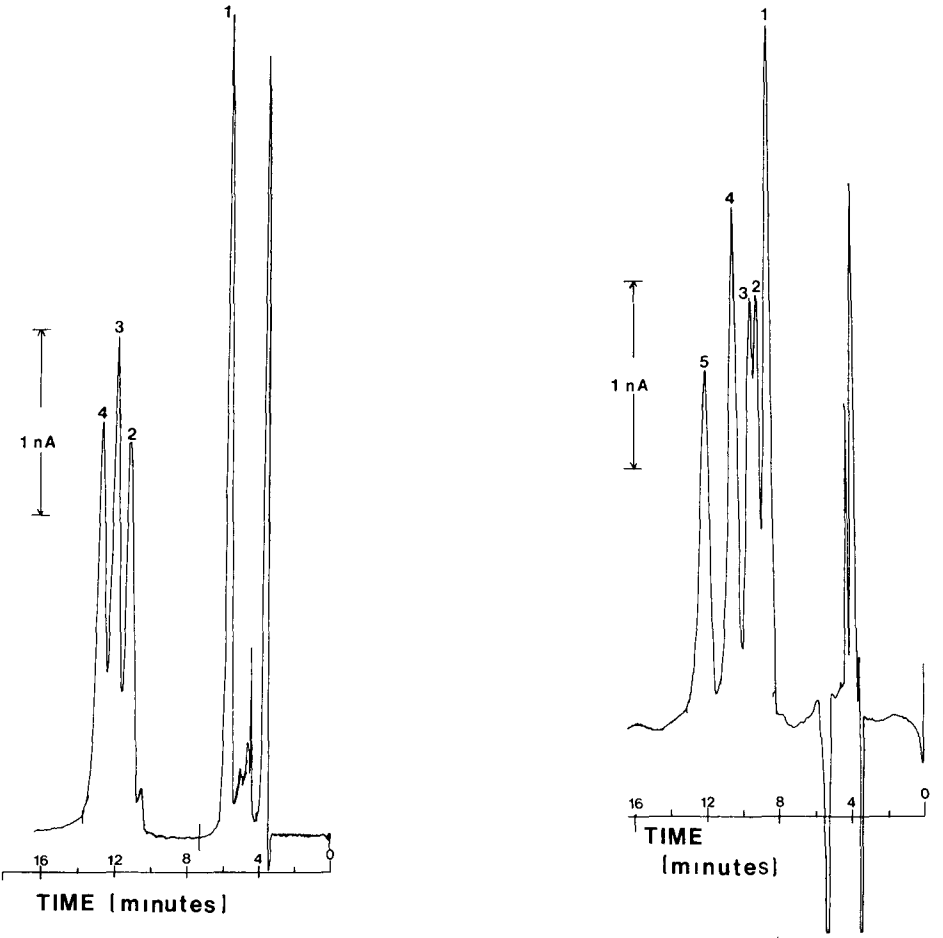

Fig. 3. Typical HPLC chromatogram obtained by using acetonitrile as the modifier, a 5-μl injection of standard mixture, a current-range setting of 5 nA f.s.d. and a potential of +1.000 V *versus* Ag/AgCl reference electrode. Peaks: 1 = Leucogentian Violet (0.101 μg/ml); 2 = N,N,N′,N′-tetramethylpararosaniline chloride (0.102 μg/ml) and N,N,N′,N″-tetramethylpararosaniline chloride (0.076 μg/ml); 3 = pentamethylpararosaniline chloride (0.114 μg/ml); 4 = Gentian Violet (0.107 μg/ml).

Fig. 4. Typical HPLC chromatogram obtained by using methanol as the modifier, a 20-μl injection of standard mixture, a current-range setting of 5 nA f.s.d. and a potential of +1.000 V *versus* Ag/AgCl reference electrode. Peaks: 1 = Leucogentian Violet (0.101 μg/ml); 2 = N,N,N′,N″-tetramethylpararosaniline chloride (0.076 μg/ml); 3 = N,N,N′,N′-tetramethylpararosaniline chloride (0.102 μg/ml); 4 = pentamethylpararosaniline chloride (0.114 μg/ml); 5 = Gentian Violet (0.107 μg/ml).

The elution order from the cyano column with methanol in the mobile phase was LGV, N″-2-TETRA, N′-1-TETRA, PENTA and GV (Fig. 4). MB had essentially the same retention time as GV.

A literature review showed no documentation on the ED of these compounds. Therefore, after establishing the HPLC conditions, the ED characteristics of the compounds of interest were evaluated. It should be noted that equilibration of the

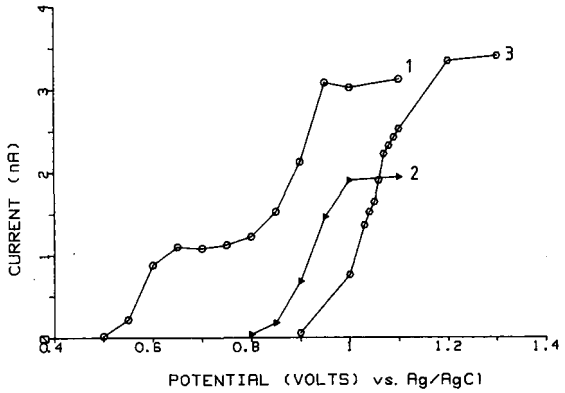

Fig. 5. Voltammogram of (1) Leucogentian Violet, (2) Gentian Violet and (3) Methylene Blue.

mobile phase with the column, for at least 16 h (overnight), was required for proper resolution when the HPLC system was initially set up.

Voltammograms were prepared by injecting standard solutions of each compound and recording the detector response at intervals of 0.050 V over a range of +1.300 to +0.500 V (Figs. 5 and 6). The plots show a very narrow range of oxidation potential, from +0.800 to +1.100 V for GV and its demethylated metabolites, with all of these compounds reaching a maximum at about +1.000 V. LGV showed a greater range of oxidation potential, with an apparent double plateau. This was verified by preparing a voltammogram using smaller increments of +0.020 and +0.010 V for LGV and GV, respectively (Fig. 7), which clearly indicates a two-phase oxidation (double plateau) for LGV. It also verifies that GV undergoes a single oxidation within the potential range of +1.100 to +0.500 V.

Although the reaction scheme is beyond the scope of this paper, a possible mechanism is suggested. The initial (phase one) or more easily oxidized state occurs at +0.650 V; at this potential the leuco (white) base is oxidized to the carbinol (colored)

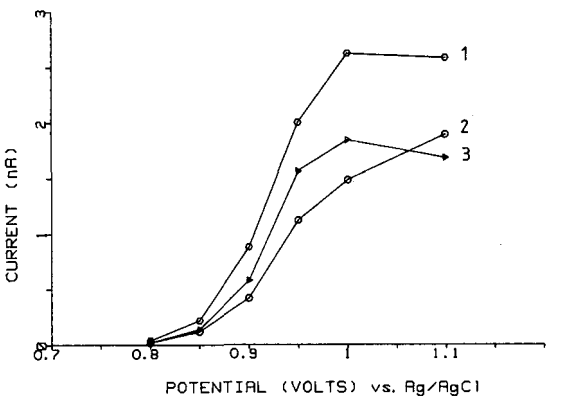

Fig. 6. Voltammogram of pentamethylpararosaniline chloride and two tetramethylpararosaniline chloride isomers. 1 = PENTA; 2 = N′-1-TETRA; 3 = N″-2-TETRA.

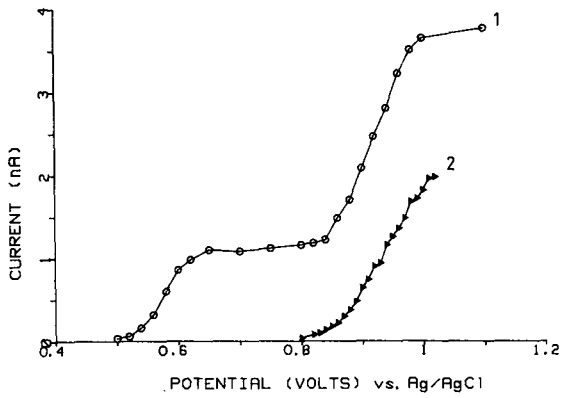

Fig. 7. Voltammogram of (1) Leucogentian Violet and (2) Gentian Violet.

base. Normally, once the triphenylmethane is oxidized to the triphenylcarbinol derivative, the reaction stops because the tertiary alcohol cannot be oxidized further without destruction of the benzene ring. Unlike the triphenylmethane, however, the N,N-dimethylaniline derivatives can be oxidized further under acidic conditions, leading to a loss of a methyl group on the dimethylaniline part of the molecule[16]. This reaction is reflected by phase two at +1.000 V.

In the case of MB, oxidation is more difficult. Although the reduction of MB to its leuco base is well documented[17], oxidation of MB has not been reported. We suspect that a demethylation of the dimethylaniline group similar to that of the methylpararosanilines is involved, but is occurring at the higher potential of +1.200 V (Fig. 6).

Linearity plots of GV, LGV and MB were prepared. Data for these plots were obtained using different current-range settings, from 2 to 50 nA f.s.d., to accommodate the wide range of amounts injected. The response was shown to be linear over the range 0.5–25 ng for GV and LGV and 5–300 ng for MB. From these plots, it was evident that the response of LGV is approximately twice that of GV, and the decreased response of MB with respect to GV and LGV is demonstrated (Table I). Linear regression data and correlation coefficients (r) for these plots are listed in Table II.

In summary, an HPLC–ED system was developed which can simultaneously detect, resolve and quantitate GV, its demethylated metabolites and LGV within 14 min. The detection limits of GV, its demethylated metabolites and LGV were

TABLE II

LINEAR REGRESSION DATA ($y = mx + b$) AND CORRELATION COEFFICIENTS (r) FOR PLOTS OF GV, LGV AND MB

Compound	m (ng^{-1})	b	r
GV	0.6475	−0.2438	0.9975
LGV	1.3008	−0.4305	0.9978
MB	0.0318	0.1973	0.9925

determined to be 0.1 pmol at a 3 × noise level at +1.000 V and a current range of 0.5 nA f.s.d. Additionally, the system has the versatility to detect and reliably quantitate MB at levels as low as 3 pmol. The system meets the requirements of sensitivity and specificity described earlier.

In future work we plan to apply this system to the determination of the residues of these compounds in animal tissues.

ACKNOWLEDGEMENTS

The authors are grateful to Dr. Jerome J. McDonald, Research Chemist, National Center for Toxicological Research, Division of Comparative Toxicology, for graciously providing the chemical standards of LGV, PENTA, N′-1-TETRA and N″-2-TETRA used in this study and for furnishing the latest toxicological data. We would also like to thank Michael L. Middleton, Research Assistant, Food and Drug Administration, Animal Drug Research Center, for the computer-generated graphics and his assistance in typing and revising this manuscript.

REFERENCES

1 *U.S. Pharmacopeia XXI–National Formulary XVI*, U.S. Pharmacopeial Convention, Rockville, MD, 1985, p. 459.
2 L. G. Rushing and M. C. Bowman, *J. Chromatogr. Sci.*, 18 (1980) 224.
3 J. J. McDonald, C. R. Breeden, B. M. North and R. W. Roth, *J. Agric. Food Chem.*, 32 (1984) 596.
4 J. J. McDonald and C. E. Cerniglia, *Drug Metab. Dispos.*, 12 (1984) 330.
5 National Center for Toxicological Research, *Final Report—Metabolism of Gentian Violet in Chickens*, NCTR Technical Report for Experiment No. 6040, May 1985.
6 D. G. MacPhee and F. P. Imray, *Mutat. Res.*, 53 (1978) 359.
7 K. T. Chung, G. E. Fulk and A. W. Andrews, *Appl. Environ. Microbiol.*, 42 (1981) 641.
8 G. Speit and W. Vogel, *Mutat. Res.*, 59 (1979) 223.
9 O. Serafimov, C. Kopp and M. Berg, *Prax. Naturwiss. Chem.*, 35 (1986) 35.
10 Rijksuniversiteit Leiden, *Neth. Appl.*, NL81 05, 758, July 1983.
11 P. S. Mandal, S. K. Talwar and P. R. Pabrai, *Indian J. Pharm. Sci.*, 43 (1981) 144.
12 S. K. Talwar, Y. K. S. Rathore and P. R. Pabrai, *Indian J. Pharm. Sci.*, 46 (1984) 179.
13 S. K. Talwar and P. R. Pabrai, *Indian J. Pharm. Sci.*, 45 (1983) 238.
14 S. L. Abidi, *J. Chromatogr.*, 255 (1983) 101.
15 L. Gagliardi, G. Cavazzutti, A. Amato, A. Basili and D. Tonelli, *J. Chromatogr.*, 394 (1987) 345.
16 C. R. Noller, *Chemistry of Organic Compounds*, W. B. Saunders, Philadelphia, London, 2nd ed., 1958, Ch. 27–31.
17 G. Papeschi, M. Costa and S. Bordi, *J. Electrochem. Soc.*, 128 (1981) 1518.

Journal of Chromatography, 467 (1989) 267–271
Elsevier Science Publishers B.V., Amsterdam — Printed in The Netherlands

CHROM. 21 362

Note

Stability of silica packing materials towards a mixed aqueous–organic eluent at alkaline pH

B. LAW* and P. F. CHAN

Safety of Medicines Department, ICI Pharmaceuticals, Alderley Park, Macclesfield, Cheshire SK10 4TG (U.K.)

(First received December 7th, 1988; revised manuscript received January 30th, 1989)

The use of silica-based packing materials with alkaline eluents is frowned upon by most practising chromatographers. It is a commonly held belief that columns used with eluents having a pH >7.5 will undergo rapid loss of performance due to dissolution of the silica matrix. This view, which can be traced back to a single report[1], has been perpetuated by a number of leading workers in the field, as well as by most manufacturers of high-performance liquid chromatography (HPLC) packing materials despite more recent reports to the contrary. Wehrli *et al.*[2] studied the dissolution of reversed-phase materials in different eluent types using atomic absorption spectrophotometry. They concluded that when using acetonitrile as the organic modifier, the rate of dissolution was very dependent on the aqueous content and the type of base in the eluent, *i.e.*, ammonia, alkylamine, sodium hydroxide or quaternary ammonium salt. Similar findings were obtained by Atwood *et al.*[3] who showed that for non-bonded silica, dissolution was reduced when the eluent had a high methanol or acetonitrile content. They also noted a sharp increase in dissolution with temperature, and they showed how the inclusion of a "sacrificial" column (often misnamed as a guard column) between pump and injector could effectively minimise silica dissolution.

In the analysis of basic compounds, the use of silica with mixed aqueous–organic eluents of high pH (typically 9 to 10) offers many advantages over reversed-phase methods. In presenting data on such systems, one of us (B.L.) has often faced scepticism from other workers on the viability of such systems due to the above mentioned belief. Apart from a report by Wheals[4], who stated that silica dissolution using such a system was not a problem providing the organic content was high and ammonia was the source of hydroxyl ions, no hard chromatographic data existed to support the stability of such systems.

The aim of the present work therefore was to produce quantitative data to demonstrate the stability of silica in the presence of an organic-rich alkaline eluent.

EXPERIMENTAL

Materials

Chromatography was carried out using a Waters 6000A HPLC pump, a Rheodyne 7125 injection valve and an LDC UV-III fixed-wavelength (254 nm) UV detec-

tor. The column was 200 × 4.6 mm I.D. packed with Spherisorb S5W silica (batch No. 5068) with characteristics typical of this type of material.

The eluent was methanol–ammonium acetate buffer (9:1), pH 9.2 measured using a Whatman PHA270 pH meter calibrated with aqueous standards. The buffer (pH 10.0) was prepared from ammonia (65 ml; 25%, w/v), acetic acid (11 ml) both AnalaR grade and water 848 ml.

Two test mixtures were used; the first to study chromatographic efficiency contained diphenylamine (t_0 marker), caffeine, propranolol, chlorcycloguanil and benzethonium chloride. The second, which was used to study changes in selectivity contained the antimalarial drugs proguanil and chlorproguanil and their metabolites, cycloguanil, 4-chlorophenylbiguanide, chlorcylcoguanil and 3,4-dichlorophenylbiguanide. These solutions were prepared in methanol and injections of approximately 10 μl were made.

Method

The column was packed using a conventional slurry technique and after conditioning with 45 ml of eluent (*ca.* 20 column volumes) tested using the two mixtures with the eluent delivered at 1 ml/min.

To simulate long and continued use, the following procedure involving recycling of the eluent was adopted.

After the initial testing 500 ml of fresh eluent was placed in the reservoir and the eluent recycled at a flow-rate of 2 ml/min, the waste from the column being fed back directly to the eluent reservoir. This system was run continuously for over three weeks, the eluent being replaced by a fresh 500-ml batch every morning, with the exception of weekends when the volume of eluent was 1 l. At appropriate intervals, using fresh eluent and a flow-rate of 1 ml/min the column was retested.

After 63 l of eluent had passed through the column, the packing material at the inlet was discoloured and showed a slight depression. The top 2–3 mm were removed and replaced with fresh packing material and the recycling process continued. The top mesh was also replaced after 3 l of eluent had passed through the column.

All measurements were made in duplicate or triplicate, efficiency (N) reduced plate height (h) and capacity factor (k') were calculated using the following standard relationships:

$$N = 5.54\,(t_R/W_{1/2})^2;\; k' = (t_R - t_0)/t_0;\; h = L/(Nd_p)$$

where t_R and t_0 are the retention times of the compound under investigation and the unretained marker, respectively. $W_{1/2}$ is the width of peak at half height, L the column length and d_p the particle diameter.

RESULTS AND DISCUSSION

It is common practice where alkaline eluents are used to employ a sacrificial or saturator column between the pump and injection valve. However, to present a worst case, this precaution was omitted in the present work. The recycling of the eluent —a common practice in some laboratories— will obviously have had some protecting effect on the column. Given the length of the experiment (over 3.5 weeks) and the fact

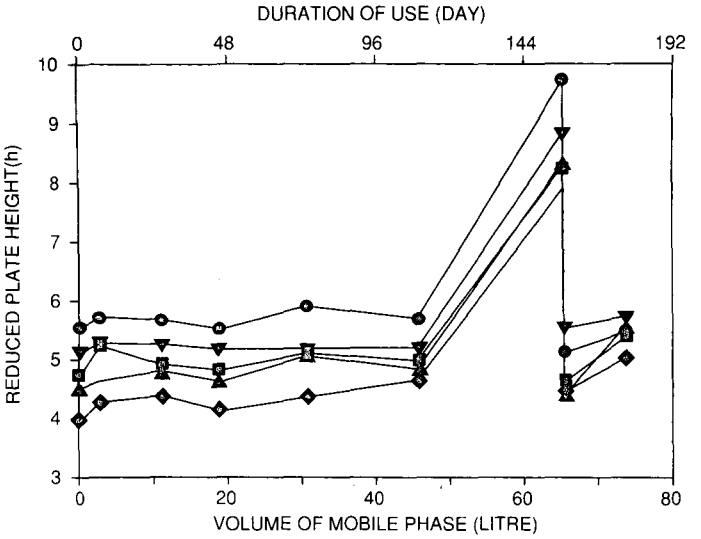

Fig. 1. The variation in reduced plate height (h) for five compounds as a function of the volume of eluent passed through the column and duration of use. ● = Diphenylamine; ▲ = caffeine; ■ = propranolol; ◆ = chlorcycloguanil; ▼ = benzethonium chloride.

that the eluent was renewed every day (except weekends) the benefit of this practice to the present case was considered to be minimal.

Efficiency

The change in chromatographic efficiency as a function of the volume of mobile phase passed through the column was measured using five compounds covering the k' range 0 (diphenylamine) to 8.6 (benzethonium). The data, reported as reduced plate height (h) are shown in Fig. 1. Although there were small variations in efficiency up to 46 l, most of these changes were not significantly different from the starting values ($p < 0.05$). Between a mobile phase volume of 46 and 65 l, however, there was a dramatic loss in efficiency as shown by increased h values. Efficiency was easily restored however, by repacking the top of the column, and with the exception of chlorcycloguanil, the restored reduced plate height values were not significantly different ($p < 0.05$) to the starting values.

The data show that there is little significant change in chromatographic efficiency when 45 l of eluent has passed through the column. Assuming a standard flow-rate of 1.0 ml/min and a 7-h working day, then this represents 107 actual days or the equivalent of 5 months continued use without significant loss in efficiency. By simply repacking the top of the column, use can be further extended to at least 74 l, 176 days, or the equivalent of nearly 9 months of routine use.

Selectivity

The biguanide mixture was chosen for this part of the study because previous experience[5] had shown these compounds to be good markers for selectivity changes using this type of HPLC system.

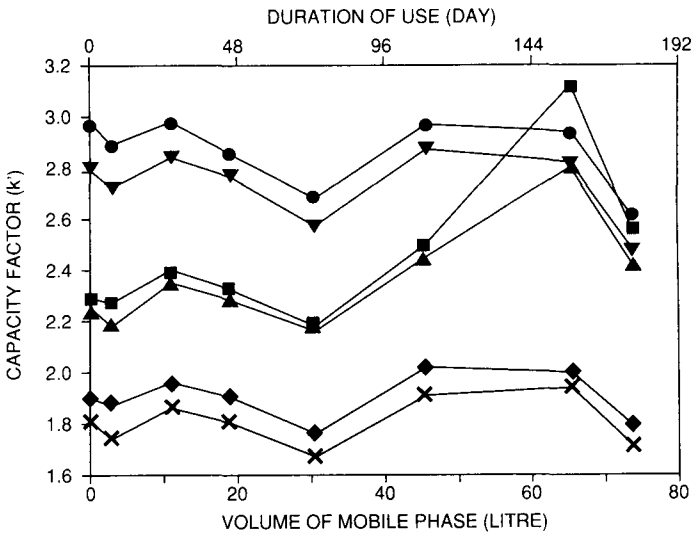

Fig. 2. The variation in capacity factor (k') for six antimalarial drugs and metabolites as a function of the volume of eluent passed through the column and duration of use. × = Proguanil, ◆ = chlorproguanil; ▲ = 3,4-dichlorophenylbiguanide; ■ = chlorophenylbiguanide; ▼ = chlorcycloguanil; ● = cycloguanil.

The variation in k' for the biguanide compounds as a function of mobile phase volume is shown in Fig. 2. Between 0.045 and 45 l (107 days) the variation in k' was relatively small (< 10% of the mean). The profiles for most of the compounds over this range were roughly parallel indicating that selectivity did not vary a great deal. Between 45 and 65 l (107 to 155 days), however, there was a significant change in k', coincidental with the loss in efficiency. At this point the retention of the two desalkyl metabolites increased relative to those of the other compounds in the mixture, resulting in a change in the order of elution. Repacking the top of the column resulted in a further change in selectivity; although the excellent separation between the four metabolites observed intially could not be regained.

Column backpressure

After 3 l of the mobile phase had passed through the column (approximately 7 days), the backpressure during the analytical phase of the work (flow-rate 1 ml/min) increased to approximately 3000 p.s.i. Replacing the top mesh re-established the pressure at 900 p.s.i. where it remained throughout the remainder of the work. This problem could be avoided in general work through the use of a sacrificial column or an in-line filter to remove particulate matter from the eluent. However, the similar backpressure at the start and end of the experiment, indicated that silica dissolution leading to settling of the bed or blocking of the bottom mesh with fines was not occurring.

CONCLUSIONS

These data indicate that contrary to popular belief silica-based packing materials can show excellent stability when used with certain types of alkaline eluent. Using

bare silica —which is more prone to dissolution than bonded materials[2,3]— with an eluent of 90% methanol, ammonia as the source of hydroxyl ions and a pH of 9.2, chromatographic efficiency was stable and reproducible for 107 days equivalent to 5 months of regular use. This could be extended to 176 days (*ca.* 9 months) by repacking the top of the column. A significant change in selectivity was observed after 107 days use which could not be restored to the original condition. It is possible that this change was due to irreversible adsorption onto the column which could be avoided by the use of a sacrificial and/or guard column in the system. These precautions were omitted in this experiment to present an aggrevated situation, although they are to be recommended for routine use.

REFERENCES

1 Cs. Horváth, W. Melander and I. Molnár, *Anal. Chem.*, 49 (1977) 142.
2 A. Wehrli, J. C. Hildenbrand, H. P. Keller, R. Stampfli and R. W. Frei, *J. Chromatogr.*, 149 (1978) 199.
3 J. G. Atwood, G. J. Schmidt and W. Slavin, *J. Chromatogr.*, 171 (1979) 109.
4 B. B. Wheals, *J. Chromatogr.*, 187 (1980) 65.
5 B. Law, unpublished results.

Journal of Chromatography, 467 (1989) 272–275
Elsevier Science Publishers B.V., Amsterdam — Printed in The Netherlands

CHROM. 21 354

Note

Use of an inexpensive low-temperature liquid crystal stationary phase for the study of volatile oil constituents with short gas chromatographic retention times

T. J. BETTS
School of Pharmacy, Curtin University of Technology, GPO Box U 1987, Perth, W. Australia 6001 (Australia)
(Received December 15th, 1988)

I have previously reported on the use of gas chromatographic (GC) relative retention times to characterise the various constituents of volatile oils: long retention time (t_R) constituents such as aromatics and sesquiterpenoids compared to geraniol[1]; and medium t_R constituents such as monoterpenoids against linolol[2,3]. Whilst the relatively shorter t_R aromatic anethole or the relatively longer t_R monoterpenoid citronellol can be examined against either geraniol or linolol, the ability of the latter to characterise monoterpene hydrocarbons with their very short t_R is limited by the discriminatory ability of the two usual stationary phases. These stationary phases are substituted polysiloxanes and polyethyleneglycols, and they function as normal liquids, which are isotropic in that the molecules of their fluids are randomly arranged, and they reveal inability to distinguish between substances such as limonene and cineole, despite their different molecular shapes. Such shapes, however, should provide discrimination for liquid phases with an ordered molecular arrangement, as is provided by liquid crystals.

The use of liquid crystals for GC stationary phases dates back to the early 1960s. Both the early studies[4,5] used azoxy-di-(aromatic ethers). Polysiloxanes with aryl, triaromatic side chains are the modern form of liquid crystal phases [6] but these all only change from the glassy to the desired smectic state, with layers of parallel molecules, at about 120°C or more. Witkiewicz[7] reviewed the situation in 1982 pointing out that "so far only thermotropic liquid crystals have been used (where) the liquid crystalline state is established after the solid is melted. The resulting liquid preserves, in a certain temperature range, properties intermediate between those of the solid and the liquid". This molecularly ordered liquid crystal is "well suited for the separation (of) many substances (*e.g.* isomers) that have identical or very similar boiling temperatures (while) their separation on ... most conventional (especially nonpolar) stationary phases ... is very difficult or impossible". He commented "that certain lyotropic systems could also find application in GC, for instance in the form of mixed phases. (These) show liquid crystalline properties over a wide range of concentrations in a suitable solvent". They should be useful at temperatures below 100°C, which are appropriate for examining the monoterpene hydrocarbons that occur in volatile oils.

0021-9673/89/$03.50

Friberg *et al.*[8] have studied the solubilization of hydrocarbons in lyotropic solutions of lecithin in ethylene glycol. Recently, Belmajdoub *et al.*[9] have recorded the phase behaviour of lyotropic solutions of cetyl-trimethylammonium bromide (CTAB) in formamide, and a 50% (w/v) solution of CTAB is examined here for its GC potential as stationary phase for resolving monoterpene hydrocarbons and other short t_R constituents of volatile oils. Byrd and Acree[10] were the first to use such a phase and found in 1988 that *p*- and *o*-xylenes were resolved on this stationary phase. They also found that nitropropane and butanone have shorter t_R than xylenes on such a column[11], which is the reverse of what occurs with conventional isotropic liquid phases.

EXPERIMENTAL

Apparatus

A Pye GCD gas chromatograph fitted with flame ionisation detector and Hewlett-Packard 3390A and 3380A recorder integrators were used. Glass columns (1.5 m × 4 mm I.D.) were packed as indicated in Table I. The weighed CTAB and formamide were dissolved in acetone and dried with the weighed support in a rotary evaporator. This column needs to be freshly prepared and not subjected to high temperature pretreatment. In contrast, the two polysiloxane columns have had extensive previous use.

Materials

The materials used are indicated in Table I.

Method

Repeated injections were made from a microsyringe which had been filled and "emptied" of materials, after rinsing with *n*-heptane. This gave a "standard" peak for the alkane along with the test solute.

TABLE I

RELATIVE RETENTION TIMES (α-PINENE = 1.00) AT 80°C ON PACKED COLUMNS

Mobile phase, nitrogen at a flow-rate of *ca.* 40 ml min^{-1} at the flame ionization detector exit.

Volatile oil constituent (and source)	t_R *vs. α-pinene (BDH)*		
	Fresh 15% CTAB–formamide (1:1)[a]	*Fully methyl polysiloxanes (old)*[b]	
		2% SP-2100	*2% OV-1*
n-Heptane[c] (Mallinckrodt)	0.31 – *0.32* – 0.33	0.37	0.49
β-Pinene (turpentine oil)	1.47 – *1.48* – 1.50	1.25	1.19
Limonene (BDH)	2.21 – *2.27* – 2.40	1.69	1.59
p-Cymene (TCI)	2.90 – *3.04* – 3.21	1.60	1.54
1,8-Cineole (Faulding)	3.17 – *3.45* – 3.72	1.69	1.58

[a] *Average* and range of six results on different columns with t_R for α-pinene 1.61 – 2.18 min. Support was Chromosorb WAW 80–100.

[b] Supports were Chromosorb WAW DCMS 80–100 for SP-2100, and Diatomite CQ 120–150 for OV-1.

[c] *n*-Heptane was used as standard.

RESULTS AND DISCUSSION

Results are presented in Table I. About 80°C was found to be the most satisfactory operating temperature for the CTAB–formamide liquid crystal phase. Formamide is presumably lost during use as the column packings needed replacing periodically to restore performance. Any such "bleed" of formamide will not affect the detector, as it does not respond to substances like formic acid. Byrd and Acree[11] indicate that a relative decrease in the formamide present may convert the mixed liquid crystal to a lamellar mesophase from the initial hexagonal one, although they found that "retention times were reproducible over a two-week period".

The non-polar fully methyl polysiloxanes should show the greatest possible discrimination between the very low polarity constituents of volatile oils examined that can be achieved with conventional liquid stationary phases. This is very poor despite their different molecular shapes and chemical natures. Limonene is a fairly flat monocyclic hydrocarbon, cymene is a flat aromatic hydrocarbon and cineole is a box-like dicyclic ether. Table I indicates that the inexpensive liquid crystal phase improves the resolution between such substances, and it was found that mixtures of these three could be resolved on a packed column of CTAB–formamide with the recorder returning nearly to baseline between the three peaks, something unachievable on the methyl polysiloxane columns.

In turpentine oil, β-pinene is clearly better resolved from α-pinene on the liquid crystal column than on methyl polysiloxane packed columns. Pumilio pine oil revealed its α- and β-pinenes and limonene amongst other early peaks on the liquid crystal. Lime oil clearly revealed its *p*-cymene content in the presence of over 50% limonene. Small amounts of *p*-cymene and limonene could also be detected in various eucalyptus oils containing 70% or more cineole, so confirming the efficiency of the CTAB–formamide liquid crystal phase. If such oils contain long t_R constituents, they will remain in the column, the packing of which should be replaced after a few days use.

For characterising the various constituents of volatile oils my procedures are currently as below, considering them in three groups, which have some overlap. (A) Short t_R, *e.g.* hydrocarbons including monoterpenes *vs.* α-pinene at 80°C, packed column of CTAB–formamide; (B) medium t_R, *e.g.* oxygenated monoterpenoids *vs.* linalol; and (C) long t_R, *e.g.* aromatics and sesquiterpenoids *vs.* geraniol. Both B and C at 135°C, capillaries of methyl–polysiloxane and polyethylene glycol 20M used.

ACKNOWLEDGEMENTS

Thanks are due to Dr. W. E. Acree, Jr. for encouragement and to Mr. B. MacKinnon for preparing the CTAB–formamide columns.

REFERENCES

1 T. J. Betts, *J. Chromatogr.*, 449 (1988) 312.
2 P. N. Breckler and T. J. Betts, *J. Chromatogr.*, 53 (1970) 163.
3 T. J. Betts, *J. Chromatogr.*, 294 (1984) 370.
4 H. Kelker, *Fresenius' Z. Anal. Chem.*, 198 (1963) 254.

5 M. J. S. Dewar and J. P. Schroeder, *J. Am. Chem. Soc.*, 86 (1964) 5235.
6 K. E. Markides, H.-C. Chang, C. M. Schregenberger, B. J. Tarbet, J. S. Bradshaw and M. L. Lee, *J. High Resolut. Chromatogr. Chromatogr. Commun.*, 8 (1985) 516.
7 Z. Witkiewicz, *J. Chromatogr.*, 251 (1982) 311.
8 S. E. Friberg, C. Solans and L. Gan Zuo, *Mol. Cryst. Liq. Cryst.*, 109 (1984) 159.
9 A. Belmajdoub, J. P. Marchal, D. Canet, I. Rico and A. Lattes, *New J. Chem. (Nouv. J. Chim.)*, 11 (1987) 415.
10 J. M. Byrd and W. E. Acree, *Mol. Cryst. Liq. Cryst. Lett.*, 5 (1988) 163.
11 J. M. Byrd and W. E. Acree, personal communication, Liquid Crystal Institute, Kent State University, Kent, OH; now at the Department of Chemistry, University of North Texas, Denton, TX.

Journal of Chromatography, 467 (1989) 276–278
Elsevier Science Publishers B.V., Amsterdam — Printed in The Netherlands

CHROM. 21 315

Note

Use of ^{1}H NMR spectroscopy in the selection of the mobile phase for high-performance liquid chromatographic monitoring of the synthesis of ibuproxam

J. ŽMITEK*, T. ŠTENDLER, B. RUSJAKOVSKI, D. KOCJAN and B. BOŽNAR
LEK, Pharmaceutical and Chemical Works, Research and Developement Department, Celovška 135, 61000 Ljubljana (Yugoslavia)
(Received January 3rd, 1989)

A convenient method for the synthesis of ibuproxam, 2-(4-isobutylphenyl)-propiohydroxamic acid (**3**), which has analgesic, antipyretic and anti-inflammatory properties[1–3], from ibuprofen (**4**)[4] via the corresponding anhydride (**2**) (Fig. 1) has been developed[5].

The developement of such a synthetic method must be supported by appropriate analytical methods capable of determining all the reactants and products quantitatively over a wide range of concentrations (even less than 1% relative). However, the instability of **2** towards solvolysis is a crucial problem for the development of a suitable high-performance liquid chromatographic (HPLC) method. Therefore, we first studied its stability by ^{1}H NMR spectroscopy.

EXPERIMENTAL

Melting points were measured on a Kofler micro hot-stage. IR, mass, UV and ^{1}H NMR spectra were obtained on a Perkin-Elmer 727B IR spectrometer, a CEC 21-110B mass spectrometer, a Hewlett-Packard 8451A diode-array UV spectrometer and Varian EM-360 60 Hz NMR spectrometer at 25°C with tetramethylsilane (TMS) as internal standard, respectively.

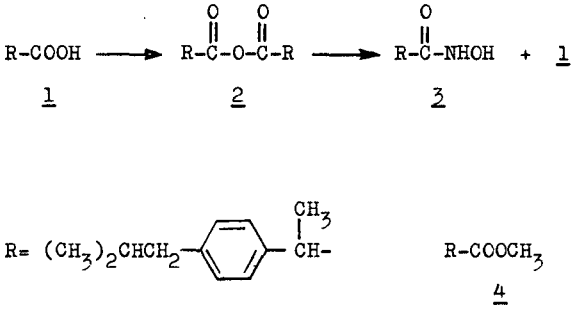

Fig. 1. Synthesis of ibuproxam.

0021-9673/89/$03.50

HPLC was carried out using an LDC/Milton Roy Constametric III pumping system with a Rheodyne 7125 sampling valve.

^{1}H NMR determinations of the stability of **2** were based on chemical shift differences for CH–CH_3 in anhydride **2** (τ 8.58), ibuprofen (**1**) and the methyl ester **4** (τ 8.53) and $COOCH_3$ in **4** (τ 6.4) in methanol (Fig. 2). The same differences were used for determinations of the stability of **2** in the presence of methanol in deuterated aprotic solvents such as chloroform, dichoromethane, carbon tetrachloride and acetonitrile, and CH–CH_3 chemical shift differences for **1** (τ 8.53) and **2** (τ 8.58) were used for studies in the same solvents in the presence of water.

Standards of **1**[4], **2**[5], **3**[1] and **4**[6] were prepared according to the literature. The UV absorption maxima obtained were 222 nm for **1** and **2** and 210 nm for **3**.

RESULTS AND DISCUSSION

Stability studies of **2** in different aprotic and protic solvents and in mixtures by ^{1}H NMR spectroscopy showed that solvolysis in methanol at 25°C is relatively fast and is completed in about 24 h, whereas **2** is stable in aprotic solvents such as chloroform, dichloromethane, carbon tetrachloride and acetonitrile when less than 5% of a protic solvent such as methanol or water is present. However, the presence of 10% of a protic solvent causes significant solvolysis.

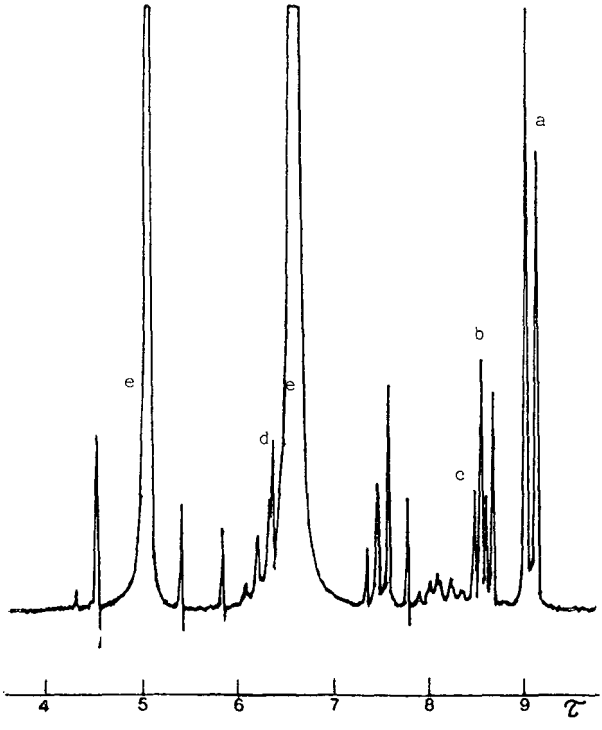

Fig. 2. ^{1}H NMR spectrum of **2** in methanol after 80 min. Signals for (a) $(CH_3)_2CHCH_2$ in **1**, **2** and **4**; (b) CH_3CH in **2**; (c) CH_3 in **1** and **4**; (d) CH_3O in **4**; (e) methanol.

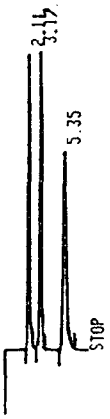

Fig. 3. Chromatogram of 0.1 mg/ml of **2** (retention time 2.11 min), ibuprofen (**1**) (3.17 min) and ibuproxam **3** (5.35 min) standards.

As shown by independent experiments, hydrolysis was catalysed by addition of $Eu(fod)_3$, to increase the chemical shift differences. Although $Eu(fod)_3$ significantly influences the chemical shifts, particularly those of the isopropionic acid part of the molecules, we were unable to use ^1H NMR as a simple and direct tool to follow the reaction course quantitatively.

From the stability of two indifferent solvents and mixtures it was clear which solvent or mixture could be used and the appropriate phase was chosen. The HPLC method developed on the basis of these results is as follows: metal column (150 × 4.6 mm I.D.), LiChrosorb NH_2 (5 μm) as stationary phase, acetonitrile–0.01 *M* tartaric acid (100:1.5) as eluent, flow-rate 1 ml/min and UV detection at 220 nm.

With the above mobile phase **2** is stable and good resolution is achieved (Fig. 3). The method shows good reproducibility (relative standard deviation = 0.5%), a wide range of linearity (from below 1 ng/ml to 0.1 mg/ml for **1**, **2** and **3**) and low detection limits (1 ng/ml for **1** and 0.1 ng/ml for **2**).

This HPLC method has been used successfully not only for the developement of the synthetic method but also for in-process control on a production scale and for the final product quality control.

REFERENCES

1 G. Orzalesi and R. Selleri, *Ger. Offen.*, DE 24 00 531, 1977.
2 S. Chemici, F. Innocenti and G. Orzalesi, *J. Pharm. Sci.*, 69 (1980) 521.
3 E. Arrigoni-Martelli, *Drugs Future*, 2 (1977) 808.
4 S. Nicholson and S. S. Adams, *G. Brit. Pat.*, GB-P 971 700, 1961.
5 *Eur. Pat.*, EP 0 203 379 A1, 1986.
6 *Ger. Pat.*, DE 26 58 610 C2, 1982.
7 C. S. Springer and R. E. Sievers, *Inorg. Chem.*, 6 (1967) 1105.

Journal of Chromatography, 467 (1989) 279–284
Elsevier Science Publishers B.V., Amsterdam — Printed in The Netherlands

CHROM. 21 239

Note

Methylation of ω-oxocarboxylic acids with diazomethane: effect of solvent on by-product formation

JOSÉ MANUEL OLÍAS*, JOSÉ J. RÍOS and MANUEL VALLE
U.E.I. Fisología y Tecnología Post-recolección, Instituto de la Grasa y sus Derivados, C.S.I.C., 41012 Sevilla (Spain)
(First received October 10th, 1988; revised manuscript received December 29th, 1988)

An essential prerequisite for the analysis of fatty acids by gas chromatography is their quantitative transformation into more volatile, less polar derivatives. Many methods for esterification have been published. Most are based on diazomethanolysis[1], acid-catalysed methanolysis with boron trifluoride–methanol[2] or hydrochloric acid–methanol[3]. Diazomethane is a particularly mild agent for methylation but its explosiveness and toxicity have discouraged the wider use it merits. However, when proper precautions are taken, the small amount involved minimizes these deterrents. Methylation is currently carried out by the introduction of gaseous diazomethane or by the addition of an ethereal solution of diazomethane to a solution of the sample[4]. The reaction proceeds at room temperature, or at 0°C, requires only a short period of time and the rate of methylation can be increased by adding various catalysts, such as methanol or water[5]. The main advantage of this method is, however, that the products do not need to be isolated.

The high reactivity of diazomethane, which is one of the reasons for its use as a derivatizing agent in organic acid analysis, can be at the same time its limitation. Diazomethane not only attacks the acidic hydrogens of acids, phenols or enols[6], but may also react with carbonyl compounds[7] and olefinic bonds[8].

ω-Oxocarboxylic acids theoretically can be converted by diazomethane into their homologous keto methyl esters. These by-products make the recognition of the original compounds rather difficult. In this paper we describe a study of the experimental conditions which might avoid undesired side reactions.

EXPERIMENTAL

Reagents and materials

All organic solvents were high-performance liquid chromatographic (HPLC) grade, from Romil Chemicals, N-methyl-N-nitroso-*p*-toluenesulphonamide (NTSA) and heptanal from Fluka, 2-(2-ethoxyethoxy)ethanol from Kodak, formic and acetic acids from Merck, boron trifluoride in methanol (14%) from Supelco, hexanal, octanal and decanal from Sigma and 10-undecenoic acid from Aldrich.

0021-9673/89/$03.50

Synthesis

ω-Oxononanoic and ω-oxodecanoic acids were synthesized from oleic and 10-undecenoic acids respectively, by hydroxylation with hydrogen peroxide–formic acid[9], followed by oxidation of the dihydroxy acid with potasium periodate, using aqueous ethanol as the solvent[10]. ω-Oxo-9-dodecenoic acid was prepared from 12,13-epoxy-9(*Z*)-octadecenoic acid (from Vernonia seed oil). The steps were: acetylation to open the epoxy group, saponification to obtain the diol[11], followed by oxidation with periodic acid[10]. ω-Oxocarboxylic acids were methylated with boron trifluoride–methanol, purified by silica gel thin-layer chromatography (TLC) and identities checked by IR and gas chromatography–mass spectrometry (GC–MS).

Esterification of ω-oxocarboxylic acids and reaction of aldehydes with diazomethane

As standard solutions, 3 mg of each ω-oxo acid or aldehyde were separately dissolved in 1 ml of an appropriate solvent. Diazomethane was prepared from NTSA according to the procedure of Cohen[12]; gaseous diazomethane was passed through each standard solution until a yellow tinge became visible against a white background. The reaction was allowed to continue at 0°C (cooling with ice–water) for 5 min, and then the excess of diazomethane was consumed by adding acetic acid diluted in diethyl ether.

GC and GC–MS

The gas chromatograph used was a Konik KNK-3000, with a flame ionization detector. A fused-silica column, 25 m × 0.22 mm, coated with OV-1/OV-101 BP, 0.25-μm film (SGE) was used; nitrogen was used as carrier gas. The column temperature was programmed from 80 (10 min) to 180°C (5 min) at 3°C/min; injector and detector temperatures, 250°C.

GC–MS analyses were conducted with a Konik KNK-2000 gas chromatograph interfaced, via an open coupling system, to an AEI-MS-30SB-VG mass spectrometer. The GC conditions were similar to those mentioned above, except that helium was used as carrier gas. The MS conditions were as follows: ionization by electron impact, 70 eV; accelerating voltage, 4 kV; emission current, 100 μA; ion source temperature, 220°C. The data were processed with a VG 11/250 data system.

RESULTS AND DISCUSSION

Simple aliphatic aldehydes react with diazomethane, usually under very mild conditions, to yield the homologous ketone along with, in most cases, the epoxide[7]. Initial work was directed at determining solvent effects on the reaction of diazomethane with the aldehydes hexanal, heptanal, octanal and decanal. Diethyl ether, hexane, dichloromethane, diethyl ether–methanol (9:1) and methanol were used as the solvents. A typical gas chromatogram of the reaction products of heptanal, in diethyl ether containing 10% methanol, is shown in Fig. 1. The electron-impact mass spectra of these compounds are presented in Fig. 2.

Peak 1, scan 27, was heptanal, identified by comparison of the mass spectrum of the authentic compound. In the mass spectrum of peak 2, scan 43, the presence of the base peak at *m/z* 43, the intense rearrangement fragment at *m/z* 58[13] and the molecular weight at 128 are compatible with hexyl methyl ketone. In the mass spectrum of peak 3,

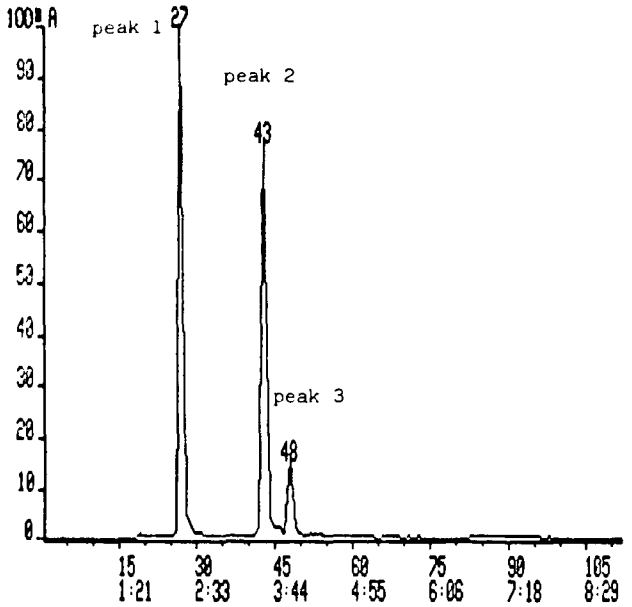

Fig. 1. Reconstructed gas chromatogram of the products of reaction between heptanal and diazomethane, in diethyl ether contaning 10% methanol. Conditions as described in the Experimental section. Total ion abundance plotted *vs.* scan number (upper line) and retention time (lower line).

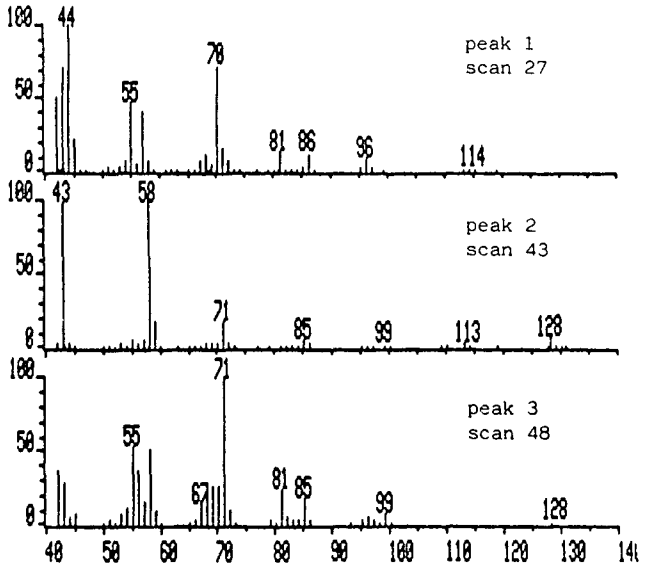

Fig. 2. Mass spectra of the compounds in peak 1, scan 27, peak 2, scan 43 and peak 3, scan 48 from the gas chromatogram shown in Fig. 1.

TABLE I
EFFECT OF SOLVENT ON THE REACTION OF HEPTANAL WITH DIAZOMETHANE AT 0°C FOR 5 min

Solvent	*Heptanal (%)*	*Hexyl methyl ketone (%)*	*1,2-Epoxyoctane (%)*
Diethyl ether	100	–	–
Hexane	100	–	–
Dichloromethane	100	–	–
Diethyl ether–methanol (9:1)	58.9[a]	34.2	6.8
Methanol	26.8[a]	49.2	23.9

[a] Average of three replicates of three determinations.

scan 48, the presence of the base peak at m/z 71 (hydrogen rearrangement with concomitant γ-scission), ions of m/z 58 and 42 (McLafferty rearrangement)[13] and the molecular weight at 128 suggest the structure of 1,2-epoxyoctane. When identical reactions were performed with hexanal, octanal or decanal, their respectives ketones and epoxides were obtained.

The relative percentages of products obtained with heptanal, in each solvent, are summarized in Table I. The results of these experiments demonstrate that inert solvents, under the assayed conditions, exert an inhibiting effect on the by-product formation, whereas methanol participates in the reaction. Similar results were obtained with hexanal, octanal and decanal. Therefore the production of ketone and

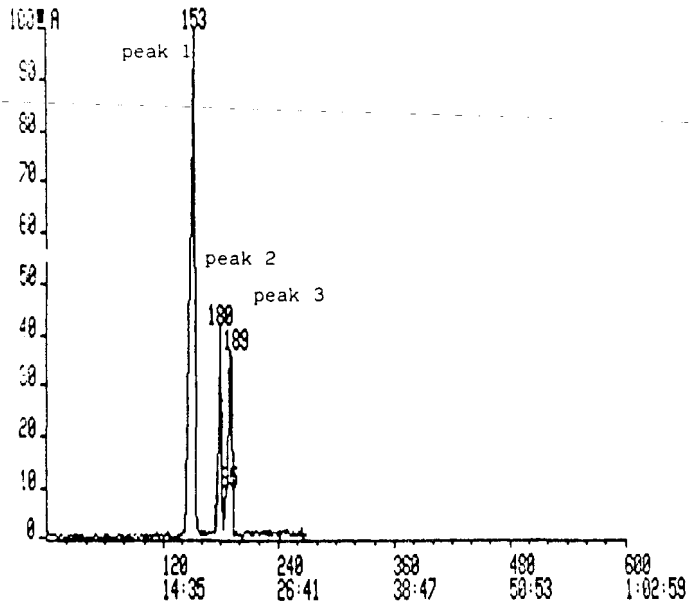

Fig. 3. Reconstructed gas chromatogram of the products of reaction between ω-oxodocecanoic acid and diazomethane, in diethyl ether containing 10% methanol. Conditions as described in the Experimental section. Total ion abundance plotted *vs.* scan number and retention time.

epoxide can be avoided by using diethyl ether, hexane or dichoromethane as the solvent.

Schlenk and Gellerman[5] have demonstrated that the esterification of long-chain fatty acids is instantaneous when gaseous diazomethane is introduced into a solution of the acids in diethyl ether containing 10% methanol. The reaction products of ω-oxodecanoic acid with diazomethane, in this solvent, were investigated. GC–MS analysis shows the presence of three compounds (Fig. 3) whose electron-impact mass spectra are presented in Fig. 4.

The mass spectrum of peak 1, scan 153, shows fragment ions of *m/z* 74, 87 and 169 ($M^+ - CH_3O$) characteristic of a methyl ester. The molecular ion peak expected (*m/z* 200) is absent. Those of *m/z* 157 ($M^+ - CHOCH_2$) and 172 ($M^+ - CO$) are ascribed to the presence of a formyl group. Therefore MS ions were consistent with methyl ω-oxodecanoate. The mass spectrum of peak 2, scan 180, presents characteristic fragments of a methyl ester, *m/z* 74, 87 and 183 ($M^+ - CH_3O$), and diagnostic peaks of an acetyl group at *m/z* 43, 58 and 157 ($M^+ - CH_3COCH_2$)[13]. The molecular ion is absent, but ions at *m/z* 183 and 157 suggest a molecular ion at *m/z* 214, therefore the compound was identified as methyl 10-oxoundecanoate. In the mass spectrum of peak 3, scan 189, fragments of a methyl ester (*m/z* 74 and 87) again appear and the fragments at *m/z* 71, 58 and 42[13] suggest the presence of a 1,2-epoxy group; the compound was tentatively identified as methyl 10,11-epoxyundecanoate.

The relative percentages of ketone and epoxide produced were 14 and 10%, respectively. In our esterification conducted in diethyl ether–methanol (9:1) with diazomethane the error in measuring the actual and desired ester product as accompanied by the by-products is greater than the errors commonly observed in measuring peak areas or in detector calibration for specific responses in GC itself.

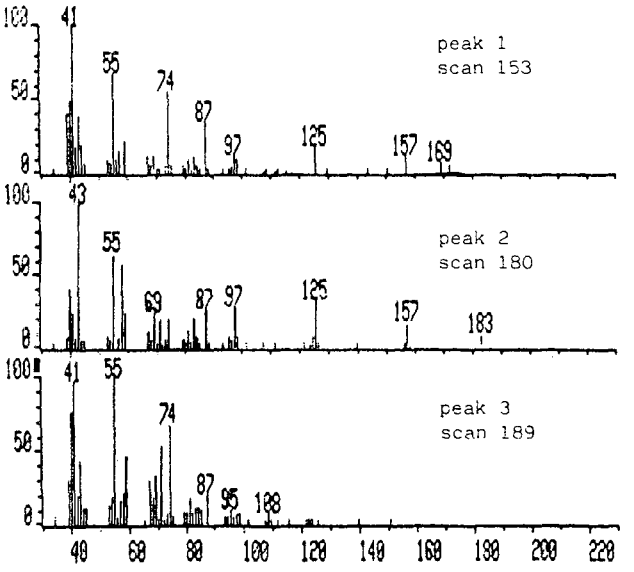

Fig. 4. Mass spectra of the compounds in peak 1, scan 153, peak 2, scan 180 and peak 3, scan 189 from the gas chromatogram shown in Fig. 3.

Therefore, we tried to see whether it was possible to stop the reaction of diazomethane with ω-oxocarboxylic acids at methyl ester. When esterification of ω-oxodecanoic acid was carried out in diethyl ether, hexane or dichloromethane, diazomethane gave quantitative recovery of the methyl ester and the formation of ketone and epoxide was negligible (less than 1%). Similar results were obtained with ω-oxononanoic acid and ω-oxo-9-dodecenoic acid.

Therefore, in the esterification of ω-oxocarboxylic acid with diazomethane, if the only desired product is the methyl ester the use of methanol must be avoided.

ACKNOWLEDGEMENTS

This study was conducted as a part of the project CCB-8509-028 supported by a grant from the U.S.–Spain Committee for Scientific and Technological Cooperation. We thank Professor E. Vioque (Inst. de la Grasa, Spain) for providing Vernonia seed oil, and M. Giménez for help in the preparation of the manuscript.

REFERENCES

1 R. Roper and T. S. Ma, *Microchem. J.*, 1 (1957) 245.
2 L. D. Metcalfe and A. A. Schmitz, *Anal. Chem.*, 33 (1961) 363.
3 H. T. Badings and C. de Jong, *J. Chromatogr.*, 279 (1983) 493.
4 A. Darbre, in K. Blau and G. King (Editors), *Handbook of Derivatives for Chromatography*, Heyden, London, 1977, Ch. 3, p. 39.
5 H. Schlenk and J. L. Gellerman, *Anal. Chem.*, 32 (1960) 1412.
6 J. S. Pizey, *Synthetic Reagents*, Vol. II, Wiley, New York, 1974, p. 70.
7 C. D. Gutsche, in R. Adams (Editor), *Organic Reactions*, Vol. VIII, J. Wiley, New York, 1954, Ch. 2, p. 364.
8 R. Huisgen and P. Eberhard, *Tetrahedron Lett.*, 45 (1971) 4343.
9 D. Swern, G. N. Billen, T. W. Findley and J. T. Scanlan, *J. Am. Chem. Soc.*, 67 (1945) 1786.
10 G. King, *J. Chem. Soc.*, (1938) 1826.
11 C. R. Smith, Jr., K. F. Koch and I. A. Wolff, *Chem. Ind. (London)*, (1959) 259.
12 J. D. Cohen, *J. Chromatogr.*, 303 (1984) 193.
13 H. Budzikiewicz, C. Djerassi and D. H. Williams, *Mass Spectrometry of Organic Compounds*, Holden-Day, San Francisco, CA, 1967, Ch. 3, p. 129; Ch. 13, p. 449.

Journal of Chromatography, 467 (1989) 285–291
Elsevier Science Publishers B.V., Amsterdam — Printed in The Netherlands

CHROM. 21 230

Note

Gas chromatographic method for enantiomeric excess determination of alcohols not requiring chiral auxiliary compounds or chiral stationary phases

A. BLINK, M. L. SUIJKERBUIJK, T. ISHIWATA and BEN L. FERINGA*
Department of Organic Chemistry, University of Groningen, Nijenborgh 16, 9747 AG Groningen (The Netherlands)
(Received November 16th, 1988)

Methodology for rapid, reliable and accurate determination of the enantiomeric composition of chiral compounds is of key importance in large areas of synthetic chemistry as the need for enantiomerically pure compounds drastically increases. The succes of enantioselective syntheses and optical resolutions and the extent of racemization during conversions of chiral synthons is quantitatively denoted by the enantiomeric excess (e.e.) of the products. In addition, e.e. determinations are often essential in natural product characterization, enzymatic conversions and mechanistic studies[1–4]. A large number of methods for e.e. determination have been developed over the last decades[2,5–7]. The majority of these methods rely on chiral auxiliary compounds. In the case of the nowadays hardly applied isotope dilution and differential microcalorimetry techniques, this prerequisite does not exist[8].

Determination of the e.e. on the enantiomers as such can be performed by NMR spectroscopy in the presence of chiral solvents[9] or paramagnetic shift reagents[10], or via chromatography on chiral stationary phases[11].

In addition NMR[12] and chromatographic analyses of diastereoisomers[11,13] prepared from enantiomers using an appropriate chiral auxiliary reagent, *e.g.*, the Mosher reagent[14], are widely applied. In the forementioned cases the formation of diastereomeric complexes or derivatives depends on the chiral auxiliary used. However, self-association in a mixture of enantiomers also creates diastereomeric relationships and coupling of enantiomers (dimerization) in a *d,l* mixture causes the formation of diastereoisomers as well[15–17]. Vigneron *et al.*[18] were the first to recognize the potential of these stereochemical phenomena for e.e. determinations. As a result of our investigations towards practical applications of enantiomeric purity determina-

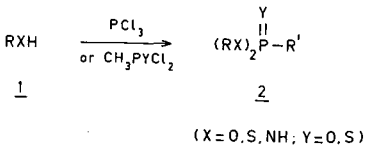

Scheme 1.

0021-9673/89/$03.50

tions without chiral auxiliary compounds, we recently described new ^{31}P NMR spectroscopic methods for e.e. determination of chiral alcohols, thiols and amines[19–23]. The principle of this e.e. determination is illustrated in Scheme 1. These methods rely on the coupling of (partly) racemic alcohols, thiols, amines and amino acid esters (**1**) using PCl_3, CH_3POCl_2 or CH_3PSCl_2 as achiral auxiliary reagents to yield diastereomeric phosphorus derivatives. In the case of enantiomerically pure substrates only one diastereoisomer of $R'PY(XR)_2$ (**2**) is formed. The diastereometric ratios of compound **2** and consequently the enantiomeric ratios of **1** are readily determined by ^{31}P NMR spectroscopy[19–23].

We now describe the application of achiral phosphorus coupling reagents in a new method for e.e. determination of chiral secondary alcohols by capillary gas chromatography (GC).

EXPERIMENTAL

Instrumentation and reagents

All GC experiments were performed on an HP 5890A gas chromatograph equipped with a split injector, a flame ionization detector and a HP 3390A integrator. Quantitative analyses were carried out on a 50 m × 0.22 mm I.D. fused-silica capillary column coated with 0.33-μm cross-linked methylsilicone gum phase (Hewlett-Packard part No. 19091A-105). For rapid optimizations of the separation conditions of the diastereoisomers, a 10 m × 0.53 mm I.D. fused-silica capillary column coated with 2.65-μm film thickness of cross-linked methylsilicone gum phase (HP part No. 19095z-121) was used. Using this column, much shorter retention times of the phosphonates were observed and a quick qualitative picture of the separation of diastereomers was achieved.

4-Dimethylaminopyridine (DMAP), triethylamine, phenylphosphonothioic dichloride, phenylphosphonic dichloride and methylphosphonic dichloride were obtained from Janssen (Beerse Belgium) and used as such. Dichloromethane and alcohols used were dried and purified as usual; the purity of alcohols exceeded 98.5% as determined by GC.

Procedure

To a solution of racemic alcohol (0.5–2.0 mmol) and triethylamine (0.55–2.2 mmol) in 0.5–2.0 ml of dichloromethane were added 5 mol % of DMAP[a]. Moisture was excluded from the solution and the phosphonic dichloride reagent (0.25–1.0 mmol) dissolved in 0.4–1.0 ml of dichloromethane was added dropwise in approximately 0.5 min by means of a syringe. In several cases, $(C_2H_5)_3N \cdot HCl$ separated from the solution after 10 min. The mixture was subsequently stirred at room temperature overnight, filtered if necessary and the solution used as such for GC analysis. Alternatively, molar stock solutions of phosphonic dichloride reagent in dry dichloromethane were used.

---

[a] DMAP is an excellent catalyst for the preparation of phosphonic acid derivatives; for its use as an acylation catalyst see ref. 24.

RESULTS AND DISCUSSION

Chiral alcohols are converted into diastereomeric (thio)phosphonates **5** via reaction with alkyl- or aryl(thio)phosphonic dichlorides **3** as shown in Scheme 2.

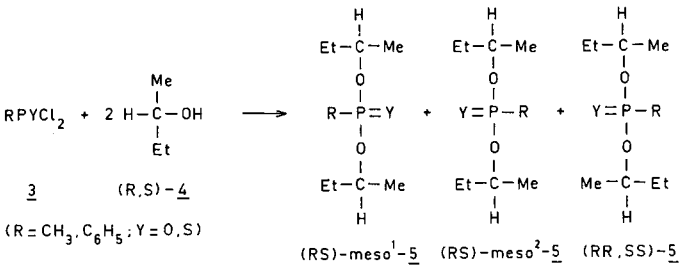

Scheme 2. Me = methyl, Et = ethyl

In the case of phosphonates **5** derived from racemic alcohols a mixture of a *d,l* pair and two meso-isomers is expected to be formed in a 50:25:25 ratio, provided no diastereoselection takes place in the coupling step. The formation of two meso-compounds is the result of the pseudoasymmetric phosphorus centre[19–23]. In the case of phosphonate **5** derived from enantiomerically pure (*S*)-alcohols only, the (*S,S*)-diastereoisomer of **5** is present. The chromatogram of the phosphonates **5** obtained from racemic *sec.*-butanol and phenylphosphonic dichloride (**3**; R = C_6H_5, Y = O) is shown in Fig. 1a. Complete baseline separation was readily achieved for the (*RR,SS*)-racemic pair and both meso-isomers of **5** with a meso/*d,l* ratio of 49.77:50.23.

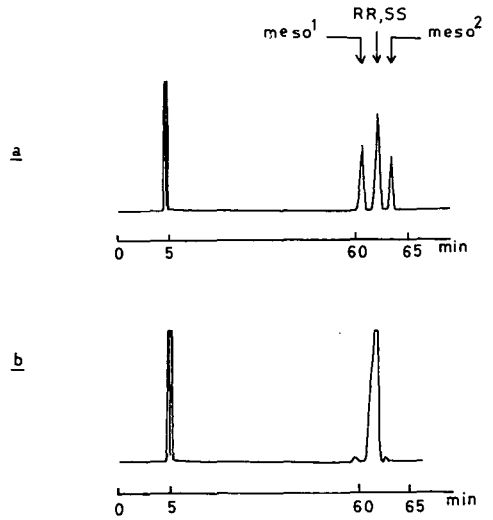

Fig. 1. GC analysis of (a) racemic $C_6H_5PO[OCH(CH_3)C_2H_5]_2$ (**5**) in dichloromethane and (b) **5** (R = C_6H_5, Y = O) derived from (*S*)-2-butanol containing 1.5% (*R*)-2-butanol.

For racemic **5** the enantiomeric purity, p, was calculated to be 0.002% from the integrated peak areas Q and Q' of the *RR(SS)*-isomer and the meso-isomers respectively (with *RR,SS*/meso ratio, $K = Q/Q'$) using Horeau's formula $p^2 = (K-1)/(K+1)$; see also refs. 18–23. These features allow accurate determination of the e.e. of partly enriched *sec.*-butanol. For this purpose a mixture of (*S*)-2-butanol containing 1.5% (*R*)-2-butanol was applied. The GC analysis is shown in Fig. 1b. An e.e. of 97.2% was calculated from the integrated peak areas. Enantiomerically pure (*S*)-2-butanol yields exclusively (*SS*)-**5** and consequently a single peak with a retention time of 62.2 min (Fig. 1).

To find the best coupling reagent for GC determinations of the enantiomeric purity of chiral alcohols a number of phosphorus derivatives were investigated. The data are summarized in Table I together with results of ^{31}P NMR spectroscopic analysis for comparison. For alcohols, the best results in ^{31}P NMR analysis, *i.e.*, the largest chemical shift differences, were obtained with the smallest alkyl substituent R in compound **5**[19–23]. In contrast herewith, the largest differences in the retention times of meso- and *d,l*-diastereoisomers of **5** were obtained with R = C_6H_5. As is the case in ^{31}P NMR analyses of phosphonates from *sec.*-alcohols, the thio derivatives (**5**, Y = S) give in general superior separations.

Furthermore, it was found that aryl(thio)phosphonates (**5**) gave superior separations compared to alkyl(thio)phosphonates. The advantage of the additional interactions possible with the π-system of an aryl-substituted compound in the chromatographic separation of diastereomers has ample precedent in the literature[13].

The results of the GC analysis of racemic alcohols using both $C_6H_5POCl_2$ and $C_6H_5PSCl_2$ as achiral derivatizing agents are summarized in Table II.

Complete baseline separations were achieved except for 2-octanol and 3-heptanol using $C_6H_5POCl_2$. The meso/*d,l* ratios are in accordance with expectation; a maximum deviation of 2% in a large number of analyses was found. This demonstrates that no substantial diastereoselection takes place during the coupling step and that accurate determination of the enantiomeric purity is possible. Furthermore, a variety of chiral *sec.*-alcohols can readily be analyzed using $C_6H_5PSCl_2$ as a reagent. Unfortunately, chiral primary and tertiary alcohols so far either did not give ade-

TABLE I

GC AND ^{31}P NMR DATA FOR RP(=Y)[OCH(CH_3)C_2H_5]$_2$

Entry	*R*	*Y*	*Column temp. (°C)*	*Retention time (min)*		*δ (Hz[a])*
				Column A	*Column B*	
1	H	O	80	8.4[b]	N.D.[c]	38, 28
2	CH_3	O	50	54.7, 55.4, 57.2[b]		2, 24
3	C_6H_5	O	115	25.2, 26.0, 26.7	60.3, 62.0, 63.2	
4	CH_3	S	–	N.D.[c]	N.D.[c]	46, 43
5	C_6H_5	S	–	N.D.[c]	84.1, 86.3, 88.0	

[a] Chemical shift differences (absolute values) between *d,l*-pair and meso-diastereomers.
[b] No baseline separation.
[c] Not determined.

TABLE II

GC DATA FOR PHOSPHONATES DERIVED FROM RACEMIC ALCOHOLS AND $C_6H_5PYCl_2$

Entry	*Alcohol*	*Y*	*Column temp. (°C)*	*Retention time (min)*	*Ratio meso/d,l (%)*
1		O	145	60.3, 62.0, 63.2	49.8 : 50.2
2		O	160	63.4, 65.1, 66.9	51.4 : 48.6
3		O	165	73.7, 76.2, 79.0	51.0 : 49.0
4	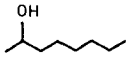	O	200	94.4, 95.5, 96.5	50.3 : 49.7[a]
5	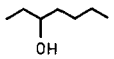	O	175	115.0, 115.9, 116.5	45.8 : 54.2[a]
6		S	145	84.2, 86.3, 88.0	52.0 : 48.0
7	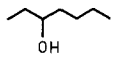	S	195	74.1, 75.4, 76.3	50.1 : 49.9
8		S	155	80.2, 82.5, 84.8	51.7 : 48.3
9		S	170	73.3, 77.6, 81.4	50.0 : 50.0
10	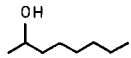	S	210	82.2, 84.7	49.3 : 50.7[b]
11	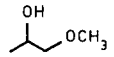	O	150	109.1, 110.8, 111.6	

[a] No complete baseline separation.
[b] *RR,SS* and meso[2] at 84.7 min.

quate GC separations or gave complex chromatograms indicating by-product formation upon derivatization with $C_6H_5PSCl_2$ or $C_6H_5POCl_2$.

In order to decrease the time necessary for the optimization of the GC condi-

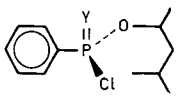

6

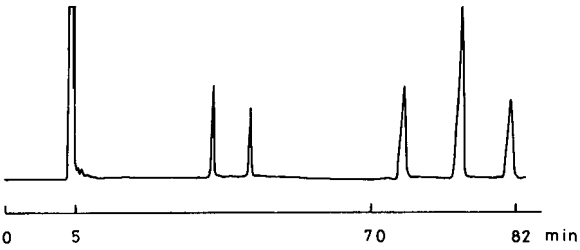

Fig. 2. GC analysis of the products of the reaction of $C_6H_5POCl_2$ with *R,S*-4-methyl-2-pentanol (after 30 min).

tions for e.e. determination and with the purpose of obtaining a quick qualitative indication of whether separation of the diastereoisomers is possible when this new technique is applied to unknown chiral alcohols, the GC analyses can be performed after a short derivatization period, for instance 30 min. In general, sufficient (thio)-phosphonate **5** will be formed during this period to allow GC determination of the isomers. The second, and often major, product present at this stage of the conversion will be the (thio)phosphonic acid monoester, *e.g.*, **6**, derived from 4-methyl-2-pentanol. This compound consists of a mixture of two diastereoisomers when obtained from racemic 4-methyl-2-pentanol. A typical GC chromatogram at partial conversion of racemic 4-methyl-2-pentanol with $C_6H_5PSCl_2$ is shown in Fig. 2. The two isomers of **6** and three isomers of **5** are well separated.

A drawback of the new method described is the relatively long retention times to achieve complete separation of diastereoisomers, which is an essential condition for accurate e.e. determination. Our results show that the resolution and accuracy of the method presented here can compete with existing GC methodology based on diastereomeric derivatives or chiral stationary phases. Currently we are investigating the lower limit to which traces of the enantiomer can be determined in a chiral alcohol. In addition we are developing on the basis of these preliminary results an efficient method to determine the enantiomeric excesses of chiral alcohols on a sub-milligram scale.

In conclusion, at present our new method allows accurate determination of enantiomeric purities of *sec.*-alcohols with $\leqslant 1.5\%$ of an enantiomer readily determined. The analysis is performed without any chiral auxiliary compound using standard capillary GC columns.

ACKNOWLEDGEMENT

We gratefully acknowledge the contributions of Dr. A. W. van Hemert and Mr. G. Brugge to the early stages of this work.

REFERENCES

1 J. D. Morrison and H. S. Mosher, *Asymmetric Organic Reactions,* Prentice-Hall, Washington, DC, 1971.
2 J. D. Morrison (Editor), *Asymmetric Synthesis,* Academic Press, New York, Vols. 1–5, 1984.
3 J. Retey and J. A. Robinson, *Stereospecificity in Organic Chemistry and Enzymology,* Monographs in Modern Chemistry 13, Verlag Chemie, Weinheim, 1982.

4 R. Scheffold (Editor), *Modern Synthetic Methods 1980,* Sälle & Sauerländer, Frankfurt, 1980.
5 V. Schurig, *Kontakte (Merck, Darmstadt)*, 1 (1985) 54.
6 V. Schurig, *Kontakte (Merck, Darmstadt)*, 2 (1985) 22.
7 J. Jacques, A. Collet and S. H. Wilen, *Enantiomers, Racemates and Resolutions,* Wiley, New York, 1981, p. 405.
8 K. K. Andersen, D. M. Gash and J. D. Robertson, in J. D. Morrison (Editor), *Asymmetric Synthesis,* Academic Press, New York, Vol. 1, 1983, Ch. 4.
9 G. R. Weisman, in J. D. Morrison (Editor), *Asymmetric Synthesis,* Academic Press, New York, Vol. 1, 1983, Ch. 8.
10 R. R. Fraser, in J. D. Morrison (Editor), *Asymmetric Synthesis,* Academic Press, New York, Vol. 1, 1983, Ch. 9.
11 V. Schurig, in J. D. Morrison (Editor), *Asymmetric Synthesis,* Academic Press, New York, Vol. 1, 1983, Ch. 5.
12 S. Yamaguchi, in J. D. Morrison (Editor), *Asymmetric Synthesis*, Academic Press, New York, Vol. 1, 1983, Ch. 7.
13 W. H. Pirkle and J. Finn, in J. D. Morrison (Editor), *Asymmetric Synthesis,* Academic Press, New York, Vol. 1, 1983, Ch. 6.
14 J. A. Dale, D. L. Dull and H. S. Mosher, *J. Org. Chem.*, 34 (1969) 2543.
15 A. Horeau, *Tetrahedron Lett.*, (1969) 3121.
16 A. Horeau and J. P. Guetté, *Tetrahedron,* (1974) 1923.
17 H. Wynberg and B. L. Feringa, *Tetrahedron,* 32 (1976) 2831.
18 J. P. Vigneron, M. Dhaenens and A. Horeau, *Tetrahedron,* 29 (1973) 1053.
19 B. L. Feringa, A. A. Smaardijk and H. Wynberg, *J. Am. Chem. Soc.* 107 (1985) 4798.
20 B. L. Feringa, A. A. Smaardijk, H. Wynberg, B. Strijtveen and R. M. Kellogg, *Tetrahedron Lett.*, 27 (1986) 997.
21 B. L. Feringa, B. Strijtveen and R. M. Kellogg, *J. Org. Chem.*, 51 (1986) 5486.
22 B. Strijtveen, B. L. Feringa and R. M. Kellogg, *Tetrahedron,* 43 (1987) 123.
23 B. L. Feringa, *J. Chem. Soc., Chem. Commun.*, (1987) 695.
24 G. Hoefle, W. Steglich and H. Vorbrueggen, *Angew. Chem., Int. Ed. Engl.*, 17 (1978) 569.

Journal of Chromatography, 467 (1989) 292–298
Elsevier Science Publishers B.V., Amsterdam — Printed in The Netherlands

CHROM. 21 322

Note

Packed column supercritical-fluid chromatography and linked supercritical-fluid chromatography–mass spectrometry for the analysis of phytoecdysteroids from *Silene nutans* and *Silene otites*

MARK W. RAYNOR, JACOB P. KITHINJI and KEITH D. BARTLE
Department of Physical Chemistry, University of Leeds, Leeds (U.K.)
DAVID E. GAMES and IAN C. MYLCHREEST
Department of Chemistry, University College, P.O. Box 78, Cardiff (U.K.)
RENÉ LAFONT
Département de Biologie, CNRS URA 117, École Normale Supérieure, 46 rue d'Ulm, Paris (France)
and
E. DAVID MORGAN* and IAN D. WILSON
Department of Chemistry, University of Keele, Staffordshire (U.K.)
(First received August 18th, 1988; revised manuscript received January 13th, 1989)

The ecdysteroids are polar, polyhydroxylated steroids which are both involatile and thermally unstable, and thus unsuitable for gas–liquid chromatography unless derivatised, as for example, by trimethylsilylation of some, or all, of the hydroxyl groups. Currently, high-performance liquid chromatography (HPLC) methods are generally used for their analysis[1]. Two recent studies have shown them to be suitable candidates for supercritical-fluid chromatography (SFC) with packed columns [2,3]. It also proved to be possible to perform linked SFC–mass spectrometry (MS) for these compounds[3]. We wish to demonstrate the advantages of SFC methods in the examination of ecdysteroids and describe here its application to the screening of plants for phytoecdysteroids (*i.e*, plant-derived ecdysteroids) by using extracts of two plants of the genus *Silene, S. nutans* and *S. otites* (Caryophyllaceae). The presence of ecdysteroids in plants is of particular interest because, although the ecdysteroids are best known for their involvement in athropod development (particurlarly moulting in insects), plants frequently provide a much wider source, both in terms of quantity and variety of structural types. These phytoecdysteroids therefore are an invaluable source of material for the study of ecdysteroid metabolism in insects and other athropods. The greater chromatographic efficiency of SFC compared with HPLC[4], and the greater compatibility of SFC mobile phases with linked chromatography–mass spectrometry, make SFC an attractive technique for the rapid screening of plant extracts for ecdysteroids, as demonstrated in this paper.

MATERIALS AND METHODS

Ecdysteroid standards were gifts from a number of sources or had been isolated and fully characterised using NMR and MS (structures are shown in Fig.1). Air dried

0021-9673/89/$03.50

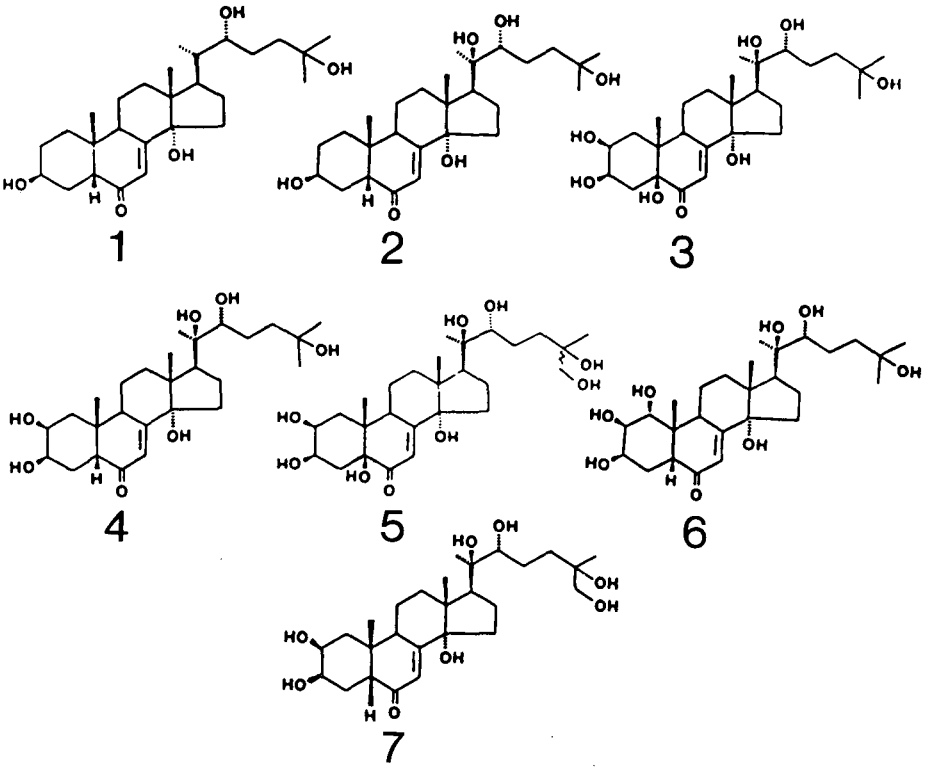

Fig. 1. Structures of the ecdysteroids present in the plant extracts described: 1 = 2-deoxyecdysone; 2 = 2-deoxy-20-hydroxyecdysone; 3 = polypodine B; 4 = 20-hydroxyecdysone; 5 = 26-hydroxypolypodine B; 6 = integristerone A; 7 = 20,26-dihydroxyecdysone.

stems and leaves of *S. nutans* and *S. otites* were extracted with methanol, solid material was removed by filtration and the extract concentrated. The further precipitate which formed was removed by centrifugation, and the filtrate was partitioned between hexane and methanol–water (85:15) (to remove neutral lipids), followed by dilution of a methanol solution with acetone to precipitate phospholipids.

HPLC separation was achieved with a Zorbax-SIL column (25 cm × 4.6 mm I.D.) using dichloromethane–isopropanol–water (125:40:3) as moving phase at 1 ml min^{-1} with detection at 254 nm.

Initial studies were performed on 5 μm cyanopropyl Spherisorb (Phase Separations, Queensferry, U.K.) packed in stainless-steel columns (25 cm × 4.6 mm I.D.) using a mobile phase provided from a cylinder of carbon dioxide containing 10% methanol. The mobile phase was delivered using a modified Varian 8500 syringe pump (Varian, Walton-on-Thames, U.K.), operating at 290 atm, approximately 3 ml min^{-1} whilst the column itself was heated, at 60°C, using a Dupont Model 860 column oven. Detection of ecdysteroids was at 235 nm using a CE 2112 variable-wavelength detector (Cecil Instruments, Cambridge, U.K.) fitted with an 8-μl high pressure stainless-steel flow cell. Samples were dissolved in methanol for injection (5 μl) via a Rheodyne 7125 injector (Altech, Carnforth, U.K.). The pressure was main-

tained with a length of stainless-steel tubing (2 m × 0.006 in. I.D.) in a water bath at 40°C.

For SFC–MS, chromatography was performed on columns packed with 3 μm silica gel (2 cm × 4.6 mm I.D., Perkin Elmer, Beaconsfield, U.K.) using a mobile phase of carbon dioxide containing 22% of methanol. The mobile phase was delivered using a Hewlett-Packard 1046B HPLC system modified for SFC as described by Games *et. al.*[5] at a flow-rate of 4 ml min^{-1} (300 bar) and column temperature of 85°C, with UV detection at 235 nm.

A T-piece was inserted after the UV detector to deliver approximately half of the flow to a modified Finnigan MAT thermospray ion source, modified for SFC as described by Games and co-workers[5,6]. For these experiments the vapouriser and jet of the mass spectrometer was set at 95°C and 180°C respectively with the repeller voltage set at +10 V and a discharge voltage of 1700 V.

RESULTS AND DISCUSSION

In previous studies capillary and packed columns were examined[2] with supercritical carbon dioxide. This mobile phase proved unsuccessful with packed columns and only low polarity ecdysteroids could be eluted from a capillary column. In order to elute more polar ecdysteroids, carbon dioxide modified with methanol was used on either uncoated silica[3] or on cyanopropyl bonded silica[2] and gave excellent results with good peak shape and short analysis times. Initial studies, with normal-phase HPLC on the two plant extracts showed the *S. otites* extract to be rich in 2-deoxyecdysone, 2-deoxy-20-hydroxyecdysone and 20-hydroxyecdysone whilst the *S. nutans* extract contained large amounts of polypodine B, and 20-hydroxyecdysone together with smaller quantities of integristerone A, 20,26-dihydroxyecdysone and 26-hydroxypolypodine B (Fig. 2). HPLC analysis required analysis times of up to 45 min. SFC on cyanopropyl-bonded silica gel gave essentially the same pattern as

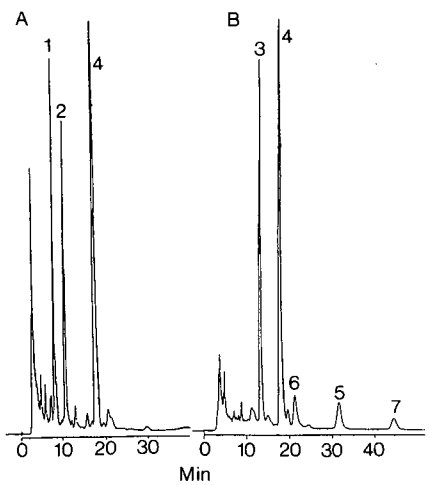

Fig. 2. Normal phase HPLC of ecdysteroid-containing plant extracts from (A) *Silene otites* and (B) *Silene nutans*. See Fig. 1 for peak identification.

normal phase HPLC. A minor exception was that 26-hydroxypolypodine B eluted before integristerone A on the cyano column in SFC and after it on silica gel in HPLC separation. A noteworthy feature was the much reduced analysis times, less than 2 min (Fig. 3A) attained with SFC with near baseline resolution for the ecdysteroids present in the *S. nutans* extract. Similarly, the results obtained for the *S. otites* extract (Fig. 3B) showed a large reduction in analysis time from over 40 min to under 3 min, albeit with the loss of resolution between the three minor components. Under the conditions described here the seven ecdysteroids studied had the following elution order and retention times: 2-deoxyecdysone, 1.4 min; 2-deoxy-20-hydroxyecdysone, 1.6 min; polypodine B, 1.7 min; 20-hydroxyecdysone, 1.9 min; 26-hydroxypolypodine B, 2.3 min; integristerone A, 2.5 min; 20,26-dihydroxyecdysone, 2.7 min. As we have observed before, there is no simple correlation between the number of a hydroxyl groups in ecdysteroids and elution order. In this SFC system, which has similar chromatographic elution order to normal phase HPLC, addition of a hydroxyl group in the 5β-position seems to reduce retention time compared to similar compounds with 5β-H. Sensitivity of detection was not examined here. Each injection contained approximately 25 μg of each major ecdysteroid. In earlier work[3] the limit of detection was found to be below 50 ng.

SFC on silica gel required both higher temperatures, and more methanol in the mobile phase. Nevertheless with such modification very short analysis times were possible. 20-Hydroxyecdysone eluted in 2.06 min using two linked 2-cm silica gel columns and in 1.15 min with a short 2-cm column. Mass spectra were obtained on the substances separated on the silica gel columns, as described below.

Supercritical-fluid chromatography linked to mass spectrometry

With the linked SFC–MS system described by Games *et al.*[5] spectra close to electron impact (EI) type are obtained with carbon dioxide, but in the presence of increasing amounts of methanol, spectra increasingly closer to chemical ionization

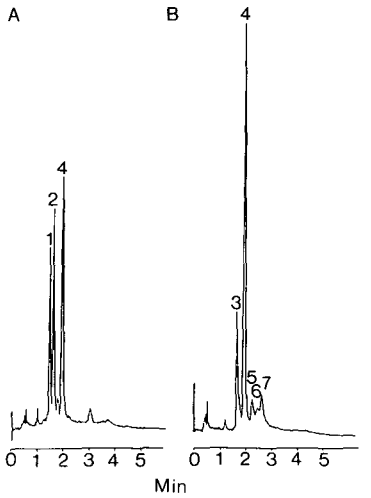

Fig. 3. SFC of ecdysteroids on 5 μm cyanopropyl bonded silica gel with carbon dioxide–methanol (9:1) as mobile phase at 3 ml min^{-1}, 60°C and 290 bar. (A) *S. nutans*, (B) *S. otites*. See Fig. 1 for peak identification.

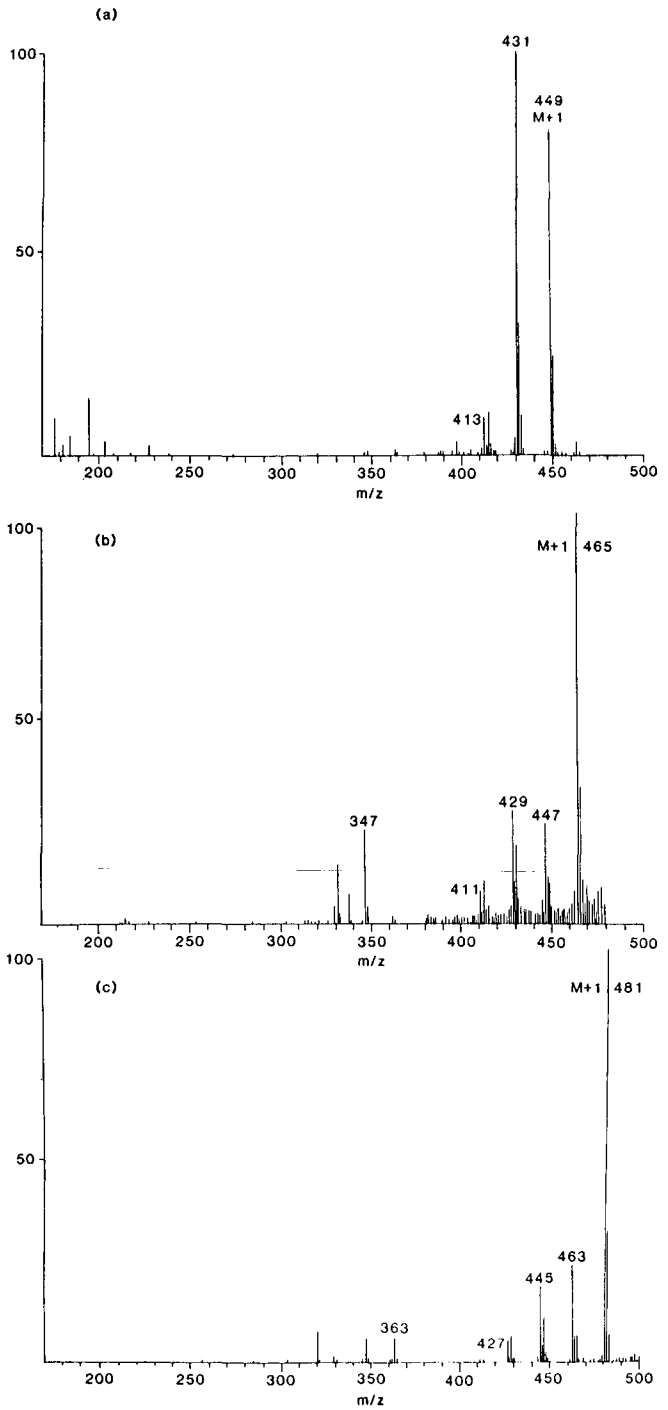

Fig. 4. Mass spectra of (a) 2-deoxyecdysone, (b) 2-deoxy-20-hydroxyecdysone and (c) 20-hydroxyecdysone from *S. otites* following SFC as described in Materials and Methods.

(CI) type are obtained. This has advantages and disadvantages. The advantage of greater sensitivity is obtained with the CI type spectra and they are useful for obtaining molecular masses, particularly with the ecdysteroids which tend to lose one, two, three or four molecules of water in the spectrometer. On the other hand, the CI spectra give little or no structural information to help identification.

From SFC–MS, spectra of the CI type (Fig. 4) were obtained for 2-deoxyecdysone, 2-deoxy-20-hydroxyecdysone and 20-hydroxyecdysone from the crude extract of *S. otites*. These spectra show prominent M + 1 ions, and losses of up to three molecules of water, the (M + 1) − 18 ion at *m/z* 431 being the base peak for 2-deoxyecdysone. Similar spectra were obtained for 20-hydroxyecdysone and polypodine B from *S. nutans*, with weak ions in the latter showing losses of four molecules of water.

In order to obtain more diagnostic fragments, the temperature of the block was raised to 260°C, which altered the spectra. That of 2-deoxyecdysone did not give many fragment ions, but in the case of 20-hydroxyecdysone (Fig. 5) and polypodine B characteristic fragment ions were obtained. All ecdysteroids with hydroxyl groups at C-20 and C-22 show a characteristic cleavage between these atoms to give prominent ions, with daughter ions at 18 and 36 a.m.u. less. Thus for 20-hydroxyecdysone the prominent ions are at *m/z* 363 ($C_{21}H_{34}O_5$), 345 and 327 from the nucleus and *m/z* 99 and 81 from the side chain. At the higher temperature *m/z* 363 became the base peak (Fig. 5) with 345 and 327 prominent. These spectra are clearly due to greater fragmentation and not pyrolysis. The result of pyrolysis of ecdysteroids is dehydration, with successive loss of the molecular ion, M − 18, M − 26, etc. The molecular ion is still clearly seen in Fig. 5 and is the strongest of that cluster of ions. The ion at *m/z* 363 arises only by fragmentation and not by dehydration. Similarly, 2-deoxy-20-hydroxyecdysone gave *m/z* 347 ($C_{21}H_{34}O_4$ base peak), 329 and 311 and polypodine B gave *m/z* 379 ($C_{21}H_{34}O_6$), 361 and 343. These fragment ions, due to cleavage between C-20 and C-22, together with the molecular ions are useful because they tell how many hydroxyl groups are in the nucleus and how many in the side chain, an impor-

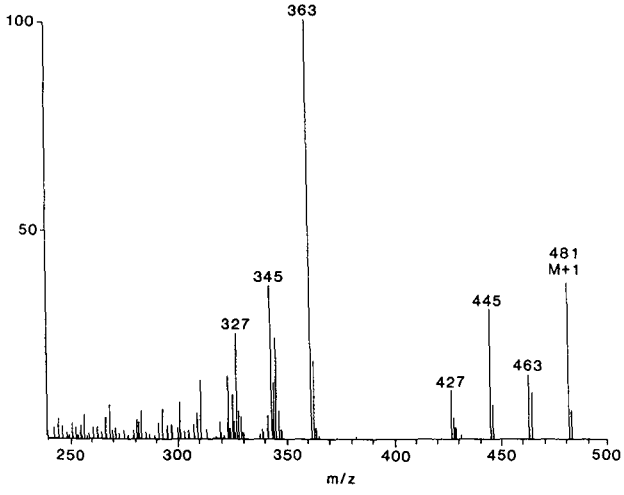

Fig. 5. SFC–MS of 20-hydroxyecdysone showing the increased fragmentation obtained with the jet block temperature set at 260°C.

tant early piece of information in identification of ecdysteroids. Spectra were not scanned to low masses because of the presence of cluster ions of carbon dioxide and methanol. We did not explore the limits of sensitivity. The spectra shown were obtained with microgram quantities.

Good quality spectra were not obtained from the minor components present in *S. nutans* extract, however this indicates the limits of the present equipment rather than the ultimate capabilities of the SFC–MS technique.

CONCLUSIONS

We have shown that supercritical-fluid chromatography can be used for very rapid separation of the polar sterols in ecdysteroid-containing plant extracts. Combined with mass spectrometry the technique can give both the molecular masses of these compounds and, by varying temperature, the characteristic fragmentation, so useful in electron impact mass spectrometry for compound identification.

ACKNOWLEDGEMENTS

I.C.M. thanks Glaxo and Finnigan MAT for financial support. D.E.G. thanks ARFC, SERC, the Royal Society and Finnigan MAT for the provision of funds for the purchase of SFC and MS equipment. M.W.R. and J.P.K. thank SERC and the Royal Society of Chemistry for financial assistance.

REFERENCES

1. R. Lafont and P. Beydon, in J. Koolman (Editor), *Ecdysone*, Georg Thieme-Verlag, Stuttgart, 1988, in press.
2. M. W. Raynor, J. P. Kithinji, I. K. Barker, K. D. Bartle and I. D. Wilson, *J. Chromatogr.*, 436 (1988) 497.
3. E. D. Morgan, S. J. Murphy, D. E. Games and I. C. Mylchreest, *J. Chromatogr.*, 441 (1988) 165.
4. D. R. Gere, R. D. Board and D. McManigill, *Anal. Chem.*, 54 (1982) 736.
5. D. E. Games, A. J. Berry, I. C. Mylchreest, J. R. Perkins and S. Pleasance. *Eur. Chromatogr. News*, 1 (1987) 10.
6. A. J. Berry, D. E. Games, I. C. Mylchreest, J. R. Perkins and S. Pleasance, *Biomed. Environ. Mass Spectrom.*, 15 (1988) 105.

Journal of Chromatography, 467 (1989) 299–303
Elsevier Science Publishers B.V., Amsterdam — Printed in The Netherlands

CHROM. 21 319

Note

High-performance hydroxyapatite chromatography of nucleic acids

YOSUKE YAMASAKI*, AKIHIRO YOKOYAMA, AKANE OHNAKA and YOSHIO KATO
Central Research Laboratory, Tosoh Corporation, 4560 Tonda, Shinnanyo-shi, Yamaguchi 746 (Japan)
and
TOMOAKI MUROTSU and KEN-ICHI MATSUBARA
Institute of Molecular and Cellular Biology, Osaka University, Yamada-oka, Suita, Osaka 565 (Japan)
(First received October 17th, 1988; revised manuscript received January 16th, 1989)

Hydroxyapatite chromatography (HAC) was developed by Tiselius *et al.*[1] and is widely used for the separation of nucleic acids[2–19]. High-performance HAC has recently been developed since smaller particles with mechanical stability could be supplied reproducibly. Although high-performance HAC has been used for the separation of proteins[20–27] and glycosides[28], the separation of nucleic acids has been limited to only total DNA and tRNA[29,30]. More recently, a new high-performance HAC column has become commercially available under the trade-name TSKgel HA-1000, which has 5-μm particles with a large pore size of 1000 Å[25]. In this work we examined the separation of various types of nucleic acids such as whole DNA, plasmids, phage RNA, tRNA and oligonucleotides on TSKgel HA-1000.

EXPERIMENTAL

All chromatographic separations were performed at 25°C with a high-performance liquid chromatograph consisting of a CCPM pump (Tosoh, Tokyo, Japan), a Model 7125 sample injector (Rheodyne, Cotati, CA, U.S.A.), a UV-8000 detector operated at 260 nm and an FBR-2 recorder (Tosoh).

Samples of 2 μg of calf thymus DNA, one before and one after heat denaturation, were separated using a 30-min linear gradient from 10 to 500 m*M* sodium phosphate (pH 6.8) containing 0.01 m*M* calcium chloride. The sample was denatured by incubation at 100°C for 5 min. A plasmid mixture containing 12 μg of M13mp8 and 11 μg of pBR322 and a 16-μg sample of MS2 phage RNA were separated with a 30-min linear gradient from 10 to 500 m*M* sodium phosphate (pH 6.8). A mixture of oligodeoxyadenylic acids containing 375 milliabsorbance units (260 nm) of $pd(A)_{40-60}$ and 15 milliabsorbance units (260 nm), of $pd(A)_{20}$ was separated with a 240-min linear gradient from 2 to 100 m*M* sodium phosphate (pH 6.8). The number of oligodeoxyadenylic acids was calculated by the injection of a pure sample of $pd(A)_{20}$. A 100-μg sample of tRNA from *E. coli* and Baker's yeast were separated with a 120-min linear gradient from 10 to 400 m*M* sodium phosphate (pH 6.8).

All columns except that used for the separation of oligodeoxyadenylic acids were

0021-9673/89/$03.50

75 × 7.5 mm I.D. with a guard column (10 × 6 or 10 × 4.6 mm I.D.). The oligodeoxyadenylic acid sample was separated on a glass column (75 × 8 mm I.D.). The dead volume between the pump and the column was 2.0 ml and the column volume was 2.8 ml. The concentration of sodium phosphate in the eluate was calculated from the linear gradient in the separation system considered with the dead volume and the column volume. The flow-rate was 1.0 ml/min. The recovery of nucleic acids was determined by measuring the absorbance of eluate at 260 nm.

Calf thymus DNA, *E. coli* and baker's yeast tRNA were purchased from Sigma (St. Louis, MO, U.S.A.). Plasmid M13mp8 was obtained from New England Biolabs. (Beverly, MA, U.S.A.). Plasmid pBR322 was prepared according to Tsurimoto and Matsubara[31]. MS2 phage RNA was purchased from Boehringer Mannheim Yamanouchi (Tokyo, Japan). The oligodeoxyadenylic acids $pd(A)_{20}$ and $pd(A)_{40-60}$ were obtained from Pharmacia (Piscataway, NJ, U.S.A.).

RESULTS AND DISCUSSION

Fig. 1 shows the separation of calf thymus DNA before and after denaturation. The sample before heat denaturation (*i.e.*, double-stranded DNA) eluted at a sodium phosphate concentration of 216 m*M* at 18 min. On the other hand, the heat-denatured sample (*i.e.*, single-stranded DNA) eluted at sodium phosphate concentration of 134 m*M* at 13 min, while a trace amount of native DNA was eluted at 18 min. Accordingly, the double- and single-stranded linear DNAs could be completely separated within 20 min. The addition of calcium chloride to the eluent did not affect the separation but it increased the lifetime of the column. The recovery of DNA was more than 88%. We examined other DNAs obtained from herring sperm and salmon testis. Native and denatured DNA in these samples could also be separated well at the same concentration of sodium phosphate as the DNA samples in Fig. 1 (data not shown).

Fig. 2 shows the separation of plasmid DNAs. The circular and single-stranded plasmid M13mp8, with 7229 bases, was eluted at a sodium phospate concentration of 150 m*M* in the eluent at 14 min. On the other hand, the circular and double-stranded

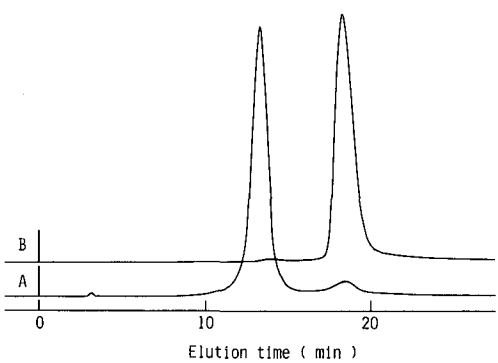

Fig. 1. Separation of calf thymus DNA by high-performance HAC before and after heat denaturation. 2 μg of calf thymus DNA (A) after and (B) before heat denaturation were separated with a 30-min linear gradient from 10 to 500 m*M* sodium phosphate (pH 6.8) containing 0.01 m*M* calcium chloride at a flow-rate of 1.0 ml/min.

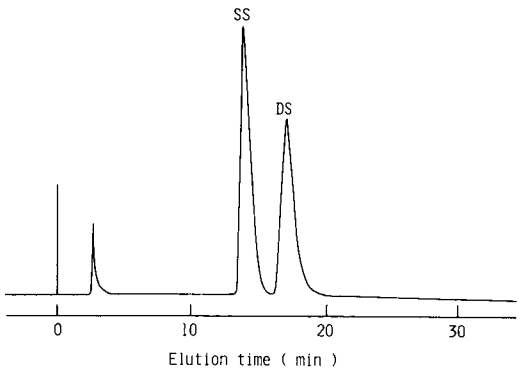

Fig. 2. Separation of single-, and double-stranded plasmid DNA by high-performance HAC. The plasmid mixture of 12 μg of M13mp8 and 11 μg of pBR322 was separated with a 30-min linear gradient from 10 to 500 m*M* sodium phosphate (pH 6.8) at a flow-rate of 1.0 ml/min.

plasmid pBR322, with 4362 base pairs, was eluted at a sodium phosphate concentration of 216 m*M* at 18 min. The total recovery of the plasmid DNAs was 90%. It was found that single- and double-stranded DNA could not only be separated in linear DNA but also in circular plasmid DNA. Hence the sodium phosphate concentration for elution was independent of the size of DNA in relatively high-molecular-weight DNA samples.

We also examined linear DNA fragments of λ DNA-Hind III digest and φX-174 RF DNA-Hae III digest. The DNA fragments, however, could not be separated with higher resolution by HAC than by ion-exchange chromatography (IEC) on the non-porous resin TSKgel DEAE-NPR[32] (data not shown).

Fig. 3 shows the separation of the oligodeoxyadenylic acids $pd(A)_{20}$ and $pd(A)_{40-60}$. These samples were found to contain many contaminant oligonucleotides of $pd(A)_{<39}$ and $pd(A)_{>60}$, and were eluted at a fairly low concentration of sodium phosphate as the oligodeoxyadenylic acids were single-stranded DNA of low molecular weight. The chromatogram showed high resolution, and the oligodeoxyadenylic acids could be separated up to at least the 70-mer. This chromatographic pattern was similar to that obtained by IEC on TSKgel DEAE-NPR[33], although HAC took much longer for separation. The total recovery of the oligonucleotides was 96%.

Fig. 4 shows the separation of MS2 phage RNA, which has a relatively high molecular weight (3569 bases) and was eluted at a sodium phosphate concentration of

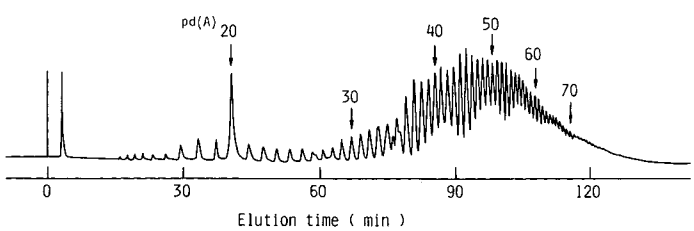

Fig. 3. Separation of oligodeoxyadenylic acid by high-performance HAC. The mixture of 15 milliabsorbance units (260 nm) of $pd(A)_{20}$ and 375 milliabsorbance units (260 nm) of $pd(A)_{40-60}$ was separated with a 240-min linear gradient from 2 to 100 m*M* sodium phosphate (pH 6.8) at a flow-rate of 1.0 ml/min.

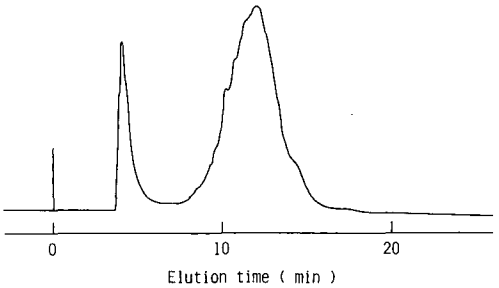

Fig. 4. Separation of MS2 phage RNA by high-performance HAC. 16 μg of MS2 phage RNA was separated with a 30-min linear gradient from 10 to 500 m*M* sodium phosphate (pH 6.8) at a flow-rate of 1.0 ml/min.

134 m*M* at 13 min. It had the same retention time as single-stranded DNA prepared from calf thymus, but it eluted as a broad peak. This may reflect the different conformation derived from the secondary and tertiary structure of RNA[2]. The total recovery of MS2 phage RNA was 95%.

Fig. 5 shows the separation of tRNAs from *E. coli* and baker's yeast. The tRNAs were eluted earlier than MS2 phage RNA at a concentration of sodium phosphate between 65 and 140 m*M* in the eluent as the tRNAs have a lower molecular weight of *ca.* 76 bases. Many peaks were observed, which suggests the multiplicity of tRNA and also the presence of secondary and tertiary structure as indicated by Kawasaki *et al.*[29]. The total recoveries of the tRNA were 91 and 96%, respectively.

As demonstrated above, various types of nucleic acids could be separated quantitatively by high-performance HAC on TSKgel HA-1000. In the case of DNA, single- and double-stranded DNA were separated completely, not only in linear DNA but also in circular plasmid DNA, within 20 min. The sodium phosphate concentration needed for elution was independent of the steric structure and molecular weight for relatively large DNA. Hydroxyapatite could discriminate the rigid helical structure of double-stranded DNA from the flexible single-stranded DNA. On the other hand, relatively small double-stranded DNA, such as DNA fragments, seemed to be separated according to the size whereas the resolution with HAC was lower than that with IEC. However, single-stranded DNAs consisting of oligodeoxynucleotides were separated according to size with the same resolution in both HAC and IEC.

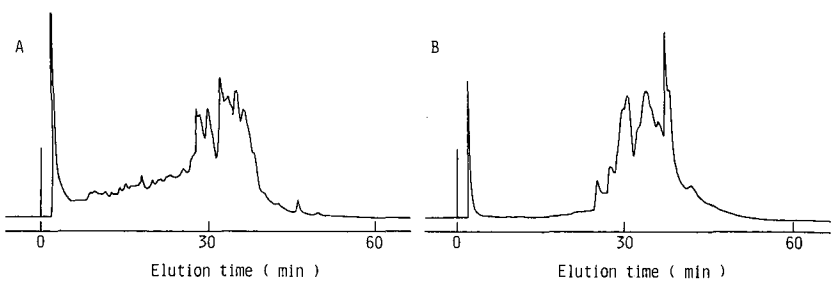

Fig. 5. Separation of tRNA by high-performance HAC. 100 μg of tRNA from (A) *E. coli* and (B) baker's yeast were separated with a 120-min linear gradient from 10 to 400 m*M* sodium phosphate (pH 6.8) at a flow-rate of 1.0 ml/min.

Large RNA such as MS2 phage RNA was eluted at the same concentration of sodium phosphate as single-stranded DNA, although it eluted as a broad peak. It is also suggested that the secondary and tertiary structure of phage RNA give rise to different interactions with hydroxyapatite. tRNAs could also be separated successfully into a number of peaks. tRNA is known to exist in a clover-leaf conformation in spite of having only *ca.* 76 bases. Therefore, differences in the secondary and tertiary structures and the base sequence may be resonsible for interactions of tRNAs with hydroxyapatite.

In conclusion, high-performance HAC on TSKgel HA-1000 should be a very useful tool for the separation of various nucleic acids. Nucleic acids can be separated effectively according to their conformation and molecular weight.

REFERENCES

1 A. Tiselius, S. Hjerten and O. Levin, *Arch. Biochem. Biophys.*, 65 (1956) 132.
2 G. Bernardi, *Methods Enzymol.*, 21 (1971) 95.
3 W. Meinke, D. A. Goldstein and M. R. Hall, *Anal. Biochem.*, 58 (1974) 82.
4 W. Pakroppa and W. Muller, *Proc. Natl. Acad. Sci. U.S.A.*, 71 (1974) 669.
5 S. Altman and B. C. Stark, *Anal. Biochem.*, 59 (1974) 547.
6 K. Grohmann, L. H. Smith and R. L. Sinsheimer, *Biochemistry*, 14 (1975) 1951.
7 W. Pakroppa, W. Goebel and W. Muller, *Anal. Biochem.*, 67 (1975) 372.
8 I. G. Ivanov, P. V. Venkov and G. G. Markov, *Prep. Biochem.*, 67 (1975) 219.
9 D. W. Sutton and J. D. Kemp, *Biochemistry*, 15 (1976) 3153.
10 M. Shoyab and A. Sen, *J. Biol. Chem.*, 254 (1978) 6654.
11 A. Colman, M. J. Byers, S. B. Primrose and A. Lyons, *Eur. J. Biochem.*, 91 (1978) 303.
12 I. P. Hesslewood, *Int. J. Radiat. Biol.*, 34 (1978) 461.
13 F. A. Beland, K. L. Dooley and D. A. Casciano, *J. Chromatogr.*, 174 (1979) 177.
14 M. G. Pluskal and S. Sarkar, *Biochemistry*, 20 (1981) 2048.
15 P. I. Andriaenssens, J. Bixler and M. W. Anderson, *Anal. Biochem.*, 123 (1982) 162.
16 G. D. Stoner, F. B. Daniel, K. M. Schenck, H. A. Schut, P. J. Goldblatt and D. W. Sanwisch, *Carcinogenesis*, 3 (1982) 195.
17 T. R. Johnson and J. Ilan, *Anal. Biochem.*, 132 (1983) 20.
18 F. O. Obi, *J. Chromatogr.*, 369 (1986) 321.
19 J. R. Milligan, L. Catz-Biro and M. C. Archer, *J. Chromatogr.*, 411 (1987) 481.
20 T. Kawasaki, S. Takahashi and K. Ikeda, *Eur. J. Biochem.*, 152 (1985) 361.
21 T. Kawasaki, W. Kobayashi, K. Ikeda, S. Takahashi and H. Monma, *Eur. J. Biochem.*, 157 (1986) 291.
22 L. D. Libera, *J. Chromatogr.*, 366 (1986) 417.
23 Y. Funae, S. Wada, S. Imaoka, S. Hirotsune, M. Tominaga, S. Tanaka, T. Kishimoto and M. Maekawa, *J. Chromatogr.*, 381 (1986) 149.
24 T. Kadoya, T. Isobe, M.Ebihara, T. Ogawa, M. Sumita, H. Kuwahara, A. Kobayashi, T. Ishikawa and T. Okuyama, *J. Liq. Chromatogr.*, 9 (1986) 3543.
25 Y. Kato, K. Nakamura and T. Hashimoto, *J. Chromatogr.*, 398 (1987) 340.
26 Y. Yamakawa and J. Chiba, *J. Liq. Chromatogr.*, 11 (1988) 665.
27 Y. Yamasaki and Y. Kato, *J. High Resolut. Chromatogr. Chromatogr. Commun.*, in press.
28 R. Kasai, H. Yamaguchi and O. Tanaka, *J. Chromatogr.*, 407 (1987) 205.
29 T. Kawasaki, K. Ikeda, S. Takahashi and Y. Kuboki, *Eur. J. Biochem.*, 155 (1986) 249.
30 S. C. Compton, *LC · GC Mag. Liq. Gas Chromatogr.*, 1 (1984) 294.
31 T. Tsurimoto and K. Matsubara, *Taisha*, 17 (1981) 81.
32 Y. Kato, Y. Yamasaki, T. Kitamura, A. Mitsui, T. Hashimoto, S. Fukushige, T. Murotsu and K. Matsubara, in preparation.
33 Y. Kato, T. Kitamura, A. Mitsui, Y. Yamasaki, T. Murotsu, K. Matsubara, T. Hashimoto and S. Fukushige, *J. Chromatogr.*, 447 (1988) 212.

Journal of Chromatography, 467 (1989) 304–308
Elsevier Science Publishers B.V., Amsterdam — Printed in The Netherlands

CHROM. 21 350

Note

Einsatz der Hochleistungsflüssigkeitschromatographie bei der Untersuchung der metallionkatalysierten Methanolyse des Phosphorsäurephenylesterdiamids

J. RADICKE, J. HARTUNG, U. POMMER* und H. BÖHLAND
Pädagogische Hochschule "Dr. Theodor Neubauer" Erfurt/Mühlhausen, Wissenschaftsbereiche Physikalische Chemie und Botanik/Pflanzenphysiologie/Biochemie, DDR-5700 Mühlhausen (D.D.R.)
(Eingegangen am 16. Januar 1989)

Der Einsatz von Phosphorsäurephenylesterdiamid (PPDA) als Ureaseinhibitor bei der Harnstoffdüngung ermöglichte eine bedeutende Senkung der Harnstoffhydrolyseraten im Boden[1,2]. Trotzdem treten bei seiner Anwendung Unsicherheiten auf, die nur teilweise durch die pH-Wert-abhängige PPDA-Hydrolyseempfindlichkeit erklärt werden können[3,4].

Es machte sich deshalb erforderlich, das PPDA-Reaktionsverhalten ausführlich zu charakterisieren. Die vorliegenden Untersuchungen an methanolischen Systemen zeigen, dass verschiedene Metallionen die selektive P–O-Bindungsspaltung am PPDA-Molekül katalysieren und damit seine Solvolyse stark beschleunigen.

Weiterführende UV-spektroskopische Arbeiten bestätigten, dass die experimentellen Befunde eindeutig auf wässrige Systeme übertragbar sind.

EXPERIMENTELLES

Reaktionsbedingungen

Zur Herstellung der methanolischen PPDA–Metallsalz-Reaktionsgemische wurden chromatographisch reine Ausgangssubstanzen verwendet. Als Katalysatoren kamen Zink-, Mangan(II)-, Cobalt(II)- und Nickel(II)-chloride bzw. -acetate zum Einsatz. Für das Reaktionsgemisch wurden folgende Stoffmengenverhältnisse gewählt: 0,050 *M* PPDA–0,025 *M* M^{2+}; 1,00 m*M* PPDA–0,50 m*M* M^{2+}; 1,00 m*M* PPDA–0,25 m*M* M^{2+}.

Die Bestimmung des pH-Wertes der Lösungen und Ermittlung der Komplexbildungskonstanten erfolgte potentiometrisch unter Verwendung entsprechender Auswerteprogramme.

Qualitative Produktanalyse

Hochleistungsflüssigkeitschromatographie (HPLC). Die HPLC-Analytik der Testansätze basierte auf folgender Gerätekombination: Chromatograph (Fa. Knauer) mit HPLC-Pumpe (Modell 52.00); Spektralfotometer (Modell 85.20); Rheodyne-Probeschleifen-Spritzenventil (Modell RH 71-25); Trennsäule (250 × 4,6 mm I.D.)

0021-9673/89/$03.50

mit LiChrosorb RP-18 (10 μm); Vorsäule (40 × 4,6 mm I.D.) mit Perisorb RP-18 (30–40 μm); Linseis-Zweikanal-Flachschreiber (Modell LS 24.70.70); Spectra-Physics-Minigrator-Rechenintegrator (Modell 23000-111).

Als Elutionsmittel diente ein Methanol–Wasser-Gemisch (20:80) bei einer Flussrate von 2,00 ml/min und einem Druck von 10 MPa. Die Detektion erfolgte bei 210 nm. Das Probeschleifenvolumen betrug 20 μl. Zu seiner Füllung wurden jeweils 100 μl Untersuchungslösung verwendet, um eventuelle Kontaminationen mit Resten vorausgegangener Analysen auszuschliessen.

Dünnschichtchromatographie. UV-Inaktive Reaktionsprodukte wurden mittels Dünnschichtchromatographie (Fertigplatten: Silufol UV 254 der Fa. Kavalier, C.S.S.R.) nachgewiesen. Als Referenzsubstanz diente Phosphorsäuremethylesterdiamid (PMDA), hergestellt nach einem modifizierten Stokes'schen Verfahren[5,6] mit anschliessender partieller Reinigung durch Tetrahydrofuranextraktion. Zur Detektion wurde Ninhydrin-Sprühreagens verwendet[7]. Für das vorliegende Trennungsproblem konnten folgende mobile Phasen von uns experimentell ermittelt werden: (I) Pentan-1-ol–Tetrahydrofuran–Propan-2-ol–Ammoniaklösung (25%) (1:3:0,5:0,5); (II) Pentan-1-ol–Aceton–Propan-2-ol–Ammoniaklösung (25%) (1:3:0,5:0,5); (III) Pentan-1-ol–1,4-Dioxan–Methanol–Ammoniaklösung (25%) (1:1:1:0,5); (IV) Pentan-1-ol–Ethanol–Ammoniaklösung (25%) (1:1:0,5).

Quantifizierung der Reaktion

Mit Hilfe der vom Integrator ausgedruckten Werte für die Peakflächen wurde im Bereich von 1,00 m*M* bis 0,05 m*M* Phenol (subl.) eine Eichgerade aufgestellt. Die eingesetzten repräsentativen Messwerte wurden aus jeweils zehn Einzelmessungen ermittelt (Fehler: 0,05 bis 0,30%). Damit war es möglich, die Reaktionskinetik zu studieren. Die methanolischen Ausgangslösungen (PPDA und Metallsalz) wurden auf 25,0°C thermostatiert und nach der Mischung in konstanten Zeitabschnitten vermessen. Die Bestimmung des Endpunktes der Reaktion erfolgte nach acht bis zehn Halbwertszeiten. Parallelmessungen am Spektralfotometer M 40 (VEB Carl-Zeiss, Jena, D.D.R.) unter Verwendung konzentrationsanaloger Grössen dienten dem Vergleich mit der chromatographisch ermittelten Reaktionsordnung und Reaktionsgeschwindigkeitskonstanten.

ERGEBNISSE UND DISKUSSION

In Zusammenhang mit präparativ-analytischen Untersuchungen[4] konnte mit der HPLC-Auftrennung des Reaktionsgemisches nachgewiesen werden, dass Phenol als Produkt gebildet wird (Fig. 1). Die Zuordnung erfolgte durch Cochromatographie der Reinsubstanz.

Das gleichzeitig entstehende PMDA wurde mittels Dünnschichtchromatographie neben Phenol identifiziert (Fig. 2).

Da das als Referenzsubstanz eingesetzte PMDA nur partiell gereinigt werden konnte, ergaben sich nach Entwicklung der Chromatogramme zusätzlich kleine, mit Ninhydrin anfärbbare Spots, die in den Darstellungen vernachlässigt wurden. Aufgrund der experimentellen Ergebnisse kann geschlussfolgert werden, dass es unter katalytischem Einfluss der getesteten Metallionen (pH-Wert: konst.) zur selektiven

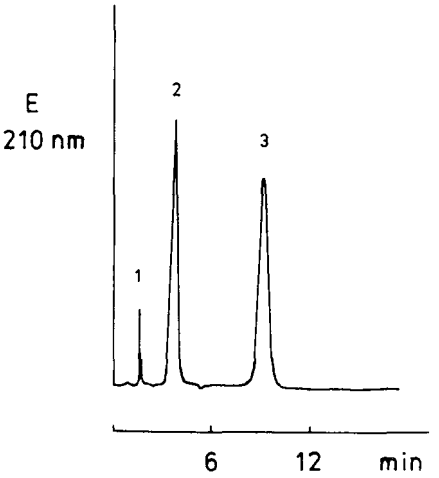

Fig. 1. HPLC-Chromatogramm während des Reaktionsverlaufes der PPDA-Methanolyse unter Verwendung von Zinkacetat als Katalysator. Peak 1 = Lösungsmittel + Katalysator; Peak 2 = PPDA; Peak 3 = Phenol.

P–O-Bindungsspaltung am PPDA und zur Methanolyse nach folgender Gleichung kommt:

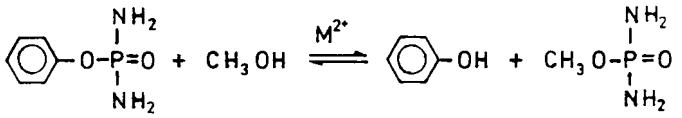

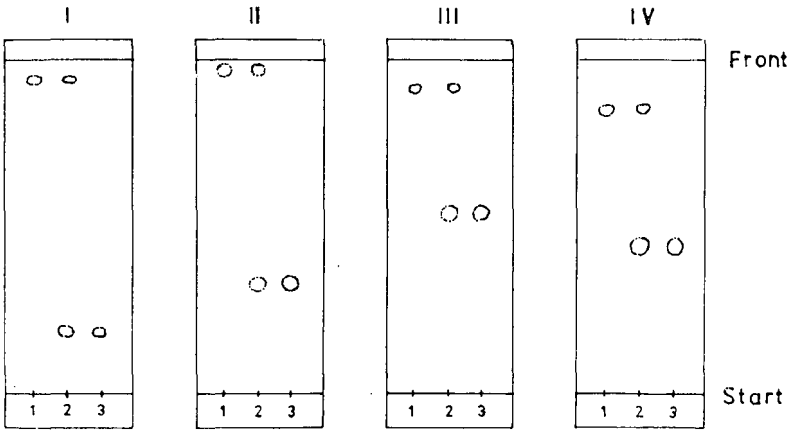

Fig. 2. Dünnschichtchromatogramme zur PPDA-Methanolyse. 1 = Phenol (UV-Detektion); 2 = Reaktionsgemisch; 3 = PMDA; I–IV = mobile Phasen (siehe Text).

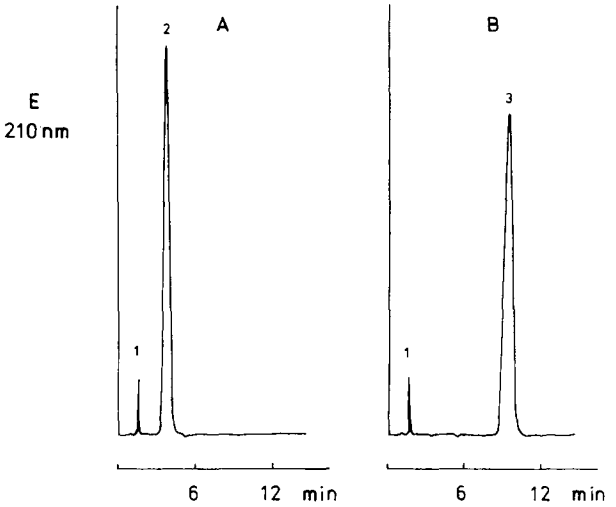

Fig. 3. HPLC-Chromatogramme zu Beginn (A) und nach Abschluss (B) der PPDA-Methanolyse unter Verwendung von Zinkacetat als Katalysator. Peak 1 = Lösungsmittel + Katalysator; Peak 2 = PPDA; Peak 3 = Phenol.

Mit Hilfe der eingesetzten Analytik wurde sichtbar, dass nach Abschluss der Methanolyse das Gleichgewicht der Reaktion vollkommen zugunsten der Produkte verschoben ist (Fig. 3).

Der Wirkungsgrad des Katalysators steht dabei in Relation zur Elektronenkonfiguration des entsprechenden Metallions. So konnte nachgewiesen werden, dass Zink- und Mangan(II)-salze eine hohe katalytische Wirksamkeit besitzen[8]. Der Ligandenaustausch am Zentralion erfolgt aufgrund der kinetischen Labilität der Komplexstrukturen wesentlich schneller als am Cobalt(II)- und Nickel(II)-ion[9]. Reaktionskinetische Untersuchungen ergaben, dass die metallionkatalysierte PPDA-Methanolyse nach dem Geschwindigkeits-Zeit-Gesetz erster Ordnung verläuft:

$$\ln \frac{c_{\text{Phenol}\,\infty}}{c_{\text{Phenol}\,\infty} - c_{\text{Phenol}}} = k't \qquad (1)$$

Hinsichtlich der Beteiligung des Lösungsmittels an der Reaktion und in bezug auf die beschriebene Katalyse handelt es sich um eine Pseudo-1.Ordnung.

Zur Bestimmung der Reaktionsgeschwindigkeitskonstanten k' mit Hilfe der Phenol-Peakflächenintegration wurden folgende Bedingungen gewählt (Katalysator: $Zn(CH_3COO)_2 \cdot 2H_2O$): $c_{\text{Kat.}} = 0{,}50$ mM; $c_{\text{PPDA}} = 1{,}00$ mM; $\theta = 25{,}0$°C; pH = 8,80.

Die aus mehreren Versuchsansätzen ermittelte Pseudo-1.Ordnung-Geschwindigkeitskonstante $\bar{k}'$ beträgt $2{,}79 \cdot 10^{-3}$ min^{-1} ($t_{1/2} = 4{,}14$ h). Der sehr hohe Katalysatorwirkungsgrad des Zinkions wie auch der anderen Metallionen konnte aufgrund der extrem grossen Zeitkonstanten für den unkatalysierten Reaktionsverlauf nicht quantifiziert werden. Die UV-spektroskopischen Messungen zur Reaktions-

kinetik ergaben unter analogen Bedingungen eine Pseudo-1.Ordnung-Geschwindigkeitskonstante $\bar{k}'$ von $3{,}09 \cdot 10^{-3}$ min^{-1} ($t_{1/2}$ = 3,74 h). Die Abweichungen vom chromatographisch ermittelten Wert sind auf gerätetechnische Unsicherheiten am verwendeten Spektralfotometer zurückzuführen. Sowohl bei der Testung der anderen genannten Metallsalze als auch bei weiterführenden spektroskopischen Untersuchungen zur metallionkatalysierten PPDA-Hydrolyse konnte Übereinstimmung hinsichtlich des beschriebenen Reaktionsmechanismus beobachtet werden.

DANK

Wir danken Herrn Dr. Heinze vom VEB Fahlberg-List Magdeburg (D.D.R.) für die Bereitstellung des PMDA-Rohproduktes.

LITERATUR

1 R. Heber, S. Muller, W. Matzel und H. Ansorge, *Arch. Ackerpflanzenbau Bodenkd.*, 4 (1979) 231.
2 B. H. Byrnes, N. K. Savant und E. T. Craswell, *Soil Sci. Soc. Am. J.*, 47 (1983) 270.
3 E. R. Austin, T. J. Bradford und M. S. Lupin, *J. Agric. Food Chem.*, 32 (1984) 1090.
4 G. König, J. Radicke, H. Böhland und H.-J. Michel, *Z. Chem.*, 27, No. 7 (1987) 261.
5 H. N. Stokes, *Am. Chem. J.*, 16 (1894) 127.
6 L. F. Audrieth und A. D. F. Toy, *J. Am. Chem. Soc.*, 63 (1941) 2117.
7 *Anfärbereagenzien für Dünnschicht- und Papier-Chromatographie*, E. Merck, Darmstadt, 1980, p. 75.
8 W. G. Penney, *Trans. Faraday Soc.*, 36 (1940) 627.
9 F. Dickert, P. Fischer, H. Hoffmann und G. Platz, *J. Chem. Soc., Chem. Commun.*, 1 (1972) 106.

Journal of Chromatography, 467 (1989) 309–314
Elsevier Science Publishers B.V., Amsterdam — Printed in The Netherlands

CHROM. 21 363

Note

Alkaline size-exclusion chromatography of lignins and coal extracts using cross-linked dextran gels

MICHAEL E. HIMMEL* and KENNETH K. OH
Applied Biological Sciences Section, Biotechnology Research Branch, Solar Fuels Research Division, Solar Energy Research Institute, 1617 Cole Boulevard, Golden, CO 80401 (U.S.A.)
DAVID R. QUIGLEY
Biotechnology Group, Idaho National Engineering Laboratory, P.O. Box 1625, Idaho Falls, ID 83415 (U.S.A.)
and
KAREL GROHMANN
Applied Biological Sciences Section, Biotechnology Research Branch, Solar Fuels Research Division, Solar Energy Research Institute, 1617 Cole Boulevard, Golden, CO 80401 (U.S.A.)
(Received September 6th, 1988)

Biochemists working with natural polymers have long been concerned with the challenge of fractionating these materials by chromatographic methods. However, many such polymers are difficult to disperse in aqueous solutions, even if made to relatively high ionic strengths at neutral pH. In the case of three classes of important biopolymers, coal extracts, humic acids and lignins, this behavior is often due to the presence of water-insoluble complexes containing aromatic or aliphatic polyphenols[1,2]. A successful solvent for these polymers was found by McNaughton *et al.*[3] and Sarkanen *et al.*[4] to be 0.1 *M* sodium hydroxide, which produces a pH of 13 at 20°C. One problem involved in adapting such a solvent–solute system to size-exclusion chromatography (SEC) is that of minimizing solute–solute interaction and solute–column gel interaction. Also, the chromatography gel must be stable for weeks in 0.1 *M* sodium hydroxide, and high-performance separations offering theoretical plates in the 10^3–10^4/m range are desirable.

Since the first descriptions of gel filtration chromatography (now more commonly referred to as SEC) in the mid-1950s by Lindqvist and Storgards[5], the separation and quantitation of a wide variety of biomacromolecules has been possible. This early work was performed with an insoluble, cross-linked polydextran gel, eventually called Sephadex™ by Pharmacia (Uppsala, Sweden). Many other "non-rigid" SEC separation gels soon became available, including the agarose gels Sepharose™ and Sepharose CL™ from Pharmacia, and Bio-Gel™ A series from Bio-Rad Labs. (Richmond, CA, U.S.A.); the dextran–bisacrylamide gels Sephacryl™ from Pharmacia; the acrylate gels Fractogel or Toyo-Pearl™ from Toyo Soda (Japan); the polyacrylamide gels Bio-Gel P series from Bio-Rad; and the agarose–acrylamide gels Ultrogel™ from LKB (Rockville, MD, U.S.A.). Since these gels are formed in the

0021-9673/89/$03.50

30–80-μm particle size range, free-packed column efficiencies are rather low. Also, only Sepharose CL is recommended[6] for use at pH values as high as 14.

Some "rigid" gels for high-pressure (HP) SEC available for the last decade include the native silica gels Porasil™ from Waters Assoc. (Milford, MA, U.S.A.), Fractosil™ from E. Merck (Darmstadt, F.R.G.) and CPG Electro-Nucleonics (Fairfield, NJ, U.S.A.); the hydrophilically bonded silica gels TSK-gel SW type from Toyo Soda, LiChrospher™ from E. Merck, Protein-Pak™ from Waters Assoc., and SynChropak™ from SynChrom (Linden, IN, U.S.A.); the acrylate polymer based gels TSK-gel PW type from Toyo Soda and OHpak™ from Showa Denko (Japan); the polyvinyl alcohol gels Ashipak™ GS series from Asahi Kasei (Japan) and the OHpak Q series from Showa Denko; the rigid polyacrylamide gel PL-aqua gel P series, Polymer Labs. (U.K.); and finally the cross-linked dextran gel Superose™ 6 HR and 12 HR from Pharmacia. Of these HPSEC gels, only TSK-gel PW and Superose offer extended stability at pH 14.

Prepacked columns of Superose gels were chosen in the study reported here, where neutral pH, aqueous extracts of lignite coal and ball-milled aspen lignin were analyzed in 0.1 *M* sodium hydroxide.

EXPERIMENTAL

Chromatography instrumentation

The system used in this study employed a Beckman Model 110B HPLC pump, a Waters Assoc. Model 440 UV detector with a 280-nm filter, and a Beckman Model 210 manual injection valve fitted with a 100-μl sample loop. Chromatograms were recorded and stored on floppy-disc media using Dynamic Solutions HPLC software and an MS-DOS compatible personal computer. The column set consisted of a Superose 6 HR (30 cm × 10 mm I.D.) and a Superose 12 HR (30 cm × 10 mm I.D.) connected in series. Samples were prepared in 0.1 *M* sodium hydroxide made with degassed, deionized water to a concentration of about 1 mg/ml. Samples were injected into the system immediately after preparation and fitration with 0.22-μm HPLC sample filters (Rainin Instruments).

Molecular weight standards

Sodium polystyrene sulfonate (NaPS) standards (peak-average molecular weight, M_p = 1200, 780, 400, 200, 100, 74, 34, 18, 8, 4.6 and 1.8 kilodaltons) were from Polymer Labs. (Church Stretton, U.K.) and sodium polyacrylate (NaPA) standards (weight-average molecular weight, M_w = 8300, 3800 and 1930) were from American Polymer Standards Corp. (Mentor, OH, U.S.A.). Tannic acid [formular weight (FW) = 1701], sodium azide (FW = 65), sodium 4,5-dihydroxynaphthalene-2,7-disulfonate (FW = 400), and sodium dihydroxybenzoate (FW= 154) were from Aldrich. Trisodium ethylenediaminetetraacetate (EDTA) (FW = 358) and 4-hydroxy-3-methoxybenzoic acid (vanillic acid) (FW = 168) were from Sigma.

Preparation of lignin and coal-extract samples

Texas lignite (coal) was oxidatively pretreated with 8 *M* nitric acid for 1 h. Resulting material was washed with deionized water until the pH of the wash water was greater than 5 and was then continuously extracted with water in a soxhlet

extraction apparatus for 6 weeks. This coal (1 g) was then repeatedly extracted with 10 ml of 50 m*M* phosphate buffer, pH 7. Initial additions of buffer resulted in immediate pH decreases, and little material was extracted. Subsequent extractions resulted in smaller decreases in pH and more material going into solution. The sample analyzed in this study resulted from an early extract. Materials from these extracts remain fully soluble at pH values above 7. Ball-milled aspen lignin was prepared following the procedure of Lundquist *et al.*[7]. The yield of purified milled wood lignin obtained was usually about 10% (w/w) that of ethanol–benzene-extracted aspen wood. The ball-milled aspen lignin was not esterified before analysis.

Analysis of chromatographic data

The elution profiles of aspen lignin and the coal extract were subjected to molecular weight distribution analysis [*e.g.*, for the number-average molecular weight (M_n), M_w and M_p] using the graphical method described by Yau *et al.*[8] after baseline correction. Values for molecular weight increment, M_i, along the elution envelope were determined from the linear portion of the column calibration curve (constructed from all standards from NaPS 400 000 through sodium tannate). Calculations for column theoretical plate analysis were from Fritz and Schenk[9].

RESULTS AND DISCUSSION

A HPSEC column system consisting of Superose 6 HR (30 cm × 10 mm I.D.) and Superose 12 HR (30 cm × 10 mm I.D.) columns connected in series was calibrated with newly available, sulphonated polystyrene and polyacrylate standards. For determination of the lower portion of the calibration curve several well characterized, alkaline soluble compounds were used, including sodium tannate, sodium vanillate and sodium dihydroxynaphthalene sulfonate. Sodium azide was used as a marker of V_t (Fig. 1). When plotted as the simple function log molecular weight *versus* elution time, the calibration standards appear to produce a reasonably linear curve over the molecular weight region $1 \cdot 10^3$–$1 \cdot 10^5$ (Fig. 1). Although many other relationships between solute molecular weight (or, more accurately, effective hydrodynamic volume) and elution volume can be proposed[8,10], the function presented here appears adequate for the scope of this preliminary study.

The lignin samples examined are irregular phenylpropane polymers that represent approximately 30% (w/w) (native lignin) of the available polymeric content of hardwood tree stems[1]. This material offers, therefore, a valuable resource that must be utilized as fully as possible if full value of harvested tree crops is to be attained. Understanding the relationship between lignin apparent molecular weight and various physical properties is of great concern. The ball-milled aspen lignin sample loaded on the alkaline Superose system was eluted as a multimodal envelope, which was graphically deconvoluted to remove the unknown component eluting after V_t (Fig. 2). The M_w was found to be 2450. This value corresponds well with numerous hardwood milled lignins studied by Faix and co-workers[11,12], where for spruce, aspen, beech and birch lignins, M_w values between 2800 and 5500 were found. Whereas previous studies of acetylated and unacetylated lignins on μStyragel columns with organic solvents show varying degrees of column–solute interaction[13,14], Superose, a non-aromatic, strongly hydrophilic chromatography gel, contributes little such interaction in the

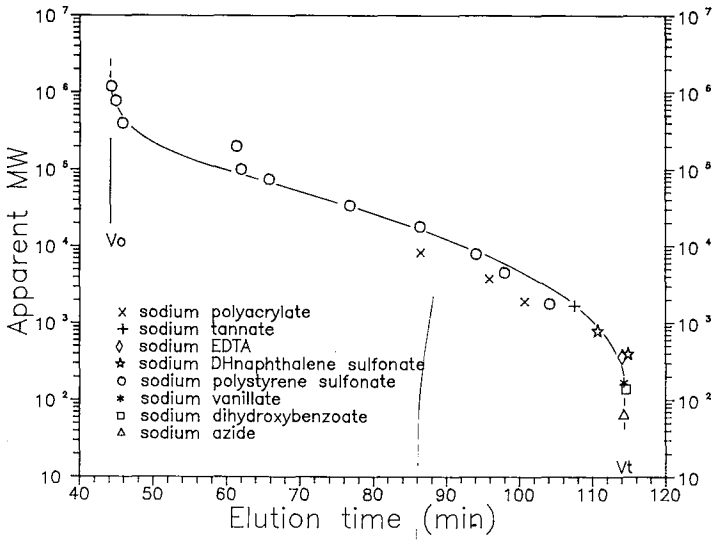

Fig. 1. Calibration of HPSEC column system consisting of one Superose™ 6 HR and one Superose 12 HR connected in series. The mobile phase was 0.1 *M* sodium hydroxide and the chromatography was conducted at 20°C. MW = Molecular weight; V_0 = the column elution volume corresponding to the interstitial volume between gel beads and V_t = the total liquid column volume; DH = dihydroxy.

presence of solvents like 0.1 *M* sodium hydroxide, which strongly dissociate both the solute and gel matrix[15], thus minimizing short-range adsorptive effects.

The coal-extract sample injected on the Superose system eluted as a narrow, symmetrical peak (Fig. 3). Graphical molecular weight distribution analysis produced values for M_n and M_w of 2800 and 3000, respectively. M_p was found to be 3900 by

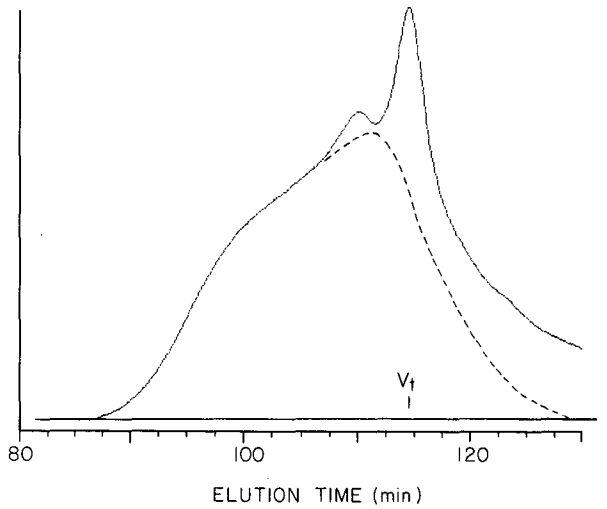

Fig. 2. Elution of ball-milled aspen lignin from Superose column system in 0.1 *M* sodium hydroxide. Column loading was 0.25 mg, the flow-rate was 0.3 ml/min and detection was at 280 nm. Dashed line shows result of graphical baseline subtraction and deconvolution of peak eluting after V_t (see text).

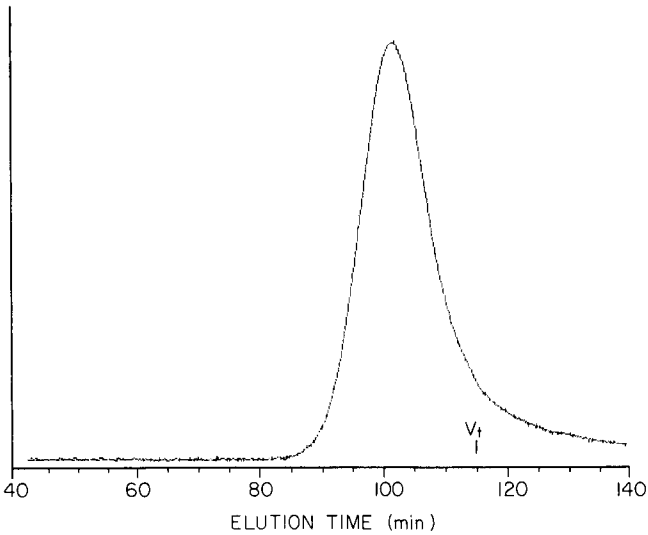

Fig. 3. Elution of acidified coal-extract from Superose column system in 0.1 *M* sodium hydroxide. Chromatography conditions as in Fig. 2.

comparison of the elution time of the peak-maximum-ordinate shown in Fig. 3 with the column calibration curve. The very low polydispersity found in the present study for this sample in sodium hydroxide (M_w/M_n = 1.03) may further reflect the low column–solute interaction available with this cross-linked dextran column packing material. Although the literature contains studies of molecular weight analyses of alkali-soluble, native coal extracts that yield molecular weights near $1 \cdot 10^6$ (ref. 16), studies describing the molecular weights of neutral pH, humic acid extracts of acid-hydrolyzed coal (as reported here) are not readily available.

In conclusion, "conventional gel permeation chromatographic" analysis was applied to Superose columns calibrated with alkali-stable standard polymers and low-molecular-weight acidic compounds. These compounds are similar in chemical structure to the polyphenolic or acidic biopolymers examined. Also, theoretical plate analysis for sodium azide elution showed the column system used in this study had $1.5 \cdot 10^4$ plates per meter, which is 10–100 times that possible with open-column type packing materials, such as Sephadex. Rigid, organic polymer-based packing materials for prepacked columns, such as TSK-gel PW series, although stable at pH 14, are quite hydrophobic and may retard the elution of polyphenol-containing polymers. Superose, the high-performance[17], alkali-stable, cross-linked dextran gel material, appears to be an ideal support matrix for SEC in strongly dissociating, high ionic strength solvents such as 0.1 *M* sodium hydroxide.

ACKNOWLEDGEMENTS

The authors wish to thank Helena Chum and David Johnson for samples of ball-milled aspen lignin. Work at the Solar Energy Research Institute was funded by the Biochemical Conversion Program at the U.S. Department of Energy Biofuels and

Municipal Waste Technology Division through FTP No. 658. This work was also funded under contract No. DE-AC07-761001570 from the U.S. Department of Energy office of Fossil Energy to the Idaho National Engineering Laboratory/EG&G Idaho, Inc.

REFERENCES

1 K. V. Sarkanen and C. H. Ludwig, *Lignins: Occurrence, Formation, Structure, and Reactions*, Wiley-Interscience, New York, 1971.
2 D. Fengel and G. Wegener, *Wood: Chemistry, Ultrastructure, Reactions*, Walter de Gruyter, Berlin, 1984.
3 J. G. McNaughton, W. Q. Yean and D. A. I. Goring, *Tappi*, 50 (1967) 548.
4 S. Sarkanen, D. C. Teller, E. Abramowski and J. L. McCarthy, *Macromolecules*, 15 (1982) 1098.
5 B. Lindqvist and T. Storgards, *Nature (London)*, 175 (1955) 511.
6 R. C. Montelaro, in P. L. Dubin (Editor), *Aqueous Size-Exclusion Chromatography*, Elsevier, Amsterdam, 1988, Ch. 10, pp. 269–296.
7 K. Lundquist, R. Ohlsson and R. Simonson, *Sven. Papperstidn*, 78(1975) 390.
8 W. W. Yau, J. J. Kirkland and D. D. Bly, *Modern Size Exclusion Chromatography*, Wiley, New York, 1979.
9 S. Fritz and G. H. Schenk, *Quantitative Analytical Chemistry*, Allyn & Bacon, Boston, 1974, p. 377.
10 M. E. Himmel and P. G. Squire, in P. L. Dubin (Editor), *Aqueous Size-Exclusion Chromatography*, Elsevier, Amsterdam, 1988, Ch. 1, pp. 3–22.
11 O. Faix, W. Lange and O. Beinhoff, *Holzforschung*, 34 (1980) 174.
12 O. Faix, W. Lange and E. C. Salud, *Holzforschung*, 35 (1981) 3.
13 H. L. Chum, D. K. Johnson, M. P. Tucker and M. E. Himmel, *Holzforschung*, 41 (1987) 97.
14 W. G. Glasser, P. C. Barnett, P. C. Muller and K. V. Sarkanen, *J. Agric. Food Chem.*, 31 (1983) 921.
15 P. L. Dubin, in P. L. Dubin (Editor), *Aqueous Size-Exclusion Chromatography*, Elsevier, Amsterdam, 1988, Ch. 3, pp. 55–75.
16 E. S. Olson, J. W. Diehl and M. L. Froehlich, *Fuel*, 66 (1987) 992.
17 T. Andersson, M. Carlsson, L. Hagel, P.-A. Pernemalm and J.-C. Janson, *J. Chromatogr.*, 326 (1985) 33.

Journal of Chromatography, 467 (1989) 315–320
Elsevier Science Publishers B.V., Amsterdam — Printed in The Netherlands

CHROM. 21 310

Note

Gas chromatographic determination of glycoprotein amino sugars as O-pentafluorobenzyloxime acetates

PIER ANTONIO BIONDI*, FRANCESCA MANCA, ARMANDO NEGRI, GABRIELLA TEDESCHI and CAMILLO SECCHI

Istituto di Fisiologia Veterinaria e Biochimica, Via Celoria 10, 20133 Milan (Italy)

(First received August 29th, 1988; revised manuscript received January 9th, 1989)

We recently introduced a method for the gas chromatographic (GC) determination of glycoprotein neutral monosaccharides[1]. The procedure requires derivatization with O-(2,3,4,5,6-pentafluorobenzyl)hydroxylamine (PFBOA) followed by acetylation to give stable pentafluorobenzyloxime acetates (Ac-PFBO). The separation of the Ac-PFBO derivatives was performed on fused-silica capillary columns coated with a polar cyanopropylsiloxane phase. However, we could not achieve a reliable simultaneous determination of the amino sugars present in glycoproteins, glucosamine (GlcN) and galactosamine (GalN). Adsorption of amino sugars on both glass and fused-silica capillary columns is a well known problem[2–4].

The aim of this work was to establish improved conditions that allow the method to be extended to the determination of both neutral and amino sugars. In addition, the reproducibility of the method was increased by using 3-O-methylglucose (OMeGlc) instead of *meso*-inositol as an internal standard for the final quantitative analysis. The glycidic content of standard glycoproteins is reported as an application of the improved procedure.

EXPERIMENTAL

Materials

PFBOA was supplied by Janssen (Beerse, Belgium), neutral and amino sugars by Fluka (Buchs, Switzerland) and standard glycoproteins by Sigma (St. Louis, MO, U.S.A.).

Apparatus

A DANI Model 3600 B gas chromatograph equipped with a flame ionization detector and adapted for capillary columns was used. Electron-impact mass spectrometric (MS) analysis was carried out with a Finnigan-MAT 1020 instrument at an ionizing voltage of 70 eV.

Chromatographic conditions

The separations were performed on a fused-silica column (6 m × 0.32 mm I.D.) wall-coated (0.2 μm) with CP-Sil 88 (Chrompack, Middelburg, The Netherlands). The

0021-9673/89/$03.50

following temperatures were applied: column, 140°C for 4 min, then 10°C/min to 240°C and held for 10 min; injector, 240°C; and detector, 250°C. Splitless injection was used (splitless time 40 s). The gas flow-rates were as follows: carrier gas (helium), 3 ml/min; hydrogen, 25 ml/min; and air, 350 ml/min. The carrier gas was purified by Gas-clean moisture and oxygen filters (Chrompack).

Derivatization

The procedure is only slightly different from that reported previously[1]. Aliquots of neutral and amino monosaccharides and of OMeGlc were withdrawn from their standard aqueous solutions (10 or 1 m*M*) and dried under vacuum over potassium hydroxide pellets. The reaction and extraction steps were carried out in PTFE-lined screw-capped vials. A 0.2-ml volume of pyridine containing 10 mg of PFBOA was added to the dried monosaccharides and the mixtures were maintained in an ultrasonic bath for 5 min. The tubes were then heated at 80°C for 20 min. After cooling, acetic anhydride (0.4 ml) was added and the samples were heated again for 20 min at 80°C. The reaction mixtures were evaporated nearly to dryness under a stream of nitrogen and the residues were dissolved in dichloromethane (3 ml) and washed with ice-cold 0.1 *M* hydrochloric acid (2 ml) and water (2 × 2 ml). The organic phases were filtered over anhydrous sodium sulphate and evaporated to dryness under a stream of nitrogen. The residues were dissolved in ethyl acetate (0.1 ml) and aliquots (1 μl) were analysed by GC.

Glycoprotein hydrolysis and determination were performed according to the previous protocol[1] with the exception of the use of OMeGlc as an internal standard. Calibration graphs were constructed in the ranges 5–500 and 10–1000 nmol for neutral and amino sugars, respectively. OMeGlc (50 nmol) was always added.

RESULTS

A typical chromatographic profile obtained from a sample containing neutral and amino sugars and OMeGlc as internal standard is shown in Fig. 1. All unknown peaks resulting from the reagents, solvents and occasional impurities are eluted before

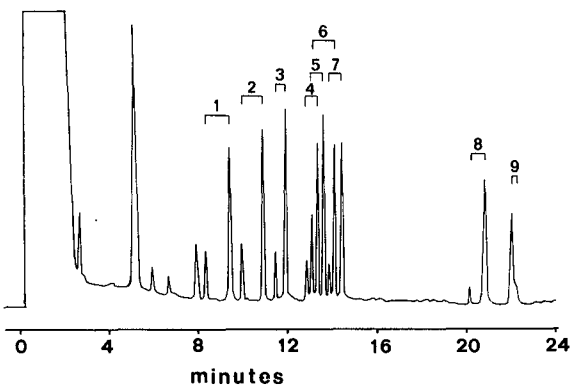

Fig. 1. Typical GC profile corresponding to a standard sample of neutral and amino sugars analysed according to the conditions described under Experimental. Peaks: 1 = fucose; 2 = arabinose; 3 = xylose; 4 = O-methylglucose; 5 = mannose; 6 = galactose; 7 = glucose; 8 = glucosamine; 9 = galactosamine.

fucose isomers. No other interferent peak hinders the analysis of the sugar derivatives, eluted with longer retention time owing to their higher molecular weight. In the profile, one of the two isomers of Ac-PFBO-GalN was present only as a shoulder on the predominant peak; nevertheless, its determination was reliable. In fact, the plot of the ratios between the height of the peak of Ac-PFBO-GalN and that of the predominant peak of Ac-PFBO-OMeGlc *versus* the amount of hexosamine was linear. The same linear relationship was obtained for the predominant isomers of all other monosaccharides. The parameters of the calibration graph are reported in Table I. The minimum detectable amount of GlcN and GalN was about 4 nmol, corresponding to 40 pmol injected.

The identity of the hexosamine derivatives was verified by MS. Mass spectra were recorded for both the minor and the predominant peaks of Ac-PFBO-GlcN and at the beginning and end of the Ac-PFBO-GalN peak. The portions of the spectra at m/z values higher than 300 are shown in Fig. 2 (the base peak was at 115 m/z for both derivatives and therefore it does not appear). The background noise is due to the high sensitivity used to show significant peaks. The structure and one of the characteristic fragmentations of hexosamine derivatives are shown in Fig. 3. No differences were found between the spectra of the two isomers of each amino sugar derivative, indicating that MS analysis allows the identity of the derivative to be established but does not distinguish between *syn* and *anti* isomers, as already observed for neutral sugars.

In order to study the stability of GlcN and GalN to trifluoroacetic acid (TFA), the standard amino sugars were subjected to derivatization with and without previous TFA treatment. By comparing the resulting peak heights, the mean recoveries ($n = 3$) for 50 nmol were 78% (range 72–84%) and 92% (range 83–95%) for GlcN and GalN, respectively.

Sugar components of some standard glycoproteins were determined as an example of the application of the modified procedure; the results are reported in Table II and a typical chromatographic profile is shown in Fig. 4.

TABLE I

CALIBRATION PARAMETERS

Calibration according to the equation $R_h = a + b$(nmoles monosaccharide), where R_h is the ratio between the height of the major peak of each monosaccharide and the major peak of OMeGlc. The regression lines for calibrations are obtained with different amounts of monosaccharides and the same amount (50 nmol) of OMeGlc as internal standard. The values reported are the means of three determinations.

Monosaccharide	*a (intercept)*	*b (slope)*	*r (correlation coefficient)*
Fucose	0.049	0.019	0.998
Arabinose	0.028	0.021	0.999
Xylose	0.042	0.024	0.999
Mannose	−0.033	0.026	0.999
Galactose	−0.009	0.020	0.999
Glucose	−0.002	0.021	0.999
Glucosamine	0.051	0.0079	0.994
Galactosamine	0.020	0.0056	0.995

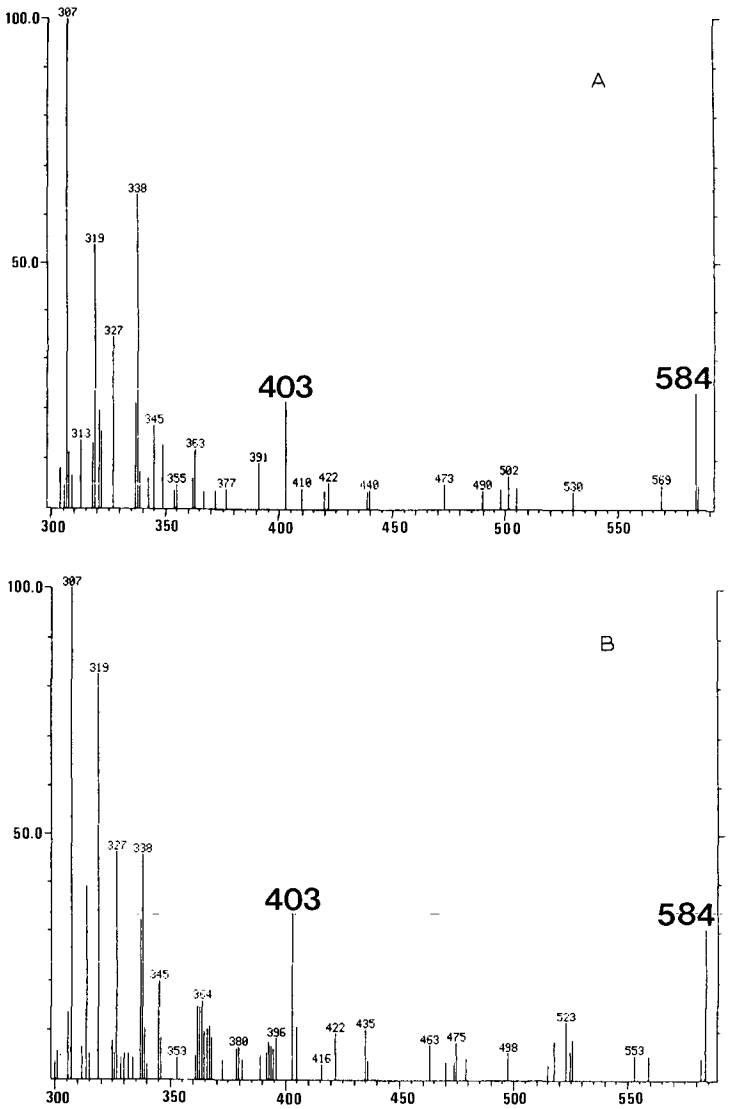

Fig. 2. Portions of mass spectra at m/z values higher than 300 of Ac-PFBO derivatives of (A) glucosamine and (B) galactosamine.

DISCUSSION

Previously, neutral sugars were separated as their Ac-PFBO derivatives on a 15-m capillary column coated with a cyanopropylsiloxane phase[1]. Under the reported conditions GlcN and GalN derivatives gave good and well resolved peaks only when brief linear high-temperature programmes (from 200 to 240°C at 15°C/min) were used. When the running time was increased by using lower initial temperatures,

TABLE II

CONTENTS OF ALDOSES AND HEXOSAMINES (%, w/w) IN SOME KNOWN GLYCOPROTEINS

Glycoprotein		*Monosaccharide*				
		Fucose	*Mannose*	*Galactose*	*N-Acetylglucos-amine*	*N-Acetylgalactos-amine*
Foetal calf serum	Found	–	2.6	4.3	6.7	1.1
asialofetuin	Ref. 5	–	2.9	4.2	5.9	1.0
Bovine thyroglobulin	Found	0.5	2.2	1.6	6.8	–
	Ref. 6	0.4	2.3	1.3	6.0	–
Bovine α_1-acid	Found	0.7	5.9	6.8	10.5	–
glycoprotein	Ref. 7	0.8	5.8	7.0	11.0	–
Ovalbumin	Found	–	2.1	0.2	1.1	–
	Ref. 8	–	2.4	0.15	1.3	–

the GlcN and GalN peaks broadened and their determination was unreliable. However, this applies only to new columns. In fact, with a column life as short as about 2 weeks the amino sugars peaks completely disappeared also using brief high-temperature programmes. This confirms the difficulties encountered by other workers with the GC analysis of amino sugars on fused-silica and especially glass capillary columns[2–4]. In our case, the use of PFBOA results in derivatives with high molecular weight and low volatility, which are more likely to be adsorbed than other derivatives commonly used in the GC analysis of monosaccharides (*e.g.*, alditol acetates, aldonitrile acetates and O-methyl oxime acetates).

In order to overcome this problem, we adjusted the length of the capillary column and increased the purity of the carrier gas. The column length was reduced from 15 to 6 m and helium was cleaned by filters retaining water and oxygen. The results were very satisfactory with regard to both efficiency and reproducibility of the amino sugar determination. The Ac-PFBO-GlcN and Ac-PFBO-GalN peaks were narrow and easily quantified at nanomole level also with the programme needed for the determination of all the monosaccharides. In fact, in spite of the use of a shorter column the separation of *syn* and *anti* isomers of the neutral sugars remained unaffected. Moreover, as the chromatographic behaviour of the hexosamine derivatives was independent of the column age, reliable routine analysis were assured for at least 4 months.

With regard to quantitative analysis, OMeGlc was preferred to the previously

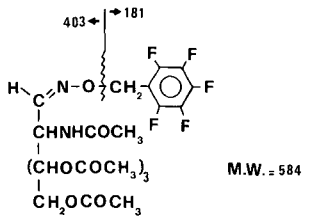

Fig. 3. Structure and a characteristic fragmentation of Ac-PFBO derivatives of hexosamines.

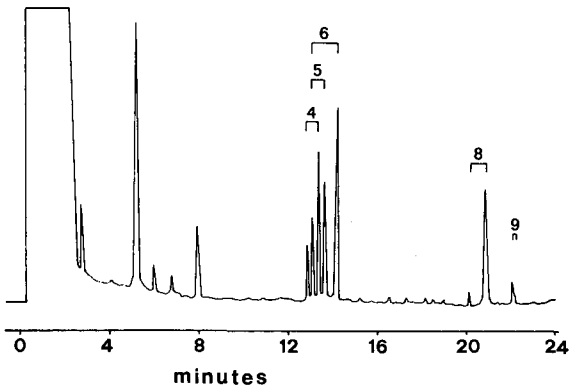

Fig. 4. Typical GC profile corresponding to a sample of foetal calf serum asialofetuin analysed according to the described procedure. Peak numbers as in Fig. 1.

used *meso*-inositol as an internal standard because it is more similar chemically to monosaccharides. The correlation coefficients of the calibration graphs for neutral sugars reported in Table I are higher than those obtained with *meso*-inositol; this can be explained by the involvement of OMeGlc in both derivatization steps, whereas *meso*-inositol was involved only in the acetylation step. The other difference from the previous procedure is the smaller volumes of pyridine and acetic anhydride in the reaction mixtures (while the amount of PFBOA used is unchanged). The use of an ultrasonic bath, in fact, ensured good solubilization of the monosaccharides in a lower volume, while the final time-consuming evaporation step was speeded up.

ACKNOWLEDGEMENTS

This work was supported by a grant from the Ministereo della Pubblica Istruzione (40% funds; project "The glycoconjugates in cellular normal and pathological processes").

REFERENCES

1 P. A. Biondi, F. Manca, A. Negri, C. Secchi and M. Montana, *J. Chromatogr.*, 411 (1987) 275.
2 J. R. Hudson, S. L. Morgan and A. Fox, *J. High Resolut. Chromatogr. Chromatogr. Commun.*, 5 (1982) 285.
3 A. Fox, S. L. Morgan, J. R. Hudson, Z. T. Zhu and P. Y. Lau, *J. Chromatogr.*, 256 (1983) 429.
4 J. R. Neeser and T. F. Schweizer, *Anal. Biochem.*, 142 (1984) 58.
5 J. R. Neeser, *Carbohydr. Res.*, 138 (1985) 189.
6 T. P. Mawhinney, M. S. Feather, G. J. Barbero and J. R. Martinez, *Anal. Biochem.*, 101 (1980) 291.
7 D. G. Pritchard and W. Niedermeier, *J. Chromatogr.*, 152 (1978) 487.
8 S. Honda and S. Suzuki, *Anal. Biochem.*, 142 (1984) 167.

Journal of Chromatography, 467 (1989) 321–326
Elsevier Science Publishers B.V., Amsterdam — Printed in The Netherlands

CHROM. 21 250

Note

Rapid high-performance liquid chromatographic method for the determination of bencetonium chloride residues in fish products; confirmation by thin-layer chromatography

Th. B. A. REUVERS*
Dpto. of Bromatologia, Centro Nacional de Alimentación y Nutrición, Majadahonda, Madrid (Spain)
G. ORTÍZ
University of Bogotá, Bogotá (Colombia)
and
M. RAMOS and M. MARTÍN DE POZUELO
Dpto. of Bromatología, Centro Nacional de Alimentación y Nutrición, Majadahonda, Madrid (Spain)
(First received February 18th, 1988; revised manuscript received January 4th, 1989)

Bencetonium chloride is a surface-active agent and exhibits antiseptic properties.

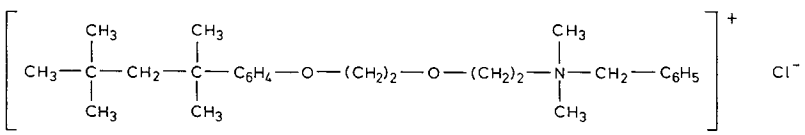

Benzyl(diisobutylphenoxyethoxyethyl)dimethylammonium chloride

It is used frequently as an algicide, bactericide and fungicide in dairies and food industries in many countries. The need for the detection and identification of its residues in food is of great importance as contamination of food with this quaternary ammonium compound (QAC) is forbidden.

Various techniques have been applied to the quantitative analysis of QACs; a common method used for the determination of QAC residues in milk[1–4] involves ion pairing of the material with an acid dye and subsequent extraction into an organic phase such as chloroform or dichloromethane, followed by spectrophotometric measurement. However, this technique does not provide any information about the QAC found and it is not very useful for residue analysis in food because of the formation of emulsions which inhibit extraction and lower recoveries.

The introduction of chromatographic techniques increased the specificity and sensitivity in the analysis of QAC, which are poor in the colorimetric method. Gas chromatography (GC) and high-performance liquid chromatography (HPLC) have been applied in distribution studies of various QACs[5–9].

Larson and Pfeiffer[10] proposed a liquid chromatographic method with indirect photometric detection using benzyltrimethylammonium salt in the mobile phase as an

0021-9673/89/$03.50

UV-absorbing counter ion. Kawase *et al.*[11] present an interesting technique based on the separation of dialkyl-type cationic surfactants by HPLC and on-line ion-pair extraction of the surfactant with bromophenol blue into an immiscible organic phase. However, these methods cannot be applied to the determination of residues of QACs in a complex matrix.

Almost no relevant methods for the detection and quantitation of QACs are available and only a few authors have reported work in this field. Pohlmann and Cohan[12] describe the detection of QACs in biological fluids by GC, and Wee and Kennedy[13] developed a liquid chromatographic method with conductometric detection for the determination of trace levels of QACs in river-water.

The determination of QACs in meat and meat products has been described by Harke *et al.*[14]: the samples were extracted with organic solvents and the residues of QACs detected by thin-layer chromatography (TLC). Rojas *et al.*[15] proposed a colorimetric method for a cationic surfactant in fish, which resulted in a determination of the total QACs, without their individual identification. These two methods show some difficulties in the extraction and isolation of the QACs from the complex matrices. Therefore, Reuvers *et al.*[16] presented an extraction method in which 1-hexanesulphonic acid was used as the counter ion during the extraction of benzalkonium chloride from fish products. TLC based on the method as described by Harke *et al.*[14] was used for the detection of the surfactant.

HPLC has not yet been employed in the detection of bencetonium chloride residues in foods. Here, we propose a method based on such a technique, using a counter ion in the extraction and chromatographic procedure.

EXPERIMENTAL

Reagents and instrumentation

All solvents were reagent grade and used as received. The counter ion 1-hexanesulphonic acid was supplied by Scharlau (F.E.R.O.S.A., Barcelona, Spain) and hexachloroplatinic(IV) acid by BDH Chemicals (U.K.).

The HPLC equipment consisted of a Waters pump, an injector (U6K) and UV absorption was monitored at 254 nm with a fixed-wavelength detector (Waters R 441 UV) at a range setting of 0.02 a.u.f.s. The HPLC column (30 cm × 3.9 mm) used throughout this work was packed with μBondapak-CN (Waters); it was used at room temperature. The eluent consisted of acetonitrile–0.1 *M* ammonium acetate (75:25) with the addition of 15 ml PIC B6 (Waters) per litre of the mobile phase. Flow-rate: 1 ml/min.

Extraction and clean up of bencetonium chloride from fish samples

A 10-g sample of minced hake, European squid or shortfin squid was mixed thoroughly with 50 ml of 96% ethanol, 0.05 ml 1-hexanesulphonic acid and 0.5 ml 2 *M* HCl. After 1 h the suspension was filtered into a 250-ml round-bottom flask. The residue was extracted with a second portion of 50 ml 96% ethanol and the ethanolic supernatant filtered into the same flask. The filter cake was pressed and washed with 25 ml of ethanol and the pooled extracts were dried in a rotatory evaporator under vacuum at $<70°C$. The dry residue was taken up in 0.5 ml 2 *M* HCl, 0.5 ml methanol, 0.05 ml 1-hexanesulphonic acid and 5 ml light petroleum (b.p. 30–40°C). The

suspension was agitated for 2 min and the mixture transferred to an extraction tube (25 ml, 3 cm I.D.). The round-bottom flask was rinsed subsequently with the same mixture and with 5 ml light petroleum; both rinses were transferred to the extraction tube.

The extracts were mixed and heated in a warm water-bath (70°C) until the organic layer had disappeared. A 2-ml volume of dichoromethane–light petroleum (1:1) was added to the retained aqueous phase followed by mixing for 1 min to achieve complete extraction of the bencetonium chloride–counter ion complex. The organic phase was used for analysis.

Detection and identification by HPLC

Different amounts of standard BC (bencetonium chloride) were injected to check the linear response of the detector. Recovery experiments were carried out on spiked samples of different fish products by injection of 5, 10 or 20 μl of the organic layer (2 ml) obtained under the conditions of extraction, purification and detection, as described above.

Confirmation by TLC

A 10-μl volume of the sample extracts was applied on Kieselgel 60 plates (20 cm $\times$ 20 cm) and eluted by *n*-butanol–acetic acid–water (4:1:1). The plates were air-dried and sprayed with the following reagent: 3 ml of 10% aqueous hexachloroplatinic(IV) acid mixed with 97 ml of water and 100 ml 6% aqueous KI. The detergent appeared inmediately as dark blue spots on a rose background.

RESULTS AND DISCUSSION

Different amounts of a 0.1% solution of bencetonium chloride in water were injected into the chromatographic system (0.02 and 0.05 a.u.f.s. $\times$ range setting) and peak heights were measured. The calibration graph was calculated using the method of least squares and can be expressed as $y = 25.8x + 15.8$, where y = BC peak height in mm at 254 nm (0.02 a.u.f.s.) and x = the amount of BC injected (on different days). The linearity was satisfactory with a correlation factor, $r = 0.983$ and was linear up to 10 μg injected. The standard deviation (S.D.) was 1.7 ng/mm at 0.02 a.u.f.s. with a coefficient of variation (C.V.) of 6.5%.

The retention time (about 6 min) of BC under these chromatographic conditions is long enough to assure the separation of the front peak in the fish samples. Fig. 1 shows a chromatogram of 2 μg of BC injected under the conditions described.

To check the validity of the proposed extraction and clean up, various commercial samples of fish products were homogenized and spiked with different amounts (up to 100 ppm) of BC and the extracts analyzed. Typical chromatograms of spiked (50 ppm) and unspiked hake extracts are shown in Fig. 2. It is seen that the separation of the BC peak from the front peak is sufficient to analyze BC in fish. Recoveries for hake are shown in Table I, based on the calibration graph.

The same procedures were carried out with commercial squid samples. The results are shown in Fig. 3 and Table II.

The "unusual" extraction and clean-up procedures are necessary to desorb and suspend all the sediments present on the walls of the flask. In our earlier extraction experiments[16], carried out without light petroleum in the extraction mixture,

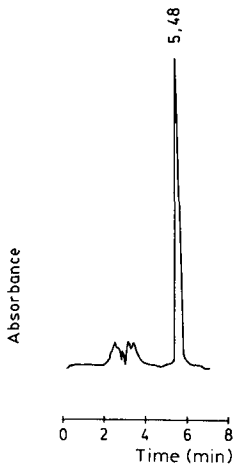

Fig. 1. Chromatogram of 2 μg bencetonium chloride.

sediments remained on the wall with BC adsorbed, resulting in very low recoveries. The presence of the counter ion in an acid medium facilitates the extraction of BC into the organic layer, which, however, does not contain all the BC present. That is the reason for the evaporation of the organic layer in the presence of the aqueous layer and

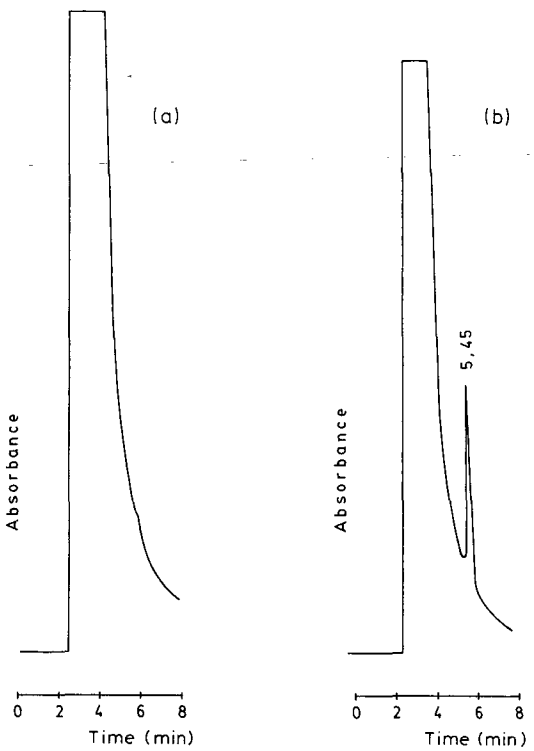

Fig. 2. Typical chromatograms of (a) unspiked and (b) spiked (50 ppm) hake extracts.

TABLE I
RECOVERY OF BENCETONIUM CHLORIDE IN HAKE

Hake	*Found mean value (ppm) (n=4)*	*Recovery (%)*	*C.V. (%)*
10 g	–	–	
10 g + 10 ppm	8.6	86.3	6.3
10 g + 25 ppm	23.0	92	13.4
10 g + 100 ppm	87.4	87.4	19.0

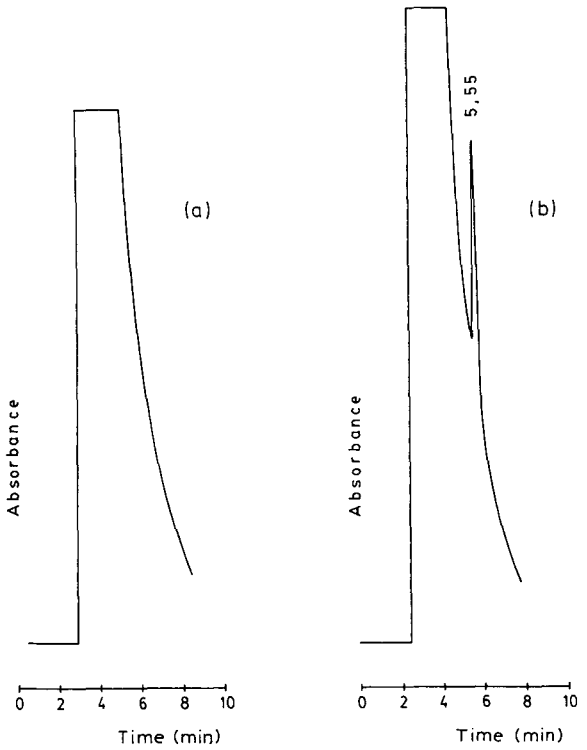

Fig. 3. Typical chromatograms of (a) unspiked and (b) spiked (50 ppm) squid extracts.

TABLE II
RECOVERY OF BENCETONIUM CHLORIDE IN SQUID

Squid	*Found mean value (ppm) (n=4)*	*Recovery (%)*	*C.V. (%)*
10 g	–		
10 g + 10 ppm	9.1	91.0	21
10 g + 25 ppm	22.1	88.4	19
10 g + 50 ppm	41.9	83.7	19
10 g + 100 ppm	88.1	88.1	9.2

its subsequent extraction with dichoromethane–light petroleum (1:1), which results in the complete transfer of the BC–counter ion complex into the organic layer. The presence of light petroleum in this mixture is necessary to assure that the organic layer is always the upper layer. The procedure described is suitable for fatty and non-fatty fish. Recoveries were satisfactory as shown in Tables I and II. The method was linear between 0 and 500 ppm, in which range BC occurs in fish products, and the detection limit is approximately 5–10 ppm.

However, the presence of BC should be confirmed. TLC may be used for the identification of BC. Under the conditions described, aliquots of 10 μl of the fish extracts and different amounts of the standard (1, 2, 5 μg) are added to the Kieselgel 60 (Merck) plate and eluted. Immediately after the development with the spray reagent, the spots are observed and quantitated by visual comparison of their intensities with these of standard spots. The detection limit is about 10 ppm and the TLC results are well in agreement with the values obtained using the HPLC method proposed. Other QACs such as benzalkonium chloride are visible, but they do not interfere because of their higher R_F values.

ACKNOWLEDGEMENTS

The authors thank N. Mendez and C. Díaz for their analytical assistance and A. Gómez for technical assistance in the preparation of the manuscript.

REFERENCES

1 G. Wildbrett and F. Einreiner, *Z. Lebensm.-Unters.-Forsch.*, 165 (1977) 34.
2 F. Munaò and O. C. Grillo, *Il Latte*, 5 (1980) 673.
3 S. G. Faber, H. G. Gasthuis, G. van der Haar and G. Veenkamp, *De Ware(n) Chemicus*, 8 (1978) 138.
4 *Methods of analysis of AOAC*, Association of Official Analytical Chemists, Washington, DC, 13th ed., 1980, method No. 20.077-20.089, pp. 333–336.
5 L.-K. Ng, M. Hupé and A. G. Harris, *J. Chromatogr.*, 351 (1986) 554.
6 S. L. Abidi, *J. Chromatogr.*, 200 (1980) 216.
7 A. Nakae, K. Kunihiro and G. Muto, *J. Chromatogr.*, 134 (1977) 459.
8 J. Kawase, Y. Takao and K. Tsuji, *J. Chromatogr.*, 262 (1983) 48.
9 R. C. Meyer, *J. Pharm. Sci.*, 69 (1980) 1148.
10 J. R. Larson and C. D. Pfeiffer, *Anal. Chem.*, 55 (1983) 393.
11 J. Kawase, Y. Takao and K. Tsuji, *J. Chromatogr.*, 262 (1983) 293.
12 J. L. W. Pohlmann and S. L. Cohan, *J. Chromatogr.*, 131 (1977) 297.
13 V. T. Wee and J. M. Kennedy, *Anal. Chem.*, 54 (1982) 1631.
14 H. P. Harke, G. Bestmann and M. Linke, *Gordian*, 1 (1978) 7.
15 E. Rojas, P. Lasa, J. J. Rivera and E. Muro, *Quím. Ind. (Madrid)*, 28 (1982) 205.
16 Th. Reuvers, G. Ortíz, M. Martín de Pozuelo and M. Ramos, *II World Congress of Food Technology, Barcelona, March 3–6, 1987.*

Journal of Chromatography, 467 (1989) 327–331
Elsevier Science Publishers B.V., Amsterdam — Printed in The Netherlands

CHROM. 21 209

Note

Rapid, sensitive high-performance liquid chromatographic method for the analysis of buflomedil hydrochloride and its potential by-products

M. GOBETTI*, M. DI BITETTO and R. ROSSI
Chemical Division R. and D. Dept., PIERREL S.p.A., Via Bisceglie 96, 20152 Milan (Italy)
(First received September 12th, 1988; revised manuscript received November 28th, 1988)

Buflomedil hydrochloride [2′,4′,6′-trimethoxy-4-(1-pyrrolidinyl)butyrophenone] is a peripheral vasodilatator[1–4] currently widely employed in the treatment of peripheral vascular diseases. The synthesis of this compound is relatively simple, but impurities may occur (Fig. 1).

We have developed a rapid, sensitive high-performance liquid chromatographic (HPLC) method for the simultaneous separation and determination of buflomedil hydrochloride and related by-products using a reversed-phase Supelcosil LC-8 3-μm column and 0.005 *M* KH_2PO_4–acetonitrile as a mobile phase. Two HPLC methods[5,6] for the determination of buflomedil hydrochloride have been reported but, in both cases, sodium lauryl sulphate was used as an ion-pair reagent and moreover the separation from related impurities was not taken into account.

EXPERIMENTAL

Apparatus

Buflomedil hydrochloride and its potential by-products were separated on an Hewlett-Packard HPLC system consisting of a Model 1084 B liquid chromatograph equipped with a variable-wavelength detector set at 230 nm and a Model 79850 B LC terminal which served as a gradient controller and data station. Samples of 20 μl, prepared by dissolving the products in the mobile phase, were injected via a Model 79841 variable volume injector and separated on Supelcosil LC-8 3 μm, 3.3 cm × 4.6 mm I.D. The mobile phase, acetonitrile–0.005 *M* KH_2PO_4 pH 3, was filtered and deaerated before use and delivered according to the gradients indicated in Fig. 2. During analysis, both the solvents and column compartment were maintained at 40°C.

Chemicals and reagents

All the solvents used were HPLC-grade (Merck, Darmstadt, F.R.G.) except water. Distilled water was deionized and filtered through a Milli-Q water purification system. Monobasic potassium phosphate, 1,3,5-trimethoxybenzene as well as the other reagents were obtained from Janssen Chimica (Beerse, Belgium).

Buflomedil hydrochloride was synthesized according to the method described[7], while the by-products were separated by liquid chromatography on a silica-gel column using ethyl acetate–hexane (20:80, v/v) as the mobile phase.

0021-9673/89/$03.50

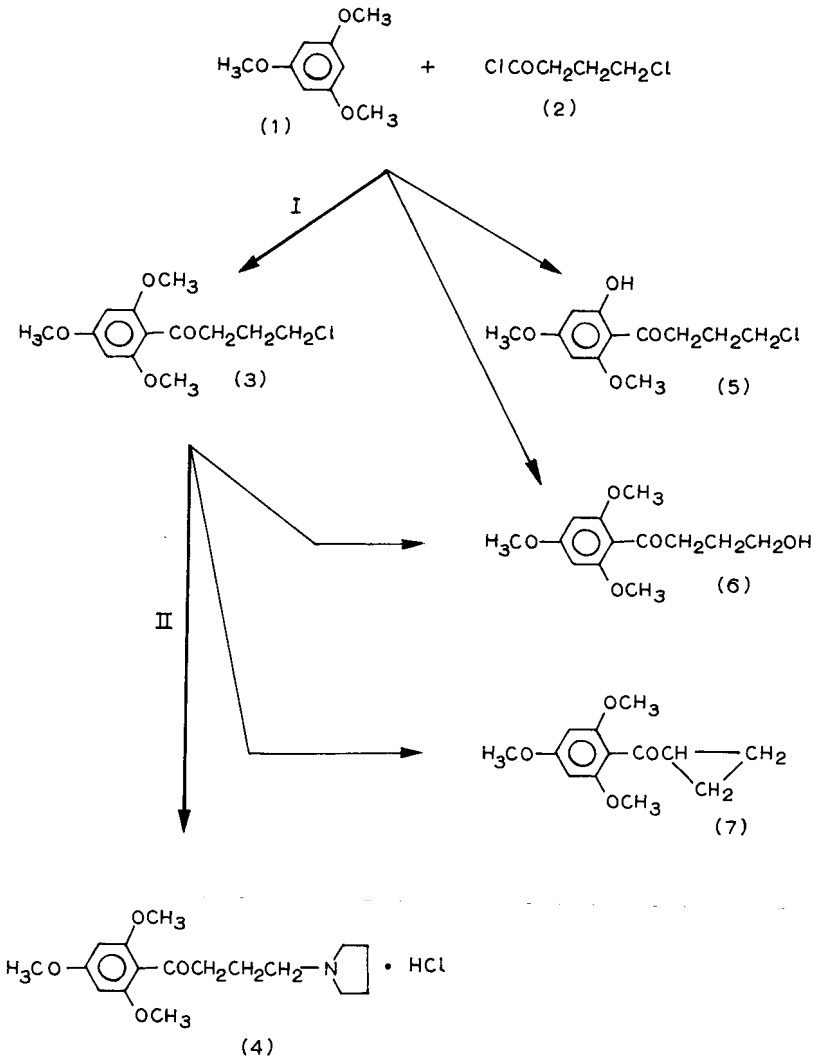

Fig. 1. Synthetic pathway for buflomedil hydrochloride, **1** = 1,3,5-trimethoxybenzene; **2** = 4-chlorobutyryl chloride; **3** = 2′,4′,6′-trimethoxy-4-chlorobutyrophenone; **4** = buflomedil hydrochloride; **5** = 2′-hydroxy-4′,6′-dimethoxy-4-chlorobutyrophenone; **6** = 2′,4′,6′-trimethoxy-4-hydroxylbutyrophenone; **7** = cyclopropyl(2,4,6-trimethoxyphenyl)methanone.

The structures were assigned by elemental analysis and ^{1}H and ^{13}C NMR spectroscopy.

Sensitivity, linearity and precision

The external standard technique was used to check the sensitivity, the linearity and the precision of the assay. The proportionality of the peak height to the amount of buflomedil hydrochloride and of all other products was measured in the range of 0–200

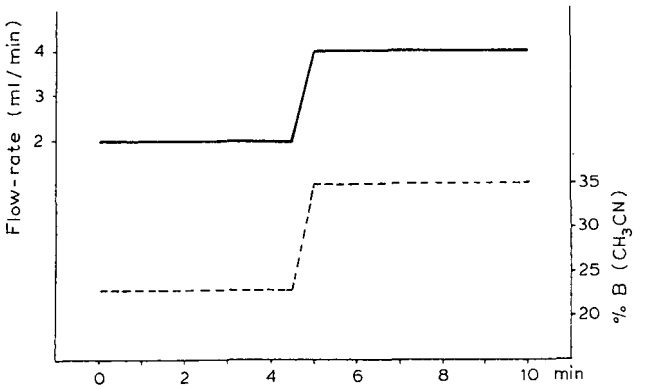

Fig. 2. Flow (———) and mobile phase (– – –) gradients.

μg/ml. The calibration graphs were linear in this range; the correlation coefficients and the detection limits for buflomedil hydrochloride and its by-products are reported in Table I.

The reproducibility of the chromatographic procedure was indicated by

TABLE I

LINEARITY AND SENSITIVITY OF THE ANALYTICAL PROCEDURE

Product[a]	*Slope*	*Correlation coefficient*	*Detection limit (μg on column)*
A	1.025	0.996	0.35
B	0.985	0.995	0.10
C	0.982	0.997	0.40
D	1.004	0.996	0.40
E	1.032	0.995	0.35
F	1.040	0.995	0.12

[a] A = 2′,4′,6′-Trimethoxy-4-hydroxybutyrophenone; B = buflomedil hydrochloride; C = 1,3,5-trimethoxybenzene; D = cyclopropyl(2,4,6-trimethoxyphenyl)methanone; E = 2′,4′,6′-trimethoxy-4-chlorobutyrophenone; F = 2′-hydroxy-4′,6′-dimethoxy-4-chlorobutyrophenone.

TABLE II

PRECISION OF THE ANALYTICAL PROCEDURE

Products as in Table I. $n = 10$. Concentration of each product was 20 μg/ml.

Product	*Rel. standard deviation (%)*
A	± 0.35
B	± 0.32
C	± 0.40
D	± 0.25
E	± 0.37
F	± 0.25

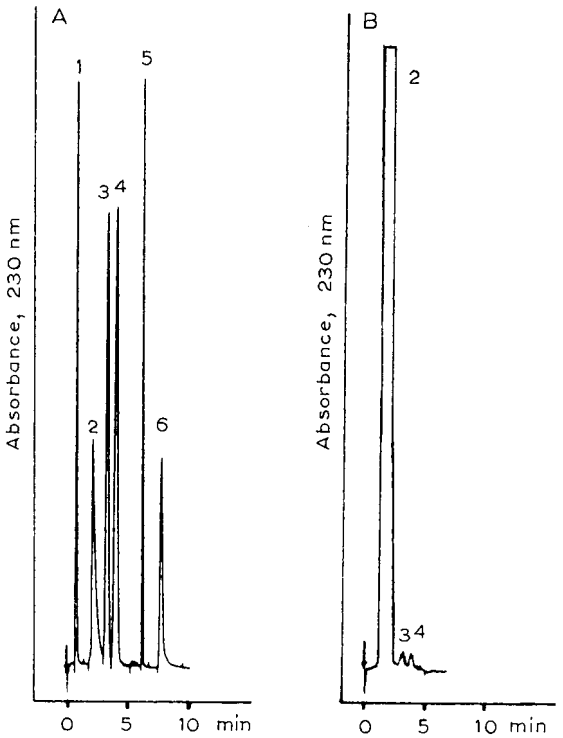

Fig. 3. Chromatograms of an artificial mixture (20 μg/ml) of each compound (A) and of 100 μg/ml of buflomedil, 0.5 μg/ml of impurities **1** and **7** (B). Peaks: 1 = 2′,4′,6′-trimethoxy-4-hydroxybutyrophenone; 2 = buflomedil hydrochloride; 3 = 1,3,5-trimethoxybenzene; 4 = cyclopropyl(2,4,6-trimethoxyphenyl)-methanone; 5 = 2′,4′,6′-trimethoxy-4-chlorobutyrophenone; 6 = 2′-hydroxy-4′,6′-dimethoxy-4-chloro-butyrophenone.

replicate injection of the same standard solutions; the relative standard deviations are reported in Table II.

RESULTS

The chromatograms shown in Fig. 3 are typical of an artificial mixture of buflomedil hydrochloride and related impurities. In chromatogram A the concentration of each product was 20 μg/ml and the attenuation was 0.0256 a.u.f.s., while in chromatogram B the concentration of buflomedil hydrochloride was 100 μg/ml while those of the impurities **1** and **7**, which are the most important were 0.5 μg/ml and the attenuation was 0.0064 a.u.f.s.

DISCUSSION

We have developed an high speed (less than 10 min) and highly sensitive HPLC method that allows the efficient and simultaneous separation and quantitation of buflomedil and synthesis-derived impurities.

According to the synthetic pathway (Fig. 1), in the first step, if the temperature is not well controlled, the presence of the Lewis acid can produce demethylation of an *o*-methoxy group with consequent formation of the impurity **5**.

In the second step there are three possible mechanisms of reaction: substitution of chlorine by pyrrolidine yields the expected product **4**; substitution of chlorine by hydroxyl, which may occur in basic media (second step) or in acidic media (first step in the presence of moisture); dehydrohalogenation with cyclization to yield impurity **7**. The impurity **7** is the most important because in raw buflomedil it is present in considerable amount and even after purification by crystallization it is possible to detect traces of this product. Some commercial samples of buflomedil, analyzed according to our method, do not show the presence of impurity **7**, nevertheless we think that it is very important to monitor this by-product.

In our method the use of KH_2PO_4 instead of sodium lauryl sulphate, and the low pH of the mobile phase, leads to a longer column life.

ACKNOWLEDGEMENTS

We thank E. Pantò, M. Inglesi and G. Fioriello for their technical assistance in the preparation of buflomedil hydrochloride and by-products.

REFERENCES

1 P. C. Braga, V. Capponi and G. Cagnetta, *Clin. Trials*, 17 (1980) 64.
2 J. Roussel and A. Oliveux, *Extract de La Vie Medicale*, 6 (1979) 1459.
3 G. Rosas, C. Cerdeyra, M. A. Lucas, I. R. Parano and J. J. Villa, *Angiology*, 32 (1981) 291.
4 P. Galley and A. de Boysson, *La Revue de Geriatrie*, 6 (1981) 151.
5 J. A. Badmin, J. L. Kumar and W. C. Mann, *J. Chromatogr.*, 172 (1979) 319.
6 E. W. Thomas, *J. Chromatogr.*, 228 (1982) 387.
7 E. W. McKellin, *U.S. Pat.*, 4 326 082 (1981).

Journal of Chromatography, 467 (1989) 332–335
Elsevier Science Publishers B.V., Amsterdam — Printed in The Netherlands

CHROM. 21 361

Note

Stability-indicating high-performance liquid chromatography assay for the anticancer drug bryostatin 1

JOHN C. BAER and JOHN A. SLACK*

Cancer Research Campaign Experimental Chemotherapy Group, Pharmaceutical Sciences Institute, Aston University, Birmingham B4 7ET (U.K.)

and

GEORGE R. PETTIT

Cancer Research Institute and Department of Chemistry, Arizona State University, Tempe, AZ 85287 (U.S.A.)

(First received October 12th, 1988: revised manuscript received January 9th, 1989)

In 1968[1] we observed that extracts of the marine bryozoan *Bugula neritina* (Linnaeus) provided exceptional antineoplastic activity (100% life extension) against the U.S. National Cancer Institute's (NCI) murine P388 lymphocytic leukemia (PS system). Fourteen years later we reported[2] the isolation and X-ray crystal structure of bryostatin 1 the most prominent member of a new series[3] of macrocyclic lactones with remarkable biological properties. For example, against the PS leukemia bryostatin 1 has provided 52–96% life extension at 10–70 μg (injection dose per kg) levels and against the NCI murine M5 ovarian carcinoma tumor regression model a 20–65% curative response at 20–40 μg/kg. With the M531 murine ovarian sarcoma [intraperitoneal (i.p.) tumor implant with i.p. treatment] bryostatin 1 afforded 31–68% life extension at 5–40 μg/kg. More recently this potentially important substance has shown exceptional selectivity against human cancer cell lines (NCI representing leukemias, non-small cell lung cancer, melanoma and renal cancer).

Furthermore, bryostatin 1 has been found capable of producing powerful antitumor promoting[4,5], immunomodulating[6,7] and normal bone marrow cell growth stimulating[8] responses. Consequently, preclinical development of bryostatin 1 has been undertaken by the Cancer Research Campaign and the NCI. This work describes the development of a stability-indicating high-performance liquid chromatographic (HPLC) assay for the drug, prior to formulation for clinical trial.

EXPERIMENTAL

Materials

Before use, the HPLC-grade solvents (from BDH, Poole, U.K.) and the deionised and distilled water were filtered. The bryostatins were isolated as previously described[1]. Cholest-4-en-3-one (internal standard) was obtained from Aldrich (Gillingham, U.K.).

The HPLC system comprised three Waters 510 pumps, a 490 UV detector and

0021-9673/89/$03.50

a 710B WISP autosampler controlled by an 840 data station. The injection volume was 0.01 ml. A Waters μBondapak Phenyl column, 10 μm particle size, 8 mm I.D., was used under radial compression.

Method development

Assay development was restricted due to the small amount of bryostatin 1 available (8 mg). An initial isocratic mobile phase containing acetonitrile–distilled water (72:28, v/v) was selected with cholest-4-en-3-one as an internal standard. Detection was at the $\lambda_{max.}$ of bryostatin 1 (266 nm) and the mobile phase flow-rate was 1.5 ml/min.

Optimization was carried out using a "Snyder triangle" separation[9] with the three isocratic solvents (A) methanol–distilled water (85:15), (B) acetonitrile–distilled water (72:28), and (C) tetrahydrofuran–distilled water (56:44). A computer plot was used to predict the optimum mobile phase in terms of resolution between, and widths of, the two peaks. Resolution was greater than 2 for all predicted solvent mixtures and the optimum, in fact, turned out to be pure solvent A.

RESULTS AND DISCUSSION

Validation

Formulated bryostatin 1 solutions containing 0.1 mg/ml in absolute ethanol were prepared. HPLC vials were prepared containing an equal volume of internal standard, 0.4 mg/ml cholest-4-en-3-one in ethanol. The internal standard solution was stored at 4°C and renewed each week. Detection was at 266 nm, range 0.2 a.u.f.s.

The reproducibility of the chromatographic separation was good, both in terms of retention times and peak areas. The coefficient of variation for injection ($n=6$) was 1.1% and between day variation ($n=21$) was 3.1%. Calibration curves were linear over the concentration range 0.025 to 0.075 mg/ml with a correlation coefficient greater than 0.998. Using UV detection, the limit of detection of bryostatin 1 was 5 ng on column.

Degradation and related compounds

Bryostatin 1 was heated at 70°C in solutions containing 0.1 *M* hydrochloric acid, 0.1 *M* sodium hydroxide, 0.1 *M* hydrogen peroxide, or water. Samples were taken from 0–4 h and analysed by HPLC. After 4 h, the compound appeared to be stable in distilled water or hydrogen peroxide but was 100% degraded in alkali and 33% degraded in acid, presumably due to cleavage of ester groups (Fig. 1). Repeating the experiment in phosphate buffer (0.1 *M*, pH 9.3) gave a number of degradation peaks. Identification of the degradation products is ongoing. Bryostatin 2 (Fig. 1) in dimethyl sulphoxide, a desacetyl analogue of bryostatin 1 and potential degradation product, was resolved from bryostatin 1 (Fig. 2).

Solubility

The solubility of bryostatin 1 in ethanol–aqueous solutions was assessed using this analysis method. Briefly, a known concentration of bryostatin 1 in ethanol was stirred with increasing volumes of 0.9% (w/v) saline solution and aliquots of the supernatant taken for analysis against a standard in ethanol. While this method is

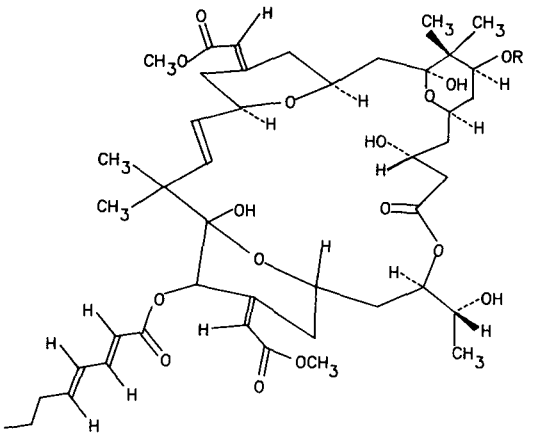

Fig. 1. Structure of bryostatin 1 (R = $-CO-CH_3$) and bryostatin 2 (R = H).

more efficient in the use of drug, however there is the possibility of supersaturation. The results are shown in Table I. Bryostatin 1 proved to be extremely insoluble in pure aqueous solvents.

Stability

The results of a pilot batch formulation, of a 0.1-mg/ml solution in absolute ethanol of the drug in glass ampoules, indicated no sign of degradation after three

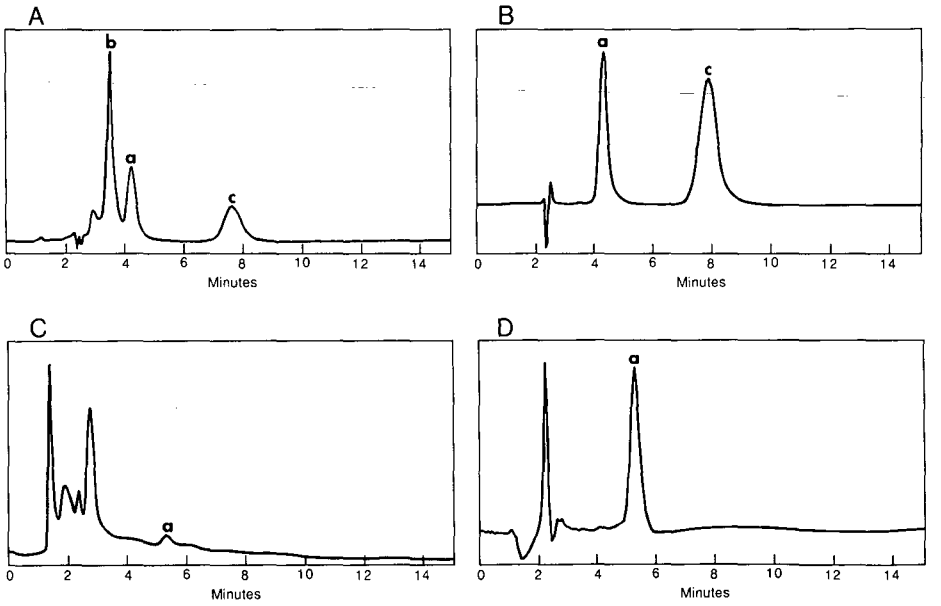

Fig. 2. (A) Chromatogram of bryostatin 1 (a), bryostatin 2 (b) and cholest-4-en-3-one (internal standard) (c). (B) Chromatogram of bryostatin 1 and internal standard. (C) Degradation of bryostatin 1 in 0.1 *M* phosphate, pH 9.3 (70°C, 1 h). (D) Degradation of bryostatin 1 in 0.1 *M* hydrochloric acid (70°C, 1.5 h).

TABLE I
SOLUBILITY OF BRYOSTATIN 1 IN ETHANOL–SALINE MIXTURES AT 20°C

Solution	*Solubility (mg/l)*
Water	0.77
0.9% (w/v) Saline	0.72
10% (v/v) Ethanol in 0.9% (w/v) saline	1.43
20% (v/v) Ethanol in 0.9% (w/v) saline	5.68
60% (v/v) Ethanol in 0.9% (w/v) saline	97.0
100% Ethanol	>4000

weeks at 50 or 20°C in daylight, or thirty weeks at −20°C. In addition a 0.06-mg/ml solution in 60% (w/v) ethanol–40% saline in a polypropylene syringe was found to be stable over a 24-h period at 20°C.

CONCLUSIONS

A stability-indicating assay for bryostatin 1 has been developed for use in formulation studies and as a basis for analysis of the drug in biological fluids.

ACKNOWLEDGEMENTS

Two of the authors (J.C.B. and J.A.S.) are grateful to the Cancer Research Campaign (grant No. SP1518) for support during the course of this work and G.R.P. wishes to acknowledge financial assistance provided by the Fannie E. Rippel Foundation, the Arizona Disease Control Research Commission, the Robert B. Dalton Endowment fund and grant No. CA16049 from the National Institutes of Health.

REFERENCES

1 G. R. Pettit, J. F. Day, J. L. Hartwell and H. B. Wood, *Nature (London)*, (1970) 962.
2 G. R. Pettit, C. L. Herald, D. L. Doubek, D. L. Herald, E. Arnold and J. Clardy, *J. Am. Chem. Soc.*, 104 (1982) 6846.
3 G. R. Pettit, J. E. Leet, C. L. Herald, Y. Kamano, F. E. Boettner, L. Baczynskyj and R. A. Nieman, *J. Org. Chem.*, 52 (1987) 2854.
4 M. L. Dell'Aquila, H. T. Nguyen, C. L. Herald, G. R. Pettit and P. M. Blumberg, *Cancer Res.*, 47 (1987) 6006.
5 M. Gscwendt, G. Furstenberger, S. Rose-John, M. Rogers, W. Kittstein, G. R. Pettit, C. L. Herald and F. Marks, *Carcinogenesis*, 9 (1988) 555.
6 G. Trenn, G. R. Pettit, H. Takayama, J. Hu-li and M. V. Sitkovsky, *J. Immunol.*, 140 (1988) 433.
7 H. Mohr, G. R. Pettit and A. Plessing-Menze, *Immunobiology*, 175 (1987) 420.
8 W. S. May, S. J. Sharkis, A. H. Esa, V. Gebbia, A. S. Kraft, G. R. Pettit and L. L. Sensenbrenner, *Proc. Natl. Acad. Sci. U.S.A.*, 84 (1987) 8483.
9 J. C. Berridge, *Techniques for the Automated Optimization of HPLC Separations*, Wiley Interscience, Chichester, 1985, pp. 192–195.

Journal of Chromatography, 467 (1989) 336–337
Elsevier Science Publishers B.V., Amsterdam — Printed in The Netherlands

CHROM. 21 349

Book Review

Analytical artifacts —GC, MS, HPLC, TLC and PC (*Journal of Chromatography Library Series*, Vol. 44), by B. S. Middleditch, Elsevier, Amsterdam, Oxford, New York, Tokyo, 1989, XXIII + 1033 pp., price Dfl. 495.00, US$ 241.50, ISBN 0-444-87158-6.

In the Preface to this volume the author states:

"This is not the place to elaborate on specific artifacts. However, it should be appropriate to give some indication of the types of problem which are considered:

- Plasticizers are present in many materials and can leach into a sample, contaminating it. Most analysts realize that they should use glass rather than plastic containers, but few of them would anticipate the possibility of plasticizer residues on glassware washed using detergent from a plastic bottle.

- A recent article in a respected journal claimed that the identity of the pheromone emitted by bitches in season to attract male dogs had been determined. What they detected was a widely-used antimicrobial agent.

- A male colleague once discovered (to his consternation) that skin oils collected from his forehead contained estrogens (female sex hormones). He was relieved to discover that they were from the hand lotion of the technician who swabbed his skin."

He then lists alphabetically the artifacts found by various workers, giving usually the mass spectrum, name, Merck Index number, retention index and a paragraph briefly outlining where the compound was encountered as an artifact, giving a total of 752 pages of information. Then follows a list of about 1000 references with full title and a very useful array of indexes.

One has the impression that the author has collected all the important work on analytical artifacts, available from the chemical literature, but one tends to ask oneself about the significance of such a collection.

If one has spent several years isolating carrier-free radioactive isotopes from natural radio-elements or cyclotron targets, one soon realises that the covalent bond is not as stable as one would like it to be. For example, when extracting UX_1 from an ethereal solution of 90 kg of uranyl nitrate, one finishes up with a beaker full of silica gel eluted from the twenty glass bottles in which the uranium solution is stored. When one elutes a lanthanum isotope from an ion-exchange column and evaporates the solution, one obtains instead of an invisible, radioactive residue several milligrams of a greyish residue, this being the resin that was solubilized during the chromatography.

Modern chromatography separates only minute amounts. This is dictated by the chromatographic process, which becomes more efficient as concentrations decrease. It should therefore be evident to the intelligent chromatographer that the usual impurities in addition to the usual decomposition products of stationary phases,

solvents, apparatus and compounds to be chromatographed will assume an important rôle. For every compound listed, and there are many, the chromatographer, if he is a chemist as well, can recall another which he encountered during his work.

Under the heading Paper Chromatography one finds the statement that

> "Preparative paper chromatography is unsuitable for trace analysis because the paper inevitably contains contaminants. An acceptable substitute is glass-fiber paper (Clark and Wotiz, 1973)".

But are not all chromatographic methods unsuitable unless the impurities are considered and eliminated?

The next entry on the same page on Parafilm states:

> "A boon to biochemists but anathema to analysts, Parafilm is a thermoplastic sealing material with a high alkane content. When it is stretched over the mouth of a vessel it is inevitable that the contents will be contaminated with a homologous series of alkanes, ranging from C_{20} to C_{35}. It was suggested by Gaskin *et al.* (1971), perhaps with tongue in cheek, that Parafilm be used as a source of alkanes for determining gas chromatographic retention index values".

This should surely be evident to any critical researcher, chemist or not.

The standard technique in criminology for detecting fingerprints is the reaction with ninhydrin; why, then, a sketchy chapter on amino acids?

The reviewer is left with some doubts about who will find this book useful in his work.

Journal of Chromatography, 467 (1989) 338
Elsevier Science Publishers B.V., Amsterdam — Printed in The Netherlands

CHROM. 21 262

Book Review

High-performance liquid chromatography of biopolymers and biooligomers, Part B: Separation of individual compound classes (*Journal of Chromatography Library Series*, Vol. 41B), by O. Mikeš, Elsevier, Amsterdam, Oxford, New York, Tokyo, 1988, XXII + 722 pp., price Dfl 360.00, US$ 189.50, ISBN 0-444-43034-2.

The reviewer of Part A of this book deplored in this journal the poor linguistic editing of the first volume. In this respect Part B is much improved and hence readable.

The book consists of 718 pages, of which 476 pages comprise the actual book, discussing in various chapters the separation of biopolymers and biooligomers according to compound classes. Then follows chapter 14, which is a register of chromatographed substances (97 pages) and the relevant bibliography (76 pages), and a subject index (57 pages), altogether about 230 pages of bibliographic material.

The Preface states that as the Register and Bibliography were slightly out-of-date, an Appendix and Addendum containing the most recent citations have been added. The most recent citations are, according to page 612, from the period 1983–86. However, in fact one finds, for example in the chapter on proteins, that of about 250 references only four are to papers published in 1986. In the chapter on enzymes, no paper is more recent than 1985.

On the one hand one sympathizes with the authors, as they collected 1304 references alone for the register. On the other hand, one is tempted to ask what purpose can be served by such an extensive compilation of the literature if it is three years or more out of date on appearance? Most of the figures show chromatograms with elution times of 30–50 min; how relevant is such information to workers in the field today?

It may be said that such delays are unavoidable in a book of this size, but this does not alter the fact that its validity as a reference book is seriously affected.

Perhaps the only answer to the problem is that as such books cannot be written without losing their usefulness on the way, they might well be superseded by computerized literature searches and consultation of the relevant bibliography sections of the appropriate journals.

Journal of Chromatography, 467 (1989) 339
Elsevier Science Publishers B.V., Amsterdam — Printed in The Netherlands

CHROM. 21 321

Book Review

Preparative-scale chromatography (*Chromatographic Science Series*, Vol. 46), edited by E. Grushka, Marcel Dekker, New York, Basle, 1989, XIV + 324 pp., price US$ 99.75 (U.S.A. and Canada), US$ 119.50 (rest of world), ISBN 0-8247-8061-2.

It is a fact of life that in any new field of applications or techniques in chromatography, sooner or later various series of symposia and several monographs appear within short intervals. Preparative-scale chromatography is certainly no exception. Two series of symposia have already been initiated and this is the fourth book on the topic to be reviewed in this journal.

This volume includes fifteen chapters by different authors and spans a wide range of techniques: theory, preparative high-performance liquid chromatography, the coil planet centrifuge, continuous chromatography and some specific applications.

The chapters on specific applications have more the character of scientific papers and hence do not survey the field but rather give concrete results. Then there are chapters by authors who have written or contributed to recent monographs, *e.g.*, V. R. Meyer, M. Verzele and Y. Ito, so that one cannot expect much new insight if one has already read their books or recent papers.

Altogether the book has more the character of a symposium volume, but it is not clear whether this is so or rather that it is a collection of invited contributions.

The contribution by Schott (pages 269–308) is largely based on papers that have appeared in this journal, mainly from Schott and Schrade, *J. Chromatogr.*, 265 (1983) 257–275. This paper is not quoted, nor are there any acknowledgements for the reproduction of Figures 1–3 from that paper.

Most of the contributions are pertinent and interesting. Nevertheless, together they do not constitute the complete survey of the field that is still lacking in the literature.

Journal of Chromatography, 467 (1989) 340
Elsevier Science Publishers B.V., Amsterdam — Printed in The Netherlands

CHROM. 21 373

Book Review

Neuromethods, Vol. 10, Analysis of psychiatric drugs, edited by A. A. Boulton, G. B. Baker and R. T. Coutts, Humana Press, Clifton, NJ, 1988, 547 pp., price US$ 79.50 (U.S.A.)/US$ 89.50 (export), ISBN 0-89603-121-7.

Not only do the twelve chapters of this book review the main methods for the analysis of psychiatric drugs, but the volume goes further in that it deals with animal models for assessing drug action, high-affinity binding of antidepressants to platelets and brain tissue and a final chapter on structure–activity relationships at the benzodiazepine receptor.

It is an excellent idea to produce a volume that contains a review of all methods as well as numerous laboratory applications, such as protein binding. All chapters give an extensive bibliography and are very readable. However, this book raises a point that should be discussed.

This volume, to take an example, is the concerted effort of twelve research groups, with the result that the complete manuscript can only be printed when the slowest authors have revised their contributions. We have cases such as the chapter on isotope derivative assays, which has about 45 references, most of which date from between 1970 and 1980 and the latest 1984. Hence this is already out of date. Similarly, some tables in the chapter on "In vitro and ex vivo neurochemical screening procedures..." pages 330–334, stop at 1985. Other chapters offer 1986 as their most recent references. The whole of this problem is one of book production. There seems to be a feeling that no undue hurry is needed and that 2 years is a reasonable time for the production of a book. That this is not necessarily so is proved by the scientific supplements in daily newspapers, which can publish figures, graphs and recent results without the gestation period of an elephant. Given the advent of desk-top publishing, why should we continue to bake stale bread?

PUBLICATION SCHEDULE FOR 1989

Journal of Chromatography and Journal of Chromatography, Biomedical Applications

MONTH	J	F	M	A	M	J	J	A	S	O	N	D
Journal of Chromatography	461 462 463/1	463/2 464/1	464/2 465/1 465/2	466 467/1 467/2	468 469 470/1 470/2	471 472/1 472/2 473/1	The publication schedule for further issues will be published later					
Bibliography Section		486/1		486/2		486/3		486/4				
Biomedical Applications	487/1	487/2	488/1 488/2	489/1 489/2	490/1 490/2	491/1	491/2	492/1	492/2 493			

INFORMATION FOR AUTHORS

(Detailed *Instructions to Authors* were published in Vol. 445, pp. 453–456. A free reprint can be obtained by application to the publisher, Elsevier Science Publishers B.V., P.O. Box 330, 1000 AH Amsterdam, The Netherlands.)

Types of Contributions. The following types of papers are published in the *Journal of Chromatography* and the section on *Biomedical Applications:* Regular research papers (Full-length papers), Notes, Review articles and Letters to the Editor. Notes are usually descriptions of short investigations and reflect the same quality of research as Full-length papers, but should preferably not exceed six printed pages. Letters to the Editor can comment on (parts of) previously published articles, or they can report minor technical improvements of previously published procedures; they should preferably not exceed two printed pages. For review articles, see inside front cover under Submission of Papers.

Submission. Every paper must be accompanied by a letter from the senior author, stating that he is submitting the paper for publication in the *Journal of Chromatography*. Please do not send a letter signed by the director of the institute or the professor unless he is one of the authors.

Manuscripts. Manuscripts should be typed in double spacing on consecutively numbered pages of uniform size. The manuscript should be preceded by a sheet of manuscript paper carrying the title of the paper and the name and full postal address of the person to whom the proofs are to be sent. Authors of papers in French or German are requested to supply an English translation of the title of the paper. As a rule, papers should be divided into sections, headed by a caption (*e.g.*, Summary, Introduction, Experimental, Results, Discussion, etc.). All illustrations, photographs, tables, etc., should be on separate sheets.

Introduction. Every paper must have a concise introduction mentioning what has been done before on the topic described, and stating clearly what is new in the paper now submitted.

Summary. Full-length papers and Review articles should have a summary of 50–100 words which clearly and briefly indicates what is new, different and significant. In the case of French or German articles an additional summary in English, headed by an English translation of the title, should also be provided. (Notes and Letters to the Editor are published without a summary.)

Illustrations. The figures should be submitted in a form suitable for reproduction, drawn in Indian ink on drawing or tracing paper. Each illustration should have a legend, all the *legends* being typed (with double spacing) together on a *separate sheet*. If structures are given in the text, the original drawings should be supplied. Coloured illustrations are reproduced at the author's expense, the cost being determined by the number of pages and by the number of colours needed. The written permission of the author and publisher must be obtained for the use of any figure already published. Its source must be indicated in the legend.

References. References should be numbered in the order in which they are cited in the text, and listed in numerical sequence on a separate sheet at the end of the article. Please check a recent issue for the layout of the reference list. Abbreviations for the titles of journals should follow the system used by *Chemical Abstracts*. Articles not yet published should be given as "in press" (journal should be specified), "submitted for publication" (journal should be specified), "in preparation" or "personal communication".

Dispatch. Before sending the manuscript to the Editor please check that the envelope contains three copies of the paper complete with references, legends and figures. One of the sets of figures must be the originals suitable for direct reproduction. Please also ensure that permission to publish has been obtained from your institute.

Proofs. One set of proofs will be sent to the author to be carefully checked for printer's errors. Corrections must be restricted to instances in which the proof is at variance with the manuscript. "Extra corrections" will be inserted at the author's expense.

Reprints. Fifty reprints of Full-length papers, Notes and Letters to the Editor will be supplied free of charge. Additional reprints can be ordered by the authors. An order form containing price quotations will be sent to the authors together with the proofs of their article.

Advertisements. Advertisement rates are available from the publisher on request. The Editors of the journal accept no responsibility for the contents of the advertisements.

Analytical Artifacts

GC, MS, HPLC, TLC and PC

by **B.S. MIDDLEDITCH**, *Dept. of Biochemical and Biophysical Sciences, University of Houston, Houston, TX, USA*

(Journal of Chromatography Library, 44)

This encyclopaedic catalogue of the pitfalls and problems that all analysts encounter in their work is destined to spend more time on the analyst's workbench than on a library shelf. The author has dedicated the book to "the innumerable scientists who made mistakes, used impure chemicals and solvents, suffered the consequences of unanticipated side-reactions, and were otherwise exposed to mayhem yet were too embarrassed to publish their findings".

Traditionally, the mass spectroscopist or gas chromatographer learnt his trade by participating in a 4-6 year apprenticeship as graduate student and post-doctoral researcher. Generally, no formal training was provided on the things that go wrong, but this information was accumulated by sharing in the experiences of colleagues. Nowadays, many novice scientists simply purchase a computerized instrument, plug it in, and use it. Much time can be wasted in studying and resolving problems due to artifacts and there is also a strong possibility that artifacts will not be recognized as such. For example, most analysts realize that they should use glass rather than plastic containers; but few of them would anticipate the possibility of plasticizer residues on glassware washed using detergent from a plastic bottle.

This book is an easy-to-use compendium of problems encountered when using various commonly used analytical techniques. Emphasis is on impurities, by-products, contaminants and other artifacts. A separate entry is provided for each artifact. For specific chemicals, this entry provides the common name, mass spectrum, gas chromatographic data, CAS name and registry number, synonyms and a narrative discussion. More than 1100 entries are included. Mass spectral data are indexed in a 6-peak index (molecular ion, base peak, second peak, third peak) and there are also formula, author and subject indexes. An extensive bibliography contains complete literature citations.

The book is designed to be *used*. It will not only allow experienced analysts to profit from the mistakes of others, but it will also be invaluable to other scientists who use analytical instruments in their work.

1989 xxiv + 1028 pages
US$ 241.50 / Dfl. 495.00
ISBN 0-444-87158-6

ELSEVIER SCIENCE PUBLISHERS

P.O. Box 211, 1000 AE Amsterdam, The Netherlands
P.O. Box 882, Madison Square Station, New York, NY 10159, USA